Karlsruher Institut für Technologie

Uncertainty principles for inverse source and inverse scattering problems

Zur Erlangung des akademischen Grades eines

Doktors der Naturwissenschaften

von der KIT-Fakultät für Mathematik
des Karlsruher Instituts für Technologie (KIT)
genehmigte

Dissertation

von

Lisa Schätzle

Referent:	Prof. Dr. Roland Griesmaier
Korreferent:	Prof. Dr. Andreas Rieder
Tag der mündlichen Prüfung:	28. Mai 2025

Acknowledgment

This thesis was funded by the Deutsche Forschungsgemeinschaft (DFG, German Research Foundation) – Project-ID 258734477 – SFB 1173.

An dieser Stelle möchte ich mich bei einer Reihe an Personen bedanken, die mich während meiner Promotion unterstützt und dadurch zu einem wesentlichen Teil zum Gelingen dieser Arbeit beigetragen haben.

Ein besonderer Dank gilt meinem Betreuer Prof. Dr. Roland Griesmaier für seine stetige Unterstützung und hilfreichen Anregungen, sowie das sorgfältige Lesen meiner Texte und die resultierenden ausführlichen Verbesserungsvorschläge. Weiter möchte ich mich bei Prof. Dr. Andreas Rieder dafür bedanken, dass er das Zweitgutachten dieser Arbeit übernommen hat.

Auch bei meinen zwei weiteren Chefs PD Dr. Tilo Arens und PD Dr. Frank Hettlich möchte ich mich bedanken, sowohl für die angenehme Zusammenarbeit in der Lehre, wie auch für die fachlichen und nichtfachlichen Gespräche und dafür, dass sie stets ein offenes Ohr für mich hatten.

Ich bedanke mich auch beim Rest meiner Arbeitsgruppe und möchte namentlich meinen Mitdoktorandinnen Leonie Fink, Eliane Kummer, und Nasim Shafieebyaneh nennen, die diese Arbeit korrekturgelesen haben. Ich hatte das Glück zeitgleich mit tollen Menschen zu promovieren und hoffe, dass wir auch in der Zukunft in Kontakt bleiben werden.

Ein großes Dankeschön geht auch an meine Eltern und meine Schwester, die mich stets unterstützt und an mich geglaubt haben, selbst in Zeiten, in denen ich mich selbst damit schwer getan habe.

Nicht zuletzt möchte ich mich bei meinem Partner Marvin Knöller für seinen stetigen Rückhalt und sein Verständnis, das Korrekturlesen dieser Arbeit und die schöne gemeinsame Zeit, bisher hier in Karlsruhe und bald endlich in Helsinki, bedanken.

Abstract

We consider scattering of time-harmonic acoustic waves by an ensemble of compactly supported inhomogeneous objects, called scatterers, in a homogeneous background medium. The scatterers are illuminated by incident plane waves along all possible illumination directions and, each time, the resulting scattered waves are detected far away along all possible observation directions. This data can be described by the far field operator, which uniquely determines the scatterers in inverse medium scattering. In practice, this given data is often noisy and possibly incomplete, which motivates the study of two related inverse problems, that are at the center of our consideration in this thesis. On the one hand, given the far field operator associated to the ensemble of scatterers, we discuss the nonlinear inverse problem to recover the far field operators associated to each of the scatterers individually. We refer to this problem as *far field operator splitting*, which involves the removal of specific multiple scattering effects. This problem is closely related to the question whether the components of the scatterer can be distinguished by means of inverse medium scattering in a stable way. On the other hand, we study the restoration of missing or inaccurate components of the observed far field operator, which we refer to as *far field operator completion*. Both problems are ill-posed without further assumptions, but we give sufficient conditions on the diameter of the supports of the scatterers, the distance between them, and the size of the missing or corrupted data component to guarantee stable recovery whenever sufficient a priori information on the location of the unknown scatterers is available. We reformulate both inverse problems as suitable splitting problems and take advantage of the fact that the arising far field operator components can be well approximated by sparse or low rank operators. This enables us to use techniques from compressed sensing and from low rank matrix completion. We provide algorithms, error estimates and a stability analysis for two as well as for three dimensions. Furthermore, we verify our theoretical predictions by numerical examples both on synthetic and on experimental data, and we test to what extent our reconstructions are suitable as an input for an inverse medium scattering problem.

Contents

CHAPTER 1

INTRODUCTION

1.1. FROM INVERSE MEDIUM SCATTERING TO FAR FIELD OPERATOR SPLITTING AND COMPLETION

The aim of research in inverse scattering theory is to detect or to identify unknown objects from measurements of associated acoustic, electromagnetic or elastic waves. In the case of scattering of time-harmonic acoustic waves by compactly supported inhomogeneous media this leads to the acoustic *inverse medium scattering problem* (see, e.g. [31, p. 439]). Here, the compactly supported inhomogeneous unknown object, called scatterer, is supposed to lie in a homogeneous background medium. Mathematically, the scatterer can be modeled by the support of a contrast function. In inverse medium scattering, the task is to determine this contrast function or at least its support from the knowledge of scattered wave data. The scatterer is illuminated along all possible illumination directions with plane waves and the resulting scattered waves are measured far away along all possible observation directions, i.e., the associated far field patterns are measured. This input data can be described by the far field operator, which maps densities of superpositions of incident plane waves to the far field patterns of the corresponding scattered waves. The determination of the scatterer given the far field operator leads to a uniquely solvable, but ill-posed inverse problem. This operator can be viewed as an idealized measurement operator for the inverse medium scattering problem, and it plays a central role in several reconstruction methods (see, e.g., [2, 28, 29, 32, 51, 64] and the monographs [16, 17, 31, 69]). In practice, the given far field data is typically noisy and often incomplete, which makes these reconstruction methods more or less challenging to apply. Scenarios are also conceivable in which the data carries artifacts that one likes to avoid and to filter out. One may think, e.g., of an ensemble of scatterers, where only the far field data corresponding to one or a few of the scatterers is of interest. Consequently, it is desirable to preprocess the data accordingly. This motivates the consideration of two related inverse problems, which we aim to focus on in this work. Assuming that a possibly noisy and incomplete version of the far field operator is available and that the scatterer may consist of several components, we ask the following questions:

(a) *Far field operator splitting:* Is it possible to reconstruct the far field operators associated to the scatterer's components individually, if we have enough a priori information on the location of these components to distinguish them from one another? In particular, is it possible to remove multiple scattering effects generated simultaneously by all scatterers?

(b) *Far field operator completion:* Can we recover missing parts of the far field operator, provided the portion of missing data is not too large, and filter possible data errors?

Both problems are uniquely solvable with exact data but severely ill-posed without further assumptions. The goal of this work is to develop reconstruction methods for solving problems (a) and (b) without solving the time-consuming and also ill-posed inverse medium scattering problem itself. Furthermore, the stability of the obtained reconstructions with respect to noise in the data is aimed to be analyzed.

In contrast to the inverse medium scattering problem with the far field operator as an input it is an open question whether a single far field pattern is already sufficient to determine the scatterer uniquely at least under some (simplifying) assumptions, see [30, Sec. 8]. The same holds for the inverse obstacle problem (see e.g. [31, Chap. 7]), but it has been proven to fail in the case of the inverse source problem, see [10]. For all three problems, nevertheless, substantial information on the support, just as the (convex) scattering support (see [75, 76, 95]), or provided the scatterer's components are small enough and far enough away from each other, the number and locations of these components can be uniquely reconstructed (see [95]). The studies on this research question motivated the considerations in [50, 54, 55, 56], that form the foundation of this thesis.

The key concept for handling the ill-posedness of problems (a) and (b) relies on sparse and low rank approximations of the far field operator components. These can be derived from (possibly partial) a priori knowledge on the localizations and sizes of the scatterer's components (for problem (a)) or on the localization and size of the whole scatterer and the configuration of non-observable data (for problem (b)). This is based on the concept of *nonevanescent far fields* as developed for the source problem in [55, 56] for the Helmholtz equation or in [57] for Maxwell's equations and Navier systems. The regularization strategy, which is called a *regularized Picard criterion* in this context, is to not recover the full far fields, but only their nonevanescent parts. These are the parts that can be radiated by a limited power source supported in a ball, which is prescribed by the a priori knowledge on the scatterer's location and size, and at the same time detectable by a receiver of a given sensitivity. The resulting sparse representations of these parts with respect to modulated Fourier bases reappear in a modified form within the sparse and low rank approximations of the far field operators in this work.

When moving from the inverse source problem to the inverse medium scattering problem, two major differences arise. The first difference is that the far field splitting problem for inverse source problems is linear, while it is nonlinear for the inverse medium scattering problem due to multiple scattering effects. Thus, it becomes an additional challenge to quantify and to remove these unintended multiple scattering contributions when solving problem (a). The Born series expansion (see e.g. [62]) of the far field operator proves to be a good tool to tackle this issue. Starting with the Born approximation, i.e. with a linearization of the problem, and gradually involving more and more scattering orders allows us to develop strategies for dealing with the full medium scattering problem. The consideration of the Born approximation provides, as a special source problem, a direct link to the existing work on far field splitting and completion for the source problem, cf. [55, 56]. This further clarifies the inclusion of the term 'source problem' in the title of this thesis. The (inverse) Born series has recently also been used directly in reconstruction methods for the inverse medium scattering problem in [35, 62, 63, 83]. In [11] (see also [42, 43]) the authors have been applying a reduced order model to transform scattering data for a time-dependent scattering problem including multiple scattering effects to observations expected in the Born approximation, i.e., multiple scattering effects are removed. Both approaches are not directly related to the results in this work. The second difference is that, while for the inverse source problem one has access to just one far field pattern radiated by the unknown source, infinitely many but correlated far field patterns are available for the inverse medium scattering problem. These correlations in the data unlock the possibility to further stabilize our reconstruction methods by incorporating the concept of low rank and the reciprocity relation (see e.g. [31, Thm. 8.8]), when working with whole far field operators instead of individual far field patterns.

To position our work within existing research, we also note that alternate methods for far field splitting for inverse source problems have been proposed in [8, 88], and that splitting problems for time-dependent waves have recently been considered in [4, 48, 58]. Data completion for far field operators as in problem (b) has been discussed in [41, 80] (see also [3, 12] for related results for the Cauchy problem for the Helmholtz equation). In contrast to our work, the authors of those works do not use sparse representations of far field patterns or far field operators with respect to modulated Fourier bases to stabilize their algorithms, which so far also lack a rigorous stability analysis.

The contribution of this thesis can be classified as follows. We extend the existing stability analysis and algorithms for splitting and completion of single far fields in inverse source problems to far field operator splitting and completion for inverse medium scattering problems, which turns out to result in an improved stability due to correlated data. In the case of far field operator splitting, this leads to new theoretical insights. On the one hand, we incorporate the reciprocity relation and the low rank property of far field operators, which both was not possible in the case of single far field patterns. On the other hand, we identify far field operator components that model multiple scattering effects with those scatterer components that first and last interact with the wave. This makes it possible to develop a criterion to filter out a large portion of unwanted multiple scattering when solving problem (a). We formulate related uncertainty principles for both inverse problems (a) and (b). Some of these are similar to those in existing literature, while others, involving above mentioned aspects, require completely new approaches. Incorporating the low rank property enables the use of a new class of algorithms for nuclear norm minimization. In addition to our tests on synthetic data, we run our methods on experimental data and examine to what extent our reconstructions are suitable as an input for the inverse medium problem.

In the following, we give a brief insight into some underlying ideas for our stability analysis, which originate from the *compressed sensing* problem (see e.g. [22, 37]) and the *matrix completion* problem (see e.g. [20, 21]) in signal processing. In [18] a survey and a comparison of these two problems can be found.

1.2. Related concepts from signal processing

In signal processing, a classical *uncertainty principle* links the measure $|T|$ of the essential support T of a signal to the measure $|W|$ of the essential support W of its Fourier transform via $|T||W| \geq 1$, so they cannot be arbitrarily localized at the same time. In quantum mechanics, this principle is also known as Heisenberg's indeterminacy principle, which states that a particle's position and momentum cannot be measured with arbitrary precision at the same time. This principle further applies in a similar way to the discrete Fourier transform, where for visualization purposes, we consider the two-dimensional case, since this is relevant throughout this work. Let the discrete two-dimensional Fourier transform of a matrix $A = (a_{m,n})_{0\leq m,n\leq N-1} \in \mathbb{C}^{N\times N}$ for $N \in \mathbb{N}$ be given by $\hat{A} = (\hat{a}_{m',n'})_{0\leq m',n'\leq N-1}$ with

$$\hat{a}_{m',n'} := \frac{1}{N}\sum_{m=0}^{N-1}\sum_{n=0}^{N-1} a_{m,n} e^{-2\pi \mathrm{i}\frac{mm'+nn'}{N^2}} \qquad \text{for } m',n' \in \{0,\dots,N-1\},$$

and let $\|A\|_{\ell^0\times\ell^0} = \{(m,n) \,|\, a_{m,n} \neq 0\}$. Consequently, the inverse discrete Fourier transform is given by $\check{A} = (\check{a}_{m,n})_{0\leq m,n\leq N-1}$ with

$$\check{a}_{m,n} := \frac{1}{N}\sum_{m'=0}^{N-1}\sum_{n'=0}^{N-1} a_{m',n'} e^{2\pi \mathrm{i}\frac{mm'+nn'}{N^2}} \qquad \text{for } m,n \in \{0,\dots,N-1\}. \tag{1.1}$$

Then, for the time-bandwidth product there holds a classical uncertainty principle of the form

$$\|A\|_{\ell^0\times\ell^0}\|\hat{A}\|_{\ell^0\times\ell^0} \geq N^2, \tag{1.2}$$

see [40, Thm. 1]. This can be proven easily as follows. For arbitrary $A, B \in \mathbb{C}^{N\times N}$ we conclude from Hölder's inequality, (1.1), the Cauchy Schwarz inequality and Parseval's identity that

$$\begin{aligned}|\langle A,B\rangle_{\ell^2\times\ell^2}| \leq \|A\|_{\ell^1\times\ell^1}\|B\|_{\ell^\infty\times\ell^\infty} &\leq \frac{1}{N}\|A\|_{\ell^1\times\ell^1}\|\hat{B}\|_{\ell^1\times\ell^1} \\ &\leq C\sqrt{\|A\|_{\ell^0\times\ell^0}\|\hat{B}\|_{\ell^0\times\ell^0}}\|A\|_{\ell^2\times\ell^2}\|B\|_{\ell^2\times\ell^2}, \end{aligned} \tag{1.3}$$

where $C = 1/N$. Choosing $A = B$ in (1.3) yields (1.2). Estimates of the form (1.3) is what we refer to as an uncertainty principle throughout this work. For $\phi, \psi \in L^2(\mathbb{R}^2)$ with $\operatorname{supp}\phi \subset T$ and $\operatorname{supp}\hat{\psi} \subset W$ and the Fourier transform on $L^2(\mathbb{R}^2)$ given by

$$\hat{\phi}(\boldsymbol{y}) := \frac{1}{2\pi} \int_{\mathbb{R}^2} \phi(\boldsymbol{x}) e^{-\mathrm{i}\boldsymbol{x}\cdot\boldsymbol{y}} \, \mathrm{d}\boldsymbol{x} \qquad \text{for } \boldsymbol{y} \in \mathbb{R}^2 ,$$

an uncertainty principle of the form (1.3) reads

$$|\langle \phi, \psi \rangle_{L^2(\mathbb{R}^2)}| \leq C \sqrt{|T||W|} \|\phi\|_{L^2(\mathbb{R}^2)} \|\psi\|_{L^2(\mathbb{R}^2)} , \tag{1.4}$$

where $C = 1/(2\pi)$. In contrast to the above, it is not possible to directly deduce a classical uncertainty principle of the form (1.2) from (1.4), since $\operatorname{supp}\phi$ and $\operatorname{supp}\hat{\phi}$ cannot be finite at the same time, so the choice $\phi = \psi$ is not admissible. Nevertheless, (1.4) can be transformed into a meaningful statement in that case by the use of essentially supported functions on certain sets, see [40, Thm. 2]. The notion of an uncertainty principle as in (1.3) and (1.4) constitutes the foundation for the development of algorithms and associated stability estimates for sparse representations of functions, see e.g. [38, 39], and for tackling the compressed sensing problem, see e.g. [22, 37]. Since for the source problem, the far field pattern radiated by a source is its restricted Fourier transform, this notion of an uncertainty principle further highly influenced the results from [55, 56, 57] for splitting and completion of single far field patterns in that situation.

In the *compressed sensing* problem, the aim is to reconstruct a signal from finitely many sampled values, which leads to an undetermined system and is thus not uniquely solvable. To relate it to the framework as introduced above, we think of the signal as an $L^2(\mathbb{R}^2)$ function. By additionally assuming its Fourier coefficients to be sparse, which means that only a few coefficients are nonzero, a good approximation of this signal can be obtained by solving a *basis pursuit* problem. Here, a minimization of the number of nonzero Fourier coefficients is replaced by a minimization of their $\ell^1 \times \ell^1$ norm. This preserves, as a convex relaxation, certain properties of the original problem, but can be solved numerically using convex optimization. Alternatively, we can think of the original problem as a *matrix completion* problem, when interpreting the Fourier coefficients as matrix entries. Instead of demanding sparsity of the Fourier coefficients, we can also assume the underlying matrix to have low rank. Similar to basis pursuit, minimizing the rank, i.e., the number of nonzero singular values of the matrix, can be relaxed to minimizing the nuclear norm, i.e., the ℓ_1 norm of the singular values, see [20, 21].

Our idea is to translate far field operator splitting (a) and far field operator completion (b) into the frameworks of compressed sensing and low rank matrix completion. This allows us to incorporate key concepts and algorithms from these research fields to develop reconstruction methods and stability analyses for our own purposes. Particularly, this involves introducing spaces of sparse or low rank far field operators, deriving suitable splits of the far field operator in these subspaces and setting up related minimization problems.

1.3. Outline of this thesis

In Chapter 2, after introducing some preliminaries, we provide the technical background on the acoustic medium scattering problem, which we end with the introduction of the far field operator. This operator is a Hilbert–Schmidt integral operator and at the center of our considerations. Some basics about Hilbert–Schmidt integral operators are collected in Appendix A. We develop sparse and low rank approximations of the far field operator with respect to modulated Fourier bases, by first examining its Born series expansion in more detail. For the Born approximations as well as for the sparse and low rank approximations we give related error estimates. The latter are essentially based on the decay behavior of Bessel functions with respect to their order and for fixed argument. Useful properties of Bessel functions and related special functions can be found in Appendix B. It

turns out that shifting the scatterer in space further improves the sparsity and low rank property of the associated far field operator, which can be modeled by introducing a translation operator.

The rest of this thesis is divided into two parts, Chapters 3 and 4 covering the far field operator splitting problem and Chapters 5 and 6 dealing with the completion problem (possibly in combination with the splitting problem).

In Chapter 3, assuming the scatterer to consist of two components, we start our theoretical investigation of far field operator splitting by further expanding the far field operator not only in terms of the scattering order, but also in terms of the scatterer's components. Based on this, we generalize our concepts from the previous chapter to develop sparse representations of far field operator components associated to multiple scattering effects involving both scatterer's components. After considering a general subspace splitting problem, we first study the problem's Born approximation, which neglects multiple scattering effects, as an ansatz equation. Later, we extend on this idea to include multiple scattering effects. We formulate related uncertainty principles and examine the stability of the reconstructions when approximating the solutions of the original splitting problem by related least squares problems, $\ell^1 \times \ell^1$ minimization problems and a coupled nuclear norm minimization problem. Two subgradients, that are needed for the proofs of the last mentioned problem formulation, are given in Appendix C. Finally, we describe how to incorporate the reciprocity principle and provide related results for more than two scatterer's components.

In Chapter 4, after explaining the implementation in detail, we provide numerical examples to test our theoretical findings from the previous chapter. Numerically, we implement the solutions of the mentioned minimization problems by using the conjugate gradient method and different variants of the fast iterative soft thresholding algorithm. The general framework and the required proximity operators are elaborated in more detail in Appendix D.

Far field operator completion is the topic of Chapter 5. Starting with solving the completion problem only, we turn to solving the completion and splitting problem simultaneously. We again give related uncertainty principles and stability analyses for least squares and $\ell^1 \times \ell^1$ minimization problem formulations.

In Chapter 6 we provide numerical tests on far field operator completion. Additionally to the theoretically investigated schemes, we implement algorithms for nuclear norm minimization. We begin, as in Chapter 4, with tests on synthetic data and then apply our algorithms to experimental data from the Fresnel Institute in the framework of missing backscattering data. Finally, we use our obtained reconstructions for missing back scattering data as an input for solving the shape identification problem by the factorization method. Here, we compare the results with the often used procedure to use the data extended by zeros as an input.

1.4. Prior publication

Some results of this work have already been published in [53]. This applies to many of the results for two dimensions excluding the findings from Subsection 3.4.2 as well as all results involving the low rank property of the far field operator.

CHAPTER 2

Far field operators for inhomogeneous acoustic medium scattering

2.1. Preliminaries

Let $d \in \{2,3\}$ denote the dimension and $D \subseteq \mathbb{R}^d$ an open set with boundary $\partial D = \overline{D} \cap (\mathbb{R}^d \setminus D)$. For $m \in \mathbb{N}_0 \cup \{\infty\}$ we define the subspaces of classical m-times differentiable functions by

$$\begin{aligned} C^m(D) &:= \{u : D \to \mathbb{C} \,|\, u \text{ is } m \text{ times continuosly differentiable}\}, \\ C_0^m(D) &:= \{u \in C^m(D) \,|\, \operatorname{supp} u \subseteq D \text{ is compact}\}, \end{aligned}$$

where $\operatorname{supp} u := \overline{\{x \in D \,|\, u(x) \neq 0\}}$ is the support of $u : D \to \mathbb{C}$.

For $1 \leq p \leq \infty$ we denote by $L^p(D)$ the standard Lebesgue space equipped with the norm

$$\|u\|_{L^p(D)} := \begin{cases} \left(\int_D |u(\boldsymbol{x})|^p \, \mathrm{d}\boldsymbol{x}\right)^{1/p} & \text{if } p < \infty, \\ \operatorname{ess\,sup}_{\boldsymbol{x} \in D} |u(\boldsymbol{x})| & \text{if } p = \infty. \end{cases}$$

The space $L^2(D)$ is a Hilbert space with the inner product

$$\langle u, v \rangle_{L^2(D)} := \int_D u(\boldsymbol{x}) \overline{v(\boldsymbol{x})} \, \mathrm{d}\boldsymbol{x}, \qquad u, v \in L^2(D).$$

Throughout this work, in our notation, inner products are always linear in the first and antilinear in the second argument. We further define for $1 \leq p \leq \infty$ the vector-valued spaces

$$L^p(D; \mathbb{C}^d) := \{u : D \to \mathbb{C}^d \,|\, u_j \in L^p(D) \text{ for } j = 1, \ldots, d\}.$$

We call $\boldsymbol{v} \in L^2(D, \mathbb{C}^d)$ the variational gradient of $u \in L^2(D)$ if

$$\int_D u \nabla \phi \, \mathrm{d}\boldsymbol{x} = -\int_D \boldsymbol{v} \phi \, \mathrm{d}\boldsymbol{x} \qquad \text{for all } \phi \in C_0^\infty(D),$$

and we write $\boldsymbol{v} = \nabla u$ in that case. We introduce the Sobolev space $H^1(D)$ by

$$H^1(D) := \{u \in L^2(D) \,|\, u \text{ has a variational gradient } \nabla u \in L^2(D, \mathbb{C}^d)\},$$

which is a Hilbert space together with the inner product

$$\langle u, v \rangle_{H^1(D)} := \langle u, v \rangle_{L^2(D)} + \langle \nabla u, \nabla v \rangle_{L^2(D)},$$

where $\langle \nabla u, \nabla v \rangle_{L^2(D)} = \int_D \nabla u(\boldsymbol{x}) \cdot \overline{\nabla v(\boldsymbol{x})} \, \mathrm{d}\boldsymbol{x}$.

For $\boldsymbol{x} = (x_1, \ldots, x_d)^\top \in \mathbb{R}^d$ we write $\boldsymbol{x}' = (x_1, \ldots, x_{d-1})^\top \in \mathbb{R}^{d-1}$. We denote by $B_R(\boldsymbol{c}) \subseteq \mathbb{R}^d$

the open d-dimensional ball of radius $R > 0$ centered at $\boldsymbol{c} \in \mathbb{R}^d$ and by $B'_R(\boldsymbol{c}') \subseteq \mathbb{R}^{d-1}$ the open $(d-1)$-dimensional ball of radius $R > 0$ centered at $\boldsymbol{c}' \in \mathbb{R}^{d-1}$. Let

$$H^1_{\mathrm{loc}}(\mathbb{R}^d) := \{u \in L^2(\mathbb{R}^d) \,|\, \chi_{B_R(\mathbf{0})} u \in H^1(B_R(\mathbf{0})) \text{ for all } R > 0\}\,.$$

We recall the definition of a Lipschitz bounded set from [70, Def. 5.1] (see also [81, Def. 3.28]).

Definition 2.1. We call an open set $D \subseteq \mathbb{R}^d$ Lipschitz bounded if there exist $J \in \mathbb{N}$ cylinders

$$U_j = \{R_j \boldsymbol{x} + \boldsymbol{z}^{(j)} \,|\, \boldsymbol{x} \in B'_{\alpha_j}(\mathbf{0}) \times (-2\beta_j, 2\beta_j)\}\,, \quad j = 1, \ldots, J\,,$$

with translation vectors $\boldsymbol{z}^{(j)} \in \mathbb{R}^d$ and rotation matrices $R_j \in \mathbb{R}^{d\times d}$ and Lipschitz continuous functions $\xi_j : B'_{\alpha_j}(\mathbf{0}) \to \mathbb{R}$ with $|\xi_j(\boldsymbol{x}')| \leq \beta_j$ for all $\boldsymbol{x}' \in B'_{\alpha_j}(\mathbf{0})$ such that $\partial D \subseteq \bigcup_{j=1}^J U_j$ and

$$\begin{aligned}
\partial D \cap U_j &= \{R_j \boldsymbol{x} + \boldsymbol{z}^{(j)} \,|\, \boldsymbol{x}' \in B'_{\alpha_j}(\mathbf{0})\,,\, x_d = \xi_j(\boldsymbol{x}')\}\,,\\
D \cap U_j &= \{R_j \boldsymbol{x} + \boldsymbol{z}^{(j)} \,|\, \boldsymbol{x}' \in B'_{\alpha_j}(\mathbf{0})\,,\, x_d < \xi_j(\boldsymbol{x}')\}\,,\\
U_j \setminus \overline{D} &= \{R_j \boldsymbol{x} + \boldsymbol{z}^{(j)} \,|\, \boldsymbol{x}' \in B'_{\alpha_j}(\mathbf{0})\,,\, x_d > \xi_j(\boldsymbol{x}')\}
\end{aligned}$$

for $j = 1, \ldots, J$. Here, without loss of generality, the cylinders are constructed in such a way that $\beta_j \geq \alpha_j$.

Roughly speaking Definition 2.1 means, that the boundary ∂D of D can be represented locally, i.e., after choosing possibly different cartesian coordinates for different parts of ∂D, as the graph of a Lipschitz function. Due to the Rademacher theorem (cf. [45, Sec. 5.8, Thm. 6]) D being Lipschitz bounded guarantees the differentiability of the local parametrizations

$$\psi_j(\boldsymbol{x}') := R_j \begin{bmatrix} \boldsymbol{x}' \\ \xi_j(\boldsymbol{x}') \end{bmatrix} + \boldsymbol{z}^{(j)}\,, \qquad \boldsymbol{x}' \in B'_{\alpha_j}(\mathbf{0})\,,\, j = 1 \ldots, J\,,$$

of ∂D almost everywhere. Therefore, particularly the unique exterior unit normal vector $\nu(\boldsymbol{x})$ exists at almost all points $\boldsymbol{x} \in \partial D$, see [70, Rem. A.8]. This regularity assumption on ∂D ensures the validity of Green's theorems as a basic tool for studying solutions of the Helmholtz equation.

Let ψ denote a parametrization of the sphere S^{d-1}, e.g. for $d = 2$

$$\psi : [0, 2\pi) \to S^1\,, \qquad \psi(\varphi) := (\cos\varphi, \sin\varphi)^\top$$

and for $d = 3$

$$\psi : [0, \pi] \times (-\pi, \pi] \to S^2\,, \qquad \psi(\vartheta, \varphi) := (\sin\vartheta\cos\varphi, \sin\vartheta\sin\varphi, \cos\vartheta)^\top\,,$$

respectively. We use this parametrization for introducing the Hilbert space $L^2(S^{d-1})$ on the sphere $S^{d-1} := \{\boldsymbol{x} \in \mathbb{R}^d \,|\, |\boldsymbol{x}| = 1\}$ as it is for example done in [73, Sec. 8.2], which is for $d = 2$ equipped with the inner product

$$\langle f, g\rangle_{L^2(S^1)} := \langle f \circ \psi, g \circ \psi\rangle_{L^2(0,2\pi)} = \int_0^{2\pi} f(\psi(\varphi))\overline{g(\psi(\varphi))}\,\mathrm{d}\varphi\,, \qquad f, g \in L^2(S^1)\,,$$

as a line integral, and for $d = 3$ it is equipped with the inner product

$$\begin{aligned}
\langle f, g\rangle_{L^2(S^2)} &:= \langle f \circ \psi, g \circ \psi\rangle_{L^2((0,\pi)\times(-\pi,\pi))}\\
&= \int_{-\pi}^{\pi}\int_0^{\pi} f(\psi(\vartheta,\varphi))\overline{g(\psi(\vartheta,\varphi))}\sin\vartheta\,\mathrm{d}\vartheta\,\mathrm{d}\varphi\,, \qquad f, g \in L^2(S^2)\,,
\end{aligned}$$

as a surface integral. The spaces $L^p(S^{d-1})$, $1 \leq p \leq \infty$, and $L^2(S^{d-1} \times S^{d-1})$ are defined analogously

by setting

$$\|f\|_{L^p(S^{d-1})} := \begin{cases} \|f \circ \psi\|_{L^p(0,2\pi)} & \text{if } d = 2\,, \\ \|f \circ \psi\|_{L^p((0,\pi)\times(-\pi,\pi))} & \text{if } d = 3\,, \end{cases}$$

and by using Fubini's theorem, respectively. For $\boldsymbol{x} \in \mathbb{R}^d$ we introduce the notation $\widehat{\boldsymbol{x}} := \boldsymbol{x}/|\boldsymbol{x}| \in S^{d-1}$ for the direction of $\boldsymbol{x}$.

2.2. Acoustic scattering by inhomogeneous media

Let $k > 0$ be the *wave number*. Furthermore, let $D \subseteq \mathbb{R}^d$ be a bounded set with Lipschitz boundary. The function $n^2 = 1 + q$ models the *index of refraction* with *contrast function* $q \in L^\infty(D)$ satisfying $q > -1$. The set D corresponds to the shape of the scatterer. This scatterer is illuminated by the *incident plane wave*

$$u^i(\boldsymbol{x}; \boldsymbol{\theta}) := e^{\mathrm{i}k\boldsymbol{x}\cdot\boldsymbol{\theta}}, \qquad \boldsymbol{x} \in \mathbb{R}^d,$$

along the *illumination direction* $\boldsymbol{\theta} \in S^{d-1}$. We mark dependencies on q with q as a subscript and dependencies on $\boldsymbol{\theta}$ with $\boldsymbol{\theta}$ as a second argument. The *total wave* u_q resulting in scattering of u^i on the scatterer D solves the following *medium scattering problem* for the *Helmholtz equation*. Find $u_q \in H^1_{\mathrm{loc}}(\mathbb{R}^d)$ with

$$\Delta u_q + k^2 n^2 u_q = 0 \qquad \text{in } \mathbb{R}^d\,, \tag{2.1a}$$

such that the corresponding *scattered wave* $u_q^s := u_q - u^i$ fulfills the *Sommerfeld radiation condition*

$$\lim_{|\boldsymbol{x}|\to\infty} |\boldsymbol{x}|^{\frac{d-1}{2}} \left(\frac{\partial u_q^s}{\partial r}(\boldsymbol{x}; \boldsymbol{\theta}) - \mathrm{i}k u_q^s(\boldsymbol{x}; \boldsymbol{\theta}) \right) = 0 \tag{2.1b}$$

uniformly with respect to the direction $\widehat{\boldsymbol{x}} = \boldsymbol{x}/|\boldsymbol{x}| \in S^{d-1}$.

Remark 2.2. Since the index of refraction n^2 is not smooth we cannot expect the solution u_q to be smooth. Therefore, the Helmholtz equation (2.1a) has to be understood in the variational sense, i.e., $u_q \in H^1_{\mathrm{loc}}(\mathbb{R}^d)$ is a solution if and only if

$$\int_{\mathbb{R}^d} \left(\nabla u_q \cdot \nabla \phi - k^2 n^2 u_q \phi \right) \mathrm{d}\boldsymbol{x} = 0 \qquad \text{for all } \phi \in C_0^\infty(\mathbb{R}^d)\,.$$

For $R > 0$ large enough such that $D \subseteq B_R(\mathbf{0})$ the restriction $u_q^s|_{\mathbb{R}^d \setminus \overline{B_R(\mathbf{0})}} \in H^1_{\mathrm{loc}}(\mathbb{R}^d \setminus \overline{B_R(\mathbf{0})})$ solves

$$\Delta u_q^s + k^2 u_q^s = 0 \qquad \text{in } \mathbb{R}^d \setminus \overline{B_R(\mathbf{0})}\,, \qquad u_q^s = u_q - u^i \qquad \text{on } \partial B_R(\mathbf{0})\,.$$

Thus, [70, Thm. 2.37] yields smoothness and even analyticity of u_q^s, so also of u_q outside $B_R(\mathbf{0})$ for $d = 3$. The case $d = 2$ can be shown analogously, see also [46, Chap. 7–8]. Therefore, the Sommerfeld radiation condition (2.1b) is well defined in classical sense. ◊

Let

$$\Phi_k(\boldsymbol{x}) := \begin{cases} \frac{\mathrm{i}}{4} H_0^{(1)}(k|\boldsymbol{x}|) & \text{if } d = 2\,, \\ \frac{1}{4\pi} \frac{e^{\mathrm{i}k|\boldsymbol{x}|}}{|\boldsymbol{x}|} & \text{if } d = 3\,, \end{cases} \tag{2.2}$$

denotes the *fundamental solution* of the Helmholtz equation at wave number k. Here, $H_0^{(1)}$ is the Hankel function of the first kind and order zero, cf. (B.5). Problem (2.1) has a unique solution, which can be represented as the solution of an integral equation, cf. [67, Thms. 6.8, 6.9] (see also [31, Thms. 8.3, 8.7] for piecewise smooth index of refraction n^2).

Theorem 2.3. *(a) Let $u_q \in H^1_{\mathrm{loc}}(\mathbb{R}^d)$ be a solution of (2.1). Then $u_q|_D \in L^2(D)$ solves the*

Lippmann–Schwinger integral equation

$$u_q(\boldsymbol{x};\boldsymbol{\theta}) \;=\; u^i(\boldsymbol{x};\boldsymbol{\theta}) + k^2 \int_{\mathbb{R}^d} q(\boldsymbol{y})\Phi_k(\boldsymbol{x}-\boldsymbol{y})u_q(\boldsymbol{y};\boldsymbol{\theta})\,\mathrm{d}\boldsymbol{y}\,, \qquad \boldsymbol{x}\in D\,. \tag{2.3}$$

(b) If, on the other hand, $u_q \in L^2(D)$ is a solution of the integral equation (2.3), then u_q can be extended by the right hand side of (2.3) to a solution $u_q \in H^1_{\mathrm{loc}}(\mathbb{R}^d)$ of (2.1).

(c) There exists a unique solution $u_q \in H^1_{\mathrm{loc}}(\mathbb{R}^d)$ of the scattering problem (2.1) or, equivalently, a unique solution $u_q \in L^2(D)$ of the integral equation (2.3).

To motivate where formula (2.3) comes from, we use $\Delta u^i + k^2 u^i = 0$ in $\mathbb{R}^d$ to rewrite (2.1a) as

$$\Delta u_q^s + k^2 u_q^s \;=\; \Delta u_q + k^2 u_q \;=\; k^2(1-n^2)u_q \;=\; -k^2 q u_q \qquad \text{in } \mathbb{R}^d\,.$$

This is a source problem for the Helmholtz equation for u_q^s with source term $-k^2 q u_q$. By applying the theory of solutions for this problem class (see [67, Thms. 6.5, 6.7]), we conclude that u_q^s is given as a volume potential with density $-k^2 q u_q$.

From the asymptotic behavior of the fundamental solution $\Phi_k(\boldsymbol{x})$ for $|\boldsymbol{x}|\to\infty$ follows that the scattered wave u_q^s satisfies the asymptotic *far field expansion*

$$u_q^s(\boldsymbol{x};\boldsymbol{\theta}) \;=\; C_d\,\frac{e^{\mathrm{i}k|\boldsymbol{x}|}}{|\boldsymbol{x}|^{(d-1)/2}}\,u_q^\infty(\widehat{\boldsymbol{x}};\boldsymbol{\theta}) + O\left(|\boldsymbol{x}|^{-\frac{d+1}{2}}\right) \qquad \text{for } |\boldsymbol{x}|\to\infty \tag{2.4}$$

uniformly with respect to the *observation direction* $\widehat{\boldsymbol{x}} = \boldsymbol{x}/|\boldsymbol{x}| \in S^{d-1}$ with

$$C_d \;:=\; \begin{cases} \frac{e^{\mathrm{i}\pi/4}}{\sqrt{8\pi}} & \text{if } d=2\,,\\ \frac{1}{4\pi} & \text{if } d=3\,. \end{cases} \tag{2.5}$$

The *far field (pattern)* $u_q^\infty \in L^2(S^{d-1}\times S^{d-1})$ in (2.4) is given by

$$u_q^\infty(\widehat{\boldsymbol{x}};\boldsymbol{\theta}) \;:=\; k^2 \int_D q(\boldsymbol{y})u_q(\boldsymbol{y};\boldsymbol{\theta})e^{-\mathrm{i}k\widehat{\boldsymbol{x}}\cdot\boldsymbol{y}}\,\mathrm{d}\boldsymbol{y}\,, \qquad \widehat{\boldsymbol{x}}\in S^{d-1}\,, \tag{2.6}$$

(cf. [67, Thm. 6.11] or [31, p. 316]). We further have the following one-to-one correspondence between the scattered field u_q^s and its far field pattern u_q^∞. There holds

$$u_q^\infty \;=\; 0 \qquad \text{if and only if} \qquad u_q^s \;=\; 0 \text{ outside } B_R(\boldsymbol{0}) \text{ for } D\subseteq B_R(\boldsymbol{0})\,,$$

see also [67, Thm. 6.11]. Superpositions of far field patterns are modeled by the associated *far field operator*, which maps densities of superpositions of incident plane waves to the far field patterns of the corresponding scattered waves, i.e.,

$$F_q : L^2(S^{d-1}) \to L^2(S^{d-1})\,, \quad (F_q g)(\widehat{\boldsymbol{x}}) \;:=\; \int_{S^{d-1}} u_q^\infty(\widehat{\boldsymbol{x}};\boldsymbol{\theta})g(\boldsymbol{\theta})\,\mathrm{d}s(\boldsymbol{\theta})\,. \tag{2.7}$$

Throughout this work, the far field operator F_q is at the center of our considerations. Some of its basic properties are collected in the following proposition (cf. e.g. [67, Thms. 6.14, 6.16] or [69, Thm. 4.4] and [31, p. 324]).

Proposition 2.4. *(a) The far field pattern u_q^∞ satisfies the* reciprocity relation

$$u_q^\infty(\widehat{\boldsymbol{x}};\boldsymbol{\theta}) \;=\; u_q^\infty(-\boldsymbol{\theta};-\widehat{\boldsymbol{x}}) \qquad \textit{for all } \widehat{\boldsymbol{x}},\boldsymbol{\theta}\in S^{d-1}\,. \tag{2.8}$$

(b) Since F_q is an integral operator with analytic kernel (see the beginning of Chapter 5), we have

that $F_q \in \mathcal{N}(L^2(S^{d-1}))$, i.e., it is trace class, so in particular Hilbert–Schmidt and compact (cf. Definitions A.3 and A.4).

(c) The far field operator F_q is normal (i.e. $F_q^* F_q = F_q F_q^*$).

(d) The scattering operator $S_q : L^2(S^{d-1}) \to L^2(S^{d-1})$ *given by*

$$S_q := I + 2\mathrm{i}k|C_d|^2 F_q \tag{2.9}$$

with C_d as in (2.5) is unitary (i.e. $S_q^* S_q = S_q S_q^* = I$), so its eigenvalues lie on the unit circle in the complex plane. For the far field operator F_q this means, that its eigenvalues lie on the circle centered at $\mathrm{i}/(2k|C_d|^2)$ of radius $1/(2k|C_d|^2)$ in the complex plane. These eigenvalues are further infinitely many provided q has no sign change (see [31, Thm. 8.16] and the proof of [31, Thm. 8.13]).

The following example illustrates how a far field operator F_q can be realized numerically for a piecewise constant contrast function q and dimension $d = 2$.

Example 2.5. Let $d = 2$. For simulating the far field operator F_q we define $L \in \mathbb{N}$ equally distributed incident and observation directions by

$$\widehat{\boldsymbol{x}}_l := \boldsymbol{\theta}_l := (\cos\psi_l, \sin\psi_l)^\top \qquad \text{with } \psi_l := (l-1)\frac{2\pi}{L} \text{ for } l = 1, \dots, L\,.$$

For resolving all relevant information it is sufficient to choose $L \gtrsim 2kR + 1$ for $R > 0$ being the smallest radius of a ball than contains D. We do not elaborate on the reason for this at this point, as it will be discussed in detail later, see Theorem 2.11 and Example 4.1 (cf. also [55]). We apply the composite trapezoidal rule on (2.7) and obtain for $g \in L^2(S^1)$

$$(F_q g)(\widehat{\boldsymbol{x}}) \approx \frac{2\pi}{L} \sum_{l=1}^{L} u_q^\infty(\widehat{\boldsymbol{x}}; \boldsymbol{\theta}_l) g(\boldsymbol{\theta}_l)\,.$$

Accordingly, the matrix

$$\boldsymbol{F}_q := \frac{2\pi}{L} \left(u_q^\infty(\widehat{\boldsymbol{x}}_m; \boldsymbol{\theta}_n) \right)_{1 \le m,n \le L} \in \mathbb{C}^{L \times L}$$

approximates F_q, and it remains the task to simulate the evaluations of the far field pattern $u_q^\infty(\widehat{\boldsymbol{x}}_m; \boldsymbol{\theta}_n)$ for $1 \le m, n \le L$. Here, the main issue is that the scattering problem (2.1) that defines u_q and consequently u_q^∞ is defined on the unbounded domain $\mathbb{R}^2$. There are two common classes of methods that treat this difficulty differently: Volume integral methods and coupled finite element and boundary element methods. At this point, we particularly emphasize one method proposed by Vainikko [97] for smooth or at least piecewise smooth contrast functions q, which is a special volume integral method that solves the Lippmann–Schwinger equation using trigonometric interpolation based on periodization and Fourier transform techniques (see also Example 3.7). Since the simulation of far field data is not the main focus of this work, we simplify the situation for our numerical purposes, and we do not use one of these methods but a Nyström method. We restrict ourselves to a piecewise constant contrast function, i.e. $q = q_0$ in D and $q = 0$ in $\mathbb{R}^2 \setminus \overline{D}$ for some constant $q_0 > -1$.

Let $k_1 := k\sqrt{1+q_0}$ be the inner and $k_2 := k$ be the outer wave number. Moreover, let u_q be the solution of the original scattering problem (2.1) and $u_q^s = u_q - u^i$ the corresponding scattered field. Then, the restrictions $v_1 = u_q|_D$ and $v_2 = u_q^s|_{\mathbb{R}^d \setminus \overline{D}}$ solve the *transmission problem*

$$\begin{aligned} \Delta v_1 + k_1^2 v_1 &= 0 && \text{in } D\,, \\ \Delta v_2 + k_2^2 v_2 &= 0 && \text{in } \mathbb{R}^d \setminus \overline{D}\,, \\ v_1^- - v_2^+ = u^i \qquad \text{and} \qquad \frac{\partial v_1^-}{\partial \nu} - \frac{\partial v_2^+}{\partial \nu} &= \frac{\partial u^i}{\partial \nu} && \text{on } \partial D\,, \end{aligned}$$

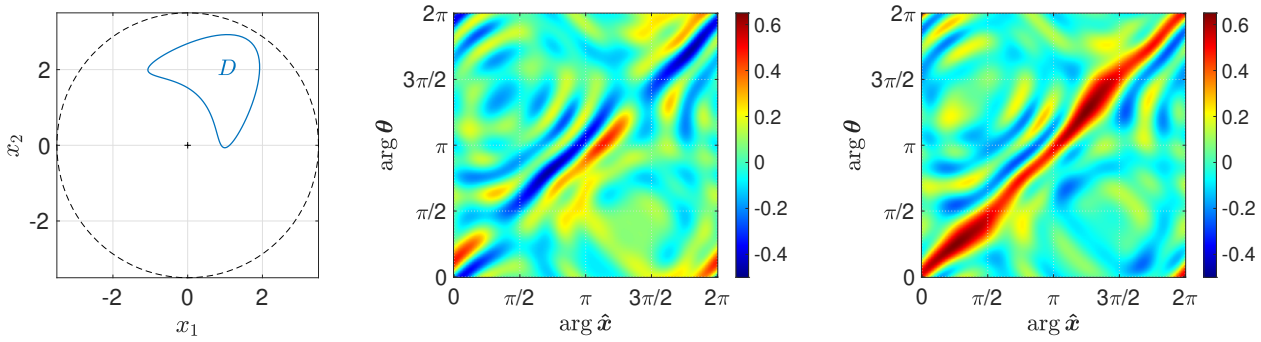

FIGURE 2.1. Left: Support of the scatterer D (solid) and ball $B_R(\mathbf{0})$ (dashed) with radius $R = 3.5$ containing D.
Real part (middle) and imaginary part (right) of the discretized far field operator $\boldsymbol{F}_q$ for $L = 256$ equally distributed illumination and observation directions.

$$\lim_{r\to\infty} r^{\frac{d-1}{2}} \left(\frac{\partial v_2}{\partial r}(\boldsymbol{x};\boldsymbol{\theta}) - \mathrm{i}k v_2(\boldsymbol{x};\boldsymbol{\theta}) \right) = 0 \tag{2.10}$$

in the classical sense. Here, the superscripts $+$ and $-$ denote the traces on the boundary ∂D from the outside and the inside of D, respectively. This problem has been studied e.g. in [74, 98] and can be reformulated as a boundary integral equation. We make a layer potential ansatz for v_1 and v_2 with coupling parameter k, i.e. we assume them to be of the form

$$v_i = \int_{\partial D} \left(\frac{\partial}{\partial \nu(\boldsymbol{y})} \Phi_{k_i}(\,\cdot\,,\boldsymbol{y}) - \mathrm{i}k \Phi_{k_i}(\,\cdot\,,\boldsymbol{y}) \right) \varphi_i(\boldsymbol{y})\, \mathrm{d}s(\boldsymbol{y}) \tag{2.11}$$

for some unknown densities $\varphi_i \in C(\partial D)$, $i = 1, 2$. By the jump relations (cf. [31, Thm. 3.1]) for the single- and double-layer potential φ_1 and φ_2 are solution of the boundary integral equation system

$$\begin{bmatrix} I - K_{k_1} + \mathrm{i}kS_{k_1} & I + K_{k_2} - \mathrm{i}kS_{k_2} \\ -T_{k_1} + \mathrm{i}k(I + K'_{k_1}) & T_{k_2} - \mathrm{i}k(-I + K'_{k_2}) \end{bmatrix} \begin{bmatrix} \varphi_1 \\ \varphi_2 \end{bmatrix} = \begin{bmatrix} -2u^i|_{\partial D} \\ -2\frac{\partial u^i}{\partial \nu}|_{\partial D} \end{bmatrix}.$$

Here, we used the transmission conditions (2.10). For given $l > 0$ the operators S_l, K_l, K'_l and T_l are the acoustic single-layer, double-layer, transposed double-layer and hypersingular boundary integral operator at wave number l, as defined in [31, (3.8)–(3.11)]. We use a Nyström method as described in [31, Sec. 3.6] for an even number L of discretization points for computing the densities φ_1 and φ_2. Using the asymptotics of the fundamental solution in (2.11) with $i = 1$ gives a formula for the far field pattern, on which again the composite trapezoidal rule can be applied.

In Figure 2.1, the real part (middle) and the imaginary part (right) of the discretized far field operator $\boldsymbol{F}_q$ is plotted for a kite shaped scatterer D as shown in Figure 2.1 (left) modeled by the contrast function q as defined above for $q_0 = 2$. The wave number is $k = 2.5$ and for $R = 3.5$ we have that $D \subseteq B_R(\mathbf{0})$, so the choice for the number of incident and observation directions $L = 256 > 18.5 = 2kR + 1$ is large enough. ◊

2.3. BORN APPROXIMATIONS

For any fixed $\boldsymbol{\theta} \in S^{d-1}$ we can interpret the Lippmann–Schwinger equation (2.3) as a fixed point equation for $u_q(\,\cdot\,;\boldsymbol{\theta})$

$$u_q(\,\cdot\,;\boldsymbol{\theta}) = u^i(\,\cdot\,;\boldsymbol{\theta}) + L_q u_q(\,\cdot\,;\boldsymbol{\theta}) \qquad \text{in } D\,,$$

where the bounded linear operator $L_q : L^2(D) \to L^2(D)$ is defined by

$$(L_q f)(\boldsymbol{x}) := k^2 \int_D q(\boldsymbol{y}) f(\boldsymbol{y}) \Phi_k(\boldsymbol{x}-\boldsymbol{y}) \, \mathrm{d}\boldsymbol{y}, \qquad \boldsymbol{x} \in D. \tag{2.12}$$

If the operator norm $\|L_q\|$ is strictly less than one, then the solution to (2.3) can be written as a Neumann series

$$u_q(\,\cdot\,;\boldsymbol{\theta}) = u^i(\,\cdot\,;\boldsymbol{\theta}) + \sum_{l=1}^{\infty} L_q^l u^i(\,\cdot\,;\boldsymbol{\theta}) \qquad \text{in } D. \tag{2.13}$$

This series is often called the *Born series* and describes the different levels of multiple scattering of the incident wave $u^i(\,\cdot\,;\boldsymbol{\theta})$ at the scatterer q. It converges in $L^2(D)$ and uniformly with respect to the incident direction $\boldsymbol{\theta} \in S^{d-1}$. The lth summand of this series, which we refer to as the *scattered field component associated to scattering processes of order $l \in \mathbb{N}$ on q* is denoted by

$$\begin{aligned} u_q^{s,(l)}(\,\cdot\,;\boldsymbol{\theta}) &:= L_q^l u^i(\,\cdot\,;\boldsymbol{\theta}) \\ &= k^{2l} \int_D \cdots \int_D q(\boldsymbol{y}_l) \cdots q(\boldsymbol{y}_1) e^{\mathrm{i}k\boldsymbol{y}_1\cdot\boldsymbol{\theta}} \Phi_k(\,\cdot\,-\boldsymbol{y}_l) \Phi_k(\boldsymbol{y}_l-\boldsymbol{y}_{l-1}) \cdots \Phi_k(\boldsymbol{y}_2-\boldsymbol{y}_1) \, \mathrm{d}\boldsymbol{y}_1 \cdots \mathrm{d}\boldsymbol{y}_l. \end{aligned}$$

Plugging the Born series (2.13) of the total wave into the representation (2.6) of the far field pattern yields

$$u_q^\infty(\widehat{\boldsymbol{x}};\boldsymbol{\theta}) = k^2 \sum_{l=1}^{\infty} \int_D q(\boldsymbol{y}) e^{-\mathrm{i}k\widehat{\boldsymbol{x}}\cdot\boldsymbol{y}} (L_q^{l-1} u^i(\,\cdot\,;\boldsymbol{\theta}))(\boldsymbol{y}) \, \mathrm{d}\boldsymbol{y}, \qquad \widehat{\boldsymbol{x}} \in S^{d-1}. \tag{2.14}$$

We write for $\widehat{\boldsymbol{x}} \in S^{d-1}$ and $l \geq 2$

$$\begin{aligned} u_q^{\infty,(l)}(\widehat{\boldsymbol{x}};\boldsymbol{\theta}) &:= k^2 \int_D q(\boldsymbol{y}) e^{-\mathrm{i}k\widehat{\boldsymbol{x}}\cdot\boldsymbol{y}} (L_q^{l-1} u^i(\,\cdot\,;\boldsymbol{\theta}))(\boldsymbol{y}) \, \mathrm{d}\boldsymbol{y} \\ &= k^{2l} \int_D \cdots \int_D q(\boldsymbol{y}_l) \cdots q(\boldsymbol{y}_1) \Phi_k(\boldsymbol{y}_l-\boldsymbol{y}_{l-1}) \cdots \Phi_k(\boldsymbol{y}_2-\boldsymbol{y}_1) e^{\mathrm{i}k(\boldsymbol{\theta}\cdot\boldsymbol{y}_1 - \widehat{\boldsymbol{x}}\cdot\boldsymbol{y}_l)} \, \mathrm{d}\boldsymbol{y}_1 \cdots \mathrm{d}\boldsymbol{y}_l \end{aligned} \tag{2.15}$$

for the lth summand in (2.14), which we refer to as *far field component associated to scattering processes of order $l \in \mathbb{N}$ on q*. Then,

$$u_q^\infty(\widehat{\boldsymbol{x}};\boldsymbol{\theta}) = \sum_{l=1}^{\infty} u_q^{\infty,(l)}(\widehat{\boldsymbol{x}};\boldsymbol{\theta}), \qquad \widehat{\boldsymbol{x}} \in S^{d-1}. \tag{2.16}$$

Taking all scattering components up to a certain scattering order $p \in \mathbb{N}$ into account leads to the *Born far field of order p*, which is given by the pth partial sum in (2.14), i.e., by

$$u_q^{\infty,(\leq p)}(\widehat{\boldsymbol{x}};\boldsymbol{\theta}) := \sum_{l=1}^{p} u_q^{\infty,(l)}(\widehat{\boldsymbol{x}};\boldsymbol{\theta}), \qquad \widehat{\boldsymbol{x}} \in S^{d-1}.$$

Recalling the definition of the far field operator (2.7) we introduce the *far field operator component associated to scattering processes of order $l \in \mathbb{N}$ on q* by

$$F_q^{(l)} : L^2(S^{d-1}) \to L^2(S^{d-1}), \quad (F_q^{(l)} g)(\widehat{\boldsymbol{x}}) := \int_{S^{d-1}} u_q^{\infty,(l)}(\widehat{\boldsymbol{x}};\boldsymbol{\theta}) g(\boldsymbol{\theta}) \, \mathrm{d}s(\boldsymbol{\theta}). \tag{2.17}$$

Accordingly, the Born series of the far field operator F_q reads as $F_q = \sum_{l=1}^{\infty} F_q^{(l)}$. For any $p \in \mathbb{N}$ we define the *Born far field operator of order p* by

$$F_q^{(\leq p)} : L^2(S^{d-1}) \to L^2(S^{d-1}), \quad (F_q^{(\leq p)} g)(\widehat{\boldsymbol{x}}) := \int_{S^{d-1}} u_q^{\infty,(\leq p)}(\widehat{\boldsymbol{x}};\boldsymbol{\theta}) g(\boldsymbol{\theta}) \, \mathrm{d}s(\boldsymbol{\theta}). \tag{2.18}$$

The operators $F_q^{(l)}$ and $F_q^{(\leq p)}$ are Hilbert–Schmidt integral operators since their integral kernels satisfy $u_q^{\infty,(l)}, u_q^{\infty,(\leq p)} \in L^2(S^{d-1} \times S^{d-1})$, see Theorem A.8. Alternatively, this follows from the estimates in Theorems 2.11 and 2.19 below, which give upper bounds for the Hilbert–Schmidt norms of these operators, see (2.20).

Remark 2.6 (Convergence of the Born series expansions). Theorem A.8 gives together with (2.14), the Cauchy Schwarz inequality and the definition of the operator norm for the approximation error of the far field operator by the Born far field operator of order $p \in \mathbb{N}$ that

$$\begin{aligned}
\|F_q - F_q^{(\leq p)}\|_{\mathrm{HS}}^2 &= \|u_q^\infty - u_q^{\infty,(\leq p)}\|_{L^2(S^{d-1}\times S^{d-1})}^2 \\
&= k^4 \int_{S^{d-1}} \int_{S^{d-1}} \Big| \sum_{l=p+1}^{\infty} \int_D q(\boldsymbol{y}) e^{\mathrm{i}k\widehat{\boldsymbol{x}}\cdot\boldsymbol{y}} (L_q^{l-1} u^i(\,\cdot\,;\boldsymbol{\theta}))(\boldsymbol{y})\, \mathrm{d}\boldsymbol{y} \Big|^2 \, \mathrm{d}s(\widehat{\boldsymbol{x}})\, \mathrm{d}s(\boldsymbol{\theta}) \\
&\leq |S^{d-1}| k^4 \|q\|_{L^2(D)}^2 \int_{S^{d-1}} \Big(\sum_{l=p+1}^{\infty} \|L_q^{l-1} u^i(\,\cdot\,;\boldsymbol{\theta})\|_{L^2(D)} \Big)^2 \, \mathrm{d}s(\boldsymbol{\theta}) \\
&\leq |S^{d-1}| k^4 \|q\|_{L^2(D)}^2 \int_{S^{d-1}} \Big(\sum_{l=p+1}^{\infty} \|L_q\|^{l-1} \|u^i(\,\cdot\,;\boldsymbol{\theta})\|_{L^2(D)} \Big)^2 \, \mathrm{d}s(\boldsymbol{\theta}) \\
&= |S^{d-1}|^2 k^4 |D|^2 \|q\|_{L^2(D)}^2 \Big(\sum_{l=p}^{\infty} \|L_q\|^l \Big)^2 \\
&\leq |S^{d-1}|^2 k^4 |D|^3 \|q\|_{L^\infty(D)}^2 \Big(\sum_{l=p}^{\infty} \|L_q\|^l \Big)^2 .
\end{aligned}$$

Here, $|D|$ and $|S^{d-1}|$ denote the volume of D and the surface area of S^{d-1}, respectively, i.e., $|S^1| = 2\pi$ and $|S^2| = 4\pi$. Provided $\|L_q\| < 1$ we can conclude from the sum of the geometric series that

$$\|F_q - F_q^{(\leq p)}\|_{\mathrm{HS}} \leq |S^{d-1}| k^2 |D|^{\frac{3}{2}} \|q\|_{L^\infty(D)} \frac{\|L_q\|^p}{1 - \|L_q\|} \longrightarrow 0 \qquad \text{for } p \to \infty .$$

Sufficient conditions on k and q for the convergence of the Born series expansions have, e.g., been discussed in [62, 68, 85, 96]. For instance, (2.12) immediately implies that

$$\begin{aligned}
\|L_q f\|_{L^2(D)}^2 &= \int_D \Big| k^2 \int_D q(\boldsymbol{y}) f(\boldsymbol{y}) \Phi_k(\boldsymbol{x} - \boldsymbol{y})\, \mathrm{d}\boldsymbol{y} \Big|^2 \, \mathrm{d}\boldsymbol{x} \\
&\leq k^4 \|f\|_{L^2(D)}^2 \int_D \int_D |q(\boldsymbol{y}) \Phi_k(\boldsymbol{x} - \boldsymbol{y})|^2 \, \mathrm{d}\boldsymbol{y}\, \mathrm{d}\boldsymbol{x}
\end{aligned}$$

for all $f \in L^2(D)$, i.e.,

$$\|L_q\|^2 \leq k^4 \int_D \int_D |q(\boldsymbol{y}) \Phi_k(\boldsymbol{x} - \boldsymbol{y})|^2 \, \mathrm{d}\boldsymbol{y}\, \mathrm{d}\boldsymbol{x} = \|L_q\|_{\mathrm{HS}}^2 , \tag{2.19}$$

see Theorem A.8. The right hand side in (2.19) is always finite. To see this, we write for $0 < r < 1$ independent of x ($B_r(\boldsymbol{x}) \not\subseteq D$ is permitted)

$$\|L_q\|_{\mathrm{HS}}^2 \leq k^4 \|q\|_{L^\infty(D)}^2 \Big(\int_D \int_{D \setminus B_r(\boldsymbol{x})} |\Phi_k(\boldsymbol{x} - \boldsymbol{y})|^2 \, \mathrm{d}\boldsymbol{y}\, \mathrm{d}\boldsymbol{x} + \int_D \int_{B_r(\boldsymbol{x})} |\Phi_k(\boldsymbol{x} - \boldsymbol{y})|^2 \, \mathrm{d}\boldsymbol{y}\, \mathrm{d}\boldsymbol{x} \Big) .$$

The first integral is finite due to the analyticity of Φ_k in $\mathbb{R}^d \setminus \{\mathbf{0}\}$ and the boundedness of D. The asymptotic behavior of the fundamental solution $\Phi_k(\boldsymbol{x} - \boldsymbol{y})$ as $|\boldsymbol{x} - \boldsymbol{y}| \to 0$ shows that the second

integral is finite as well. We can bound

$$|\Phi_k(\boldsymbol{x}-\boldsymbol{y})| \leq \begin{cases} C \ln\left(\frac{1}{|\boldsymbol{x}-\boldsymbol{y}|}\right) & \text{if } d=2\,, \\ C\frac{1}{|\boldsymbol{x}-\boldsymbol{y}|} & \text{if } d=3\,, \end{cases}$$

for $|\boldsymbol{x}-\boldsymbol{y}| \to 0$ and $C>0$ (see [31, (3.107)] for $d=2$). For $d=2$ this implies together with Lebesgue's theorem that

$$\int_D \int_{B_r(x)} |\Phi_k(\boldsymbol{x}-\boldsymbol{y})|^2 \,\mathrm{d}\boldsymbol{y}\,\mathrm{d}\boldsymbol{x} \leq C^2|D| \int_0^{2\pi}\int_0^r t\ln^2 t\,\mathrm{d}t\,\mathrm{d}\varphi = \frac{\pi}{2}C^2|D|r^2(2\ln^2 r - 2\ln r + 1)\,,$$

which tends to zero for $r \to 0$. For $d=3$ we obtain again with Lebesgue's theorem that

$$\int_D \int_{B_r(x)} |\Phi_k(\boldsymbol{x}-\boldsymbol{y})|^2 \,\mathrm{d}\boldsymbol{y}\,\mathrm{d}\boldsymbol{x} \leq C^2|D| \int_{-\pi}^{\pi}\int_0^{\pi}\int_0^r \frac{1}{t^2} t^2 \sin\vartheta \,\mathrm{d}t\,\mathrm{d}\vartheta\,\mathrm{d}\varphi = 4\pi C^2|D|r \longrightarrow 0$$

for $r \to 0$. Overall, L_q is a Hilbert–Schmidt operator, and the Born series of the far field operator converges when $\|L_q\|_{\mathrm{HS}} < 1$, which we assume henceforth. ◊

2.4. Sparse and low rank representations of far field operators

Let the support of the scatterer be contained in some ball $B_R(\mathbf{0}) \subseteq \mathbb{R}^d$ centered at the origin, i.e. $D \subseteq B_R(\mathbf{0})$. We show that the far field operator components $F_q^{(l)}$ associated to scattering processes of order $l \in \mathbb{N}$ can be well approximated by operators that have a finite expansion or are of finite rank. Here, it turns out that the number of expansion coefficients or the rank is directly linked to the quantity kR, respectively. Therefore, for kR not too large we obtain sparse or low rank approximations of these far field operator components. Due to the different structure of the underlying series expansions we tackle the two- and three-dimensional case separately.

The two-dimensional case

Notation 2.7. We denote by $\boldsymbol{e}_n := (e^{\mathrm{i}n\arg(\,\cdot\,)}/\sqrt{2\pi})_{n\in\mathbb{Z}}$ the standard Fourier basis of $L^2(S^1)$, which is an orthonormal basis and satisfies $\mathbb{Y}_n^2 = \operatorname{span}\{\boldsymbol{e}_n, \boldsymbol{e}_{-n}\}$ (cf. Section B.1). Here, $\mathbb{Y}_n^2$ is the space of spherical harmonics of degree $n \in \mathbb{N}_0$ in $\mathbb{R}^2$, see (B.1). Consequently, $(\boldsymbol{e}_{m,n})_{m,n}$ given by $\boldsymbol{e}_{m,n}(\widehat{\boldsymbol{x}};\boldsymbol{\theta}) := \boldsymbol{e}_m(\widehat{\boldsymbol{x}})\boldsymbol{e}_{-n}(\boldsymbol{\theta})$, $\widehat{\boldsymbol{x}},\boldsymbol{\theta} \in S^1$, $m,n \in \mathbb{Z}$, provides an orthonormal basis for $L^2(S^1\times S^1)$. We expand the kernel $\kappa_G \in L^2(S^1\times S^1)$ of a Hilbert–Schmidt operator $G \in \mathrm{HS}(L^2(S^1))$ in terms of $(\boldsymbol{e}_{m,n})_{m,n}$ and obtain for $g \in L^2(S^1)$ that

$$Gg = \int_{S^1} \kappa_G(\,\cdot\,;\boldsymbol{\theta})g(\boldsymbol{\theta})\,\mathrm{d}s(\boldsymbol{\theta}) = \sum_{m\in\mathbb{Z}}\sum_{n\in\mathbb{Z}} \langle \kappa_G, \boldsymbol{e}_{m,n}\rangle_{L^2(S^1\times S^1)} \boldsymbol{e}_m \langle g, \boldsymbol{e}_n\rangle_{L^2(S^1)}\,.$$

With the notations

$$\|G\|_{L^p} := \|\kappa_G\|_{L^p(S^1\times S^1)} \qquad \text{and} \qquad \|G\|_{\ell^p\times\ell^p} := \|(\langle \kappa_G, \boldsymbol{e}_{m,n}\rangle_{L^2(S^1\times S^1)})_{m,n}\|_{\ell^p\times\ell^p}$$

for $1 \leq p \leq \infty$, we conclude from Parseval's identity and Theorem A.8 that

$$\|G\|_{\mathrm{HS}} = \|G\|_{L^2} = \|G\|_{\ell^2\times\ell^2}\,. \tag{2.20}$$

Based on this we identify $G \in \mathrm{HS}(L^2(S^1))$ with its kernel $\kappa_G \in L^2(S^1 \times S^1)$ as well with its expansion coefficients $(\langle \kappa_G, \boldsymbol{e}_{m,n} \rangle_{L^2(S^1\times S^1)})_{m,n} \in \ell^2 \times \ell^2$, which satisfy

$$\langle \kappa_G, \boldsymbol{e}_{m,n} \rangle_{L^2(S^1\times S^1)} = \int_{S^1} \int_{S^1} \kappa_G(\widehat{\boldsymbol{x}}; \boldsymbol{\theta}) \boldsymbol{e}_{-m}(\widehat{\boldsymbol{x}}) \boldsymbol{e}_n(\boldsymbol{\theta}) \, \mathrm{d}s(\widehat{\boldsymbol{x}}) \, \mathrm{d}s(\boldsymbol{\theta}) = \langle G\boldsymbol{e}_n, \boldsymbol{e}_m \rangle_{L^2(S^1)} .$$

We refer to the essential support of the integral kernel κ_G as the *L^0-support*

$$\operatorname{supp}_{L^0} G := \operatorname{supp} \kappa_G \subseteq S^1 \times S^1$$

of G and denote its measure by $\|G\|_{L^0}$. Analogously, we call the index set of the nonzero Fourier coefficients $(\langle G\boldsymbol{e}_n, \boldsymbol{e}_m \rangle_{L^2(S^1)})_{m,n}$ the *$\ell^0 \times \ell^0$-support*

$$\operatorname{supp}_{\ell^0\times\ell^0} G := \Big\{ (m,n) \in \mathbb{Z}^2 \,|\, \langle G\boldsymbol{e}_n, \boldsymbol{e}_m \rangle_{L^2(S^1)} \neq 0 \Big\}$$

of G and denote the number of these indices by $\|G\|_{\ell^0\times\ell^0}$. Moreover, let $\|G\|_{\mathrm{nuc}}$ be the nuclear norm of G (cf. (A.5)), and let $\operatorname{rank} G$ be its rank (cf. Definition A.6). For $W \subseteq \mathbb{Z}^2$ and $1 \leq p \leq \infty$ we further define $\ell^p \times \ell^p(W) := \{(a_{m,n})_{m,n} \in \ell^p \times \ell^p \,|\, \operatorname{supp}(a_{m,n})_{m,n} \subseteq W\}$ as a subspace of $\ell^p \times \ell^p$, and we write

$$\|G\|_{\ell^p\times\ell^p(W)} := \|(\langle G\boldsymbol{e}_m, \boldsymbol{e}_n \rangle_{L^2(S^1\times S^1)})_{m,n}\|_{\ell^p\times\ell^p(W)} .$$

Lemma 2.8. *The far field component $u_q^{\infty,(l)}$ in (2.15) and the far field operator component $F_q^{(l)}$ in (2.17) associated to scattering processes of order $l \in \mathbb{N}$ can be expanded as a Fourier series via*

$$u_q^{\infty,(l)} = \sum_{m\in\mathbb{Z}} \sum_{n\in\mathbb{Z}} a_{m,n}^{(l)} \boldsymbol{e}_{m,n} \qquad \text{and} \qquad F_q^{(l)} g = \sum_{m\in\mathbb{Z}} \sum_{n\in\mathbb{Z}} a_{m,n}^{(l)} \boldsymbol{e}_m \langle g, \boldsymbol{e}_n \rangle_{L^2(S^1)}$$

for $g \in L^2(S^1)$ with Fourier coefficients given by

$$a_{m,n}^{(l)} = 2\pi k^{2l} \mathrm{i}^{n-m} \int_D \cdots \int_D q(\boldsymbol{y}_l) \cdots q(\boldsymbol{y}_1) \Phi_k(\boldsymbol{y}_l - \boldsymbol{y}_{l-1}) \cdots \Phi_k(\boldsymbol{y}_2 - \boldsymbol{y}_1) \times e^{-\mathrm{i}(m \arg \boldsymbol{y}_l - n \arg \boldsymbol{y}_1)} J_m(k|\boldsymbol{y}_l|) J_n(k|\boldsymbol{y}_1|) \, \mathrm{d}\boldsymbol{y}_1 \cdots \mathrm{d}\boldsymbol{y}_l . \quad (2.21)$$

Here, J_m and J_n denote the Bessel functions of order m and n, respectively (see Appendix B.1).

Proof. By the Jacobi–Anger expansion (B.12) the plane wave terms in (2.15) can be rewritten as

$$e^{\mathrm{i}k(\boldsymbol{\theta}\cdot\boldsymbol{y}_1 - \widehat{\boldsymbol{x}}\cdot\boldsymbol{y}_l)} = \sum_{m\in\mathbb{Z}} \sum_{n\in\mathbb{Z}} \mathrm{i}^{n-m} e^{-\mathrm{i}(m \arg \boldsymbol{y}_l - n \arg \boldsymbol{y}_1)} J_m(k|\boldsymbol{y}_l|) J_n(k|\boldsymbol{y}_1|) e^{\mathrm{i}m \arg \widehat{\boldsymbol{x}}} e^{-\mathrm{i}n \arg \widehat{\boldsymbol{x}}} .$$

Substituting this into (2.15) yields the result. □

Definition 2.9. Let $N \in \mathbb{N}$ with $N \gtrsim kR$, which throughout this work means that $N = N(kR)$ is somewhat larger than kR. We define the *subspace of sparse far field operators associated to scatterers supported in $B_R(\mathbf{0}) \subseteq \mathbb{R}^2$* by

$$\mathcal{V}_N := \Big\{ G \in \mathrm{HS}(L^2(S^1)) \;\Big|\; Gg = \sum_{|m|\leq N} \sum_{|n|\leq N} a_{m,n} \, \boldsymbol{e}_m \langle g, \boldsymbol{e}_n \rangle_{L^2(S^1)} , \, a_{m,n} \in \mathbb{C} \Big\} . \quad (2.22)$$

Furthermore, we denote by

$$\mathcal{W}_N := \Big\{ G \in \mathrm{HS}(L^2(S^1)) \;\Big|\; Gg = \sum_{|n|\leq N} \Big(\boldsymbol{e}_n \langle g, \alpha_n \rangle_{L^2(S^1)} + \beta_n \langle g, \boldsymbol{e}_n \rangle_{L^2(S^1)} \Big) , \, \alpha_n, \beta_n \in L^2(S^1) \Big\} . \quad (2.23)$$

the *subspace of low rank far field operators associated to scatterers supported in* $B_R(\mathbf{0}) \subseteq \mathbb{R}^2$. By $\mathcal{P}_{\mathcal{V}_N} : \mathrm{HS}(L^2(S^1)) \to \mathcal{V}_N$ and $\mathcal{P}_{\mathcal{W}_N} : \mathrm{HS}(L^2(S^1)) \to \mathcal{W}_N$ we denote the orthogonal projections onto $\mathcal{V}_N$ and $\mathcal{W}_N$ with respect to $\langle \cdot, \cdot \rangle_{\mathrm{HS}}$, respectively.

The following remark relates the two subspaces $\mathcal{V}_N$ and $\mathcal{W}_N$ to each other.

Remark 2.10. (i) By definition we have for $G \in \mathcal{V}_N$ that

$$\operatorname{supp}_{\ell^0 \times \ell^0} G \subseteq [-N, N]^2 .$$

To identify the $\ell^0 \times \ell^0$-support of $G \in \mathcal{W}_N$, we rewrite G given as in (2.23) in the form (2.22), i.e., we expand for all n the functions α_n and β_n in terms of $(\boldsymbol{e}_m)_m$ and obtain

$$\begin{aligned} Gg = \sum_{|m|\le N} \sum_{n\in\mathbb{Z}} a_{m,n}\, \boldsymbol{e}_m \langle g, \boldsymbol{e}_n \rangle_{L^2(S^1)} + \sum_{m\in\mathbb{Z}} \sum_{|n|\le N} a_{m,n}\, \boldsymbol{e}_m \langle g, \boldsymbol{e}_n \rangle_{L^2(S^1)} \\ - \sum_{|m|\le N} \sum_{|n|\le N} a_{m,n}\, \boldsymbol{e}_m \langle g, \boldsymbol{e}_n \rangle_{L^2(S^1)} , \end{aligned} \tag{2.24a}$$

where

$$a_{m,n} = \begin{cases} \langle \boldsymbol{e}_n, \alpha_m \rangle_{L^2(S^1)} & \text{if } |m| \le N, |n| > N , \\ \langle \beta_n, \boldsymbol{e}_m \rangle_{L^2(S^1)} & \text{if } |m| > N, |n| \le N , \\ \langle \boldsymbol{e}_n, \alpha_m \rangle_{L^2(S^1)} + \langle \beta_n, \boldsymbol{e}_m \rangle_{L^2(S^1)} & \text{if } |m| \le N, |n| \le N . \end{cases} \tag{2.24b}$$

We conclude that $G \in \mathcal{W}_N$ if and only if

$$\operatorname{supp}_{\ell^0 \times \ell^0} G \subseteq ([-N, N] \times \mathbb{Z}) \cup (\mathbb{Z} \times [-N, N]) ,$$

which particularly implies $\mathcal{W}_N \not\subseteq \mathcal{V}_N$.

(ii) Let $G \in \mathcal{V}_N$ be given as in (2.22). Then, G can be rewritten in form (2.23) by choosing, e.g., $\alpha_n = 0$ and $\beta_n = \sum_{|m|\le N} a_{m,n} \boldsymbol{e}_m$ for all n. This implies $\mathcal{V}_N \subseteq \mathcal{W}_N$.

(iii) Let $N \in \mathbb{N}$ be not too large. Then, operators in $\mathcal{V}_N$ have a sparse representation with respect to $(\boldsymbol{e}_{m,n})_{m,n}$ because $\operatorname{supp}_{\ell^0 \times \ell^0} G \subseteq [-N, N]^2$ (see (i)), so $\|G\|_{\ell^0 \times \ell^0} \le (2N+1)^2$ for $G \in \mathcal{V}_N$. In contrast to that, operators in $\mathcal{W}_N$ are not necessarily sparse with respect to $(\boldsymbol{e}_{m,n})_{m,n}$ since $\|G\|_{\ell^0 \times \ell^0}$ does not even need to be finite anymore (see (i)). Nevertheless, operators in $\mathcal{W}_N$ are of low rank because $\operatorname{rank} G \le 2N + 1$ for $G \in \mathcal{W}_N$. Due the (ii) the same holds for operators in $\mathcal{V}_N$. This clarifies the naming of $\mathcal{V}_N$ as subspace of 'sparse' and of $\mathcal{W}_N$ as subspace of 'low rank' far field operators. Both generalize the concept of *non-evanescent far field patterns* as introduced in [55].

(iv) By definition we have $G \in \mathcal{V}_N$ if and only if $\mathcal{N}(G)^\perp \subseteq \bigoplus_{n=0}^N \mathbb{Y}_n^2$ and $\mathcal{R}(G) \subseteq \bigoplus_{n=0}^N \mathbb{Y}_n^2$. Denoting by $\mathcal{W}_N^\perp$ the subspace orthogonal to $\mathcal{W}_N$ in $\mathrm{HS}(L^2(S^1))$, which is given by

$$\mathcal{W}_N^\perp = \Big\{ G \in \mathrm{HS}(L^2(S^1)) \;\Big|\; Gg = \sum_{|m|>N} \sum_{|n|>N} a_{m,n}\, \boldsymbol{e}_m \langle g, \boldsymbol{e}_n \rangle_{L^2(S^1)} , \, a_{m,n} \in \mathbb{C} \Big\} ,$$

we make a similar observation for $\mathcal{W}_N^\perp$. It holds $G \in \mathcal{W}_N^\perp$ if and only if $\mathcal{N}(G) \subseteq \bigoplus_{n=0}^N \mathbb{Y}_n^2$ and $\mathcal{R}(G)^\perp \subseteq \bigoplus_{n=0}^N \mathbb{Y}_n^2$ (cf. [24, Sec. 4] for the finite dimensional case). ◊

Next, we turn to the central result of this section, which states that the far field operator components $F_q^{(l)}$, $l \ge 1$, and hence also $F_q^{(\le p)}$, $p \ge 1$, and F_q (cf. Remark 2.12 (ii)) can be well approximated in the subspaces $\mathcal{V}_N$ and $\mathcal{W}_N$.

Theorem 2.11. *Suppose that* $\|L_q\|_{\mathrm{HS}} < 1$ *and let* $l \geq 1$. *For* $N \in \mathbb{N}$ *with* $N \gtrsim kR$ *we have the error estimates*

$$\|F_q^{(l)} - \mathcal{P}_{\mathcal{V}_N} F_q^{(l)}\|_{\mathrm{HS}} \leq 4\pi^{\frac{3}{2}} kR \|q\|_{L^\infty(D)} \|L_q\|_{\mathrm{HS}}^{l-1} \Big(\sum_{n>N} \|J_n(|\cdot|)\|^2_{L^2(B_{kR}(\mathbf{0}))} \Big)^{\frac{1}{2}} \tag{2.25}$$

and

$$\|F_q^{(l)} - \mathcal{P}_{\mathcal{W}_N} F_q^{(l)}\|_{\mathrm{HS}} \leq 4\pi \|q\|_{L^\infty(D)} \|L_q\|_{\mathrm{HS}}^{l-1} \sum_{n>N} \|J_n(|\cdot|)\|^2_{L^2(B_{kR}(\mathbf{0}))} \,. \tag{2.26}$$

Both upper bounds decay superlinearly in N, *more precisely faster than any power of* N^{-1}.

Proof. Taking the absolute value in (2.21) and applying Hölder's inequality and the Cauchy Schwarz inequality several times shows that

$$\begin{aligned}
|a_{m,n}^{(l)}| &\leq 2\pi k^{2l} \|q\|_{L^\infty(D)} \Big| \int_D J_m(k|\boldsymbol{y}_l|) \int_D \cdots \int_D q(\boldsymbol{y}_{l-1}) \cdots q(\boldsymbol{y}_1) \Phi_k(\boldsymbol{y}_l - \boldsymbol{y}_{l-1}) \cdots \Phi_k(\boldsymbol{y}_2 - \boldsymbol{y}_1) \\
&\qquad \times e^{-\mathrm{i}(m \arg \boldsymbol{y}_l - n \arg \boldsymbol{y}_1)} J_n(k|\boldsymbol{y}_1|) \, \mathrm{d}\boldsymbol{y}_1 \cdots \mathrm{d}\boldsymbol{y}_{l-1} \, \mathrm{d}\boldsymbol{y}_l \Big| \\
&\leq 2\pi k^{2l} \|q\|_{L^\infty(D)} \|J_m(k|\cdot|)\|_{L^2(D)} \Big(\int_D \Big| \int_D q(\boldsymbol{y}_{l-1}) \Phi_k(\boldsymbol{y}_l - \boldsymbol{y}_{l-1}) \int_D \cdots \int_D q(\boldsymbol{y}_{l-2}) \cdots q(\boldsymbol{y}_1) \\
&\quad \times \Phi_k(\boldsymbol{y}_{l-1} - \boldsymbol{y}_{l-2}) \cdots \Phi_k(\boldsymbol{y}_2 - \boldsymbol{y}_1) e^{\mathrm{i}n \arg \boldsymbol{y}_1} J_n(k|\boldsymbol{y}_1|) \, \mathrm{d}\boldsymbol{y}_1 \cdots \mathrm{d}\boldsymbol{y}_{l-1} \Big|^2 \mathrm{d}\boldsymbol{y}_l \Big)^{\frac{1}{2}} \\
&\leq 2\pi k^{2l} \|q\|_{L^\infty(D)} \|J_m(k|\cdot|)\|_{L^2(D)} \Big(\int_D \int_D |q(\boldsymbol{y}) \Phi_k(\boldsymbol{x} - \boldsymbol{y})|^2 \, \mathrm{d}\boldsymbol{y} \, \mathrm{d}\boldsymbol{x} \Big)^{\frac{1}{2}} \\
&\quad \times \Big(\int_D \Big| \int_D \cdots \int_D q(\boldsymbol{y}_{l-2}) \cdots q(y_1) \Phi_k(\boldsymbol{y}_{l-1} - \boldsymbol{y}_{l-2}) \cdots \Phi_k(\boldsymbol{y}_2 - \boldsymbol{y}_1) \\
&\qquad \times e^{\mathrm{i}n \arg \boldsymbol{y}_1} J_n(k|\boldsymbol{y}_1|) \, \mathrm{d}\boldsymbol{y}_1 \cdots \mathrm{d}\boldsymbol{y}_{l-2} \Big|^2 \mathrm{d}\boldsymbol{y}_{l-1} \Big)^{\frac{1}{2}} \\
&\leq \cdots \\
&\leq 2\pi k^2 \|q\|_{L^\infty(D)} \|J_m(k|\cdot|)\|_{L^2(D)} \|J_n(k|\cdot|)\|_{L^2(D)} \Big(k^4 \int_D \int_D \Big| q(\boldsymbol{y}) \Phi_k(\boldsymbol{x} - \boldsymbol{y}) \Big|^2 \, \mathrm{d}\boldsymbol{y} \, \mathrm{d}\boldsymbol{x} \Big)^{\frac{l-1}{2}} \\
&= 2\pi k^2 \|q\|_{L^\infty(D)} \|L_q\|_{\mathrm{HS}}^{l-1} \|J_m(k|\cdot|)\|_{L^2(D)} \|J_n(k|\cdot|)\|_{L^2(D)} \,.
\end{aligned}$$

Since $I - \mathcal{P}_{\mathcal{V}_N} = \mathcal{P}_{\mathcal{V}_N^\perp}$ and $I - \mathcal{P}_{\mathcal{W}_N} = \mathcal{P}_{\mathcal{W}_N^\perp}$ the summation areas for the estimates below are defined by the $\ell^0 \times \ell^0$-supports of operators in $\mathcal{V}_N^\perp$ and $\mathcal{W}_N^\perp$, respectively. These are visualized in Figure 2.2. From above upper bound for $|a_{m,n}^{(l)}|$ we conclude for $\mathcal{W}_N$ under consideration of Remark 2.10 (iv) that

$$\begin{aligned}
\|F_q^{(l)} - \mathcal{P}_{\mathcal{W}_N} F_q^{(l)}\|_{\mathrm{HS}}^2 &= \sum_{|m|>N} \sum_{|n|>N} |a_{m,n}^{(l)}|^2 \\
&\leq \Big(2\pi \|q\|_{L^\infty(D)} \|L_q\|_{\mathrm{HS}}^{l-1} \sum_{|n|>N} k^2 \|J_n(k|\cdot|)\|^2_{L^2(D)} \Big)^2 \\
&= \Big(4\pi \|q\|_{L^\infty(D)} \|L_q\|_{\mathrm{HS}}^{l-1} \sum_{n>N} k^2 \|J_n(k|\cdot|)\|^2_{L^2(D)} \Big)^2 \\
&\leq \Big(4\pi \|q\|_{L^\infty(D)} \|L_q\|_{\mathrm{HS}}^{l-1} \sum_{n>N} \|J_n(|\cdot|)\|^2_{L^2(B_{kR}(\mathbf{0}))} \Big)^2 \,.
\end{aligned} \tag{2.27}$$

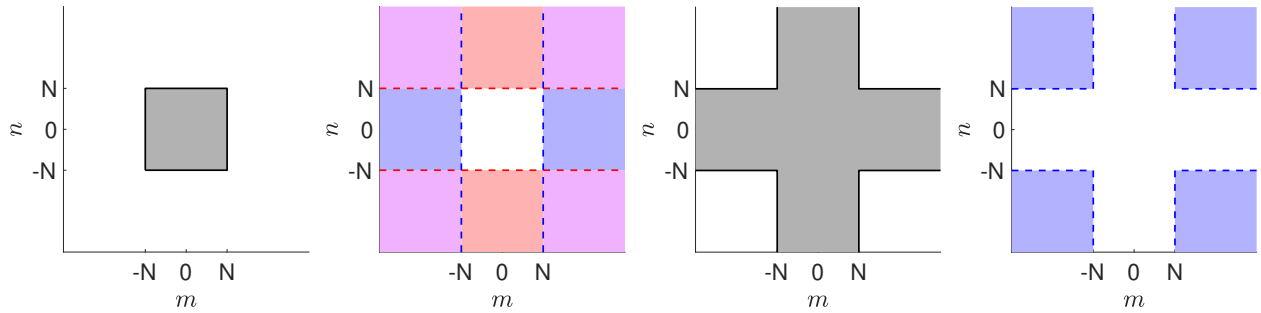

FIGURE 2.2. $\ell^0 \times \ell^0$-supports of operators in $\mathcal{V}_N$ (left) and of operators in $\mathcal{W}_N$ (middle right). Middle left: Partitioning of $\ell^0 \times \ell^0$-support of operators in $\mathcal{V}_N^\perp$ as sum of part marked in red and part marked in blue, minus part marked in both colors. Right: $\ell^0 \times \ell^0$-support of operators in $\mathcal{W}_N^\perp$.

For the last equality we used that $\|J_{-n}(k|\cdot|)\|_{L^2(D)} = \|J_n(k|\cdot|)\|_{L^2(D)}$ due to formula (B.7). We make a similar estimation for $\mathcal{V}_N$ and obtain

$$\begin{aligned}
\|F_q^{(l)} - \mathcal{P}_{\mathcal{V}_N} F_q^{(l)}\|_{\mathrm{HS}}^2 &= \sum_{m\in\mathbb{Z}} \sum_{|n|>N} |a_{m,n}^{(l)}|^2 + \sum_{|m|>N} \sum_{n\in\mathbb{Z}} |a_{m,n}^{(l)}|^2 - \sum_{|m|>N} \sum_{|n|>N} |a_{m,n}^{(l)}|^2 \\
&\le \sum_{m\in\mathbb{Z}} \sum_{|n|>N} |a_{m,n}^{(l)}|^2 + \sum_{|m|>N} \sum_{n\in\mathbb{Z}} |a_{m,n}^{(l)}|^2 \\
&\le 2\left(2\pi\|q\|_{L^\infty(D)}\|L_q\|_{\mathrm{HS}}^{l-1}\right)^2 \sum_{|n|>N} k^2\|J_n(k|\cdot|)\|_{L^2(D)}^2 \sum_{m\in\mathbb{Z}} k^2\|J_m(k|\cdot|)\|_{L^2(D)}^2 \\
&\le 2\pi\left(2\pi kR\|q\|_{L^\infty(D)}\|L_q\|_{\mathrm{HS}}^{l-1}\right)^2 \sum_{|n|>N} k^2\|J_n(k|\cdot|)\|_{L^2(D)}^2 \\
&= 4\pi\left(2\pi kR\|q\|_{L^\infty(D)}\|L_q\|_{\mathrm{HS}}^{l-1}\right)^2 \sum_{n>N} k^2\|J_n(k|\cdot|)\|_{L^2(D)}^2 \\
&\le 4\pi\left(2\pi kR\|q\|_{L^\infty(D)}\|L_q\|_{\mathrm{HS}}^{l-1}\right)^2 \sum_{n>N} \|J_n(|\cdot|)\|_{L^2(B_{kR}(\mathbf{0}))}^2 . \qquad (2.28)
\end{aligned}$$

For the third inequality we used that

$$\sum_{m\in\mathbb{Z}} k^2\|J_m(k|\cdot|)\|_{L^2(D)}^2 \le \sum_{m\in\mathbb{Z}} k^2\|J_m(k|\cdot|)\|_{L^2(B_R(\mathbf{0}))}^2 = \sum_{m\in\mathbb{Z}} \|J_m(|\cdot|)\|_{L^2(B_{kR}(\mathbf{0}))}^2 = \pi(kR)^2 , \qquad (2.29)$$

see [55, (3.7)]. The decay of $(\|J_n(|\cdot|)\|_{L^2(B_{kR}(\mathbf{0}))})_n$ in $n \in \mathbb{N}$ for $n \gtrsim kR$ has been studied in [55]. It holds that

$$\begin{aligned}
\|J_n(|\cdot|)\|_{L^2(B_{kR}(\mathbf{0}))} &\le \frac{\pi^{\frac{1}{2}} 2^{\frac{1}{3}}}{3^{\frac{2}{3}}\Gamma(\frac{2}{3})} n^{\frac{1}{3}} \left(1+\frac{1}{2n}\right)^{\frac{n+1}{2}} \frac{kR}{n} \left(\left(\frac{kR}{n}\right)^2 e^{1-\left(\frac{kR}{n}\right)^2}\right)^{\frac{n}{2}} \\
&\le b_0\, n^{\frac{1}{3}} \left(1+\frac{1}{2n}\right)^{\frac{n+1}{2}} \frac{kR}{n} \left(\left(\frac{kR}{n}\right)^2 e^{1-\left(\frac{kR}{n}\right)^2}\right)^{\frac{n}{2}}
\end{aligned}$$

with $b_0 \approx 0.7928$, so $(\|J_n(|\cdot|)\|_{L^2(B_{kR}(\mathbf{0}))})_n$ decays in n faster than any power of n^{-1}, which carries over to the two upper bounds in (2.27) and (2.28). □

Remark 2.12. (i) Our numerical tests in Example 4.3 show that the choice $N = \lceil ekR/2 \rceil$ is appropriate as a truncation index in terms of kR.

(ii) By summing over l we obtain similar upper bounds for approximating $F_q^{(\le p)}$ and F_q in $\mathcal{V}_N$

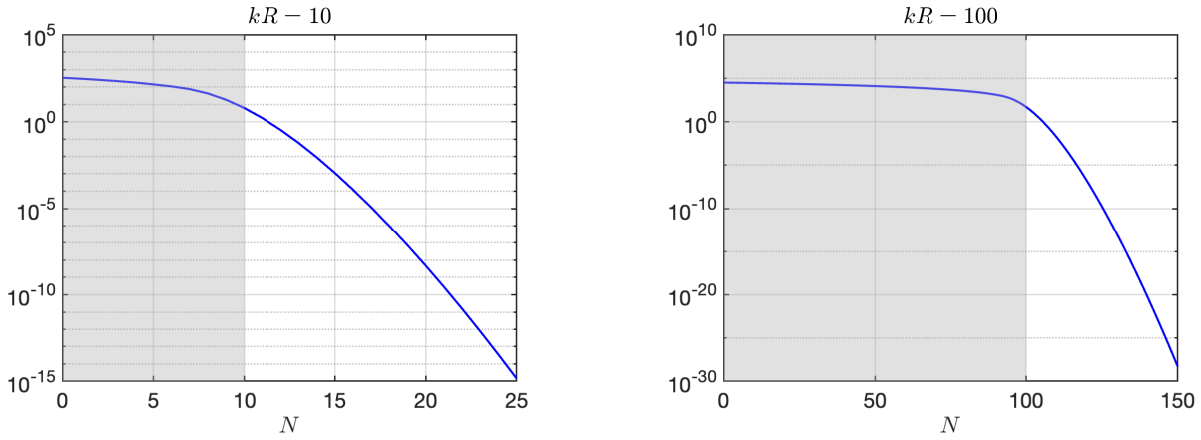

FIGURE 2.3. Plots of the factor $\sum_{|n|>N} \|J_n(|\cdot|)\|^2_{L^2(B_{kR}(\mathbf{0}))}$ in (2.25) and (2.26) as a function of $N \in \mathbb{N}$ for $kR = 10$ (left) and for $kR = 100$ (right)

and $\mathcal{W}_N$, respectively. The superlinear decay of these bounds in N is preserved.

(iii) In [55] it has been proved additionally that

$$\lim_{kR\to\infty} \frac{\|J_{\lceil \nu kR\rceil}(|\cdot|)\|^2_{L^2(B_{kR}(\mathbf{0}))}}{2kR} = \begin{cases} \sqrt{1-\nu^2} & \text{if } \nu \le 1\,, \\ 0 & \text{else}\,. \end{cases} \tag{2.30}$$

Consequently, the term $\|J_n(|\cdot|)\|^2_{L^2(B_{kR}(\mathbf{0}))}$ approaches the asymptote $2\sqrt{(kR)^2 - n^2}$ for large values of kR. Numerical tests in [55] confirm that this already happens for moderate values of kR and that these terms decay quickly for $n \gtrsim kR$. This observation further underpins that the essential support of the expansion coefficients (2.21) is contained in $[-N, N]^2$ with $N \gtrsim kR$ and their decay behavior from a different perspective.

(iv) We note that (B.6) shows that

$$\|J_n(|\cdot|)\|^2_{L^2(B_{kR}(\mathbf{0}))} = \pi(kR)^2\big(J_n^2(kR) - J_{n-1}(kR)J_{n+1}(kR)\big)\,, \qquad n \in \mathbb{Z}\,,$$

which provides explicit representations of the upper bounds (2.25) and (2.26), that can be implemented directly without any approximations needed.

Figure 2.3 illustrates the decay of the factor $\sum_{|n|>N} \|J_n(|\cdot|)\|^2_{L^2(B_{kR}(\mathbf{0}))}$ by plotting the term $\sum_{|n|=N+1}^{1000} \|J_n(|\cdot|)\|^2_{L^2(B_{kR}(\mathbf{0}))}$ as a function of $N \in \mathbb{N}$ for the choices $kR = 10$ (left) and $kR = 100$ (right). In both situations superlinear decay starts at about $N = kR$, and it is more rapid for larger kR. ◊

Example 2.13. To further illustrate this approximations, we consider an analytical example by choosing $q = \chi_{B_R(\mathbf{0})}$ for the contrast function, i.e., the refractive index n^2 is piecewise constant with value $n^2 = 2$ in $D = B_R(\mathbf{0})$ and $n^2 = 1$ in $\mathbb{R}^2 \setminus \overline{B_R(\mathbf{0})}$. Then, the Fourier coefficients $(a^{(1)}_{m,n})_{m,n}$ from (2.21) with $l = 1$ satisfy

$$\begin{aligned} a^{(1)}_{m,n} &= 2\pi k^2 (-\mathrm{i})^{m-n} \int_{B_R(\mathbf{0})} e^{-\mathrm{i}(m-n)\arg \boldsymbol{y}} J_m(k|\boldsymbol{y}|) J_n(k|\boldsymbol{y}|)\, \mathrm{d}\boldsymbol{y} \\ &= 2\pi k^2 (-\mathrm{i})^{m-n} \int_0^R J_m(kr) J_n(kr) r\, \mathrm{d}r \underbrace{\int_0^{2\pi} e^{-\mathrm{i}(m-n)\varphi}\, \mathrm{d}\varphi}_{=2\pi\delta^m_n} \end{aligned}$$

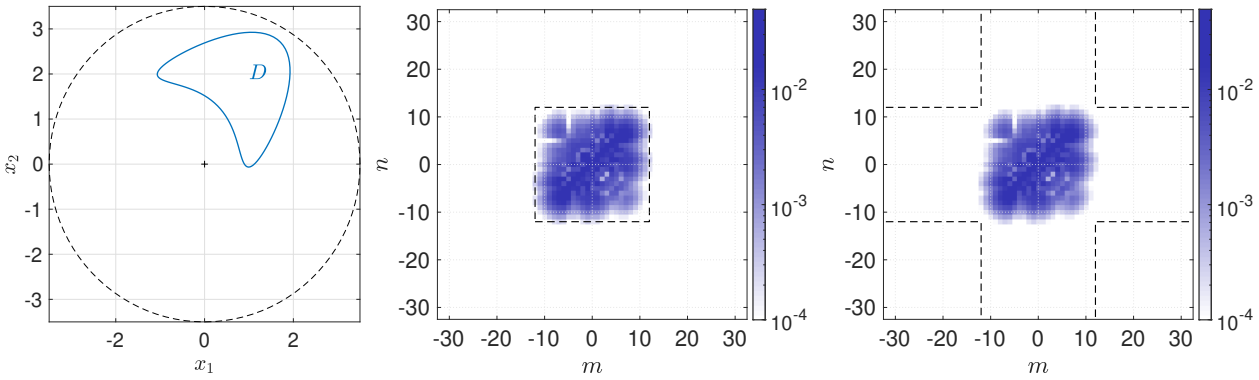

Figure 2.4. Left: Support of the scatterer D (solid) and ball $B_R(\mathbf{0})$ with radius $R = 3.5$ containing D.
Absolute values of Fourier coefficients $(a_{m,n})_{m,n}$ of far field operator F_q at wave number $k = 2.5$ together with dashed square corresponding to its sparse approximation in $\mathcal{V}_N$ (middle) and with the dashed cross-shaped index set corresponding to its low rank approximation in $\mathcal{W}_N$ (right) for $N = 12$.

$$= \begin{cases} 2\pi \|J_n(|\cdot|)\|^2_{L^2(B_{kR}(\mathbf{0}))} & \text{if } n = m\,, \\ 0 & \text{else}\,, \end{cases}$$

with δ_n^m denoting the Kronecker delta. Recalling (2.30), this shows that the cut-off parameter N in Theorem 2.11 cannot be chosen smaller than kR. ◊

Example 2.14. We illustrate our findings by a numerical example and consider the same scattering object D as in Example 2.5, i.e. a kite-shaped scatterer as depicted in Figure 2.4 (left) at wave number $k = 2.5$. The contrast function is given by $q = 2\chi_D$, and we simulate the far field operator as explained in Example 2.5, which yields a matrix $\boldsymbol{F}_q = 2\pi/L(u_q^\infty(\widehat{\boldsymbol{x}}_m; \boldsymbol{\theta}_n))_{m,n} \in \mathbb{C}^{L\times L}$ for $L = 256$. Taking the two-dimensional fast Fourier transform of this matrix gives an approximation of the Fourier coefficients $(a_{m,n})_{m,n}$ of F_q with respect to $(e_{m,n})_{m,n}$.

In Figure 2.4 (middle, right) the absolute values of these Fourier coefficients are plotted for $-32 \le m, n \le 32$ on a logarithmic color scale. The dashed square in Figure 2.4 (middle) corresponds to the support of the Fourier coefficients of operators in $\mathcal{V}_N$, the dashed cross in Figure 2.4 (right) to the support of the Fourier coefficients of operators in $\mathcal{W}_N$. Here, we choose $N = \lceil ekR/2 \rceil = 12$ with $R = 3.5$. It is nicely confirmed that the Fourier coefficients are essentially supported inside the marked square and in the cross-shaped area, respectively. ◊

The three-dimensional case

Notation 2.15. We denote by $(Y_n^p)_{|p|\le n}$ the orthonormal basis of the space of spherical harmonics $\mathbb{Y}_n^3$ of order n in $\mathbb{R}^3$ as introduced in (B.14). By Theorem B.3 we know that

$$((\widehat{\boldsymbol{x}}, \boldsymbol{\theta}) \mapsto Y_m^o(\widehat{\boldsymbol{x}}) Y_n^p(\boldsymbol{\theta}))_{|o|\le m, |p|\le n} \qquad \text{and} \qquad ((\widehat{\boldsymbol{x}}, \boldsymbol{\theta}) \mapsto Y_m^o(\widehat{\boldsymbol{x}}) Y_n^p(\boldsymbol{\theta}))_{\substack{m\in\mathbb{N}_0, |o|\le m,\\ n\in\mathbb{N}_0, |p|\le n}}$$

form a orthonormal basis in $\mathbb{Y}_m^3 \times \mathbb{Y}_n^3$ and in $L^2(S^2 \times S^2) = \bigoplus_{m,n\in\mathbb{N}_0} \mathbb{Y}_m^3 \times \mathbb{Y}_n^3$, respectively. So, by the same theorem every kernel $\kappa_G \in L^2(S^2 \times S^2)$ of a Hilbert–Schmidt operator $G \in \mathrm{HS}(L^2(S^2))$ can be expanded as a Fourier–Laplace series

$$\kappa_G = \sum_{m=0}^{\infty} \sum_{n=0}^{\infty} \alpha_{m,n} \qquad \text{with } \alpha_{m,n} \in \mathbb{Y}_m^3 \times \mathbb{Y}_n^3\,.$$

For $m, n \in \mathbb{N}_0$ the (m,n)th spherical harmonics component $\alpha_{m,n}$ of κ_G is the orthogonal projection of κ_G onto the space $\mathbb{Y}^3_m \times \mathbb{Y}^3_n$, which is given by formula (B.19). We use the notations

$$\|G\|_{L^p} := \|\kappa_G\|_{L^p(S^2\times S^2)} \qquad \text{for } 1 \le p \le \infty\,,$$

$$\|G\|_{\ell^p\times\ell^p} := \|(\alpha_{m,n})_{m,n}\|_{(\ell^p\times\ell^p)(L^2(S^2\times S^2))} := \Bigg(\sum_{m,n=0}^{\infty} \|\alpha_{m,n}\|^p_{L^2(S^2\times S^2)}\Bigg)^{\frac{1}{p}} \qquad \text{for } 1 \le p < \infty$$

and

$$\|G\|_{\ell^\infty\times\ell^\infty} := \|(\alpha_{m,n})_{m,n}\|_{(\ell^\infty\times\ell^\infty)(L^2(S^2\times S^2))} := \operatorname*{ess\,sup}_{m,n\in\mathbb{N}_0} \|\alpha_{m,n}\|_{L^2(S^2\times S^2)}\,,$$

and we conclude from Parseval's identity and Theorem B.3 that

$$\|G\|_{\mathrm{HS}} = \|G\|_{L^2} = \|G\|_{\ell^2\times\ell^2}\,. \tag{2.31}$$

Particularly, we have that $(\alpha_{m,n})_{m,n} \in (\ell^2\times\ell^2)(L^2(S^2\times S^2))$, where

$$(\ell^p\times\ell^p)(L^2(S^2\times S^2)) := \{(\beta_{m,n})_{m,n} \,|\, \beta_{m,n} \in \mathbb{Y}^3_m \times \mathbb{Y}^3_n \text{ for all } m,n\in\mathbb{N}_0 \text{ and } \|(\beta_{m,n})_{m,n}\|_{\ell^p\times\ell^p} < \infty\}$$

for $1 \le p \le \infty$. We refer to the essential support of the integral kernel κ_G as the *L^0-support*

$$\operatorname{supp}_{L^0} G := \operatorname{supp}\kappa_G \subseteq S^2\times S^2$$

of G and denote its measure by $\|G\|_{L^0}$. We further call the index set of the nonvanishing spherical harmonics components $(\alpha_{m,n})_{m,n}$ the *$\ell^0\times\ell^0$-support*

$$\operatorname{supp}_{\ell^0\times\ell^0} G = \{(m,n)\in\mathbb{N}_0^2 \,|\, \alpha_{m,n} \neq 0\}$$

of G and denote the number of these indices by $\|G\|_{\ell^0\times\ell^0}$. Moreover, we introduce the following *weighted $\ell^p\times\ell^p$ spaces*, which are of special importance when investigating the mapping properties of the translation operator in Subsection 2.5. Given two sequences of weights $w = (w_n)_n \subseteq [0,\infty)$ and $v = (v_n)_n \subseteq [0,\infty)$, we define

$$(\ell^p_w\times\ell^p_v)(L^2(S^2\times S^2)) := \{(\beta_{m,n})_{m,n} \,|\, \beta_{m,n} \in \mathbb{Y}^3_m \times \mathbb{Y}^3_n \text{ for all } m,n\in\mathbb{N}_0 \text{ and } \|(\beta_{m,n})_{m,n}\|_{\ell^p_w\times\ell^p_v} < \infty\}\,,$$

where for $1 \le p < \infty$,

$$\|G\|_{\ell^p_w\times\ell^p_v} := \|(\alpha_{m,n})_{m,n}\|_{(\ell^p_w\times\ell^p_v)(L^2(S^2\times S^2))} := \Bigg(\sum_{m,n=0}^{\infty} w_m v_n \|\alpha_{m,n}\|^p_{L^2(S^2\times S^2)}\Bigg)^{\frac{1}{p}}$$

and

$$\|G\|_{\ell^\infty_w\times\ell^\infty_v} := \|(\alpha_{m,n})_{m,n}\|_{(\ell^\infty_w\times\ell^\infty_v)(L^2(S^2\times S^2))} := \sup_{m,n\in\mathbb{N}_0} \Big(w_m v_n \|\alpha_{m,n}\|_{L^2(S^2\times S^2)}\Big)\,.$$

If it is clear from the context, we use $\ell^p\times\ell^p$ and $\ell^p_w\times\ell^p_v$ as an abbreviation for $(\ell^p\times\ell^p)(L^2(S^2\times S^2))$ and $(\ell^p_w\times\ell^p_v)(L^2(S^2\times S^2))$, respectively. Moreover, let $\|G\|_{\mathrm{nuc}}$ be the nuclear norm of G (cf. (A.5)), and let $\operatorname{rank} G$ be its rank (cf. Definition A.6). For $W \subseteq \mathbb{N}_0^2$, $w = (w_n)_n, v = (v_n)_n \subseteq (0,\infty]$ and $1 \le p \le \infty$ we further define $\ell^p_w\times\ell^p_v(W) := \{(\beta_{m,n})_{m,n} \in \ell^p_w\times\ell^p_v \,|\, \operatorname{supp}(\beta_{m,n})_{m,n} \subseteq W\}$ as a subspace of $\ell^p_w\times\ell^p_v$, and we write

$$\|G\|_{\ell^p_w\times\ell^p_v(W)} := \|(\alpha_{m,n})_{m,n}\|_{\ell^p_w\times\ell^p_v(W)}\,.$$

The following lemma gives an explicit expansion of far field patterns and represents the analogue of Lemma 2.8 in the three-dimensional case.

Lemma 2.16. *The far field component* (2.15) *associated to scattering processes of order* $l \in \mathbb{N}$ *can be expanded as a Fourier–Laplace series via*

$$u_q^{\infty,(l)}(\widehat{\boldsymbol{x}};\boldsymbol{\theta}) = \sum_{m=0}^{\infty}\sum_{n=0}^{\infty} \alpha_{m,n}^{(l)}(\widehat{\boldsymbol{x}};\boldsymbol{\theta}) \,, \qquad \widehat{\boldsymbol{x}},\boldsymbol{\theta} \in S^2 \,, \tag{2.32}$$

with

$$\begin{aligned}\alpha_{m,n}^{(l)}(\widehat{\boldsymbol{x}};\boldsymbol{\theta}) = k^{2l}\frac{(2m+1)^2(2n+1)^2}{16\pi^2}\mathrm{i}^{n-m}\int_D\cdots\int_D q(\boldsymbol{y}_l)\cdots q(\boldsymbol{y}_1)\Phi_k(\boldsymbol{y}_l-\boldsymbol{y}_{l-1})\cdots\Phi_k(\boldsymbol{y}_2-\boldsymbol{y}_1)\\ \times j_m(k|\boldsymbol{y}_l|)j_n(k|\boldsymbol{y}_1|)\langle P_m^{\widehat{\boldsymbol{x}}}, P_m^{\widehat{\boldsymbol{y}}_l}\rangle_{L^2(S^2)}\langle P_n^{\boldsymbol{\theta}}, P_n^{\widehat{\boldsymbol{y}}_1}\rangle_{L^2(S^2)}\,\mathrm{d}\boldsymbol{y}_1\cdots\mathrm{d}\boldsymbol{y}_l \,.\end{aligned} \tag{2.33}$$

Here, $\alpha_{m,n}^{(l)} \in \mathbb{Y}_m^3 \times \mathbb{Y}_n^3$ *is the* (m,n)*th spherical harmonics component of* $u_q^{\infty,(l)}$ *and* $P_n^{\widehat{\boldsymbol{x}}} = P_n(\widehat{\boldsymbol{x}}\cdot(\,\cdot\,))$. *The functions* P_n *and* j_n *are the* Legendre polynomial of degree n *and the* spherical Bessel function of order n, *see Section B.2.*

Proof. Plugging the Jacobi–Anger expansion (B.24) twice into (2.15) yields

$$\begin{aligned}u_q^{\infty,(l)}(\widehat{\boldsymbol{x}};\boldsymbol{\theta}) = k^{2l}\int_D\cdots\int_D q(\boldsymbol{y}_l)\cdots q(\boldsymbol{y}_1)\Phi_k(\boldsymbol{y}_l-\boldsymbol{y}_{l-1})\cdots\Phi_k(\boldsymbol{y}_2-\boldsymbol{y}_1)\\ \times\sum_{o=0}^{\infty}\sum_{p=0}^{\infty}\mathrm{i}^{p-o}(2o+1)(2p+1)j_o(k|\boldsymbol{y}_l|)j_p(k|\boldsymbol{y}_1|)P_o(\widehat{\boldsymbol{y}}_l\cdot\widehat{\boldsymbol{x}})P_p(\widehat{\boldsymbol{y}}_1\cdot\boldsymbol{\theta})\,\mathrm{d}\boldsymbol{y}_1\cdots\mathrm{d}\boldsymbol{y}_l \,.\end{aligned} \tag{2.34}$$

From (B.19) we know, that we can represent the (m,n)th spherical harmonics component $\alpha_{m,n}^{(l)}$ of $u_q^{\infty,(l)}$ by

$$\alpha_{m,n}^{(l)}(\widehat{\boldsymbol{x}};\boldsymbol{\theta}) = \frac{(2m+1)(2n+1)}{16\pi^2}\int_{S^2}P_m(\widehat{\boldsymbol{x}}\cdot\boldsymbol{\omega})\int_{S^2}P_n(\boldsymbol{\theta}\cdot\boldsymbol{\upsilon})u_q^{\infty,(l)}(\boldsymbol{\omega};\boldsymbol{\upsilon})\,\mathrm{d}s(\boldsymbol{\upsilon})\,\mathrm{d}s(\boldsymbol{\omega}) \,.$$

We insert (2.34) and use that

$$\int_{S^2}P_m(\widehat{\boldsymbol{x}}\cdot\boldsymbol{\omega})P_n(\widehat{\boldsymbol{y}}\cdot\boldsymbol{\omega})\,\mathrm{d}s(\boldsymbol{\omega}) = 0 \qquad \text{for all } \widehat{\boldsymbol{x}},\widehat{\boldsymbol{y}} \in S^2,\ m \neq n \,,$$

due to the mutually orthogonality of $\mathbb{Y}_n^3$, $n \in \mathbb{N}_0$ (see (B.3)). Together with Remark B.2 this gives (2.32)–(2.33). □

The following definition is the counterpart to Definition 2.9 in three dimensions.

Definition 2.17. For $N \in \mathbb{N}$ with $N \gtrsim kR$ we define the *subspace of sparse far field operators associated to scatterers supported in* $B_R(\mathbf{0}) \subseteq \mathbb{R}^3$ by

$$\mathcal{V}_N := \Big\{G \in \mathrm{HS}(L^2(S^2)) \;\Big|\; Gg = \sum_{m=0}^{N}\sum_{n=0}^{N}\int_{S^2}\alpha_{m,n}(\,\cdot\,;\boldsymbol{\theta})g(\boldsymbol{\theta})\,\mathrm{d}s(\boldsymbol{\theta}),\ \alpha_{m,n} \in \mathbb{Y}_m^3\times\mathbb{Y}_n^3\Big\} \,. \tag{2.35}$$

Furthermore, we denote by

$$\begin{aligned}\mathcal{W}_N := \Big\{G \in \mathrm{HS}(L^2(S^2)) \;\Big|\; Gg = \sum_{n=0}^{N}\int_{S^2}(\alpha_n(\,\cdot\,;\boldsymbol{\theta})+\beta_n(\,\cdot\,;\boldsymbol{\theta}))g(\boldsymbol{\theta})\,\mathrm{d}s(\boldsymbol{\theta}),\\ \alpha_n \in \mathbb{Y}_n^3\times L^2(S^2),\ \beta_n \in L^2(S^2)\times\mathbb{Y}_n^3\Big\} \,.\end{aligned} \tag{2.36}$$

the *subspace of low rank far field operators associated to scatterers supported in* $B_R(\mathbf{0}) \subseteq \mathbb{R}^3$. By $\mathcal{P}_{\mathcal{V}_N} : \mathrm{HS}(L^2(S^2)) \to \mathcal{V}_N$ and $\mathcal{P}_{\mathcal{W}_N} : \mathrm{HS}(L^2(S^2)) \to \mathcal{W}_N$ we denote the orthogonal projections onto $\mathcal{V}_N$ and $\mathcal{W}_N$ with respect to $\langle \cdot, \cdot \rangle_{\mathrm{HS}}$, respectively.

As an analogue to Remark 2.10, the following remark relates the two subspaces $\mathcal{V}_N$ and $\mathcal{W}_N$ to each other.

Remark 2.18. (i) We can expand the (m,n)th spherical harmonics component (2.33) further in terms of the orthonormal basis $((\widehat{\boldsymbol{x}}, \boldsymbol{\theta}) \mapsto Y_m^o(\widehat{\boldsymbol{x}}) Y_n^{-p}(\boldsymbol{\theta}))_{|p|\leq n, |o|\leq m}$ of $\mathbb{Y}_m^3 \times \mathbb{Y}_n^3$. We insert the addition theorem (B.16) twice and take the orthonormality of $\{Y_m^o\}_{|o|\leq m}$ into account to conclude

$$\begin{aligned}\langle P_m^{\widehat{\boldsymbol{x}}}, P_m^{\widehat{\boldsymbol{y}}_l} \rangle_{L^2(S^2)} &= \frac{16\pi^2}{(2m+1)^2} \sum_{o,p=-m}^{m} \int_{S^2} Y_m^o(\widehat{\boldsymbol{x}}) Y_m^{-o}(\boldsymbol{\omega}) Y_m^{-p}(\widehat{\boldsymbol{y}}_l) Y_m^p(\boldsymbol{\omega}) \, \mathrm{d}s(\boldsymbol{\omega}) \\ &= \frac{16\pi^2}{(2m+1)^2} \sum_{o=-m}^{m} Y_m^o(\widehat{\boldsymbol{x}}) Y_m^{-o}(\widehat{\boldsymbol{y}}_l) \,.\end{aligned}$$

Here, we used that due to the definition (B.14) of Y_m^o it holds $\overline{Y_m^o} = Y_m^{-o}$. Analogously, we have that

$$\langle P_n^{\boldsymbol{\theta}}, P_n^{\widehat{\boldsymbol{y}}_1} \rangle_{L^2(S^2)} = \frac{16\pi^2}{(2n+1)^2} \sum_{p=-n}^{n} Y_n^{-p}(\boldsymbol{\theta}) Y_n^p(\widehat{\boldsymbol{y}}_1) \,.$$

We insert both into (2.33) and obtain

$$\alpha_{m,n}^{(l)}(\widehat{\boldsymbol{x}}; \boldsymbol{\theta}) = \sum_{o=-m}^{m} \sum_{p=-n}^{n} a_{m,n}^{o,p,(l)} Y_m^o(\widehat{\boldsymbol{x}}) Y_n^{-p}(\boldsymbol{\theta})$$

with

$$\begin{aligned}a_{m,n}^{o,p,(l)} := k^{2l} 16\pi^2 \mathrm{i}^{n-m} \int_D \cdots \int_D q(\boldsymbol{y}_l) \cdots q(\boldsymbol{y}_1) \Phi_k(\boldsymbol{y}_l - \boldsymbol{y}_{l-1}) \cdots \Phi_k(\boldsymbol{y}_2 - \boldsymbol{y}_1) \\ \times j_m(k|\boldsymbol{y}_l|) Y_m^{-o}(\widehat{\boldsymbol{y}}_l) j_n(k|\boldsymbol{y}_1|) Y_n^p(\widehat{\boldsymbol{y}}_1) \, \mathrm{d}\boldsymbol{y}_1 \cdots \mathrm{d}\boldsymbol{y}_l \,.\end{aligned}$$

This reveals the same structure as in (2.21) for the two-dimensional case and the far field operator component $F_q^{(l)}$ associated to scattering processes of order l can in the same manner for $g \in L^2(S^2)$ be written as

$$F_q^{(l)} g = \sum_{m=0}^{\infty} \sum_{n=0}^{\infty} \sum_{o=-m}^{m} \sum_{p=-n}^{n} a_{m,n}^{o,p,(l)} Y_m^o \langle g, Y_n^p \rangle_{L^2(S^2)} \,. \tag{2.37}$$

Accordingly, we can rewrite $\mathcal{V}_N$ as

$$\mathcal{V}_N = \left\{ G \in \mathrm{HS}(L^2(S^2)) \;\middle|\; Gg = \sum_{m=0}^{N} \sum_{n=0}^{N} \sum_{o=-m}^{m} \sum_{p=-n}^{n} a_{m,n}^{o,p} Y_m^o \langle g, Y_n^p \rangle_{L^2(S^2)} \,,\; a_{m,n}^{o,p} \in \mathbb{C} \right\},$$

and the analogue can be done for $\mathcal{W}_N$.

(ii) By definition we have for $G \in \mathcal{V}_N$ that

$$\mathrm{supp}_{\ell^0 \times \ell^0} G \subseteq [0, N]^2 \,.$$

For the $\ell^0 \times \ell^0$-support of $G \in \mathcal{W}_N$ we find as in Remark 2.10 (i) that

$$\mathrm{supp}_{\ell^0 \times \ell^0} G \subseteq ([0, N] \times \mathbb{N}_0) \cup (\mathbb{N}_0 \times [0, N]) \,.$$

(iii) As in Remark 2.10 (i)-(ii) we observe that $\mathcal{V}_N \subseteq \mathcal{W}_N$ but $\mathcal{W}_N \not\subseteq \mathcal{V}_N$.

(iv) Suppose N is not too large. Due to (ii) we have $\|G\|_{\ell^0\times\ell^0} \leq (N+1)^2$ for $G \in \mathcal{V}_N$, which reveals the sparsity of such operators. Operators in $\mathcal{W}_N$ are not necessarily sparse, since their $\ell^0 \times \ell^0$-support may be infinite.

(v) Let $G \in \mathcal{W}_N$ be given as in (2.36) for some $\alpha_n \in \mathbb{Y}_n^3 \times L^2(S^2)$ and $\beta_n \in L^2(S^2) \times \mathbb{Y}_n^3$, $n \in \mathbb{N}_0$, which can be expanded according to

$$\alpha_n(\widehat{\boldsymbol{x}};\boldsymbol{\theta}) = \sum_{m=-n}^{n} \langle \alpha_n(\cdot\,;\boldsymbol{\theta}), Y_n^m\rangle_{L^2(S^2)} Y_n^m(\widehat{\boldsymbol{x}})\,,\ \beta_n(\widehat{\boldsymbol{x}};\boldsymbol{\theta}) = \sum_{m=-n}^{n} \langle \beta_n(\widehat{\boldsymbol{x}};\,\cdot\,), Y_n^m\rangle_{L^2(S^2)} Y_n^m(\boldsymbol{\theta})$$

for $\widehat{\boldsymbol{x}}, \boldsymbol{\theta} \in S^2$. Plugging these representations into the formula for G from (2.36) yields

$$\operatorname{rank} G \leq \sum_{n=0}^{N}\sum_{m=-n}^{n} 1 = \sum_{n=0}^{N}(2n+1) = 2\,\frac{N(N+1)}{2} + (N+1) = (N+1)^2\,. \tag{2.38}$$

The same holds for $G \in \mathcal{V}_N$. Consequently, if N is not too large operators in $\mathcal{W}_N$ as well as in $\mathcal{V}_N$ are of low rank.

(vi) Finally, we make similar observations as in Remark 2.10 (iv), namely that $G \in \mathcal{V}_N$ if and only if $\mathcal{N}(G)^\perp \subseteq \bigoplus_{n=0}^N \mathbb{Y}_n^3$ and $\mathcal{R}(G) \subseteq \bigoplus_{n=0}^N \mathbb{Y}_n^3$. For $\mathcal{W}_N^\perp$ denoting the orthogonal subspace to $\mathcal{W}_N$ in $\mathrm{HS}(L^2(S^2))$ we further have that $G \in \mathcal{W}_N^\perp$ if and only if $\mathcal{N}(G) \subseteq \bigoplus_{n=0}^N \mathbb{Y}_n^3$ and $\mathcal{R}(G)^\perp \subseteq \bigoplus_{n=0}^N \mathbb{Y}_n^3$. ◊

The following approximation theorem underpins that the far field operator component $F_q^{(l)}$, $l \geq 1$, as well as $F_q^{(\leq p)}$, $p \geq 1$, and F_q (cf. Remark 2.20 (i)) can be well approximated in the subspaces $\mathcal{V}_N$ and $\mathcal{W}_N$. It represents the counterpart to Theorem 2.11.

Theorem 2.19. *Suppose that $\|L_q\|_{\mathrm{HS}} < 1$ and let $l \geq 1$. For $N \in \mathbb{N}$ with $N \gtrsim kR$ there holds the error estimate*

$$\|F_q^{(l)} - \mathcal{P}_{\mathcal{V}_N} F_q^{(l)}\|_{\mathrm{HS}} \leq \frac{4\pi}{k}\|q\|_{L^\infty(D)}\|L_q\|_{\mathrm{HS}}^{l-1}\left(2M(kR)\sum_{n=N+1}^{\infty}(2n+1)^2\|j_n(|\,\cdot\,|)\|^2_{L^2(B_{kR}(\mathbf{0}))}\right)^{\frac{1}{2}}. \tag{2.39}$$

and

$$\|F_q^{(l)} - \mathcal{P}_{\mathcal{W}_N} F_q^{(l)}\|_{\mathrm{HS}} \leq \frac{4\pi}{k}\|q\|_{L^\infty(D)}\|L_q\|_{\mathrm{HS}}^{l-1}\sum_{n=N+1}^{\infty}(2n+1)^2\|j_n(|\,\cdot\,|)\|^2_{L^2(B_{kR}(\mathbf{0}))}\,. \tag{2.40}$$

Here, $M(kR) := \sum_{n=0}^{\infty}(2n+1)^2\|j_n(|\,\cdot\,|)\|^2_{L^2(B_{kR}(\mathbf{0}))}$. Both upper bounds decay superlinearly in N, more precisely faster than any power of N^{-1}.

Proof. We proceed similar to the proof of Theorem 2.11. The Cauchy Schwarz inequality together with (B.17) yields

$$\int_{S^2}\sup_{\boldsymbol{y}\in D}\left|\langle P_m^{\widehat{\boldsymbol{x}}}, P_m^{\widehat{\boldsymbol{y}}}\rangle_{L^2(S^2)}\right|^2 \mathrm{d}s(\widehat{\boldsymbol{x}}) \leq |S^2|\left(\frac{4\pi}{2m+1}\right)^2 = \frac{(4\pi)^3}{(2m+1)^2}\,, \tag{2.41}$$

from which we deduce by using (2.33) and Hölder's inequality and the Cauchy Schwarz inequality several times that

$$\begin{aligned}&\|\alpha_{m,n}^{(l)}\|^2_{L^2(S^2\times S^2)}\\ &= k^{4l}\frac{(2m+1)^4(2n+1)^4}{(4\pi)^4}\int_{S^2}\int_{S^2}\left|\int_D\cdots\int_D q(\boldsymbol{y}_l)\cdots q(\boldsymbol{y}_1)\Phi_k(\boldsymbol{y}_l-\boldsymbol{y}_{l-1})\cdots\Phi_k(\boldsymbol{y}_2-\boldsymbol{y}_1)\right.\end{aligned}$$

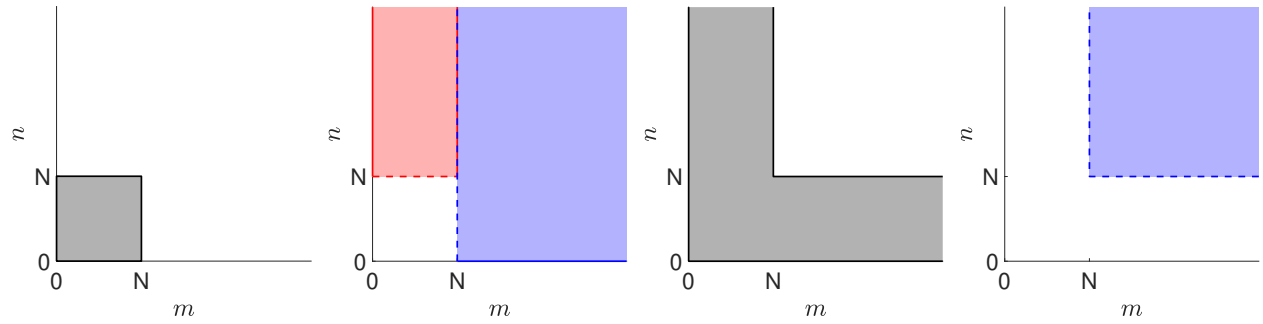

FIGURE 2.5. $\ell^0 \times \ell^0$-supports of operators in $\mathcal{V}_N$ (left) and of operators in $\mathcal{W}_N$ (middle right). Middle left: Partitioning of $\ell^0 \times \ell^0$-support of operators in $\mathcal{V}_N^\perp$ as sum of part marked in red and part in blue. Right: $\ell^0 \times \ell^0$-support of operators in $\mathcal{W}_N^\perp$.

$$
\begin{aligned}
&\times j_m(k|\boldsymbol{y}_l|) j_n(k|\boldsymbol{y}_1|) \langle P_m^{\widehat{\boldsymbol{x}}}, P_m^{\widehat{\boldsymbol{y}}_l} \rangle_{L^2(S^2)} \langle P_n^{\boldsymbol{\theta}}, P_n^{\widehat{\boldsymbol{y}}_1} \rangle_{L^2(S^2)} \, \mathrm{d}\boldsymbol{y}_1 \cdots \mathrm{d}\boldsymbol{y}_l \Big|^2 \, \mathrm{d}s(\widehat{\boldsymbol{x}}) \, \mathrm{d}s(\boldsymbol{\theta}) \\
&\leq k^{4l} \frac{(2m+1)^4 (2n+1)^4}{(4\pi)^4} \|q\|_{L^\infty(D)}^2 \Big(\int_{S^2} \sup_{\boldsymbol{y} \in D} \big| \langle P_m^{\widehat{\boldsymbol{x}}}, P_m^{\widehat{\boldsymbol{y}}} \rangle_{L^2(S^2)} \big|^2 \, \mathrm{d}s(\widehat{\boldsymbol{x}}) \Big) \|j_m(k|\,\cdot\,|)\|_{L^2(D)}^2 \\
&\quad \times \int_{S^2} \int_D \Big| \int_D q(\boldsymbol{y}_{l-1}) \Phi_k(\boldsymbol{y}_l - \boldsymbol{y}_{l-1}) \int_D \cdots \int_D q(\boldsymbol{y}_{l-2}) \cdots q(\boldsymbol{y}_1) \Phi_k(\boldsymbol{y}_{l-1} - \boldsymbol{y}_{l-2}) \cdots \Phi_k(\boldsymbol{y}_2 - \boldsymbol{y}_1) \\
&\quad \times j_n(k|\boldsymbol{y}_1|) \langle P_n^{\boldsymbol{\theta}}, P_n^{\widehat{\boldsymbol{y}}_1} \rangle_{L^2(S^2)} \, \mathrm{d}\boldsymbol{y}_1 \cdots \mathrm{d}\boldsymbol{y}_{l-1} \Big|^2 \, \mathrm{d}\boldsymbol{y}_l \, \mathrm{d}s(\boldsymbol{\theta}) \\
&\leq k^{4l} \frac{(2m+1)^4 (2n+1)^4}{(4\pi)^4} \|q\|_{L^\infty(D)}^2 \Big(\int_{S^2} \sup_{\boldsymbol{y} \in D} \big| \langle P_m^{\widehat{\boldsymbol{x}}}, P_m^{\widehat{\boldsymbol{y}}} \rangle_{L^2(S^2)} \big|^2 \, \mathrm{d}s(\widehat{\boldsymbol{x}}) \Big) \|j_m(k|\,\cdot\,|)\|_{L^2(D)}^2 \\
&\quad \times \Big(\int_D \int_D |q(\boldsymbol{y}) \Phi_k(\boldsymbol{x} - \boldsymbol{y})|^2 \, \mathrm{d}\boldsymbol{y} \, \mathrm{d}\boldsymbol{x} \Big) \int_{S^2} \int_D \Big| \int_D \cdots \int_D q(\boldsymbol{y}_{l-2}) \cdots q(\boldsymbol{y}_1) \Phi_k(\boldsymbol{y}_{l-1} - \boldsymbol{y}_{l-2}) \cdots \\
&\quad \times \Phi_k(\boldsymbol{y}_2 - \boldsymbol{y}_1) j_n(k|\boldsymbol{y}_1|) \langle P_n^{\boldsymbol{\theta}}, P_n^{\widehat{\boldsymbol{y}}_1} \rangle_{L^2(S^2)} \, \mathrm{d}\boldsymbol{y}_1 \cdots \mathrm{d}\boldsymbol{y}_{l-2} \Big|^2 \, \mathrm{d}\boldsymbol{y}_{l-1} \, \mathrm{d}s(\boldsymbol{\theta}) \\
&\leq \cdots \\
&\leq k^4 \frac{(2m+1)^4 (2n+1)^4}{(4\pi)^4} \|q\|_{L^\infty(D)}^2 \Big(\int_{S^2} \sup_{\boldsymbol{y} \in D} \big| \langle P_m^{\widehat{\boldsymbol{x}}}, P_m^{\widehat{\boldsymbol{y}}} \rangle_{L^2(S^2)} \big|^2 \, \mathrm{d}s(\widehat{\boldsymbol{x}}) \Big) \|j_m(k|\,\cdot\,|)\|_{L^2(D)}^2 \\
&\quad \times \Big(\int_{S^2} \sup_{\boldsymbol{y} \in D} \big| \langle P_n^{\boldsymbol{\theta}}, P_n^{\widehat{\boldsymbol{y}}} \rangle_{L^2(S^2)} \big|^2 \, \mathrm{d}s(\widehat{\boldsymbol{x}}) \Big) \|j_n(k|\,\cdot\,|)\|_{L^2(D)}^2 \Big(k^4 \int_D \int_D \Big| q(\boldsymbol{y}) \Phi_k(\boldsymbol{x} - \boldsymbol{y}) \Big|^2 \, \mathrm{d}\boldsymbol{y} \, \mathrm{d}\boldsymbol{x} \Big)^{l-1} \\
&\leq \frac{(4\pi)^2}{k^2} (2m+1)^2 (2n+1)^2 \|q\|_{L^\infty(D)}^2 \|L_q\|_{\mathrm{HS}}^{2(l-1)} k^3 \|j_m(k|\,\cdot\,|)\|_{L^2(D)}^2 k^3 \|j_n(k|\,\cdot\,|)\|_{L^2(D)}^2 .
\end{aligned}
$$

Therewith, we conclude from (2.31) for $\mathcal{W}_N$ that

$$
\begin{aligned}
\|F_q^{(l)} - \mathcal{P}_{\mathcal{W}_N} F_q^{(l)}\|_{\mathrm{HS}}^2 &= \Big\| \sum_{m=N+1}^{\infty} \sum_{n=N+1}^{\infty} \alpha_{m,n}^{(l)} \Big\|_{L^2(S^2 \times S^2)}^2 = \sum_{m=N+1}^{\infty} \sum_{n=N+1}^{\infty} \|\alpha_{m,n}^{(l)}\|_{L^2(S^2 \times S^2)}^2 \\
&\leq \frac{(4\pi)^2}{k^2} \|q\|_{L^\infty(D)}^2 \|L_q\|_{\mathrm{HS}}^{2(l-1)} \Big(\sum_{n=N+1}^{\infty} (2n+1)^2 k^3 \|j_n(k|\,\cdot\,|)\|_{L^2(D)}^2 \Big)^2 \\
&\leq \frac{(4\pi)^2}{k^2} \|q\|_{L^\infty(D)}^2 \|L_q\|_{\mathrm{HS}}^{2(l-1)} \Big(\sum_{n=N+1}^{\infty} (2n+1)^2 \|j_n(|\,\cdot\,|)\|_{L^2(B_{kR}(\mathbf{0}))}^2 \Big)^2 .
\end{aligned}
$$

Here, the summation area is given by the $\ell^0 \times \ell^0$-support of operators in $\mathcal{W}_N^\perp$, and the analogue holds for $\mathcal{V}_N$ in the estimate below. These supports are visualized in Figure 2.5. We obtain for $\mathcal{V}_N$

with (2.31) and Parseval's identity that

$$\begin{aligned}
\|F_q^{(l)} - \mathcal{P}_{\mathcal{V}_N} F_q^{(l)}\|_{\mathrm{HS}}^2 &= \Big\| \sum_{m=N+1}^{\infty} \sum_{n=0}^{\infty} \alpha_{m,n}^{(l)} + \sum_{m=0}^{N} \sum_{n=N+1}^{\infty} \alpha_{m,n}^{(l)} \Big\|_{L^2(S^2\times S^2)}^2 \\
&= \sum_{m=N+1}^{\infty} \sum_{n=0}^{\infty} \|\alpha_{m,n}^{(l)}\|_{L^2(S^2\times S^2)}^2 + \sum_{m=0}^{N} \sum_{n=N+1}^{\infty} \|\alpha_{m,n}^{(l)}\|_{L^2(S^2\times S^2)}^2 \\
&\le \sum_{m=N+1}^{\infty} \sum_{n=0}^{\infty} \|\alpha_{m,n}^{(l)}\|_{L^2(S^2\times S^2)}^2 + \sum_{m=0}^{\infty} \sum_{n=N+1}^{\infty} \|\alpha_{m,n}^{(l)}\|_{L^2(S^2\times S^2)}^2 \\
&\le \frac{2(4\pi)^2}{k^2} \|q\|_{L^\infty(D)}^2 M(kR) \|L_q\|_{\mathrm{HS}}^{2(l-1)} \sum_{n=N+1}^{\infty} (2n+1)^2 k^3 \|j_n(k|\cdot|)\|_{L^2(D)}^2 \\
&\le \frac{2(4\pi)^2}{k^2} \|q\|_{L^\infty(D)}^2 M(kR) \|L_q\|_{\mathrm{HS}}^{2(l-1)} \sum_{n=N+1}^{\infty} (2n+1)^2 \|j_n(|\cdot|)\|_{L^2(B_{kR}(\mathbf{0}))}^2 ,
\end{aligned}$$

where $M(kR) := \sum_{n=0}^{\infty} (2n+1)^2 \|j_n(|\cdot|)\|_{L^2(B_{kR}(\mathbf{0}))}^2$. The decay of $(\|j_n(|\cdot|)\|_{L^2(B_{kR}(\mathbf{0}))}^2)_n$ in $n \in \mathbb{N}_0$ has been studied in [56]. For $n \gtrsim kR$ there holds

$$\begin{aligned}
\|j_n(|\cdot|)\|_{L^2(B_{kR}(\mathbf{0}))}^2 &\le \frac{16\pi^2}{6^{\frac{4}{3}} (\Gamma(\frac{2}{3}))^2 \sqrt{e}} kR \Big(n+\frac{1}{2}\Big)^{\frac{2}{3}} \Big(\Big(\frac{kR}{n+1}\Big)^2 e^{1-(\frac{kR}{n+1})^2} \Big)^{n+1} \\
&\le b_1 kR \Big(n+\frac{1}{2}\Big)^{\frac{2}{3}} \Big(\Big(\frac{kR}{n+1}\Big)^2 e^{1-(\frac{kR}{n+1})^2} \Big)^{n+1}
\end{aligned}$$

with $b_1 \approx 4.791$, so $(\|j_n(|\cdot|)\|_{L^2(B_{kR}(\mathbf{0}))}^2)_n$ decays in n faster than any power of n^{-1}, which carries over to the two upper bounds. □

As in Remark 2.12 additional features of the upper bounds in (2.39) and (2.40) can be shown.

Remark 2.20. (i) By summing over l we obtain similar upper bounds for approximating $F_q^{(\le p)}$ and F_q in $\mathcal{V}_N$ and $\mathcal{W}_N$, respectively. The superlinear decay of these bounds in N is preserved.

(ii) From [56] we recall that

$$\lim_{kR\to\infty} \frac{\|j_{\lceil(\nu+1/2)kR\rceil}(|\cdot|)\|_{L^2(B_{kR}(\mathbf{0}))}^2}{2\pi kR} = \begin{cases} \sqrt{1-(\nu+\frac{1}{2})^2} & \text{if } \nu \le \frac{1}{2}, \\ 0 & \text{else}. \end{cases}$$

(iii) An explicit representation formula for implementation is given by

$$\begin{aligned}
\|j_n(|\cdot|)\|_{L^2(B_{kR}(\mathbf{0}))}^2 &= \frac{(\pi R)^2}{k} \big(J_{n+1/2}^2(kR) - J_{n-1/2}(kR) J_{n+3/2}(kR)\big) \\
&= 2\pi R^3 \big(j_n^2(kR) - j_{n-1}(kR) j_{n+1}(kR)\big), \qquad n \in \mathbb{N},
\end{aligned}$$

which can be obtained by using the relation (B.21) between j_n and $J_{n+1/2}$ and the product formula (B.6).

Figure 2.6 illustrates the decay of the factor $\sum_{n>N} (2n+1)^2 \|j_n(|\cdot|)\|_{L^2(B_{kR}(\mathbf{0}))}^2$ by plots of $\sum_{n=N+1}^{1000} (2n+1)^2 \|j_n(|\cdot|)\|_{L^2(B_{kR}(\mathbf{0}))}^2$ as function of $N \in \mathbb{N}$ for the choices $kR = 10$ (left) and $kR = 100$ (right). Similar to Figure 2.3, the superlinear decay starts in both situations at about $N = kR$, and it is more rapid for the larger value of kR. ◊

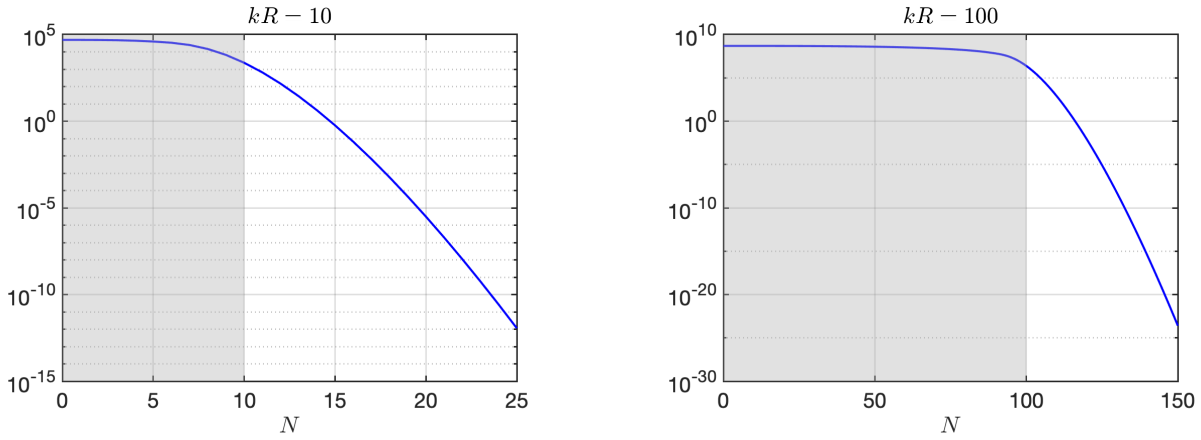

FIGURE 2.6. Plots of the factor $\sum_{n>N}(2n+1)^2\|j_n(|\cdot|)\|^2_{L^2(B_{kR}(\mathbf{0}))}$ in (2.39) and (2.40) as a function of $N \in \mathbb{N}$ for $kR = 10$ (left) and for $kR = 100$ (right)

2.5. FAR FIELD OPERATOR TRANSLATION

To reduce R and consequently N in the sparse and low rank representations of the previous section, which involves a reduction of the $\ell^0 \times \ell^0$-support or of the rank of the corresponding operators, it is often helpful to shift the scatterer in space. If the support of the scatterer is contained in some ball $B_R(\boldsymbol{c}) \subseteq \mathbb{R}^d$ with $\boldsymbol{c} \in \mathbb{R}^d$ and $R > 0$, then the support of the shifted scatterer modelled by $q(\cdot + \boldsymbol{c})$ is contained in $B_R(\mathbf{0})$. Thus, for the shifted contrast $q(\cdot + \boldsymbol{c})$ our theoretical findings from the previous section apply, which means, that the far field operator associated to $q(\cdot + \boldsymbol{c})$ can be well approximated in $\mathcal{V}_N$ and in $\mathcal{W}_N$, respectively, where $N \gtrsim kR$. We define the *contrast function shifted by* $\boldsymbol{c}$ as

$$q_{\boldsymbol{c}}(\boldsymbol{x}) := q(\boldsymbol{x} + \boldsymbol{c}), \qquad \boldsymbol{x} \in \mathbb{R}^d.$$

With this notation, it remains to investigate how the far field operators F_q and $F_{q_{\boldsymbol{c}}}$ are related. The definition of the far field pattern (2.6) for fixed $\boldsymbol{\theta} \in S^{d-1}$ can be viewed as $u_q^\infty(\cdot\,;\boldsymbol{\theta})$ being the Fourier transform of $qu_q(\cdot\,;\boldsymbol{\theta})$ restricted to the sphere kS^{d-1}. This suggests that the translation property of the Fourier transform somehow carries over to the far field pattern and to the far field operator associated to $q_{\boldsymbol{c}}$. We calculate

$$\begin{aligned} u_{q_{\boldsymbol{c}}}^\infty(\widehat{\boldsymbol{x}};\boldsymbol{\theta}) &= k^2 \int_{\mathbb{R}^d} q_{\boldsymbol{c}}(\boldsymbol{y}) u_{q_{\boldsymbol{c}}}(\boldsymbol{y};\boldsymbol{\theta}) e^{-\mathrm{i}k\widehat{\boldsymbol{x}}\cdot\boldsymbol{y}}\,\mathrm{d}\boldsymbol{y} = k^2 \int_{\mathbb{R}^d} q(\boldsymbol{y}+\boldsymbol{c}) u_{q_{\boldsymbol{c}}}(\boldsymbol{y};\boldsymbol{\theta}) e^{-\mathrm{i}k\widehat{\boldsymbol{x}}\cdot\boldsymbol{y}}\,\mathrm{d}\boldsymbol{y} \\ &= k^2 e^{\mathrm{i}k\boldsymbol{c}\cdot\widehat{\boldsymbol{x}}} \int_{\mathbb{R}^d} q(\boldsymbol{y}) u_{q_{\boldsymbol{c}}}(\boldsymbol{y}-\boldsymbol{c};\boldsymbol{\theta}) e^{-\mathrm{i}k\widehat{\boldsymbol{x}}\cdot\boldsymbol{y}}\,\mathrm{d}\boldsymbol{y}, \qquad \widehat{\boldsymbol{x}} \in S^{d-1}. \end{aligned} \tag{2.42}$$

By the Lippmann–Schwinger equation (2.3) and the definition of u^i we obtain for $u_{q_{\boldsymbol{c}}}(\boldsymbol{x}-\boldsymbol{c};\boldsymbol{\theta})$ that

$$\begin{aligned} u_{q_{\boldsymbol{c}}}(\boldsymbol{x}-\boldsymbol{c};\boldsymbol{\theta}) &= u^i(\boldsymbol{x}-\boldsymbol{c};\boldsymbol{\theta}) + k^2 \int_{\mathbb{R}^d} q(\boldsymbol{y}+\boldsymbol{c}) \Phi_k(\boldsymbol{x}-\boldsymbol{c}-\boldsymbol{y}) u_{q_{\boldsymbol{c}}}(\boldsymbol{y};\boldsymbol{\theta})\,\mathrm{d}\boldsymbol{y} \\ &= e^{-\mathrm{i}k\boldsymbol{c}\cdot\boldsymbol{\theta}} u^i(\boldsymbol{x};\boldsymbol{\theta}) + k^2 \int_{\mathbb{R}^d} q(\boldsymbol{y}) \Phi_k(\boldsymbol{x}-\boldsymbol{y}) u_{q_{\boldsymbol{c}}}(\boldsymbol{y}-\boldsymbol{c};\boldsymbol{\theta})\,\mathrm{d}\boldsymbol{y}, \qquad \boldsymbol{x} \in D, \end{aligned}$$

and consequently

$$e^{\mathrm{i}k\boldsymbol{c}\cdot\boldsymbol{\theta}} u_{q_{\boldsymbol{c}}}(\boldsymbol{x}-\boldsymbol{c};\boldsymbol{\theta}) = u^i(\boldsymbol{x};\boldsymbol{\theta}) + k^2 \int_{\mathbb{R}^d} q(\boldsymbol{y}) \Phi_k(\boldsymbol{x}-\boldsymbol{y}) \left(e^{\mathrm{i}k\boldsymbol{c}\cdot\boldsymbol{\theta}} u_{q_{\boldsymbol{c}}}(\boldsymbol{y}-\boldsymbol{c};\boldsymbol{\theta}) \right) \mathrm{d}\boldsymbol{y}, \qquad \boldsymbol{x} \in D. \tag{2.43}$$

From Theorem 2.3 (b) we conclude that $e^{\mathrm{i}k\boldsymbol{c}\cdot\boldsymbol{\theta}} u_{q_{\boldsymbol{c}}}(\cdot - \boldsymbol{c};\boldsymbol{\theta})$ can be extended by the right hand side of (2.43) to a solution of (2.1) which is uniquely determined due to Theorem 2.3 (c). Hence, we

have that

$$u_{q_{\boldsymbol{c}}}(\boldsymbol{x}-\boldsymbol{c};\boldsymbol{\theta}) = e^{-\mathrm{i}k\boldsymbol{c}\cdot\boldsymbol{\theta}}u_q(\boldsymbol{x};\boldsymbol{\theta}) \qquad \text{and} \qquad u^s_{q_{\boldsymbol{c}}}(\boldsymbol{x}-\boldsymbol{c};\boldsymbol{\theta}) = e^{-\mathrm{i}k\boldsymbol{c}\cdot\boldsymbol{\theta}}u^s_q(\boldsymbol{x};\boldsymbol{\theta})\,, \qquad \boldsymbol{x}\in\mathbb{R}^d\,. \tag{2.44}$$

By plugging (2.44) into (2.42) we obtain

$$u^\infty_{q_{\boldsymbol{c}}}(\widehat{\boldsymbol{x}};\boldsymbol{\theta}) = e^{-\mathrm{i}k\boldsymbol{c}\cdot(\boldsymbol{\theta}-\widehat{\boldsymbol{x}})}u^\infty_q(\widehat{\boldsymbol{x}};\boldsymbol{\theta})\,, \qquad \widehat{\boldsymbol{x}}\in S^{d-1}\,.$$

For the corresponding far field operator this means that

$$(F_{q_{\boldsymbol{c}}}g)(\widehat{\boldsymbol{x}}) = \int_{S^{d-1}} g(\boldsymbol{\theta})u^\infty_{q_{\boldsymbol{c}}}(\widehat{\boldsymbol{x}};\boldsymbol{\theta})\,\mathrm{d}s(\boldsymbol{\theta}) = e^{\mathrm{i}k\boldsymbol{c}\cdot\widehat{\boldsymbol{x}}}\int_{S^{d-1}} e^{-\mathrm{i}k\boldsymbol{c}\cdot\boldsymbol{\theta}}g(\boldsymbol{\theta})u^\infty_q(\widehat{\boldsymbol{x}};\boldsymbol{\theta})\,\mathrm{d}s(\boldsymbol{\theta})\,, \qquad \widehat{\boldsymbol{x}}\in S^{d-1}\,.$$

To formalize this dependency we introduce the linear operators

$$T_{\boldsymbol{c}} : L^2(S^{d-1}) \to L^2(S^{d-1})\,, \quad (T_{\boldsymbol{c}}g)(\widehat{\boldsymbol{x}}) := e^{\mathrm{i}k\boldsymbol{c}\cdot\widehat{\boldsymbol{x}}}g(\widehat{\boldsymbol{x}})\,, \tag{2.45}$$

and

$$\mathcal{T}_{\boldsymbol{c}} : \mathrm{HS}(L^2(S^{d-1})) \to \mathrm{HS}(L^2(S^{d-1}))\,, \quad \mathcal{T}_{\boldsymbol{c}}G := T_{\boldsymbol{c}}\circ G\circ T_{-\boldsymbol{c}}\,, \tag{2.46}$$

which we call *translation operators*. We have that $F_{q_{\boldsymbol{c}}} = \mathcal{T}_{\boldsymbol{c}}F_q$. We also use the notation $\mathcal{T}_{\boldsymbol{c}}$ for the effect of $\mathcal{T}_{\boldsymbol{c}}$ on the integral kernel and on the sequence of Fourier coefficients (for $d=2$) or spherical harmonics components (for $d=3$) of a Hilbert–Schmidt operator. In this sense, we also understand $\mathcal{T}_{\boldsymbol{c}}$ as a mapping $L^2(S^{d-1}\times S^{d-1}) \to L^2(S^{d-1}\times S^{d-1})$ and $\ell^2\times\ell^2 \to \ell^2\times\ell^2$ (for $d=2$) or $\ell^2\times\ell^2(L^2(S^2\times S^2)) \to \ell^2\times\ell^2(L^2(S^2\times S^2))$ (for $d=3$), respectively.

Definition and Corollary 2.21. Given $\boldsymbol{c}\in\mathbb{R}^d$ and $N\in\mathbb{N}$ with $N\gtrsim kR$ we define the *subspace of sparse far field operators associated to scatterers supported in* $B_R(\boldsymbol{c})\subseteq\mathbb{R}^d$ by

$$\mathcal{V}_N^{\boldsymbol{c}} := \{G\in\mathrm{HS}(L^2(S^{d-1})) \mid \mathcal{T}_{\boldsymbol{c}}G\in\mathcal{V}_N\} \tag{2.47}$$

and the *subspace of low rank far field operators associated to scatterers supported in* $B_R(\boldsymbol{c})\subseteq\mathbb{R}^d$ by

$$\mathcal{W}_N^{\boldsymbol{c}} := \{G\in\mathrm{HS}(L^2(S^{d-1})) \mid \mathcal{T}_{\boldsymbol{c}}G\in\mathcal{W}_N\}\,. \tag{2.48}$$

Here, the subspaces $\mathcal{V}_N$ and $\mathcal{W}_N$ are given as in Definitions 2.9 and 2.17. The approximation results of Theorems 2.11 and 2.19 are directly transferrable to the subspaces $\mathcal{V}_N^{\boldsymbol{c}}$ and $\mathcal{W}_N^{\boldsymbol{c}}$. Provided $\operatorname{supp} q\subseteq B_R(\boldsymbol{c})$, the right hand sides of (2.25), (2.26), (2.39) and (2.40) remain unchanged when replacing $\mathcal{P}_{\mathcal{V}_N}$ by $\mathcal{P}_{\mathcal{V}_N^{\boldsymbol{c}}}$ and $\mathcal{P}_{\mathcal{W}_N}$ by $\mathcal{P}_{\mathcal{W}_N^{\boldsymbol{c}}}$, respectively.

Proof. For $d=2$ we conclude from the Jacobi–Anger expansion (B.12) and simple linear transformations that the Fourier coefficients $(a^{(l)}_{m,n})_{m,n}$ of $\mathcal{T}_{\boldsymbol{c}}u_q^{\infty,(l)}$ are given as in (2.21) by

$$\begin{aligned} a^{(l)}_{m,n} = 2\pi k^{2l}\mathrm{i}^{n-m}\int_D\cdots\int_D q(\boldsymbol{y}_l)\cdots q(\boldsymbol{y}_1)\Phi_k(\boldsymbol{y}_l-\boldsymbol{y}_{l-1})\cdots\Phi_k(\boldsymbol{y}_2-\boldsymbol{y}_1) \\ \times e^{-\mathrm{i}(m\arg(\boldsymbol{y}_l-\boldsymbol{c})-n\arg(\boldsymbol{y}_1-\boldsymbol{c}))}J_m(k|\boldsymbol{y}_l-\boldsymbol{c}|)J_n(k|\boldsymbol{y}_1-\boldsymbol{c}|)\,\mathrm{d}\boldsymbol{y}_1\cdots\mathrm{d}\boldsymbol{y}_l\,. \end{aligned} \tag{2.49}$$

Proceeding as in the proof of Theorem 2.11, yields the result since $|e^{-\mathrm{i}(m\arg(\boldsymbol{y}-\boldsymbol{c})-n\arg(\boldsymbol{x}-\boldsymbol{c}))}| = 1$ for all $\boldsymbol{x},\boldsymbol{y}\in\mathbb{R}^2$ and $\|J_n(k|\cdot-\boldsymbol{c}|)\|_{L^2(D)} \le \|J_n(k|\cdot|)\|_{L^2(B_R(\boldsymbol{0}))}$.

For $d=3$ we conclude with the same techniques that the spherical harmonics components $(\alpha^{(l)}_{m,n})_{m,n}$ of $\mathcal{T}_{\boldsymbol{c}}u_q^{\infty,(l)}$ are given by

$$\begin{aligned} \alpha^{(l)}_{m,n}(\widehat{\boldsymbol{x}};\boldsymbol{\theta}) = k^{2l}\frac{(2m+1)^2(2n+1)^2}{16\pi^2}\mathrm{i}^{n-m}\int_D\cdots\int_D q(\boldsymbol{y}_l)\cdots q(\boldsymbol{y}_1)\Phi_k(\boldsymbol{y}_l-\boldsymbol{y}_{l-1})\cdots\Phi_k(\boldsymbol{y}_2-\boldsymbol{y}_1) \\ \times j_m(k|\boldsymbol{y}_l-\boldsymbol{c}|)j_n(k|\boldsymbol{y}_1-\boldsymbol{c}|)\langle P_m^{\widehat{\boldsymbol{x}}}, P_m^{\widehat{\boldsymbol{y}_l-\boldsymbol{c}}}\rangle_{L^2(S^2)}\langle P_n^{\boldsymbol{\theta}}, P_m^{\widehat{\boldsymbol{y}_1-\boldsymbol{c}}}\rangle_{L^2(S^2)}\,\mathrm{d}\boldsymbol{y}_1\cdots\mathrm{d}\boldsymbol{y}_l\,. \end{aligned} \tag{2.50}$$

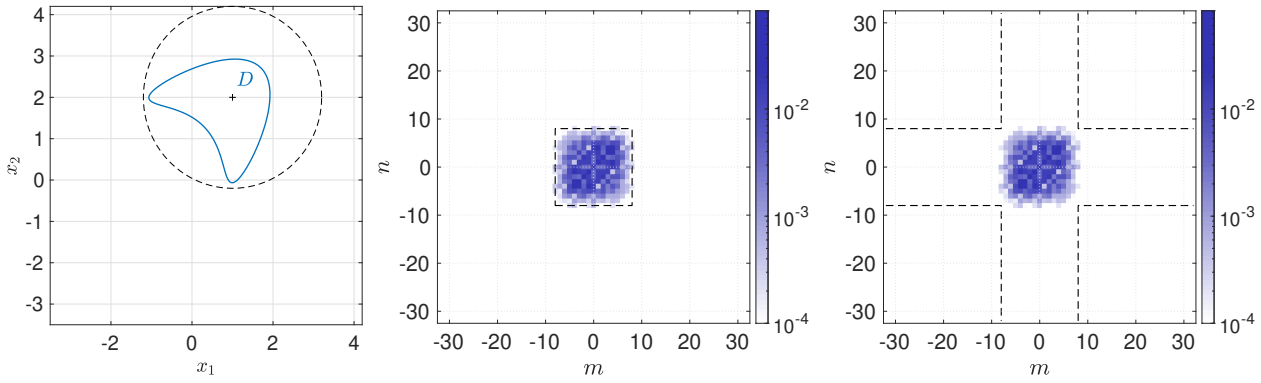

FIGURE 2.7. Left: Support of the scatterer D (solid) and ball $B_R(\boldsymbol{c})$ centered at $\boldsymbol{c} = (1,2)^\top$ with radius $R = 2.2$ containing D. Middle: Absolute values of Fourier coefficients $(a^{\boldsymbol{c}}_{m,n})_{m,n}$ of the translated far field operator $\mathcal{T}_{\boldsymbol{c}} F_q$ at wave number $k = 2.5$ together with dashed square corresponding to sparse approximation of F_q in $\mathcal{V}^{\boldsymbol{c}}_N$ (middle) and with dashed cross-shaped index set corresponding to low rank approximation of F_q in $\mathcal{W}^{\boldsymbol{c}}_N$ (right) for $N = 8$.

Since we have that

$$\int_{S^2} \sup_{\boldsymbol{y}\in D} |\langle P^{\boldsymbol{\theta}}_n, P^{\widehat{\boldsymbol{y}-\boldsymbol{c}}}_n \rangle_{L^2(S^2)}|^2 \, \mathrm{d}s(\boldsymbol{\theta}) \leq \frac{(4\pi)^3}{(2n+1)^2} \quad \text{and} \quad \|j_n(k|\cdot - \boldsymbol{c}|)\|_{L^2(D)} \leq \|j_n(k|\cdot|)\|_{L^2(B_R(\boldsymbol{0}))},$$

see (2.41), the result follows similar to the proof of Theorem 2.19. □

Remark 2.22. By construction (2.47) of $\mathcal{V}^{\boldsymbol{c}}_N$ and (2.48) of $\mathcal{W}^{\boldsymbol{c}}_N$, the translation operator $\mathcal{T}_{-\boldsymbol{c}}$ provides the modulation factor, with which spherical harmonics expansions as introduced in Notations 2.7 and 2.15 has to be multiplied to generate sparse or low rank representations of operators in $\mathcal{V}^{\boldsymbol{c}}_N$ or in $\mathcal{W}^{\boldsymbol{c}}_N$, respectively. In this context, the support of the required Fourier coefficients or of the required spherical harmonics components can be localized by suitably choosing $\boldsymbol{c}$. This is why we speak of modulated Fourier bases at this point. ◊

Example 2.23. We illustrate our findings by a numerical example in two dimensions. We consider the same scattering object D as in Examples 2.5 and 2.14, i.e., a kite shaped scatterer as depicted in Figure 2.7 (left) at wave number $k = 2.5$ with $q = 2\chi_D$. Taking the two-dimensional fast Fourier transform of the discretized translated far field operator $\mathcal{T}_{\boldsymbol{c}} \boldsymbol{F}_q$ gives an approximation of the Fourier coefficients of $\mathcal{T}_{\boldsymbol{c}} F_q$ with respect to $(e_{m,n})_{m,n}$.

In Figure 2.7 (middle, right) the absolute values of these Fourier coefficients are plotted for $-32 \leq m, n \leq 32$ on a logarithmic color scale. The dashed square in Figure 2.7 (middle) corresponds to the support of the Fourier coefficients of $\mathcal{T}_{\boldsymbol{c}} F$ for operators $F \in \mathcal{V}^{\boldsymbol{c}}_N$, the dashed cross in Figure 2.7 (right) to the support of the Fourier coefficients of $\mathcal{T}_{\boldsymbol{c}} F$ for operators $F \in \mathcal{W}^{\boldsymbol{c}}_N$. Here, we choose $N = \lceil ekR/2 \rceil = 8$ with $R = 2.2$. It is nicely confirmed that the Fourier coefficients are essentially supported inside the marked square and inside the cross-shaped area, respectively, and that the sizes of these supports can be reduced by applying $\mathcal{T}_{\boldsymbol{c}}$ in comparison to the plots in Figure 2.4, where we chose $N = 12$. ◊

In the following, we summarize the essential properties of the translation operator $\mathcal{T}_{\boldsymbol{c}}$, that will be needed in the rest of this work. Since the corresponding proofs differ significantly in structure, we once again consider the two- and three-dimensional case separately. We refer to Notations 2.7 and 2.15 for the used notations.

The two-dimensional case

Lemma 2.24. *Let $\boldsymbol{c} \in \mathbb{R}^2 \setminus \{\boldsymbol{0}\}$. Then, for $\mathcal{T}_{\boldsymbol{c}} \in \mathcal{L}(\mathrm{HS}(L^2(S^1)))$ the following holds.*

(a) The operator $\mathcal{T}_{\boldsymbol{c}}$ acts as a multiplication operator on the kernel κ_G and as a convolution operator on the Fourier coefficients $(a_{m,n})_{m,n}$ of $G \in \mathrm{HS}(L^2(S^1))$, more precisely there holds

$$(\mathcal{T}_{\boldsymbol{c}}\kappa_G)(\widehat{\boldsymbol{x}};\boldsymbol{\theta}) \;=\; e^{\mathrm{i}k(\widehat{\boldsymbol{x}}-\boldsymbol{\theta})\cdot\boldsymbol{c}}\kappa_G(\widehat{\boldsymbol{x}};\boldsymbol{\theta})\,, \qquad \widehat{\boldsymbol{x}},\boldsymbol{\theta} \in S^1\,,$$

and $\mathcal{T}_{\boldsymbol{c}}((a_{m,n})_{m,n}) = (a^{\boldsymbol{c}}_{m,n})_{m,n}$ with

$$a^{\boldsymbol{c}}_{m,n} \;=\; \sum_{m'\in\mathbb{Z}}\sum_{n'\in\mathbb{Z}} a_{m-m',n-n'}\big(\mathrm{i}^{m'-n'}e^{-\mathrm{i}(m'-n')\arg\boldsymbol{c}}J_{m'}(k|\boldsymbol{c}|)J_{n'}(k|\boldsymbol{c}|)\big)\,, \qquad m,n\in\mathbb{Z}\,. \tag{2.51}$$

(b) The operator $\mathcal{T}_{\boldsymbol{c}}$ is unitary with $\mathcal{T}_{\boldsymbol{c}}^* = \mathcal{T}_{-\boldsymbol{c}} = \mathcal{T}_{\boldsymbol{c}}^{-1}$. Moreover, for all $1 \le p \le \infty$,

$$\|\mathcal{T}_{\boldsymbol{c}}G\|_{L^p} \;=\; \|G\|_{L^p}\,, \qquad G \in \mathrm{HS}(L^2(S^1)) \cap L^p(S^1\times S^1)\,, \tag{2.52}$$

(c) We have that

$$\|\mathcal{T}_{\boldsymbol{c}}G\|_{\ell^\infty\times\ell^\infty} \;\le\; (k|\boldsymbol{c}|)^{-\frac{2}{3}}\|G\|_{\ell^1\times\ell^1}\,, \qquad G \in \mathrm{HS}(L^2(S^1)) \cap \ell^1\times\ell^1\,. \tag{2.53}$$

If in addition $k|\boldsymbol{c}| > 2(M+N+1)$ for some $M,N\in\mathbb{N}$, then

$$\|\mathcal{T}_{\boldsymbol{c}}G\|_{\ell^\infty\times\ell^\infty([-M,M]^2)} \;\le\; (k|\boldsymbol{c}|)^{-1}\|G\|_{\ell^1\times\ell^1([-N,N]^2)} \tag{2.54}$$

for $G \in \mathrm{HS}(L^2(S^1)) \cap \ell^1\times\ell^1([-N,N]^2)$.

(d) We have that

$$\|G\|_{L^\infty} \;\le\; \frac{1}{2\pi}\|G\|_{\ell^1\times\ell^1}\,, \qquad G \in \mathrm{HS}(L^2(S^1)) \cap \ell^1\times\ell^1\,. \tag{2.55}$$

Proof. Let $G \in \mathrm{HS}(L^2(S^1))$ with associated Hilbert–Schmidt kernel $\kappa_G \in L^2(S^1\times S^1)$ and Fourier coefficients $(a_{m,n})_{m,n} \in \ell^2\times\ell^2$.

(a) The effect of $\mathcal{T}_{\boldsymbol{c}}$ on κ_G is immediately clear by definition. It operates on the Fourier coefficients $(a_{m,n})_{m,n}$ of G as a convolution operator, since we obtain by a short calculation using the Jacobi–Anger expansion (B.12) for the Fourier coefficients $(a^{\boldsymbol{c}}_{m,n})_{m,n}$ of $\mathcal{T}_{\boldsymbol{c}}G$ that

$$a^{\boldsymbol{c}}_{m,n} \;=\; \sum_{m'\in\mathbb{Z}}\sum_{n'\in\mathbb{Z}} a_{m-m',n-n'}\big(\mathrm{i}^{m'-n'}e^{-\mathrm{i}(m'-n')\arg\boldsymbol{c}}J_{m'}(k|\boldsymbol{c}|)J_{n'}(k|\boldsymbol{c}|)\big)\,, \qquad m,n\in\mathbb{Z}\,.$$

(b) By definition the adjoint of $T_{\boldsymbol{c}}$ from (2.45) is given by $T_{\boldsymbol{c}}^* = T_{-\boldsymbol{c}} = T_{\boldsymbol{c}}^{-1}$, which implies together with (a) that for any $H \in \mathrm{HS}(L^2(S^1))$ with associated kernel $\kappa_H \in L^2(S^1\times S^1)$ we have that

$$\begin{aligned}
\langle\mathcal{T}_{\boldsymbol{c}}G, H\rangle_{\mathrm{HS}} \;&=\; \langle\mathcal{T}_{\boldsymbol{c}}\kappa_G, \kappa_H\rangle_{L^2(S^1\times S^1)} \;=\; \int_{S^1\times S^1} e^{\mathrm{i}k\boldsymbol{c}\cdot(\widehat{\boldsymbol{x}}-\boldsymbol{\theta})}\kappa_G(\widehat{\boldsymbol{x}},\boldsymbol{\theta})\overline{\kappa_H(\widehat{\boldsymbol{x}},\boldsymbol{\theta})}\,\mathrm{d}s(\widehat{\boldsymbol{x}},\boldsymbol{\theta}) \\
&=\; \int_{S^1\times S^1} \kappa_G(\widehat{\boldsymbol{x}},\boldsymbol{\theta})\overline{e^{\mathrm{i}k(-\boldsymbol{c})\cdot(\widehat{\boldsymbol{x}}-\boldsymbol{\theta})}\kappa_H(\widehat{\boldsymbol{x}},\boldsymbol{\theta})}\,\mathrm{d}s(\widehat{\boldsymbol{x}},\boldsymbol{\theta}) \;=\; \langle\kappa_G, \mathcal{T}_{-\boldsymbol{c}}\kappa_H\rangle_{L^2(S^1\times S^1)} \\
&=\; \langle G, \mathcal{T}_{-\boldsymbol{c}}H\rangle_{\mathrm{HS}}\,.
\end{aligned}$$

This shows that $\mathcal{T}_{\boldsymbol{c}}^* = \mathcal{T}_{-\boldsymbol{c}}$, which is the same as $\mathcal{T}_{\boldsymbol{c}}^{-1}$. On operator level, this identity can also be concluded from $\mathrm{tr}(GH) = \mathrm{tr}(HG)$, see [90, Thm. VI.25], as it is done in the proof of [53, Lem. 3.3].

The isometry property (2.52) follows immediately by definition (2.46) and (2.45), since $|e^{\mathrm{i}k\boldsymbol{c}\cdot\widehat{\boldsymbol{x}}}| = 1$ for all $\widehat{\boldsymbol{x}} \in S^1$.

(c) Suppose $(a_{m,n})_{m,n} \in \ell^1 \times \ell^1$. Recalling that $|J_n(t)| < b_0|t|^{-1/3}$ for any $t \neq 0$ and $b_0 \approx 0.7857$, see (B.8) and (b), we find that

$$\|\mathcal{T}_{\boldsymbol{c}} G\|_{\ell^\infty \times \ell^\infty} \leq \|(J_n(k|\boldsymbol{c}|))_n\|_{\ell^\infty}^2 \|(a_{m,n})_{m,n}\|_{\ell^1 \times \ell^1} \leq (k|\boldsymbol{c}|)^{-\frac{2}{3}} \|G\|_{\ell^1 \times \ell^1}, \tag{2.56}$$

which shows (2.53).

Assuming additionally that $\operatorname{supp}_{\ell^0 \times \ell^0} G \subseteq [-N, N]^2$ we obtain similar to (2.56) that

$$\|\mathcal{T}_{\boldsymbol{c}} G\|_{\ell^\infty \times \ell^\infty([-M,M]^2)} \leq \|(J_n(k|\boldsymbol{c}|))_n\|_{\ell^\infty([-M-N,M+N])}^2 \|(a_{m,n})_{m,n}\|_{\ell^1 \times \ell^1([-N,N]^2)}. \tag{2.57}$$

Supposing that $k|\boldsymbol{c}| > 2(M+N+1)$ for some $M, N \in \mathbb{N}$ we know from (B.9) that

$$\sup_{|n| \leq M+N} |J_n(k|\boldsymbol{c}|)| \leq b_1 |\boldsymbol{c}|^{-\frac{1}{2}} \qquad \text{with } b_1 \approx 0.7595.$$

Substituting this into (2.57) yields (2.54).

(d) Let $(a_{m,n})_{m,n} \in \ell^1 \times \ell^1$. The mapping property (2.55) then follows from Hölder's inequality, which gives together with $|\boldsymbol{e}_{m,n}(\widehat{\boldsymbol{x}}; \boldsymbol{\theta})| = 1/(2\pi)$ for all $m, n \in \mathbb{Z}$ and $\widehat{\boldsymbol{x}}, \boldsymbol{\theta} \in S^1$ that

$$\|G\|_{L^\infty} = \Big\| \sum_{m \in \mathbb{Z}} \sum_{n \in \mathbb{Z}} a_{m,n}\, \boldsymbol{e}_{m,n} \Big\|_{L^\infty(S^1 \times S^1)} \leq \frac{1}{2\pi} \|G\|_{\ell^1 \times \ell^1}.$$

□

THE THREE-DIMENSIONAL CASE

Lemma 2.25. *Let $\boldsymbol{c} \in \mathbb{R}^3 \setminus \{\boldsymbol{0}\}$. Then, for $\mathcal{T}_{\boldsymbol{c}} \in \mathcal{L}(\mathrm{HS}(L^2(S^2)))$ the following holds.*

(a) The operator $\mathcal{T}_{\boldsymbol{c}}$ acts as a multiplication operator on the kernel κ_G of $G \in \mathrm{HS}(L^2(S^2))$ by

$$(\mathcal{T}_{\boldsymbol{c}} \kappa_G)(\widehat{\boldsymbol{x}}; \boldsymbol{\theta}) = e^{\mathrm{i}k(\widehat{\boldsymbol{x}} - \boldsymbol{\theta}) \cdot \boldsymbol{c}} \kappa_G(\widehat{\boldsymbol{x}}; \boldsymbol{\theta}), \qquad \widehat{\boldsymbol{x}}, \boldsymbol{\theta} \in S^2,$$

and on the spherical harmonics components $(\alpha_{m,n})_{m,n}$ of G by $\mathcal{T}_{\boldsymbol{c}}((\alpha_{m,n})_{m,n}) = (\alpha^{\boldsymbol{c}}_{m,n})_{m,n}$ with

$$\begin{aligned} \alpha^{\boldsymbol{c}}_{m,n}(\widehat{\boldsymbol{x}}, \boldsymbol{\theta}) = \frac{(2m+1)(2n+1)}{16\pi^2} \sum_{o,p,r,s=0}^{\infty} \mathrm{i}^{o-p} (2o+1)(2p+1) j_o(k|\boldsymbol{c}|) j_p(k|\boldsymbol{c}|) \\ \times \int_{S^2} P_m^{\widehat{\boldsymbol{x}}}(\boldsymbol{\omega}) P_o^{\widehat{\boldsymbol{c}}}(\boldsymbol{\omega}) \int_{S^2} P_n^{\boldsymbol{\theta}}(\boldsymbol{\upsilon}) P_p^{\widehat{\boldsymbol{c}}}(\boldsymbol{\upsilon}) \alpha_{r,s}(\boldsymbol{\omega}; \boldsymbol{\upsilon}) \, \mathrm{d}s(\boldsymbol{\upsilon}) \, \mathrm{d}s(\boldsymbol{\omega}) \end{aligned} \tag{2.58}$$

for $\widehat{\boldsymbol{x}}, \boldsymbol{\theta} \in S^2$ and $m, n \in \mathbb{N}_0$.

(b) The operator $\mathcal{T}_{\boldsymbol{c}}$ is unitary with $\mathcal{T}_{\boldsymbol{c}}^* = \mathcal{T}_{-\boldsymbol{c}} = \mathcal{T}_{\boldsymbol{c}}^{-1}$. Moreover, for all $1 \leq p \leq \infty$,

$$\|\mathcal{T}_{\boldsymbol{c}} G\|_{L^p} = \|G\|_{L^p}, \qquad G \in \mathrm{HS}(L^2(S^2)) \cap L^p(S^2 \times S^2). \tag{2.59}$$

(c) We have that

$$\|\mathcal{T}_{\boldsymbol{c}} G\|_{\ell^\infty_{1/(2n+1)} \times \ell^\infty_{1/(2n+1)}} \leq (k|\boldsymbol{c}|)^{-\frac{5}{3}} \|G\|_{\ell^1_{2n+1} \times \ell^1_{2n+1}}, \qquad G \in \mathrm{HS}(L^2(S^2)) \cap \ell^1_{2n+1} \times \ell^1_{2n+1}. \tag{2.60}$$

[1] *If in addition* $k|c| > 2(M+N+3/2)$ *for some* $M, N \in \mathbb{N}$, *then*

$$\|\mathcal{T}_c G\|_{\ell^\infty_{1/(2n+1)}\times\ell^\infty_{1/(2n+1)}([0,M]^2)} \leq (k|c|)^{-1}\|G\|_{\ell^1_{2n+1}\times\ell^1_{2n+1}([0,N]^2)} \tag{2.61}$$

for $G \in \mathrm{HS}(L^2(S^2)) \cap \ell^1_{2n+1} \times \ell^1_{2n+1}([0,N]^2)$.

(d) We have that

$$\|G\|_{L^\infty} \leq \frac{1}{4\pi}\|G\|_{\ell^1_{\sqrt{2n+1}}\times\ell^1_{\sqrt{2n+1}}}, \qquad G \in \mathrm{HS}(L^2(S^2)) \cap \ell^1_{\sqrt{2n+1}} \times \ell^1_{\sqrt{2n+1}}. \tag{2.62}$$

Proof. Let $G \in \mathrm{HS}(L^2(S^2))$ with associated Hilbert–Schmidt kernel $\kappa_G \in L^2(S^2 \times S^2)$ and spherical harmonics components $(\alpha_{m,n})_{m,n} \in \mathbb{Y}^3_m \times \mathbb{Y}^3_n$.

(a) The effect of $\mathcal{T}_c$ on κ_G follows immediately by definition This gives together with the Jacobi–Anger expansion (B.24) for expanding the plane wave term $e^{\mathrm{i}k(\widehat{\boldsymbol{x}}-\boldsymbol{\theta})\cdot\boldsymbol{c}}$ that

$$\begin{aligned}(\mathcal{T}_c\kappa_G)(\widehat{\boldsymbol{x}};\boldsymbol{\theta}) &= \sum_{r,s=0}^{\infty}(\mathcal{T}_c\alpha_{r,s})(\widehat{\boldsymbol{x}},\boldsymbol{\theta}) = \sum_{r,s=0}^{\infty} e^{\mathrm{i}k(\widehat{\boldsymbol{x}}-\boldsymbol{\theta})\cdot\boldsymbol{c}}\alpha_{r,s}(\widehat{\boldsymbol{x}},\boldsymbol{\theta}) \\ &= \sum_{o,p,r,s=0}^{\infty} \mathrm{i}^{o-p}(2o+1)(2p+1)j_o(k|\boldsymbol{c}|)j_p(k|\boldsymbol{c}|)P_o^{\widehat{\boldsymbol{c}}}(\widehat{\boldsymbol{x}})P_p^{\widehat{\boldsymbol{c}}}(\boldsymbol{\theta})\alpha_{r,s}(\widehat{\boldsymbol{x}},\boldsymbol{\theta}).\end{aligned}$$

We compute the (m,n)th spherical harmonics component $\alpha^{\boldsymbol{c}}_{m,n}$ of $\mathcal{T}_{\boldsymbol{c}}\kappa_G$ by using formula (B.19), which gives representation (2.58).

(b) The proof of Lemma 2.24 (b) can be transferred immediately to three dimensions.

(c) We proceed similar to the proof of [56, Lem. 4.2]. Let $(\alpha^{\boldsymbol{c}}_{m,n})_{m,n}$ denote the spherical harmonics components of $\mathcal{T}_{\boldsymbol{c}}G$ and suppose that $(\alpha_{m,n})_{m,n} \in \ell^1_{2n+1} \times \ell^1_{2n+1}$. By formulas (B.19) and (2.58), we obtain for $m, n \in \mathbb{N}_0$

$$\begin{aligned}\|\alpha^{\boldsymbol{c}}_{m,n}\|^2_{L^2(S^2\times S^2)} &= |\langle \alpha^{\boldsymbol{c}}_{m,n}, \alpha^{\boldsymbol{c}}_{m,n}\rangle_{L^2(S^2\times S^2)}| \\ &= \frac{(2m+1)(2n+1)}{16\pi^2}\Bigg|\sum_{o,p,r,s=0}^{\infty}\mathrm{i}^{o-p}(2o+1)(2p+1)j_o(k|\boldsymbol{c}|)j_p(k|\boldsymbol{c}|)\int_{S^2}\int_{S^2}\overline{\alpha^{\boldsymbol{c}}_{m,n}(\widehat{\boldsymbol{x}},\boldsymbol{\theta})} \\ &\quad\times\int_{S^2}P_m^{\widehat{\boldsymbol{x}}}(\boldsymbol{\omega})P_o^{\widehat{\boldsymbol{c}}}(\boldsymbol{\omega})\int_{S^2}P_n^{\boldsymbol{\theta}}(\boldsymbol{v})P_p^{\widehat{\boldsymbol{c}}}(\boldsymbol{v})\alpha_{r,s}(\boldsymbol{\omega},\boldsymbol{v})\,\mathrm{d}s(\boldsymbol{v})\,\mathrm{d}s(\boldsymbol{\omega})\,\mathrm{d}s(\boldsymbol{\theta})\,\mathrm{d}s(\widehat{\boldsymbol{x}})\Bigg| \\ &= \Bigg|\sum_{o,p,r,s=0}^{\infty}\mathrm{i}^{o-p}(2o+1)(2p+1)j_o(k|\boldsymbol{c}|)j_p(k|\boldsymbol{c}|) \\ &\quad\times\int_{S^2}P_o^{\widehat{\boldsymbol{c}}}(\boldsymbol{\omega})\int_{S^2}P_p^{\widehat{\boldsymbol{c}}}(\boldsymbol{v})\alpha_{r,s}(\boldsymbol{\omega},\boldsymbol{v})\overline{\alpha^{\boldsymbol{c}}_{m,n}(\boldsymbol{\omega},\boldsymbol{v})}\,\mathrm{d}s(\boldsymbol{v})\,\mathrm{d}s(\boldsymbol{\omega})\Bigg|.\end{aligned}$$

Due to Lemma B.4 all summands vanish for $o > m+r$ or $o < |m-r|$ or $p > n+s$ or $p < |n-s|$. Thus, we can estimate by using the triangle inequality, Hölder's inequality and the Cauchy Schwarz inequality

$$\begin{aligned}\|\alpha^{\boldsymbol{c}}_{m,n}\|^2_{L^2(S^2\times S^2)} \leq \sum_{r,s=0}^{\infty}\sum_{o=|m-r|}^{m+r}\sum_{p=|n-s|}^{n+s}(2o+1)(2p+1)|j_o(k|\boldsymbol{c}|)||j_p(k|\boldsymbol{c}|)| \\ \times\Bigg|\int_{S^2}P_o^{\widehat{\boldsymbol{c}}}(\boldsymbol{\omega})\int_{S^2}P_p^{\widehat{\boldsymbol{c}}}(\boldsymbol{v})\alpha_{r,s}(\boldsymbol{\omega},\boldsymbol{v})\overline{\alpha^{\boldsymbol{c}}_{m,n}(\boldsymbol{\omega},\boldsymbol{v})}\,\mathrm{d}s(\boldsymbol{v})\,\mathrm{d}s(\boldsymbol{\omega})\Bigg|\end{aligned}$$

[1] According to Notation 2.15, we should actually write $\ell^\infty_{(1/(2n+1))_n}\times\ell^\infty_{(1/(2n+1))_n}$ and $\ell^1_{(2n+1)_n}\times\ell^1_{(2n+1)_n}$ instead of $\ell^\infty_{1/(2n+1)}\times\ell^\infty_{1/(2n+1)}$ and $\ell^1_{2n+1}\times\ell^1_{2n+1}$, but for the sake of readability we omit the brackets at this point.

$$\leq \Bigg(\sum_{r,s=0}^{\infty} \|\alpha_{r,s}\|_{L^2(S^2\times S^2)} \Bigg(\sum_{o=|m-r|}^{m+r} (2o+1)|j_o(k|\boldsymbol{c}|)| \|P_o^{\widehat{\boldsymbol{c}}}\|_{L^\infty(S^2)} \Bigg) \times \Bigg(\sum_{p=|n-s|}^{n+s} (2p+1)|j_p(k|\boldsymbol{c}|)| \|P_p^{\widehat{\boldsymbol{c}}}\|_{L^\infty(S^2)} \Bigg) \Bigg) \|\alpha_{m,n}^{\boldsymbol{c}}\|_{L^2(S^2\times S^2)} \,.$$

We use formula (B.17) and divide by $\|\alpha_{m,n}^{\boldsymbol{c}}\|_{L^2(S^2\times S^2)}$, which yields

$$\|\alpha_{m,n}^{\boldsymbol{c}}\|_{L^2(S^2\times S^2)} \leq \sum_{r,s=0}^{\infty} \|\alpha_{r,s}\|_{L^2(S^2\times S^2)} \Bigg(\sum_{o=|m-r|}^{m+r} (2o+1)|j_o(k|\boldsymbol{c}|)| \Bigg) \Bigg(\sum_{p=|n-s|}^{n+s} (2p+1)|j_p(k|\boldsymbol{c}|)| \Bigg) .$$

From (B.22) we know that $|j_n(t)| \leq b_2|t|^{-5/6}$ for any $t \neq 0$ and $b_2 \approx 0.9848$ and consequently

$$\|\alpha_{m,n}^{\boldsymbol{c}}\|_{L^2(S^2\times S^2)} \leq (k|\boldsymbol{c}|)^{-\frac{5}{3}} \sum_{r,s=0}^{\infty} \|\alpha_{r,s}\|_{L^2(S^2\times S^2)} \Bigg(\sum_{o=|m-r|}^{m+r} (2o+1) \Bigg) \Bigg(\sum_{p=|n-s|}^{n+s} (2p+1) \Bigg) .$$

Suppose $m, r \in \mathbb{N}_0$, and let without loss of generality be $m > r$ (otherwise switch the roles of m and r). Then, there holds

$$\begin{aligned} \sum_{o=|m-r|}^{m+r} (2o+1) &= \sum_{o=m-r}^{m+r} (2o+1) = \sum_{o=0}^{2r} (2(o+m-r)+1) \\ &= 2\,\frac{2r(2r+1)}{2} + (2(m-r)+1)(2r+1) = (2m+1)(2r+1) \,, \end{aligned} \tag{2.63}$$

which gives us

$$\|\alpha_{m,n}^{\boldsymbol{c}}\|_{L^2(S^2\times S^2)} \leq (k|\boldsymbol{c}|)^{-\frac{5}{3}} (2m+1)(2n+1) \sum_{r,s=0}^{\infty} (2r+1)(2s+1) \|\alpha_{r,s}\|_{L^2(S^2\times S^2)} \,.$$

All in all, we obtain (3.9) since we can estimate

$$\begin{aligned} \|\mathcal{T}_{\boldsymbol{c}} G\|_{\ell^\infty_{1/(2n+1)}\times\ell^\infty_{1/(2n+1)}} &= \sup_{m,n\in\mathbb{N}_0} \frac{\|\alpha_{m,n}^{\boldsymbol{c}}\|_{L^2(S^2\times S^2)}}{(2m+1)(2n+1)} \\ &\leq (k|\boldsymbol{c}|)^{-\frac{5}{3}} \sum_{r,s=0}^{\infty} (2r+1)(2s+1) \|\alpha_{r,s}\|_{L^2(S^2\times S^2)} \\ &= (k|\boldsymbol{c}|)^{-\frac{5}{3}} \|G\|_{\ell^1_{2n+1}\times\ell^1_{2n+1}} \,. \end{aligned}$$

Let additionally the support of $(\alpha_{m,n})_{m,n}$ be contained in $[0,N]^2$ and $k|\boldsymbol{c}| > 2(M+N+3/2)$ for some $M, N \in \mathbb{N}$. Then, we know from (B.23) that

$$\sup_{0\leq n\leq M+N} |j_n(k|\boldsymbol{c}|)| \leq b_3 |\boldsymbol{c}|^{-1} \qquad \text{with } b_3 \approx 0.9519 \,.$$

Substituting this instead of (B.22) into above calculation yields (2.62).

(d) Let $(\alpha_{m,n})_{m,n} \in \ell^1_{\sqrt{2n+1}} \times \ell^1_{\sqrt{2n+1}}$. By the triangle inequality, Cauchy Schwarz, (B.19) and the fact that $\|P_m^{\widehat{\boldsymbol{x}}}\|_{L^2(S^2)} = \sqrt{4\pi/(2m+1)}$, see (B.17), we can bound

$$\|G\|_{L^\infty} = \|\kappa_G\|_{L^\infty(S^2\times S^2)} \leq \sum_{m,n=0}^{\infty} \|\alpha_{m,n}\|_{L^\infty(S^2\times S^2)}$$

$$= \sum_{m,n=0}^{\infty} \frac{(2m+1)(2n+1)}{16\pi^2} \operatorname*{ess\,sup}_{\widehat{\boldsymbol{x}},\boldsymbol{\theta}\in S^2} \left| \int_{S^2} P_m^{\widehat{\boldsymbol{x}}}(\boldsymbol{\omega}) \int_{S^2} P_n^{\boldsymbol{\theta}}(\boldsymbol{\upsilon}) \kappa_G(\boldsymbol{\omega};\boldsymbol{\upsilon}) \, \mathrm{d}s(\boldsymbol{\upsilon}) \, \mathrm{d}s(\boldsymbol{\omega}) \right|$$

$$\leq \sum_{m,n=0}^{\infty} \frac{\sqrt{(2m+1)(2n+1)}}{4\pi} \|\alpha_{m,n}\|_{L^2(S^2\times S^2)} = \frac{1}{4\pi} \|\kappa_G\|_{\ell^1_{\sqrt{2n+1}}\times\ell^1_{\sqrt{2n+1}}} .$$

This finishes the proof.

□

CHAPTER 3

FAR FIELD OPERATOR SPLITTING

Before introducing our first inverse problem, that will be in the focus of this chapter, we summarize some key assumptions on the geometry of the scatterer.

Assumption 3.1. *We suppose that the scatterer consists of $J \in \mathbb{N}$, $J \geq 2$,* well-separated *components, i.e., $D = \bigcup_{j=1}^{J} D_j$ for some Lipschitz bounded open sets $D_j \subseteq B_{R_j}(\boldsymbol{c}_j)$ with $\boldsymbol{c}_j \in \mathbb{R}^d$ and $R_j > 0$, $j = 1, \ldots, J$, such that $|\boldsymbol{c}_{j_1} - \boldsymbol{c}_{j_2}| > R_{j_1} + R_{j_2}$ for all $j_1 \neq j_2$. This means that the scatterer's components are contained in pairwise disjointly supported balls. Let $q_j := q|_{D_j}$ denote the contrast function of the jth scatterer's component, $j = 1, \ldots, J$.*

For simplicity we assume $J = 2$ henceforth, but refer to Subsection 3.6.3, which covers the general case $J \geq 2$.

The goal of **far field operator splitting** is to recover the far field operators F_{q_1} and F_{q_2} corresponding to the two components of the scatterer from F_q.

Since $q = q_1 + q_2$ is uniquely determined by F_q (see [14, 84, 86, 89]), this inverse problem is uniquely solvable, whenever sufficient a priori information on the locations of the scatterers D_1 and D_2 is available to determine q_1 and q_2 from q. However, this is an ill-posed problem since F_{q_1} and F_{q_2} may depend discontinuously on F_q. This is due to the fact that the far field operators F_{q_1} and F_{q_2}, so that $\operatorname{supp} q_j \subseteq D_j$, $j = 1, 2$, satisfy Assumption 3.1, can look arbitrarily similar. Therefore, small noise in F_q may lead to large perturbations in F_{q_1} and F_{q_2}.

Furthermore, by (2.7) this problem is nonlinear in q_1 and q_2, which is due to multiple scattering effects involving both scatterer's components. The task is to somehow quantify these multiple scattering effects. This is done in Section 3.1 below based on the Born series (2.16). We will discuss the structure of the remaining chapters after we have derived the Born series expansion of F_q.

Beforehand, we illustrate with a concrete example how the far field operator F_q is decomposed when dealing with far field operator splitting.

Example 3.2. Let $d = 2$. We choose the wave number $k = 0.5$, and we set the contrast function $q = \chi_{D_1} + 2\chi_{D_2}$ for a nut shaped scatterer D_1 and a kite shaped scatterer D_2 as shown in Figure 3.1 (top left). We use a Nyström method as described in Example 2.5 for $L = 150$ equally distributed observation and illumination directions on S^1 to compute approximations $\boldsymbol{F}_q$, $\boldsymbol{F}_{q_1}$ and $\boldsymbol{F}_{q_2}$ for the far field operators F_q, F_{q_1} and F_{q_2} corresponding to both scatterer's components, to the nut shaped scatterer only and to the kite shaped scatterer only, respectively. The real parts of these operators are plotted in Figure 3.1 (top right, bottom left and bottom middle). We further compute the difference $\boldsymbol{D} := \boldsymbol{F}_q - \boldsymbol{F}_{q_1} - \boldsymbol{F}_{q_2}$, whose real part is shown in Figure 3.1 (bottom right). The matrix $\boldsymbol{D}$ models the part of $\boldsymbol{F}_q$ which is related to multiple scattering effects involving both scatterer's components, and it must be removed when solving the far field operator splitting problem. By construction there holds

$$\boldsymbol{F}_q = \boldsymbol{F}_{q_1} + \boldsymbol{F}_{q_2} + \boldsymbol{D}\,.$$

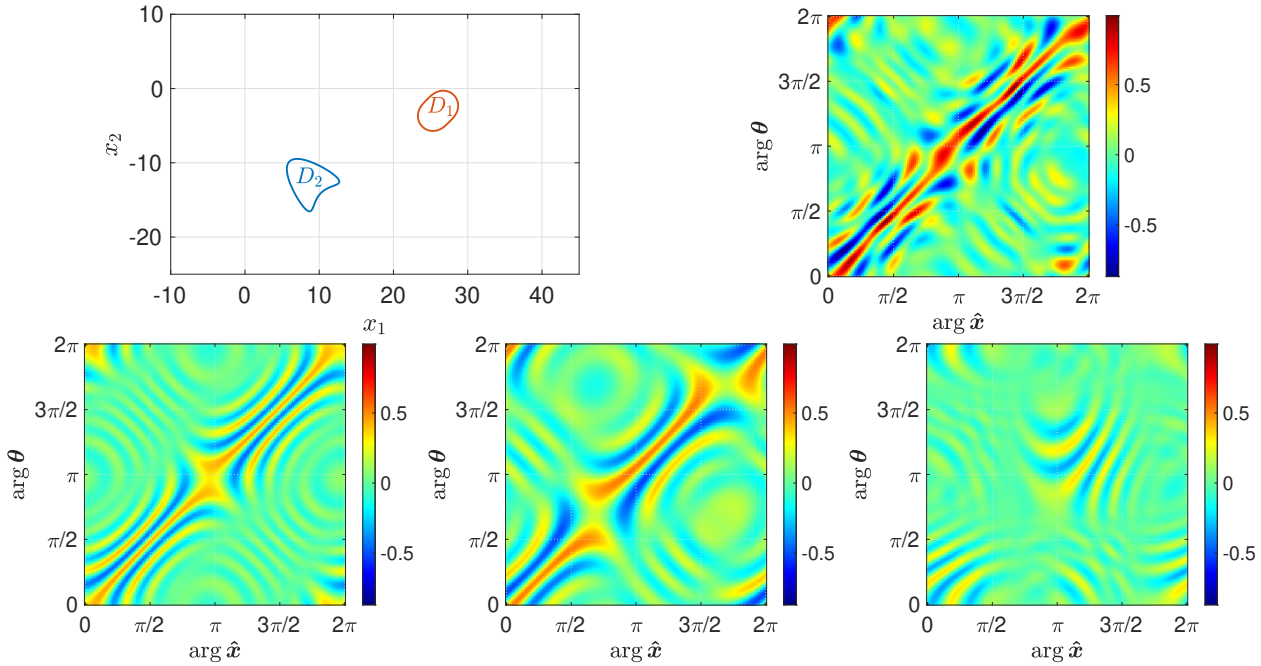

FIGURE 3.1. Top left: Supports of the scatterer's components. Real parts of discretized far field operators $\boldsymbol{F}_q$ (top right), $\boldsymbol{F}_{q_1}$ (bottom left) and $\boldsymbol{F}_{q_2}$ (bottom middle). Bottom right: Real part of difference $\boldsymbol{D} = \boldsymbol{F}_q - \boldsymbol{F}_{q_1} - \boldsymbol{F}_{q_2}$.

We further calculate the relative ratios

$$\frac{\|\boldsymbol{F}_{q_1}\|_{\mathrm{HS}}}{\|\boldsymbol{F}_q\|_{\mathrm{HS}}} \approx 0.626\,, \qquad \frac{\|\boldsymbol{F}_{q_2}\|_{\mathrm{HS}}}{\|\boldsymbol{F}_q\|_{\mathrm{HS}}} \approx 0.807 \qquad \text{and} \qquad \frac{\|\boldsymbol{D}\|_{\mathrm{HS}}}{\|\boldsymbol{F}_q\|_{\mathrm{HS}}} \approx 0.406\,,$$

measured in the Hilbert–Schmidt norm, which is also known as the Frobenius norm in finite dimensions. This gives an intuition how large the additive effects of the individual parts of $\boldsymbol{F}_q$ are in this situation. Although, the relative ratio of $\boldsymbol{D}$ is smaller than the ones of $\boldsymbol{F}_1$ and $\boldsymbol{F}_2$ for this example, it is not negligible, so it seems reasonable to invest effort into the quantification of multiple scattering. ♢

3.1. EXPANSIONS IN TERMS OF THE SCATTERER'S COMPONENTS

Under Assumption 3.1 each summand in the Born series (2.16) for the far field pattern can be further decomposed. For $j, l \in \{1, 2\}$ we define $L_{q,j,l} : L^2(D_j) \to L^2(D_l)$ by

$$(L_{q,j,l} f)(\boldsymbol{x}) := k^2 \int_{D_j} q(\boldsymbol{y}) f(\boldsymbol{y}) \Phi_k(\boldsymbol{x} - \boldsymbol{y}) \, \mathrm{d}\boldsymbol{y}\,, \qquad \boldsymbol{x} \in D_l\,.$$

Recalling formula (2.15) for the lth summand in (2.16) we have that

$$u_q^{\infty,(l)}(\widehat{\boldsymbol{x}}; \boldsymbol{\theta}) = \sum_{j_l=1}^{2} \cdots \sum_{j_1=1}^{2} u_{q_{j_l},\ldots,q_{j_1}}^{\infty,(l)}(\widehat{\boldsymbol{x}}; \boldsymbol{\theta})\,, \qquad \widehat{\boldsymbol{x}}, \boldsymbol{\theta} \in S^{d-1}\,,$$

with

$$u_{q_{j_l},\ldots,q_{j_1}}^{\infty,(l)}(\widehat{\boldsymbol{x}}; \boldsymbol{\theta}) := k^2 \int_{D_{j_l}} q_{j_l}(\boldsymbol{y}_l) e^{-\mathrm{i}k\widehat{\boldsymbol{x}}\cdot\boldsymbol{y}_l} \big(L_{q,j_{l-1},j_l}(\cdots(L_{q,j_1,j_2} u^i(\cdot\,; \boldsymbol{\theta})))\big)(\boldsymbol{y}_l) \, \mathrm{d}\boldsymbol{y}_l$$

$$= k^{2l} \int_{D_{j_l}} \cdots \int_{D_{j_1}} q_{j_l}(\boldsymbol{y}_l) \cdots q_{j_1}(\boldsymbol{y}_1) \Phi_k(\boldsymbol{y}_l - \boldsymbol{y}_{l-1}) \cdots \Phi_k(\boldsymbol{y}_2 - \boldsymbol{y}_1) e^{\mathrm{i}k(\boldsymbol{\theta}\cdot\boldsymbol{y}_1 - \widehat{\boldsymbol{x}}\cdot\boldsymbol{y}_l)} \, \mathrm{d}\boldsymbol{y}_1 \cdots \mathrm{d}\boldsymbol{y}_l \quad (3.1)$$

for $\widehat{\boldsymbol{x}}, \boldsymbol{\theta} \in S^{d-1}$ and $j_1, \ldots, j_l \in \{1, 2\}$. As indicated by our notation, the term $u^{\infty,(l)}_{q_{j_l},\ldots,q_{j_1}}$ describes the component of the far field pattern associated to the part of the scattered wave that results from l scattering processes starting at q_{j_1}, followed by q_{j_2} and so forth, until q_{j_l}.

We define the associated far field operator components by

$$F^{(l)}_{q_{j_l},\ldots,q_{j_1}} : L^2(S^{d-1}) \to L^2(S^{d-1}), \quad (F^{(l)}_{q_{j_l},\ldots,q_{j_1}} g)(\widehat{\boldsymbol{x}}) := \int_{S^{d-1}} u^{\infty,(l)}_{q_{j_l},\ldots,q_{j_1}}(\widehat{\boldsymbol{x}}; \boldsymbol{\theta}) g(\boldsymbol{\theta}) \, \mathrm{d}s(\boldsymbol{\theta}).$$

Therewith, we can rewrite the Born far field operator of order p from (2.18) as

$$\begin{aligned} F_q^{(\leq p)} &= \sum_{l=1}^{p} F_q^{(l)} = \sum_{l=1}^{p} \Bigg(\sum_{j_l=1}^{2} \cdots \sum_{j_1=1}^{2} F^{(l)}_{q_{j_l},\ldots,q_{j_1}} \Bigg) \\ &= F_{q_1}^{(\leq p)} + F_{q_2}^{(\leq p)} + \Bigg(\sum_{l=1}^{p} \sum_{(j_1,\ldots,j_l) \in \{1,2\}^l \setminus \left(\{1\}^l \cup \{2\}^l\right)} F^{(l)}_{q_{j_l},\ldots,q_{j_1}} \Bigg). \end{aligned} \quad (3.2)$$

Suppose that the Born series expansion of F_q converges, which is the case provided $\|L_q\|_{\mathrm{HS}} < 1$, see Remark 2.6. For increasing p, the Born far field operator $F_q^{(\leq p)}$ on the left hand side of (3.2) is an increasingly accurate approximation of the far field operator F_q corresponding to the system of two scatterers, while the first two terms $F_{q_1}^{(\leq p)}$ and $F_{q_2}^{(\leq p)}$ on the right hand side of (3.2) approximate the far field operators F_{q_1} and F_{q_2} corresponding to the two individual scatterers in D_1 and D_2 increasingly well. Furthermore, the terms in brackets on the right hand side of (3.2) approximate multiple scattering effects involving both q_1 and q_2.

Formula (3.2) represents the basis for all splitting problem formulations in this chapter. We recall the goal of far field operator splitting, which is to recover F_{q_1} and F_{q_2} from F_q. To this end, we split F_q into three components, two corresponding to the first two terms on the right hand side of (3.2), and one corresponding to the terms in brackets on the right hand side of this equation.

The rest of this chapter is structured as follows. First, we generalize in Section 3.2 the concepts from Sections 2.4 and 2.5 to identify subspaces of a similar structure, in which the components in brackets on the right hand side of (3.2) can be well approximated. As a first approach, we search for solutions of the splitting problem in these subspaces. The least squares problems considered here are always of the same structure. In Section 3.3 we consequently investigate the general problem of splitting a Hilbert Schmidt operator into two or more components individually lying in arbitrary subspaces. For $p = 1$, the term in brackets on the right hand side of (3.2) vanishes, so no summand that approximates multiple scattering effects has to be taken into account. This situation is taken as an ansatz for our findings in Section 3.4. In contrast to that, for $p \geq 2$, the term in brackets does not vanish, so multiple scattering effects do have an impact. The special case $p = 2$ is chosen as an starting point for our methods from Section 3.5. In Section 3.6 we comment on the transferability of our results to the case $p \geq 3$, and we elaborate related results for $J \geq 2$ scatterer's components. Finally, we explain how the reciprocity principle (cf. Proposition 2.4 (a)) can be incorporated for further improving the stability of our developed methods.

3.2. Generalized subspaces of non-evanescent far field operators and translation

We have already seen in Theorems 2.11 and 2.19 that the far field operator components $F_{q_1}^{(\leq p)}$ and $F_{q_2}^{(\leq p)}$ in (3.2) have sparse approximations in the subspaces $\mathcal{V}_{N_1}^{\boldsymbol{c}_1}$ and $\mathcal{V}_{N_2}^{\boldsymbol{c}_2}$ and low rank approximations in the subspaces $\mathcal{W}_{N_1}^{\boldsymbol{c}_1}$ and $\mathcal{W}_{N_2}^{\boldsymbol{c}_2}$ with $N_1 \gtrsim kR_1$ and $N_2 \gtrsim kR_2$, respectively. In fact,

the same reasoning shows that any term in brackets on the right hand side of (3.2) that is of the form $F^{(l)}_{q_1,q_{j_2},\dots,q_{j_{l-1}},q_1}$ or $F^{(l)}_{q_2,q_{j_2},\dots,q_{j_{l-1}},q_2}$, i.e., the first and the last interaction takes place at the same component of the scatterer, can be well approximated in $\mathcal{V}^{\boldsymbol{c}_1}_{N_1}$ and $\mathcal{W}^{\boldsymbol{c}_1}_{N_1}$ or $\mathcal{V}^{\boldsymbol{c}_2}_{N_2}$ and $\mathcal{W}^{\boldsymbol{c}_2}_{N_2}$, respectively (see also Theorem 3.4 below). To obtain sparse approximations of the remaining terms in brackets on the right hand side of (3.2), which are all of the form $F^{(l)}_{q_1,q_{j_2},\dots,q_{j_{l-1}},q_2}$ or $F^{(l)}_{q_2,q_{j_2},\dots,q_{j_{l-1}},q_1}$, we need to adjust our concepts from Sections 2.4 and 2.5 by allowing mutually distinct cut-off parameters and modulation factors in $\widehat{\boldsymbol{x}}$ and in $\boldsymbol{\theta}$ direction.

The following definition is a counterpart to Definitions 2.9 and 2.17 and to Definition and Corollary 2.21.

Definition 3.3. Let $M, N \in \mathbb{N}$ and $\boldsymbol{b}, \boldsymbol{c} \in \mathbb{R}^d$.

(a) We define the *generalized subspace of sparse far field operators* for $d = 2$ by

$$\mathcal{V}_{M,N} := \left\{ G \in \mathrm{HS}(L^2(S^1)) \;\middle|\; Gg = \sum_{|m|\le M} \sum_{|n|\le N} a_{m,n}\, \boldsymbol{e}_m \langle g, \boldsymbol{e}_n \rangle_{L^2(S^1)},\ a_{m,n} \in \mathbb{C} \right\}$$

and for $d = 3$ by

$$\mathcal{V}_{M,N} := \left\{ G \in \mathrm{HS}(L^2(S^2)) \;\middle|\; Gg = \sum_{m=0}^{M} \sum_{n=0}^{N} \int_{S^2} \alpha_{m,n}(\,\cdot\,;\boldsymbol{\theta}) g(\boldsymbol{\theta})\, \mathrm{d}s(\boldsymbol{\theta}),\ \alpha_{m,n} \in \mathbb{Y}^3_m \times \mathbb{Y}^3_n \right\}.$$

By $\mathcal{P}_{\mathcal{V}_{M,N}} : \mathrm{HS}(L^2(S^{d-1})) \to \mathcal{V}_{M,N}$ we mean the orthogonal projection onto $\mathcal{V}_{M,N}$ with respect to $\langle \cdot, \cdot \rangle_{\mathrm{HS}}$. We note that $\mathcal{V}_{N,N} = \mathcal{V}_N$ from (2.22) or (2.35).

(b) We further define the *generalized translation operator* by

$$\mathcal{T}_{\boldsymbol{b},\boldsymbol{c}} : \mathrm{HS}(L^2(S^{d-1})) \to \mathrm{HS}(L^2(S^{d-1})), \quad \mathcal{T}_{\boldsymbol{b},\boldsymbol{c}} G := T_{\boldsymbol{b}} \circ G \circ T_{-\boldsymbol{c}}, \tag{3.3}$$

where $T_{\boldsymbol{b}}$ and $T_{-\boldsymbol{c}}$ are defined as in (2.45). Then, $\mathcal{T}_{\boldsymbol{c},\boldsymbol{c}} = \mathcal{T}_{\boldsymbol{c}}$ from (2.46).

(c) Finally, we introduce

$$\mathcal{V}^{\boldsymbol{b},\boldsymbol{c}}_{M,N} := \{ G \in \mathrm{HS}(L^2(S^{d-1})) \mid \mathcal{T}_{\boldsymbol{b},\boldsymbol{c}} G \in \mathcal{V}_{M,N} \}. \tag{3.4}$$

Again, we note that $\mathcal{V}^{\boldsymbol{c},\boldsymbol{c}}_{N,N} = \mathcal{V}^{\boldsymbol{c}}_N$ from (2.47).

As can be deduced from the following theorem, far field operator components of the form $F^{(l)}_{q_{j_1},\dots,q_{j_l}}$ for given $l \in \mathbb{N}$ and $j_1, \dots, j_l \in \{1, 2\}$ can be well approximated in the subspace $\mathcal{V}^{\boldsymbol{c}_{j_1},\boldsymbol{c}_{j_l}}_{N_{j_1},N_{j_l}}$. This should be compared to Theorems 2.11 and 2.19, which cover the case $j_1 = \dots = j_l$.

Theorem 3.4. *Suppose* $\|L_q\| < 1$ *and let* $l \in \mathbb{N}$, $j_1, \dots, j_l \in \{1, 2\}$ *and* $N_1, N_2 \in \mathbb{N}$ *with* $N_1 \gtrsim kR_1$ *and* $N_2 \gtrsim kR_2$. *Then, we have for* $d = 2$ *the error estimate*

$$\begin{aligned} \|F^{(l)}_{q_{j_1},\dots,q_{j_l}} - \mathcal{P}_{\mathcal{V}^{\boldsymbol{c}_{j_1},\boldsymbol{c}_{j_l}}_{N_{j_1},N_{j_l}}} F^{(l)}_{q_{j_1},\dots,q_{j_l}} \|_{\mathrm{HS}} &\le 2\pi^{\frac{3}{2}} \|q_{j_l}\|_{L^\infty(D_{j_l})} \|L_{q,j_1,j_2}\|_{\mathrm{HS}} \cdots \|L_{q,j_{l-1},j_l}\|_{\mathrm{HS}} \\ &\times \left((kR_{j_l})^2 \sum_{|n|>N_{j_1}} \|J_n(|\,\cdot\,|)\|^2_{L^2(B_{kR_{j_1}}(\mathbf{0}))} + (kR_{j_1})^2 \sum_{|n|>N_{j_l}} \|J_n(|\,\cdot\,|)\|^2_{L^2(B_{kR_{j_l}}(\mathbf{0}))} \right)^{\frac{1}{2}}, \end{aligned} \tag{3.5}$$

and for $d = 3$ *we have that*

$$\|F^{(l)}_{q_{j_1},\dots,q_{j_l}} - \mathcal{P}_{\mathcal{V}^{\boldsymbol{c}_{j_1},\boldsymbol{c}_{j_l}}_{N_{j_1},N_{j_l}}} F^{(l)}_{q_{j_1},\dots,q_{j_l}} \|_{\mathrm{HS}} \le \frac{4\pi}{k} \|q_{j_l}\|_{L^\infty(D_{j_l})} \|L_{q,j_1,j_2}\|_{\mathrm{HS}} \cdots \|L_{q,j_{l-1},j_l}\|_{\mathrm{HS}}$$

$$\times \Bigg(M(kR_{j_1}) \sum_{m=N_{j_l}+1}^{\infty} (2m+1)^2 \|j_m(|\cdot|)\|^2_{L^2(B_{kR_{j_l}}(\mathbf{0}))} + M(kR_{j_l}) \sum_{n=N_{j_1}+1}^{\infty} (2n+1)^2 \|j_n(|\cdot|)\|^2_{L^2(B_{kR_{j_1}}(\mathbf{0}))} \Bigg)^{\frac{1}{2}} . \tag{3.6}$$

Here, we recall $M(kR_j) = \sum_{n=0}^{\infty}(2n+1)^2\|j_n(|\cdot|)\|^2_{L^2(B_{kR_j}(\mathbf{0}))}$ *for* $j = 1, 2$ *from Theorem 2.19.*

Proof. We first observe that $\|L_q\| < 1$ implies $\|L_{q,j,l}\|_{\mathrm{HS}} < 1$ for all $j, l \in \{1, 2\}$. As in (2.49), the expansion coefficients $(a^{(l)}_{m,n})_{m,n}$ of $\mathcal{T}_{\boldsymbol{c}_{j_1},\boldsymbol{c}_{j_l}} u^{\infty,(l)}_{q_{j_l},\dots,q_{j_1}}$ from (3.1) are for $d = 2$ given by

$$a^{(l)}_{m,n} = 2\pi k^{2l} \mathrm{i}^{n-m} \int_{D_{j_l}} \cdots \int_{D_{j_1}} q_{j_l}(\boldsymbol{y}_l) \cdots q_{j_1}(\boldsymbol{y}_1) \Phi_k(\boldsymbol{y}_l - \boldsymbol{y}_{l-1}) \cdots \Phi_k(\boldsymbol{y}_2 - \boldsymbol{y}_1) \times e^{-\mathrm{i}(m \arg(\boldsymbol{y}_l - \boldsymbol{c}_{j_l}) - n \arg(\boldsymbol{y}_1 - \boldsymbol{c}_{j_1}))} J_m(k|\boldsymbol{y}_l - \boldsymbol{c}_{j_l}|) J_n(k|\boldsymbol{y}_1 - \boldsymbol{c}_{j_1}|) \, \mathrm{d}\boldsymbol{y}_1 \cdots \mathrm{d}\boldsymbol{y}_l .$$

Therefore, we can estimate analogously to the proof of Theorem 2.11 and obtain

$$\begin{aligned} \|F^{(l)}_{q_{j_1},\dots,q_{j_l}} - \mathcal{P}_{\mathcal{V}^{\boldsymbol{c}_{j_1},\boldsymbol{c}_{j_l}}_{N_{j_1},N_{j_l}}} F^{(l)}_{q_{j_1},\dots,q_{j_l}}\|^2_{\mathrm{HS}} &\le \sum_{m\in\mathbb{Z}} \sum_{|n|>N_{j_1}} |a^{(l)}_{m,n}|^2 + \sum_{|m|>N_{j_l}} \sum_{n\in\mathbb{Z}} |a^{(l)}_{m,n}|^2 \\ &\le 4\pi^2 \|q_{j_l}\|^2_{L^\infty(D_{j_l})} \|L_{q,j_1,j_2}\|^2_{\mathrm{HS}} \cdots \|L_{q,j_{l-1},j_l}\|^2_{\mathrm{HS}} \\ &\quad \times \Bigg(\sum_{m\in\mathbb{Z}} \|J_m(|\cdot|)\|^2_{L^2(B_{kR_{j_l}}(\mathbf{0}))} \sum_{|n|>N_{j_1}} \|J_n(|\cdot|)\|^2_{L^2(B_{kR_{j_1}}(\mathbf{0}))} \\ &\quad + \sum_{|m|>N_{j_l}} \|J_m(|\cdot|)\|^2_{L^2(B_{kR_{j_l}}(\mathbf{0}))} \sum_{n\in\mathbb{Z}} \|J_n(|\cdot|)\|^2_{L^2(B_{kR_{j_1}}(\mathbf{0}))} \Bigg), \end{aligned}$$

which together with

$$\sum_{m\in\mathbb{Z}} \|J_m(|\cdot|)\|^2_{L^2(B_{kR_{j_l}}(\mathbf{0}))} = \pi(kR_{j_l})^2 \qquad \text{and} \qquad \sum_{n\in\mathbb{Z}} \|J_n(|\cdot|)\|^2_{L^2(B_{kR_{j_1}}(\mathbf{0}))} = \pi(kR_{j_1})^2 ,$$

see (2.29), yields (3.5).

For $d = 3$, as in (2.50), the related spherical harmonics components $(\alpha^{(l)}_{m,n})_{m,n}$ can be written as

$$\alpha^{(l)}_{m,n}(\widehat{\boldsymbol{x}};\boldsymbol{\theta}) = k^{2l} \frac{(2m+1)^2(2n+1)^2}{16\pi^2} \mathrm{i}^{n-m} \int_{D_{j_l}} \cdots \int_{D_{j_1}} q_{j_l}(\boldsymbol{y}_l) \cdots q_{j_1}(\boldsymbol{y}_1) \Phi_k(\boldsymbol{y}_l - \boldsymbol{y}_{l-1}) \cdots$$
$$\times \Phi_k(\boldsymbol{y}_2 - \boldsymbol{y}_1) j_m(k|\boldsymbol{y}_l - \boldsymbol{c}_{j_l}|) j_n(k|\boldsymbol{y}_1 - \boldsymbol{c}_{j_1}|) \langle P^{\widehat{\boldsymbol{x}}}_m, P^{\widehat{\boldsymbol{y}_l - \boldsymbol{c}_{j_l}}}_m \rangle_{L^2(S^2)} \langle P^{\boldsymbol{\theta}}_n, P^{\widehat{\boldsymbol{y}_1 - \boldsymbol{c}_{j_1}}}_n \rangle_{L^2(S^2)} \, \mathrm{d}\boldsymbol{y}_1 \cdots \mathrm{d}\boldsymbol{y}_l .$$

To obtain (3.6), we consequently can estimate as in the proof of Theorem 2.19

$$\|F^{(l)}_{q_{j_1},\dots,q_{j_l}} - \mathcal{P}_{\mathcal{V}^{\boldsymbol{c}_{j_1},\boldsymbol{c}_{j_l}}_{N_{j_1},N_{j_l}}} F^{(l)}_{q_{j_1},\dots,q_{j_l}}\|^2_{\mathrm{HS}} \le \sum_{m=N_{j_l}+1}^{\infty} \sum_{n=0}^{\infty} \|\alpha^{(l)}_{m,n}\|^2_{L^2(S^2\times S^2)} + \sum_{m=0}^{\infty} \sum_{n=N_{j_1}+1}^{\infty} \|\alpha^{(l)}_{m,n}\|^2_{L^2(S^2\times S^2)}$$
$$\le \frac{16\pi^2}{k^2} \|q_{j_l}\|^2_{L^\infty(D_{j_l})} \|L_{q,j_1,j_2}\|^2_{\mathrm{HS}} \cdots \|L_{q,j_{l-1},j_l}\|^2_{\mathrm{HS}}$$
$$\times \Bigg(\sum_{m=N_{j_l}+1}^{\infty} (2m+1)^2 \|j_m(|\cdot|)\|^2_{L^2(B_{kR_{j_l}}(\mathbf{0}))} \sum_{n=0}^{\infty} (2n+1)^2 \|j_n(|\cdot|)\|^2_{L^2(B_{kR_{j_1}}(\mathbf{0}))}$$

$$+\sum_{m=0}^{\infty}(2m+1)^2\|j_m(|\cdot|)\|^2_{L^2(B_{kR_{j_l}}(\mathbf{0}))}\sum_{n=N_{j_1}+1}^{\infty}(2n+1)^2\|j_n(|\cdot|)\|^2_{L^2(B_{kR_{j_1}}(\mathbf{0}))}\Big).$$

□

Since we do not need generalized subspaces of low rank far field operators for our later purposes, we do not introduce them in the same manner, although this would provide a meaningful definition. Nevertheless, we have the following approximation theorem which states that far field operator components of the form $F^{(l)}_{q_{j_1},\dots,q_{j_l}}$ for given $l\in\mathbb{N}$ and $j_1,\dots,j_l\in\{1,2\}$ can be well approximated in the subspaces $\mathcal{W}^{\boldsymbol{c}_{j_1}}_{N_{j_1}}$ and $\mathcal{W}^{\boldsymbol{c}_{j_l}}_{N_{j_l}}$ of low rank operators.

Theorem 3.5. *Suppose $\|L_q\|<1$ and let $l\in\mathbb{N}$, $j_1,\dots,j_l\in\{1,2\}$ and $N_1,N_2\in\mathbb{N}$ with $N_1\gtrsim kR_1$ and $N_2\gtrsim kR_2$. Then, we have for $d=2$ the error estimate*

$$\|F^{(l)}_{q_{j_1},\dots,q_{j_l}}-\mathcal{P}_{\mathcal{W}^{\boldsymbol{c}_{j_1}}_{N_{j_1}}}F^{(l)}_{q_{j_1},\dots,q_{j_l}}\|_{\mathrm{HS}}\le 2\pi^{\frac{3}{2}}\|q_{j_l}\|_{L^\infty(D_{j_l})}\|L_{q,j_1,j_2}\|_{\mathrm{HS}}\cdots\|L_{q,j_{l-1},j_l}\|_{\mathrm{HS}}$$
$$\times kR_{j_l}\Big(\sum_{|n|>N_{j_1}}\|J_n(|\cdot|)\|^2_{L^2(B_{kR_{j_1}}(\mathbf{0}))}\Big)^{\frac{1}{2}},$$

and for $d=3$ we have that

$$\|F^{(l)}_{q_{j_1},\dots,q_{j_l}}-\mathcal{P}_{\mathcal{W}^{\boldsymbol{c}_{j_1}}_{N_{j_1}}}F^{(l)}_{q_{j_1},\dots,q_{j_l}}\|_{\mathrm{HS}}\le\frac{4\pi}{k}\|q_{j_l}\|_{L^\infty(D_{j_l})}\|L_{q,j_1,j_2}\|_{\mathrm{HS}}\cdots\|L_{q,j_{l-1},j_l}\|_{\mathrm{HS}}$$
$$\times\Big(M(kR_{j_l},k(\boldsymbol{c}_{j_l}-\boldsymbol{c}_{j_1}))\sum_{n=N_{j_1}+1}^{\infty}(2n+1)^2\|j_n(|\cdot|)\|^2_{L^2(B_{kR_{j_1}}(\mathbf{0}))}\Big)^{\frac{1}{2}},$$

where $M(kR_{j_l},k(\boldsymbol{c}_{j_l}-\boldsymbol{c}_{j_1})):=\sum_{m=0}^{\infty}(2m+1)^2\|j_m(|\cdot|)\|^2_{L^2(B_{kR_{j_l}}(k(\boldsymbol{c}_{j_l}-\boldsymbol{c}_{j_1})))}$.

For $\mathcal{W}^{\boldsymbol{c}_{j_l}}_{N_{j_l}}$ we obtain the analogous bounds by interchanging the roles of j_1 and j_l.

Proof. To show this one can proceed as in the proofs of Theorems 3.5, 2.11 and 2.19. For $d=2$ we use that for all $\boldsymbol{c}=(c_1,c_2)^\top\in\mathbb{R}^2$ and $R>0$ there holds due to (B.10) that

$$\sum_{m\in\mathbb{Z}}\|J_m(|\cdot|)\|^2_{L^2(B_R(\boldsymbol{c}))}=\sum_{m\in\mathbb{Z}}\int_{B_R(\boldsymbol{c})}J_m^2(|\boldsymbol{x}|)\,\mathrm{d}\boldsymbol{x}$$
$$=\sum_{m\in\mathbb{Z}}\int_0^{2\pi}\int_0^R J_m^2\Big(\sqrt{r^2+|\boldsymbol{c}|^2+2r(c_1\cos\varphi+c_2\sin\varphi)}\Big)\,r\,\mathrm{d}r\,\mathrm{d}\varphi=\int_0^{2\pi}\int_0^R r\,\mathrm{d}r\,\mathrm{d}\varphi=\pi R^2$$

independently on $\boldsymbol{c}$. □

Remark 3.6. Since we have that $\mathcal{V}^{\boldsymbol{c}_{j_1},\boldsymbol{c}_{j_l}}_{N_{j_1},N_{j_l}}\subsetneq\mathcal{W}^{\boldsymbol{c}_{j_1}}_{N_{j_1}}$ and $\mathcal{V}^{\boldsymbol{c}_{j_1},\boldsymbol{c}_{j_l}}_{N_{j_1},N_{j_l}}\subsetneq\mathcal{W}^{\boldsymbol{c}_{j_l}}_{N_{j_l}}$ we expect a smaller approximation error, when projecting $F^{(l)}_{q_{j_1},\dots,q_{j_l}}$ onto $\mathcal{W}^{\boldsymbol{c}_{j_1}}_{N_{j_1}}$ or onto $\mathcal{W}^{\boldsymbol{c}_{j_l}}_{N_{j_l}}$ compared to Theorem 3.4. For $d=2$ this is indeed the case, but for $d=3$ this reduction of the upper bound is not directly visible. Consequently, for $d=3$ it can be assumed that $M(kR_{j_l},k(\boldsymbol{c}_{j_l}-\boldsymbol{c}_{j_1}))$ can be simplified even further in order to eliminate the dependence on $\boldsymbol{c}_{j_l}$ and $\boldsymbol{c}_{j_1}$.

Example 3.7. We consider a numerical example for $d=2$ with $q=-0.5\chi_{D_1}+2\chi_{D_2}$ for a nut shaped scatterer D_1 and a kite shaped scatterer D_2, as shown in Figure 3.2 (left). We choose the wave number $k=5$ and approximate the far field component $u^{\infty,(2)}_{q_2,q_1}(\widehat{\boldsymbol{x}}_m;d_n)$, given as in (3.1), for $L=256$ equidistant observation and illumination directions on S^1 using trigonometric interpolation as described in [93, 97].

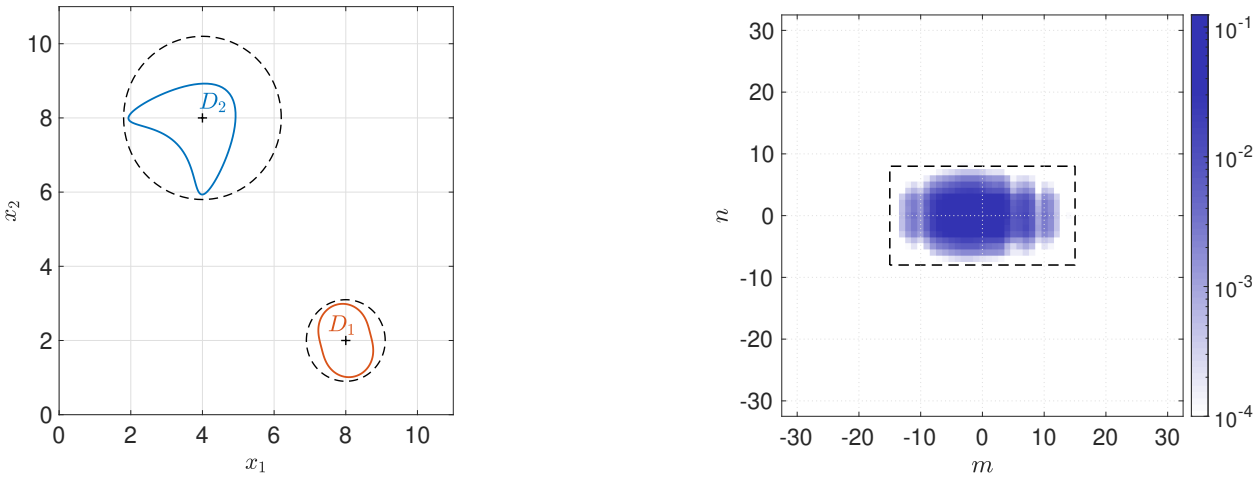

Figure 3.2. Left: Supports of two scatterers D_1 and D_2 (solid) and balls $B_{R_1}(\boldsymbol{c}_1)$ and $B_{R_2}(\boldsymbol{c}_2)$ (dashed). Right: Absolute values of modulated Fourier coefficients $(a^{(2)}_{m,n})_{m,n}$ of $F^{(2)}_{q_2,q_1}$ at $k = 5$. Dashed rectangle corresponds to coefficients used by sparse approximation of $F^{(2)}_{q_2,q_1}$ in $\mathcal{V}^{\boldsymbol{c}_2,\boldsymbol{c}_1}_{N_2,N_1}$ with $N_1 = 7$ and $N_2 = 13$.

The scatterers D_1 and D_2 are contained in balls $B_{R_1}(\boldsymbol{c}_1)$ and $B_{R_2}(\boldsymbol{c}_2)$ of radius $R_1 = 1.1$ and $R_2 = 2.2$ centered at $\boldsymbol{c}_1 = (8,2)^\top$ and $\boldsymbol{c}_2 = (4,8)^\top$, respectively. Both are shown in Figure 3.2 (left).

A two-dimensional fast Fourier transform of the shifted far field patterns

$$\frac{2\pi}{L}\left(e^{-\mathrm{i}k(\boldsymbol{c}_1\cdot\boldsymbol{\theta}_n-\boldsymbol{c}_2\cdot\widehat{\boldsymbol{x}}_m)}u^{\infty,(2)}_{q_2,q_1}(\widehat{\boldsymbol{x}}_m;\boldsymbol{\theta}_n)\right)_{m,n}\in\mathbb{C}^{L\times L}$$

yields an approximation of the Fourier coefficients $(a^{(2)}_{m,n})_{m,n}$ of $\mathcal{T}_{\boldsymbol{c}_2,\boldsymbol{c}_1}F^{\infty,(2)}_{q_2,q_1}$ with respect to $(e_{m,n})_{m,n}$. In Figure 3.2 (right) the absolute values of these expansion coefficients are plotted for $-32 \le m,n \le 32$ on a logarithmic color scale. It is confirmed that these coefficients are essentially supported in the dashed marked rectangle $[-N_2,N_2]\times[-N_1,N_1]$ with $N_1 = \lceil ekR_1/2\rceil = 8$ and $N_2 = \lceil ekR_1/2\rceil = 15$. ◊

Analogously to Lemmas 2.24 and 2.25, we have the following properties of the generalized translation operator.

Lemma 3.8. *Let $\boldsymbol{b},\boldsymbol{c}\in\mathbb{R}^d\setminus\{\boldsymbol{0}\}$. Then, for $\mathcal{T}_{\boldsymbol{b},\boldsymbol{c}}\in\mathcal{L}(\mathrm{HS}(L^2(S^{d-1})))$ the following holds.*

(a) The operator $\mathcal{T}_{\boldsymbol{b},\boldsymbol{c}}$ is unitary with $\mathcal{T}^*_{\boldsymbol{b},\boldsymbol{c}} = \mathcal{T}_{-\boldsymbol{b},-\boldsymbol{c}} = \mathcal{T}^{-1}_{\boldsymbol{b},\boldsymbol{c}}$. Moreover, for all $1\le p\le\infty$,

$$\|\mathcal{T}_{\boldsymbol{b},\boldsymbol{c}}G\|_{L^p} = \|G\|_{L^p}\,,\qquad G\in\mathrm{HS}(L^2(S^{d-1}))\cap L^p(S^{d-1}\times S^{d-1})\,, \tag{3.7}$$

(b) In both dimensions, the operator $\mathcal{T}_{\boldsymbol{b},\boldsymbol{c}}$ acts via

$$\mathcal{T}_{\boldsymbol{b},\boldsymbol{c}}\kappa_G(\widehat{\boldsymbol{x}},\boldsymbol{\theta}) = e^{\mathrm{i}k(\boldsymbol{b}\cdot\widehat{\boldsymbol{x}}-\boldsymbol{c}\cdot\boldsymbol{\theta})}\kappa_G(\widehat{\boldsymbol{x}},\boldsymbol{\theta})\,,\qquad \widehat{\boldsymbol{x}},\boldsymbol{\theta}\in S^{d-1}\,,$$

as a multiplication operator on the kernel κ_G of $G\in\mathrm{HS}(L^2(S^{d-1}))$. It further acts for $d=2$ as a convolution operator on the Fourier coefficients $(a_{m,n})_{m,n}$ of G by $\mathcal{T}_{\boldsymbol{b},\boldsymbol{c}}((a_{m,n})_{m,n}) = (a^{\boldsymbol{b},\boldsymbol{c}}_{m,n})_{m,n}$ with

$$a^{\boldsymbol{b},\boldsymbol{c}}_{m,n} = \sum_{m'\in\mathbb{Z}}\sum_{n'\in\mathbb{Z}} a_{m-m',n-n'}\left(\mathrm{i}^{m'-n'}e^{-\mathrm{i}m'\arg\boldsymbol{b}}e^{\mathrm{i}n'\arg\boldsymbol{c}}J_{m'}(k|\boldsymbol{b}|)J_{n'}(k|\boldsymbol{c}|)\right)\,,\qquad m,n\in\mathbb{Z}\,.$$

For $d=3$ its effect on the spherical harmonics components $(\alpha_{m,n})_{m,n}$ of G is described

by $\mathcal{T}_{\boldsymbol{b},\boldsymbol{c}}((\alpha_{m,n})_{m,n}) = (\alpha_{m,n}^{\boldsymbol{b},\boldsymbol{c}})_{m,n}$ *with*

$$\alpha_{m,n}^{\boldsymbol{b},\boldsymbol{c}}(\widehat{\boldsymbol{x}},\boldsymbol{\theta}) = \frac{(2m+1)(2n+1)}{16\pi^2} \sum_{o,p,r,s=0}^{\infty} \mathrm{i}^{o-p}(2o+1)(2p+1) j_o(k|\boldsymbol{b}|) j_p(k|\boldsymbol{c}|) \times \int_{S^2} P_m^{\widehat{\boldsymbol{x}}}(\boldsymbol{\omega}) P_o^{\widehat{\boldsymbol{b}}}(\boldsymbol{\omega}) \int_{S^2} P_n^{\boldsymbol{\theta}}(\boldsymbol{v}) P_p^{\widehat{\boldsymbol{c}}}(\boldsymbol{v}) \alpha_{r,s}(\boldsymbol{\omega};\boldsymbol{v}) \, \mathrm{d}s(\boldsymbol{v}) \, \mathrm{d}s(\boldsymbol{\omega})$$

for $\widehat{\boldsymbol{x}}, \boldsymbol{\theta} \in S^2$ *and* $m, n \in \mathbb{N}_0$.

(c) We have for $d = 2$ *and any* $G \in \mathrm{HS}(L^2(S^1)) \cap \ell^1 \times \ell^1$ *that*

$$\|\mathcal{T}_{\boldsymbol{b},\boldsymbol{c}} G\|_{\ell^\infty \times \ell^\infty} \leq \begin{cases} (k^2|\boldsymbol{b}||\boldsymbol{c}|)^{-\frac{1}{3}} \|G\|_{\ell^1 \times \ell^1} & \text{if } \boldsymbol{b}, \boldsymbol{c} \neq \boldsymbol{0}\,, \\ (k|\boldsymbol{b}|)^{-\frac{1}{3}} \|G\|_{\ell^1 \times \ell^1} & \text{if } \boldsymbol{b} \neq \boldsymbol{0}\,,\ \boldsymbol{c} = \boldsymbol{0}\,, \\ (k|\boldsymbol{c}|)^{-\frac{1}{3}} \|G\|_{\ell^1 \times \ell^1} & \text{if } \boldsymbol{b} = \boldsymbol{0}\,,\ \boldsymbol{c} \neq \boldsymbol{0}\,, \end{cases} \tag{3.8}$$

and we have for $d = 3$ *and any* $G \in \mathrm{HS}(L^2(S^2)) \cap \ell^1_{2n+1} \times \ell^1_{2n+1}$ *that*

$$\|\mathcal{T}_{\boldsymbol{b},\boldsymbol{c}} G\|_{\ell^\infty_{1/(2n+1)} \times \ell^\infty_{1/(2n+1)}} \leq \begin{cases} (k^2|\boldsymbol{b}||\boldsymbol{c}|)^{-\frac{5}{6}} \|G\|_{\ell^1_{2n+1} \times \ell^1_{2n+1}} & \text{if } \boldsymbol{b}, \boldsymbol{c} \neq \boldsymbol{0}\,, \\ (k|\boldsymbol{b}|)^{-\frac{5}{6}} \|G\|_{\ell^1_{2n+1} \times \ell^1_{2n+1}} & \text{if } \boldsymbol{b} \neq \boldsymbol{0}\,,\ \boldsymbol{c} = \boldsymbol{0}\,, \\ (k|\boldsymbol{c}|)^{-\frac{5}{6}} \|G\|_{\ell^1_{2n+1} \times \ell^1_{2n+1}} & \text{if } \boldsymbol{b} = \boldsymbol{0}\,,\ \boldsymbol{c} \neq \boldsymbol{0}\,. \end{cases} \tag{3.9}$$

Proof. This follows similar to the proofs of Lemmas 2.24 and 2.25.

For (c) we note that $J_0(0) = j_0(0) = 1$ and that $J_n(0) = 0$ for all $n \in \mathbb{Z} \setminus \{0\}$ and $j_n(0) = 0$ for all $n \in \mathbb{N}$. □

3.3. The general subspace splitting problem

In this section, let $\mathcal{V}_1, \mathcal{V}_2 \subseteq \mathrm{HS}(L^2(S^{d-1}))$ denote two arbitrary finite or infinite-dimensional closed subspaces. Moreover, denote for $j = 1, 2$ by $\mathcal{P}_j : \mathrm{HS}(L^2(S^{d-1})) \to \mathcal{V}_j$ the orthogonal projection onto $\mathcal{V}_j$ with respect to $\langle \cdot, \cdot \rangle_{\mathrm{HS}}$, which maps each operator $G \in \mathrm{HS}(L^2(S^{d-1}))$ to its uniquely determined nearest operator in $\mathcal{V}_j$, i.e.,

$$\|G - \mathcal{P}_j G\|_{\mathrm{HS}} = d(G, \mathcal{V}_j) := \inf\{\|G - H\|_{\mathrm{HS}} : H \in \mathcal{V}_j\}\,.$$

We consider the general **subspace splitting problem** to recover $F_1 \in \mathcal{V}_1$ and $F_2 \in \mathcal{V}_2$ from $F \in \mathrm{HS}(L^2(S^{d-1}))$ such that $F = F_1 + F_2$.

In general, neither existence nor uniqueness of this split is given. For ensuring existence we need that $F \in \mathcal{V}_1 + \mathcal{V}_2$ and for uniqueness that $\mathcal{V}_1 \cap \mathcal{V}_2 = \{0\}$. Here, the sum of these two subspaces is given by

$$\mathcal{V}_1 + \mathcal{V}_2 := \{G + H : G \in \mathcal{V}_1\,,\ H \in \mathcal{V}_2\}\,,$$

which is again a subspace, but not necessarily closed (see e.g. [94, Exa. 2.2] for a counter example). Provided $\mathcal{V}_1 \cap \mathcal{V}_2 = \{0\}$ we call this sum direct and write $\mathcal{V}_1 \oplus \mathcal{V}_2$.

A more detailed investigation of the uniqueness of this problem as well of its stability requires to introduce the concept of the minimal angle.

Definition 3.9. The *minimal angle* θ between $\mathcal{V}_1$ and $\mathcal{V}_2$ is the angle in $[0, \pi/2]$ whose cosine is given by

$$\cos\theta = \sup_{G \in \mathcal{V}_1, H \in \mathcal{V}_2} \frac{\langle G, H \rangle_{\mathrm{HS}}}{\|G\|_{\mathrm{HS}} \|H\|_{\mathrm{HS}}}\,.$$

From [36, Lem. 10, Thm. 12] we have the following properties of the cosine of the minimal angle.

Lemma 3.10. *(a) We have that* $\cos\theta = \|\mathcal{P}_1\mathcal{P}_2\| = \|\mathcal{P}_1\mathcal{P}_2\mathcal{P}_1\|^{\frac{1}{2}}$.

(b) In general it holds $0 \leq \cos\theta \leq 1$.

(c) It is $\cos\theta = 0$ *if and only if* $\mathcal{V}_1 \perp \mathcal{V}_2$.

(d) The following statements are equivalent

(i) $\cos\theta < 1$;

(ii) $\mathcal{V}_1 \cap \mathcal{V}_2 = \{0\}$ *and* $\mathcal{V}_1 + \mathcal{V}_2$ *is closed;*

(iii) $\inf\{d(G, \mathcal{V}_2) : G \in \mathcal{V}_1\,,\ \|G\|_{\mathrm{HS}} = 1\} > 0$.

(e) For all $G \in \mathcal{V}_1$ *and* $H \in \mathcal{V}_2$ *we have the* sharpened Schwarz inequality

$$|\langle G, H\rangle_{\mathrm{HS}}| \leq \cos\theta \|G\|_{\mathrm{HS}}\|H\|_{\mathrm{HS}}\,. \tag{3.10}$$

Remark 3.11. By comparing the sharpened Schwarz inequality (3.10) with the uncertainty principle (1.4), we recognize a close connection between the cosine of the minimal angle of two subspaces and the uncertainty principle, which holds between operators of these subspaces. More precisely, a corresponding uncertainty principle provides an upper bound for the cosine of the minimal angle, which comes with a concrete interpretation, namely assumptions on the support of operators lying in these subspaces. ◊

In the following, we give a stability estimate for the subspace splitting problem provided $F \in \mathcal{V}_1 + \mathcal{V}_2$, see [56, Thm. 1.1].

Theorem 3.12. *Suppose that* $F = F_1 + F_2$ *for* $F_1 \in \mathcal{V}_1$ *and* $F_2 \in \mathcal{V}_2$ *and that* $\cos\theta < 1$. *Then,*

$$\|F_j\|_{\mathrm{HS}}^2 \leq \frac{1}{1-\cos^2\theta}\|F\|_{\mathrm{HS}}^2 \qquad \text{for } j = 1, 2\,.$$

Proof. We estimate by using (3.10)

$$\begin{aligned}\|F\|_{\mathrm{HS}}^2 &= \|F_1 + F_2\|_{\mathrm{HS}}^2 = \|F_1\|_{\mathrm{HS}}^2 + \|F_2\|_{\mathrm{HS}}^2 + 2\,\mathrm{Re}\langle F_1, F_2\rangle_{\mathrm{HS}} \\ &\geq \|F_1\|_{\mathrm{HS}}^2 + \|F_2\|_{\mathrm{HS}}^2 - 2|\langle F_1, F_2\rangle_{\mathrm{HS}}| \geq \|F_1\|_{\mathrm{HS}}^2 + \|F_2\|_{\mathrm{HS}}^2 - 2\cos\theta\|F_1\|_{\mathrm{HS}}\|F_2\|_{\mathrm{HS}} \\ &= \left(\cos\theta\|F_1\|_{\mathrm{HS}} - \|F_2\|_{\mathrm{HS}}\right)^2 + (1-\cos^2\theta)\|F_1\|_{\mathrm{HS}}^2 \geq (1-\cos^2\theta)\|F_1\|_{\mathrm{HS}}^2\,.\end{aligned}$$

Interchanging the roles of F_2 and F_2 yields the second inequality. □

Theorem 3.12 provides an absolute condition number, given by the cosecant of θ, of the splitting operator that maps F onto (F_1, F_2) in the meaning of a measure for the error propagation when applying this splitting operator to a noisy version F^δ of F. This can be seen from the theorem below.

Since for $F^0, F^\delta \in \mathrm{HS}(L^2(S^{d-1}))$, we cannot expect the original splitting problem as introduced above to be solvable, we replace it by the associated *least squares problem.*

Theorem 3.13. *Suppose that* $F^0, F^\delta \in \mathrm{HS}(L^2(S^{d-1}))$ *and that* $\cos\theta < 1$. *Furthermore, denote by* F_1^0, F_2^0 *and* F_1^δ, F_2^δ *the solutions of the least squares problems*

$$F^0 \overset{\mathrm{LS}}{=} F_1^0 + F_2^0\,, \qquad F_1^0 \in \mathcal{V}_1\,,\ F_2^0 \in \mathcal{V}_2\,, \tag{3.11a}$$

$$F^\delta \overset{\mathrm{LS}}{=} F_1^\delta + F_2^\delta\,, \qquad F_1^\delta \in \mathcal{V}_1\,,\ F_2^\delta \in \mathcal{V}_2\,, \tag{3.11b}$$

respectively. Then, for $j = 1, 2$,

$$\|F_j^0 - F_j^\delta\|_{\mathrm{HS}}^2 \leq \frac{1}{1-\cos^2\theta}\|F^0 - F^\delta\|_{\mathrm{HS}}^2\,.$$

Proof. We proceed as in the proof of [55, Thm. 5.3]. Due to the equivalence of (i) and (ii) in Lemma 3.10 (d) the subspace $\mathcal{V}_1 + \mathcal{V}_2 = \mathcal{V}_1 \oplus \mathcal{V}_2$ is closed and consequently we can decompose each $G \in \mathrm{HS}(L^2(S^{d-1}))$ uniquely into $G = H + H^\perp$ with parts $H \in \mathcal{V}_1 \oplus \mathcal{V}_2$ and $H^\perp \in (\mathcal{V}_1 \oplus \mathcal{V}_2)^\perp$ that fulfill

$$\|G\|_{\mathrm{HS}}^2 \;=\; \|H\|_{\mathrm{HS}}^2 + \|H^\perp\|_{\mathrm{HS}}^2 \,.$$

Here, $(\mathcal{V}_1 \oplus \mathcal{V}_2)^\perp$ denotes the orthogonal complement of $\mathcal{V}_1 \oplus \mathcal{V}_2$ with respect to $\langle \cdot, \cdot \rangle_{\mathrm{HS}}$. Due to the least squares property (3.11) we have that $(F_1^0 - F_1^\delta) + (F_2^0 - F_2^\delta) \in \mathcal{V}_1 \oplus \mathcal{V}_2$ as well as that $(F^0 - F^\delta) - ((F_1^0 - F_1^\delta) + (F_2^0 - F_2^\delta)) \in (\mathcal{V}_1 \oplus \mathcal{V}_2)^\perp$, so

$$\begin{aligned} \|F^0 - F^\delta\|_{\mathrm{HS}}^2 \;&=\; \|(F_1^0 - F_1^\delta) + (F_2^0 - F_2^\delta)\|_{\mathrm{HS}}^2 + \|(F^0 - F^\delta) - ((F_1^0 - F_1^\delta) + (F_2^0 - F_2^\delta))\|_{\mathrm{HS}}^2 \\ &\geq\; \|(F_1^0 - F_1^\delta) + (F_2^0 - F_2^\delta)\|_{\mathrm{HS}}^2 \,. \end{aligned}$$

Therefore, by using (3.10) and the arithmetic-geometric mean inequality we obtain

$$\begin{aligned} \|F^0 - F^\delta\|_{\mathrm{HS}}^2 \;&\geq\; \|F_1^0 - F_1^\delta\|_{\mathrm{HS}}^2 + \|F_2^0 - F_2^\delta\|_{\mathrm{HS}}^2 - 2|\langle F_1^0 - F_1^\delta, F_2^0 - F_2^\delta \rangle_{\mathrm{HS}}| \\ &\geq\; \|F_1^0 - F_1^\delta\|_{\mathrm{HS}}^2 + \|F_2^0 - F_2^\delta\|_{\mathrm{HS}}^2 - 2\cos\theta \|F_1^0 - F_1^\delta\|_{\mathrm{HS}} \|F_2^0 - F_2^\delta\|_{\mathrm{HS}} \\ &\geq\; \|F_1^0 - F_1^\delta\|_{\mathrm{HS}}^2 + \|F_2^0 - F_2^\delta\|_{\mathrm{HS}}^2 - \cos^2\theta \|F_1^0 - F_1^\delta\|_{\mathrm{HS}}^2 - \|F_2^0 - F_2^\delta\|_{\mathrm{HS}}^2 \\ &=\; (1 - \cos^2\theta) \|F_1^0 - F_1^\delta\|_{\mathrm{HS}}^2 \,. \end{aligned} \tag{3.12}$$

Interchanging the roles of $(F_1^0 - F_1^\delta)$ and $(F_2^0 - F_2^\delta)$ in the last estimate shows the second inequality. □

Given $F \in \mathrm{HS}(L^2(S^{d-1}))$ solving the least squares problem as introduced above is equivalent to seeking for $F_j \in \mathcal{V}_j$, $j = 1, 2$, satisfying the Galerkin condition

$$\langle F, \phi \rangle_{\mathrm{HS}} \;=\; \langle F_1, \phi \rangle_{\mathrm{HS}} + \langle F_2, \phi \rangle_{\mathrm{HS}} \qquad \text{for all } \phi \in \mathcal{V}_1 + \mathcal{V}_2 \,.$$

Equivalently, we can also find $F_j \in \mathcal{V}_j$, $j = 1, 2$, by solving

$$\begin{bmatrix} I & \mathcal{P}_1\mathcal{P}_2 \\ \mathcal{P}_2\mathcal{P}_1 & I \end{bmatrix} \begin{bmatrix} F_1 \\ F_2 \end{bmatrix} = \begin{bmatrix} \mathcal{P}_1 F \\ \mathcal{P}_2 F \end{bmatrix} , \tag{3.13}$$

which is basically the associated normal equation $\mathscr{A}^*\mathscr{A}(F_1, F_2) = \mathscr{A}^*(F)$ for

$$\mathscr{A} : \mathcal{V}_1 \times \mathcal{V}_2 \to \mathrm{HS}(L^2(S^{d-1})) \qquad (F_1, F_2) \;\mapsto\; \mathcal{P}_1 F_1 + \mathcal{P}_2 F_2 \,,$$

and consequently

$$\mathscr{A}^* : \mathrm{HS}(L^2(S^{d-1})) \to \mathcal{V}_1 \times \mathcal{V}_2 \,, \qquad F \;\mapsto\; (\mathcal{P}_1 F, \mathcal{P}_2 F) \,.$$

In principle, we could omit $\mathcal{P}_2$ in the first row and $\mathcal{P}_1$ in the second row of the left side of (3.13) and let the system unchanged. Adding these terms makes the linear operator on the left side of (3.13) hermitian, since there holds $(\mathcal{P}_1\mathcal{P}_2)^* = (\mathcal{P}_2)^*(\mathcal{P}_1)^* = \mathcal{P}_2\mathcal{P}_1$. Let $(G, H) \in \mathrm{HS}(L^2(S^{d-1}))^2 \setminus \{0\}$ and without loss of generality suppose $G \neq 0$. Provided $\cos\theta < 1$ the positive definiteness of this operator follows from

$$\begin{aligned} \langle G + \mathcal{P}_1\mathcal{P}_2 H, G \rangle_{\mathrm{HS}} + \langle \mathcal{P}_2\mathcal{P}_1 G + H, H \rangle_{\mathrm{HS}} \;&=\; \|G\|_{\mathrm{HS}}^2 + \|H\|_{\mathrm{HS}}^2 + 2\,\mathrm{Re}\langle \mathcal{P}_2\mathcal{P}_1 G, H \rangle_{\mathrm{HS}} \\ &\geq\; \|G\|_{\mathrm{HS}}^2 + \|H\|_{\mathrm{HS}}^2 - 2\cos\theta \|G\|_{\mathrm{HS}} \|H\|_{\mathrm{HS}} \\ &\geq\; (1 - \cos^2\theta) \|G\|_{\mathrm{HS}}^2 \;>\; 0 \,, \end{aligned}$$

cf. (3.12). Consequently, problem (3.13) can be solved numerically by using, e.g., conjugate gradients (see Subsections 4.1.4 and 6.1.2). The solutions of (3.13) can for $\cos\theta < 1$ also be computed explicitly

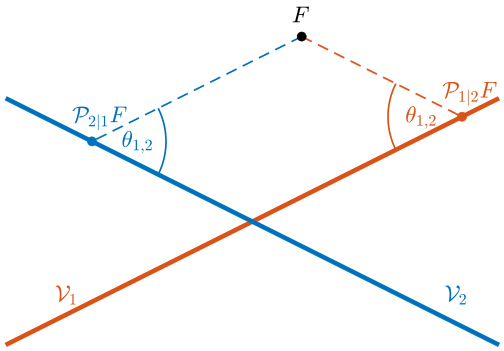

FIGURE 3.3. Sketch of the solution $(\mathcal{P}_{1|2}F, \mathcal{P}_{2|1}F)$ of the general splitting problem.

by

$$F_1 = \mathcal{P}_{1|2}F := (I - \mathcal{P}_1\mathcal{P}_2)^{-1}\mathcal{P}_1(I - \mathcal{P}_2)F\,,$$
$$F_2 = \mathcal{P}_{1|2}F := (I - \mathcal{P}_2\mathcal{P}_1)^{-1}\mathcal{P}_2(I - \mathcal{P}_1)F\,,$$

cf. [55, Sec. 7], where the inverse operators on the right hand sides exist due to a Neumann series argument since $\|\mathcal{P}_1\mathcal{P}_2\| = \|\mathcal{P}_2\mathcal{P}_1\| = \cos\theta < 1$. The operator $\mathcal{P}_{j|l}$, $j \neq l$, is the projection operator onto $\mathcal{V}_j$ along $\mathcal{V}_l$, which is visualized in Figure 3.3.

Finally, we generalize the above result for splitting a Hilbert–Schmidt operator not only into two but into multiple $J \geq 3$ components. For this purpose, let $\mathcal{V}_1, \ldots, \mathcal{V}_J \subseteq \mathrm{HS}(L^2(S^{d-1}))$ denote closed finite- or infinite-dimensional subspaces. Moreover, we denote by $\theta_{j,l}$ the minimal angle between $\mathcal{V}_j$ and $\mathcal{V}_l$ for $j, l \in \{1, \ldots, J\}$, $j \neq l$, as introduced in Definition 3.9. For guaranteeing the closednes of $\mathcal{V}_1 \oplus \ldots \oplus \mathcal{V}_J$ we assume that at most one of the subspaces is infinite-dimensional. This is needed for the proof of Theorem 3.15 and shown in the proposition below. Since this will also be the case later in all considered least squares problem formulations, it is a reasonable assumption.

Proposition 3.14. *Suppose that* $\cos\theta_{j,l} < 1$ *for all* $j, l \in \{1, \ldots, J\}$ *with* $j \neq l$.
Then, $\mathcal{V}_1 + \ldots + \mathcal{V}_J = \mathcal{V}_1 \oplus \ldots \oplus \mathcal{V}_J$ *is a closed subspace.*

Proof. From Lemma 3.10 (d) we already know that $\mathcal{V}_j \cap \mathcal{V}_l = \{0\}$ as well as that $\mathcal{V}_j + \mathcal{V}_l$ are pairwise closed for $j \neq l$. Consequently, it must hold $\mathcal{V}_1 \cap \ldots \cap \mathcal{V}_J = \{0\}$, so it remains to show that $\mathcal{V}_1 + \ldots + \mathcal{V}_J$ is closed. If all $\mathcal{V}_j$ are finite-dimensional this is already clear. Therefore, we suppose that $\mathcal{V}_{j^*}$ is infinite-dimensional and that $\mathcal{V}_j$ is finite-dimensional for all $j \neq j^*$. Then, $\mathcal{V} := \oplus_{j \neq j^*}\mathcal{V}_j$ is closed and again finite-dimensional, which implies the compactness of $\{G \in \mathcal{V} : \|G\|_{\mathrm{HS}} = 1\}$. Since this set is also disjoint to $\mathcal{V}_{j^*}$ we have that

$$\inf\{d(G, \mathcal{V}_{j^*}) : G \in \mathcal{V}\,,\ \|G\|_{\mathrm{HS}} = 1\} > 0\,,$$

due to the continuity of the distance mapping $G \mapsto d(G, \mathcal{V}_{j^*})$. The equivalence of (iii) and (ii) in Lemma 3.10 (d) yields the result. □

The following theorem provides a condition number of the operator that splits F into $J \geq 3$ components individually lying in one of the subspaces $\mathcal{V}_j$, $j \in \{1, \ldots, J\}$, by solving the associated least squares problem. It is structured as in Theorem 3.13.

Theorem 3.15. *Suppose that* $F^0, F^\delta \in \mathrm{HS}(L^2(S^{d-1}))$ *and that for each* $j \in \{1, \ldots, J\}$

$$\sum_{l \neq j} \cos\theta_{j,l} < 1\,.$$

Furthermore, denote by F_j^0 *and* F_j^δ *for* $j \in \{1,\dots,J\}$ *the solutions of the least squares problems*

$$F^0 \overset{\text{LS}}{=} \sum_{j=1}^{J} F_j^0\,, \qquad F_j^0 \in \mathcal{V}_j\,, j = \{1,\dots,J\}\,, \tag{3.14a}$$

$$F^\delta \overset{\text{LS}}{=} \sum_{j=1}^{J} F_j^\delta\,, \qquad F_j^\delta \in \mathcal{V}_j\,, j = \{1,\dots,J\}\,, \tag{3.14b}$$

respectively. Then, for $j = \{1,\dots,J\}$,

$$\|F_j^0 - F_j^\delta\|_{\text{HS}}^2 \le \left(1 - \sum_{l\neq j} \cos\theta_{j,l}\right)^{-1} \|F^0 - F^\delta\|_{\text{HS}}^2\,. \tag{3.15}$$

Proof. We first mention that due to Proposition 3.14 the subspace $\mathcal{V}_1 + \ldots + \mathcal{V}_J = \mathcal{V}_1 \oplus \ldots \oplus \mathcal{V}_J$ is closed, which guarantees the required existence and uniqueness of the orthogonal projection onto it. We proceed as in the proof of [55, Thm. 5.8] and conclude from the least squares property (3.14) that

$$\|F^0 - F^\delta\|_{\text{HS}}^2 = \left\|\sum_{j=1}^{J}(F_j^0 - F_j^\delta)\right\|_{\text{HS}}^2 + \left\|(F^0 - F^\delta) - \sum_{j=1}^{J}(F_j^0 - F_j^\delta)\right\|_{\text{HS}}^2 \ge \left\|\sum_{j=1}^{J}(F_j^0 - F_j^\delta)\right\|_{\text{HS}}^2.$$

Therefore, using the arithmetic-geometric mean inequality and the sharpened Schwarz inequality (3.10) yields

$$\begin{aligned}
\|F^0 - F^\delta\|_{\text{HS}}^2 &\ge \sum_{j=1}^{J} \|F_j^0 - F_j^\delta\|_{\text{HS}}^2 - \sum_{j=1}^{J}\sum_{l\neq j} |\langle F_j^0 - F_j^\delta, F_l^0 - F_l^\delta\rangle_{\text{HS}}| \\
&\ge \sum_{j=1}^{J} \|F_j^0 - F_j^\delta\|_{\text{HS}}^2 - \sum_{j=1}^{J}\sum_{l\neq j} \cos\theta_{j,l}\|F_j^0 - F_j^\delta\|_{\text{HS}}\|F_l^0 - F_l^\delta\|_{\text{HS}} \\
&\ge \sum_{j=1}^{J}\left(1 - \frac{1}{2}\sum_{l\neq j}\cos\theta_{j,l}\right)\|F_j^0 - F_j^\delta\|_{\text{HS}}^2 - \frac{1}{2}\sum_{j=1}^{J}\sum_{l\neq j}\cos\theta_{j,l}\|F_l^0 - F_l^\delta\|_{\text{HS}}^2 \\
&= \sum_{j=1}^{J}\left(1 - \frac{1}{2}\sum_{l\neq j}\cos\theta_{j,l}\right)\|F_j^0 - F_j^\delta\|_{\text{HS}}^2 - \frac{1}{2}\sum_{j=1}^{J}\sum_{l\neq j}\cos\theta_{j,l}\|F_j^0 - F_j^\delta\|_{\text{HS}}^2 \\
&= \sum_{j=1}^{J}\left(1 - \sum_{l\neq j}\cos\theta_{j,l}\right)\|F_j^0 - F_j^\delta\|_{\text{HS}}^2\,.
\end{aligned}$$

□

Remark 3.16. In principal, one can apply above result for $J = 2$ components, too. However, this clearly worsens the condition number. This observation as well as our numerical tests in Examples 4.4 and 4.5 for the conjugate gradient method suggest that the estimates in the proof of Theorem 3.15 are not sharp. ◊

3.4. Splitting in Born approximation of order one

For $p = 1$, expansion (3.2) reduces to

$$F_q^{(\le 1)} = F_{q_1}^{(\le 1)} + F_{q_2}^{(\le 1)}\,, \tag{3.16}$$

and as already observed the term in brackets on the right hand side of (3.2) vanishes.

From Theorems 2.11 and 2.19 we know that $F_{q_j}^{(\leq 1)} = F_{q_j}^{(1)}$ has a sparse approximation in the subspace $\mathcal{V}_{N_j}^{\boldsymbol{c}_j}$ and a low rank approximation in the subspace $\mathcal{W}_{N_j}^{\boldsymbol{c}_j}$ of far field operators associated to scatterers supported in $B_{R_j}(\boldsymbol{c}_j)$ with $N_j \gtrsim kR_j$ and for $j = 1, 2$. We take expansion (3.16) as an approach for solving the original far field operator splitting problem as introduced in the beginning of this chapter, and we approximate the solutions of this problem by solving suitable minimization problems. More precisely, we either search for them in these subspaces $\mathcal{V}_{N_j}^{\boldsymbol{c}_j}$ or $\mathcal{W}_{N_j}^{\boldsymbol{c}_j}$, $j = 1, 2$, or we enforce their sparsity or low rank property in another way.

Remark 3.17. Using the procedure described above, we treat the Born approximation (of order $p = 1$) of the scattering problem (2.1) exactly, so the linearization of this problem with respect to q. We replace all q dependent quantities u_q, u_q^s, u_q^∞ and F_q by their Born approximations $u_q^{(\leq 1)}$, $u_q^{s,(\leq 1)}$, $u_q^{\infty,(\leq 1)}$ and $F_q^{(\leq 1)}$ of order $p = 1$, respectively, and we observe that the scattered field $u_q^{s,(\leq 1)}(\,\cdot\,;\boldsymbol{\theta})$ for fixed $\boldsymbol{\theta} \in S^{d-1}$ then solves

$$\Delta u_q^{s,(\leq 1)}(\,\cdot\,;\boldsymbol{\theta}) + k^2 u_q^{s,(\leq 1)}(\,\cdot\,;\boldsymbol{\theta}) \;=\; -k^2 q u^i(\,\cdot\,;\boldsymbol{\theta}) \qquad \text{in } \mathbb{R}^d\,,$$

so indeed is a solution of the source problem for the Helmholtz equation with source term $-k^2 q u^i(\,\cdot\,;\boldsymbol{\theta})$. The splitting problem for this problem class has already been studied extensively in the case of single far field patterns in [50, 54, 55, 56]. We note that the concept of far field operators does not exist for source problems. Nevertheless, this link allows us to compare our results for far field operator splitting to the corresponding results for splitting individual far field patterns (cf. Remarks 3.21 (ii) and 3.25 (iii)). ◊

3.4.1. Sparsity-sparsity splitting

Splitting by solving a least squares problem

As a first approach, we seek approximations $\widetilde{F}_{q_1} \in \mathcal{V}_{N_1}^{c_1}$ and $\widetilde{F}_{q_2} \in \mathcal{V}_{N_2}^{c_2}$ of the far field operators F_{q_1} and F_{q_2}, corresponding to the individual components of the scatterer, satisfying the *least squares (LS) problem*

$$F_q \overset{\text{LS}}{=} \widetilde{F}_{q_1} + \widetilde{F}_{q_2} \qquad \text{in } \mathrm{HS}(L^2(S^{d-1}))\,. \tag{3.17}$$

The following two propositions give related uncertainty principles, from which we can conclude stability estimates for problem (3.17) due to Theorem 3.13. The notations that we use here have been introduced in Notations 2.7 and 2.15.

Proposition 3.18. *Let $d = 2$ and suppose that $G \in \mathcal{V}_{N_1}^{\boldsymbol{c}_1}$ and $H \in \mathcal{V}_{N_2}^{\boldsymbol{c}_2}$ for some $\boldsymbol{c}_1, \boldsymbol{c}_2 \in \mathbb{R}^2$ and $N_1, N_2 \in \mathbb{N}$. Then,*

$$\frac{|\langle G, H\rangle_{\mathrm{HS}}|}{\|G\|_{\mathrm{HS}}\|H\|_{\mathrm{HS}}} \leq \frac{\sqrt{\|\mathcal{T}_{\boldsymbol{c}_1} G\|_{\ell^0\times\ell^0}\|\mathcal{T}_{\boldsymbol{c}_2} H\|_{\ell^0\times\ell^0}}}{(k|\boldsymbol{c}_2 - \boldsymbol{c}_1|)^{\frac{2}{3}}} \leq \frac{(2N_1+1)(2N_2+1)}{(k|\boldsymbol{c}_1 - \boldsymbol{c}_2|)^{\frac{2}{3}}}\,. \tag{3.18}$$

If in addition $k|\boldsymbol{c}_1 - \boldsymbol{c}_2| > 2(N_1 + N_2 + 1)$, then

$$\frac{|\langle G, H\rangle_{\mathrm{HS}}|}{\|G\|_{\mathrm{HS}}\|H\|_{\mathrm{HS}}} \leq \frac{\sqrt{\|\mathcal{T}_{\boldsymbol{c}_1} G\|_{\ell^0\times\ell^0}\|\mathcal{T}_{\boldsymbol{c}_2} H\|_{\ell^0\times\ell^0}}}{k|c_2 - c_1|} \leq \frac{(2N_1+1)(2N_2+1)}{k|c_1 - c_2|}\,. \tag{3.19}$$

Proof. Using the Hölder's inequality and the mapping properties (2.53) and (2.52) of $\mathcal{T}_{\boldsymbol{c}}$ from Lemma 2.24 gives

$$\begin{aligned}|\langle G, H\rangle_{\mathrm{HS}}| \;&=\; |\langle \mathcal{T}_{\boldsymbol{c}_2} G, \mathcal{T}_{\boldsymbol{c}_2} H\rangle_{\ell^2\times\ell^2}| \;\leq\; \|\mathcal{T}_{\boldsymbol{c}_2} G\|_{\ell^\infty\times\ell^\infty}\|\mathcal{T}_{\boldsymbol{c}_2} H\|_{\ell^1\times\ell^1} \\ &=\; \|\mathcal{T}_{\boldsymbol{c}_2-\boldsymbol{c}_1}\mathcal{T}_{\boldsymbol{c}_1} G\|_{\ell^\infty\times\ell^\infty}\|\mathcal{T}_{\boldsymbol{c}_2} H\|_{\ell^1\times\ell^1} \;\leq\; \frac{1}{(k|\boldsymbol{c}_2 - \boldsymbol{c}_1|)^{\frac{2}{3}}}\|\mathcal{T}_{\boldsymbol{c}_1} G\|_{\ell^1\times\ell^1}\|\mathcal{T}_{\boldsymbol{c}_2} H\|_{\ell^1\times\ell^1}\end{aligned}$$

$$\leq \frac{\sqrt{\|\mathcal{T}_{\boldsymbol{c}_1} G\|_{\ell^0\times\ell^0}\|\mathcal{T}_{\boldsymbol{c}_2} H\|_{\ell^0\times\ell^0}}}{(k|\boldsymbol{c}_2-\boldsymbol{c}_1|)^{\frac{2}{3}}}\|\mathcal{T}_{\boldsymbol{c}_1} G\|_{\ell^2\times\ell^2}\|\mathcal{T}_{\boldsymbol{c}_2} H\|_{\ell^2\times\ell^2}$$
$$\leq \frac{(2N_1+1)(2N_2+1)}{(k|\boldsymbol{c}_2-\boldsymbol{c}_1|)^{\frac{2}{3}}}\|G\|_{\mathrm{HS}}\|H\|_{\mathrm{HS}}\,.$$

If in addition $k|\boldsymbol{c}_2-\boldsymbol{c}_1| > 2(N_1+N_2+1)$ and $N_1, N_2 \geq 1$, then using (2.54) instead of (2.53) gives (3.19). □

Proposition 3.19. *Let $d=3$ and suppose that $G \in \mathcal{V}_{N_1}^{\boldsymbol{c}_1}$ and $H \in \mathcal{V}_{N_2}^{\boldsymbol{c}_2}$ for some $\boldsymbol{c}_1, \boldsymbol{c}_2 \in \mathbb{R}^3$ and $N_1, N_2 \in \mathbb{N}$. Furthermore, denote $W_1 := \operatorname{supp}_{\ell^0\times\ell^0}(\mathcal{T}_{\boldsymbol{c}_1} G)$ and $W_2 := \operatorname{supp}_{\ell^0\times\ell^0}(\mathcal{T}_{\boldsymbol{c}_2} H)$. Then,*

$$\frac{|\langle G,H\rangle_{\mathrm{HS}}|}{\|G\|_{\mathrm{HS}}\|H\|_{\mathrm{HS}}} \leq \frac{\left(\sum_{(m,n)\in W_1}(2m+1)^2(2n+1)^2\right)^{\frac{1}{2}}\left(\sum_{(m,n)\in W_2}(2m+1)^2(2n+1)^2\right)^{\frac{1}{2}}}{(k|\boldsymbol{c}_1-\boldsymbol{c}_2|)^{\frac{5}{3}}}$$
$$\leq \frac{16}{9}\frac{(N_1+\frac{1}{2})(N_1+1)(N_1+\frac{3}{2})(N_2+\frac{1}{2})(N_2+1)(N_2+\frac{3}{2})}{(k|\boldsymbol{c}_1-\boldsymbol{c}_2|)^{\frac{5}{3}}}\,. \tag{3.20}$$

If in addition $k|\boldsymbol{c}_1-\boldsymbol{c}_2| > 2(N_1+N_2+3/2)$, then

$$\frac{|\langle G,H\rangle_{\mathrm{HS}}|}{\|G\|_{\mathrm{HS}}\|H\|_{\mathrm{HS}}} \leq \frac{\left(\sum_{(m,n)\in W_1}(2m+1)^2(2n+1)^2\right)^{\frac{1}{2}}\left(\sum_{(m,n)\in W_2}(2m+1)^2(2n+1)^2\right)^{\frac{1}{2}}}{(k|\boldsymbol{c}_1-\boldsymbol{c}_2|)^{2}}$$
$$\leq \frac{16}{9}\frac{(N_1+\frac{1}{2})(N_1+1)(N_1+\frac{3}{2})(N_2+\frac{1}{2})(N_2+1)(N_2+\frac{3}{2})}{(k|\boldsymbol{c}_1-\boldsymbol{c}_2|)^{2}}\,. \tag{3.21}$$

Proof. We proceed similarly to the proof of Proposition 3.18 and use Hölder's inequality and the mapping properties (2.60) and (2.59) of $\mathcal{T}_{\boldsymbol{c}}$ from Lemma 2.25 to obtain

$$\begin{aligned}
|\langle G,H\rangle_{\mathrm{HS}}| &= |\langle \mathcal{T}_{\boldsymbol{c}_2} G, \mathcal{T}_{\boldsymbol{c}_2} H\rangle_{\ell^2\times\ell^2}| \leq \|\mathcal{T}_{\boldsymbol{c}_2} G\|_{\ell^\infty_{1/(2n+1)}\times\ell^\infty_{1/(2n+1)}}\|\mathcal{T}_{\boldsymbol{c}_2} H\|_{\ell^1_{2n+1}\times\ell^1_{2n+1}}\\
&= \|\mathcal{T}_{\boldsymbol{c}_2-\boldsymbol{c}_1}\mathcal{T}_{\boldsymbol{c}_1} G\|_{\ell^\infty_{1/(2n+1)}\times\ell^\infty_{1/(2n+1)}}\|\mathcal{T}_{\boldsymbol{c}_2} H\|_{\ell^1_{2n+1}\times\ell^1_{2n+1}}\\
&\leq \frac{1}{(k|\boldsymbol{c}_2-\boldsymbol{c}_1|)^{\frac{5}{3}}}\|\mathcal{T}_{\boldsymbol{c}_1} G\|_{\ell^1_{2n+1}\times\ell^1_{2n+1}}\|\mathcal{T}_{\boldsymbol{c}_2} H\|_{\ell^1_{2n+1}\times\ell^1_{2n+1}}\\
&\leq \frac{\left(\sum_{(m,n)\in W_1}(2m+1)^2(2n+1)^2\right)^{\frac{1}{2}}\left(\sum_{(m,n)\in W_2}(2m+1)^2(2n+1)^2\right)^{\frac{1}{2}}}{(k|\boldsymbol{c}_1-\boldsymbol{c}_2|)^{\frac{5}{3}}}\|\mathcal{T}_{\boldsymbol{c}_1} G\|_{\ell^2\times\ell^2}\|\mathcal{T}_{\boldsymbol{c}_2} H\|_{\ell^2\times\ell^2}\\
&\leq \frac{16}{9}\frac{(N_1+\frac{1}{2})(N_1+1)(N_1+\frac{3}{2})(N_2+\frac{1}{2})(N_2+1)(N_2+\frac{3}{2})}{(k|\boldsymbol{c}_1-\boldsymbol{c}_2|)^{\frac{5}{3}}}\|G\|_{\mathrm{HS}}\|H\|_{\mathrm{HS}}\,.
\end{aligned}$$

Here, we used that, due to the second formula of Faulhaber $\sum_{j=1}^n j^2 = \frac{1}{6}n(n+1)(2n+1)$ (cf. e.g. [71]), it holds for $j=1,2$ that

$$\left(\sum_{(m,n)\in W_j}(2m+1)^2(2n+1)^2\right)^{\frac{1}{2}} \leq \sum_{n=0}^{N_j}(2n+1)^2 = \frac{4}{3}(N_j+\tfrac{1}{2})(N_j+1)(N_j+\tfrac{3}{2})\,, \tag{3.22}$$

see the proof of [56, Thm. 4.3]. For (3.21) we again have to replace (2.60) by its improved version (2.61). □

In the following theorem F_q^δ denotes a noisy observation of the exact far field operator F_q. We assume that a priori information on the approximate location of the individual scatterer's components is available, i.e., that the balls $B_{R_1}(\boldsymbol{c}_1)$ and $B_{R_2}(\boldsymbol{c}_2)$ are known. Accordingly, we choose $N_1 \gtrsim kR_1$

and $N_2 \gtrsim kR_2$ in the least squares problem (3.17) and compare the results for exact and noisy far field operators to establish a stability estimate. This generalizes the stability result for far field patterns from [55, Thm. 5.3] in two dimensions and [56, Thm. 5.1] in three dimensions to far field operators. The proof follows immediately from Theorem 3.13 and Propositions 3.18 and 3.19 under consideration of Remark 3.11.

Theorem 3.20. *Suppose that* $F_q, F_q^\delta \in \mathrm{HS}(L^2(S^{d-1}))$, *and let* $\boldsymbol{c}_1, \boldsymbol{c}_2 \in \mathbb{R}^d$ *and* $N_1, N_2 \in \mathbb{N}$ *with* $N_1 \gtrsim kR_1$ *and* $N_2 \gtrsim kR_2$ *such that* $C < 1$, *where*

$$C := \begin{cases} \frac{(2N_1+1)(2N_2+1)}{(k|\boldsymbol{c}_1-\boldsymbol{c}_2|)^{\frac{2}{3}}} & \text{if } d = 2\,, \\ \frac{16}{9}\,\frac{(N_1+\frac{1}{2})(N_1+1)(N_1+\frac{3}{2})(N_2+\frac{1}{2})(N_2+1)(N_2+\frac{3}{2})}{(k|\boldsymbol{c}_1-\boldsymbol{c}_2|)^{\frac{5}{3}}} & \text{if } d = 3\,. \end{cases}$$

Denote by $\widetilde{F}_{q_1}, \widetilde{F}_{q_2}$ *and* $\widetilde{F}_{q_1}^\delta, \widetilde{F}_{q_2}^\delta$ *the solutions to the least squares problems*

$$F_q \overset{\mathrm{LS}}{=} \widetilde{F}_{q_1} + \widetilde{F}_{q_2}\,, \qquad \widetilde{F}_{q_1} \in \mathcal{V}_{N_1}^{\boldsymbol{c}_1}\,,\ \widetilde{F}_{q_2} \in \mathcal{V}_{N_2}^{\boldsymbol{c}_2}\,, \tag{3.23a}$$

$$F_q^\delta \overset{\mathrm{LS}}{=} \widetilde{F}_{q_1}^\delta + \widetilde{F}_{q_2}^\delta\,, \qquad \widetilde{F}_{q_1}^\delta \in \mathcal{V}_{N_1}^{\boldsymbol{c}_1}\,,\ \widetilde{F}_{q_2}^\delta \in \mathcal{V}_{N_2}^{\boldsymbol{c}_2}\,, \tag{3.23b}$$

respectively. Then, for $j = 1, 2$,

$$\|\widetilde{F}_{q_j} - \widetilde{F}_{q_j}^\delta\|_{\mathrm{HS}}^2 \le (1 - C^2)^{-1}\|F_q - F_q^\delta\|_{\mathrm{HS}}^2\,. \tag{3.24}$$

Remark 3.21. If $k|\boldsymbol{c}_1 - \boldsymbol{c}_2| > 2(N_1 + N_2 + d/2)$ in Theorem 3.20, then the stability estimate (3.24) can be improved by replacing $C < 1$ by $\widetilde{C} < 1$, where

$$\widetilde{C} := \begin{cases} \frac{(2N_1+1)(2N_2+1)}{(k|\boldsymbol{c}_1-\boldsymbol{c}_2|)} & \text{if } d = 2\,, \\ \frac{16}{9}\,\frac{(N_1+\frac{1}{2})(N_1+1)(N_1+\frac{3}{2})(N_2+\frac{1}{2})(N_2+1)(N_2+\frac{3}{2})}{(k|\boldsymbol{c}_1-\boldsymbol{c}_2|)^2} & \text{if } d = 3\,. \end{cases}$$

This can be obtained by replacing (3.18) by (3.19) and (3.20) by (3.21) in Theorem 3.13, respectively. ◊

Splitting by solving an $\ell^1 \times \ell^1$ minimization problem

If a priori knowledge of the sizes R_j of the individual scatterers $D_j \subseteq B_{R_j}(\boldsymbol{c}_j)$, $j = 1, 2$, which is required to determine the cut-off parameters $N_j \gtrsim kR_j$ of the ansatz spaces in the least squares formulation (3.17), is not available but at least the approximate positions $\boldsymbol{c}_1$ and $\boldsymbol{c}_2$ are known, then (3.17) can be replaced by an $\ell^1 \times \ell^1$ *minimization problem*. Let

$$F_q \approx \widetilde{F}_{q_1}^0 + \widetilde{F}_{q_2}^0 \tag{3.25}$$

be an approximate decomposition of the exact far field operator with $\widetilde{F}_{q_1}^0 \in \mathcal{V}_{N_1}^{\boldsymbol{c}_1}$ and $\widetilde{F}_{q_2}^0 \in \mathcal{V}_{N_2}^{\boldsymbol{c}_2}$ for some $N_1 \gtrsim kR_1$ and $N_2 \gtrsim kR_2$, which could be the least squares solution of (3.17) but does not have to be computed. In (3.11), we replaced the original ill-posed far field operator splitting problem by a well-posed finite dimensional problem (cf. Theorem 3.20). The projection onto closed ansatz spaces has a regularizing effect. We now take a different approach and consider a Tikhonov regularization with an $\ell^1 \times \ell^1$ penalty term.

In two-dimensional case, we obtain the following $\ell^1 \times \ell^1$ penalized least squares problem. Given the far field operator F_q determine the solution $(\widetilde{F}_{q_1}, \widetilde{F}_{q_2}) \in \mathrm{HS}(L^2(S^1))^2$ of

$$\underset{(\widetilde{F}_{q_1}, \widetilde{F}_{q_2})}{\text{minimize}} \quad \|F_q - (\widetilde{F}_{q_1} + \widetilde{F}_{q_2})\|_{\mathrm{HS}}^2 + \mu(\|\mathcal{T}_{\boldsymbol{c}_1}\widetilde{F}_{q_1}\|_{\ell^1\times\ell^1} + \|\mathcal{T}_{\boldsymbol{c}_2}\widetilde{F}_{q_2}\|_{\ell^1\times\ell^1})\,. \tag{3.26}$$

Indeed the objective function of (3.26) is the Tikhonov functional of the following constrained $\ell^1 \times \ell^1$ minimization problem with Lagrange multiplier $1/\mu$. Given the far field operator F_q and a noise level $\delta > 0$ determine the solution $(\widetilde{F}_{q_1}, \widetilde{F}_{q_2}) \in \mathrm{HS}(L^2(S^1))^2$ of

$$\underset{(\widetilde{F}_{q_1},\widetilde{F}_{q_2})}{\text{minimize}} \quad \|\mathcal{T}_{\boldsymbol{c}_1}\widetilde{F}_{q_1}\|_{\ell^1\times\ell^1} + \|\mathcal{T}_{\boldsymbol{c}_2}\widetilde{F}_{q_1}\|_{\ell^1\times\ell^1} \quad \text{subject to} \quad \|F_q - (\widetilde{F}_{q_1} + \widetilde{F}_{q_2})\|_{\mathrm{HS}} \le \delta\,. \tag{3.27}$$

In literature this approach is known as *basis pursuit*, cf. [38, 26]. A more detailed discussion of the two problems (3.26) and (3.27) and how to solve them numerically can be found in Subsection 4.1.5.

In Theorem 3.23 below we establish a stability result for the $\ell^1 \times \ell^1$ minimization problem (3.27). For its proof we need the following lemma, for which we refer to [55, Lem. SM5.1].

Lemma 3.22. *For $J \in \mathbb{N}$ and $a_1, \dots, a_J \in \mathbb{R}$ there holds*

$$\sum_{j=1}^{J}\sum_{l\neq j} a_j a_l \;\le\; \frac{J-1}{J}\Big(\sum_{j=1}^{J} a_j\Big)^2 \;\le\; (J-1)\sum_{j=1}^{J} a_j^2\,.$$

As before, F_q^δ represents a noisy observation of the exact far field operator F_q. The bound $\delta_0 > 0$ in (3.28) describes the accuracy of the approximate exact solution from (3.25), which in case of the least squares solution corresponds to the error of the first order Born approximation and projection errors as in (2.25) and (2.39). The optimization problem (3.30) seeks an approximate decomposition of the given noisy far field operator F_q^δ that is close to the approximate exact solution and, thus, can be well approximated in the subspaces $\mathcal{V}_{N_1}^{\boldsymbol{c}_1}$ and $\mathcal{V}_{N_2}^{\boldsymbol{c}_2}$, without specifying $N_1, N_2 > 0$ in advance. Here, the assumption (3.29) guarantees that the approximate split (3.25) is feasible. The noise level $\delta > 0$ results from the data error combined with the accuracy δ_0 of the approximate exact solution.

Theorem 3.23. *Let $d = 2$ and suppose that $F_q \in \mathrm{HS}(L^2(S^1))$, let $\boldsymbol{c}_1, \boldsymbol{c}_2 \in \mathbb{R}^2$ and $N_1, N_2 \in \mathbb{N}$ with $N_1 \gtrsim kR_1$ and $N_2 \gtrsim kR_2$ such that for $j \in \{1,2\}$ it holds $C_j := 4(2N_j+1)^2(k|\boldsymbol{c}_1 - \boldsymbol{c}_2|)^{-2/3} < 1$. We assume that $\widetilde{F}_{q_1}^0 \in \mathcal{V}_{N_1}^{\boldsymbol{c}_1}$ and $\widetilde{F}_{q_2}^0 \in \mathcal{V}_{N_2}^{\boldsymbol{c}_2}$ are such that*

$$\|F_q - (\widetilde{F}_{q_1}^0 + \widetilde{F}_{q_2}^0)\|_{\mathrm{HS}} \;<\; \delta_0 \tag{3.28}$$

for some $\delta_0 > 0$. Moreover, suppose that $F_q^\delta \in \mathrm{HS}(L^2(S^1))$ and $\delta > 0$ satisfy

$$\delta \ge \delta_0 + \|F_q - F_q^\delta\|_{\mathrm{HS}} \tag{3.29}$$

and let $(\widetilde{F}_{q_1}^\delta, \widetilde{F}_{q_2}^\delta) \in \mathrm{HS}(L^2(S^1))^2$ denote the solution to

$$\underset{(\widetilde{F}_{q_1},\widetilde{F}_{q_2})}{\text{minimize}} \quad \|\mathcal{T}_{\boldsymbol{c}_1}\widetilde{F}_{q_1}\|_{\ell^1\times\ell^1} + \|\mathcal{T}_{\boldsymbol{c}_2}\widetilde{F}_{q_2}\|_{\ell^1\times\ell^1} \quad \text{subject to} \quad \|F_q^\delta - (\widetilde{F}_{q_1} + \widetilde{F}_{q_2})\|_{\mathrm{HS}} \le \delta\,. \tag{3.30}$$

Then,

$$\|\widetilde{F}_{q_j}^0 - \widetilde{F}_{q_j}^\delta\|_{\mathrm{HS}}^2 \;\le\; (1-C_j)^{-1}4\delta^2\,, \qquad j = 1,2\,. \tag{3.31}$$

Proof. We proceed as in the proof of [55, Thm. 6.1] and define $\widetilde{F}_1 := \widetilde{F}_{q_1}^0 - \widetilde{F}_{q_1}^\delta$ and $\widetilde{F}_2 := \widetilde{F}_{q_2}^0 - \widetilde{F}_{q_2}^\delta$. Moreover, we denote the $\ell^0 \times \ell^0$-support of $\mathcal{T}_{\boldsymbol{c}_1}\widetilde{F}_{q_1}^0$ and $\mathcal{T}_{\boldsymbol{c}_2}\widetilde{F}_{q_2}^0$ by W_1 and W_2, respectively. We estimate for $j \in \{1,2\}$

$$\begin{aligned}
\|\mathcal{T}_{\boldsymbol{c}_j}\widetilde{F}_{q_j}^\delta\|_{\ell^1\times\ell^1} &= \|\mathcal{T}_{\boldsymbol{c}_j}(\widetilde{F}_{q_j}^0 - \widetilde{F}_j)\|_{\ell^1\times\ell^1} = \|\mathcal{T}_{\boldsymbol{c}_j}(\widetilde{F}_{q_j}^0 - \widetilde{F}_j)\|_{\ell^1\times\ell^1(W_j)} + \|\mathcal{T}_{\boldsymbol{c}_j}\widetilde{F}_j\|_{\ell^1\times\ell^1(W_j^c)} \\
&= \|\mathcal{T}_{\boldsymbol{c}_j}(\widetilde{F}_{q_j}^0 - \widetilde{F}_j)\|_{\ell^1\times\ell^1(W_j)} + \|\mathcal{T}_{\boldsymbol{c}_j}\widetilde{F}_j\|_{\ell^1\times\ell^1} - \|\mathcal{T}_{\boldsymbol{c}_j}\widetilde{F}_j\|_{\ell^1\times\ell^1(W_j)} \\
&\ge \|\mathcal{T}_{\boldsymbol{c}_j}\widetilde{F}_{q_j}^0\|_{\ell^1\times\ell^1(W_j)} + \|\mathcal{T}_{\boldsymbol{c}_j}\widetilde{F}_j\|_{\ell^1\times\ell^1} - 2\|\mathcal{T}_{\boldsymbol{c}_j}\widetilde{F}_j\|_{\ell^1\times\ell^1(W_j)}\,.
\end{aligned}$$

Solving these inequalities for $\|\mathcal{T}_{\boldsymbol{c}_j}\widetilde{F}_j\|_{\ell^1\times\ell^1}$ and adding them up gives together with (3.30)

$$\|\mathcal{T}_{\boldsymbol{c}_1}\widetilde{F}_1\|_{\ell^1\times\ell^1}+\|\mathcal{T}_{\boldsymbol{c}_2}\widetilde{F}_2\|_{\ell^1\times\ell^1}\ \le\ 2\big(\|\mathcal{T}_{\boldsymbol{c}_1}\widetilde{F}_1\|_{(\ell^1\times\ell^1)(W_1)}+\|\mathcal{T}_{\boldsymbol{c}_2}\widetilde{F}_2\|_{(\ell^1\times\ell^1)(W_2)}\big)\,. \tag{3.32}$$

By using (3.28)–(3.30), we obtain

$$\begin{aligned}4\delta^2\ &\ge\ (\|F_q-F_q^\delta\|_{\mathrm{HS}}+\delta_0+\delta)^2\\ &\ge\ (\|F_q-F_q^\delta\|_{\mathrm{HS}}+\|F_q-(\widetilde{F}_{q_1}^0+\widetilde{F}_{q_2}^0)\|_{\mathrm{HS}}+\|F_q^\delta-(\widetilde{F}_{q_1}^\delta+\widetilde{F}_{q_2}^\delta)\|_{\mathrm{HS}})^2\ \ge\ \|\widetilde{F}_1+\widetilde{F}_2\|_{\mathrm{HS}}^2\\ &\ge\ \|\widetilde{F}_1\|_{\mathrm{HS}}^2+\|\widetilde{F}_2\|_{\mathrm{HS}}^2-2|\langle\widetilde{F}_1,\widetilde{F}_2\rangle_{\mathrm{HS}}|\ =\ \|\widetilde{F}_1\|_{\mathrm{HS}}^2+\|\widetilde{F}_2\|_{\mathrm{HS}}^2-2|\langle\mathcal{T}_{\boldsymbol{c}_2-\boldsymbol{c}_1}\mathcal{T}_{\boldsymbol{c}_1}\widetilde{F}_1,\mathcal{T}_{\boldsymbol{c}_2}\widetilde{F}_2\rangle_{\mathrm{HS}}|\,.\end{aligned}$$

For $a,b\ge 0$ the inequality of arithmetic and geometric means shows that $4ab\le(a+b)^2$. Further, it holds $(a+b)^2\le 2(a^2+b^2)$ by the second inequality of Lemma 3.22 for $J=2$. This implies together with (2.53), (3.32) and Hölder's inequality that

$$\begin{aligned}|\langle\mathcal{T}_{\boldsymbol{c}_2-\boldsymbol{c}_1}\mathcal{T}_{\boldsymbol{c}_1}\widetilde{F}_1,\mathcal{T}_{\boldsymbol{c}_2}\widetilde{F}_2\rangle_{\mathrm{HS}}|\ &\le\ \|\mathcal{T}_{\boldsymbol{c}_2-\boldsymbol{c}_1}\mathcal{T}_{\boldsymbol{c}_1}\widetilde{F}_1\|_{\ell^\infty\times\ell^\infty}\|\mathcal{T}_{\boldsymbol{c}_2}\widetilde{F}_2\|_{\ell^1\times\ell^1}\\ &\le\ (k|\boldsymbol{c}_1-\boldsymbol{c}_2|)^{-\frac{2}{3}}\|\mathcal{T}_{\boldsymbol{c}_1}\widetilde{F}_1\|_{\ell^1\times\ell^1}\|\mathcal{T}_{\boldsymbol{c}_2}\widetilde{F}_2\|_{\ell^1\times\ell^1}\\ &\le\ \frac{1}{4(k|\boldsymbol{c}_1-\boldsymbol{c}_2|)^{\frac{2}{3}}}\Big(\|\mathcal{T}_{\boldsymbol{c}_1}\widetilde{F}_1\|_{\ell^1\times\ell^1}+\|\mathcal{T}_{\boldsymbol{c}_2}\widetilde{F}_2\|_{\ell^1\times\ell^1}\Big)^2\\ &\le\ \frac{1}{(k|\boldsymbol{c}_1-\boldsymbol{c}_2|)^{\frac{2}{3}}}\Big(\|\mathcal{T}_{\boldsymbol{c}_1}\widetilde{F}_1\|_{\ell^1\times\ell^1(W_1)}+\|\mathcal{T}_{\boldsymbol{c}_2}\widetilde{F}_2\|_{\ell^1\times\ell^1(W_2)}\Big)^2\\ &\le\ \frac{1}{(k|\boldsymbol{c}_1-\boldsymbol{c}_2|)^{\frac{2}{3}}}\Big(\|\mathcal{T}_{\boldsymbol{c}_1}\widetilde{F}_1\|_{\ell^0\times\ell^0}^{\frac12}\|\widetilde{F}_1\|_{\mathrm{HS}}+\|\mathcal{T}_{\boldsymbol{c}_2}\widetilde{F}_2\|_{\ell^0\times\ell^0}^{\frac12}\|\widetilde{F}_2\|_{\mathrm{HS}}\Big)^2\\ &\le\ \frac{2}{(k|\boldsymbol{c}_1-\boldsymbol{c}_2|)^{\frac{2}{3}}}\Big(\|\mathcal{T}_{\boldsymbol{c}_1}\widetilde{F}_1\|_{\ell^0\times\ell^0}\|\widetilde{F}_1\|_{\mathrm{HS}}^2+\|\mathcal{T}_{\boldsymbol{c}_2}\widetilde{F}_2\|_{\ell^0\times\ell^0}\|\widetilde{F}_2\|_{\mathrm{HS}}^2\Big)\\ &=\ \frac12\Big(C_1\|\widetilde{F}_1\|_{\mathrm{HS}}^2+C_2\|\widetilde{F}_2\|_{\mathrm{HS}}^2\Big)\,.\end{aligned} \tag{3.33}$$

Overall, this first gives

$$4\delta^2\ \ge\ (1-C_1)\|\widetilde{F}_1\|_{\mathrm{HS}}^2+(1-C_2)\|\widetilde{F}_2\|_{\mathrm{HS}}^2$$

and then (3.31) by dropping one of the summands . □

In the three-dimensional case, we have to modify the considered minimization problem (3.27) according to the mapping properties of the translation operator in Lemma 2.25. This leads to the following *weighted $\ell^1\times\ell^1$ minimization problem*. Given the far field operator F_q and a noise level $\delta>0$ determine the solution $(\widetilde{F}_{q_1},\widetilde{F}_{q_2})\in\mathrm{HS}(L^2(S^2))^2$ of

$$\underset{(\widetilde{F}_{q_1},\widetilde{F}_{q_2})}{\text{minimize}}\quad \|\mathcal{T}_{\boldsymbol{c}_1}\widetilde{F}_{q_1}\|_{\ell^1_{2n+1}\times\ell^1_{2n+1}}+\|\mathcal{T}_{\boldsymbol{c}_2}\widetilde{F}_{q_1}\|_{\ell^1_{2n+1}\times\ell^1_{2n+1}}\quad\text{subject to}\quad \|F_q-(\widetilde{F}_{q_1}+\widetilde{F}_{q_2})\|_{\mathrm{HS}}\le\delta\,. \tag{3.34}$$

In Theorem 3.24 below we establish an associated stability result, that is structured as in Theorem 3.23.

Theorem 3.24. *Let $d=3$ and suppose that $F_q\in\mathrm{HS}(L^2(S^2))$, let $\boldsymbol{c}_1,\boldsymbol{c}_2\in\mathbb{R}^3$ and $N_1,N_2\in\mathbb{N}$ with $N_1\gtrsim kR_1$ and $N_2\gtrsim kR_2$ such that for $j\in\{1,2\}$,*

$$C_j:=\frac{64}{9}\,\frac{(N_j+\frac12)^2(N_j+1)^2(N_j+\frac32)^2}{(k|\boldsymbol{c}_1-\boldsymbol{c}_2|)^{\frac53}}<1\,.$$

We assume that $\widetilde{F}_{q_1}^0\in\mathcal{V}_{N_1}^{\boldsymbol{c}_1}$ and $\widetilde{F}_{q_2}^0\in\mathcal{V}_{N_2}^{\boldsymbol{c}_2}$ are such that

$$\|F_q-(\widetilde{F}_{q_1}^0+\widetilde{F}_{q_2}^0)\|_{\mathrm{HS}}\ <\ \delta_0$$

for some $\delta_0 > 0$. *Moreover, suppose that* $F_q^\delta \in \mathrm{HS}(L^2(S^2))$ *and* $\delta > 0$ *satisfy*

$$\delta \geq \delta_0 + \|F_q - F_q^\delta\|_{\mathrm{HS}}$$

and let $(\widetilde{F}_{q_1}^\delta, \widetilde{F}_{q_2}^\delta) \in \mathrm{HS}(L^2(S^2))^2$ *denote the solution to*

$$\underset{(F_{q_1},F_{q_2})}{\text{minimize}} \quad \|\mathcal{T}_{\boldsymbol{c}_1} F_{q_1}\|_{\ell^1_{2n+1}\times\ell^1_{2n+1}} + \|\mathcal{T}_{\boldsymbol{c}_2} F_{q_2}\|_{\ell^1_{2n+1}\times\ell^1_{2n+1}} \quad \text{subject to} \quad \|F_q^\delta - (F_{q_1} + F_{q_2})\|_{\mathrm{HS}} \leq \delta\,.$$

Then,

$$\|\widetilde{F}_{q_j}^0 - \widetilde{F}_{q_j}^\delta\|_{\mathrm{HS}}^2 \leq (1 - C_j)^{-1} 4\delta^2\,, \qquad j = 1, 2\,. \tag{3.35}$$

Proof. We define $\widetilde{F}_1 := \widetilde{F}_{q_1}^0 - \widetilde{F}_{q_1}^\delta$ and $\widetilde{F}_2 := \widetilde{F}_{q_2}^0 - \widetilde{F}_{q_2}^\delta$, and we denote the $\ell^0 \times \ell^0$-support of $\mathcal{T}_{c_1}\widetilde{F}_{q_1}^0$ and $\mathcal{T}_{c_2}\widetilde{F}_{q_2}^0$ by W_1 and W_2, respectively. Then, as in the proof of Theorem 3.23 (cf. (3.32)) we can show

$$\|\mathcal{T}_{c_1}\widetilde{F}_1\|_{\ell^1_{2n+1}\times\ell^1_{2n+1}} + \|\mathcal{T}_{c_2}\widetilde{F}_2\|_{\ell^1_{2n+1}\times\ell^1_{2n+1}} \leq 2\big(\|\mathcal{T}_{c_1}\widetilde{F}_1\|_{(\ell^1_{2n+1}\times\ell^1_{2n+1})(W_1)} + \|\mathcal{T}_{c_2}\widetilde{F}_2\|_{(\ell^1_{2n+1}\times\ell^1_{2n+1})(W_2)}\big)\,. \tag{3.36}$$

Analogously to (3.33), we obtain, by using (2.60) and (3.36) instead of (2.53) and (3.32), that

$$\begin{aligned}
|\langle \mathcal{T}_{\boldsymbol{c}_2-\boldsymbol{c}_1}\mathcal{T}_{\boldsymbol{c}_1}\widetilde{F}_1, \mathcal{T}_{\boldsymbol{c}_2}\widetilde{F}_2\rangle_{\mathrm{HS}}| &\leq \|\mathcal{T}_{\boldsymbol{c}_2-\boldsymbol{c}_1}\mathcal{T}_{\boldsymbol{c}_1}\widetilde{F}_1\|_{\ell^\infty_{1/(2n+1)}\times\ell^\infty_{1/(2n+1)}} \|\mathcal{T}_{\boldsymbol{c}_2}\widetilde{F}_2\|_{\ell^1_{2n+1}\times\ell^1_{2n+1}} \\
&\leq (k|\boldsymbol{c}_1 - \boldsymbol{c}_2|)^{-\frac{5}{3}} \|\mathcal{T}_{\boldsymbol{c}_1}\widetilde{F}_1\|_{\ell^1_{2n+1}\times\ell^1_{2n+1}} \|\mathcal{T}_{\boldsymbol{c}_2}\widetilde{F}_2\|_{\ell^1_{2n+1}\times\ell^1_{2n+1}} \\
&\leq \frac{1}{4(k|\boldsymbol{c}_1 - \boldsymbol{c}_2|)^{\frac{5}{3}}} \Big(\|\mathcal{T}_{\boldsymbol{c}_1}\widetilde{F}_1\|_{\ell^1_{2n+1}\times\ell^1_{2n+1}} + \|\mathcal{T}_{\boldsymbol{c}_2}\widetilde{F}_2\|_{\ell^1_{2n+1}\times\ell^1_{2n+1}}\Big)^2 \\
&\leq \frac{1}{(k|\boldsymbol{c}_1 - \boldsymbol{c}_2|)^{\frac{5}{3}}} \Big(\|\mathcal{T}_{\boldsymbol{c}_1}\widetilde{F}_1\|_{\ell^1_{2n+1}\times\ell^1_{2n+1}(W_1)} + \|\mathcal{T}_{\boldsymbol{c}_2}\widetilde{F}_2\|_{\ell^1_{2n+1}\times\ell^1_{2n+1}(W_2)}\Big)^2 \\
&\leq \frac{1}{2}\Big(C_1\|\widetilde{F}_1\|_{\mathrm{HS}}^2 + C_2\|\widetilde{F}_2\|_{\mathrm{HS}}^2\Big)\,.
\end{aligned}$$

For the last step, we used that

$$\begin{aligned}
\|\mathcal{T}_{c_j}\widetilde{F}_j\|_{\ell^1_{2n+1}\times\ell^1_{2n+1}(W_j)} &\leq \Big(\sum_{(m,n)\in W_j} (2m+1)^2(2n+1)^2\Big)^{\frac{1}{2}} \|\widetilde{F}_j\|_{\mathrm{HS}} \\
&\leq \frac{4}{3}(N_j + \tfrac{1}{2})(N_j + 1)(N_j + \tfrac{3}{2})\|\widetilde{F}_j\|_{\mathrm{HS}}
\end{aligned}$$

for $j \in \{1, 2\}$, due to (3.22). Proceeding as in the proof of Theorem 3.23 yields the result. □

Remark 3.25. (i) If $k|\boldsymbol{c}_1 - \boldsymbol{c}_2| > 2(N_1 + N_2 + d/2)$ in Theorems 3.23 and 3.24, then the related stability estimates can as in Remark 3.21 be improved by replacing $C_j < 1$ by $\widetilde{C_j} < 1$ for $j = 1, 2$, where

$$\widetilde{C_j} := \begin{cases} \frac{4(2N_j+1)^2}{k|\boldsymbol{c}_1-\boldsymbol{c}_2|} & \text{if } d = 2\,, \\ \frac{64}{9}\,\frac{(N_j+\frac{1}{2})^2(N_j+1)^2(N_j+\frac{3}{2})^2}{(k|\boldsymbol{c}_1-\boldsymbol{c}_2|)^2} & \text{if } d = 3\,. \end{cases}$$

(ii) Let $C < 1$ in Theorem 3.20 and $C_j < 1$, $j = 1, 2$, in Theorems 3.23 and 3.24. We compare the asymptotic behavior of the stability bound (3.24) with those of the bounds (3.31) and (3.35). For all choices of N_1, N_2 and $\boldsymbol{c}_1, \boldsymbol{c}_2$ such that above assumptions hold, we have that $C < C_j$, $j = 1, 2$. This means, that at some point solving the least squares problem is always more stable than solving the $\ell^1 \times \ell^1$ minimization problem. This remains true, when inserting the improved constants $\widetilde{C}$ and $\widetilde{C}_j$, $j = 1, 2$.

(iii) Recalling (2.7), it would be possible to split the far field operator F_q by splitting the far field patterns $u_q^\infty(\,\cdot\,;\boldsymbol{\theta})$ for each incident direction $\boldsymbol{\theta} \in S^{d-1}$ individually. This can be realized by applying the methods developed in [50, 54, 55], cf. Remark 3.17. However, comparing the stability estimate of single far field patterns $u_q^\infty(\,\cdot\,;\boldsymbol{\theta})$ established in [55, Thms. 5.3, 6.1] for two dimensions and in [56, Thm. 5.1] for three dimensions with the related stability estimate for splitting of whole far field operator F_q, we find that the latter is more stable. The stability estimates are of the same structure but the constants C, $\widetilde{C}$, C_j and $\widetilde{C}_j$, $j = 1, 2$, developed in this work are the squares of the corresponding constants in [55, 56]. Considering the additional improvement achieved by applying the reciprocity relation as will be outlined in Subsection 3.6.1 below, this demonstrates a significant advantage of the algorithms developed in this work when it comes to splitting entire far field operators. Furthermore, the improved version of the splitting scheme, which takes multiple scattering into account and which we discuss in the next subsection, is not applicable for splitting single far field patterns at all. ◊

3.4.2. Rank-sparsity splitting

So far, we used that $F_{q_1}^{(\leq 1)}$ can be well approximated by a sparse operator in the subspace $\mathcal{V}_{N_1}^{\boldsymbol{c}_1}$ associated to the scatterer's component supported in $B_{R_1}(\boldsymbol{c}_1)$ with $N_1 \gtrsim kR_1$. From Theorems 2.11 and 2.19 we further know that $F_{q_1}^{(\leq 1)}$ has a low rank approximation in the subspace $\mathcal{W}_{N_1}^{\boldsymbol{c}_1}$. Therefore, again taking equation (3.16) as an approach, we replace the original far field operator splitting problem by the problem of splitting F_q into a low rank component in $\mathcal{W}_{N_1}^{\boldsymbol{c}_1}$ and a sparse component in $\mathcal{V}_{N_2}^{\boldsymbol{c}_2}$. In signal processing, such a problem, to decompose a given matrix into a low rank and a sparse component, is known as *Principal Component Analysis* or *robust Principal Component Analysis* if, as in our situation, possible additive noise is included in consideration. In this context, the singular functions of the low rank component are called *principal components* (cf. e.g. [19, Subsec. 1.4]). It will turn out that considering this problem has the advantage that only the position $\boldsymbol{c}_2$ of the second scatterer's component needs to be known in advance for determining the modulated Fourier basis with respect to which the associated far field operator component F_{q_2} is sparse. If it is the other way around, i.e., if only $\boldsymbol{c}_1$ is known, switch the roles of q_1 and q_2. Thus, compared to the $\ell^1 \times \ell^1$ minimization problem (3.27), this further reduces the required a priori knowledge on the scatterer's location. The reason for this lies in the invariance of the rank and the nuclear norm with respect to the translation operator $\mathcal{T}_{\boldsymbol{c}_1}$. This is proven in the lemma below. In contrast to that, the (weighted) $\ell^1 \times \ell^1$ norm is affected by the translation operator, which is indicated by formula (2.51) for the translated Fourier coefficients (for $d = 2$) or formula (2.58) for the translated spherical harmonics components (for $d = 3$), respectively.

Lemma 3.26. *For all $\boldsymbol{c} \in \mathbb{R}^d$ and $G \in \mathrm{HS}(L^2(S^{d-1}))$ we have, that*

$$\operatorname{rank}(\mathcal{T}_{\boldsymbol{c}} G) \;=\; \operatorname{rank} G \qquad \textit{and} \qquad \|\mathcal{T}_{\boldsymbol{c}} G\|_{\mathrm{nuc}} \;=\; \|G\|_{\mathrm{nuc}}\,.$$

Proof. Let $(\sigma_n; u_n, v_n)_{1 \leq n \leq \operatorname{rank} G}$ denote a singular system for $G \in \mathrm{HS}(L^2(S^{d-1}))$ (see Theorem A.1). Then, for arbitrary $\boldsymbol{c} \in \mathbb{R}^d$ there holds

$$\mathcal{T}_{\boldsymbol{c}} G \;=\; \sum_{n=1}^{\operatorname{rank} G} \sigma_n T_{\boldsymbol{c}} u_n \langle\,\cdot\,, T_{\boldsymbol{c}} v_n\rangle_{L^2(S^{d-1})}\,.$$

From

$$\langle T_{\boldsymbol{c}} u_n, T_{\boldsymbol{c}} u_m\rangle_{L^2(S^{d-1})} \;=\; \langle T_{\boldsymbol{c}-\boldsymbol{c}} u_n, u_m\rangle_{L^2(S^{d-1})} \;=\; \langle u_n, u_m\rangle_{L^2(S^{d-1})} \;=\; \delta_n^m \qquad \text{for all } n, m\,,$$

we conclude that $(T_{\boldsymbol{c}} u_n)_n$ as well as $(T_{\boldsymbol{c}} v_n)_n$ are again orthonormal systems. Thus, a singular system for $\mathcal{T}_{\boldsymbol{c}} G$ is given by $(\sigma_n; T_{\boldsymbol{c}} u_n, T_{\boldsymbol{c}} v_n)_{1 \leq n \leq \operatorname{rank} G}$, which finishes the proof. □

SPLITTING BY SOLVING A LEAST SQUARES PROBLEM

Based on the above observation, we consider as a first approach the following *least squares problem*, which fits into the general framework of Section 3.3. Given the exact far field operator F_q find approximations $\widetilde{F}_{q_1} \in \mathcal{W}_{N_1}^{\boldsymbol{c}_1}$ and $\widetilde{F}_{q_2} \in \mathcal{V}_{N_2}^{\boldsymbol{c}_2}$ for the far field operators F_{q_1} and F_{q_2} such that

$$F_q \overset{\text{LS}}{=} \widetilde{F}_{q_1} + \widetilde{F}_{q_2} \qquad \text{in } \mathrm{HS}(L^2(S^{d-1}))\,. \tag{3.37}$$

We clarify that problem (3.37) is of no practical relevance, but for free after developing the associated uncertainty principles in Propositions 3.27 and 3.28. Compared to the least squares problem (3.23), it provides a worse stability bound that comes with the same a priori required knowledge (cf. Theorem 3.20 and Corollary 3.30).

The following propositions give uncertainty principles that involve the subspaces $\mathcal{W}_{N_1}^{\boldsymbol{c}_1}$ and $\mathcal{V}_{N_2}^{\boldsymbol{c}_2}$.

Proposition 3.27. *Let $d = 2$ and suppose that $G \in \mathcal{W}_{N_1}^{\boldsymbol{c}_1}$ and $H \in \mathcal{V}_{N_2}^{\boldsymbol{c}_2}$ for some $\boldsymbol{c}_1, \boldsymbol{c}_2 \in \mathbb{R}^2$ and $N_1, N_2 \in \mathbb{N}$. Then,*

$$\begin{aligned}\frac{|\langle G, H\rangle_{\mathrm{HS}}|}{\|G\|_{\mathrm{HS}}\|H\|_{\mathrm{HS}}} &\le 2\sup_{o\in\mathbb{Z}}\left(\sum_{|m-o|\le \operatorname{rank} G} J_m^2(k|\boldsymbol{c}_1-\boldsymbol{c}_2|)\|\mathcal{T}_{\boldsymbol{c}_2}H\|_{\ell^0\times\ell^0}\right)^{\frac{1}{2}}\\ &\le \frac{2\sqrt{2N_1+1}(2N_2+1)}{(k|\boldsymbol{c}_1-\boldsymbol{c}_2|)^{\frac{1}{3}}}\,.\end{aligned} \tag{3.38}$$

Proof. Since we have $G \in \mathcal{W}_{N_1}^{\boldsymbol{c}_1}$, there holds $\mathcal{T}_{\boldsymbol{c}_2}G \in \mathcal{W}_{N_1}^{\boldsymbol{c}_1-\boldsymbol{c}_2}$. We estimate

$$\begin{aligned}|\langle G, H\rangle_{\mathrm{HS}}| &= |\langle \mathcal{T}_{\boldsymbol{c}_2}G, \mathcal{T}_{\boldsymbol{c}_2}H\rangle_{\ell^2\times\ell^2}| \le \|\mathcal{T}_{\boldsymbol{c}_2}G\|_{\ell^\infty\times\ell^\infty}\|\mathcal{T}_{\boldsymbol{c}_2}H\|_{\ell^1\times\ell^1}\\ &\le \|\mathcal{P}_{\mathcal{W}_{N_1}^{\boldsymbol{c}_1-\boldsymbol{c}_2}}(\mathcal{T}_{\boldsymbol{c}_2}G)\|_{\ell^\infty\times\ell^\infty}\sqrt{\|\mathcal{T}_{\boldsymbol{c}_2}H\|_{\ell^0\times\ell^0}}\|\mathcal{T}_{\boldsymbol{c}_2}H\|_{\mathrm{HS}}\\ &\le (2N_2+1)\|\mathcal{P}_{\mathcal{W}_{N_1}^{\boldsymbol{c}_1-\boldsymbol{c}_2}}(\mathcal{T}_{\boldsymbol{c}_2}G)\|_{\ell^\infty\times\ell^\infty}\|H\|_{\mathrm{HS}}\,,\end{aligned} \tag{3.39}$$

so it remains to bound $\|\mathcal{P}_{\mathcal{W}_{N_1}^{\boldsymbol{c}_1-\boldsymbol{c}_2}}(\mathcal{T}_{\boldsymbol{c}_2}G)\|_{\ell^\infty\times\ell^\infty}$ in terms of $\|G\|_{\mathrm{HS}}$. We use the abbreviation $\boldsymbol{c} := \boldsymbol{c}_1 - \boldsymbol{c}_2$ and proceed similarly to the proof of [25, Prop. 4]. Based on expansion (2.24), we decompose the orthogonal projection $\mathcal{P}_{\mathcal{W}_{N_1}^{\boldsymbol{c}}}$ onto $\mathcal{W}_{N_1}^{\boldsymbol{c}}$ according to

$$\mathcal{P}_{\mathcal{W}_{N_1}^{\boldsymbol{c}}}F = P_{V_{N_1}^{\boldsymbol{c}}}\circ F + F\circ P_{V_{N_1}^{\boldsymbol{c}}} - P_{V_{N_1}^{\boldsymbol{c}}}\circ F\circ P_{V_{N_1}^{\boldsymbol{c}}}\,, \qquad F\in\mathrm{HS}(L^2(S^1))\,, \tag{3.40a}$$

where $P_{V_{N_1}^{\boldsymbol{c}}} : L^2(S^1) \to L^2(S^1)$ is given by $P_{V_{N_1}^{\boldsymbol{c}}}g := \sum_{|n|\le N_1} T_{-\boldsymbol{c}}\boldsymbol{e}_n\langle g, T_{-\boldsymbol{c}}\boldsymbol{e}_n\rangle_{L^2(S^1)}$ (cf. Remark 2.22) Consequently, there holds for arbitrary $F \in \mathrm{HS}(L^2(S^1))$ and $g \in L^2(S^1)$

$$(P_{V_{N_1}^{\boldsymbol{c}}}\circ F)g = P_{V_{N_1}^{\boldsymbol{c}}}(Fg) = \sum_{|m|\le N_1} T_{-\boldsymbol{c}}\boldsymbol{e}_m\langle Fg, T_{-\boldsymbol{c}}\boldsymbol{e}_m\rangle_{L^2(S^1)}\,, \tag{3.40b}$$

$$(F\circ P_{V_{N_1}^{\boldsymbol{c}}})g = F(P_{V_{N_1}^{\boldsymbol{c}}}g) = \sum_{|n|\le N_1} F(T_{-\boldsymbol{c}}\boldsymbol{e}_n)\langle g, T_{-\boldsymbol{c}}\boldsymbol{e}_n\rangle_{L^2(S^1)}\,, \tag{3.40c}$$

$$(P_{V_{N_1}^{\boldsymbol{c}}}\circ F\circ P_{V_{N_1}^{\boldsymbol{c}}})g = (\mathcal{P}_{\mathcal{V}_{N_1}^{\boldsymbol{c}}}F)g = \sum_{|m|\le N_1}\sum_{|n|\le N_1}\langle F(T_{-\boldsymbol{c}}\boldsymbol{e}_n), T_{-\boldsymbol{c}}\boldsymbol{e}_m\rangle_{L^2(S^1)}\,T_{-\boldsymbol{c}}\boldsymbol{e}_m\langle g, T_{-\boldsymbol{c}}\boldsymbol{e}_n\rangle_{L^2(S^1)}\,. \tag{3.40d}$$

Using (3.40a) and the triangle inequality, we continue to estimate

$$\|\mathcal{P}_{\mathcal{W}_{N_1}^{\boldsymbol{c}}}(\mathcal{T}_{\boldsymbol{c}_2}G)\|_{\ell^\infty\times\ell^\infty} \le \|P_{V_{N_1}^{\boldsymbol{c}}}\circ(\mathcal{T}_{\boldsymbol{c}_2}G)\|_{\ell^\infty\times\ell^\infty} + \|(I-P_{V_{N_1}^{\boldsymbol{c}}})\circ(\mathcal{T}_{\boldsymbol{c}_2}G)\circ P_{V_{N_1}^{\boldsymbol{c}}}\|_{\ell^\infty\times\ell^\infty}\,. \tag{3.41}$$

Bound for the first summand in (3.41): By expanding (3.40b) for $g \in L^2(S^1)$, we obtain that

$$P_{V_{N_1}^{\boldsymbol{c}}} \circ (\mathcal{T}_{\boldsymbol{c}_2} G) g = \sum_{|m| \le N_1} T_{-\boldsymbol{c}} \boldsymbol{e}_m \langle (\mathcal{T}_{\boldsymbol{c}_2} G) g, T_{-\boldsymbol{c}} \boldsymbol{e}_m \rangle_{L^2(S^1)}$$
$$= \sum_{o,l \in \mathbb{Z}} \left(\sum_{|m| \le N_1} \langle T_{-\boldsymbol{c}} \boldsymbol{e}_m, \boldsymbol{e}_o \rangle_{L^2(S^1)} \langle (\mathcal{T}_{\boldsymbol{c}_2} G) \boldsymbol{e}_l, T_{-\boldsymbol{c}} \boldsymbol{e}_m \rangle_{L^2(S^1)} \right) \boldsymbol{e}_o \langle g, \boldsymbol{e}_l \rangle_{L^2(S^1)} .$$

Together with the Cauchy Schwarz inequality and Parseval's identity this yields

$$\| P_{V_{N_1}^{\boldsymbol{c}}} \circ (\mathcal{T}_{\boldsymbol{c}_2} G) \|_{\ell^\infty \times \ell^\infty} = \sup_{o,l \in \mathbb{Z}} \left| \sum_{|m| \le N_1} \langle T_{-\boldsymbol{c}} \boldsymbol{e}_m, \boldsymbol{e}_o \rangle_{L^2(S^1)} \langle (\mathcal{T}_{\boldsymbol{c}_2} G) \boldsymbol{e}_l, T_{-\boldsymbol{c}} \boldsymbol{e}_m \rangle_{L^2(S^1)} \right|$$
$$\le \sup_{o \in \mathbb{Z}} \left(\sum_{|m| \le N_1} |\langle T_{-\boldsymbol{c}} \boldsymbol{e}_m, \boldsymbol{e}_o \rangle_{L^2(S^1)}|^2 \right)^{\frac{1}{2}} \sup_{l \in \mathbb{Z}} \left(\sum_{|m| \le N_1} |\langle (\mathcal{T}_{\boldsymbol{c}_2} G) \boldsymbol{e}_l, T_{-\boldsymbol{c}} \boldsymbol{e}_m \rangle_{L^2(S^1)}|^2 \right)^{\frac{1}{2}}$$
$$\le \sup_{o \in \mathbb{Z}} \left(\sum_{|m| \le N_1} |\langle T_{-\boldsymbol{c}} \boldsymbol{e}_m, \boldsymbol{e}_o \rangle_{L^2(S^1)}|^2 \right)^{\frac{1}{2}} \sup_{l \in \mathbb{Z}} \| (\mathcal{T}_{\boldsymbol{c}_2} G) \boldsymbol{e}_l \|_{L^2(S^1)} .$$

The second factor can be bounded by $\|\mathcal{T}_{\boldsymbol{c}_2} G\| \le \|\mathcal{T}_{\boldsymbol{c}_2} G\|_{\mathrm{HS}} = \|G\|_{\mathrm{HS}}$ by using the definition of the operator norm, (A.7) and (2.52). For the first factor, we conclude from the Jacobi–Anger expansion (B.12) that

$$|\langle T_{-\boldsymbol{c}} \boldsymbol{e}_m, \boldsymbol{e}_o \rangle_{L^2(S^1)}| = \left| \sum_{n \in \mathbb{Z}} (-\mathrm{i})^n J_n(k|\boldsymbol{c}|) e^{-\mathrm{i} n \arg c} \underbrace{\langle \boldsymbol{e}_n, \boldsymbol{e}_{o-m} \rangle_{L^2(S^1)}}_{=\delta^n_{o-m}} \right| = |J_{o-m}(k|\boldsymbol{c}|)| . \tag{3.42}$$

All in all, the first summand in (3.41) can be bounded by

$$\| P_{V_{N_1}^{\boldsymbol{c}}} \circ (\mathcal{T}_{\boldsymbol{c}_2} G) \|_{\ell^\infty \times \ell^\infty} \le \sup_{o \in \mathbb{Z}} \left(\sum_{|m| \le N_1} J^2_{o-m}(k|\boldsymbol{c}|) \right)^{\frac{1}{2}} \|G\|_{\mathrm{HS}} = \sup_{o \in \mathbb{Z}} \left(\sum_{|m-o| \le N_1} J^2_m(k|\boldsymbol{c}|) \right)^{\frac{1}{2}} \|G\|_{\mathrm{HS}} .$$

Bound for the second summand in (3.41): By expanding (3.40c)–(3.40d), we obtain that

$$((I - P_{V_{N_1}^{\boldsymbol{c}}}) \circ (\mathcal{T}_{\boldsymbol{c}_2} G) \circ P_{V_{N_1}^{\boldsymbol{c}}}) g$$
$$= \sum_{|m| > N_1} \sum_{|n| \le N_1} \langle (\mathcal{T}_{\boldsymbol{c}_2} G)(T_{-\boldsymbol{c}} \boldsymbol{e}_n), T_{-\boldsymbol{c}} \boldsymbol{e}_m \rangle_{L^2(S^1)} T_{-\boldsymbol{c}} \boldsymbol{e}_m \langle g, T_{-\boldsymbol{c}} \boldsymbol{e}_n \rangle_{L^2(S^1)} = \sum_{o,l \in \mathbb{Z}} b_{o,l} \, \boldsymbol{e}_o \langle g, \boldsymbol{e}_l \rangle_{L^2(S^1)}$$

with

$$b_{o,l} = \sum_{|m| > N_1} \sum_{|n| \le N_1} \langle \boldsymbol{e}_l, T_{-\boldsymbol{c}} \boldsymbol{e}_n \rangle_{L^2(S^1)} \langle T_{-\boldsymbol{c}} \boldsymbol{e}_m, \boldsymbol{e}_o \rangle_{L^2(S^1)} \langle (\mathcal{T}_{\boldsymbol{c}_2} G) T_{-\boldsymbol{c}} \boldsymbol{e}_n, T_{-\boldsymbol{c}} \boldsymbol{e}_m \rangle_{L^2(S^1)}$$

for $o, l \in \mathbb{Z}$. We apply the Cauchy Schwarz inequality to conclude

$$\| (I - P_{V_{N_1}^{\boldsymbol{c}}}) \circ (\mathcal{T}_{\boldsymbol{c}_2} G) \circ P_{V_{N_1}^{\boldsymbol{c}}} \|_{\ell^\infty \times \ell^\infty} = \sup_{o,l \in \mathbb{Z}} |b_{o,l}|$$
$$= \sup_{o,l \in \mathbb{Z}} \left| \sum_{|m| > N_1} \sum_{|n| \le N_1} \langle \boldsymbol{e}_l, T_{-\boldsymbol{c}} \boldsymbol{e}_n \rangle_{L^2(S^1)} \langle T_{-\boldsymbol{c}} \boldsymbol{e}_m, \boldsymbol{e}_o \rangle_{L^2(S^1)} \langle (\mathcal{T}_{\boldsymbol{c}_2} G) T_{-\boldsymbol{c}} \boldsymbol{e}_n, T_{-\boldsymbol{c}} \boldsymbol{e}_m \rangle_{L^2(S^1)} \right|$$

$$
\begin{aligned}
&\leq \sup_{o,l\in\mathbb{Z}} \left(\sum_{|m|>N_1} \sum_{|n|\leq N_1} |\langle \boldsymbol{e}_l, T_{-\boldsymbol{c}} \boldsymbol{e}_n \rangle_{L^2(S^1)} \langle T_{-\boldsymbol{c}} \boldsymbol{e}_m, \boldsymbol{e}_o \rangle_{L^2(S^1)}|^2 \right)^{\frac{1}{2}} \\
&\qquad \times \left(\sum_{|m|>N_1} \sum_{|n|\leq N_1} |\langle (\mathcal{T}_{\boldsymbol{c}_2} G) T_{-\boldsymbol{c}} \boldsymbol{e}_n, T_{-\boldsymbol{c}} \boldsymbol{e}_m \rangle_{L^2(S^1)}|^2 \right)^{\frac{1}{2}} \\
&= \sup_{l\in\mathbb{Z}} \left(\sum_{|n|\leq N_1} |\langle \boldsymbol{e}_l, T_{-\boldsymbol{c}} \boldsymbol{e}_n \rangle_{L^2(S^1)}|^2 \right)^{\frac{1}{2}} \sup_{o\in\mathbb{Z}} \left(\sum_{|m|>N_1} |\langle T_{-\boldsymbol{c}} \boldsymbol{e}_m, \boldsymbol{e}_o \rangle_{L^2(S^1)}|^2 \right)^{\frac{1}{2}} \\
&\quad \times \left(\sum_{|m|>N_1} \sum_{|n|\leq N_1} |\langle (\mathcal{T}_{\boldsymbol{c}_2} G) T_{-\boldsymbol{c}} \boldsymbol{e}_n, T_{-\boldsymbol{c}} \boldsymbol{e}_m \rangle_{L^2(S^1)}|^2 \right)^{\frac{1}{2}} .
\end{aligned}
$$

By using Parseval's identity, the first formula in (A.6) for the Hilbert–Schmidt norm, (3.42) and (2.52), we further estimate

$$
\begin{aligned}
&\| (I - P_{V^{\mathbf{c}}_{N_1}}) \circ (\mathcal{T}_{\boldsymbol{c}_2} G) \circ P_{V^{\mathbf{c}}_{N_1}} \|_{\ell^\infty \times \ell^\infty} \\
&\leq \sup_{l\in\mathbb{Z}} \left(\sum_{|n|\leq N_1} J_{l-n}^2(k|\boldsymbol{c}|) \right)^{\frac{1}{2}} \sup_{o\in\mathbb{Z}} \|\boldsymbol{e}_o\|_{L^2(S^1)} \left(\sum_{n\in\mathbb{Z}} \|(\mathcal{T}_{\boldsymbol{c}_2} G) T_{-\boldsymbol{c}} \boldsymbol{e}_n\|_{L^2(S^1)}^2 \right)^{\frac{1}{2}} \\
&= \sup_{l\in\mathbb{Z}} \left(\sum_{|n-l|\leq N_1} J_n^2(k|\boldsymbol{c}|) \right)^{\frac{1}{2}} \|\mathcal{T}_{\boldsymbol{c}_2} G\|_{\mathrm{HS}} = \sup_{l\in\mathbb{Z}} \left(\sum_{|n-l|\leq N_1} J_n^2(k|\boldsymbol{c}|) \right)^{\frac{1}{2}} \|G\|_{\mathrm{HS}} .
\end{aligned}
$$

Altogether, this yields

$$
\|\mathcal{P}_{\mathcal{W}^{\mathbf{c}}_{N_1}} (\mathcal{T}_{\boldsymbol{c}_2} G)\|_{\ell^\infty \times \ell^\infty} \leq 2 \sup_{o\in\mathbb{Z}} \left(\sum_{|n-o|\leq N_1} J_n^2(k|\boldsymbol{c}|) \right)^{\frac{1}{2}} \|G\|_{\mathrm{HS}} \leq \frac{2\sqrt{2N_1+1}}{(k|\boldsymbol{c}|)^{\frac{1}{3}}} \|G\|_{\mathrm{HS}} ,
$$

due to the bound (B.8) for $|J_n(k|\boldsymbol{c}|)|$. Substituting this into (3.39) ends the proof. □

Proposition 3.28. *Let $d = 3$ and suppose that $G \in \mathcal{W}^{\boldsymbol{c}_1}_{N_1}$ and $H \in \mathcal{V}^{\boldsymbol{c}_2}_{N_2}$ for some $\boldsymbol{c}_1, \boldsymbol{c}_2 \in \mathbb{R}^2$ and $N_1, N_2 \in \mathbb{N}$. Then,*

$$
\frac{|\langle G, H \rangle_{\mathrm{HS}}|}{\|G\|_{\mathrm{HS}} \|H\|_{\mathrm{HS}}} \leq \frac{4(2N_1+1)\sqrt{2(N_1^2+2N_1+\frac{1}{2})}(2N_2+1)^2(N_2^2+2N_2+\frac{1}{2})}{(k|\boldsymbol{c}_1-\boldsymbol{c}_2|)^{\frac{5}{6}}} . \tag{3.43}
$$

Proof. We use the abbreviation $\boldsymbol{c} := \boldsymbol{c}_1 - \boldsymbol{c}_2$ and denote by W_2 the $\ell^0 \times \ell^0$-support of $\mathcal{T}_{\boldsymbol{c}_2} H$. We obtain similarly to the previous proof that

$$
\begin{aligned}
|\langle G, H \rangle_{\mathrm{HS}}| &\leq \|\mathcal{T}_{\boldsymbol{c}_2} G\|_{\ell^\infty_{(2n+1)^{-3/2}} \times \ell^\infty_{(2n+1)^{-3/2}}} \|\mathcal{T}_{\boldsymbol{c}_2} H\|_{\ell^1_{(2n+1)^{3/2}} \times \ell^1_{(2n+1)^{3/2}}} \\
&\leq \|\mathcal{P}_{\mathcal{W}^{\mathbf{c}}_{N_1}} (\mathcal{T}_{\boldsymbol{c}_2} G)\|_{\ell^\infty_{(2n+1)^{-3/2}} \times \ell^\infty_{(2n+1)^{-3/2}}} \left(\sum_{(m,n)\in W_2} (2m+1)^3 (2n+1)^3 \right)^{\frac{1}{2}} \|H\|_{\mathrm{HS}} .
\end{aligned}
$$

As in (3.22), we bound the second factor with the third formula of Faulhaber $\sum_{j=1}^n j^3 = n^2(n+1)^2/4$ (cf. e.g. [71]) according to

$$
\left(\sum_{(m,n)\in W_2} (2m+1)^3 (2n+1)^3 \right)^{\frac{1}{2}} \leq \sum_{n=0}^{N_2} (2n+1)^3 = 2(N_2+1)^2(N_2^2+2N_2+\tfrac{1}{2}) ,
$$

which yields

$$|\langle G, H\rangle_{\mathrm{HS}}| \leq 2(N_2+1)^2(N_2^2+2N_2+\tfrac{1}{2})\|\mathcal{P}_{\mathcal{W}^{\boldsymbol{c}}_{N_1}}(\mathcal{T}_{\boldsymbol{c}_2}G)\|_{\ell^\infty_{(2n+1)^{-3/2}}\times\ell^\infty_{(2n+1)^{-3/2}}}\|H\|_{\mathrm{HS}}\,. \tag{3.44}$$

It remains to bound $\|\mathcal{P}_{\mathcal{W}^{\boldsymbol{c}}_{N_1}}(\mathcal{T}_{\boldsymbol{c}_2}G)\|_{\ell^\infty_{(2n+1)^{-3/2}}\times\ell^\infty_{(2n+1)^{-3/2}}}$ in terms of $\|G\|_{\mathrm{HS}}$. Similar to the previous proof we decompose

$$\mathcal{P}_{\mathcal{W}^{\boldsymbol{c}}_{N_1}}F \;=\; P^{\boldsymbol{c}}_{N_1}\circ F + F\circ P^{\boldsymbol{c}}_{N_1} - P^{\boldsymbol{c}}_{N_1}\circ F\circ P^{\boldsymbol{c}}_{N_1}\,,\qquad F\in\mathrm{HS}(L^2(S^2))\,,$$

where $P_{V^{\boldsymbol{c}}_{N_1}}:L^2(S^2)\to L^2(S^2)$ is due to (B.16) given by

$$P_{V^{\boldsymbol{c}}_{N_1}}g := \sum_{n=0}^{N_1}\sum_{m=-n}^{n}\langle g, T_{-\boldsymbol{c}}Y^m_n\rangle_{L^2(S^2)}T_{-\boldsymbol{c}}Y^m_n \;=\; \sum_{n=0}^{N_1}\frac{4\pi}{2n+1}\int_{S^2}e^{\mathrm{i}kc\cdot(\boldsymbol{\omega}-\,\cdot\,)}P_n((\,\cdot\,)\cdot\boldsymbol{\omega})g(\boldsymbol{\omega})\,\mathrm{d}s(\boldsymbol{\omega})\,.$$

Consequently, it holds for arbitrary $F\in\mathrm{HS}(L^2(S^2))$ and $g\in L^2(S^2)$

$$(P_{V^{\boldsymbol{c}}_{N_1}}\circ F)g \;=\; P^{\boldsymbol{c}}_{N_1}(Fg) \;=\; \sum_{m=0}^{N_1}\sum_{o=-m}^{m}T_{-\boldsymbol{c}}Y^o_m\langle Fg, T_{-\boldsymbol{c}}Y^o_m\rangle_{L^2(S^2)}\,, \tag{3.45a}$$

$$(F\circ P_{V^{\boldsymbol{c}}_{N_1}})g \;=\; F(P^{\boldsymbol{c}}_{N_1}g) \;=\; \sum_{n=0}^{N_1}\sum_{p=-n}^{n}F(T_{-\boldsymbol{c}}Y^p_n)\langle g, T_{-\boldsymbol{c}}Y^p_n\rangle_{L^2(S^2)}\,, \tag{3.45b}$$

$$(P_{V^{\boldsymbol{c}}_{N_1}}\circ F\circ P_{V^{\boldsymbol{c}}_{N_1}})g \;=\; (\mathcal{P}_{\mathcal{V}^{\boldsymbol{c}}_{N_1}}F)g \tag{3.45c}$$

$$\;=\; \sum_{m,n=0}^{N_1}\sum_{o=-m}^{m}\sum_{p=-n}^{n}\langle F(T_{-\boldsymbol{c}}Y^p_n), T_{-\boldsymbol{c}}Y^o_m\rangle_{L^2(S^2)}\,T_{-\boldsymbol{c}}Y^o_m\langle g, T_{-\boldsymbol{c}}Y^p_n\rangle_{L^2(S^2)}\,, \tag{3.45d}$$

see (2.37). As in (3.41) we have

$$\begin{aligned}&\|\mathcal{P}_{\mathcal{W}^{\boldsymbol{c}}_{N_1}}(\mathcal{T}_{\boldsymbol{c}_2}G)\|_{\ell^\infty_{(2n+1)^{-3/2}}\times\ell^\infty_{(2n+1)^{-3/2}}}\\ &\quad\leq \|P_{V^{\boldsymbol{c}}_{N_1}}\circ(\mathcal{T}_{\boldsymbol{c}_2}G)\|_{\ell^\infty_{(2n+1)^{-3/2}}\times\ell^\infty_{(2n+1)^{-3/2}}} + \|(I-P_{V^{\boldsymbol{c}}_{N_1}})\circ(\mathcal{T}_{\boldsymbol{c}_2}G)\circ P_{V^{\boldsymbol{c}}_{N_1}}\|_{\ell^\infty_{(2n+1)^{-3/2}}\times\ell^\infty_{(2n+1)^{-3/2}}}\,.\end{aligned} \tag{3.46}$$

Bound for the first summand in (3.46): Since the (r,s)th spherical harmonics component of the operator in the first summand of (3.46) is due to (3.45a) and (B.19) given by

$$\frac{(2r+1)(2s+1)}{16\pi^2}\sum_{m=0}^{N_1}\sum_{o=-m}^{m}\langle T_{-\boldsymbol{c}}Y^o_m, P^{\widehat{\boldsymbol{x}}}_r\rangle_{L^2(S^2)}\langle(\mathcal{T}_{\boldsymbol{c}}G)P^{\boldsymbol{\theta}}_s, T_{-\boldsymbol{c}}Y^o_m\rangle_{L^2(S^2)}\,,$$

we can estimate

$$\begin{aligned}&\|P_{V^{\boldsymbol{c}}_{N_1}}\circ(\mathcal{T}_{\boldsymbol{c}_2}G)\|_{\ell^\infty_{(2n+1)^{-3/2}}\times\ell^\infty_{(2n+1)^{-3/2}}}\\ &= \frac{1}{16\pi^2}\sup_{r,s\in\mathbb{N}_0}\frac{1}{\sqrt{(2r+1)(2s+1)}}\\ &\quad\times\left(\int_{S^2}\int_{S^2}\left|\sum_{m=0}^{N_1}\sum_{o=-m}^{m}\langle T_{-\boldsymbol{c}}Y^o_m, P^{\widehat{\boldsymbol{x}}}_r\rangle_{L^2(S^2)}\langle(\mathcal{T}_{\boldsymbol{c}}G)P^{\boldsymbol{\theta}}_s, T_{-\boldsymbol{c}}Y^o_m\rangle_{L^2(S^2)}\right|^2\mathrm{d}s(\boldsymbol{\theta})\,\mathrm{d}s(\widehat{\boldsymbol{x}})\right)^{\frac{1}{2}}\\ &\leq \frac{1}{16\pi^2}\sup_{r\in\mathbb{N}_0}\left(\frac{1}{2r+1}\int_{S^2}\sum_{m=0}^{N_1}\sum_{o=-m}^{m}|\langle T_{-\boldsymbol{c}}Y^o_m, P^{\widehat{\boldsymbol{x}}}_r\rangle_{L^2(S^2)}|^2\,\mathrm{d}s(\widehat{\boldsymbol{x}})\right)^{\frac{1}{2}}\end{aligned}$$

$$\times \sup_{s\in\mathbb{N}_0}\left(\frac{1}{2s+1}\int_{S^2}\sum_{m=0}^{N_1}\sum_{o=-m}^{m}|\langle(\mathcal{T}_{\boldsymbol{c}}G)P_s^{\boldsymbol{\theta}},T_{-\boldsymbol{c}}Y_m^o\rangle_{L^2(S^2)}|^2\,\mathrm{d}s(\boldsymbol{\theta})\right)^{\frac{1}{2}}.$$

By using Parseval's identity, the definition of the operator norm and (B.17) we bound the second factor by

$$\begin{aligned}\sup_{s\in\mathbb{N}_0}\left(\frac{1}{2s+1}\int_{S^2}\|(\mathcal{T}_{\boldsymbol{c}}G)P_s^{\boldsymbol{\theta}}\|_{L^2(S^2)}^2\,\mathrm{d}s(\boldsymbol{\theta})\right)^{\frac{1}{2}} &\le \sup_{s\in\mathbb{N}_0}\left(\frac{1}{2s+1}\int_{S^2}\|P_s^{\boldsymbol{\theta}}\|_{L^2(S^2)}^2\,\mathrm{d}s(\boldsymbol{\theta})\right)^{\frac{1}{2}}\|G\|\\ &\le 4\pi\sup_{s\in\mathbb{N}_0}\left(\frac{1}{2s+1}\right)\|G\|_{\mathrm{HS}} = 4\pi\|G\|_{\mathrm{HS}}.\end{aligned}$$

For the first factor, we obtain using the Jacobi–Anger expansion (B.24), Lemma B.4, formulas (B.17) and (2.63) and the bound (B.22) for $|j_p(k|\boldsymbol{c}|)|$ that

$$\begin{aligned}|\langle T_{-\boldsymbol{c}}Y_m^o,P_r^{\widehat{\boldsymbol{x}}}\rangle_{L^2(S^2)}| &= \left|\sum_{p=|m-r|}^{m+r}\mathrm{i}^p(2p+1)j_p(k|\boldsymbol{c}|)\langle\widehat{P_p^{-\boldsymbol{c}}}Y_m^o,P_r^{\widehat{\boldsymbol{x}}}\rangle_{L^2(S^2)}\right|\\ &\le \|Y_m^o\|_{L^2(S^2)}\sum_{p=|m-r|}^{m+r}(2p+1)|j_p(k|\boldsymbol{c}|)|\|\widehat{P_p^{-\boldsymbol{c}}}\|_{L^\infty(S^2))}\|P_r^{\widehat{\boldsymbol{x}}}\|_{L^2(S^2)}\\ &\le \frac{\sqrt{4\pi}}{\sqrt{2r+1}(k|\boldsymbol{c}|)^{\frac{5}{6}}}\sum_{p=|m-r|}^{m+r}(2p+1) = \frac{\sqrt{4\pi(2r+1)}(2m+1)}{(k|\boldsymbol{c}|)^{\frac{5}{6}}}.\end{aligned}$$

Altogether, the first summand in (3.46) can be bounded by

$$\begin{aligned}\|P_{V_{N_1}^{\boldsymbol{c}}}\circ(\mathcal{T}_{\boldsymbol{c}_2}G)\|_{\ell^\infty_{(2n+1)^{-3/2}}\times\ell^\infty_{(2n+1)^{-3/2}}} &\le \frac{1}{(k|\boldsymbol{c}|)^{\frac{5}{6}}}\left(\sum_{m=0}^{N_1}(2m+1)^3\right)^{\frac{1}{2}}\|G\|_{\mathrm{HS}}\\ &= \frac{(2N_1+1)\sqrt{2(N_1^2+2N_1+\frac{1}{2})}}{(k|\boldsymbol{c}|)^{\frac{5}{6}}}\|G\|_{\mathrm{HS}}.\end{aligned}$$

Bound for the second summand in (3.46): We expand (3.45b)–(3.45c) by using (B.16) and obtain that the (r,s)th spherical harmonics component of the operator in the second summand of (3.46) is given by

$$\begin{aligned}&\frac{(2r+1)(2s+1)}{16\pi^2}\sum_{m=N_1+1}^{\infty}\sum_{n=0}^{N_1}\sum_{o=-m}^{m}\sum_{p=-n}^{n}\langle T_{-\boldsymbol{c}}Y_m^o,P_r^{\widehat{\boldsymbol{x}}}\rangle_{L^2(S^2)}\\ &\qquad\times\langle P_s^{\boldsymbol{\theta}},T_{-\boldsymbol{c}}Y_n^p\rangle_{L^2(S^2)}\langle(\mathcal{T}_{\boldsymbol{c}_2}G)T_{-\boldsymbol{c}}Y_n^p,T_{-\boldsymbol{c}}Y_m^o\rangle_{L^2(S^2)},\end{aligned}$$

so

$$\begin{aligned}&\|(I-P_{V_{N_1}^{\boldsymbol{c}}})\circ(\mathcal{T}_{\boldsymbol{c}_2}G)\circ P_{V_{N_1}^{\boldsymbol{c}}}\|_{\ell^\infty_{(2n+1)^{-3/2}}\times\ell^\infty_{(2n+1)^{-3/2}}}\\ &= \frac{1}{16\pi^2}\sup_{r,s\in\mathbb{N}_0}\frac{1}{\sqrt{(2r+1)(2s+1)}}\left(\int_{S^2}\int_{S^2}\left|\sum_{m=N_1+1}^{\infty}\sum_{n=0}^{N_1}\sum_{o=-m}^{m}\sum_{p=-n}^{n}\langle T_{-\boldsymbol{c}}Y_m^o,P_r^{\widehat{\boldsymbol{x}}}\rangle_{L^2(S^2)}\right.\right.\\ &\quad\left.\left.\times\langle P_s^{\boldsymbol{\theta}},T_{-\boldsymbol{c}}Y_n^p\rangle_{L^2(S^2)}\langle(\mathcal{T}_{\boldsymbol{c}}G)T_{-\boldsymbol{c}}Y_n^p,T_{-\boldsymbol{c}}Y_m^o\rangle_{L^2(S^2)}\right|^2\mathrm{d}s(\boldsymbol{\theta})\,\mathrm{d}s(\widehat{\boldsymbol{x}})\right)^{\frac{1}{2}}\end{aligned}$$

$$\leq \frac{1}{16\pi^2} \sup_{s\in\mathbb{N}_0} \left(\frac{1}{2s+1} \int_{S^2} \sum_{n=0}^{N_1} \sum_{p=-n}^{n} |\langle P_s^{\boldsymbol{\theta}}, T_{-\boldsymbol{c}} Y_n^p \rangle_{L^2(S^2)}|^2 \, \mathrm{d}s(\boldsymbol{\theta}) \right)^{\frac{1}{2}}$$
$$\times \sup_{r\in\mathbb{N}_0} \left(\frac{1}{2r+1} \int_{S^2} \sum_{m=N_1+1}^{\infty} \sum_{o=-m}^{m} |\langle T_{-\boldsymbol{c}} Y_m^o, P_r^{\widehat{\boldsymbol{x}}} \rangle_{L^2(S^2)}|^2 \, \mathrm{d}s(\widehat{\boldsymbol{x}}) \right)^{\frac{1}{2}}$$
$$\times \left(\sum_{m=N_1+1}^{\infty} \sum_{n=0}^{N_1} \sum_{o=-m}^{m} \sum_{p=-n}^{n} |\langle (\mathcal{T}_{\boldsymbol{c}_2} G) T_{-\boldsymbol{c}} Y_n^p, T_{-\boldsymbol{c}} Y_m^o \rangle_{L^2(S^2)}|^2 \right)^{\frac{1}{2}}.$$

With the same techniques, which we used in the first part of this proof, we can estimate the first factor by

$$\sup_{s\in\mathbb{N}_0} \left(\frac{1}{2s+1} \int_{S^2} \sum_{n=0}^{N_1} \sum_{p=-n}^{n} |\langle P_s^{\boldsymbol{\theta}}, T_{-\boldsymbol{c}} Y_n^p \rangle_{L^2(S^2)}|^2 \, \mathrm{d}s(\boldsymbol{\theta}) \right)^{\frac{1}{2}} \leq \frac{4\pi(2N_1+1)\sqrt{2(N_1^2+2N_1+\frac{1}{2})}}{(k|\boldsymbol{c}|)^{\frac{5}{6}}}$$

and the second factor by

$$\sup_{r\in\mathbb{N}_0} \left(\frac{1}{2r+1} \int_{S^2} \sum_{m=N_1+1}^{\infty} \sum_{o=-m}^{m} |\langle T_{-\boldsymbol{c}} Y_m^o, P_r^{\widehat{\boldsymbol{x}}} \rangle_{L^2(S^2)}|^2 \, \mathrm{d}s(\widehat{\boldsymbol{x}}) \right)^{\frac{1}{2}} \leq 4\pi \,.$$

For the third factor we use Parseval's identity and formula (A.6) for the Hilbert–Schmidt norm to bound

$$\sum_{m=N_1+1}^{\infty} \sum_{n=0}^{N_1} \sum_{o=-m}^{m} \sum_{p=-n}^{n} |\langle (\mathcal{T}_{\boldsymbol{c}_2} G) T_{-\boldsymbol{c}} Y_n^p, T_{-\boldsymbol{c}} Y_m^o \rangle_{L^2(S^2)}|^2 \leq \sum_{n=0}^{N_1} \sum_{p=-n}^{n} \|(\mathcal{T}_{\boldsymbol{c}_2} G) T_{-\boldsymbol{c}} Y_n^p\|_{L^2(S^2)}^2 \leq \|G\|_{\mathrm{HS}}^2 \,.$$

All in all, we obtain the same upper bound as for the first summand in (3.46). Substituting this into (3.44) ends the proof. □

Remark 3.29. (i) If in Propositions 3.27 and 3.28 in addition $k|\boldsymbol{c}_1 - \boldsymbol{c}_2| > 2(N_1 + N_2 + d/2)$, then we have

$$\frac{|\langle G, H \rangle_{\mathrm{HS}}|}{\|G\|_{\mathrm{HS}} \|H\|_{\mathrm{HS}}} \leq \begin{cases} \frac{2\sqrt{2N_1+1}(2N_2+1)}{(k|\boldsymbol{c}_1-\boldsymbol{c}_2|)^{\frac{1}{2}}} & \text{if } d=2\,, \\ \frac{4(2N_1+1)\sqrt{2(N_1^2+2N_1+\frac{1}{2})}(2N_2+1)^2(N_2^2+2N_2+\frac{1}{2})}{k|\boldsymbol{c}_1-\boldsymbol{c}_2|} & \text{if } d=3\,. \end{cases}$$

This can be shown by replacing (B.8) by (B.9) in the proof of Proposition 3.27 or (B.22) by (B.23) in the proof of Proposition 3.28, respectively.

(ii) Provided the upper bounds in Propositions 3.27 and 3.28 are smaller than 1, then the derived upper bounds in the uncertainty principles (3.18) or (3.20) involving the subspaces $\mathcal{V}_{N_1}^{\boldsymbol{c}_1}$ and $\mathcal{V}_{N_2}^{\boldsymbol{c}_2}$ are always smaller than the upper bounds in the uncertainty principle (3.38) or (3.43) involving $\mathcal{W}_{N_1}^{\boldsymbol{c}_1}$ and $\mathcal{V}_{N_2}^{\boldsymbol{c}_2}$, respectively. This goes well with $\mathcal{V}_N^{\boldsymbol{c}} \subseteq \mathcal{W}_N^{\boldsymbol{c}}$ (cf. Remarks 2.10 (ii) and 2.18 (iii) and Definition and Corollary 2.21).

(iii) In literature (cf. [24, 25]), our notion of an uncertainty principle is substituted by the concept of *rank-sparsity incoherence*. This is based on the quantities

$$\xi := \sup_{G\in\mathcal{W}_{N_1}^{\boldsymbol{c}_1-\boldsymbol{c}_2},\, \|G\|\leq 1} \|G\|_{\ell^\infty\times\ell^\infty} \qquad \text{and} \qquad \mu := \sup_{G\in\mathcal{V}_{N_2},\, \|G\|_{\ell^\infty\times\ell^\infty}\leq 1} \|G\| \,.$$

A sufficient condition for $\mathcal{W}_{N_1}^{\boldsymbol{c}_1} \cap \mathcal{V}_{N_2}^{\boldsymbol{c}_2} = \{0\}$ or equivalently $\mathcal{W}_{N_1}^{\boldsymbol{c}_1-\boldsymbol{c}_2} \cap \mathcal{V}_{N_2} = \{0\}$ is then given

by $\xi\mu < 1$. On the one hand, ξ being small means that the Fourier coefficients of operators in $\mathcal{W}_{N_1}^{\boldsymbol{c}_1-\boldsymbol{c}_2}$ are 'diffuse' in the sense that they cannot become too large in scales of their largest singular value. On the other hand, μ being small means that the spectrum of operators in $\mathcal{V}_{N_2}$ is 'diffuse' in the sense that their singular values are small in scales of their largest Fourier coefficient.

Comparing our proof of Theorems 3.27 and 3.28 with the proof [25, Prop. 4] clarifies that $\xi\mu < 1$ is a more restrictive assumption. This suggests that our later developed stability estimates will not be sharp. However, these upper bounds in (3.38) and in (3.43) have a concrete meaning regarding the scatterer's geometry. In terms of the wave number k, the sizes of the scatterer's components must be sufficiently small, and their mutual distances must be sufficiently large, such that these bounds are strictly smaller than one. ◊

The following theorem provides a stability result for the least squares problem (3.37). This follows immediately from Theorem 3.13 together with Propositions 3.27 and 3.28. As mentioned above, it is of no practical relevance and is presented just for completeness.

Corollary 3.30. *Suppose that* $F_q, F_q^\delta \in \mathrm{HS}(L^2(S^{d-1}))$, *and let* $\boldsymbol{c}_1, \boldsymbol{c}_2 \in \mathbb{R}^d$ *and* $N_1, N_2 \in \mathbb{N}$ *with* $N_1 \gtrsim kR_1$ *and* $N_2 \gtrsim kR_2$ *such that* $C < 1$, *where*

$$C := \begin{cases} \frac{2\sqrt{2N_1+1}(2N_2+1)}{(k|\boldsymbol{c}_1-\boldsymbol{c}_2|)^{\frac{1}{3}}} & \text{if } d = 2\,, \\ \frac{4(2N_1+1)\sqrt{2(N_1^2+2N_1+\frac{1}{2})}(2N_2+1)^2(N_2^2+2N_2+\frac{1}{2})}{(k|\boldsymbol{c}_1-\boldsymbol{c}_2|)^{\frac{5}{6}}} & \text{if } d = 3\,. \end{cases}$$

Denote by $\widetilde{F}_{q_1}, \widetilde{F}_{q_2}$ *and* $\widetilde{F}_{q_1}^\delta, \widetilde{F}_{q_2}^\delta$ *the solutions to the least squares problems*

$$F_q \overset{\mathrm{LS}}{=} \widetilde{F}_{q_1} + \widetilde{F}_{q_2}\,, \qquad \widetilde{F}_{q_1} \in \mathcal{W}_{N_1}^{\boldsymbol{c}_1}\,,\ \widetilde{F}_{q_2} \in \mathcal{V}_{N_2}^{\boldsymbol{c}_2}\,,$$
$$F_q^\delta \overset{\mathrm{LS}}{=} \widetilde{F}_{q_1}^\delta + \widetilde{F}_{q_2}^\delta\,, \qquad \widetilde{F}_{q_1}^\delta \in \mathcal{W}_{N_1}^{\boldsymbol{c}_1}\,,\ \widetilde{F}_{q_2}^\delta \in \mathcal{V}_{N_2}^{\boldsymbol{c}_2}\,,$$

respectively. Then, for $j = 1, 2$,

$$\|\widetilde{F}_{q_j} - \widetilde{F}_{q_j}^\delta\|_{\mathrm{HS}}^2 \le (1-C^2)^{-1}\|F_q - F_q^\delta\|_{\mathrm{HS}}^2\,. \tag{3.47}$$

Remark 3.31. If $k|\boldsymbol{c}_1 - \boldsymbol{c}_2| > 2(N_1 + N_2 + d/2)$ in Corollary 3.30, then as in Remark 3.21 the stability estimate (3.47) can be improved by replacing $C < 1$ by $\widetilde{C} < 1$, where

$$\widetilde{C} := \begin{cases} \frac{2\sqrt{2N_1+1}(2N_2+1)}{(k|\boldsymbol{c}_1-\boldsymbol{c}_2|)^{\frac{1}{2}}} & \text{if } d = 2\,, \\ \frac{4(2N_1+1)\sqrt{2(N_1^2+2N_1+\frac{1}{2})}(2N_2+1)^2(N_2^2+2N_2+\frac{1}{2})}{k|\boldsymbol{c}_1-\boldsymbol{c}_2|} & \text{if } d = 3\,. \end{cases}$$

◊

SPLITTING BY SOLVING A COUPLED NUCLEAR NORM AND $\ell^1 \times \ell^1$ MINIMIZATION

In this subsection, we restrict ourselves to two dimensions. In principle, the results below can also be extended to three dimensions. However, since the two-dimensional case already turns out to be highly technical and involved, we do not pursue this in this thesis.

We apply $\mathcal{T}_{\boldsymbol{c}_2}$ on expansion (3.16) and obtain

$$\mathcal{T}_{\boldsymbol{c}_2} F_q^{(\le 1)} = \mathcal{T}_{\boldsymbol{c}_2} F_{q_1}^{(\le 1)} + \mathcal{T}_{\boldsymbol{c}_2} F_{q_2}^{(\le 1)}\,, \tag{3.48}$$

which we choose as an approach for the following investigation. This translation of the whole equation is not necessary but improves the readability without worsening the results. For technical

reasons in the later proof it turns out to be necessary to replace the exact translated far field operator $\mathcal{T}_{\boldsymbol{c}_2} F_q$ by some finite-dimensional approximation. Our observations in Section 2.4 ensure that $\operatorname{supp} q \subseteq B_R(\boldsymbol{c}_2)$ for some $R > 0$ implies that F_q can be well–approximated in $\mathcal{V}_N^{\boldsymbol{c}_2}$ and consequently $\mathcal{T}_{\boldsymbol{c}_2} F_q$ in $\mathcal{V}_N$ with $N \gtrsim kR$. As before, given $N_2 \gtrsim kR_2$ with $\operatorname{supp} q_2 \subseteq B_{R_2}(\boldsymbol{c}_2)$, we further know that F_{q_2} can be well approximated in $\mathcal{V}_{N_2}^{\boldsymbol{c}_2}$, so $\mathcal{T}_{\boldsymbol{c}_2} F_{q_2}$ in $\mathcal{V}_{N_2} \subseteq \mathcal{V}_N$. Finally, the fact that F_{q_1} can be well approximated in $\mathcal{W}_{N_1}^{\boldsymbol{c}_1}$ for some $N_1 \gtrsim kR_1$ with $\operatorname{supp} q_1 \subseteq B_{R_1}(\boldsymbol{c}_1)$ yields that it makes sense to search $\mathcal{T}_{\boldsymbol{c}_2} F_{q_1}$ in $\mathcal{W}_{N_1}^{\boldsymbol{c}_1 - \boldsymbol{c}_2}$. We cannot even expect a general element of $\mathcal{W}_{N_1}^{\boldsymbol{c}_1 - \boldsymbol{c}_2}$ and to be well approximated in $\mathcal{V}_N$. Therefore, we impose an additional assumption on the low rank component to ensure that it can be well approximated in $\mathcal{V}_N$.

This is reflected in the following framework. Let $M^0 \in \mathcal{V}_N$ be an approximation of $\mathcal{T}_{\boldsymbol{c}_2} F_q$, and let

$$M^0 \approx \widetilde{L}^0 + \widetilde{S}^0 \tag{3.49}$$

be an approximate split into a low rank component $\widetilde{L}^0 \in \mathcal{W}_{N_1}^{\boldsymbol{c}_1 - \boldsymbol{c}_2}$ and a sparse component $\widetilde{S}^0 \in \mathcal{V}_{N_2}$, such that the low rank component can be well approximated in $\mathcal{V}_{M_1}^{\boldsymbol{c}_1 - \boldsymbol{c}_2}$ for some $M_1 \geq N_1$ with $N > M_1 + k|\boldsymbol{c}_1 - \boldsymbol{c}_2|$.

Remark 3.32. We cannot expect the decomposition (3.49) to exist in an exact way since $M^0, S^0 \in \mathcal{V}_N$ but probably $\widetilde{L}^0 \notin \mathcal{V}_N$. However, Proposition 3.33 below shows that under above additional assumption on $\widetilde{L}^0$ and for N large enough $\widetilde{L}^0$ can at least be reliably well approximated in $\mathcal{V}_N$. To see this suppose $\|\widetilde{L}^0 - \widehat{L}\|_{\mathrm{HS}} \leq \varepsilon$ for some $\widehat{L} \in \mathcal{V}_{M_1}^{\boldsymbol{c}_1 - \boldsymbol{c}_2}$ and $\varepsilon > 0$. Then, Proposition 3.33 yields

$$\begin{aligned}\|(I - \mathcal{P}_{\mathcal{V}_N})\widetilde{L}^0\|_{\mathrm{HS}} &\leq \|(I - \mathcal{P}_{\mathcal{V}_N})\widehat{L}\|_{\mathrm{HS}} + \|(I - \mathcal{P}_{\mathcal{V}_N})(\widetilde{L}^0 - \widehat{L})\|_{\mathrm{HS}} \\ &\leq \|\widehat{L}\|_{\mathrm{HS}} \left(2(2M_1 + 1) \sum_{|n| > N} \sum_{|m| \leq M} J_{n-m}^2(k|\boldsymbol{c}_1 - \boldsymbol{c}_2|) \right)^{\frac{1}{2}} + \varepsilon \,,\end{aligned}$$

and the first summand on the right hand side can be made arbitrarily small by choosing N large enough. The operator $(I - \mathcal{P}_{\mathcal{V}_N})$ is linear and thus cannot increase the rank of $\widetilde{L}^0$. Consequently, above estimate further gives a upper bound for $\|(I - \mathcal{P}_{\mathcal{V}_N})\widetilde{L}^0\|_{\mathrm{nuc}}$ according to

$$\begin{aligned}\|(I - \mathcal{P}_{\mathcal{V}_N})\widetilde{L}^0\|_{\mathrm{nuc}} &\leq \sqrt{\operatorname{rank}((I - \mathcal{P}_{\mathcal{V}_N})\widetilde{L}^0)}\|(I - \mathcal{P}_{\mathcal{V}_N})\widetilde{L}^0\|_{\mathrm{HS}} \\ &\leq \sqrt{\operatorname{rank} \widetilde{L}^0}\|(I - \mathcal{P}_{\mathcal{V}_N})\widetilde{L}^0\|_{\mathrm{HS}} = \sqrt{2N_1 + 1}\|(I - \mathcal{P}_{\mathcal{V}_N})\widetilde{L}^0\|_{\mathrm{HS}} \,.\end{aligned}$$

◊

Proposition 3.33. *Let $M, N \in \mathbb{N}$ and $\boldsymbol{c} \in \mathbb{R}^2 \setminus \{\mathbf{0}\}$ such that $N > M + k|\boldsymbol{c}|$. Then, it holds*

$$\|(I - \mathcal{P}_{\mathcal{V}_N})G\|_{\mathrm{HS}} \leq \|G\|_{\mathrm{HS}} \left(2(2M + 1) \sum_{|n| > N} \sum_{|m| \leq M} J_{n-m}^2(k|\boldsymbol{c}|) \right)^{\frac{1}{2}}, \qquad G \in \mathcal{V}_M^{\boldsymbol{c}} \,.$$

For $|n| > N$ and $|m| \leq M$ we have that $|n - m| > N - M > k|\boldsymbol{c}|$. Consequently, according to the proof of Theorem 2.11, the upper bound decays superlinearly in N, more precisely faster than any power of N^{-1}.

Proof. We assume $G \in \mathcal{V}_M^{\boldsymbol{c}}$ and expand

$$\begin{aligned}G &= \sum_{|m|,|n| \leq M} a_{m,n} T_{-\boldsymbol{c}} \boldsymbol{e}_m \langle \cdot \,, T_{-\boldsymbol{c}} \boldsymbol{e}_n \rangle_{L^2(S^1)} \\ &= \sum_{o,l \in \mathbb{Z}} \sum_{|m|,|n| \leq M} a_{m,n} \langle \boldsymbol{e}_l, T_{-\boldsymbol{c}} \boldsymbol{e}_n \rangle_{L^2(S^1)} \langle T_{-\boldsymbol{c}} \boldsymbol{e}_m, \boldsymbol{e}_o \rangle_{L^2(S^1)} \boldsymbol{e}_o \langle \cdot \,, \boldsymbol{e}_l \rangle_{L^2(S^1)} \,.\end{aligned}$$

This yields as in (2.28) together with the Cauchy Schwarz inequality that

$$\begin{aligned}
\|G - \mathcal{P}_{\mathcal{V}_N} G\|_{\mathrm{HS}}^2 &= \|G - \mathcal{P}_{\mathcal{V}_N} G\|_{\ell^2 \times \ell^2}^2 \\
&\leq \sum_{o \in \mathbb{Z}, |l| > N} \Big| \sum_{|m|,|n| \leq M} a_{m,n} \langle \boldsymbol{e}_l, T_{-\boldsymbol{c}} \boldsymbol{e}_n \rangle_{L^2(S^1)} \langle T_{-\boldsymbol{c}} \boldsymbol{e}_m, \boldsymbol{e}_o \rangle_{L^2(S^1)} \Big|^2 \\
&\quad + \sum_{|o| > N, l \in \mathbb{Z}} \Big| \sum_{|m|,|n| \leq M} a_{m,n} \langle \boldsymbol{e}_l, T_{-\boldsymbol{c}} \boldsymbol{e}_n \rangle_{L^2(S^1)} \langle T_{-\boldsymbol{c}} \boldsymbol{e}_m, \boldsymbol{e}_o \rangle_{L^2(S^1)} \Big|^2 \\
&\leq 2\|G\|_{\mathrm{HS}}^2 \Big(\sum_{n \in \mathbb{Z}} \sum_{|m| \leq M} |\langle \boldsymbol{e}_n, T_{-\boldsymbol{c}} \boldsymbol{e}_m \rangle_{L^2(S^1)}|^2 \Big) \Big(\sum_{|n| > N} \sum_{|m| \leq M} |\langle \boldsymbol{e}_n, T_{-\boldsymbol{c}} \boldsymbol{e}_m \rangle_{L^2(S^1)}|^2 \Big) \\
&= 2\|G\|_{\mathrm{HS}}^2 \Big(\sum_{n \in \mathbb{Z}} \sum_{|m| \leq M} J_{n-m}^2(k|\boldsymbol{c}|) \Big) \Big(\sum_{|n| > N} \sum_{|m| \leq M} J_{n-m}^2(k|\boldsymbol{c}|) \Big) \\
&= 2\|G\|_{\mathrm{HS}}^2 (2M+1) \Big(\sum_{|n| > N} \sum_{|m| \leq M} J_{n-m}^2(k|\boldsymbol{c}|) \Big),
\end{aligned}$$

where we used that due to (B.10)

$$\sum_{n \in \mathbb{Z}} \sum_{|m| \leq M} J_{n-m}^2(k|\boldsymbol{c}|) = \sum_{|m| \leq M} \sum_{n \in \mathbb{Z}} J_{n-m}^2(k|\boldsymbol{c}|) = 2M+1 .$$

This finishes the proof. □

The split (3.49) does not have to be computed explicitly. Our additional assumption on the decay of the Fourier coefficients of $\mathcal{T}_{\boldsymbol{c}_1 - \boldsymbol{c}_2} \widetilde{L}^0$ causes that such an approximate split cannot be obtained by solving the least squares problem (3.37), where we require only $\widetilde{L}^0 \in \mathcal{W}_{N_1}^{\boldsymbol{c}_1 - \boldsymbol{c}_2}$. However, since $\mathcal{V}_{N_1}^{\boldsymbol{c}_1 - \boldsymbol{c}_2} \subseteq \mathcal{W}_{N_1}^{\boldsymbol{c}_1 - \boldsymbol{c}_2}$ (see Remark 2.10 (ii)) it can e.g. be obtained by solving problem (3.17), where we require $\widetilde{L}^0 \in \mathcal{V}_{N_1}^{\boldsymbol{c}_1 - \boldsymbol{c}_2}$. Due to $\mathcal{V}_{N_1}^{\boldsymbol{c}_1 - \boldsymbol{c}_2} + \mathcal{V}_{N_1, N_2}^{\boldsymbol{c}_1 - \boldsymbol{c}_2, \boldsymbol{0}} + \mathcal{V}_{N_2, N_1}^{\boldsymbol{0}, \boldsymbol{c}_1 - \boldsymbol{c}_2} \subseteq \mathcal{W}_{N_1}^{\boldsymbol{c}_1 - \boldsymbol{c}_2}$ (cf. Theorem 3.5), Subsection 3.5 below provides an alternative least squares problem (3.67) for computing such a split. The required decay of the Fourier coefficients can be justified as in Proposition 3.33. At this point, we also refer to Subsection 3.6.2, where it is explained how the procedure of this Subsection can be transferred to Born approximations of order $p \geq 2$.

As proposed in [101], $\widetilde{L}^0$ and $\widetilde{S}^0$ can be approximated by solving *robust Principal Component Pursuit (RPCP)*, i.e.,

$$\underset{(L,S) \in \mathcal{V}_N^2}{\text{minimize}} \|L\|_{\mathrm{nuc}} + \lambda \|S\|_{\ell^1 \times \ell^1} \qquad \text{subject to} \qquad \|M^0 - L - S\|_{\mathrm{HS}} \leq \delta \tag{3.50}$$

for some coupling parameter $\lambda > 0$ and some noise level $\delta > 0$, which is combination of the approximation errors for $\mathcal{T}_{\boldsymbol{c}_2} F_{q_1}$ and $\mathcal{T}_{\boldsymbol{c}_2} F_{q_2}$. As before, this choice of the objective function promotes sparsity of the Fourier coefficients of $\widetilde{S}^0$. An overview of possible alternative minimization problem formulations is given in [13].

In the following, we fix a singular system $(\sigma_n; u_n, v_n)_{1 \leq n \leq 2N_1+1}$ for $\widetilde{L}^0$ and the Fourier coefficients $(a_{m,n})_{|m|,|n| \leq N_2}$ of $\widetilde{S}^0$ to define the operators

$$\Lambda := \sum_{n=1}^{2N_1+1} u_n \langle \cdot, v_n \rangle_{L^2(S^1)} \qquad \text{and} \qquad \Sigma := \sum_{|m|,|n| \leq N_2} \frac{\overline{a_{m,n}}}{|a_{m,n}|} \boldsymbol{e}_m \langle \cdot, \boldsymbol{e}_n \rangle_{L^2(S^1)} . \tag{3.51}$$

Given $\widetilde{M}^0 := \widetilde{L}^0 + \widetilde{S}^0$ and $\lambda \in (0,1)$ the pair $(\widetilde{L}^0, \widetilde{S}^0)$ is the unique solution of the *Principal*

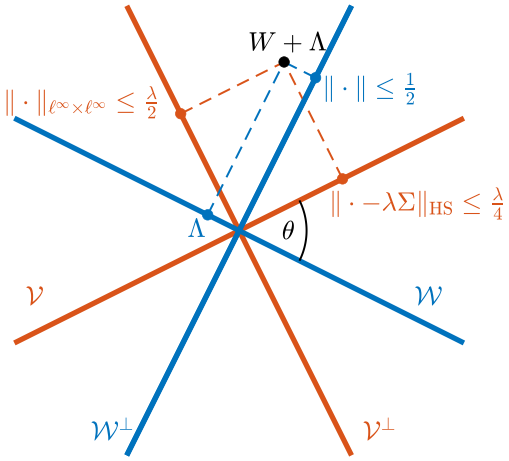

FIGURE 3.4. Geometric visualization of the dual certificate W as introduced in (3.53). The dashed lines mark the four involved orthogonal projections of $W+\Lambda$. Each of these projections must fulfill an optimality condition. Intuitively, it seems easier all conditions to be satisfied simultaneously if the minimal angle θ between $\mathcal{W}:=\mathcal{W}_{N_1}^{\boldsymbol{c}_1-\boldsymbol{c}_2}$ and $\mathcal{V}:=\mathcal{V}_{N_2}$ is large, i.e., if $\|\mathcal{P}_{\mathcal{V}}\mathcal{P}_{\mathcal{W}}\|$ is small. Here, we mention that $\mathcal{P}_{\mathcal{W}^\perp}(W+\Lambda)=W$.

Component Pursuit problem

$$\underset{(\widetilde{L}^0,\widetilde{S}^0)\in\mathrm{HS}(L^2(S^1))^2}{\text{minimize}}\ \|\widetilde{L}^0\|_{\mathrm{nuc}}+\lambda\|\widetilde{S}^0\|_{\ell^1\times\ell^1}\qquad\text{subject to}\qquad\widetilde{M}^0=\widetilde{L}^0+\widetilde{S}^0 \tag{3.52}$$

if $\|\mathcal{P}_{\mathcal{V}_{N_2}}\mathcal{P}_{\mathcal{W}_{N_1}^{\boldsymbol{c}_1-\boldsymbol{c}_2}}\|\leq 1/2$ and if there exists a *dual certificate* $W\in\mathrm{HS}(L^2(S^1))$ satisfying

$$\begin{cases}\mathcal{P}_{\mathcal{W}_{N_1}^{\boldsymbol{c}_1-\boldsymbol{c}_2}}W=0\,, & \|W\|<\frac{1}{2}\,,\\ \|\mathcal{P}_{\mathcal{V}_{N_2}}(\Lambda+W-\lambda\Sigma)\|_{\mathrm{HS}}\leq\frac{\lambda}{4}\,,\\ \|(I-\mathcal{P}_{\mathcal{V}_{N_2}})(\Lambda+W)\|_{\ell^\infty\times\ell^\infty}\leq\frac{\lambda}{2}\,,\end{cases} \tag{3.53}$$

cf. [19, Lem. 2.5 and (2.4)]. The optimization problem (3.52) has also been investigated in [25].

We again mention that $\widetilde{L}^0\notin\mathcal{V}_N$ and consequently $\widetilde{M}^0\notin\mathcal{V}_N$. The proof of [19, Lem. 2.5] is formulated for the matrix case. The matrix dimension does not come into play at any point in this proof. Furthermore, the subdifferential of the nuclear norm and $\ell^1\times\ell^1$ norm remains structurally unchanged when transitioning from matrices to Hilbert–Schmidt operators (cf. Example D.2). Consequently, this proof can be directly applied to the infinite-dimensional case.

Above optimality condition (3.53) is visualized in Figure 3.4, and it plays an essential role in the development of a stability estimate for problem (3.50) as it is done in Theorem 3.34 below, which is of a similar structure than Theorems 3.23 and 3.24.

The operator M^δ represents an approximation of a noisy observation of $\mathcal{T}_{\boldsymbol{c}_2}F_q^{(\leq 1)}$ in $\mathcal{V}_N$. The bound δ_0 in (3.55) below models the accuracy of the approximate exact solution. In case of (3.49) this consists of the error of the first order Born approximation and all involved projection errors. Particularly, δ_0 controls how far the approximate exact low rank component L^0 is from lying in $\mathcal{V}_N$. At this point, we refer to Subsection 3.6.2, where it is examined that in fact, only the error of the second order Born approximation plays a role, provided we are only interested in the reconstruction of F_{q_2} and not of F_{q_1}. The total noise level δ consists of the data error and twice the accuracy δ_0 of the approximate exact solution. The proof of Theorem 3.34 is similar to the proof of [101, Prop. 4]. We mention that, on the one hand, some modifications are needed since $\mathcal{W}_{N_1}^{\boldsymbol{c}_1-\boldsymbol{c}_2}\not\subseteq\mathcal{V}_N$ and, on the other hand, the assumption $\|\mathcal{P}_{\mathcal{V}_{N_2}}\mathcal{P}_{\mathcal{W}_{N_1}^{\boldsymbol{c}_1-\boldsymbol{c}_2}}\|<1/2$ in [101, Prop. 4] is replaced by our uncertainty principle from Proposition 3.27.

Theorem 3.34. *Suppose that $M^0, M^\delta \in \mathcal{V}_N$ for $N \in \mathbb{N}$ with $N \gtrsim kR$, and let $\boldsymbol{c}_1, \boldsymbol{c}_2 \in \mathbb{R}^2$ and $N_1, N_2 \in \mathbb{N}$ with $N_1, N_2 < N$, $N_1 \gtrsim kR_1$ and $N_2 \gtrsim kR_2$, such that $C < 1/4$, where*

$$C := \frac{2\sqrt{2N_1+1}(2N_2+1)}{(k|\boldsymbol{c}_1 - \boldsymbol{c}_2|)^{\frac{1}{3}}}. \tag{3.54}$$

We assume that $\widetilde{L}^0 \in \mathcal{W}_{N_1}^{\boldsymbol{c}_1-\boldsymbol{c}_2}$ and $\widetilde{S}^0 \in \mathcal{V}_{N_2}$ are such that

$$\|M^0 - (\widetilde{L}^0 + \widetilde{S}^0)\|_{\ell^1\times\ell^1} \le \delta_0\,, \qquad \|M^0 - (\widetilde{L}^0 + \widetilde{S}^0)\|_{\mathrm{nuc}} \le \delta_0\,, \qquad \|(I - \mathcal{P}_{\mathcal{V}_N})\widetilde{L}^0\|_{\mathrm{nuc}} \le \delta_0 \tag{3.55}$$

for some $\delta_0 \ge 0$ and that there exists a dual certificate $W \in \mathrm{HS}(L^2(S^1))$ satisfying (3.53).

Moreover, suppose that $\delta > 0$ satisfies

$$\delta \ge 2\delta_0 + \|M^0 - M^\delta\|_{\mathrm{HS}} \tag{3.56}$$

and let $(\widetilde{L}^\delta, \widetilde{S}^\delta) \in \mathcal{V}_N^2$ for $\lambda = 1/\sqrt{2N+1}$ denote the solution to

$$\underset{(L,S)}{\text{minimize}}\, \|L\|_{\mathrm{nuc}} + \lambda\|S\|_{\ell^1\times\ell^1} \qquad \text{subject to} \qquad \|M^\delta - (L+S)\|_{\mathrm{HS}} \le \delta\,. \tag{3.57}$$

Then, for $j = 1, 2$,

$$\|\widetilde{L}^0 - \widetilde{L}^\delta\|_{\mathrm{HS}}^2 \le 2\left(1 + 40\left(1 + 2(1-C)^{-1}\right)(2N+1)^2\right)\delta^2\,, \tag{3.58a}$$

$$\|\widetilde{S}^0 - \widetilde{S}^\delta\|_{\mathrm{HS}}^2 \le 2\left(1 + 40\left(1 + 2(1-C)^{-1}\right)(2N+1)^2\right)\delta^2\,. \tag{3.58b}$$

Proof. We use the abbreviations $\widetilde{L} := \widetilde{L}^0 - \widetilde{L}^\delta$, $\widetilde{S} := \widetilde{S}^0 - \widetilde{S}^\delta$, $\mathcal{W} := \mathcal{W}_{N_1}^{\boldsymbol{c}_1-\boldsymbol{c}_2}$ and $\mathcal{V} := \mathcal{V}_{N_2}$ and estimate by using the parallelogram identity

$$\begin{aligned}
\|\widetilde{S}^0 - \widetilde{S}^\delta\|_{\mathrm{HS}}^2 &\le \|\widetilde{L}\|_{\mathrm{HS}}^2 + \|\widetilde{S}\|_{\mathrm{HS}}^2 = \frac{1}{2}\|\widetilde{L}+\widetilde{S}\|_{\mathrm{HS}}^2 + \frac{1}{2}\|\widetilde{L}-\widetilde{S}\|_{\mathrm{HS}}^2 \\
&= \frac{1}{2}\|\widetilde{L}+\widetilde{S}\|_{\mathrm{HS}}^2 + \frac{1}{4}\left(\|\mathcal{P}_{\mathcal{V}}(\widetilde{L}-\widetilde{S})\|_{\mathrm{HS}}^2 + \|\mathcal{P}_{\mathcal{W}}(\widetilde{L}-\widetilde{S})\|_{\mathrm{HS}}^2\right) \\
&\quad + \frac{1}{4}\left(\|\mathcal{P}_{\mathcal{V}^\perp}(\widetilde{L}-\widetilde{S})\|_{\mathrm{HS}}^2 + \|\mathcal{P}_{\mathcal{W}^\perp}(\widetilde{L}-\widetilde{S})\|_{\mathrm{HS}}^2\right).
\end{aligned} \tag{3.59}$$

The term $\|\widetilde{L}^0 - \widetilde{L}^\delta\|_{\mathrm{HS}}^2$ can be controlled by the same upper bound. In the following, we estimate the three summands in (3.59) individually.

Bound for the first summand in (3.59): As in the proof of Theorem 3.23, we obtain by using (3.55)–(3.57) and (A.7) that

$$\frac{1}{2}\|\widetilde{L}+\widetilde{S}\|_{\mathrm{HS}}^2 \le \frac{1}{2}\left(\|M^0 - (\widetilde{L}^0+\widetilde{S}^0)\|_{\mathrm{HS}} + \|M^0 - M^\delta\|_{\mathrm{HS}} + \|M^\delta - (\widetilde{L}^\delta+\widetilde{S}^\delta)\|_{\mathrm{HS}}\right)^2 \le 2\delta^2\,. \tag{3.60}$$

Bound for the second summand in (3.59): Let $0 < C < 1$ be given as in (3.54). We conclude from the uncertainty principle (3.38) and from $a^2 + b^2 - 2Cab \ge (1-C)(a^2+b^2)$ for all $a, b \ge 0$ that

$$\begin{aligned}
&\|\mathcal{P}_{\mathcal{V}}(\widetilde{L}-\widetilde{S}) - \mathcal{P}_{\mathcal{W}}(\widetilde{L}-\widetilde{S})\|_{\mathrm{HS}}^2 \\
&= \|\mathcal{P}_{\mathcal{V}}(\widetilde{L}-\widetilde{S})\|_{\mathrm{HS}}^2 + \|\mathcal{P}_{\mathcal{W}}(\widetilde{L}-\widetilde{S})\|_{\mathrm{HS}}^2 - 2\langle\mathcal{P}_{\mathcal{V}}(\widetilde{L}-\widetilde{S}), \mathcal{P}_{\mathcal{W}}(\widetilde{L}-\widetilde{S})\rangle_{\mathrm{HS}} \\
&\ge \|\mathcal{P}_{\mathcal{V}}(\widetilde{L}-\widetilde{S})\|_{\mathrm{HS}}^2 + \|\mathcal{P}_{\mathcal{W}}(\widetilde{L}-\widetilde{S})\|_{\mathrm{HS}}^2 - 2C\|\mathcal{P}_{\mathcal{V}}(\widetilde{L}-\widetilde{S})\|_{\mathrm{HS}}\|\mathcal{P}_{\mathcal{W}}(\widetilde{L}-\widetilde{S})\|_{\mathrm{HS}} \\
&\ge (1-C)\left(\|\mathcal{P}_{\mathcal{V}}(\widetilde{L}-\widetilde{S})\|_{\mathrm{HS}}^2 + \|\mathcal{P}_{\mathcal{W}}(\widetilde{L}-\widetilde{S})\|_{\mathrm{HS}}^2\right).
\end{aligned}$$

This is equivalent to

$$\frac{1}{4}\left(\|\mathcal{P}_{\mathcal{V}}(\widetilde{L}-\widetilde{S})\|_{\mathrm{HS}}^2+\|\mathcal{P}_{\mathcal{W}}(\widetilde{L}-\widetilde{S})\|_{\mathrm{HS}}^2\right) \leq \frac{1}{4(1-C)}\|\mathcal{P}_{\mathcal{V}}(\widetilde{L}-\widetilde{S})-\mathcal{P}_{\mathcal{W}}(\widetilde{L}-\widetilde{S})\|_{\mathrm{HS}}^2 .$$

Since we can decompose

$$0 = (\widetilde{L}-\widetilde{S})-(\widetilde{L}-\widetilde{S}) = \mathcal{P}_{\mathcal{V}}(\widetilde{L}-\widetilde{S})-\mathcal{P}_{\mathcal{W}}(\widetilde{L}-\widetilde{S})+\mathcal{P}_{\mathcal{V}^\perp}(\widetilde{L}-\widetilde{S})-\mathcal{P}_{\mathcal{W}^\perp}(\widetilde{L}-\widetilde{S})$$

we deduce from the parallelogram identity that

$$\begin{aligned}\frac{1}{4}\left(\|\mathcal{P}_{\mathcal{V}}(\widetilde{L}-\widetilde{S})\|_{\mathrm{HS}}^2+\|\mathcal{P}_{\mathcal{W}}(\widetilde{L}-\widetilde{S})\|_{\mathrm{HS}}^2\right) &\leq \frac{1}{4(1-C)}\|\mathcal{P}_{\mathcal{V}^\perp}(\widetilde{L}-\widetilde{S})-\mathcal{P}_{\mathcal{W}^\perp}(\widetilde{L}-\widetilde{S})\|_{\mathrm{HS}}^2 \\ &\leq \frac{1}{2(1-C)}\left(\|\mathcal{P}_{\mathcal{V}^\perp}(\widetilde{L}-\widetilde{S})\|_{\mathrm{HS}}^2+\|\mathcal{P}_{\mathcal{W}^\perp}(\widetilde{L}-\widetilde{S})\|_{\mathrm{HS}}^2\right) .\end{aligned}$$

The obtained upper bound is a multiple of the third summand in (3.59). Thus, it remains to bound this third summand in (3.59).

Bound for third summand in (3.59): We use (A.7) and $\|\cdot\|_{\mathrm{HS}} \leq \|\cdot\|_{\ell^1\times\ell^1}$ (since $\ell^1 \subseteq \ell^2$), and we choose $\lambda = 1/\sqrt{2N+1}$ to obtain

$$\begin{aligned}&\frac{1}{4}\left(\|\mathcal{P}_{\mathcal{V}^\perp}(\widetilde{L}-\widetilde{S})\|_{\mathrm{HS}}^2+\|\mathcal{P}_{\mathcal{W}^\perp}(\widetilde{L}-\widetilde{S})\|_{\mathrm{HS}}^2\right) \leq \frac{1}{4}\left(\|\mathcal{P}_{\mathcal{V}^\perp}(\widetilde{L}-\widetilde{S})\|_{\mathrm{HS}}+\|\mathcal{P}_{\mathcal{W}^\perp}(\widetilde{L}-\widetilde{S})\|_{\mathrm{HS}}\right)^2 \\ &\leq \frac{1}{4}\left(\sqrt{2N+1}\|\mathcal{P}_{\mathcal{V}^\perp}(\widetilde{L}-\widetilde{S})\|_{\mathrm{nuc}}+\|\mathcal{P}_{\mathcal{W}^\perp}(\widetilde{L}-\widetilde{S})\|_{\ell^1\times\ell^1}\right)^2 \\ &= \frac{2N+1}{4}\left(\|\mathcal{P}_{\mathcal{V}^\perp}(\widetilde{L}-\widetilde{S})\|_{\mathrm{nuc}}+\lambda\|\mathcal{P}_{\mathcal{W}^\perp}(\widetilde{L}-\widetilde{S})\|_{\ell^1\times\ell^1}\right)^2 .\end{aligned}$$

Since we can decompose

$$\widetilde{L} = \frac{1}{2}(\widetilde{L}-\widetilde{S})+\frac{1}{2}(\widetilde{L}+\widetilde{S}) \qquad \text{and} \qquad \widetilde{S} = \frac{1}{2}(\widetilde{S}-\widetilde{L})+\frac{1}{2}(\widetilde{S}+\widetilde{L}) ,$$

we conclude with the reverse triangle inequality that

$$\begin{aligned}&\|\widetilde{L}^0-\widetilde{L}\|_{\mathrm{nuc}}+\lambda\|\widetilde{S}^0-\widetilde{S}\|_{\ell^1\times\ell^1} \\ &= \|\widetilde{L}^0+\frac{1}{2}(\widetilde{S}-\widetilde{L})-\frac{1}{2}(\widetilde{L}+\widetilde{S})\|_{\mathrm{nuc}}+\lambda\|\widetilde{S}^0+\frac{1}{2}(\widetilde{L}-\widetilde{S})-\frac{1}{2}(\widetilde{L}+\widetilde{S})\|_{\mathrm{nuc}} \\ &\geq \|\widetilde{L}^0+\frac{1}{2}(\widetilde{S}-\widetilde{L})\|_{\mathrm{nuc}}+\lambda\|\widetilde{S}^0+\frac{1}{2}(\widetilde{L}-\widetilde{S})\|_{\ell^1\times\ell^1}-\frac{1}{2}\left(\|\widetilde{L}+\widetilde{S}\|_{\mathrm{nuc}}+\lambda\|\widetilde{L}+\widetilde{S}\|_{\ell^1\times\ell^1}\right) .\end{aligned}$$

From

$$\begin{aligned}\|M^\delta-(\mathcal{P}_{\mathcal{V}_N}\widetilde{L}^0+\widetilde{S}^0)\|_{\mathrm{HS}} &\leq \|M^\delta-M^0\|_{\mathrm{HS}}+\|M^0-(\widetilde{L}^0+\widetilde{S}^0)\|_{\mathrm{HS}}+\|(I-\mathcal{P}_{\mathcal{V}_N})\widetilde{L}^0\|_{\mathrm{HS}} \\ &\leq \|M^\delta-M^0\|_{\mathrm{HS}}+\|M^0-(\widetilde{L}^0+\widetilde{S}^0)\|_{\mathrm{HS}}+\|(I-\mathcal{P}_{\mathcal{V}_N})\widetilde{L}^0\|_{\mathrm{nuc}} \\ &\leq \|M^\delta-M^0\|_{\mathrm{HS}}+2\delta_0 \leq \delta ,\end{aligned}$$

due to (A.7), (3.55), and (3.56), we know that $(\mathcal{P}_{\mathcal{V}_N}\widetilde{L}^0, \widetilde{S}^0)$ is feasible for (3.57). Thus, (3.55) gives us that

$$\begin{aligned}\|\widetilde{L}^0-\widetilde{L}\|_{\mathrm{nuc}}+\lambda\|\widetilde{S}^0-\widetilde{S}\|_{\ell^1\times\ell^1} &= \|\widetilde{L}^\delta\|_{\mathrm{nuc}}+\lambda\|\widetilde{S}^\delta\|_{\ell^1\times\ell^1} \leq \|\mathcal{P}_{\mathcal{V}_N}\widetilde{L}^0\|_{\mathrm{nuc}}+\lambda\|\widetilde{S}^0\|_{\ell^1\times\ell^1} \\ &\leq \|\widetilde{L}^0\|_{\mathrm{nuc}}+\lambda\|\widetilde{S}^0\|_{\ell^1\times\ell^1}+\|(I-\mathcal{P}_{\mathcal{V}_N})\widetilde{L}^0\|_{\mathrm{nuc}} \leq \|\widetilde{L}^0\|_{\mathrm{nuc}}+\lambda\|\widetilde{S}^0\|_{\ell^1\times\ell^1}+\delta_0 .\end{aligned}$$

We choose $H_1 = -H_2 = \frac{1}{2}(\widetilde{S} - \widetilde{L})$ in Lemma 3.35 below and obtain that

$$\begin{aligned}
&\frac{1}{8}\left(\|\mathcal{P}_{\mathcal{V}^\perp}(\widetilde{L}-\widetilde{S})\|_{\text{nuc}} + \lambda\|\mathcal{P}_{\mathcal{W}^\perp}(\widetilde{L}-\widetilde{S})\|_{\ell^1\times\ell^1}\right)\\
&\leq \|\widetilde{L}^0 + \frac{1}{2}(\widetilde{S}-\widetilde{L})\|_{\text{nuc}} + \lambda\|\widetilde{S}^0 + \frac{1}{2}(\widetilde{L}-\widetilde{S})\|_{\ell^1\times\ell^1} - \left(\|\widetilde{L}^0\|_{\text{nuc}} + \lambda\|\widetilde{S}^0\|_{\ell^1\times\ell^1}\right)\\
&\leq \|\widetilde{L}^0 - \widetilde{L}\|_{\text{nuc}} + \lambda\|\widetilde{S}^0 - \widetilde{S}\|_{\ell^1\times\ell^1} - \left(\|\widetilde{L}^0\|_{\text{nuc}} + \lambda\|\widetilde{L}^0\|_{\ell^1\times\ell^1} + \delta_0\right)\\
&\quad + \frac{1}{2}\left(\|\widetilde{L}+\widetilde{S}\|_{\text{nuc}} + \lambda\|\widetilde{L}+\widetilde{S}\|_{\ell^1\times\ell^1} + 2\delta_0\right)\\
&\leq \frac{1}{2}\left(\|\widetilde{L}+\widetilde{S}\|_{\text{nuc}} + \lambda\|\widetilde{L}+\widetilde{S}\|_{\ell^1\times\ell^1} + 2\delta_0\right),
\end{aligned}$$

so

$$\frac{1}{4}\left(\|\mathcal{P}_{\mathcal{V}^\perp}(\widetilde{L}-\widetilde{S})\|_{\text{nuc}} + \lambda\|\mathcal{P}_{\mathcal{W}^\perp}(\widetilde{L}-\widetilde{S})\|_{\ell^1\times\ell^1}\right)^2 \leq 4\left(\|\widetilde{L}+\widetilde{S}\|_{\text{nuc}} + \lambda\|\widetilde{L}+\widetilde{S}\|_{\ell^1\times\ell^1} + 2\delta_0\right)^2,$$

which yields by using (3.55) for the fourth estimate, $\lambda(2N+1) = \sqrt{2N+1}$ for the first equality and (3.56)–(3.57) for the sixth estimate

$$\begin{aligned}
&\frac{1}{4}\left(\|\mathcal{P}_{\mathcal{V}^\perp}(\widetilde{L}-\widetilde{S})\|_{\text{HS}}^2 + \|\mathcal{P}_{\mathcal{W}^\perp}(\widetilde{L}-\widetilde{S})\|_{\text{HS}}^2\right)\\
&\leq (2N+1)\frac{1}{4}\left(\|\mathcal{P}_{\mathcal{V}^\perp}(\widetilde{L}-\widetilde{S})\|_{\text{nuc}} + \lambda\|\mathcal{P}_{\mathcal{W}^\perp}(\widetilde{L}-\widetilde{S})\|_{\ell^1\times\ell^1}\right)^2\\
&\leq 4(2N+1)\left(\|\widetilde{L}+\widetilde{S}\|_{\text{nuc}} + \lambda\|\widetilde{L}+\widetilde{S}\|_{\ell^1\times\ell^1} + 2\delta_0\right)^2\\
&\leq 4(2N+1)\Big(\|M^0 - (\widetilde{L}^\delta + \widetilde{S}^\delta)\|_{\text{nuc}} + \lambda\|M^0 - (\widetilde{L}^\delta + \widetilde{S}^\delta)\|_{\ell^1\times\ell^1}\\
&\qquad\qquad + \|M^0 - (\widetilde{L}^0 + \widetilde{S}^0)\|_{\text{nuc}} + \|M^0 - (\widetilde{L}^0 + \widetilde{S}^0)\|_{\ell^1\times\ell^1} + 2\delta_0\Big)^2\\
&\leq 4(2N+1)\left(\sqrt{2N+1}\|M^0 - (\widetilde{L}^\delta + \widetilde{S}^\delta)\|_{\text{HS}} + \lambda(2N+1)\|M^0 - (\widetilde{L}^\delta + \widetilde{S}^\delta)\|_{\text{HS}} + 4\delta_0\right)^2\\
&= 4(2N+1)\left(2\sqrt{2N+1}\|M^0 - (\widetilde{L}^\delta + \widetilde{S}^\delta)\|_{\text{HS}} + 4\delta_0\right)^2\\
&\leq 4(2N+1)\left(2\sqrt{2N+1}(\|M^0 - M^\delta\|_{\text{HS}} + \|M^\delta - (\widetilde{L}^\delta + \widetilde{S}^\delta)\|_{\text{HS}}) + 4\delta_0\right)^2\\
&\leq 4(2N+1)\left(2\sqrt{2N+1}(2\delta - \delta_0) + 4\delta_0\right)^2 = 4(2N+1)(\underbrace{4\sqrt{2N+1}\delta}_{\geq 0} - \underbrace{2(\sqrt{2N+1}-2)\delta_0}_{\geq 0})^2.
\end{aligned}$$

Since there holds $(a-b)^2 \leq a^2 + b^2$ for $a, b \geq 0$ and $\delta_0 \leq \delta$ because of (3.56), we further estimate

$$\begin{aligned}
\frac{1}{4}\left(\|\mathcal{P}_{\mathcal{V}^\perp}(\widetilde{L}-\widetilde{S})\|_{\text{HS}}^2 + \|\mathcal{P}_{\mathcal{W}^\perp}(\widetilde{L}-\widetilde{S})\|_{\text{HS}}^2\right) &\leq 4(2N+1)\left(16(2N+1)\delta^2 + 4(\sqrt{2N+1}-2)^2\delta_0^2\right)\\
&\leq 4(16+4)(2N+1)^2\delta^2 = 80(2N+1)^2\delta^2,
\end{aligned} \tag{3.61}$$

where we used that $(a-2)^2 = 4 - 4a + a^2 \leq a^2$ for $a \geq 1$ and $\delta_0 \leq \delta$.

All in all, summing up (3.60)–(3.61) finishes the proof. □

The following lemma is similar to [101, Lem. 5] and is needed as an auxiliary result in the proof of Theorem 3.34 above.

Lemma 3.35. *Suppose $\lambda \leq 1/2$ and that C as defined in (3.54) satisfies $C \leq 1/4$. Moreover, let $W \in \text{HS}(L^2(S^1))$ be a dual certificate associated to $\widetilde{L}^0 \in \mathcal{W}_{N_1}^{c_1-c_2}$ and $\widetilde{S}^0 \in \mathcal{V}_{N_1}$ as introduced in (3.51) and (3.53).*

Then, for all $H_1, H_2 \in \mathrm{HS}(L^2(S^1))$ with $H_1 + H_2 = 0$ we have that

$$\|\widetilde{L}^0 + H_1\|_{\mathrm{nuc}} + \lambda\|\widetilde{S}^0 + H_2\|_{\ell^1\times\ell^1} \geq \|\widetilde{L}^0\|_{\mathrm{nuc}} + \lambda\|\widetilde{S}^0\|_{\ell^1\times\ell^1} + \frac{1}{4}\left(\|(I - \mathcal{P}_{\mathcal{W}_{N_1}^{c_1-c_2}})H_1\|_{\mathrm{nuc}} + \lambda\|(I - \mathcal{P}_{\mathcal{V}_{N_2}})H_2\|_{\ell^1\times\ell^1}\right).$$

Proof. We use the abbreviations $\mathcal{W} := \mathcal{W}_{N_1}^{c_1-c_2}$ and $\mathcal{V} := \mathcal{V}_{N_2}$ and suppose that $Z_1 \in \partial(\lambda\|\widetilde{L}^0\|_{\mathrm{nuc}})$ and $Z_2 \in \partial\|\widetilde{S}^0\|_{\ell^1\times\ell^1}$. From Example C.2 and Lemma C.3 we know that these subdifferentials satisfy

$$\begin{aligned} Z_1 &= \Lambda + W' && \text{with} && \mathcal{P}_{\mathcal{W}}W' = 0 && \text{and} && \|W'\| \leq 1\,, \\ Z_2 &= \lambda(\Sigma + F) && \text{with} && \mathcal{P}_{\mathcal{V}}F = 0 && \text{and} && \|F\|_{\ell^\infty\times\ell^\infty} \leq 1\,, \end{aligned}$$

where Λ and Σ are defined as in (3.51) in dependence on a fixed singular system $(\sigma_n; u_n, v_n)_{1\leq n\leq 2N_1+1}$ for $\widetilde{L}^0$ and on the Fourier coefficients $(a_{m,n})_{|m|,|n|\leq N_2}$ of $\widetilde{S}^0$, respectively. Furthermore, due to Definition C.1 of a subgradient we have

$$\|\widetilde{L}^0 + H_1\|_{\mathrm{nuc}} + \lambda\|\widetilde{S}^0 + H_2\|_{\ell^1\times\ell^1} \geq \|\widetilde{L}^0\|_{\mathrm{nuc}} + \lambda\|\widetilde{S}^0\|_{\ell^1\times\ell^1} + \langle Z_1, H_1\rangle_{\mathrm{HS}} + \langle Z_2, H_2\rangle_{\mathrm{HS}}\,.$$

Consequently, it remains to show

$$\langle Z_1, H_1\rangle_{\mathrm{HS}} + \langle Z_2, H_2\rangle_{\mathrm{HS}} \geq \frac{1}{4}\left(\|\mathcal{P}_{\mathcal{W}^\perp}H_1\|_{\mathrm{nuc}} + \lambda\|\mathcal{P}_{\mathcal{V}^\perp}H_2\|_{\ell^1\times\ell^1}\right). \tag{3.62}$$

We rewrite Z_1 and Z_2 by adding and subtracting the dual certificate W from (3.53) and using $\mathcal{P}_{\mathcal{W}}W = 0$ as well as $W' = \mathcal{P}_{\mathcal{W}^\perp}Z_1$, $\mathcal{P}_{\mathcal{W}^\perp}\Lambda = 0$, $\mathcal{P}_{\mathcal{V}}(\lambda\Sigma) = \lambda\Sigma$ and $\lambda F = \mathcal{P}_{\mathcal{V}^\perp}Z_2$ according to

$$\begin{aligned} Z_1 &= (\Lambda + W) + (W' - W) = (\Lambda + W) + \mathcal{P}_{\mathcal{W}^\perp}(Z_1 - \Lambda - W)\,, \\ Z_2 &= (\Lambda + W) - (\mathcal{P}_{\mathcal{V}}(\Lambda + W) - \lambda\Sigma) + (\lambda F - \mathcal{P}_{\mathcal{V}^\perp}(\Lambda + W)) \\ &= (\Lambda + W) - \mathcal{P}_{\mathcal{V}}(\Lambda + W - \lambda\Sigma) + \mathcal{P}_{\mathcal{V}^\perp}(Z_2 - \Lambda - W)\,, \end{aligned}$$

which yields

$$\begin{aligned} &\langle Z_1, H_1\rangle_{\mathrm{HS}} + \langle Z_2, H_2\rangle_{\mathrm{HS}} \\ &= \langle \mathcal{P}_{\mathcal{W}^\perp}(Z_1 - \Lambda - W), H_1\rangle_{\mathrm{HS}} + \langle \mathcal{P}_{\mathcal{V}^\perp}(Z_2 - \Lambda - W), H_2\rangle_{\mathrm{HS}} - \langle \mathcal{P}_{\mathcal{V}}(\Lambda + W - \lambda\Sigma), H_2\rangle_{\mathrm{HS}}\,. \end{aligned} \tag{3.63}$$

Here, we used that $H_1 + H_2 = 0$. In the following, we bound the three summands on the right hand side of (3.63) individually.

Bounds for the first and second summand in (3.63): Since we know that $\|\cdot\|$ and $\|\cdot\|_{\mathrm{nuc}}$ as well as $1/\lambda\|\cdot\|_{\ell^\infty\times\ell^\infty}$ and $\lambda\|\cdot\|_{\ell^1\times\ell^1}$ are dual norms, respectively, we have that

$$\|\mathcal{P}_{\mathcal{W}^\perp}H_1\|_{\mathrm{nuc}} = \sup_{\|G\|\leq 1}\langle G, \mathcal{P}_{\mathcal{W}^\perp}H_1\rangle_{\mathrm{HS}} \qquad \text{and} \qquad \lambda\|\mathcal{P}_{\mathcal{V}^\perp}H_2\|_{\ell^1\times\ell^1} = \sup_{\|G\|_{\ell^\infty\times\ell^\infty}\leq\lambda}\langle G, \mathcal{P}_{\mathcal{V}^\perp}H_2\rangle_{\mathrm{HS}}\,.$$

Consequently, we can choose Z_1 and Z_2 such that $\|Z_1\| \leq 1$, $\|Z_2\|_{\ell^\infty\times\ell^\infty} \leq \lambda$,

$$\langle Z_1, \mathcal{P}_{\mathcal{W}^\perp}H_1\rangle_{\mathrm{HS}} = \|\mathcal{P}_{\mathcal{W}^\perp}H_1\|_{\mathrm{nuc}} \qquad \text{and} \qquad \langle Z_2, \mathcal{P}_{\mathcal{V}^\perp}H_2\rangle_{\mathrm{HS}} = \lambda\|\mathcal{P}_{\mathcal{V}^\perp}H_2\|_{\ell^1\times\ell^1}\,.$$

For the first summand in (3.63), this implies together with the first line in (3.53) that

$$\begin{aligned} &\langle \mathcal{P}_{\mathcal{W}^\perp}(Z_1 - \Lambda - W), H_1\rangle_{\mathrm{HS}} = \langle Z_1, \mathcal{P}_{\mathcal{W}^\perp}H_1\rangle_{\mathrm{HS}} - \langle \mathcal{P}_{\mathcal{W}^\perp}(\Lambda + W), \mathcal{P}_{\mathcal{W}^\perp}H_1\rangle_{\mathrm{HS}} \\ &\geq (1 - \|\mathcal{P}_{\mathcal{W}^\perp}(\Lambda + W)\|)\,\|\mathcal{P}_{\mathcal{W}^\perp}H_1\|_{\mathrm{nuc}} = (1 - \|W\|)\,\|\mathcal{P}_{\mathcal{W}^\perp}H_1\|_{\mathrm{nuc}} \geq \frac{1}{2}\|\mathcal{P}_{\mathcal{W}^\perp}H_1\|_{\mathrm{nuc}}\,. \end{aligned} \tag{3.64}$$

For the second summand in (3.63), we obtain analogously by using the third instead of the first line (3.53) that

$$\langle \mathcal{P}_{\mathcal{V}^\perp}(Z_2 - \Lambda - W), H_2\rangle_{\mathrm{HS}} \;\geq\; (\lambda - \|\mathcal{P}_{\mathcal{V}^\perp}(\Lambda + W)\|_{\ell^\infty\times\ell^\infty})\,\|\mathcal{P}_{\mathcal{V}^\perp}H_2\|_{\ell^1\times\ell^1} \;\geq\; \frac{\lambda}{2}\|\mathcal{P}_{\mathcal{V}^\perp}H_2\|_{\ell^1\times\ell^1}\,.$$

Bound for the third summand in (3.63): We can use the second line in (3.53) to estimate

$$\langle \mathcal{P}_{\mathcal{V}}(\Lambda + W - \lambda\Sigma), H_2\rangle_{\mathrm{HS}} \;=\; \langle \mathcal{P}_{\mathcal{V}}(\Lambda + W - \lambda\Sigma), \mathcal{P}_{\mathcal{V}}H_2\rangle_{\mathrm{HS}} \;\leq\; \frac{\lambda}{4}\|\mathcal{P}_{\mathcal{V}}H_2\|_{\mathrm{HS}}\,.$$

From $\|\mathcal{P}_{\mathcal{V}}\mathcal{P}_{\mathcal{W}}\| \leq \sqrt{C}$ and $\|\mathcal{P}_{\mathcal{V}}\| \leq 1$ we further conclude that

$$\begin{aligned}\|\mathcal{P}_{\mathcal{V}}H_2\|_{\mathrm{HS}} \;\leq\; \|\mathcal{P}_{\mathcal{V}}\mathcal{P}_{\mathcal{W}}H_2\|_{\mathrm{HS}} + \|\mathcal{P}_{\mathcal{V}}\mathcal{P}_{\mathcal{W}^\perp}H_2\|_{\mathrm{HS}} &\leq \sqrt{C}\|H_2\|_{\mathrm{HS}} + \|\mathcal{P}_{\mathcal{W}^\perp}H_2\|_{\mathrm{HS}}\\ &= \sqrt{C}\,(\|\mathcal{P}_{\mathcal{V}}H_2\|_{\mathrm{HS}} + \|\mathcal{P}_{\mathcal{V}^\perp}H_2\|_{\mathrm{HS}}) + \|\mathcal{P}_{\mathcal{W}^\perp}H_2\|_{\mathrm{HS}}\,.\end{aligned}$$

We solve this inequality for $\|\mathcal{P}_{\mathcal{V}}H_2\|_{\mathrm{HS}}$ and obtain together with $\|\mathcal{P}_{\mathcal{V}^\perp}H_2\|_{\mathrm{HS}} \leq \|\mathcal{P}_{\mathcal{V}^\perp}H_2\|_{\mathrm{nuc}}$ (see (A.7)) and $\|\mathcal{P}_{\mathcal{W}^\perp}H_2\|_{\mathrm{HS}} = \|\mathcal{P}_{\mathcal{W}^\perp}H_1\|_{\mathrm{HS}} \leq \|\mathcal{P}_{\mathcal{W}^\perp}H_1\|_{\ell^1\times\ell^1}$ (since $\ell^1 \subseteq \ell^2$) that

$$\begin{aligned}\langle \mathcal{P}_{\mathcal{V}}(\Lambda + W - \lambda\Sigma), H_2\rangle_{\mathrm{HS}} \;\leq\; \frac{\lambda}{4(1-\sqrt{C})}\|\mathcal{P}_{\mathcal{W}^\perp}H_1\|_{\ell^1\times\ell^1} + \frac{\lambda\sqrt{C}}{4(1-\sqrt{C})}\|\mathcal{P}_{\mathcal{V}^\perp}H_2\|_{\mathrm{nuc}}\\ \leq\; \frac{1}{4}\|\mathcal{P}_{\mathcal{W}^\perp}H_1\|_{\ell^1\times\ell^1} + \frac{\lambda}{4}\|\mathcal{P}_{\mathcal{V}^\perp}H_2\|_{\mathrm{nuc}}\,. \quad (3.65)\end{aligned}$$

Finally, we add (3.64)–(3.65) to obtain the upper bound in the lemma. □

Remark 3.36. (i) We first observe that the stability bound (3.58) depends linearly on $(1-C)^{-1}$, i.e., it depends in the same way on the bound C for the cosine of the related minimal angle as before. Furthermore as expected, less a priori knowledge on the locations of the scatterer's components comes at the expense of poorer stability properties compared to the other schemes (cf. Theorems 3.20 and 3.23).

(ii) If $k|\boldsymbol{c}_1 - \boldsymbol{c}_2| > 2(N_1+N_2+1)$ in Theorem 3.34 then the stability estimate can, as in Remarks 3.21 and 3.25, be improved by replacing $C < 1$ by $\widetilde{C} < 1$, where

$$\widetilde{C} := \frac{2\sqrt{2N_1+1}(2N_2+1)}{(k|\boldsymbol{c}_1 - \boldsymbol{c}_2|)^{\frac{1}{2}}}\,.$$

(iii) The assumptions in Theorem 3.34 suggest to choose N large enough so that the data error is sufficiently small and the exact low rank component $\widetilde{L}^0$ is sufficiently well approximated in $\mathcal{V}_N$, but at the same time not larger than necessary. The reduced stability with increasing N is unsatisfying, since a larger N is linked to a better approximation of the full far field operator, i.e. of the data. Since we can already resolve the far field operator in $\mathcal{V}_N$ sufficiently well for $N \gtrsim kR$ with $R > 0$ denoting the radius of the smallest ball containing D (cf. Example 4.1), it is a tolerable restriction. Our numerical tests in Chapter 4 clarify that the dependence of the stability constant in (3.58) on N arises due to the specific choice of $\lambda = 1/\sqrt{2N+1}$. By selecting λ as optimally as possible through trial and error, we can eliminate this dependence in practice. It is ongoing research to improve above stability theorem in this regard . ◊

3.5. Splitting in Born approximation of order two

We consider the quadratic approximation of the scattering problem (2.1) with respect to q, that is obtained by replacing all q dependent quantities u_q, u_q^s, u_q^∞ and F_q by their Born approxima-

tions $u_q^{(\leq 2)}$, $u_q^{s,(\leq 2)}$, $u_q^{\infty,(\leq 2)}$ and $F_q^{(\leq 2)}$ of order $p = 2$, respectively.

Expansion (3.2) then reduces to

$$F_q^{(\leq 2)} \;=\; F_{q_1}^{(\leq 2)} + F_{q_2}^{(\leq 2)} + \big(F_{q_1,q_2}^{(2)} + F_{q_2,q_1}^{(2)}\big)\,, \tag{3.66}$$

which we take as an approach for our investigation in this section. In contrast to (3.16) the term in brackets on the right hand side of (3.2) does not vanish, i.e., multiple scattering is included (at least partly) in our consideration. From Definition and Corollary 2.21 we know that $F_{q_j}^{(\leq 2)} = F_{q_j}^{(1)} + F_{q_j,q_j}^{(2)}$ has a sparse approximation in the subspace $\mathcal{V}_{N_j}^{\boldsymbol{c}_j}$ of far field operators associated to scatterers supported in $B_{R_j}(c_j)$ with $N_j \gtrsim kR_j$, for $j = 1, 2$. Furthermore, we know from Theorem 3.4 that $F_{q_1,q_2}^{(2)}$ and $F_{q_2,q_1}^{(2)}$ have sparse approximations in the related generalized subspaces $\mathcal{V}_{N_1,N_2}^{\boldsymbol{c}_1,\boldsymbol{c}_2}$ and $\mathcal{V}_{N_2,N_1}^{\boldsymbol{c}_2,\boldsymbol{c}_1}$, respectively. In the following, we proceed similar to Section 3.4 before, but we additionally include the subspaces $\mathcal{V}_{N_1,N_2}^{\boldsymbol{c}_1,\boldsymbol{c}_2}$ and $\mathcal{V}_{N_2,N_1}^{\boldsymbol{c}_2,\boldsymbol{c}_1}$ into our schemes.

Splitting by solving a least squares problem

Analogously to (3.17), expansion (3.66) motivates to consider the following *least squares problem* formulation. Given the far field operator F_q we seek approximations $\widetilde{F}_{q_1} \in \mathcal{V}_{N_1}^{\boldsymbol{c}_1}$ and $\widetilde{F}_{q_2} \in \mathcal{V}_{N_2}^{\boldsymbol{c}_2}$ of the far field operators F_{q_1} and F_{q_2}, corresponding to the individual components of the scatterer, satisfying

$$F_q \overset{\text{LS}}{=} \widetilde{F}_{q_1} + \widetilde{F}_{q_2} + \widetilde{F}_{q_1,q_2} + \widetilde{F}_{q_2,q_1} \qquad \text{in } \mathrm{HS}(L^2(S^{d-1})) \tag{3.67}$$

for some $\widetilde{F}_{q_1,q_2} \in \mathcal{V}_{N_1,N_2}^{\boldsymbol{c}_1,\boldsymbol{c}_2}$ and $\widetilde{F}_{q_2,q_1} \in \mathcal{V}_{N_2,N_1}^{\boldsymbol{c}_2,\boldsymbol{c}_1}$. To discuss the conditioning of (3.67), we need the following uncertainty principles, which involve the generalized subspaces from (3.4). They are generalizations of Propositions 3.18 and 3.19.

Proposition 3.37. *Let $d = 2$ and suppose that $G \in \mathcal{V}_{N_1,N_2}^{\boldsymbol{c}_1,\boldsymbol{c}_2}$ and $H \in \mathcal{V}_{N_1',N_2'}^{\boldsymbol{c}_1',\boldsymbol{c}_2'}$ for $\boldsymbol{c}_1, \boldsymbol{c}_1', \boldsymbol{c}_2, \boldsymbol{c}_2' \in \mathbb{R}^2$ and $N_1, N_1', N_2, N_2' \in \mathbb{N}$. Then,*

$$\frac{|\langle G, H\rangle_{\mathrm{HS}}|}{\|G\|_{\mathrm{HS}}\|H\|_{\mathrm{HS}}} \;\leq\; \begin{cases} \frac{\sqrt{(2N_1+1)(2N_2+1)(2N_1'+1)(2N_2'+1)}}{(k^2|\boldsymbol{c}_1-\boldsymbol{c}_1'||\boldsymbol{c}_2-\boldsymbol{c}_2'|)^{\frac{1}{3}}} & \text{if } \boldsymbol{c}_1 \neq \boldsymbol{c}_1' \text{ and } \boldsymbol{c}_2 \neq \boldsymbol{c}_2'\,, \\ \frac{\sqrt{(2N_1+1)(2N_2+1)(2N_1'+1)(2N_2'+1)}}{(k|\boldsymbol{c}_1-\boldsymbol{c}_1'|)^{\frac{1}{3}}} & \text{if } \boldsymbol{c}_1 \neq \boldsymbol{c}_1' \text{ and } \boldsymbol{c}_2 = \boldsymbol{c}_2'\,, \\ \frac{\sqrt{(2N_1+1)(2N_2+1)(2N_1'+1)(2N_2'+1)}}{(k|\boldsymbol{c}_2-\boldsymbol{c}_2'|)^{\frac{1}{3}}} & \text{if } \boldsymbol{c}_1 = \boldsymbol{c}_1' \text{ and } \boldsymbol{c}_2 \neq \boldsymbol{c}_2'\,. \end{cases} \tag{3.68}$$

Proof. Suppose that $\boldsymbol{c}_1 \neq \boldsymbol{c}_1'$ and $\boldsymbol{c}_2 \neq \boldsymbol{c}_2'$. We proceed similarly to the proof of Proposition 3.18 and use Hölder's inequality and (3.8) and (3.7) from Lemma 3.8 to obtain

$$\begin{aligned} |\langle G, H\rangle_{\mathrm{HS}}| \;&\leq\; \|\mathcal{T}_{\boldsymbol{c}_1'-\boldsymbol{c}_1,\boldsymbol{c}_2'-\boldsymbol{c}_2}\mathcal{T}_{\boldsymbol{c}_1,\boldsymbol{c}_2}G\|_{\ell^\infty\times\ell^\infty}\|\mathcal{T}_{\boldsymbol{c}_1',\boldsymbol{c}_2'}H\|_{\ell^1\times\ell^1} \\ &\leq\; \frac{1}{(k|\boldsymbol{c}_1-\boldsymbol{c}_1'|)^{\frac{1}{3}}(k|\boldsymbol{c}_2-\boldsymbol{c}_2'|)^{\frac{1}{3}}}\|\mathcal{T}_{\boldsymbol{c}_1,\boldsymbol{c}_2}G\|_{\ell^1\times\ell^1}\|\mathcal{T}_{\boldsymbol{c}_1',\boldsymbol{c}_2'}H\|_{\ell^1\times\ell^1} \\ &\leq\; \frac{\sqrt{\|\mathcal{T}_{\boldsymbol{c}_1,\boldsymbol{c}_2}G\|_{\ell^0\times\ell^0}\|\mathcal{T}_{\boldsymbol{c}_1',\boldsymbol{c}_2'}H\|_{\ell^0\times\ell^0}}}{(k|\boldsymbol{c}_1-\boldsymbol{c}_1'|)^{\frac{1}{3}}(k|\boldsymbol{c}_2-\boldsymbol{c}_2'|)^{\frac{1}{3}}}\|\mathcal{T}_{\boldsymbol{c}_1,\boldsymbol{c}_2}G\|_{\ell^2\times\ell^2}\|\mathcal{T}_{\boldsymbol{c}_1',\boldsymbol{c}_2'}H\|_{\ell^2\times\ell^2} \\ &=\; \frac{\sqrt{(2N_1+1)(2N_2+1)(2N_1'+1)(2N_2'+1)}}{(k|\boldsymbol{c}_1-\boldsymbol{c}_1'|)^{\frac{1}{3}}(k|\boldsymbol{c}_2-\boldsymbol{c}_2'|)^{\frac{1}{3}}}\|G\|_{\mathrm{HS}}\|H\|_{\mathrm{HS}}\,. \end{aligned}$$

This shows the first inequality in (3.68), and the other two inequalities follow by using the corresponding estimates in (3.8) in above calculation. □

Proposition 3.38. *Let $d = 3$ and suppose that $G \in \mathcal{V}_{N_1,N_2}^{\boldsymbol{c}_1,\boldsymbol{c}_2}$ and $H \in \mathcal{V}_{N_1',N_2'}^{\boldsymbol{c}_1',\boldsymbol{c}_2'}$ for $\boldsymbol{c}_1, \boldsymbol{c}_1', \boldsymbol{c}_2, \boldsymbol{c}_2' \in \mathbb{R}^3$ and $N_1, N_1', N_2, N_2' \in \mathbb{N}$. Then,*

$$\frac{|\langle G, H\rangle_{\mathrm{HS}}|}{\|G\|_{\mathrm{HS}}\|H\|_{\mathrm{HS}}} \leq \begin{cases} \frac{16}{9}\frac{\prod_{i=1}^3\sqrt{(N_1+\frac{i}{2})(N_2+\frac{i}{2})(N_1'+\frac{i}{2})(N_2'+\frac{i}{2})}}{(k^2|\boldsymbol{c}_1-\boldsymbol{c}_1'||\boldsymbol{c}_2-\boldsymbol{c}_2'|)^{\frac{5}{6}}} & \text{if } \boldsymbol{c}_1 \neq \boldsymbol{c}_1' \text{ and } \boldsymbol{c}_2 \neq \boldsymbol{c}_2', \\ \frac{16}{9}\frac{\prod_{i=1}^3\sqrt{(N_1+\frac{i}{2})(N_2+\frac{i}{2})(N_1'+\frac{i}{2})(N_2'+\frac{i}{2})}}{(k|\boldsymbol{c}_1-\boldsymbol{c}_1'|)^{\frac{5}{6}}} & \text{if } \boldsymbol{c}_1 \neq \boldsymbol{c}_1' \text{ and } \boldsymbol{c}_2 = \boldsymbol{c}_2', \\ \frac{16}{9}\frac{\prod_{i=1}^3\sqrt{(N_1+\frac{i}{2})(N_2+\frac{i}{2})(N_1'+\frac{i}{2})(N_2'+\frac{i}{2})}}{(k|\boldsymbol{c}_2-\boldsymbol{c}_2'|)^{\frac{5}{6}}} & \text{if } \boldsymbol{c}_1 = \boldsymbol{c}_1' \text{ and } \boldsymbol{c}_2 \neq \boldsymbol{c}_2'. \end{cases}$$

Proof. As in the previous proof, adapting the proof of Proposition 3.19 by replacing the mapping properties (2.60) and (2.59) of $\mathcal{T}_{\boldsymbol{c}}$ from Lemma 2.25 by the corresponding mapping properties (3.9) and (3.7) of $\mathcal{T}_{\boldsymbol{b},\boldsymbol{c}}$ from Lemma 3.8 yields the result. □

The following theorem gives a stability result for the least squares problem (3.67), which should be compared with Theorem 3.20.

Theorem 3.39. *Suppose that $F_q, F_q^\delta \in \mathrm{HS}(L^2(S^{d-1}))$, let $\boldsymbol{c}_1, \boldsymbol{c}_2 \in \mathbb{R}^d$ and $N_1, N_2 \in \mathbb{N}$ with $N_1 \gtrsim kR_1$ and $N_2 \gtrsim kR_2$, and define*

$$C := \begin{cases} \frac{(2N_1+1)(2N_2+1)}{(k|\boldsymbol{c}_1-\boldsymbol{c}_2|)^{\frac{2}{3}}} & \text{if } d = 2, \\ \frac{16}{9}\frac{\prod_{i=1}^3(N_1+\frac{i}{2})(N_2+\frac{i}{2})}{(k|\boldsymbol{c}_1-\boldsymbol{c}_2|)^{\frac{5}{3}}} & \text{if } d = 3. \end{cases}$$

We assume that, for all $(j,l) \in \{1,2\}^2$,

$$M_j := \begin{cases} \sqrt{C}(\sqrt{C} + 2(2N_j+1)) < 1 & \text{if } d = 2, \\ \sqrt{C}(\sqrt{C} + \frac{8}{3}\prod_{i=1}^3(N_j+\frac{i}{2})) < 1 & \text{if } d = 3. \end{cases}$$

Denote by $\widetilde{F}_{q_1}, \widetilde{F}_{q_2}, \widetilde{F}_{q_1,q_2}, \widetilde{F}_{q_2,q_1}$ and $\widetilde{F}_{q_1}^\delta, \widetilde{F}_{q_2}^\delta, \widetilde{F}_{q_1,q_2}^\delta, \widetilde{F}_{q_2,q_1}^\delta$ the solutions to the least squares problems

$$F_q \overset{\mathrm{LS}}{=} \widetilde{F}_{q_1} + \widetilde{F}_{q_2} + \widetilde{F}_{q_1,q_2} + \widetilde{F}_{q_2,q_1}, \qquad \widetilde{F}_{q_j} \in \mathcal{V}_{N_j}^{\boldsymbol{c}_j}, \ \widetilde{F}_{q_j,q_l} \in \mathcal{V}_{N_j,N_l}^{\boldsymbol{c}_j,\boldsymbol{c}_l}, \tag{3.69a}$$

$$F_q^\delta \overset{\mathrm{LS}}{=} \widetilde{F}_{q_1}^\delta + \widetilde{F}_{q_2}^\delta + \widetilde{F}_{q_1,q_2}^\delta + \widetilde{F}_{q_2,q_1}^\delta, \qquad \widetilde{F}_{q_j}^\delta \in \mathcal{V}_{N_j}^{\boldsymbol{c}_j}, \ \widetilde{F}_{q_j,q_l}^\delta \in \mathcal{V}_{N_j,N_l}^{\boldsymbol{c}_j,\boldsymbol{c}_l}, \tag{3.69b}$$

respectively. Then,

$$\|\widetilde{F}_{q_j} - \widetilde{F}_{q_j}^\delta\|_{\mathrm{HS}}^2 \leq (1-M_j)^{-1}\|F_q - F_q^\delta\|_{\mathrm{HS}}^2, \qquad j = 1,2. \tag{3.70}$$

Proof. We choose $\mathcal{V}_1 = \mathcal{V}_{N_1}^{\boldsymbol{c}_1}$, $\mathcal{V}_2 = \mathcal{V}_{N_2}^{\boldsymbol{c}_2}$, $\mathcal{V}_3 = \mathcal{V}_{N_1,N_2}^{\boldsymbol{c}_1,\boldsymbol{c}_2}$ and $\mathcal{V}_4 = \mathcal{V}_{N_2,N_1}^{\boldsymbol{c}_2,\boldsymbol{c}_1}$ in Theorem 3.15. Summing up the upper bounds from Propositions 3.37 and 3.38 for the cosine of the minimal angle between these subspaces as specified in the stability estimate (3.15) yields the result. □

Remark 3.40. Provided $k|\boldsymbol{c}_1 - \boldsymbol{c}_2| < 2(N_1 + N_2 + d/2)$, the stability bound can be improved by replacing $C < 1$ by $\widetilde{C} < 1$ with $\widetilde{C}$ given as in Remark 3.21. ◊

SPLITTING BY SOLVING AN $\ell^1 \times \ell^1$ MINIMIZATION PROBLEM

As in the previous section, we can replace the least squares formulation (3.67) by a *(weighted) $\ell^1 \times \ell^1$ minimization problem*. This again has the benefit, that only a priori knowledge on the positions $\boldsymbol{c}_j$ of the individual scatterers $D_j \subseteq B_{R_j}(\boldsymbol{c}_j)$ is required, not of the cut-off parameters $N_j \gtrsim kR_j$, $j = 1, 2$.

Compared to (3.27) and (3.34), we modify the objective functions by adding penalty terms, which promote sparsity in the subspaces $\mathcal{V}_{N_1,N_2}^{\boldsymbol{c}_1,\boldsymbol{c}_2}$ and $\mathcal{V}_{N_2,N_1}^{\boldsymbol{c}_2,\boldsymbol{c}_1}$. Given the far field operator F_q and a noise level $\delta > 0$, we seek $(\widetilde{F}_{q_1}, \widetilde{F}_{q_2}, \widetilde{F}_{q_1,q_2}, \widetilde{F}_{q_2,q_1}) \in \mathrm{HS}(L^2(S^{d-1}))^4$ as the solution of

$$\begin{aligned} \underset{(\widetilde{F}_{q_1},\widetilde{F}_{q_2},\widetilde{F}_{q_1,q_2},\widetilde{F}_{q_2,q_1})}{\text{minimize}} \quad & \Psi(\widetilde{F}_{q_1}, \widetilde{F}_{q_2}, \widetilde{F}_{q_1,q_2}, \widetilde{F}_{q_2,q_1}) \\ \text{subject to} \quad & \|F_q^\delta - (\widetilde{F}_{q_1} + \widetilde{F}_{q_2} + \widetilde{F}_{q_1,q_2} + \widetilde{F}_{q_2,q_1})\|_{\mathrm{HS}} \le \delta\,, \end{aligned} \tag{3.71}$$

where for $d = 2$

$$\Psi(\widetilde{F}_{q_1}, \widetilde{F}_{q_2}, \widetilde{F}_{q_1,q_2}, \widetilde{F}_{q_2,q_1}) := \|\mathcal{T}_{\boldsymbol{c}_1}\widetilde{F}_{q_1}\|_{\ell^1\times\ell^1} + \|\mathcal{T}_{\boldsymbol{c}_2}\widetilde{F}_{q_2}\|_{\ell^1\times\ell^1} + \|\mathcal{T}_{\boldsymbol{c}_1,\boldsymbol{c}_2}\widetilde{F}_{q_1,q_2}\|_{\ell^1\times\ell^1} + \|\mathcal{T}_{\boldsymbol{c}_2,\boldsymbol{c}_1}\widetilde{F}_{q_2,q_1}\|_{\ell^1\times\ell^1} \tag{3.72a}$$

and for $d = 3$

$$\begin{aligned} &\Psi(\widetilde{F}_{q_1}, \widetilde{F}_{q_2}, \widetilde{F}_{q_1,q_2}, \widetilde{F}_{q_2,q_1}) \\ &:= \|\mathcal{T}_{\boldsymbol{c}_1}\widetilde{F}_{q_1}\|_{\ell^1_{2n+1}\times\ell^1_{2n+1}} + \|\mathcal{T}_{\boldsymbol{c}_2}\widetilde{F}_{q_2}\|_{\ell^1_{2n+1}\times\ell^1_{2n+1}} + \|\mathcal{T}_{\boldsymbol{c}_1,\boldsymbol{c}_2}\widetilde{F}_{q_1,q_2}\|_{\ell^1_{2n+1}\times\ell^1_{2n+1}} + \|\mathcal{T}_{\boldsymbol{c}_2,\boldsymbol{c}_1}\widetilde{F}_{q_2,q_1}\|_{\ell^1_{2n+1}\times\ell^1_{2n+1}}\,. \end{aligned} \tag{3.72b}$$

Theorem 3.41 below gives a corresponding stability result, which is structured as in Theorems 3.23 and 3.24.

Theorem 3.41. *Suppose that $F_q \in \mathrm{HS}(L^2(S^{d-1}))$ and let $\boldsymbol{c}_1, \boldsymbol{c}_2 \in \mathbb{R}^d$ and $N_1, N_2 \in \mathbb{N}$ with $N_1 \gtrsim kR_1$ and $N_2 \gtrsim kR_2$ such that for all $(j,l) \in \{1,2\}^2$,*

$$C_{j,l} := \begin{cases} \frac{12(2N_j+1)(2N_l+1)}{(k|\boldsymbol{c}_1-\boldsymbol{c}_2|)^{\frac{1}{3}}} < 1 & \text{if } d = 2\,, \\ \frac{64}{3}\frac{\prod_{i=1}^3 (N_j+\frac{i}{2})(N_l+\frac{i}{2})}{(k|\boldsymbol{c}_1-\boldsymbol{c}_2|)^{\frac{5}{6}}} < 1 & \text{if } d = 3\,. \end{cases}$$

We assume that $\widetilde{F}_{q_1}^0 \in \mathcal{V}_{N_1}^{\boldsymbol{c}_1}$, $\widetilde{F}_{q_2}^0 \in \mathcal{V}_{N_2}^{\boldsymbol{c}_2}$, $\widetilde{F}_{q_1,q_2}^0 \in \mathcal{V}_{N_1,N_2}^{\boldsymbol{c}_1,\boldsymbol{c}_2}$, and $\widetilde{F}_{q_2,q_1}^0 \in \mathcal{V}_{N_2,N_1}^{\boldsymbol{c}_2,\boldsymbol{c}_1}$ are such that

$$\|F_q - (\widetilde{F}_{q_1}^0 + \widetilde{F}_{q_2}^0 + \widetilde{F}_{q_1,q_2}^0 + \widetilde{F}_{q_2,q_1}^0)\|_{\mathrm{HS}} < \delta_0 \tag{3.73}$$

for some $\delta_0 \ge 0$. Moreover, suppose that $F_q^\delta \in \mathrm{HS}(L^2(S^{d-1}))$ and $\delta \ge 0$ satisfy

$$\delta \ge \delta_0 + \|F_q - F_q^\delta\|_{\mathrm{HS}}\,.$$

Let $(\widetilde{F}_{q_1}^\delta, \widetilde{F}_{q_2}^\delta, \widetilde{F}_{q_1,q_2}^\delta, \widetilde{F}_{q_2,q_1}^\delta) \in \mathrm{HS}(L^2(S^{d-1}))^4$ denote the solution to

$$\begin{aligned} \underset{(\widetilde{F}_{q_1},\widetilde{F}_{q_2},\widetilde{F}_{q_1,q_2},\widetilde{F}_{q_2,q_1})}{\text{minimize}} \quad & \Psi(\widetilde{F}_{q_1}, \widetilde{F}_{q_2}, \widetilde{F}_{q_1,q_2}, \widetilde{F}_{q_2,q_1}) \\ \text{subject to} \quad & \|F_q^\delta - (\widetilde{F}_{q_1} + \widetilde{F}_{q_2} + \widetilde{F}_{q_1,q_2} + \widetilde{F}_{q_2,q_1})\|_{\mathrm{HS}} \le \delta \end{aligned} \tag{3.74}$$

with Ψ from (3.72). Then,

$$\|\widetilde{F}_{q_j}^0 - \widetilde{F}_{q_j}^\delta\|_{\mathrm{HS}}^2 \le (1 - C_{j,j})^{-1} 4\delta^2\,, \qquad j = 1,2\,. \tag{3.75}$$

Proof. For $j,l = 1,2$, $j \ne l$, we use the abbreviations $\widetilde{F}_j := \widetilde{F}_{q_j}^0 - \widetilde{F}_{q_j}^\delta$ and $\widetilde{F}_{j,l} := \widetilde{F}_{q_j,q_l}^0 - \widetilde{F}_{q_j,q_l}^\delta$. Moreover, we denote the $\ell^0 \times \ell^0$-support of $\mathcal{T}_{\boldsymbol{c}_j}\widetilde{F}_{q_j}^0$ and of $\mathcal{T}_{\boldsymbol{c}_j,\boldsymbol{c}_l}\widetilde{F}_{q_j,q_l}^0$ by W_j and by $W_{j,l}$, respectively.

We estimate as in the proofs of Theorems 3.23 and 3.24 for $d = 2$

$$\begin{aligned} \Psi(\widetilde{F}_1, \widetilde{F}_2, \widetilde{F}_{1,2}, \widetilde{F}_{2,1}) \le 2\big(&\|\mathcal{T}_{\boldsymbol{c}_1}\widetilde{F}_1\|_{(\ell^1\times\ell^1)(W_1)} + \|\mathcal{T}_{\boldsymbol{c}_2}\widetilde{F}_2\|_{(\ell^1\times\ell^1)(W_2)} \\ &+ \|\mathcal{T}_{\boldsymbol{c}_1,\boldsymbol{c}_2}\widetilde{F}_{1,2}\|_{(\ell^1\times\ell^1)(W_{1,2})} + \|\mathcal{T}_{\boldsymbol{c}_2,\boldsymbol{c}_1}\widetilde{F}_{2,1}\|_{(\ell^1\times\ell^1)(W_{2,1})}\big) \end{aligned} \tag{3.76}$$

and for $d = 3$

$$\Psi(\widetilde{F}_1, \widetilde{F}_2, \widetilde{F}_{1,2}, \widetilde{F}_{2,1}) \leq 2(\|\mathcal{T}_{\boldsymbol{c}_1}\widetilde{F}_1\|_{(\ell^1_{2n+1}\times\ell^1_{2n+1})(W_1)} + \|\mathcal{T}_{\boldsymbol{c}_2}\widetilde{F}_2\|_{(\ell^1_{2n+1}\times\ell^1_{2n+1})(W_2)} + \|\mathcal{T}_{\boldsymbol{c}_1,\boldsymbol{c}_2}\widetilde{F}_{1,2}\|_{(\ell^1_{2n+1}\times\ell^1_{2n+1})(W_{1,2})} + \|\mathcal{T}_{\boldsymbol{c}_2,\boldsymbol{c}_1}\widetilde{F}_{2,1}\|_{(\ell^1_{2n+1}\times\ell^1_{2n+1})(W_{2,1})}). \quad (3.77)$$

Using (3.73)–(3.74) and (3.8), we obtain in the two-dimensional case

$$\begin{aligned}
4\delta^2 &\geq \|\widetilde{F}_1\|_{\mathrm{HS}}^2 + \|\widetilde{F}_2\|_{\mathrm{HS}}^2 + \|\widetilde{F}_{1,2}\|_{\mathrm{HS}}^2 + \|\widetilde{F}_{2,1}\|_{\mathrm{HS}}^2 \\
&\quad - 2|\langle\widetilde{F}_1, \widetilde{F}_2\rangle_{\mathrm{HS}}| - 2|\langle\widetilde{F}_1, \widetilde{F}_{1,2}\rangle_{\mathrm{HS}}| - 2|\langle\widetilde{F}_1, \widetilde{F}_{2,1}\rangle_{\mathrm{HS}}| \\
&\quad - 2|\langle\widetilde{F}_2, \widetilde{F}_{1,2}\rangle_{\mathrm{HS}}| - 2|\langle\widetilde{F}_2, \widetilde{F}_{2,1}\rangle_{\mathrm{HS}}| - 2|\langle\widetilde{F}_{1,2}, \widetilde{F}_{2,1}\rangle_{\mathrm{HS}}| \\
&\geq \|\widetilde{F}_1\|_{\mathrm{HS}}^2 + \|\widetilde{F}_2\|_{\mathrm{HS}}^2 + \|\widetilde{F}_{1,2}\|_{\mathrm{HS}}^2 + \|\widetilde{F}_{2,1}\|_{\mathrm{HS}}^2 \\
&\quad - \frac{2}{(k|\boldsymbol{c}_1 - \boldsymbol{c}_2|)^{\frac{2}{3}}}(\|\mathcal{T}_{\boldsymbol{c}_1}\widetilde{F}_1\|_{\ell^1\times\ell^1}\|\mathcal{T}_{\boldsymbol{c}_2}\widetilde{F}_2\|_{\ell^1\times\ell^1} + \|\mathcal{T}_{\boldsymbol{c}_1,\boldsymbol{c}_2}\widetilde{F}_{1,2}\|_{\ell^1\times\ell^1}\|\mathcal{T}_{\boldsymbol{c}_2,\boldsymbol{c}_1}\widetilde{F}_{2,1}\|_{\ell^1\times\ell^1}) \\
&\quad - \frac{2}{(k|\boldsymbol{c}_1 - \boldsymbol{c}_2|)^{\frac{1}{3}}}(\|\mathcal{T}_{\boldsymbol{c}_1}\widetilde{F}_1\|_{\ell^1\times\ell^1}\|\mathcal{T}_{\boldsymbol{c}_1,\boldsymbol{c}_2}\widetilde{F}_{1,2}\|_{\ell^1\times\ell^1} + \|\mathcal{T}_{\boldsymbol{c}_1}\widetilde{F}_1\|_{\ell^1\times\ell^1}\|\mathcal{T}_{\boldsymbol{c}_2,\boldsymbol{c}_1}\widetilde{F}_{2,1}\|_{\ell^1\times\ell^1} \\
&\qquad + \|\mathcal{T}_{\boldsymbol{c}_2}\widetilde{F}_2\|_{\ell^1\times\ell^1}\|\mathcal{T}_{\boldsymbol{c}_1,\boldsymbol{c}_2}\widetilde{F}_{1,2}\|_{\ell^1\times\ell^1} + \|\mathcal{T}_{\boldsymbol{c}_2}\widetilde{F}_2\|_{\ell^1\times\ell^1}\|\mathcal{T}_{\boldsymbol{c}_2,\boldsymbol{c}_1}\widetilde{F}_{2,1}\|_{\ell^1\times\ell^1}) \\
&\geq \|\widetilde{F}_1\|_{\mathrm{HS}}^2 + \|\widetilde{F}_2\|_{\mathrm{HS}}^2 + \|\widetilde{F}_{1,2}\|_{\mathrm{HS}}^2 + \|\widetilde{F}_{2,1}\|_{\mathrm{HS}}^2 \\
&\quad - \frac{2}{(k|\boldsymbol{c}_1 - \boldsymbol{c}_2|)^{\frac{1}{3}}}(\|\mathcal{T}_{\boldsymbol{c}_1}\widetilde{F}_1\|_{\ell^1\times\ell^1}\|\mathcal{T}_{\boldsymbol{c}_2}\widetilde{F}_2\|_{\ell^1\times\ell^1} + \|\mathcal{T}_{\boldsymbol{c}_1,\boldsymbol{c}_2}\widetilde{F}_{1,2}\|_{\ell^1\times\ell^1}\|\mathcal{T}_{\boldsymbol{c}_2,\boldsymbol{c}_1}\widetilde{F}_{2,1}\|_{\ell^1\times\ell^1}) \\
&\qquad \|\mathcal{T}_{\boldsymbol{c}_1}\widetilde{F}_1\|_{\ell^1\times\ell^1}\|\mathcal{T}_{\boldsymbol{c}_1,\boldsymbol{c}_2}\widetilde{F}_{1,2}\|_{\ell^1\times\ell^1} + \|\mathcal{T}_{\boldsymbol{c}_1}\widetilde{F}_1\|_{\ell^1\times\ell^1}\|\mathcal{T}_{\boldsymbol{c}_2,\boldsymbol{c}_1}\widetilde{F}_{2,1}\|_{\ell^1\times\ell^1} \\
&\qquad + \|\mathcal{T}_{\boldsymbol{c}_2}\widetilde{F}_2\|_{\ell^1\times\ell^1}\|\mathcal{T}_{\boldsymbol{c}_1,\boldsymbol{c}_2}\widetilde{F}_{1,2}\|_{\ell^1\times\ell^1} + \|\mathcal{T}_{\boldsymbol{c}_2}\widetilde{F}_2\|_{\ell^1\times\ell^1}\|\mathcal{T}_{\boldsymbol{c}_2,\boldsymbol{c}_1}\widetilde{F}_{2,1}\|_{\ell^1\times\ell^1}).
\end{aligned}$$

According to Lemma 3.22, we have that $2\sum_i\sum_{j<i} a_ia_j = \sum_i\sum_{j\neq i} a_ia_j \leq \frac{3}{4}(\sum_i a_i)^2 \leq 3\sum_i a_i^2$ for all $a_1, a_2, a_3, a_4 \in \mathbb{R}$. Together with (3.76) and the Cauchy Schwarz inequality this implies

$$\begin{aligned}
4\delta^2 &\geq \|\widetilde{F}_1\|_{\mathrm{HS}}^2 + \|\widetilde{F}_2\|_{\mathrm{HS}}^2 + \|\widetilde{F}_{1,2}\|_{\mathrm{HS}}^2 + \|\widetilde{F}_{2,1}\|_{\mathrm{HS}}^2 - \frac{3}{4(k|\boldsymbol{c}_1 - \boldsymbol{c}_2|)^{\frac{1}{3}}}\Psi^2(\widetilde{F}_1, \widetilde{F}_2, \widetilde{F}_{1,2}, \widetilde{F}_{2,1}) \\
&\geq \|\widetilde{F}_1\|_{\mathrm{HS}}^2 + \|\widetilde{F}_2\|_{\mathrm{HS}}^2 + \|\widetilde{F}_{1,2}\|_{\mathrm{HS}}^2 + \|\widetilde{F}_{2,1}\|_{\mathrm{HS}}^2 \\
&\quad - \frac{3}{(k|\boldsymbol{c}_1 - \boldsymbol{c}_2|)^{\frac{1}{3}}}(\|\mathcal{T}_{\boldsymbol{c}_1}\widetilde{F}_1\|_{\ell^1\times\ell^1(W_1)} + \|\mathcal{T}_{\boldsymbol{c}_2}\widetilde{F}_2\|_{\ell^1\times\ell^1(W_2)} \\
&\qquad + \|\mathcal{T}_{\boldsymbol{c}_1,\boldsymbol{c}_2}\widetilde{F}_{1,2}\|_{\ell^1\times\ell^1(W_{1,2})} + \|\mathcal{T}_{\boldsymbol{c}_2,\boldsymbol{c}_1}\widetilde{F}_{2,1}\|_{\ell^1\times\ell^1(W_{2,1})})^2 \\
&\geq \|\widetilde{F}_1\|_{\mathrm{HS}}^2 + \|\widetilde{F}_2\|_{\mathrm{HS}}^2 + \|\widetilde{F}_{1,2}\|_{\mathrm{HS}}^2 + \|\widetilde{F}_{2,1}\|_{\mathrm{HS}}^2 \\
&\quad - \frac{3}{(k|\boldsymbol{c}_1 - \boldsymbol{c}_2|)^{\frac{1}{3}}}(|W_1|^{\frac{1}{2}}\|\widetilde{F}_1\|_{\mathrm{HS}} + |W_2|^{\frac{1}{2}}\|\widetilde{F}_2\|_{\mathrm{HS}} + |W_{1,2}|^{\frac{1}{2}}\|\widetilde{F}_{1,2}\|_{\mathrm{HS}} + |W_{2,1}|^{\frac{1}{2}}\|\widetilde{F}_{2,1}\|_{\mathrm{HS}})^2 \\
&\geq \|\widetilde{F}_1\|_{\mathrm{HS}}^2 + \|\widetilde{F}_2\|_{\mathrm{HS}}^2 + \|\widetilde{F}_{1,2}\|_{\mathrm{HS}}^2 + \|\widetilde{F}_{2,1}\|_{\mathrm{HS}}^2 \\
&\quad - \frac{12}{(k|\boldsymbol{c}_1 - \boldsymbol{c}_2|)^{\frac{1}{3}}}(|W_1|\|\widetilde{F}_1\|_{\mathrm{HS}}^2 + |W_2|\|\widetilde{F}_2\|_{\mathrm{HS}}^2 + |W_{1,2}|\|\widetilde{F}_{1,2}\|_{\mathrm{HS}}^2 + |W_{2,1}|\|\widetilde{F}_{2,1}\|_{\mathrm{HS}}^2) \\
&= (1 - C_{1,1})\|\widetilde{F}_1\|_{\mathrm{HS}}^2 + (1 - C_{2,2})\|\widetilde{F}_2\|_{\mathrm{HS}}^2 + (1 - C_{1,2})(\|\widetilde{F}_{1,2}\|_{\mathrm{HS}}^2 + \|\widetilde{F}_{2,1}\|_{\mathrm{HS}}^2). \quad (3.78)
\end{aligned}$$

In the three-dimensional case, we do the same calculations, but we replace (3.8) by (3.9). We further

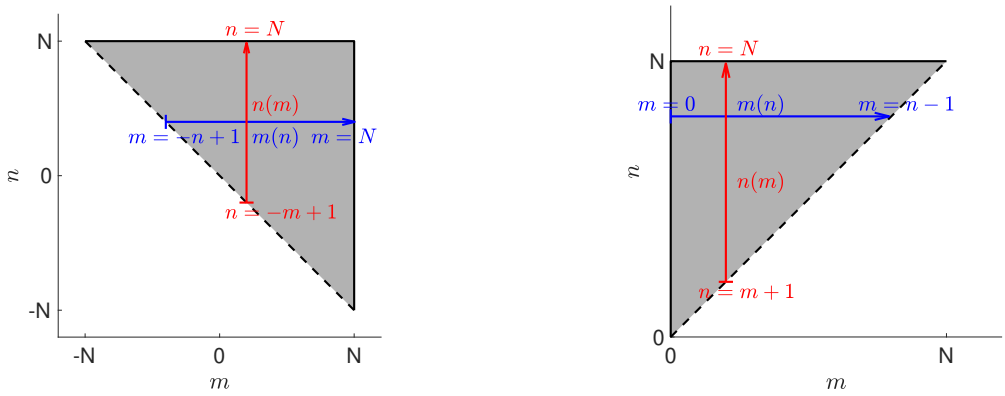

Figure 3.5. Summation over index set of operators in $\widetilde{\mathcal{V}}_N$ for two (left) and three (right) dimensions.

use (3.22) in the last step. This gives (3.78) with the constants

$$C_{j,l} = \frac{12}{(k|\boldsymbol{c}_1-\boldsymbol{c}_2|)^{\frac{5}{6}}}\frac{16}{9}\prod_{i=1}^{3}(N_j+\tfrac{i}{2})(N_l+\tfrac{i}{2}) = \frac{64}{3}\frac{\prod_{i=1}^{3}(N_j+\frac{i}{2})(N_l+\frac{i}{2})}{(k|\boldsymbol{c}_1-\boldsymbol{c}_2|)^{\frac{5}{6}}}, \qquad j,l=1,2\,.$$

□

3.6. Generalizations and further improvements

3.6.1. Taking the reciprocity relation into account

The reciprocity relation (2.8) of the far field pattern u_q^∞ carries over to the lth summand (2.15) in its Born series expansion of the far field as well as to its component (3.1) for $l \geq 1$ and $j_1,\dots,j_l \in \{1,2\}$, so

$$u_q^{\infty,(l)}(\widehat{\boldsymbol{x}};\boldsymbol{\theta}) = u_q^{\infty,(l)}(-\boldsymbol{\theta};-\widehat{\boldsymbol{x}}) \qquad \text{and} \qquad u_{q_{j_1},\dots,q_{j_l}}^{\infty,(l)}(\widehat{\boldsymbol{x}};\boldsymbol{\theta}) = u_{q_{j_l},\dots,q_{j_1}}^{\infty,(l)}(-\boldsymbol{\theta};-\widehat{\boldsymbol{x}}) \tag{3.79}$$

for all $\widehat{\boldsymbol{x}},\boldsymbol{\theta} \in S^{d-1}$. This principle states that it is equivalent to illuminate the scattering object along $\boldsymbol{\theta}$ and measure the generated far field (or far field component) along $\widehat{\boldsymbol{x}}$, or to illuminate along $-\widehat{\boldsymbol{x}}$ and measure along $-\boldsymbol{\theta}$. This symmetry property carries over to the associated expansion coefficients as we show in the following.

First, we examine those far field operator components where only a single component of the scatterer is involved. For $d=2$, let the Fourier coefficients (2.21) of $u_q^{\infty,(l)}$ be denoted by $(a_{m,n}^{(l)})_{m,n}$. We have for $\widehat{\boldsymbol{x}},\boldsymbol{\theta} \in S^1$ that

$$\begin{aligned} u_q^{\infty,(l)}(-\boldsymbol{\theta};-\widehat{\boldsymbol{x}}) &= \sum_{m\in\mathbb{Z}}\sum_{n\in\mathbb{Z}} a_{m,n}^{(l)}\boldsymbol{e}_m(-\boldsymbol{\theta})\overline{\boldsymbol{e}_n(-\widehat{\boldsymbol{x}})} \\ &= \sum_{m\in\mathbb{Z}}\sum_{n\in\mathbb{Z}}(-1)^{n-m}a_{m,n}^{(l)}\boldsymbol{e}_{-n}(\widehat{\boldsymbol{x}})\overline{\boldsymbol{e}_{-m}(\boldsymbol{\theta})} = \sum_{m\in\mathbb{Z}}\sum_{n\in\mathbb{Z}}(-1)^{m-n}a_{-n,-m}^{(l)}\boldsymbol{e}_m(\widehat{\boldsymbol{x}})\overline{\boldsymbol{e}_n(\boldsymbol{\theta})}\,. \end{aligned}$$

The reciprocity relation (3.79) then gives by equating coefficients

$$a_{m,n}^{(l)} = (-1)^{m+n}a_{-n,-m}^{(l)} \qquad \text{for } m,n\in\mathbb{Z}\,. \tag{3.80}$$

The same holds for the Fourier coefficients of u_q^∞.

Analogously for $d=3$, let $\alpha_{m,n}^{(l)}$ denote the (m,n)th spherical harmonics component of $u_q^{\infty,(l)}$. From (B.15) we conclude with the chain rule that $P_m(-t) = (-1)^m P_m(t)$ for $t \in [-1,1]$. This yields

together with (2.50)

$$\alpha_{m,n}^{(l)}(-\boldsymbol{\theta};-\widehat{\boldsymbol{x}}) = (-1)^{m+n}k^{2l}\frac{(2m+1)^2(2n+1)^2}{16\pi^2}\mathrm{i}^{n-m}\int_D\cdots\int_D q(\boldsymbol{y}_l)\cdots q(\boldsymbol{y}_1)$$
$$\times\,\Phi_k(\boldsymbol{y}_l-\boldsymbol{y}_{l-1})\cdots\Phi_k(\boldsymbol{y}_2-\boldsymbol{y}_1)j_m(k|\boldsymbol{y}_l|)j_n(k|\boldsymbol{y}_1|)\langle P_m^{\boldsymbol{\theta}},P_m^{\widehat{\boldsymbol{y}}_l}\rangle_{L^2(S^2)}\langle P_n^{\widehat{\boldsymbol{x}}},P_n^{\widehat{\boldsymbol{y}}_1}\rangle_{L^2(S^2)}\,\mathrm{d}\boldsymbol{y}_1\cdots\mathrm{d}\boldsymbol{y}_l$$

for $\widehat{\boldsymbol{x}},\boldsymbol{\theta}\in S^2$. Again, the reciprocity relation (3.79) gives by equating coefficients

$$\alpha_{m,n}^{(l)} = (-1)^{m+n}\alpha_{n,m}^{(l)} \qquad \text{for } m,n\in\mathbb{N}_0\,, \tag{3.81}$$

as well as the same for the spherical harmonics components of u_q^∞.

Now, we turn our attention to the far field components that model multiple scattering, potentially involving different scatterer's components. Suppose $d=2$ and let $(a_{m,n}^{(l)})_{m,n}$ denote the Fourier coefficients of $u_{q_{j_1},\dots,q_{j_l}}^{\infty,(l)}$ and $(b_{m,n}^{(l)})_{m,n}$ the Fourier coefficients $u_{q_{j_l},\dots,q_{j_1}}^{\infty,(l)}$. Then, the same calculation as above shows that

$$a_{m,n}^{(l)} = (-1)^{m+n}b_{-n,-m}^{(l)} \qquad \text{for } m,n\in\mathbb{Z}\,. \tag{3.82}$$

In the same way, we obtain for $d=3$ that

$$\alpha_{m,n}^{(l)} = (-1)^{m+n}\beta_{n,m}^{(l)} \qquad \text{for } m,n\in\mathbb{N}_0\,, \tag{3.83}$$

where $\alpha_{m,n}^{(l)}$ and $\beta_{m,n}^{(l)}$ denote the (m,n)th spherical harmonics component of $u_{q_{j_1},\dots,q_{j_l}}^{\infty,(l)}$ and of $u_{q_{j_l},\dots,q_{j_1}}^{\infty,(l)}$, respectively.

We can take the symmetry properties (3.80) and (3.81) into account when defining the related subspaces of sparse far field operators.

In two dimensions, any $G\in\mathcal{V}_N$ with

$$Gg = \sum_{|m|\le N}\sum_{|n|\le N} a_{m,n}\,\boldsymbol{e}_m\langle g,\boldsymbol{e}_n\rangle_{L^2(S^1)}\,, \qquad g\in L^2(S^1)\,,$$

that satisfies (3.80) can be rewritten as

$$\begin{aligned}
Gg &= \sum_{|m|\le N}\sum_{n=-m}^{N} a_{m,n}\boldsymbol{e}_m\langle g,\boldsymbol{e}_n\rangle_{L^2(S^1)} + \sum_{|m|\le N}\sum_{n=-N}^{-m-1} a_{m,n}\boldsymbol{e}_m\langle g,\boldsymbol{e}_n\rangle_{L^2(S^1)}\\
&= \sum_{|m|\le N}\sum_{n=-m}^{N} a_{m,n}\boldsymbol{e}_m\langle g,\boldsymbol{e}_n\rangle_{L^2(S^1)} + \sum_{|m|\le N}\sum_{n=-N}^{-m-1} (-1)^{m+n}a_{-n,-m}\boldsymbol{e}_m\langle g,\boldsymbol{e}_n\rangle_{L^2(S^1)}\\
&= \sum_{|m|\le N}\sum_{n=-m}^{N} a_{m,n}\boldsymbol{e}_m\langle g,\boldsymbol{e}_n\rangle_{L^2(S^1)} + \sum_{|n|\le N}\sum_{m=-n+1}^{N} (-1)^{m+n}a_{m,n}\overline{\boldsymbol{e}_n}\langle g,\overline{\boldsymbol{e}_m}\rangle_{L^2(S^1)}\\
&= \sum_{|m|\le N}\sum_{n=-m}^{N} a_{m,n}\boldsymbol{e}_m\langle g,\boldsymbol{e}_n\rangle_{L^2(S^1)} + \sum_{|m|\le N}\sum_{n=-m+1}^{N} (-1)^{m+n}a_{m,n}\overline{\boldsymbol{e}_n}\langle g,\overline{\boldsymbol{e}_m}\rangle_{L^2(S^1)}\\
&= \sum_{|m|\le N}\sum_{n=-m}^{N} a_{m,n}\Big(1-\frac{1}{2}\delta_n^{-m}\Big)\Big(\boldsymbol{e}_m\langle g,\boldsymbol{e}_n\rangle_{L^2(S^{d-1})} + (-1)^{m+n}\overline{\boldsymbol{e}_n}\langle g,\overline{\boldsymbol{e}_m}\rangle_{L^2(S^1)}\Big)\,.
\end{aligned}$$

Here, δ_n^{-m} denotes the Kronecker delta. We did index transformations in the third step and changed the summation direction as shown in Figure 3.5 (left) in the fourth step. Accordingly, we define for any $\boldsymbol{c}\in\mathbb{R}^2$ and $N\in\mathbb{N}$ the finite-dimensional subspace

$$\widetilde{\mathcal{V}}_N^{\boldsymbol{c}} := \{G\in\mathrm{HS}(L^2(S^1)) \mid \mathcal{T}_{\boldsymbol{c}}G\in\widetilde{\mathcal{V}}_N\} \tag{3.84}$$

with

$$\widetilde{\mathcal{V}}_N := \Big\{ G \in \mathrm{HS}(L^2(S^1)) \;\Big|\; Gg = \sum_{|m|\le N} \sum_{n=-m}^{N} a_{m,n} \Big(1 - \frac{1}{2}\delta_n^{-m}\Big) \Big(\boldsymbol{e}_m \langle g, \boldsymbol{e}_n \rangle_{L^2(S^1)} + (-1)^{m+n} \overline{\boldsymbol{e}_n} \langle g, \overline{\boldsymbol{e}_m} \rangle_{L^2(S^1)} \Big) \,,\; a_{m,n} \in \mathbb{C} \Big\}. \tag{3.85}$$

Analogously in three dimensions, any $G \in \mathcal{V}_N$ with

$$Gg = \sum_{m=0}^{N} \sum_{n=0}^{N} \int_{S^2} \alpha_{m,n}(\,\cdot\,;\boldsymbol{\theta}) g(\boldsymbol{\theta}) \,\mathrm{d}s(\boldsymbol{\theta}) \,, \qquad g \in L^2(S^2) \,,$$

that satisfies (3.81) can be rewritten as

$$\begin{aligned}
Gg &= \sum_{m=0}^{N} \sum_{n=m}^{N} \int_{S^2} \alpha_{m,n}(\,\cdot\,;\boldsymbol{\theta}) g(\boldsymbol{\theta}) \,\mathrm{d}s(\boldsymbol{\theta}) + \sum_{m=0}^{N} \sum_{n=0}^{m-1} \int_{S^2} \alpha_{m,n}(\,\cdot\,;\boldsymbol{\theta}) g(\boldsymbol{\theta}) \,\mathrm{d}s(\boldsymbol{\theta}) \\
&= \sum_{m=0}^{N} \sum_{n=m}^{N} \int_{S^2} \alpha_{m,n}(\,\cdot\,;\boldsymbol{\theta}) g(\boldsymbol{\theta}) \,\mathrm{d}s(\boldsymbol{\theta}) + \sum_{m=0}^{N} \sum_{n=0}^{m-1} (-1)^{m+n} \int_{S^2} \alpha_{n,m}(\,\cdot\,;\boldsymbol{\theta}) g(\boldsymbol{\theta}) \,\mathrm{d}s(\boldsymbol{\theta}) \\
&= \sum_{m=0}^{N} \sum_{n=m}^{N} \int_{S^2} \alpha_{m,n}(\,\cdot\,;\boldsymbol{\theta}) g(\boldsymbol{\theta}) \,\mathrm{d}s(\boldsymbol{\theta}) + \sum_{n=0}^{N} \sum_{m=0}^{n-1} (-1)^{m+n} \int_{S^2} \alpha_{m,n}(\,\cdot\,;\boldsymbol{\theta}) g(\boldsymbol{\theta}) \,\mathrm{d}s(\boldsymbol{\theta}) \\
&= \sum_{m=0}^{N} \sum_{n=m}^{N} \int_{S^2} \alpha_{m,n}(\,\cdot\,;\boldsymbol{\theta}) g(\boldsymbol{\theta}) \,\mathrm{d}s(\boldsymbol{\theta}) + \sum_{m=0}^{N} \sum_{n=m+1}^{N} (-1)^{m+n} \int_{S^2} \alpha_{m,n}(\,\cdot\,;\boldsymbol{\theta}) g(\boldsymbol{\theta}) \,\mathrm{d}s(\boldsymbol{\theta}) \\
&= \sum_{m=0}^{N} \sum_{n=m}^{N} \Big(1 + (-1)^{m+n} - \delta_n^m\Big) \int_{S^2} \alpha_{m,n}(\,\cdot\,;\boldsymbol{\theta}) g(\boldsymbol{\theta}) \,\mathrm{d}s(\boldsymbol{\theta}) \,.
\end{aligned}$$

Here, we changed the summation direction in the fourth step as shown in Figure 3.5 (right). As before, we define for any $\boldsymbol{c} \in \mathbb{R}^3$ and $N \in \mathbb{N}$ the finite-dimensional subspace

$$\widetilde{\mathcal{V}}_N^{\boldsymbol{c}} := \{ G \in \mathrm{HS}(L^2(S^2)) \mid \mathcal{T}_{\boldsymbol{c}} G \in \widetilde{\mathcal{V}}_N \} \,,$$

with

$$\tilde{\mathcal{V}}_N := \Big\{ G \in \mathrm{HS}(L^2(S^2)) \;\Big|\; Gg = \sum_{m=0}^{N} \sum_{n=0}^{m} \Big(1 + (-1)^{m+n}\Big) \int_{S^2} \alpha_{m,n}(\,\cdot\,;\boldsymbol{\theta}) g(\boldsymbol{\theta}) \,\mathrm{d}s(\boldsymbol{\theta}) \,,\; \alpha_{m,n} \in \mathbb{Y}_m^3 \times \mathbb{Y}_n^3 \Big\}. \tag{3.86}$$

For both cases, $d = 2$ and $d = 3$, we have that $\widetilde{\mathcal{V}}_N^{\boldsymbol{c}} \subseteq \mathcal{V}_N^{\boldsymbol{c}}$.

Example 3.42. We illustrate above observations by a numerical example, and we consider the same kite shaped scatterer $D \subseteq \mathbb{R}^2$ as in Examples 2.5, 2.14 and 2.23, i.e., we have that $k = 2.5$ and $q = 2\chi_D$. In Figure 3.6 (middle), the real part of the corresponding discretized far field operator $\boldsymbol{F}_q$ is plotted for $L = 256$ equally distributed observation and illumination directions. The symmetry axis

$$\{(\widehat{\boldsymbol{x}}, \boldsymbol{\theta}) \in S^1 \times S^1 \mid \arg \boldsymbol{\theta} = \arg(-\widehat{\boldsymbol{x}})\} = \{(\widehat{\boldsymbol{x}}, \boldsymbol{\theta}) \in S^1 \times S^1 \mid \arg \boldsymbol{\theta} = \arg \widehat{\boldsymbol{x}} + \pi\}$$

is added by two dashed black lines. The expansion coefficients $(a_{m,n})_{m,n}$ of $\mathcal{T}_{\boldsymbol{c}} \boldsymbol{F}_q$ with respect to the basis from (3.85) are shown in Figure 3.6 (right) on a logarithmic color scale. Here, we choose $\boldsymbol{c} = (1, 2)^\top$ and $R = 2.2$, which leads to $N = \lceil ekR/2 \rceil = 8$. The support of the expansion

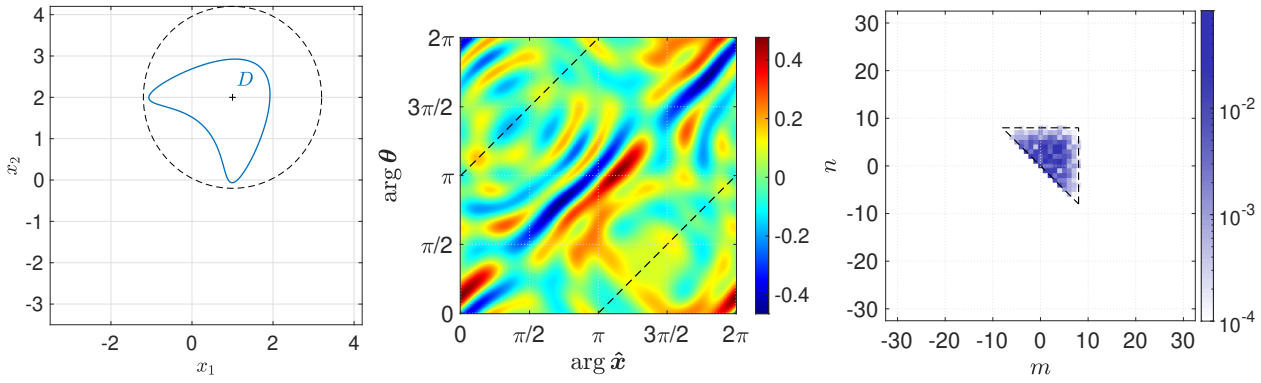

FIGURE 3.6. Left: Support of scatterer D (solid) and ball containing D (dashed). Middle: Real part of discretized far field operator $\boldsymbol{F}_q$ with symmetry axis $\{(\widehat{\boldsymbol{x}}, \boldsymbol{\theta}) \,|\, \arg \boldsymbol{\theta} = \arg(-\widehat{\boldsymbol{x}})\}$. Right: Absolute values of expansion coefficients $(a_{m,n})_{m,n}$ with respect to basis from (3.84) of far field operator $\mathcal{T}_{\boldsymbol{c}} \boldsymbol{F}_q$ together with dashed triangle corresponding to its sparse approximation in $\widetilde{\mathcal{V}}_N$ for $N = 8$.

coefficients belonging to the sparse approximation of $\mathcal{T}_{\boldsymbol{c}} \boldsymbol{F}_q$ in $\widetilde{\mathcal{V}}_N$ is marked by a dashed black triangle, and it is nicely confirmed that these are essentially support in this triangle. ◊

For $d = 2$ and $G \in \widetilde{\mathcal{V}}_N$ given as in (3.85), $(2N + 1)(N + 1)$ Fourier coefficients are required to represent G, so approximately half as many coefficients compared to (2.22). Accordingly, given $\boldsymbol{c}_1, \boldsymbol{c}_2 \in \mathbb{R}^2$ and $N_1, N_2 \in \mathbb{N}$, and replacing $\mathcal{V}_{N_1}^{\boldsymbol{c}_1}$ and $\mathcal{V}_{N_2}^{\boldsymbol{c}_2}$ by $\widetilde{\mathcal{V}}_{N_1}^{\boldsymbol{c}_1}$ and $\widetilde{\mathcal{V}}_{N_2}^{\boldsymbol{c}_2}$ in the least squares problems (3.23) yields the improved constants

$$C := \frac{\sqrt{(2N_1 + 1)(N_1 + 1)(2N_2 + 1)(N_2 + 1)}}{(k|c_1 - c_2|)^{\frac{2}{3}}},$$
$$\widetilde{C} := \frac{\sqrt{(2N_1 + 1)(N_1 + 1)(2N_2 + 1)(N_2 + 1)}}{k|c_1 - c_2|}$$

in (3.24). These constants are better by a factor of about $1/2$. The same qualitative improvement can be obtained in Theorem 3.23.

For taking the symmetry properties (3.82) and (3.83) into account, we further define in case of $d = 2$ for $\boldsymbol{b}, \boldsymbol{c} \in \mathbb{R}^2$ and $M, N \in \mathbb{N}$ the finite-dimensional subspace

$$\widetilde{\mathcal{V}}_{M,N}^{\boldsymbol{b},\boldsymbol{c}} := \Big\{ G \in \mathrm{HS}(L^2(S^1)) \,\Big|\, Gg = \sum_{|m| \le N} \sum_{|n| \le M} a_{m,n} \big(T_{\boldsymbol{b}} \boldsymbol{e}_m \langle g, T_{\boldsymbol{c}} \boldsymbol{e}_n \rangle_{L^2(S^1)} + (-1)^{m+n} T_{\boldsymbol{c}} \overline{\boldsymbol{e}_n} \langle g, T_{\boldsymbol{b}} \overline{\boldsymbol{e}_m} \rangle_{L^2(S^1)} \big) \,,\, a_{m,n} \in \mathbb{C} \Big\}. \quad (3.87)$$

In case of $d = 3$, we set for $\boldsymbol{b}, \boldsymbol{c} \in \mathbb{R}^3$ and $M, N \in \mathbb{N}$

$$\widetilde{\mathcal{V}}_{M,N}^{\boldsymbol{b},\boldsymbol{c}} := \Big\{ G \in \mathrm{HS}(L^2(S^2)) \,\Big|\, Gg = \sum_{m=0}^{M} \sum_{n=0}^{N} \int_{S^2} \Big(\mathcal{T}_{\boldsymbol{b},\boldsymbol{c}} + (-1)^{m+n} \mathcal{T}_{\boldsymbol{c},\boldsymbol{b}} \Big) \alpha_{m,n}(\,\cdot\,; \boldsymbol{\theta}) g(\boldsymbol{\theta}) \, \mathrm{d}s(\boldsymbol{\theta}) \,,\, \alpha_{m,n} \in \mathbb{Y}_m^3 \times \mathbb{Y}_n^3 \Big\}. \quad (3.88)$$

By replacing $\mathcal{V}_{N_1}^{\boldsymbol{c}_1}$, $\mathcal{V}_{N_2}^{\boldsymbol{c}_2}$ and $\mathcal{V}_{N_1,N_2}^{\boldsymbol{c}_1,\boldsymbol{c}_2} \oplus \mathcal{V}_{N_2,N_1}^{\boldsymbol{c}_2,\boldsymbol{c}_1}$ by $\widetilde{\mathcal{V}}_{N_1}^{\boldsymbol{c}_1}$, $\widetilde{\mathcal{V}}_{N_2}^{\boldsymbol{c}_2}$ and $\widetilde{\mathcal{V}}_{N_1,N_2}^{\boldsymbol{c}_1,\boldsymbol{c}_2}$ in the least squares problem (3.69), we again can improve the constant C by a factor of about $1/2$, and the same can be done in Theorem 3.41.

In three dimensions, the stability gain described above is even more significant, but technically more involved. To see this, we replace $W_j \subseteq [0, N_j]^2$ in the estimate (3.22) by $\widetilde{W}_j \subseteq \{(m, n) \in W_j \,|\, n \le m\}$

and obtain

$$\sum_{(m,n)\in\widetilde{W}_j}(2m+1)^2(2n+1)^2 \le \sum_{m=0}^{N_j}(2m+1)^2\sum_{n=0}^{m}(2n+1)^2 = \frac{1}{3}\sum_{m=0}^{N_j}(2m+1)^2(m+1)(2m+3)$$
$$= \frac{1}{30}(N_j+1)(N_j+2)(16N_j^3+62N_j^2+62N_j+15)\,, \quad (3.89)$$

where we used the upper bound from (3.22) as well as the first four formulas of Faulhaber. The fourth formula of Faulhaber reads $\sum_{j=1}^{n} j^4 = \frac{1}{30}n(n+1)(2n+1)(3n^2+3n-1)$ (cf. e.g. [71]). To examine by what factor the stability constants improve when replacing W_j with $\widetilde{W}_j$, we divide the square root of the upper bound in (3.89) by the upper bound in (3.22). Here, we obtain a term that decreases strictly monotonically in $N_j \in \mathbb{N}$, so achieves its largest value for $N_j = 1$. This yields that the constants C in Theorems 3.39 and 3.41 can be improved by approximately a factor of $1/4$. We further recognize that the order of these constants in N_j can be reduced from $O(N_j^3)$ to $O(N_j^{5/2})$.

3.6.2. Splitting in Born approximation of higher order

Our criterion from Section 3.5 for identifying multiple scattering effects involving both q_1 and q_2, namely that the corresponding summands have sparse representations in the subspaces $\mathcal{V}_{N_1,N_2}^{\boldsymbol{c}_1,\boldsymbol{c}_2}$ or $\mathcal{V}_{N_2,N_1}^{\boldsymbol{c}_2,\boldsymbol{c}_1}$, see (3.66), no longer works for scattering orders p larger than 2. This is because a scattering process is no longer uniquely determined by which component the wave was first scattered on and last scattered on. For example, the summand $F_{q_1,q_2,q_1}^{(l)}$ can no longer be distinguished from the summand $F_{q_1,q_1,q_1}^{(l)}$ in the expansion (3.2). They are both assigned to the far field operator $F_{q_1}^{(\le p)}$, which is associated to q_1, i.e., $F_{q_1,q_2,q_1}^{(l)}$ is wrongly assigned. To get an impression of how many summands are incorrectly assigned, we write out the expansion (3.2) for $p = 3$ and $p = 4$, and we mark these wrongly assigned summands with boxes. For $p = 3$ we obtain

$$F_q^{(\le 3)} = F_{q_1}^{(\le 3)} + F_{q_2}^{(\le 3)} + \Big(F_{q_1,q_2}^{(2)} + F_{q_2,q_1}^{(2)} + F_{q_1,q_1,q_2}^{(3)} + \boxed{F_{q_1,q_2,q_1}^{(3)}} + F_{q_1,q_2,q_2}^{(3)} + F_{q_2,q_1,q_1}^{(3)} + \boxed{F_{q_2,q_1,q_2}^{(3)}} + F_{q_2,q_2,q_1}^{(3)}\Big)$$

and for $p = 4$

$$\begin{aligned} F_q^{(\le 4)} = F_{q_1}^{(\le 4)} + F_{q_2}^{(\le 4)} + \Big(&F_{q_1,q_2}^{(2)} + F_{q_2,q_1}^{(2)} \\ &+ F_{q_1,q_1,q_2}^{(3)} + \boxed{F_{q_1,q_2,q_1}^{(3)}} + F_{q_1,q_2,q_2}^{(3)} + F_{q_2,q_1,q_1}^{(3)} + \boxed{F_{q_2,q_1,q_2}^{(3)}} + F_{q_2,q_2,q_1}^{(3)} \\ &+ F_{q_1,q_1,q_1,q_2}^{(4)} + \boxed{F_{q_1,q_1,q_2,q_1}^{(4)}} + F_{q_1,q_1,q_2,q_2}^{(4)} + \boxed{F_{q_1,q_2,q_1,q_1}^{(4)}} + F_{q_1,q_2,q_1,q_2}^{(4)} \\ &+ \boxed{F_{q_1,q_2,q_2,q_1}^{(4)}} + F_{q_1,q_2,q_2,q_2}^{(4)} + F_{q_2,q_1,q_1,q_1}^{(4)} + \boxed{F_{q_2,q_1,q_1,q_2}^{(4)}} + F_{q_2,q_1,q_2,q_1}^{(4)} \\ &+ \boxed{F_{q_2,q_1,q_2,q_2}^{(4)}} + F_{q_2,q_2,q_1,q_1}^{(4)} + \boxed{F_{q_2,q_2,q_1,q_2}^{(4)}} + F_{q_2,q_2,q_2,q_1}^{(4)}\Big)\,. \end{aligned}$$

We conclude that for arbitrary scattering order $p \ge 3$ in total absolutely

$$2\sum_{l=3}^{p}(2^{l-2}-1) = 2\sum_{l=0}^{p-2}2^l - 2(p-1) = 2^p - 2p$$

and relatively

$$\frac{2^p-2p}{\sum_{l=1}^{p}2^l} = \frac{2^p-2p}{2^{p+1}-2} \in [\tfrac{1}{7},\tfrac{1}{2})$$

summands of the expansion (3.2) are wrongly assigned, so in the limit case $p \to \infty$ half of the summands in the Born series expansion, splitted half-half between F_{q_1} and F_{q_2}. These considerations relate to the problem formulations from Subsection 3.4.1 and Section 3.5.

For the RPCP formulation from Subsection 3.4.2 the situation is different. We modify the aim of this problem formulation, namely to recover the far field operator F_{q_2} corresponding to the second scatterer's component from F_q by approximating this component in $\mathcal{V}_{N_2}^{\mathbf{c}_2}$ and the difference $F_q - F_{q_2}$ in $\mathcal{W}_{N_1}^{\mathbf{c}_1}$, cf. (3.48). Particularly, we no longer suppose the low rank component to approximate F_{q_1}. For $p \geq 3$ only summands of the form $F^{(l)}_{q_2,\dots,q_1,\dots,q_2}$ are wrongly assigned since summands of the form $F^{(l)}_{q_1,\dots,q_1}$, $F^{(l)}_{q_1,\dots,q_2}$ and $F^{(l)}_{q_2,\dots,q_1}$ can be well approximated in $\mathcal{W}_{N_1}^{\mathbf{c}_1}$, see Theorems 2.11, 2.19 and 3.5. As above, we conclude that for arbitrary scattering order $p \geq 3$ in total absolutely $(2^p - 2p)/2 = 2^{p-1} - p$, so relatively

$$\frac{2^{p-1} - p}{\sum_{l=1}^{p} 2^l} = \frac{2^{p-1} - p}{2^{p+1} - 2} \in [\tfrac{1}{14}, \tfrac{1}{4})$$

and in the limit case $p \to \infty$ quarter of the summands in the Born series expansion are wrongly assigned. Of course, for the operator part F_{q_2}, which we want to reconstruct, this means the same number of incorrect assignments as before.

At first glance, it seems unattractive to use our developed methods for high values of p or even for the full far field operator F_q due to the large ratio of wrongly assigned summands in the Born series expansion. However, if we look at the formula (3.1) for $u^{\infty,(l)}_{q_{j_1},\dots,q_{j_l}}$, we realize that due to the decay behavior of the fundamental solution (cf. e.g. [31, (3.105)] for $d = 2$) and the disjoint support of the scatterer's components, each change of the scatterer's component during a scattering process leads to a damping of the corresponding summand in the Born series. For those summands that are incorrectly assigned, such a change of the scatterer's component occurs at least twice and the average number of changes per summand in the Born series also grows with p. This leads us to assume that, although for the full far field operator F_q half or quarter of the summands in its Born series expansion are wrongly assigned, these summands only make a little contribution already for moderate values of p. In fact, this is validated by our numerical tests in Chapter 4.

3.6.3. GENERALIZATIONS FOR $J \geq 2$ SCATTERER COMPONENTS

In this section we no longer restrict ourselves to the case $J = 2$ but permit the scatterer D to consist of $J \geq 2$ components, see Assumption 3.1.

In this situation, the Born far field operator of order $p \in \mathbb{N}$ associated to q can be expanded as

$$F_q^{(\leq p)} = \sum_{j=1}^{J} F_{q_j}^{(\leq p)} + \left(\sum_{l=1}^{p} \sum_{(j_1,\dots,j_l) \in \{1,\dots,J\}^l \setminus \left(\cup_{j=1}^{J} \{j\}^l\right)} F^{(l)}_{q_{j_1},\dots,q_{j_l}} \right),$$

which reads for $p = 2$

$$F_q^{(\leq 2)} = \sum_{j=1}^{J} F_{q_j}^{(\leq 2)} + \left(\sum_{(j_1,j_2) \in \{1,\dots,J\}^2 \setminus \{(j,j) \,|\, 1 \leq j \leq J\}} F^{(2)}_{q_{j_1},q_{j_l}} \right). \tag{3.90}$$

Based on (3.90), we consider a similar least squares problem as (3.67), for which the theorem below gives a stability result. For $J = 2$ this theorem coincides with Theorem 3.39.

Theorem 3.43. *Suppose that $F_q, F_q^\delta \in \mathrm{HS}(L^2(S^{d-1}))$, let $\mathbf{c}_j \in \mathbb{R}^d$ and $N_j \in \mathbb{N}$ with $N_j \gtrsim kR_j$*

for $j = 1, \dots, J$ and define for $j \neq l$

$$C_{j,l} := \begin{cases} \frac{(2N_j+1)(2N_l+1)}{(k|\boldsymbol{c}_j - \boldsymbol{c}_l|)^{\frac{2}{3}}} & \text{if } d = 2\,, \\ \frac{16}{9} \frac{\prod_{i=1}^{3}(N_j+\frac{i}{2})(N_l+\frac{i}{2})}{(k|\boldsymbol{c}_j - \boldsymbol{c}_l|)^{\frac{5}{3}}} & \text{if } d = 3\,. \end{cases}$$

We assume that, for $j = 1, \dots, J$,

$$M_j := \begin{cases} \sum\limits_{l \neq j} \sqrt{C_{j,l}} \big(\sqrt{C_{j,l}} + 2(2N_j + 1) + \sum\limits_{m \neq j\,,\, m \neq l} \sqrt{C_{j,m}} \big) < 1 & \text{if } d = 2\,, \\ \sum\limits_{l \neq j} \sqrt{C_{j,l}} \big(\sqrt{C_{j,l}} + \frac{8}{3} \prod_{i=1}^{3}(N_j + \frac{i}{2}) + \sum\limits_{m \neq j\,,\, m \neq l} \sqrt{C_{j,m}} \big) < 1 & \text{if } d = 3\,. \end{cases}$$

Denote by $\widetilde{F}_{q_j}, \widetilde{F}_{q_j,q_l}$ and $\widetilde{F}^{\delta}_{q_j}, \widetilde{F}^{\delta}_{q_j,q_l}$, $j, l = 1, \dots, J$, $j \neq l$, the solutions to the least squares problems

$$F_q \overset{\text{LS}}{=} \sum_{j=1}^{J} \widetilde{F}_{q_j} + \sum_{j=1}^{J} \sum_{l \neq j} \widetilde{F}_{q_j,q_l}\,, \qquad \widetilde{F}_{q_j} \in \mathcal{V}_{N_j}^{\boldsymbol{c}_j}\,,\ \widetilde{F}_{q_j,q_l} \in \mathcal{V}_{N_j,N_l}^{\boldsymbol{c}_j,\boldsymbol{c}_l}\,,$$

$$F^{\delta}_q \overset{\text{LS}}{=} \sum_{j=1}^{J} \widetilde{F}^{\delta}_{q_j} + \sum_{j=1}^{J} \sum_{l \neq j} \widetilde{F}^{\delta}_{q_j,q_l}\,, \qquad \widetilde{F}^{\delta}_{q_j} \in \mathcal{V}_{N_j}^{\boldsymbol{c}_j}\,,\ \widetilde{F}^{\delta}_{q_j,q_l} \in \mathcal{V}_{N_j,N_l}^{\boldsymbol{c}_j,\boldsymbol{c}_l}\,,$$

respectively. Then,

$$\|\widetilde{F}_{q_j} - \widetilde{F}^{\delta}_{q_j}\|^2_{\text{HS}} \leq (1 - M_j)^{-1} \|F_q - F^{\delta}_q\|^2_{\text{HS}}\,, \qquad j = 1, \dots, J\,.$$

Proof. Choosing $\mathcal{V}_j = \mathcal{V}_{N_j}^{\boldsymbol{c}_j}$ for $j = 1, \dots, J$, and $\mathcal{V}_{J+1} = \mathcal{V}_{N_1,N_2}^{\boldsymbol{c}_1,\boldsymbol{c}_2}, \dots, \mathcal{V}_{J^2} = \mathcal{V}_{N_J,N_{J-1}}^{\boldsymbol{c}_J,\boldsymbol{c}_{J-1}}$ in Theorem 3.15 and summing up the upper bounds for the cosine of the minimal angle between these subspaces as given by Propositions 3.37 and 3.38 yields the result. □

Analogously to (3.71), we further consider a related (weighted) $\ell^1 \times \ell^1$ minimization problem, whose stability is covered by the theorem below. For $J = 2$ it coincides with Theorem 3.41. For this purpose, we modify the objective function $\Psi : \text{HS}(L^2(S^{d-1}))^{(J^2)} \to [0, \infty)$ by

$$\begin{aligned} &\Psi(\widetilde{F}_{q_1}, \dots, \widetilde{F}_{q_J}, \widetilde{F}_{q_1,q_2}, \dots, \widetilde{F}_{q_J,q_{J-1}}) \\ &\qquad := \begin{cases} \sum\limits_{j=1}^{J} \|\mathcal{T}_{\boldsymbol{c}_j} \widetilde{F}_{q_j}\|_{\ell^1 \times \ell^1} + \sum\limits_{j=1}^{J} \sum\limits_{l \neq j} \|\mathcal{T}_{\boldsymbol{c}_j,\boldsymbol{c}_l} \widetilde{F}_{q_j,q_l}\|_{\ell^1 \times \ell^1} & \text{if } d = 2\,, \\ \sum\limits_{j=1}^{J} \|\mathcal{T}_{\boldsymbol{c}_j} \widetilde{F}_{q_j}\|_{\ell^1_{2n+1} \times \ell^1_{2n+1}} + \sum\limits_{j=1}^{J} \sum\limits_{l \neq j} \|\mathcal{T}_{\boldsymbol{c}_j,\boldsymbol{c}_l} \widetilde{F}_{q_j,q_l}\|_{\ell^1_{2n+1} \times \ell^1_{2n+1}} & \text{if } d = 3\,. \end{cases} \end{aligned} \tag{3.91}$$

Theorem 3.44. *Suppose that $F_q \in \text{HS}(L^2(S^{d-1}))$, let $\boldsymbol{c}_j \in \mathbb{R}^d$ and $N_j \in \mathbb{N}$ with $N_j \gtrsim kR_j$ for $j = 1, \dots, J$, such that*

$$C_j := \begin{cases} \frac{4(J^2-1)(2N_j+1)^2}{\min_{l \neq m}(k|\boldsymbol{c}_l - \boldsymbol{c}_m|)^{\frac{1}{3}}} < 1 & \text{if } d = 2\,, \\ \frac{64(J^2-1)}{9} \frac{\prod_{i=1}^{3}(N_j+\frac{i}{2})^2}{\min_{l \neq m}(k|\boldsymbol{c}_l - \boldsymbol{c}_m|)^{\frac{5}{6}}} < 1 & \text{if } d = 3\,. \end{cases}$$

We assume that $\widetilde{F}^0_{q_j} \in \mathcal{V}_{N_j}^{\boldsymbol{c}_j}$ and $\widetilde{F}^0_{q_j,q_l} \in \mathcal{V}_{N_j,N_l}^{\boldsymbol{c}_j,\boldsymbol{c}_l}$, $j, l = 1, \dots, J$, $j \neq l$, are such that

$$\Big\| F_q - \Big(\sum_{j=1}^{J} \widetilde{F}^0_{q_j} + \sum_{j=1}^{J} \sum_{l \neq j} \widetilde{F}^0_{q_j,q_l} \Big) \Big\|_{\text{HS}} < \delta_0$$

for some $\delta_0 \geq 0$. *Moreover, suppose that* $F_q^\delta \in \mathrm{HS}(L^2(S^{d-1}))$ *and* $\delta \geq 0$ *satisfy*

$$\delta \geq \delta_0 + \|F_q - F_q^\delta\|_{\mathrm{HS}}\,,$$

and let $(\widetilde{F}_{q_1}^\delta, \dots, \widetilde{F}_{q_J}^\delta, \widetilde{F}_{q_1,q_2}^\delta, \dots, \widetilde{F}_{q_J,q_{J-1}}^\delta) \in \mathrm{HS}(L^2(S^{d-1}))^{(J^2)}$ *denote the solution to*

$$\underset{(\widetilde{F}_{q_1},\dots,\widetilde{F}_{q_J},\widetilde{F}_{q_1,q_2},\dots,\widetilde{F}_{q_J,q_{J-1}})}{\text{minimize}} \quad \Psi(\widetilde{F}_{q_1},\dots,\widetilde{F}_{q_J},F_{q_1,q_2},\dots,F_{q_J,q_{J-1}})$$
$$\text{subject to} \quad \Big\|F_q^\delta - \Big(\sum_{j=1}^J \widetilde{F}_{q_j} + \sum_{j=1}^J \sum_{l\neq j} \widetilde{F}_{q_j,q_l}\Big)\Big\|_{\mathrm{HS}} \leq \delta$$

with Ψ *from* (3.91). *Then,*

$$\|\widetilde{F}_{q_j}^0 - \widetilde{F}_{q_j}^\delta\|_{\mathrm{HS}}^2 \leq (1-C_j)^{-1} 4\delta^2\,, \qquad j = 1,\dots,J\,.$$

Proof. The theorem follows similar to Theorem 3.41 from the mapping properties (3.8) and (3.9) of the generalized translation operator and from Lemma 3.22, see also the proof of [55, Thm. 6.5]. □

Remark 3.45. (a) As before, provided $k|\boldsymbol{c}_j - \boldsymbol{c}_l| < 2(N_j + N_l + d/2)$ for $j,l = 1,\dots,J$, $j \neq l$, the stability bounds in Theorems 3.43 and 3.44 can be improved when replacing $C_{j,l}$ by

$$\widetilde{C}_{j,l} := \begin{cases} \frac{(2N_j+1)(2N_l+1)}{k|\boldsymbol{c}_j-\boldsymbol{c}_l|} & \text{if } d=2\,,\\ \frac{16}{9}\frac{\prod_{i=1}^3 (N_j+\frac{i}{2})(N_l+\frac{i}{2})}{(k|\boldsymbol{c}_j-\boldsymbol{c}_l|)^2} & \text{if } d=3\,, \end{cases}$$

and C_j by

$$\widetilde{C}_j := \begin{cases} \frac{4(J^2-1)(2N_j+1)^2}{\min_{l\neq m}(k|\boldsymbol{c}_l-\boldsymbol{c}_m|)^{\frac{1}{2}}} < 1 & \text{if } d=2\,,\\ \frac{64(J^2-1)}{9}\frac{\prod_{i=1}^3 (N_j+\frac{i}{2})^2}{\min_{l\neq m} k|\boldsymbol{c}_l-\boldsymbol{c}_m|} < 1 & \text{if } d=3\,. \end{cases}$$

(b) Further improvements can be obtained by taking reciprocity into account as it is described in Subsection 3.6.1. This involves replacing the subspaces $\mathcal{V}_{N_j}^{\boldsymbol{c}_j}$ and $\mathcal{V}_{N_j,N_l}^{\boldsymbol{c}_j,\boldsymbol{c}_l} \oplus \mathcal{V}_{N_l,N_j}^{\boldsymbol{c}_l,\boldsymbol{c}_j}$ for $j,l = 1,\dots,J$ with $j \neq l$, by $\widetilde{\mathcal{V}}_{N_j}^{\boldsymbol{c}_j}$ from (3.85)–(3.86) and by $\widetilde{\mathcal{V}}_{N_j,N_l}^{\boldsymbol{c}_j,\boldsymbol{c}_l}$ from (3.87)–(3.88), respectively.

The RPCP formulation of the far field operator splitting problem from (3.50) can be generalized to $J \geq 2$ scatterer's components by modifying the objective function similar to (3.72). In order to do so, we suppose $d = 2$, and we assume to have a priori knowledge on the location of $K < J$ scatterer's components D_j for $j \in \{j_1,\dots,j_K\}$, such that there exists a ball $B_{R^{\mathrm{LR}}}(\boldsymbol{c}^{\mathrm{LR}})$ satisfying

$$D_j \subseteq B_{R^{\mathrm{LR}}}(\boldsymbol{c}^{\mathrm{LR}})\,,\ j \in \{1,\dots,J\}\setminus\{j_1,\dots,j_K\} \quad \text{and} \quad |\boldsymbol{c}^{\mathrm{LR}} - \boldsymbol{c}_j| > R^{\mathrm{LR}} + R_j\,,\ j = j_1,\dots,j_K\,.$$

This assumption is similar to Assumption 3.1, and it is visualized in Figure 3.7 for a concrete example, where $J = 4$, $K = 2$, $j_1 = 1$ and $j_2 = 4$. As a consequence, F_{q_j} can be well approximated in the subspace $\mathcal{V}_{N_j}^{\boldsymbol{c}_j}$ with $N_j \gtrsim kR_j$ for $j = j_1,\dots,j_K$ and the remaining part of the far field operator $F_q - \sum_{j,l\in\{j_1,\dots,j_K\},j\neq l}(F_{q_j} + F_{q_j,q_l})$ can be well approximated in $\mathcal{W}_{N^{\mathrm{LR}}}^{\boldsymbol{c}^{\mathrm{LR}}}$ with $N^{\mathrm{LR}} \gtrsim kR^{\mathrm{LR}}$. Here, F_{q_j,q_l} are the approximations of multiscattering components in $\mathcal{V}_{N_j,N_l}^{\boldsymbol{c}_j,\boldsymbol{c}_l}$ for $j \neq l$. This motivates to modify the objective function in (3.57) for $\lambda > 0$ according to

$$(L, \widetilde{F}_{q_{j_1}},\dots,\widetilde{F}_{q_{j_K}},\widetilde{F}_{q_{j_1},q_{j_2}},\dots,\widetilde{F}_{q_{j_{K-1}},q_{j_K}})$$
$$\mapsto \|L\|_{\mathrm{nuc}} + \lambda \sum_{j,l\in\{j_1,\dots,j_K\},j\neq l} \Big(\|\mathcal{T}_{\boldsymbol{c}_j}\widetilde{F}_{q_j}\|_{\ell^1\times\ell^1} + \|\mathcal{T}_{\boldsymbol{c}_j,\boldsymbol{c}_l}\widetilde{F}_{q_j,q_l}\|_{\ell^1\times\ell^1}\Big)\,.$$

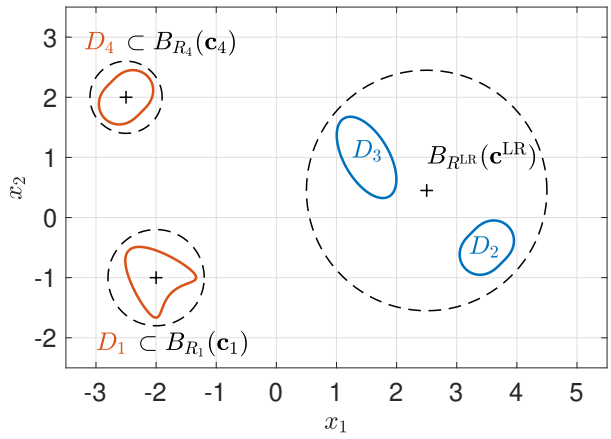

Figure 3.7. Scatterer consisting of $J = 4$ components D_j, $j = 1, 2, 3, 4$, (solid) with balls containing D_1,D_4 and $D_2 \cup D_3$, respectively (dashed).

By solving the associated minimization problem we obtain approximations of all far field operator components F_{q_j}, $j = j_1, \ldots, j_K$, with a priori known position. The remaining far field operator components are assigned to the low rank component and thus not accessible. As the stability analysis was already technically involved for only one sparse component, we do not establish a stability result for this approach, but we provide a numerical example, see Example 4.7.

CHAPTER 4

NUMERICAL TESTS FOR FAR FIELD OPERATOR SPLITTING

Before we present and discuss concrete examples to illustrate the performance of the far field operator splitting methods proposed in Sections 3.4 and 3.5, we comment on their numerical implementation. At this point, we restrict ourselves to the two-dimensional case. With exception of the final Example 4.7, the scatterer $D = D_1 \cup D_2$ is supposed to consist of two well-separated components, i.e., $D_j \subset B_{R_j}(\boldsymbol{c}_j)$ for some $\boldsymbol{c}_j \in \mathbb{R}^2$ and $R_j > 0$, $j = 1, 2$, with $|\boldsymbol{c}_1 - \boldsymbol{c}_2| > R_1 + R_2$ (cf. Assumption 3.1). We set $q_1 := q|_{D_1}$ and $q_2 := q|_{D_2}$. To simplify our simulation of the far field operator, cf. Example 2.5, we assume q to be piecewise constant by considering constant functions q_1 and q_2.

4.1. REMARKS ON THE IMPLEMENTATION

4.1.1. SIMULATION OF THE (NOISY) FAR FIELD OPERATOR

Let $N \in \mathbb{N}$ be large enough such that $N \gtrsim kR$, where $R > 0$ satisfies $\operatorname{supp} q \subset B_R(\mathbf{0})$. We simulate the exact far field operator F_q by a Nyström method as described in detail in Example 2.5 to obtain an approximation

$$\boldsymbol{F}_q := \frac{2\pi}{L} \left(u_q^\infty(\widehat{\boldsymbol{x}}_m; \boldsymbol{\theta}_n) \right)_{1 \le m,n \le L} \in \mathbb{C}^{L \times L} .$$

Here, we set $L := 2(N+1)$ and

$$\widehat{\boldsymbol{x}}_l := \boldsymbol{\theta}_l := (\cos \psi_l, \sin \psi_l)^\top \qquad \text{with } \psi_l := (l-1)\frac{2\pi}{L} \text{ for } l = 1, \dots, L .$$

This choice of L guarantees $L \ge 2N + 1$ and L even. Moreover, we specify a relative noise level $\delta_{\mathrm{rel}} \in [0, 1)$ and simulate a complex uniformly distributed random matrix $\boldsymbol{N} \in \mathbb{C}^{L \times L}$, whose Frobenius norm is given by $\delta_{\mathrm{rel}} \|\boldsymbol{F}_q\|_{\mathrm{HS}}$. By setting $\boldsymbol{F}_q^\delta := \boldsymbol{F}_q + \boldsymbol{N}$ we obtain a noisy version $\boldsymbol{F}_q^\delta$ of $\boldsymbol{F}_q$ to the absolute noise level $\delta_{\mathrm{rel}} \|\boldsymbol{F}_q\|_{\mathrm{HS}}$.

We also simulate the far field operator components

$$\boldsymbol{F}_{q_j} := \frac{2\pi}{L} \left(u_{q_j}^\infty(\widehat{\boldsymbol{x}}_m; \boldsymbol{\theta}_n) \right)_{1 \le m,n \le L} \in \mathbb{C}^{L \times L} , \qquad j = 1, 2 ,$$

corresponding to the two scatterer's components individually by using the Nyström method for the choices $q = q_j$, $j = 1, 2$, and we compare them to the results $\widetilde{\boldsymbol{F}}_{q_j}$, $j = 1, 2$, of our reconstruction methods by evaluating the relative reconstruction errors

$$\varepsilon_{\mathrm{rel}}^j := \frac{\|\boldsymbol{F}_{q_j} - \widetilde{\boldsymbol{F}}_{q_j}\|_{\mathrm{HS}}}{\|\boldsymbol{F}_{q_j}\|_{\mathrm{HS}}} .$$

4.1.2. DISCRETE FAR FIELD OPERATOR TRANSLATION AND FOURIER COEFFICIENTS

Given $\boldsymbol{c} \in \mathbb{R}^2$ we define the discrete version of $T_{\boldsymbol{c}}$ from (2.45) by

$$\boldsymbol{F} \mapsto \boldsymbol{T}_{\boldsymbol{c}}\boldsymbol{F} \qquad \text{for } \boldsymbol{F} \in \mathbb{C}^{L\times L} \qquad \text{with} \qquad \boldsymbol{T}_{\boldsymbol{c}} := \operatorname{diag}\left(e^{\mathrm{i}k\widehat{\boldsymbol{x}}_1\cdot\boldsymbol{c}}, \dots, e^{\mathrm{i}k\widehat{\boldsymbol{x}}_L\cdot\boldsymbol{c}}\right) \in \mathbb{C}^{L\times L}.$$

Given $\boldsymbol{b}, \boldsymbol{c} \in \mathbb{R}^2$ we then obtain the discrete version of $\mathcal{T}_{\boldsymbol{b},\boldsymbol{c}}$ from (3.3) by

$$\boldsymbol{F} \mapsto \mathcal{T}_{\boldsymbol{b},\boldsymbol{c}}\boldsymbol{F} := \boldsymbol{T}_{\boldsymbol{b}}\boldsymbol{F}\boldsymbol{T}_{\boldsymbol{c}}^* \qquad \text{for } \boldsymbol{F} \in \mathbb{C}^{L\times L}$$

with $\boldsymbol{T}_{\boldsymbol{c}}^* = (\overline{\boldsymbol{T}_{\boldsymbol{c}}})^\top = \overline{\boldsymbol{T}_{\boldsymbol{c}}} = \boldsymbol{T}_{-\boldsymbol{c}}$ denoting the conjugate transpose of $\boldsymbol{T}_{\boldsymbol{c}}$. We further write $\mathcal{T}_{\boldsymbol{c}} := \mathcal{T}_{\boldsymbol{c},\boldsymbol{c}}$.

For having access to the Fourier coefficients $\boldsymbol{A} = (a_{m-N-2,n-N-2})_{1\le m,n\le L}$ of a far field matrix $\boldsymbol{F}$ as introduced in the beginning of Section 2.4 we define for the Lth root of unity $\omega := e^{-\mathrm{i}\frac{2\pi}{L}}$ the Fourier matrix

$$\boldsymbol{F}_L := \left[\begin{array}{ccccc} \omega^0 & \omega^{-(N+1)} & \omega^{-2(N+1)} & \dots & \omega^{-(N+1)(2N+1)} \\ \omega^0 & \omega^{-N} & \omega^{-2N} & \dots & \omega^{-N(2N+1)} \\ \vdots & \vdots & \vdots & & \vdots \\ \omega^0 & \omega^{-1} & \omega^{-2} & \dots & \omega^{-(2N+1)} \\ \hline \omega^0 & \omega^0 & \omega^0 & \dots & \omega^0 \\ \omega^0 & \omega^1 & \omega^2 & \dots & \omega^{2N} \\ \vdots & \vdots & \vdots & & \vdots \\ \omega^0 & \omega^N & \omega^{2N+1} & \dots & \omega^{N(2N+1)} \end{array}\right] \in \mathbb{C}^{L\times L}.$$

We then have the relations $\boldsymbol{A} = \mathcal{F}_L\boldsymbol{F}$ and $\boldsymbol{F} = \mathcal{F}_L^{-1}\boldsymbol{A}$ by using the definitions

$$\mathcal{F}_L\boldsymbol{G} := \frac{2\pi}{L^2}\boldsymbol{F}_L\boldsymbol{G}\boldsymbol{F}_L^* \qquad \text{and} \qquad \mathcal{F}_L^{-1}\boldsymbol{G} := \frac{1}{2\pi}\boldsymbol{F}_L^*\boldsymbol{G}\boldsymbol{F}_L \qquad \text{for } \boldsymbol{G} \in \mathbb{C}^{L\times L}.$$

Here, we mention that due to the choice of L as an even number, the $(0,0)$th mode in the Fourier space is at the position $m = n = L/2 + 1 = N + 2$. Practically, $\mathcal{F}_L$ (and $\mathcal{F}_L^{-1}$) can, up to scaling, up to swapping halves of each column in the definition of $\boldsymbol{F}_L$, as indicated by the horizontal line, realized by the (fast) Fourier transform. Since we fixed the basis $((\widehat{\boldsymbol{x}},\boldsymbol{\theta}) \mapsto \boldsymbol{e}_m(\widehat{\boldsymbol{x}})\boldsymbol{e}_{-n}(\boldsymbol{\theta}))_{m,n}$ of $L^2(S^1\times S^1)$ and not $((\widehat{\boldsymbol{x}},\boldsymbol{\theta}) \mapsto \boldsymbol{e}_m(\widehat{\boldsymbol{x}})\boldsymbol{e}_n(\boldsymbol{\theta}))_{m,n}$ in the beginning of Section 2.4, the here generated Fourier coefficients must be mirrored at the axis $\{n = 0\}$.

4.1.3. MATRIX NORMS

We are consistent with our norm notations of the previous chapters as introduced in Notation 2.7, i.e., the matrix norms used here coincide with the operator norms noted in the same way when interpreting a matrix $\boldsymbol{F} \in \mathbb{C}^{L\times L}$ as a finite dimensional operator. In this sense, we mean by $\|\boldsymbol{F}\|_{\ell^1\times\ell^1}$ the entrywise $\ell^1\times\ell^1$ norm of $\mathcal{F}_L\boldsymbol{F}$, so of the matrix of Fourier coefficients of $\boldsymbol{F}$. We further denote by $\|\boldsymbol{F}\|_{\mathrm{HS}}$ the Frobenius norm of $\boldsymbol{F}$, by $\|\boldsymbol{F}\|$ the spectral norm of $\boldsymbol{F}$, so its largest singular value, and by $\|\boldsymbol{F}\|_{\mathrm{nuc}}$ the nuclear (or trace) norm of $\boldsymbol{F}$, which is the ℓ^1 norm of its singular values. Finally, we denote by $\|\boldsymbol{F}\|_{L^1}$ the entrywise $\ell^1\times\ell^1$ norm of $\boldsymbol{F}$.

4.1.4. SPLITTING BY THE CONJUGATE GRADIENT METHOD

We assume approximate knowledge about the locations of the individual scatterer components to be given, i.e., we assume to know $\boldsymbol{c}_j \in \mathbb{R}^2$ and $R_j > 0$ such that $D_j \subset B_{R_j}(\boldsymbol{c}_j)$, $j = 1, 2$. To

ensure $N_j \gtrsim kR_j$, we make the choice

$$N_j := \lceil \tfrac{e}{2} kR_j \rceil \qquad \text{for } j = 1, 2\,, \tag{4.1}$$

which in earlier works turned out to be suitable, cf. [50, Lem. 3.2], see also Remark 2.12 (i) and Example 4.3 below.

In the following we use the abbreviations $\mathcal{V}_j := \mathcal{V}_{N_j}^{\boldsymbol{c}_j}$ and $\mathcal{V}_{j,l} := \mathcal{V}_{N_j,N_l}^{\boldsymbol{c}_j,\boldsymbol{c}_l}$ for $j, l = 1, 2$, $j \neq l$, and introducing the *truncation* or *cut-off functions* $\mathcal{Q}_{N_j}$ and $\mathcal{Q}_{N_j,N_l}$ for $j, l = 1, 2$ by

$$(\mathcal{Q}_{N_j,N_l}\boldsymbol{F})_{m,n} := \begin{cases} f_{m,n} & \text{if } |m - N - 2| \leq N_j \text{ and } |n - N - 2| \leq N_l\,, \\ 0 & \text{else}\,, \end{cases} \qquad \text{for } \boldsymbol{F} = (f_{m,n})_{1 \leq m,n \leq L}$$

and $\mathcal{Q}_{N_j} := \mathcal{Q}_{N_j,N_j}$. With the help of these definitions, we decompose the orthogonal projection onto $\mathcal{V}_{j,l}$ on the discrete level by

$$\mathcal{P}_{j,l} : \mathbb{C}^{L\times L} \to \mathbb{C}^{L\times L}\,, \qquad \boldsymbol{F} \mapsto \mathcal{P}_{j,l}\boldsymbol{F} := (\mathcal{T}_{-\boldsymbol{c}_j,-\boldsymbol{c}_l} \circ \mathcal{F}_L^{-1} \circ \mathcal{Q}_{N_j,N_l} \circ \mathcal{F}_L \circ \mathcal{T}_{\boldsymbol{c}_j,\boldsymbol{c}_l})(\boldsymbol{F})$$

and the one onto $\mathcal{V}_j$ by setting $\mathcal{P}_j := \mathcal{P}_{j,j}$.

We know from Section 3.3 that the least squares problems (3.17) and (3.67) are equivalent to solving the corresponding linear block system, cf. (3.13). For (3.17), this leads to computing $\boldsymbol{F}_1, \boldsymbol{F}_2 \in \mathbb{C}^{L\times L}$ such that

$$\begin{bmatrix} \boldsymbol{I} & \mathcal{P}_1\mathcal{P}_2 \\ \mathcal{P}_2\mathcal{P}_1 & \boldsymbol{I} \end{bmatrix} \begin{bmatrix} \boldsymbol{F}_1 \\ \boldsymbol{F}_2 \end{bmatrix} = \begin{bmatrix} \mathcal{P}_1\boldsymbol{F}_q^\delta \\ \mathcal{P}_2\boldsymbol{F}_q^\delta \end{bmatrix}. \tag{4.2}$$

Analogously, the least squares problem (3.67) can be tackled by computing $\boldsymbol{F}_1, \boldsymbol{F}_2 \in \mathbb{C}^{L\times L}$ such that

$$\begin{bmatrix} \boldsymbol{I} & \mathcal{P}_1\mathcal{P}_2 & \mathcal{P}_1\mathcal{P}_{1,2} & \mathcal{P}_1\mathcal{P}_{2,1} \\ \mathcal{P}_2\mathcal{P}_1 & \boldsymbol{I} & \mathcal{P}_2\mathcal{P}_{1,2} & \mathcal{P}_2\mathcal{P}_{2,1} \\ \mathcal{P}_{1,2}\mathcal{P}_1 & \mathcal{P}_{1,2}\mathcal{P}_2 & \boldsymbol{I} & \mathcal{P}_{1,2}\mathcal{P}_{2,1} \\ \mathcal{P}_{2,1}\mathcal{P}_1 & \mathcal{P}_{2,1}\mathcal{P}_2 & \mathcal{P}_{2,1}\mathcal{P}_{1,2} & \boldsymbol{I} \end{bmatrix} \begin{bmatrix} \boldsymbol{F}_1 \\ \boldsymbol{F}_2 \\ \boldsymbol{F}_{1,2} \\ \boldsymbol{F}_{2,1} \end{bmatrix} = \begin{bmatrix} \mathcal{P}_1\boldsymbol{F}_q^\delta \\ \mathcal{P}_2\boldsymbol{F}_q^\delta \\ \mathcal{P}_{1,2}\boldsymbol{F}_q^\delta \\ \mathcal{P}_{2,1}\boldsymbol{F}_q^\delta \end{bmatrix} \tag{4.3}$$

for some $\boldsymbol{F}_{1,2}, \boldsymbol{F}_{2,1} \in \mathbb{C}^{L\times L}$. Since the block operators on the left hand sides of (4.2) and (4.3) are hermitian and positive definite under the assumptions of Theorems 3.20 and 3.39, we solve these systems with the conjugate gradient (cg) method. This is described for the second system in Algorithm 1, cf. e.g. [60]. Here, we denote the block operator on the left hand side of (4.3) by $\mathcal{M}$. The block structure can be realized by using cell-arrays and defining customized functions for the Frobenius norm and inner product, the addition and the product with scalars. The a priori known data error is given by $\delta = \delta_{\text{rel}}\|\boldsymbol{F}_q\|_{\text{HS}}$. Since $\boldsymbol{F}_q^\delta$ is not necessarily in $\mathcal{V}_1 + \mathcal{V}_2 + \mathcal{V}_{1,2} + \mathcal{V}_{2,1}$ and therefore not necessarily in the range of the block operator $\mathcal{M}$, we use the discrepancy principle as a stopping criterion for preventing data overfit, cf. [44, Sec. 7.3]. We cannot expect our reconstructions to be arbitrarily accurate. On one hand, this is due to the fact that the exact far field operators $\boldsymbol{F}_{q_j}$, that we aim to recover, are not in $\mathcal{V}_j$, $j = 1, 2$. On the other hand, as explained in Section 3.6.3, some parts of the Born series expansion (3.90) are wrongly assigned when solving the least squares problem (3.67).

To incorporate the reciprocity relation we define

$$\mathcal{R}_1 : \mathbb{C}^{L\times L} \to \mathbb{C}^{L\times L}\,, \qquad \boldsymbol{F} \mapsto \mathcal{R}_1\boldsymbol{F} := \frac{1}{2}\left(\boldsymbol{F} + \boldsymbol{P}. * \operatorname{flip}((\operatorname{flip}(\boldsymbol{F}, 2))^\top, 2)\right),$$

where $.*$ denotes the elementwise (or Hadamard) product of matrices, $\boldsymbol{P} := ((-1)^{m+n})_{1\leq m,n\leq L}$, and $\operatorname{flip}(\cdot, 2)$ mirrors a matrix along its second dimension. The operator $\mathcal{R}_1$ ensures the symmetry of the Fourier coefficients according to (3.80). Consequently, we obtain for the exact discretized far field operator that $\mathcal{R}_1\boldsymbol{F}_q = \boldsymbol{F}_q$. Furthermore, this symmetry according to (3.80) is preserved under addition, under scalar multiplication or under application of projections $\mathcal{P}_j$ and $\mathcal{P}_{j,l} + \mathcal{P}_{l,j}$ for

Algorithm 1 Far field operator splitting by conjugate gradient method

Input: Noisy far field matrix $\boldsymbol{F}_q^\delta$, wave number k, a priori knowledge on locations $\boldsymbol{c}_1$, $\boldsymbol{c}_2$, R_1 and R_2, maximum number of cg iterations $l_{\max}$, absolute noise level $\delta > 0$ and fudge parameter $\tau > 1$.
Output: Approximations $\widetilde{\boldsymbol{F}}_{q_1}$ and $\widetilde{\boldsymbol{F}}_{q_2}$ to far field matrix components $\boldsymbol{F}_{q_1}$ and $\boldsymbol{F}_{q_2}$.

Set $N_j = \lceil ekR_j/2 \rceil$ for $j = 1, 2$.
Initialize $\boldsymbol{R}^{(0)} = [\mathcal{P}_1\boldsymbol{F}_q^\delta, \mathcal{P}_2\boldsymbol{F}_q^\delta, \mathcal{P}_{1,2}\boldsymbol{F}_q^\delta, \mathcal{P}_{2,1}\boldsymbol{F}_q^\delta]$, $\boldsymbol{D}^{(0)} = \boldsymbol{R}^{(0)}$ and $\boldsymbol{F}^{(0)} = [\boldsymbol{0}, \boldsymbol{0}, \boldsymbol{0}, \boldsymbol{0}]$.
for $l = 0, 1, 2, \cdots, l_{\max}$ **do**
  Update $\alpha_l = \|\boldsymbol{R}^{(l)}\|_{\mathrm{HS}}^2 / \langle \boldsymbol{D}^{(l)}, \mathcal{M}\boldsymbol{D}^{(l)} \rangle_{\mathrm{HS}}$,
    $\boldsymbol{F}^{(l+1)} = \boldsymbol{F}^{(l)} + \alpha_k \boldsymbol{D}^{(l)}$,
    $\boldsymbol{R}^{(l+1)} = \boldsymbol{R}^{(l)} - \alpha_k \mathcal{M}\boldsymbol{D}^{(l)}$,
    $\beta_l = \|\boldsymbol{R}^{(l+1)}\|_{\mathrm{HS}}^2 / \|\boldsymbol{R}^{(l)}\|_{\mathrm{HS}}^2$ and
    $\boldsymbol{D}^{(l+1)} = \boldsymbol{R}^{(l+1)} + \beta_k \boldsymbol{D}^{(l)}$.
  if $\|\boldsymbol{R}^{(l+1)}\|_{\mathrm{HS}} \leq \tau\delta$ **then**
    Set $l_{\max} = l$.
  end if
end for
Set $[\widetilde{\boldsymbol{F}}_{q_1}, \widetilde{\boldsymbol{F}}_{q_2}, \sim, \sim] = \boldsymbol{F}^{(l_{\max}+1)}$.

$j, l = 1, 2$, $j \neq l$. If the exact far field operator $\boldsymbol{F}_q$ is provided in Algorithm 1 as an input, then the cg approximations satisfy the symmetry (3.80) as well and no modification of the algorithm is required.

If, on the other hand, a noisy version $\boldsymbol{F}_q^\delta$ is given, replacing $\boldsymbol{F}_q^\delta$ by $\mathcal{R}_1\boldsymbol{F}_q^\delta$ enforces the approximations to fulfill (3.80). Alternatively, projecting onto the modified subspaces $\widetilde{\mathcal{V}}_{N_j}^{\boldsymbol{c}_j}$ and $\widetilde{\mathcal{V}}_{N_j,N_l}^{\boldsymbol{c}_j,\boldsymbol{c}_l}$ from (3.84) and (3.87), $j, l = 1, 2$, $j \neq l$, can be used for noise filtering. Here, we replace $\mathcal{P}_{j,j}$ by

$$\widetilde{\mathcal{P}}_{j,j} : \mathbb{C}^{L\times L} \to \mathbb{C}^{L\times L}, \qquad \boldsymbol{F} \mapsto \widetilde{\mathcal{P}}_{j,j}\boldsymbol{F} := (\mathcal{T}_{-\boldsymbol{c}_j} \circ \mathcal{F}_L^{-1} \circ \mathcal{R}_1 \circ \mathcal{Q}_{N_j} \circ \mathcal{F}_L \circ \mathcal{T}_{\boldsymbol{c}_j})(\boldsymbol{F}).$$

For taking (3.82) into account we consider the pair $(\boldsymbol{F}_{1,2}, \boldsymbol{F}_{2,1})$ as one object. We simply evaluate $\mathcal{P}_{1,2}$ and use its result to determine the related evaluation $\mathcal{P}_{2,1}$. This means that we leave $\mathcal{P}_{1,2}$ unchanged while substituting $\mathcal{P}_{2,1}$ with

$$\widetilde{\mathcal{P}}_{2,1} : \mathbb{C}^{L\times L} \to \mathbb{C}^{L\times L}, \qquad \boldsymbol{F} \mapsto \widetilde{\mathcal{P}}_{2,1}\boldsymbol{F} := (\mathcal{T}_{-\boldsymbol{c}_2,-\boldsymbol{c}_1} \circ \mathcal{F}_L^{-1} \circ \mathcal{R}_2 \circ \mathcal{F}_L \circ \mathcal{T}_{\boldsymbol{c}_1,\boldsymbol{c}_2})(\boldsymbol{F}). \tag{4.4}$$

Here, $\mathcal{R}_2$ is given by

$$\mathcal{R}_2 : \mathbb{C}^{L\times L} \to \mathbb{C}^{L\times L}, \qquad \boldsymbol{F} \mapsto \mathcal{R}_2\boldsymbol{F} := \boldsymbol{P}. * \mathrm{flip}((\mathrm{flip}(\boldsymbol{F}, 2))^\top, 2).$$

In case of $J > 2$ scatterer's components, a modification of the block structure is required. The block system (4.3) then becomes

$$\begin{bmatrix} \boldsymbol{I} & \dots & \mathcal{P}_1\mathcal{P}_J & \mathcal{P}_1\mathcal{P}_{1,2} & \dots & \mathcal{P}_1\mathcal{P}_{J,J-1} \\ \vdots & \ddots & \vdots & \vdots & \ddots & \vdots \\ \mathcal{P}_J\mathcal{P}_1 & \dots & \boldsymbol{I} & \mathcal{P}_J\mathcal{P}_{1,2} & \dots & \mathcal{P}_J\mathcal{P}_{J,J-1} \\ \mathcal{P}_{1,2}\mathcal{P}_1 & \dots & \mathcal{P}_{1,2}\mathcal{P}_J & \boldsymbol{I} & \dots & \mathcal{P}_{1,2}\mathcal{P}_{J,J-1} \\ \vdots & \ddots & \vdots & \vdots & \ddots & \vdots \\ \mathcal{P}_{J,J-1}\mathcal{P}_1 & \dots & \mathcal{P}_{J,J-1}\mathcal{P}_J & \mathcal{P}_{J,J-1}\mathcal{P}_{1,2} & \dots & \boldsymbol{I} \end{bmatrix} \begin{bmatrix} \boldsymbol{F}_1 \\ \vdots \\ \boldsymbol{F}_J \\ \boldsymbol{F}_{1,2} \\ \vdots \\ \boldsymbol{F}_{J,J-1} \end{bmatrix} = \begin{bmatrix} \mathcal{P}_1\boldsymbol{F}_q^\delta \\ \vdots \\ \mathcal{P}_J\boldsymbol{F}_q^\delta \\ \mathcal{P}_{1,2}\boldsymbol{F}_q^\delta \\ \vdots \\ \mathcal{P}_{J,J-1}\boldsymbol{F}_q^\delta \end{bmatrix}.$$

Accordingly, every cg iterate can be realized by a cell-array consisting of J^2 matrices of dimension $L \times L$.

4.1.5. Splitting by Fast Iterative Soft Thresholding

Algorithm 2 Far field operator splitting by FISTA

Input: Noisy far field matrix $\boldsymbol{F}_q^\delta$, wave number k, a priori knowledge on positions $\boldsymbol{c}_1$ and $\boldsymbol{c}_2$, maximum number of FISTA iterations $l_{\max}$, regularization parameter $\mu > 0$, initial guess $\boldsymbol{F} = [\boldsymbol{F}_1, \boldsymbol{F}_2, \boldsymbol{F}_{1,2}, \boldsymbol{F}_{2,1}]$, tolerance $\varepsilon > 0$.

Output: Approximations $\widetilde{\boldsymbol{F}}_{q_1}$ and $\widetilde{\boldsymbol{F}}_{q_2}$ to far field matrix components $\boldsymbol{F}_{q_1}$ and $\boldsymbol{F}_{q_2}$.

Set $\omega = 1/5$.
Initialize $\boldsymbol{H}^{(1)} = [\boldsymbol{H}_1^{(1)}, \boldsymbol{H}_2^{(1)}, \boldsymbol{H}_{1,2}^{(1)}, \boldsymbol{H}_{2,1}^{(1)}] = \boldsymbol{F}$,
$\boldsymbol{F}^{(0)} = [\boldsymbol{F}_1^{(0)}, \boldsymbol{F}_2^{(0)}, \boldsymbol{F}_{1,2}^{(0)}, \boldsymbol{F}_{2,1}^{(0)}] = \boldsymbol{F}$,
$\boldsymbol{R}^{(1)} = \boldsymbol{F}_q^\delta - (\boldsymbol{H}_1^{(1)} + \boldsymbol{H}_2^{(1)} + \boldsymbol{H}_{1,2}^{(1)} + \boldsymbol{H}_{2,1}^{(1)})$ and
$t_1 = 1$.
for $l = 1, 2, \cdots, l_{\max}$ **do**
  Update $\boldsymbol{F}^{(l)} = [\boldsymbol{F}_1^{(l)}, \boldsymbol{F}_2^{(l)}, \boldsymbol{F}_{1,2}^{(l)}, \boldsymbol{F}_{2,1}^{(l)}]$ with $\boldsymbol{F}_1^{(l)} = \mathcal{M}_{\omega\mu,\boldsymbol{c}_1,\boldsymbol{c}_1}(\boldsymbol{H}_1^{(l)} + \omega\boldsymbol{R}^{(l)})$,
  $\boldsymbol{F}_2^{(l)} = \mathcal{M}_{\omega\mu,\boldsymbol{c}_2,\boldsymbol{c}_2}(\boldsymbol{H}_2^{(l)} + \omega\boldsymbol{R}^{(l)})$,
  $\boldsymbol{F}_{1,2}^{(l)} = \mathcal{M}_{\omega\mu,\boldsymbol{c}_1,\boldsymbol{c}_2}(\boldsymbol{H}_{1,2}^{(l)} + \omega\boldsymbol{R}^{(l)})$ and
  $\boldsymbol{F}_{2,1}^{(l)} = \mathcal{M}_{\omega\mu,\boldsymbol{c}_2,\boldsymbol{c}_1}(\boldsymbol{H}_{2,1}^{(l)} + \omega\boldsymbol{R}^{(l)})$,
  $t_{l+1} = \frac{1+\sqrt{1+4t_l^2}}{2}$,
  $\boldsymbol{H}^{(l+1)} = [\boldsymbol{H}_1^{(l+1)}, \boldsymbol{H}_2^{(l+1)}, \boldsymbol{H}_{1,2}^{(l+1)}, \boldsymbol{H}_{2,1}^{(l+1)}] = \boldsymbol{F}^{(l)} + \frac{t_l - 1}{t_{l+1}}(\boldsymbol{F}^{(l)} - \boldsymbol{F}^{(l-1)})$ and
  $\boldsymbol{R}^{(l+1)} = \boldsymbol{F}_q^\delta - (\boldsymbol{H}_1^{(l+1)} + \boldsymbol{H}_2^{(l+1)} + \boldsymbol{H}_{1,2}^{(l+1)} + \boldsymbol{H}_{2,1}^{(l+1)})$
  if $\|\boldsymbol{R}^{(l+1)}\|_{\mathrm{HS}} \leq \varepsilon$ **then**
    Set $l_{\max} = l$.
  end if
end for
Set $[\widetilde{\boldsymbol{F}}_{q_1}, \widetilde{\boldsymbol{F}}_{q_2}, \sim, \sim] = \boldsymbol{F}^{(l_{\max})}$.

We only assume approximate knowledge on the positions $\boldsymbol{c}_j \in \mathbb{R}^2$ of the scatterer components to be given, i.e., we do not need any knowledge about their sizes $R_j > 0$, $j = 1, 2$. As proposed in Sections 3.4 and 3.5 we can then solve the $\ell^1 \times \ell^1$ minimization problems (3.27) and (3.71), whose Tikhonov functionals read on the discrete level

$$(\boldsymbol{F}_1, \boldsymbol{F}_2) \mapsto \|\boldsymbol{F}_q^\delta - (\boldsymbol{F}_1 + \boldsymbol{F}_2)\|_{\mathrm{HS}}^2 + \mu\Big(\|\mathcal{T}_{\boldsymbol{c}_1}\boldsymbol{F}_1\|_{\ell^1\times\ell^1} + \|\mathcal{T}_{\boldsymbol{c}_2}\boldsymbol{F}_2\|_{\ell^1\times\ell^1}\Big)$$

and

$$\begin{aligned}(\boldsymbol{F}_1, \boldsymbol{F}_2, \boldsymbol{F}_{1,2}, \boldsymbol{F}_{2,1}) \mapsto \|\boldsymbol{F}_q^\delta - (\boldsymbol{F}_1 + \boldsymbol{F}_2 + \boldsymbol{F}_{1,2} + \boldsymbol{F}_{2,1})\|_{\mathrm{HS}}^2 + \mu\Big(&\|\mathcal{T}_{\boldsymbol{c}_1}\boldsymbol{F}_1\|_{\ell^1\times\ell^1} \\ &+ \|\mathcal{T}_{\boldsymbol{c}_2}\boldsymbol{F}_2\|_{\ell^1\times\ell^1} + \|\mathcal{T}_{\boldsymbol{c}_1,\boldsymbol{c}_2}\boldsymbol{F}_{1,2}\|_{\ell^1\times\ell^1} + \|\mathcal{T}_{\boldsymbol{c}_2,\boldsymbol{c}_1}\boldsymbol{F}_{2,1}\|_{\ell^1\times\ell^1}\Big)\end{aligned}$$

with $\|\cdot\|_{\ell^1\times\ell^1}$ given as in Subsection 4.1.3. For a suitably chosen regularization parameter $\mu > 0$, it is equivalent to compute the unique minimizer of these related Tikhonov functionals, cf. [49, Prop. 2.2]. From (D.2) together with Example D.2 (ii) we know that these minimizers satisfy the fixed point equations

$$\begin{bmatrix} \boldsymbol{F}_1 \\ \boldsymbol{F}_2 \end{bmatrix} = \begin{bmatrix} (\mathcal{T}_{-\boldsymbol{c}_1} \circ \mathcal{F}_L^{-1} \circ \mathcal{S}_{\omega\mu} \circ \mathcal{F}_L \circ \mathcal{T}_{\boldsymbol{c}_1})(\boldsymbol{F}_1 + \omega(\boldsymbol{F}_q^\delta - (\boldsymbol{F}_1 + \boldsymbol{F}_2))) \\ (\mathcal{T}_{-\boldsymbol{c}_2} \circ \mathcal{F}_L^{-1} \circ \mathcal{S}_{\omega\mu} \circ \mathcal{F}_L \circ \mathcal{T}_{\boldsymbol{c}_2})(\boldsymbol{F}_2 + \omega(\boldsymbol{F}_q^\delta - (\boldsymbol{F}_1 + \boldsymbol{F}_2))) \end{bmatrix}$$

for $0 < \omega < 1/2$ and

$$\begin{bmatrix} \boldsymbol{F}_1 \\ \boldsymbol{F}_2 \\ \boldsymbol{F}_{1,2} \\ \boldsymbol{F}_{2,1} \end{bmatrix} = \begin{bmatrix} (\mathcal{T}_{-\boldsymbol{c}_1} \circ \mathcal{F}_L^{-1} \circ \mathcal{S}_{\omega\mu} \circ \mathcal{F}_L \circ \mathcal{T}_{\boldsymbol{c}_1})(\boldsymbol{F}_1 + \omega(\boldsymbol{F}_q^\delta - (\boldsymbol{F}_1 + \boldsymbol{F}_2 + \boldsymbol{F}_{1,2} + \boldsymbol{F}_{2,1}))) \\ (\mathcal{T}_{-\boldsymbol{c}_2} \circ \mathcal{F}_L^{-1} \circ \mathcal{S}_{\omega\mu} \circ \mathcal{F}_L \circ \mathcal{T}_{\boldsymbol{c}_2})(\boldsymbol{F}_2 + \omega(\boldsymbol{F}_q^\delta - (\boldsymbol{F}_1 + \boldsymbol{F}_2 + \boldsymbol{F}_{1,2} + \boldsymbol{F}_{2,1}))) \\ (\mathcal{T}_{-\boldsymbol{c}_1,-\boldsymbol{c}_2} \circ \mathcal{F}_L^{-1} \circ \mathcal{S}_{\omega\mu} \circ \mathcal{F}_L \circ \mathcal{T}_{\boldsymbol{c}_1,\boldsymbol{c}_2})(\boldsymbol{F}_{1,2} + \omega(\boldsymbol{F}_q^\delta - (\boldsymbol{F}_1 + \boldsymbol{F}_2 + \boldsymbol{F}_{1,2} + \boldsymbol{F}_{2,1}))) \\ (\mathcal{T}_{-\boldsymbol{c}_2,-\boldsymbol{c}_1} \circ \mathcal{F}_L^{-1} \circ \mathcal{S}_{\omega\mu} \circ \mathcal{F}_L \circ \mathcal{T}_{\boldsymbol{c}_2,\boldsymbol{c}_1})(\boldsymbol{F}_{2,1} + \omega(\boldsymbol{F}_q^\delta - (\boldsymbol{F}_1 + \boldsymbol{F}_2 + \boldsymbol{F}_{1,2} + \boldsymbol{F}_{2,1}))) \end{bmatrix}$$

for $0 < \omega < 1/4$, respectively. Here, the nonlinear thresholding function $\mathcal{S}_{\omega\mu}$ is given as in (D.3). To simplify the notation we define for $j, l = 1, 2$ and $\omega\mu > 0$

$$\mathcal{M}_{\omega\mu,\boldsymbol{c}_j,\boldsymbol{c}_l} := \mathcal{T}_{-\boldsymbol{c}_j,-\boldsymbol{c}_l} \circ \mathcal{F}_L^{-1} \circ \mathcal{S}_{\omega\mu} \circ \mathcal{F}_L \circ \mathcal{T}_{\boldsymbol{c}_j,\boldsymbol{c}_l}\,. \tag{4.5}$$

The minimizer of the previously defined Tikhonov functionals can be approximated as in (D.5) by the *Iterative Soft Thresholding Algorithm (ISTA)*, which in its original formulation computes for an initial guess $\boldsymbol{F}^{(0)} = [\boldsymbol{F}_1^{(0)}, \boldsymbol{F}_1^{(0)}]$ a sequence of iterates according to

$$\boldsymbol{F}^{(l+1)} = \begin{bmatrix} \boldsymbol{F}_1^{(l+1)} \\ \boldsymbol{F}_2^{(l+1)} \end{bmatrix} = \begin{bmatrix} \mathcal{M}_{\omega\mu,\boldsymbol{c}_1,\boldsymbol{c}_1}(\boldsymbol{F}_1^{(l)} + \omega(\boldsymbol{F}_q^\delta - (\boldsymbol{F}_1^{(l)} + \boldsymbol{F}_2^{(l)}))) \\ \mathcal{M}_{\omega\mu,\boldsymbol{c}_2,\boldsymbol{c}_2}(\boldsymbol{F}_2^{(l)} + \omega(\boldsymbol{F}_q^\delta - (\boldsymbol{F}_1^{(l)} + \boldsymbol{F}_2^{(l)}))) \end{bmatrix}, \quad l = 0, 1, 2, \dots,$$

and in the second situation for an initial guess $\boldsymbol{F}^{(0)} = [\boldsymbol{F}_1^{(0)}, \boldsymbol{F}_1^{(0)}, \boldsymbol{F}_{1,2}^{(0)}, \boldsymbol{F}_{2,1}^{(0)}]$ according to

$$\boldsymbol{F}^{(l+1)} = \begin{bmatrix} \boldsymbol{F}_1^{(l+1)} \\ \boldsymbol{F}_2^{(l+1)} \\ \boldsymbol{F}_{1,2}^{(l+1)} \\ \boldsymbol{F}_{2,1}^{(l+1)} \end{bmatrix} = \begin{bmatrix} \mathcal{M}_{\omega\mu,\boldsymbol{c}_1,\boldsymbol{c}_1}(\boldsymbol{F}_1^{(l)} + \omega(\boldsymbol{F}_q^\delta - (\boldsymbol{F}_1^{(l)} + \boldsymbol{F}_2^{(l)} + \boldsymbol{F}_{1,2}^{(l)} + \boldsymbol{F}_{2,1}^{(k)}))) \\ \mathcal{M}_{\omega\mu,\boldsymbol{c}_2,\boldsymbol{c}_2}(\boldsymbol{F}_2^{(l)} + \omega(\boldsymbol{F}_q^\delta - (\boldsymbol{F}_1^{(l)} + \boldsymbol{F}_2^{(l)} + \boldsymbol{F}_{1,2}^{(l)} + \boldsymbol{F}_{2,1}^{(l)}))) \\ \mathcal{M}_{\omega\mu,\boldsymbol{c}_1,\boldsymbol{c}_2}(\boldsymbol{F}_{1,2}^{(l)} + \omega(\boldsymbol{F}_q^\delta - (\boldsymbol{F}_1^{(l)} + \boldsymbol{F}_2^{(l)} + \boldsymbol{F}_{1,2}^{(l)} + \boldsymbol{F}_{2,1}^{(l)}))) \\ \mathcal{M}_{\omega\mu,\boldsymbol{c}_2,\boldsymbol{c}_1}(\boldsymbol{F}_{2,1}^{(l)} + \omega(\boldsymbol{F}_q^\delta - (\boldsymbol{F}_1^{(l)} + \boldsymbol{F}_2^{(l)} + \boldsymbol{F}_{1,2}^{(l)} + \boldsymbol{F}_{2,1}^{(l)}))) \end{bmatrix}$$

for $l = 0, 1, 2, \dots$. In [34, Thm. 3.1] the strong convergence of the ISTA iterates to the unique minimizer is shown. As suggested in [6], this method can be accelerated by applying $\mathcal{M}_{\omega\mu,\boldsymbol{c}_j,\boldsymbol{c}_l}$ in each step not to the previous iterate, but to a carefully selected linear combination $\boldsymbol{H}^{(l)}$ of the two previous iterates. This leads to the *Fast Iterative Soft Thresholding Algorithm (FISTA)*, which is described in Algorithm 2 for the second situation. As in the previous subsection, the iterates and auxiliary iterates can be realized by cell-arrays, which requires customized functions for the addition and the product with scalars. We use Morozov's discrepancy principle as a stopping criterion. The case of $J > 2$ scatterer's components can be implemented similarly to the previous method by modifying the cell-arrays no longer consisting of 4 but of J^2 matrices each. The reciprocity relation can be implemented by replacing $\mathcal{M}_{\omega\mu,\boldsymbol{c}_j,\boldsymbol{c}_j}$ by

$$\widetilde{\mathcal{M}}_{\omega\mu,\boldsymbol{c}_j,\boldsymbol{c}_j} := \mathcal{T}_{-\boldsymbol{c}_j,-\boldsymbol{c}_j} \circ \mathcal{F}_L^{-1} \circ \mathcal{R}_1 \circ \mathcal{S}_{\omega\mu} \circ \mathcal{F}_L \circ \mathcal{T}_{\boldsymbol{c}_j,\boldsymbol{c}_j}\,, \qquad j = 1, 2\,,$$

and by viewing $(\boldsymbol{F}_{1,2}, \boldsymbol{F}_{2,1})$ as one object, letting $\mathcal{M}_{\omega\mu,\boldsymbol{c}_1,\boldsymbol{c}_2}$ unchanged and substituting $\mathcal{M}_{\omega\mu,\boldsymbol{c}_2,\boldsymbol{c}_1}$ by $\widetilde{\mathcal{P}}_{2,1}$ from (4.4).

4.1.6. SPLITTING BY SOLVING RPCP WITH A FISTA TYPE METHOD

We further lower our required knowledge on the scatterer's geometry in the sense that we only assume to know the position $\boldsymbol{c}_2 \in \mathbb{R}^2$ of the second scatterer's component, i.e., the position $\boldsymbol{c}_1 \in \mathbb{R}^2$ of the first component is unknown. As proposed in Section 3.4 we then can solve RPCP by solving the coupled minimization problem from Theorem 3.34. The choice of λ in this theorem corresponds to $\lambda = L^{-3/2}$, due to scaling of the Fourier transform. As before, for a suitably chosen regularization parameter $\mu > 0$, it is equivalent to minimize the related Tikhonov functional

$$(\boldsymbol{L}, \boldsymbol{S}) \mapsto \|\boldsymbol{F}_q^\delta - (\boldsymbol{L} + \boldsymbol{S})\|_{\mathrm{HS}}^2 + \mu\Big(\|\boldsymbol{L}\|_{\mathrm{nuc}} + \lambda\|\mathcal{T}_{\boldsymbol{c}_2}\boldsymbol{S}\|_{\ell^1\times\ell^1}\Big)$$

Algorithm 3 Far field operator splitting by solving RPCP via FISTA type method

Input: Noisy far field matrix $\boldsymbol{F}_q^\delta$, wave number k, a priori knowledge on position $\boldsymbol{c}_2$, maximum number of proximal gradient iterations $l_{\max}$, regularization parameter $\mu > 0$, coupling parameter $\lambda > 0$, initial guess $\boldsymbol{F} = [\boldsymbol{F}_{1,2}, \boldsymbol{F}_2]$, absolute noise level $\delta > 0$ and fudge parameter $\tau > 0$.

Output: Approximations $\widetilde{\boldsymbol{F}}_{q_2}$ and $\widetilde{\boldsymbol{F}}_{q_1,q_2}$ to far field matrix component $\boldsymbol{F}_{q_2}$ and to difference $\boldsymbol{F}_q - \boldsymbol{F}_{q_2}$.

Set $\omega = 1/3$.
Initialize $\boldsymbol{H}^{(1)} = [\boldsymbol{H}_L^{(1)}, \boldsymbol{H}_S^{(1)}] = \boldsymbol{F}$,
$\boldsymbol{F}^{(1)} = [\boldsymbol{L}^{(1)}, \boldsymbol{S}^{(1)}] = \boldsymbol{F}$,
$\boldsymbol{R}^{(1)} = \boldsymbol{F}_q^\delta - (\boldsymbol{H}_L^{(1)} + \boldsymbol{H}_S^{(1)})$ and
$t_1 = 1$.
for $l = 1, 2, \cdots, l_{\max}$ **do**
  Update $\boldsymbol{F}^{(l)} = [\boldsymbol{L}^{(l)}, \boldsymbol{S}^{(l)}]$ with $\boldsymbol{L}^{(l)} = \mathcal{D}_{\omega\mu}(\boldsymbol{H}_L^{(l)} + \omega\boldsymbol{R}^{(l)})$ and
  $\boldsymbol{S}^{(l)} = \mathcal{M}_{\omega\lambda\mu,\boldsymbol{c}_2,\boldsymbol{c}_2}(\boldsymbol{H}_S^{(l)} + \omega\boldsymbol{R}^{(l)})$,
  $t_{l+1} = \frac{1+\sqrt{1+4t_l^2}}{2}$,
  $\boldsymbol{H}^{(l+1)} = [\boldsymbol{H}_L^{(l+1)}, \boldsymbol{H}_S^{(l+1)}] = \boldsymbol{F}^{(l)} + \frac{t_l - 1}{t_{l+1}}(\boldsymbol{F}^{(l)} - \boldsymbol{F}^{(l-1)})$ and
  $\boldsymbol{R}^{(l+1)} = \boldsymbol{F}_q^\delta - (\boldsymbol{H}_L^{(l+1)} + \boldsymbol{H}_S^{(l+1)})$.
  if $\|\boldsymbol{R}^{(l+1)}\|_{\mathrm{HS}} \leq \tau\delta$ **then**
    Set $l_{\max} = l$.
  end if
  Set $[\widetilde{\boldsymbol{F}}_{q_1,q_2}, \widetilde{\boldsymbol{F}}_{q_2}] = \boldsymbol{F}^{(l_{\max})}$.
end for

to obtain an approximation $\boldsymbol{S}$ of $\boldsymbol{F}_{q_2}$. From (D.2) and Example D.2 (ii)–(iii) we conclude that the unique minimizer of this functional fulfills for all $0 < \omega < 1/2$ the fixed point equation

$$\begin{bmatrix} \boldsymbol{L} \\ \boldsymbol{S} \end{bmatrix} = \begin{bmatrix} \mathcal{D}_{\omega\mu}(\boldsymbol{L} + \omega(\boldsymbol{F}_q^\delta - (\boldsymbol{L} + \boldsymbol{S})) \\ \mathcal{M}_{\omega\lambda\mu,\boldsymbol{c}_2,\boldsymbol{c}_2}(\boldsymbol{S} + \omega(\boldsymbol{F}_q^\delta - (\boldsymbol{L} + \boldsymbol{S})) \end{bmatrix}$$

with singular value thresholding function $\mathcal{D}_{\omega\mu}$ given as in (D.4) and $\mathcal{M}_{\omega\lambda\mu,\boldsymbol{c}_2,\boldsymbol{c}_2}$ given as in (4.5). The resulting method, as it is proposed in [100, 79], is described in Algorithm 3 below. We further implement the acceleration from [79]. Alternative methods for solving RPCP numerically are collected and compared in [13].

In general we cannot expect to reconstruct the far field operator $\boldsymbol{F}_{q_1}$ to the first component, unless we are in the situation that the Born approximation is already a sufficiently good approximation to the full problem. Therefore, in most of the cases it does not make sense to compare the approximation $\widetilde{\boldsymbol{F}}_{q_1,q_2}$ of the low rank part from Algorithm 3 with $\boldsymbol{F}_{q_1}$. What we are actually approximating here is $\boldsymbol{F}_q - \boldsymbol{F}_{q_2}$. For this reason, we do not plot $\varepsilon_{\mathrm{rel}}^1$ in our numerical tests for this method and instead calculate

$$\varepsilon_{\mathrm{rel}}^{1,2} := \frac{\|(\boldsymbol{F}_q - \boldsymbol{F}_{q_2}) - \widetilde{\boldsymbol{F}}_{q_1,q_2}\|_{\mathrm{HS}}}{\|\boldsymbol{F}_q - \boldsymbol{F}_{q_2}\|_{\mathrm{HS}}}$$

as a measure for the reconstruction quality of the low rank component. The situation of $J > 2$ scatterer's components, of with $K < J$ locations are known a priori, can be realized as described in the end of Subsection 3.6.2. This involves the implementation of cell-arrays consisting of $K^2 + 1$ matrices each, one matrix for the low rank component and one matrix for the sparse components each.

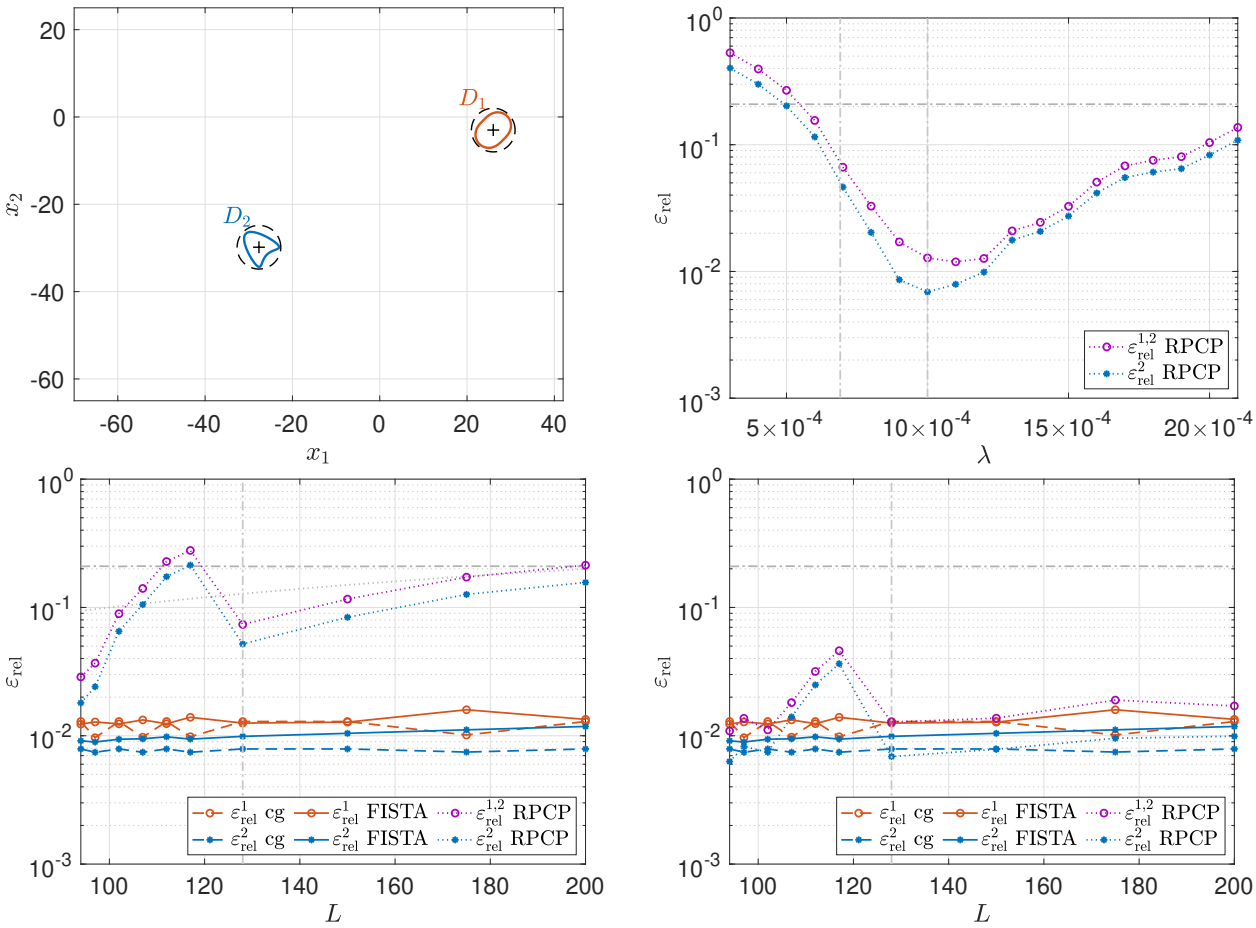

FIGURE 4.1. Top left: Geometry of scatterer (solid) and a priori information on location and size of components (dashed) for varying number L of discretization points (Example 4.1), varying wave number k (Example 4.2) and varying relative noise level δ_{rel} (Example 4.6). Top right: Relative errors of far field operator splitting for RPCP formulation in Example 4.1 for varying λ and fixed $L = 128$. Bottom: Relative errors of far field operator splitting for varying number L of discretization points in Example 4.1. Left: Choice of $\lambda = L^{-3/2}$ according to Theorem 3.34. Right: Optimal choices of λ by trial and error up to accuracy 10^{-4}.

4.2. NUMERICAL TESTS

We study the accuracy of our numerical reconstructions by the three methods as described in Subsections 4.1.4–4.1.6, depending on the different quantities that occur in the associated stability results in Chapter 3. Although all these methods are based on simplified situations, we choose the full discretized far field operator $\boldsymbol{F}_q$ (cf. Examples 4.1–4.5) or its noisy version $\boldsymbol{F}_q^\delta$ (cf. Example 4.6) as an input, i.e., we do not replace this operator by its Born approximation of order two. We have discussed in Section 3.6 that by this procedure a large number of components in the Born series are nevertheless assigned correctly, and the components that are not only have little impact, which is reflected by the resulting relative reconstruction errors. To get an impression of how large the effect of multiple scattering is in the individual examples, we also compute the relative error

$$\frac{\|\boldsymbol{F}_q - (\boldsymbol{F}_{q_1} + \boldsymbol{F}_{q_2})\|_{\mathrm{HS}}}{\|\boldsymbol{F}_q\|_{\mathrm{HS}}},$$

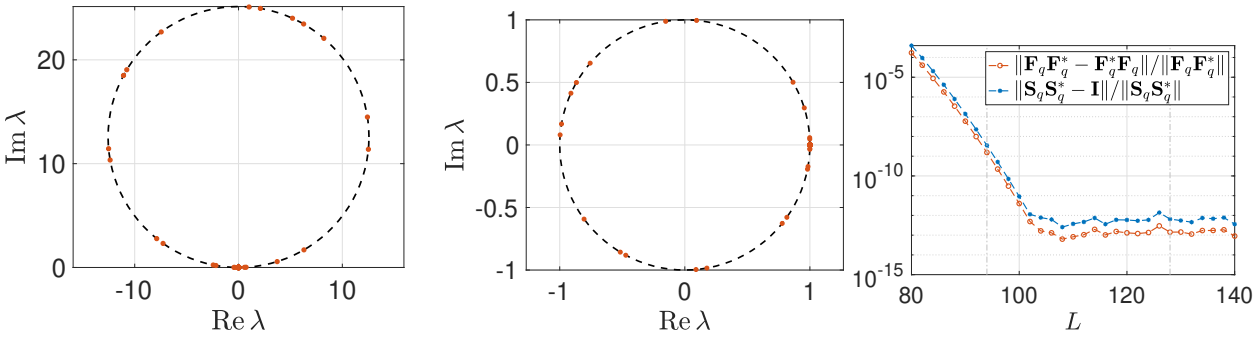

FIGURE 4.2. Eigenvalues λ of $\boldsymbol{F}_q$ (left) and of $\boldsymbol{S}_q = \boldsymbol{I} + \mathrm{i}k/(4\pi)\boldsymbol{F}_q$ (middle) for the scatterer from Example 4.1 for $L = 94$. Right: Errors of $\boldsymbol{F}_q$ being normal and of $\boldsymbol{S}_q$ being unitary for varying L.

and we add it in gray into the error plots. We create double logarithmic plots for those examples for which we want to analyze orders of the relative errors in certain quantities. Otherwise, we only present the relative errors on a logarithmic scale.

In the first three examples we fix the same geometrical setup for the scatterer as depicted in Figure 4.1 (left). Here, we set $q := -0.5\chi_{D_1} + \chi_{D_2}$, i.e., the associated index of refraction n^2 is piecewise constant with value 0.5 on D_1, value 2 on D_2 and value 1 outside D. The actual sharply chosen size of both objects is $R_1 = R_2 = 5$, and their distance is $|\boldsymbol{c}_1 - \boldsymbol{c}_2| = 60$. We investigate the performance of our methods for varying number of discretization points L, for varying wave number k and for varying quality of the a priori information. Hereby, the investigation depending on the radius also involves the investigation of the rule (4.1) for choosing the subspace dimension in the cg method.

We mention that in all examples below the assumptions of the related stability Theorems 3.39, 3.41 and 3.34 are not fulfilled. Nevertheless, the three methods converge in all considered cases, which suggests that our developed stability results are not optimal.

Example 4.1 (Varying number L of discretization points)**.** As a first example, we study the sensitivity of our methods with respect to the number L of discretization points. We fix $k = 1$. The minimal radius $R > 0$ such that $\operatorname{supp} q \subset B_R(\mathbf{0})$ is approximately given by $R = 46$. Consequently, choices of L larger than 93 are meaningful and we choose different values of L between 94 and 200, as shown in Figure 4.1 (bottom).

Before discussing the results of our methods, we want to substantiate that it is sufficient to resolve the far field operator $\boldsymbol{F}_q$ with $L = 94$ or at least with $L = 128 = 2(\lceil ekR/2 \rceil + 1)$ discretization points, where the latter is suggested by (4.1). Doing so we plot the eigenvalues of the far field operator $\boldsymbol{F}_q$ and of the scattering operator $\boldsymbol{S}_q$ from (2.9) for $L = 94$ in Figure 4.2 (left, middle). From Proposition 2.4 (d) we know that the eigenvalues of $\boldsymbol{F}_q$ lie on the circle of radius $4\pi/k$ centered at $\mathrm{i}4\pi/k$ in the complex plane and that $\boldsymbol{S}_q$ is a unitary operator, so its eigenvalues must lie on the complex unit circle. This is visually fulfilled for both plots. From Proposition 2.4 (c) we also know that $\boldsymbol{F}_q$ is a normal operator. Therefore, we further plot the relative errors, measured in the operator norm $\|\cdot\|$,

$$\frac{\|\boldsymbol{F}_q\boldsymbol{F}_q^* - \boldsymbol{F}_q^*\boldsymbol{F}_q\|}{\|\boldsymbol{F}_q\boldsymbol{F}_q^*\|} \quad \text{and} \quad \frac{\|\boldsymbol{S}_q\boldsymbol{S}_q^* - \boldsymbol{I}\|}{\|\boldsymbol{S}_q\boldsymbol{S}_q^*\|}$$

for $\boldsymbol{F}_q$ being normal and for $\boldsymbol{S}_q$ being unitary, respectively, against L in Figure 4.2 (right). It can be seen that both curves decay rapidly in L, and that they already reach very small values of the order of magnitude of 10^{-9} at $L = 94$ and of 10^{-13} at $L = 128$. The locations $L = 94$ and $L = 128$ are marked by vertical gray lines.

We make the following assumptions and parameter choices. For the cg method we assume the dashed circles in Figure 4.1 (left) to be known a priori, and we choose according to (4.1) as subspace

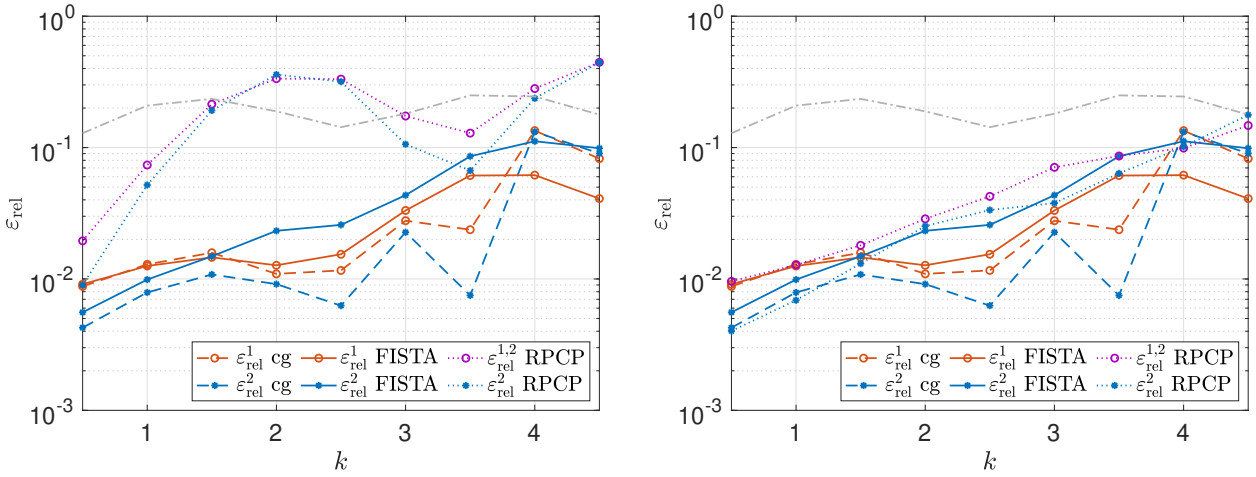

FIGURE 4.3. Relative errors of far field operator splitting for varying wave number k in Example 4.2 and L according to (4.1), i.e. $L = 2(\lceil ekR/2 \rceil + 1)$. Left: Choice of $\lambda = L^{-3/2}$ according to Theorem 3.34. Right: Optimal choices of λ by trial and error up to accuracy 10^{-4}.

dimensions $2N_1 + 1 = 2N_2 + 1 = 2\lceil 5e/2 \rceil + 1 = 15$. For FISTA we assume the positions marked by crosses in Figure 4.1 (left) to be known a priori. We further choose $\mu = 3 \times 10^{-4}$. Finally, for the third method, we assume only the position marked by a cross inside the kite to be known a priori, and we choose $\lambda = L^{-3/2}$ and $\mu = 3 \times 10^{-4}/\lambda$.

The relative errors of the resulting reconstructions are shown in Figure 4.1 (bottom left). It can be seen clearly that the results of the first two methods are nearly independent of the choice of L, whereas the third method is very sensitive in regards to this choice. The RPCP method works best for small L, but does not achieve the accuracy of the other two methods in all cases for this choice of λ. The accuracy of the cg method and FISTA is at about 1% relative error. This described behavior of the relative errors is consistent with the dependence on N in the stability bounds (3.70), (3.75) and (3.58). The dotted gray line illustrates $O(L)$, which is the theoretically expected order of the error curves for the RPCP method. The difference $\boldsymbol{F}_q - \boldsymbol{F}_{q_2}$ for small L is also well approximated by this method, as can be seen from the purple curve.

To examine whether the choice of λ given by Theorem 3.34 is optimal, we fix the number of discretization points at $L = 128$ and run the third method again for $\lambda \in [3 \times 10^{-4}, 21 \times 10^{-4}]$. This choice of L is marked in the other two error plots by vertical gray lines in order to link the three plots with each other. The results are shown in Figure 4.1 (top right). The suggested choice $\lambda = 128^{-3/2} \approx 7 \times 10^{-4}$ from Theorem 3.34 and the optimal choice $\lambda = 1 \times 10^{-3}$ are marked by vertical gray lines. For the relative error associated with the kite we observe a reduction of the relative error of around 5% to 0.7% when reducing λ from $\lambda = 128^{-3/2}$ to $\lambda = 1 \times 10^{-3}$. It is an open question how such an optimal choice of the regularization and coupling parameter can be generally constructed.

Consequently, we test the RPCP method against L for a second time. This time, we do not choose λ as in Theorem 3.34 but instead determine it as best as possible through trial and error, up to an accuracy of 10^{-4}. The plots of the resulting errors in Figure 4.1 clarify that the RPCP method is, with a few exceptions, nearly independent of L when proceeding as described, and it produces in most of the cases comparably good reconstructions of the second far field operator component to the other two methods. In both error plots in Figure 4.1 (bottom), a peak in the error curve of the RPCP method stands out at $L = 118$, which cannot be explained by our stability Theorem 3.34. ◊

Example 4.2 (Varying wave number k)**.** We further study the performance of our methods for varying wave number k. We again fix the geometrical setup as shown in Figure 4.1 (left), and we choose k uniformly distributed between 0.5 and 4.5. For each k we define the number L of

discretization points according to (4.1), i.e. $L = 2(\lceil ekR/2 \rceil + 1)$ for $R = 46$, and we assume the same a priori knowledge as in Example 4.1. For FISTA, in all runs we set $\mu = 3 \times 10^{-4}$ and for the RPCP method we set as a first test $\lambda = L^{-3/2}$ and $\mu = 3 \times 10^{-4}/\lambda$ and as a second test we maintain this selection rule for μ, but choose λ optimal by trial and error up to accuracy 10^{-4}.

The results are shown in Figure 4.3. We first note that all three methods work best for small values of k, which is reasonable due to the associated stability bounds, but it is difficult to identify an order in k from the plots. The cg method yields, especially for larger values of k, slightly better reconstructions than the other two methods, and these reconstructions are satisfying up to $k = 3.5$. FISTA already starts generating unsatisfying results for $k = 2.5$. When comparing the left and the right plot, we again observe that for the RPCP method, the selection rule for λ from Theorem 3.34 is not optimal. In the right plot the RPCP method reaches a similar accuracy to FISTA. Another interesting observation is that the relative measure of the multiple scattering effects oscillates slowly with values between 12% and 25% and remains at the same level on average. In the right plot, all relative errors appear to approximately follow these oscillations, but they increase on average. This illustrates the correlation between the approximation quality of the solutions of the splitting problem by the solutions of the minimization problems and the amount of multiple scattering. Numerical tests, that are not shown here, clarify that the relative measure for multiple scattering effects tends to zero for $k \to 0$. ◊

Example 4.3 (Varying quality of a priori knowledge $B_{R_j}(\boldsymbol{c}_j)$, $j = 1, 2$)**.** In the previous examples, we assumed very sharp information about the localizations of the scatterer's components. It may not always be possible to obtain this. Therefore, we next investigate how sensitive our methods are to less optimal knowledge on the position and on the size of one of the components, see Figure 4.4 (top left). We again fix $k = 1$. The radius of the smallest ball $B_R(\mathbf{0})$ containing all dashed circles in Figure 4.4 (top left) is approximately given by $R = 52$, so we choose in all tests $L = 2(\lceil ekR/2 \rceil + 1) = 144$ discretization points. In the first test, we assume to have access to the black marked circle around the nut shaped scatterer, and at the same time we vary the assumed knowledge on the position of the kite shaped scatterer marked in gray. Hereby, we only change the first coordinate $c \in \mathbb{R}$ of $\boldsymbol{c}_2$, and we choose R_2 as small as possible such that the kite shaped scatterer is still contained in $B_{R_2}(\boldsymbol{c}_2)$. If we were to leave R_2 unchanged, the cg method would be at a clear disadvantage. This can be seen from the second test in this example: We fix the black marked information about the localization of the kite shaped scatterer, and at the same time we vary the known size of the nut shaped scatterer as marked in gray. This means we change R_1 while leaving $\boldsymbol{c}_1$ unchanged, which clearly only affects the cg method.

In the first test, we run all three methods, and we plot their relative errors against c as shown in Figure 4.4 (bottom). At this point, we select the regularization and coupling parameters as in Examples 4.1 and 4.2. For the RPCP method this means two scenarios, setting $\lambda = L^{-3/2}$ (cf. Figure 4.4 (bottom left)) or choosing λ optimally by trial and error (cf. Figure 4.4 (bottom right)). As expected, all methods yield their best reconstruction for the kite shaped scatterer for $c = 35$, since this choice leads to a circle with the smallest possible radius R_2, which is reflected by the best possible sparsity property of the associated far field operator component. For smaller and larger c the reconstruction quality of the kite shaped scatterer gets gradually worse, where the cg method and the RPCP method are more sensitive than FISTA. The reconstruction quality for the nut shaped scatterer seems to be relatively robust in the cases of the cg method and FISTA. By comparing the left and right plots, we observe that the RPCP method achieves the accuracy of the other two methods only when the optimal choice $c = 35$ is used. All in all, the RPCP method in particular, but also the cg method, turn out to be sensitive to the choice of c.

Since only the cg method requires a priori knowledge on R_1, we only run this method for the second test. We compute N_1 according to (4.1) and plot the relative errors against N_1. This is shown in Figure 4.4 (top right), and it also allows us to decide whether our selection rule for N_1 is appropriate. The reconstruction quality for the kite shaped component remains unchanged provided R_1 and thus N_1 are chosen large enough to ensure $D_1 \subset B_{R_1}(\boldsymbol{c}_1)$ and $N_1 \geq kR_1$. For $N_1 \in [5, 13]$ the

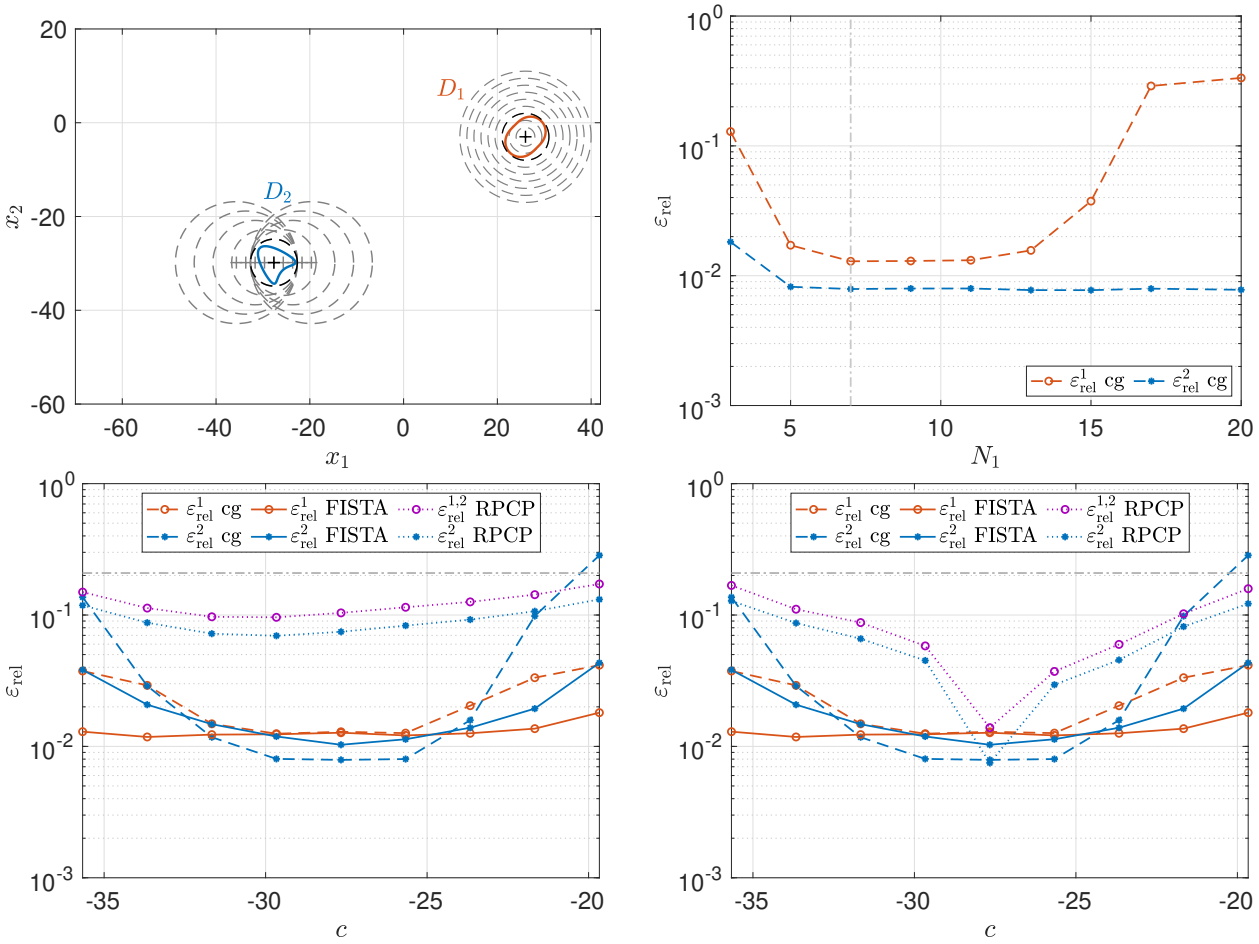

FIGURE 4.4. Top left: Geometry of scatterer (solid) and varying quality of a priori information on locations $B_{R_j}(\boldsymbol{c}_j)$ of its components (dashed) in Example 4.3 (optimal choices highlighted). Top right: Relative errors of far field operator splitting by cg method for varying a priori knowledge on size of nut shaped scatterer in Example 4.3. Bottom: Relative errors of far field operator splitting for varying a priori knowledge on position of kite shaped scatterer in Example 4.3. Left: Choice of $\lambda = L^{-3/2}$ according to Theorem 3.34. Right: Optimal choices of λ by trial and error up to accuracy 10^{-4}.

approximation quality for the nut shaped scatterer is convincing, whereas the choice $N_1 = 7$, which comes about due to (4.1), leads to the smallest relative error. This optimal choice is marked by a gray vertical line. It turns out to be less problematic to choose N_1 too large then too small, where we can choose it about twice as large as necessary until the reconstruction gradually fails. ◊

So far, we have always considered the same geometry of the scatterer. We now change this by first varying the distance between the two components in Example 4.4 and then varying the size of one of the components in Example 4.5, and we analyze how the relative errors of the reconstructions are affected by this. Here, we choose $k = 1$ and the regularization and coupling parameters in the same way as before.

We briefly comment on how the orders in R_j, $j = 1, 2$, and $|\boldsymbol{c}_1 - \boldsymbol{c}_2|$ in the stability bounds from (3.70), (3.75) and (3.58) link to the slopes of the error curves when plotting them on a logarithmic scale. For $s \in \{R_1, R_2, |\boldsymbol{c}_1 - \boldsymbol{c}_2|^{-1}\}$ these bounds are qualitatively all of the form $g(s^\beta) := (1 - \alpha s^\beta)^{-1/2}\delta$ with $s^\beta \in (0, 1/\alpha)$ for some $\alpha, \beta, \delta > 0$. For s small enough, ex-

panding $\ln g(s^\beta)$ as a Taylor series around $s^\beta = 0$ yields

$$\ln g(s^\beta) = \ln \delta + \frac{\alpha}{2} s^\beta + O(s^{2\beta}) .$$

Actually, we observe for certain areas of the error curves dependencies of the form $\beta \ln s$. These cannot be linked to our theoretical results, but enables a comparison of the three methods with each other. We reiterate that in all tests, we are not in situations where the assumptions of our stability theorems hold, i.e., in the above modulation, $\alpha s^\beta < 1$ would not be guaranteed.

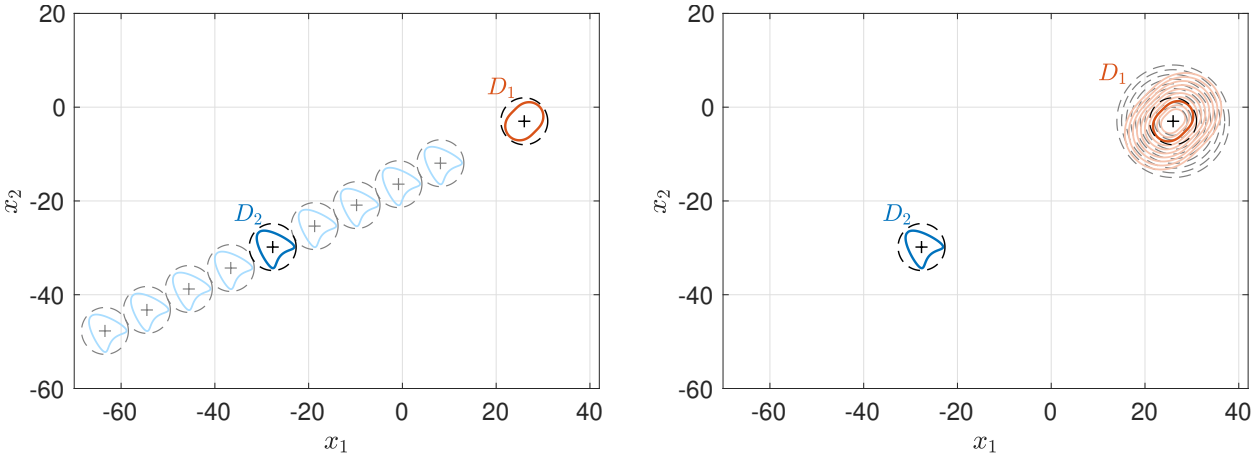

Figure 4.5. Geometry of scatterer (solid) and a priori information on location and size of components (dashed) for varying distance $|\boldsymbol{c}_1 - \boldsymbol{c}_2|$ in Example 4.4 ($|\boldsymbol{c}_1 - \boldsymbol{c}_2| = 60$ highlighted) and for varying size of nut shaped component in Example 4.5 ($R_1 = 5$ highlighted).

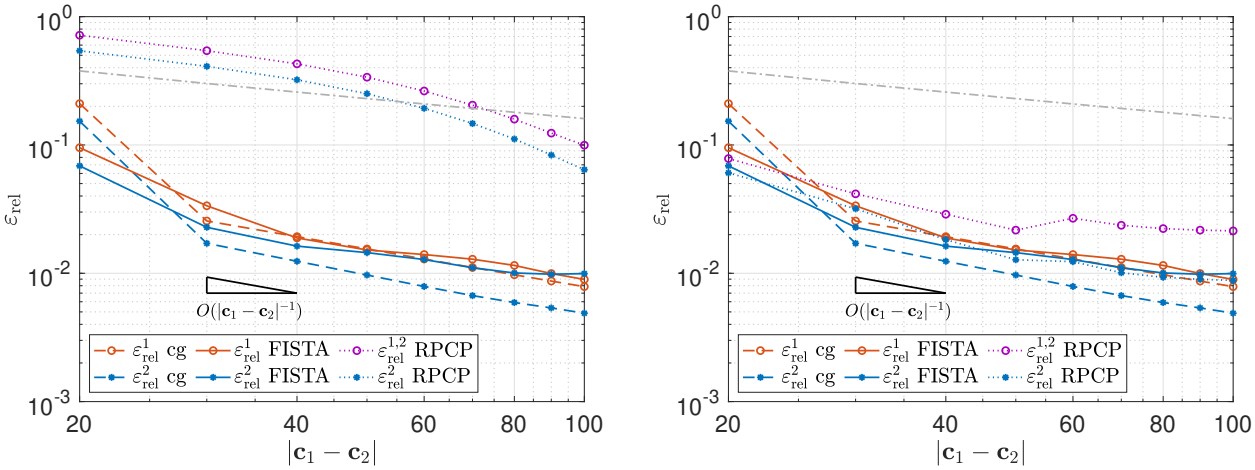

Figure 4.6. Relative errors of far field operator splitting for varying distance $|\boldsymbol{c}_1 - \boldsymbol{c}_2|$ in Example 4.4. Left: Choice of $\lambda = L^{-3/2}$ according to Theorem 3.34. Right: Optimal choices of λ by trial and error up to accuracy 10^{-4}.

Example 4.4 (Varying distance $|\boldsymbol{c}_1 - \boldsymbol{c}_2|$ between scatterer's components)**.** We study the accuracy of our numerical reconstructions depending on the distance $|\boldsymbol{c}_1 - \boldsymbol{c}_2|$ between the two components of the scatterer. We fix their sizes as well as the position of the nut shaped scatterer and vary the position of the kite shaped scatterer as shown in Figure 4.5 (left). The radius of the smallest ball $B_R(\mathbf{0})$ that contains all dashed balls is approximately given by $R = 85$. Therefore it is meaningful to run all tests with $L = 150$ discretization points. For the cg method we assume the dashed circles

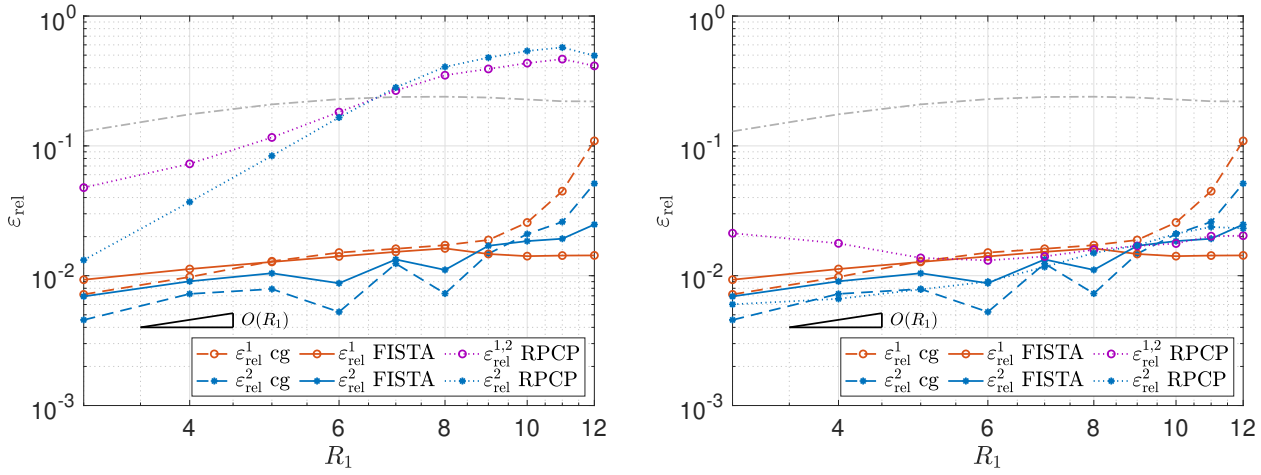

FIGURE 4.7. Relative errors of far field operator splitting for varying size of nut shaped component in Example 4.5. Left: Choice of $\lambda = L^{-3/2}$ according Theorem 3.34. Right: Optimal choices of λ by trial and error up to accuracy 10^{-4}.

in Figure 4.5 (left) to be known a priori. Accordingly, we choose the subspace dimensions given by (4.1) as $2N_1 + 1 = 2N_2 + 1 = 2\lceil 5e/2 \rceil + 1 = 15$. For the FISTA algorithm we assume the positions marked by crosses in Figure 4.5 (left) to be known a priori. Finally, for the RPCP method, we assume only the positions marked by crosses inside the kites to be known a priori.

In Figure 4.6 the corresponding relative errors are shown. As can be assumed from the related stability estimates in Chapter 3, all reconstructions improve with increasing distance between the components. The errors of the cg method behave for distances $|\boldsymbol{c}_1 - \boldsymbol{c}_2|$ larger than about 30 like $O(|\boldsymbol{c}_1 - \boldsymbol{c}_2|^{-1})$. The FISTA errors decrease a bit more slowly for increasing distance. As a consequence, the cg method yields slightly better reconstructions than FISTA for $|\boldsymbol{c}_1 - \boldsymbol{c}_2|$ large enough. However, FISTA seems a bit more robust for smaller values of $|\boldsymbol{c}_1 - \boldsymbol{c}_2|$. It is nicely confirmed that our relative measure for multiple scattering also decreases for increasing values of $|\boldsymbol{c}_1 - \boldsymbol{c}_2|$. For the far field operator of the kite shaped scatterer, the RPCP method reaches the same accuracy as the other two methods, when setting λ optimally by trial and error. An order in $|\boldsymbol{c}_1 - \boldsymbol{c}_2|$ is hard to identify from the plots for this method, but it seems comparable to FISTA in case of the kite shaped scatterer. ◊

Example 4.5 (Varying size R_1 of the first scatterer's component)**.** Next we investigate the reconstruction quality depending on the size of one of the scatterer's components by varying the size of the nut shaped scatterer while leaving the kite shaped scatterer unchanged as depicted in Figure 4.5 (right). Here, we fix $|\boldsymbol{c}_1 - \boldsymbol{c}_2| = 60$, and we choose

$$R_1 \in \{3, 4, 5, 6, 7, 8, 9, 10, 11, 12\}\,, \qquad \text{so} \qquad N_1 \in \{5, 6, 7, 9, 10, 11, 13, 14, 15, 17\}$$

according to (4.1) in the cg method. We resolve the far field operators by $L = 150$ discretization points, which is meaningful since the whole scatterer is contained in the ball of radius $R = 46$ centered at the origin. For FISTA and the RPCP method, assume the a priori knowledge on the positions of the components as in Figure 4.5 (right).

The associated relative errors are plotted in Figure 4.7 on a double logarithmic scale. As expected from the stability bounds in Chapter 3 the errors grow with increasing R_1. In case of the cg method we observe both error curves to behave more or less like $O(R_1)$ for R_1 small enough. In the case of FISTA both error curves increase a bit more slowly in R_1. For the kite shaped scatterer the stability bound (3.75) suggests the related relative error to be independent of R_1, which we clearly do not observe. At least for the kite shaped scatterer the third method reaches the accuracy of the other methods when defining λ by trial and error. All reconstructions appear to be successful up to

approximately $R_1 = 9$. For larger values of R_1, in particular the cg method starts to fail, whereas the other two methods seem to be more robust for larger values of R_1. The RPCP method provides worse reconstructions of the low rank component for smaller values of R_1, which is not explainable by our theory. ◊

We proceed by investigating in Example 4.6 below how the reconstructions change when we include additional noise in the data.

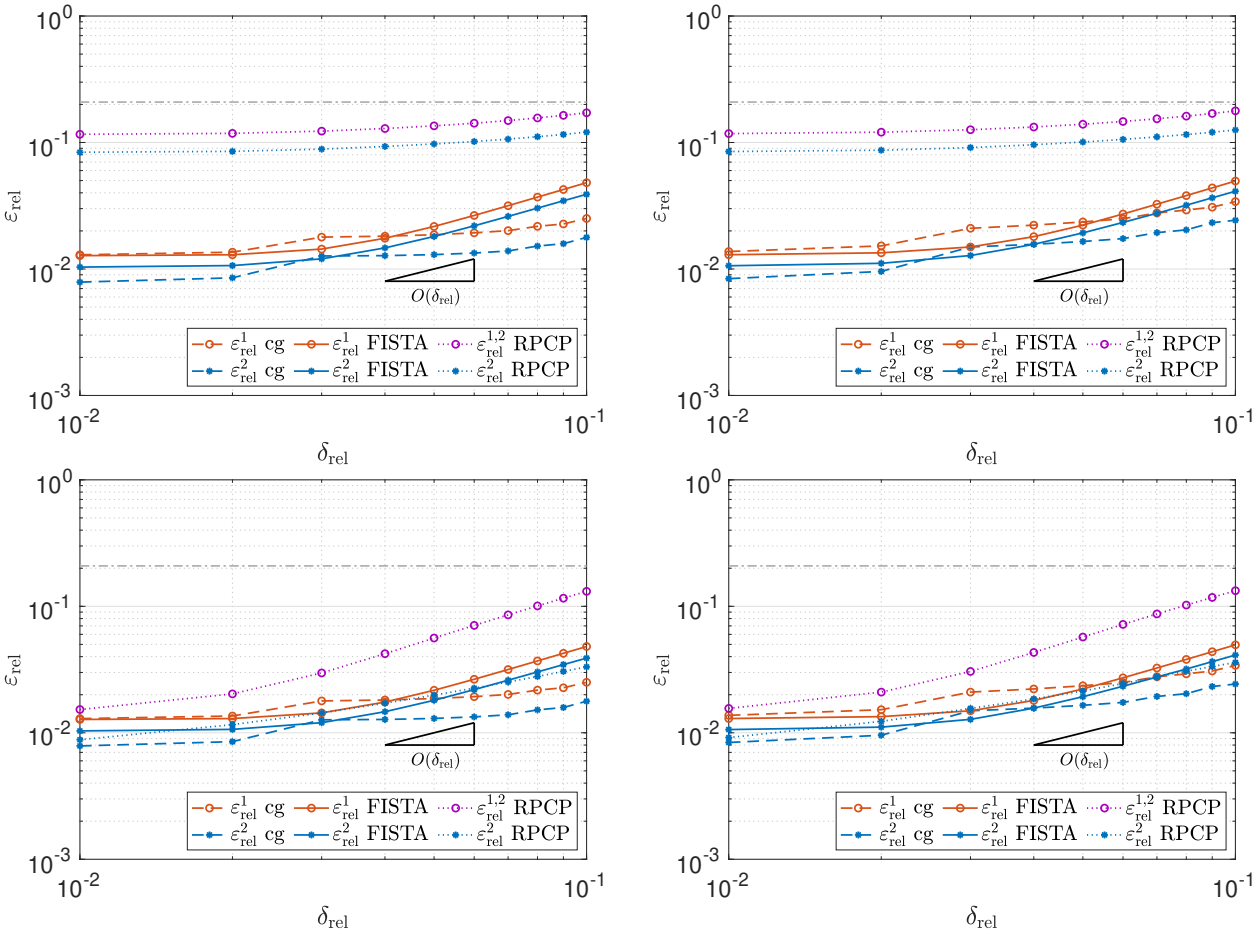

FIGURE 4.8. Relative errors for varying relative noise level δ_{rel} in Example 4.6, best (left) and worst (right) results of 15 runs.
Top: Choice of $\lambda = L^{-3/2}$ according to Theorem 3.34. Bottom: Optimal choice of $\lambda = 9 \times 10^{-4}$ by trial and error.

Example 4.6 (Varying relative noise level δ_{rel})**.** We fix the same geometrical setup as in Examples 4.1, 4.2 and 4.3, which is shown in Figure 4.1 (left), and we assume the same a priori knowledge on the scatterer's location as in Examples 4.1 and 4.2. Further, we specify uniformly distributed relative noise levels δ_{rel} between 1% and 10% and we simulate for each of them a related noisy version $\boldsymbol{F}_q^\delta$ of $\boldsymbol{F}_q$ as described in Subsection 4.1.1 for $L = 150$ discretization points. Here, for every δ_{rel} we run our three methods 15 times, in each run generating a different complex uniformly distributed noise matrix $\boldsymbol{N}$, and we calculate the relative errors of the best and the worst reconstructions. As a stopping criterion in the cg method we use the a priori known absolute noise level $\delta = \delta_{\text{rel}} \|\boldsymbol{F}_q\|_{\text{HS}}$. For FISTA we choose the same regularization parameter as before, so $\mu = 3 \times 10^{-4}$, and for the RPCP method we set λ optimally for the noise free case as investigated in Example 4.1, i.e. $\lambda = 9 \times 10^{-3}$ and $\mu = 3 \times 10^{-4}/\lambda$. The results are shown in Figure 4.8.

It can be seen that both FISTA curves as well as the error curve of the low rank component of the third method increase with the same order 1 in δ_{rel}, and that the other error curves grow less

quickly. For all methods we expect their errors to behave like $O(\delta_{\text{rel}}) = O(\delta) = O(\|\boldsymbol{F}_q - \boldsymbol{F}_q^\delta\|_{\text{HS}})$, see (3.70), (3.75) and (3.58). While for the second and third method, the curves of the best and worst cases look nearly the same, the cg method slightly depends on the actual pattern of the noise not only on its magnitude measured in the Frobenius norm. The third method again does not give useful reconstructions for $\lambda = L^{-3/2}$. ◊

The final example below covers the generalization of our methods to more than two scatterer's components as described in Subsection 3.6.3.

Example 4.7 (Three scatterer's components)**.** We consider a scatterer consisting of three components, a nut shaped scatterer D_1, a kite shaped scatterer D_2 and an elliptic scatterer D_3 as shown in Figure 4.9 (top left) by defining the contrast function $q = 0.5(\chi_{D_1} + \chi_{D_2} + \chi_{D_3})$. We fix the wave number $k = 1$, and we vary the individual distances between the scatterer's components by varying the first coordinate c of the position $\boldsymbol{c}_2 = (c, -25)^\top$ of the kite shaped scatterer between $c = -50$ and $c = 50$. For all runs we choose $L = 160$ discretization points, which is meaningful since the ball of radius $R = 58$ centered at the origin contains all dashed balls in Figure 4.9 (top left). For the cg method we assume the dashed circles from Figure 4.9 (top left) to be known a priori. According to (4.1), these choices $R_1 = R_3 = 3$ and $R_2 = 4$ lead to the subspace dimensions $2N_1 + 1 = 2N_3 + 1 = 7$ and $2N_2 + 1 = 9$. While the distance between D_1 and D_3 is fixed at $|\boldsymbol{c}_1 - \boldsymbol{c}_3| = 60$, the distances between D_1 and D_2 and between D_2 and D_3 vary with smallest values of about 42.4 and largest values of about 85.4, respectively. For FISTA we assume all three positions marked by crosses in Figure 4.9 (top left) to be known a priori and we choose $\mu = 13 \times 10^{-5}$ as a regularization parameter. For the RPCP method we only assume the positions of the kite and the elliptic shaped scatterer to be known a priori. Furthermore, we set $\lambda = L^{-3/2}$ according to Theorem 3.34 and $\mu = 13 \times 10^{-5}/\lambda$ as a first test and then, as a second test, $\mu = 13 \times 10^{-5}/\lambda$ and λ optimally by trial and error up to accuracy 10^{-5} such that the relative error of the kite shaped scatterer is as small as possible. The resulting relative errors can be found in Figure 4.9 (top right, bottom left). Finally, we set λ and μ as in the second test, but we add 5% complex uniformly distributed noise to the data as described in Subsection 4.1.1. The results are shown in Figure 4.9 (bottom right). For the cg method and FISTA we further calculate the relative reconstruction errors $\varepsilon_{\text{rel}}^3$ of the third component, and for the RPCP method we compute

$$\varepsilon_{\text{rel}}^{1,2,3} := \frac{\|(\boldsymbol{F}_q - \boldsymbol{F}_{q_1} - \boldsymbol{F}_{q_2}) - (\widetilde{\boldsymbol{F}}_{q_1,q_2,q_3} + \widetilde{\boldsymbol{F}}_{q_1,q_2} + \widetilde{\boldsymbol{F}}_{q_2,q_1})\|_{\text{HS}}}{\|\boldsymbol{F}_q - \boldsymbol{F}_{q_1} - \boldsymbol{F}_{q_2}\|_{\text{HS}}}$$

instead of $\varepsilon_{\text{rel}}^{1,2}$ as a relative reconstruction error of the low rank component. The gray curve, as a measure for the magnitude of multiple scattering effects, corresponds to

$$\frac{\|\boldsymbol{F}_q - (\boldsymbol{F}_{q_1} - \boldsymbol{F}_{q_2} - \boldsymbol{F}_{q_3})\|_{\text{HS}}}{\|\boldsymbol{F}_q\|_{\text{HS}}}.$$

It can be clearly seen that for all three runs the cg method works best, followed by FISTA. For the kite shaped component, the RPCP method produces slightly worse reconstructions, but for the nut shaped component, the reconstructions of the RPCP method and FISTA are almost equally good. Even for optimally chosen λ by trial and error, see Figure 4.9 (bottom), the relative errors of the kite shaped component are for the RPCP method worse than for the other two methods. The here achieved improvement is for all three curves less significant than in the previous examples. Concerning FISTA, the minimal distance of a scatterer's component to the other components seems to slightly affect the reconstruction quality of the related far field operator component in the noise free case. For example the FISTA curve of $\varepsilon_{\text{rel}}^2$ has little bumps for $c = -30$ and $c = 30$, which corresponds to the nearest positions of the kite to the ellipse and to the nut, respectively. The bump for $c = -30$ is also observable for the related error curve of the RPCP method. On average, the ellipse's far field operator component reconstruction of FISTA becomes better the further away

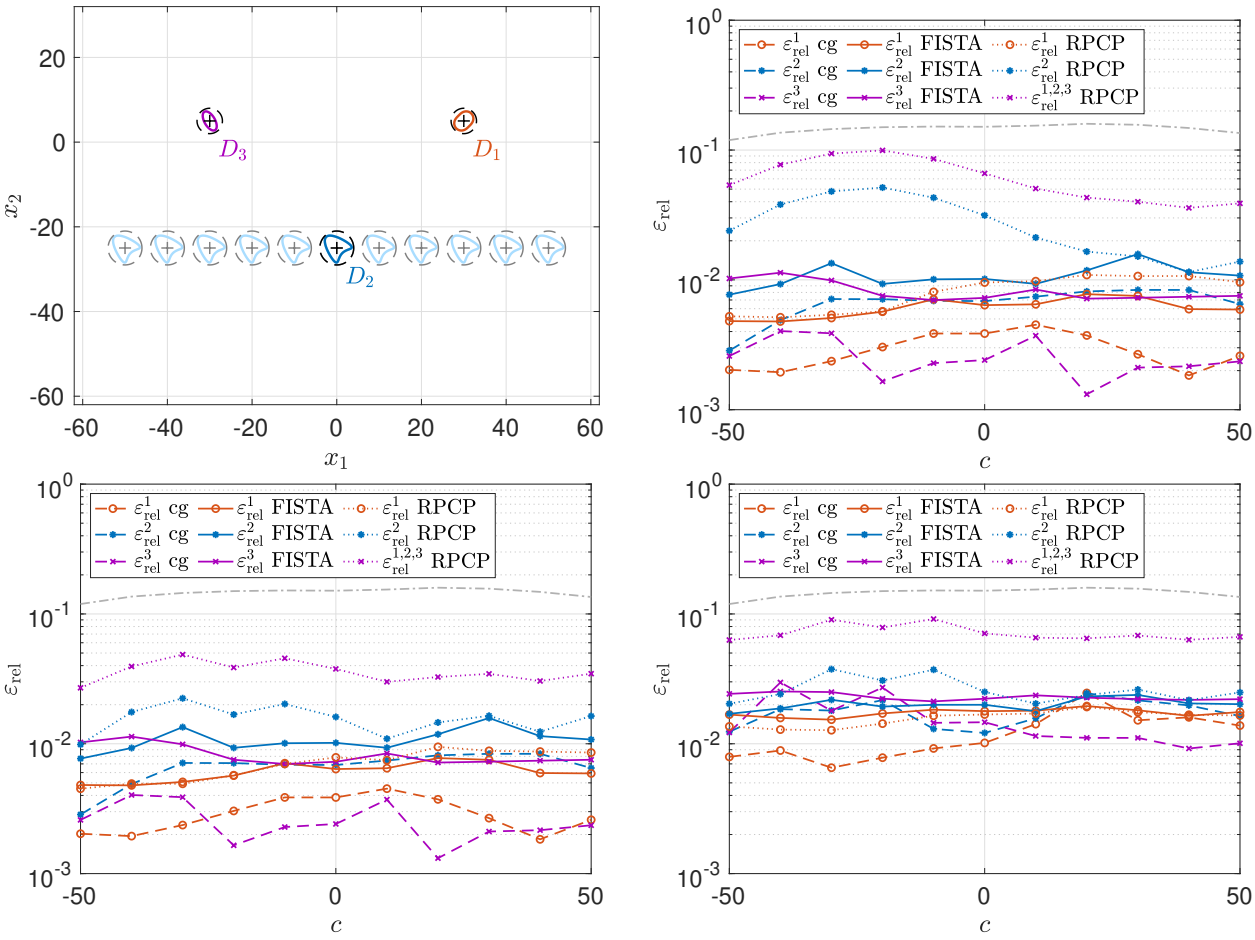

Figure 4.9. Top left: Geometry of scatterer (solid) and a priori information on location and size of components (dashed) for varying position of kite shaped component in Example 4.7 ($\boldsymbol{c}_2 = (0, -25)^\top$ highlighted). Relative errors of far field operator splitting. Top right: Noise free data, choice of $\lambda = L^{-3/2}$ according Theorem 3.34. Bottom left: Noise free data, optimal choices of λ by trial and error up to accuracy 10^{-5}. Bottom right: 5% complex uniformly distributed noise added to data, optimal choices of λ in noise free case.

the kite is. Both no longer occurs in the noisy case, where no c dependence of the FISTA curves is observable. There is no clear trend concerning the c dependence of the cg errors curves identifiable in the noise free case. In the noisy case we observe little bumps of the cg error curve of the kite shaped scatterer around $c = -30$ and $c = 30$, and the reconstruction quality of the other two components improves as the distance between the kite and these components increases. ◊

CHAPTER 5

Far field operator completion

Assumption 5.1. *We suppose that the scatterer $D \subseteq B_R(\boldsymbol{c})$ is contained in some ball with radius $R > 0$ centered at $\boldsymbol{c} \in \mathbb{R}^d$. Here, the scatterer may consist of several disjointly supported components but, unless otherwise assumed, is viewed as one component.*

Moreover, we assume that u_q^∞ cannot be observed on some $\Omega \subset S^{d-1} \times S^{d-1}$. We mention that $(\widehat{\boldsymbol{x}}, \boldsymbol{\theta}) \in \Omega$ means, that far field measurements cannot be observed along direction $\widehat{\boldsymbol{x}}$ when illuminating along direction $\boldsymbol{\theta}$.

Definition 5.2. Given the *non-observable set* $\Omega \subset S^1 \times S^1$ we define the infinite dimensional subspace

$$\mathcal{V}_\Omega := \left\{ G \in \mathrm{HS}(L^2(S^{d-1})) \;\middle|\; Gg = \int_{S^{d-1}} \chi_\Omega(\,\cdot\,, \boldsymbol{\theta}) \alpha(\cdot; \boldsymbol{\theta}) g(\boldsymbol{\theta}) \, \mathrm{d}s(\boldsymbol{\theta}) \,,\ \alpha \in L^2(S^{d-1} \times S^{d-1}) \right\},$$

which we refer to as *subspace of non-observable far field operators*. With $\mathcal{P}_{\mathcal{V}_\Omega} : \mathrm{HS}(L^2(S^{d-1})) \to \mathcal{V}_\Omega$ we mean the orthogonal projection onto $\mathcal{V}_\Omega$ with respect to $\langle \,\cdot\,, \,\cdot\, \rangle_{\mathrm{HS}}$, which restricts the integral kernel of a Hilbert Schmidt integral operator onto Ω.

We define the associated *restricted* or *observable far field operator* by $F_q|_{\Omega^c} := (I - \mathcal{P}_{\mathcal{V}_\Omega}) F_q$. With this notation, the goal of **far field operator completion** is to recover F_q from $F_q|_{\Omega^c}$. Particularly, this involves the restoration of the *non-observable part* $B_q := F_q|_{\Omega^c} - F_q$.

From formula (2.6) we can conclude for fixed $\boldsymbol{\theta} \in S^{d-1}$ that the far field pattern $u_q^\infty(\,\cdot\,; \boldsymbol{\theta})$ is a real analytic function on S^{d-1} as a multiple of the Fourier transform of $q u_q(\,\cdot\,; \boldsymbol{\theta})$ restricted to kS^{d-1}. Due to the reciprocity relation we further obtain analyticity of $u_q^\infty(\widehat{\boldsymbol{x}}; \,\cdot\,)$ on S^{d-1} for fixed $\widehat{\boldsymbol{x}} \in S^{d-1}$. In [52] it has been shown that u_q^∞ is even joint real analytic on $S^{d-1} \times S^{d-1}$, which indeed is a stronger result that cannot be deduced from the analyticity with respect to both variables individually. Consequently, the completion problem has a unique solution as long as $(S^{d-1} \times S^{d-1}) \setminus \Omega$ has an interior point, and this solution can be obtained by analytic continuation due to the identity theorem for analytic functions (cf. [61, Cor. 1.2.9, Thm. 2.2.6]). Nevertheless, this is a well-known ill-posed problem due to the non-continuity of the related inverse, i.e., small errors in the observed data can lead to big errors in the completed data (cf. e.g. [78, Chap. 2] or [59, Chap. 3]). This justifies the need for regularization.

Since we view D as one individual scatterer this problem is already linear and, consequently, it is not necessary to take the Born series into account when solving the completion problem only. This is investigated in Section 5.1.

However, it turns out that solving the splitting and the completion problem simultaneously, which is covered by Section 5.2, improves the stability of the developed problem formulations for certain configurations of the scatterer. This again requires a consideration of the associated Born series due to the nonlinearity of the problem. The results stated here are a combination of the results obtained in Sections 3.4 and 3.5 for splitting only and Section 5.1 for completion only.

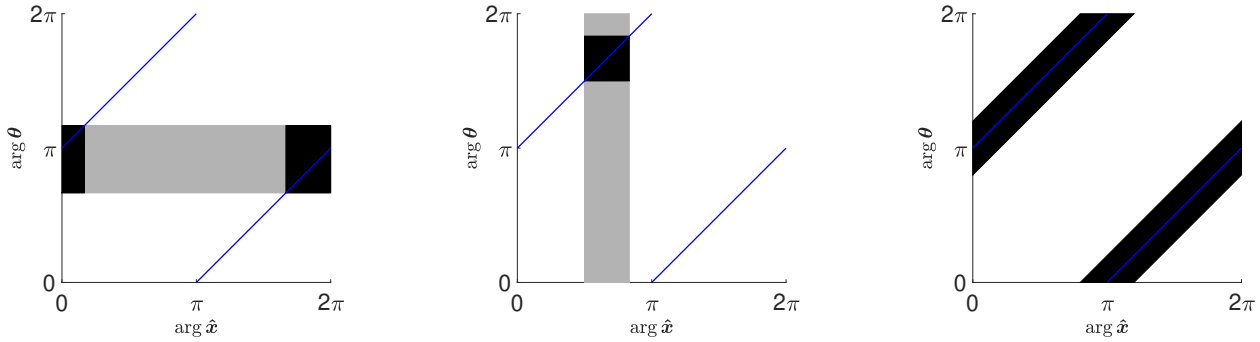

FIGURE 5.1. Non-observable set Ω before (gray) and after (black) taking reciprocity into account together with corresponding symmetry axis (blue). Left: Missing far field measurements for certain $\boldsymbol{\theta}$. Middle: Missing far field measurements for certain $\widehat{\boldsymbol{x}}$. Right: Missing backscattering data withing certain angular range.

Assumption 5.3. *In order to take the reciprocity relation (2.8) into account we impose a further assumption on Ω, namely that its complement $\Omega^c := (S^{d-1} \times S^{d-1}) \setminus \Omega$ is symmetric in the sense of reciprocity, i.e.,*

$$\Omega^c = \Omega^{c,r} \qquad \text{with} \qquad \Omega^{c,r} := \{(-\boldsymbol{\theta}, -\widehat{\boldsymbol{x}}) \in S^{d-1} \times S^{d-1} \mid (\widehat{\boldsymbol{x}}, \boldsymbol{\theta}) \in \Omega^c\}\,. \tag{5.1}$$

If this is not the case we can extend the kernel of the observable far field operator $F_q|_{\Omega^c}$ by (2.8) from Ω^c to $\Omega^{c,r}$. Consequently, this is no restriction.

Example 5.4. We illustrate the extent to which taking the reciprocity relation (2.8) into account reduces the size of the non-observable set Ω in two dimensions by three examples, as shown in Figure 5.1. In all situations the original Ω, with Ω^c possibly not satisfying (5.1), is plotted in gray, and the reduced Ω, by extending the data by reciprocity as it is described in Assumption 5.3, is plotted in black. Furthermore, a blue line marking the symmetry axis for the reciprocity is added to the plots. In Figure 5.1 (left) we choose

$$\Omega := \left\{(\widehat{\boldsymbol{x}}, \boldsymbol{\theta}) \in S^1 \times S^1 \,|\, (\arg \widehat{\boldsymbol{x}}, \arg \boldsymbol{\theta}) \in [0, 2\pi] \times [\tfrac{2\pi}{3}, \tfrac{7\pi}{6}]\right\},$$

which corresponds to missing far field data along illumination directions $\boldsymbol{\theta}$ for $\arg \boldsymbol{\theta} \in [2\pi/3, 7\pi/6]$. By taking reciprocity into account the relative size $|\Omega|/(4\pi^2)$ of Ω is reduced from $1/4$ to $1/16$ so by a factor $1/4$. In Figure 5.1 (middle) we choose

$$\Omega := \left\{(\widehat{\boldsymbol{x}}, \boldsymbol{\theta}) \in S^1 \times S^1 \,|\, (\arg \widehat{\boldsymbol{x}}, \arg \boldsymbol{\theta}) \in [\tfrac{\pi}{2}, \tfrac{5\pi}{6}] \times [0, 2\pi]\right\}.$$

This means that for all illumination directions $\boldsymbol{\theta} \in S^{d-1}$ the far field is non-observable along $\widehat{\boldsymbol{x}}$ with $\arg \widehat{\boldsymbol{x}} \in [\pi/2, 5\pi/6]$. In this situation, taking reciprocity into account reduces $|\Omega|/(4\pi^2)$ from $1/6$ to $1/36$ so by a factor $1/6$. In the last case as shown in Figure 5.1 (right) we choose

$$\Omega := \left\{(\widehat{\boldsymbol{x}}, \boldsymbol{\theta}) \in S^1 \times S^1 \,|\, |\arg \boldsymbol{\theta} - (\arg \widehat{\boldsymbol{x}} + \pi)| \le \tfrac{\pi}{5}\right\}.$$

This corresponds to missing backscattering data within an angular range of $2\pi/5$. Since Ω is already symmetric to the blue line, the relative size $|\Omega|/(4\pi^2) = 1/5$ of Ω cannot be reduced by taking reciprocity into account. ◊

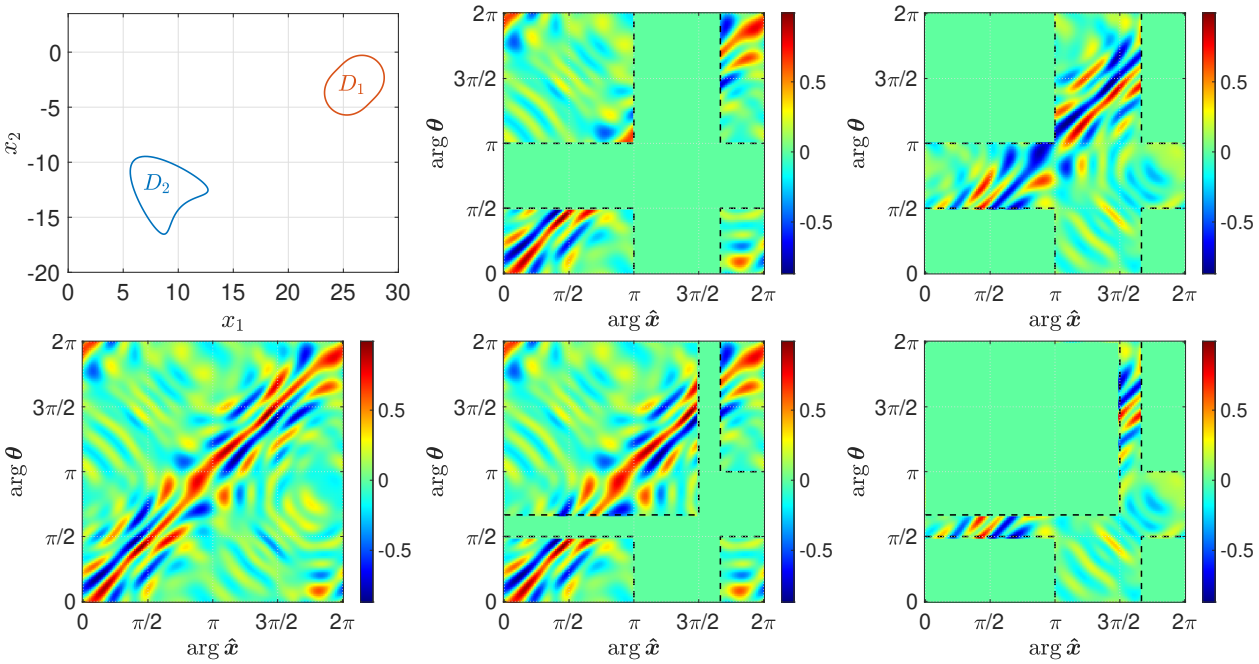

Figure 5.2. Top left: Support of scatterer. Bottom left: Real part of discretized full far field operator $\boldsymbol{F}_q$. Middle: Real parts of discretized observable far field operator $\boldsymbol{F}_q|_{\Omega^c}$ before (top) and after (bottom) taking reciprocity into account. Right: Real parts of discretized non-observable part $\boldsymbol{B}_q$ before (top) and after (bottom) taking reciprocity into account.

5.1. Completion only

Before we proceed to our theoretical investigations, we consider a numerical example for the underlying split of the far field operator completion problem in two dimensions.

Example 5.5. Suppose $d = 2$ and choose the wave number $k = 0.5$ and the contrast function q as in Example 3.2, i.e., $q = \chi_{D_1} + 2\chi_{D_2}$ for a kite shaped scatterer D_1 and a nut shaped scatterer D_2 as shown in Figure 5.2 (top left). We simulate the discretized far field operator $\boldsymbol{F}_q$ with $L = 150$ equally distributed illumination and observation directions, which is shown in Figure 5.2 (bottom left). In contrast to Example 3.2 we assume that we cannot observe all entries of $\boldsymbol{F}_q$. We suppose to have no measurements of the far field pattern available for illumination directions $\boldsymbol{\theta}$ with $\arg \boldsymbol{\theta} \in [\pi/2, \pi]$ and for observation directions $\hat{\boldsymbol{x}}$ with $\arg \hat{\boldsymbol{x}} \in [\pi, 5\pi/3]$, i.e., the non-observable set is given by

$$\Omega := \left\{ (\hat{\boldsymbol{x}}, \boldsymbol{\theta}) \in S^1 \times S^1 \,|\, (\arg \hat{\boldsymbol{x}}, \arg \boldsymbol{\theta}) \in \left([\pi, \tfrac{5\pi}{3}] \times [0, 2\pi] \right) \cup \left([0, 2\pi] \times [\tfrac{\pi}{2}, \pi] \right) \right\} .$$

We define the discretized observable far field operator $\boldsymbol{F}_q|_{\Omega^c} := (f_{m,n})_{m,n}$ as it is shown in Figure 5.2 (top middle) by

$$f_{m,n} := \begin{cases} \frac{2\pi}{L} u_q^\infty(\hat{\boldsymbol{x}}_m; \boldsymbol{\theta}_n) & \text{if } (\hat{\boldsymbol{x}}_m, \boldsymbol{\theta}_n) \notin \Omega \,, \\ 0 & \text{if } (\hat{\boldsymbol{x}}_m, \boldsymbol{\theta}_n) \in \Omega \,, \end{cases}$$

with $\hat{\boldsymbol{x}}_l$, $\boldsymbol{\theta}_l$ given as in Example 2.5, $l = 1, \ldots, L$. By setting the related non-observable part as $\boldsymbol{B}_q := \boldsymbol{F}_q|_{\Omega^c} - \boldsymbol{F}_q$ (cf. Figure 5.2 (top right)) we have that

$$\boldsymbol{F}_q|_{\Omega^c} = \boldsymbol{F}_q + \boldsymbol{B}_q \,.$$

We further extend $\boldsymbol{F}_q|_{\Omega^c}$ as described in Assumption 5.3 by taking the reciprocity relation into

account, see Figure 5.2 (bottom middle). The corresponding non-observable part is shown in Figure 5.2 (bottom right). ◊

From Definition and Corollary 2.21 we know that F_q can be well approximated in $\mathcal{V}_N^{\boldsymbol{c}}$. Furthermore by definition, non-observable part of the far field operator fulfills $B_q \in \mathcal{V}_\Omega$. We will exploit these two properties in the following. We begin again with a least squares formulation, followed by a (weighted) $\ell^1 \times \ell^1$ minimization and a coupled L_1 and $\ell^1 \times \ell^1$ minimization.

5.1.1. Completion by solving a least squares problem

Given the observed far field operator $F_q|_{\Omega^c}$, the non-observable set $\Omega \subseteq S^{d-1} \times S^{d-1}$ and $N \in \mathbb{N}$ such that $N \gtrsim kR$, we seek approximations $\widetilde{F}_q \in \mathcal{V}_N^{\boldsymbol{c}}$ and $\widetilde{B}_q \in \mathcal{V}_\Omega$ of the far field operator F_q and of its non-observable part B_q satisfying the least squares problem

$$F_q|_{\Omega_c} \overset{\text{LS}}{=} \widetilde{F}_q + \widetilde{B}_q \qquad \text{in } \mathrm{HS}(L^2(S^{d-1}))\,. \tag{5.2}$$

As elaborated in Section 3.3, the condition number of (5.2) is given by the cosecant of the minimal angle between $\mathcal{V}_N^{\boldsymbol{c}}$ and $\mathcal{V}_\Omega$, which can be related to an uncertainty principle. This is given in the proposition below.

Proposition 5.6. *Suppose that $G \in \mathcal{V}_N^{\boldsymbol{c}}$ and $H \in \mathcal{V}_\Omega$ for some $\boldsymbol{c} \in \mathbb{R}^d$, $N \in \mathbb{N}$, and $\Omega \subseteq S^{d-1} \times S^{d-1}$. Then,*

$$\frac{|\langle G, H\rangle_{\mathrm{HS}}|}{\|G\|_{\mathrm{HS}}\|H\|_{\mathrm{HS}}} \leq \begin{cases} \frac{(2N+1)\sqrt{|\Omega|}}{2\pi} & \text{if } d = 2\,, \\ \frac{(N+1)^2\sqrt{|\Omega|}}{4\pi} & \text{if } d = 3\,. \end{cases}$$

Proof. For $d = 2$, using Hölder's inequality, (2.52) with $p = \infty$, (2.55) and the Cauchy-Schwarz inequality yields

$$\begin{aligned} |\langle G, H\rangle_{\mathrm{HS}}| &= |\langle G, H\rangle_{L^2}| \leq \|G\|_{L^\infty}\|H\|_{L^1} = \|\mathcal{T}_{\boldsymbol{c}} G\|_{L^\infty}\|H\|_{L^1} \leq \frac{1}{2\pi}\|\mathcal{T}_{\boldsymbol{c}} G\|_{\ell^1\times\ell^1}\|H\|_{L^1} \\ &\leq \frac{\sqrt{\|\mathcal{T}_{\boldsymbol{c}} G\|_{\ell^0\times\ell^0}\|H\|_{L^0}}}{2\pi}\|\mathcal{T}_{\boldsymbol{c}} G\|_{\ell^2\times\ell^2}\|H\|_{L^2} \leq \frac{(2N+1)\sqrt{|\Omega|}}{2\pi}\|G\|_{\mathrm{HS}}\|H\|_{\mathrm{HS}}\,. \end{aligned}$$

For the last estimate we used that $\|\mathcal{T}_{\boldsymbol{c}} G\|_{\ell^0\times\ell^0} \leq (2N+1)^2$ according to Remark 2.10 (iii).

For $d = 3$, we set $W := \operatorname{supp}_{\ell^0\times\ell^0}(\mathcal{T}_{\boldsymbol{c}} G) \subseteq [0, N]^2$ (cf. Remark 2.18 (ii)). Then, the same calculations but replacing (2.55) by (2.62) lead to

$$\begin{aligned} |\langle G, H\rangle_{\mathrm{HS}}| &\leq \frac{1}{4\pi}\|\mathcal{T}_{\boldsymbol{c}} G\|_{\ell^1_{\sqrt{2n+1}}\times\ell^1_{\sqrt{2n+1}}}\|H\|_{L^1} \leq \frac{\sqrt{|\Omega|}}{4\pi}\Big(\sum_{(m,n)\in W}(2m+1)(2n+1)\Big)^{\frac{1}{2}}\|G\|_{\mathrm{HS}}\|H\|_{\mathrm{HS}} \\ &\leq \frac{\sqrt{|\Omega|}}{4\pi}\sum_{n=0}^{N}(2n+1)\|G\|_{\mathrm{HS}}\|H\|_{\mathrm{HS}} = \frac{(N+1)^2\sqrt{|\Omega|}}{4\pi}\|G\|_{\mathrm{HS}}\|H\|_{\mathrm{HS}}\,. \end{aligned}$$

Here, the last equality follows due to (2.38). □

In the following theorem, $F_q^\delta|_{\Omega^c}$ denotes a noisy version of a restricted far field operator $F_q|_{\Omega^c}$, which cannot be observed on $\Omega \subseteq S^{d-1} \times S^{d-1}$. This means, that $F_q^\delta|_{\Omega^c} = (I - \mathcal{P}_{\mathcal{V}_\Omega})F_q^\delta$ for some noisy version F_q^δ of F_q. We assume that a priori information on the approximate location and size of the scatterer is available, i.e., that the ball $B_R(\boldsymbol{c})$ is known, and we establish a stability estimate for the least squares problem (5.2) for $N \in \mathbb{N}$ such that $N \gtrsim kR$. This can be concluded from Theorem 3.13 together with Proposition 5.6.

Theorem 5.7. *Suppose that* $F_q, F_q^\delta \in \mathrm{HS}(L^2(S^{d-1}))$, $\Omega \subseteq S^{d-1} \times S^{d-1}$, $N \in \mathbb{N}$ *with* $N \gtrsim kR$ *and* $\boldsymbol{c} \in \mathbb{R}^d$ *such that* $C < 1$, *where*

$$C := \begin{cases} \frac{(2N+1)\sqrt{|\Omega|}}{2\pi} & \text{if } d = 2\,, \\ \frac{(N+1)^2\sqrt{|\Omega|}}{4\pi} & \text{if } d = 3\,. \end{cases}$$

Set $F_q^\delta|_{\Omega^c} := (I - \mathcal{P}_{\mathcal{V}_\Omega})F_q^\delta$ *and denote by* $\widetilde{F}_q$ *and* $\widetilde{F}_q^\delta$ *the solutions to the least squares problems*

$$F_q|_{\Omega^c} \overset{\mathrm{LS}}{=} \widetilde{F}_q + \widetilde{B}_q\,, \qquad \widetilde{F}_q \in \mathcal{V}_N^{\boldsymbol{c}}\,,\ \widetilde{B}_q \in \mathcal{V}_\Omega\,, \tag{5.3a}$$

$$F_q^\delta|_{\Omega^c} \overset{\mathrm{LS}}{=} \widetilde{F}_q^\delta + \widetilde{B}_q^\delta\,, \qquad \widetilde{F}_q^\delta \in \mathcal{V}_N^{\boldsymbol{c}}\,,\ \widetilde{B}_q^\delta \in \mathcal{V}_\Omega\,, \tag{5.3b}$$

respectively. Then,

$$\|\widetilde{F}_q^\delta - \widetilde{F}_q\|_{\mathrm{HS}}^2 \le (1 - C^2)^{-1}\|F_q^\delta|_{\Omega^c} - F_q|_{\Omega^c}\|_{\mathrm{HS}}^2\,, \tag{5.4a}$$

$$\|\widetilde{B}_q^\delta - \widetilde{B}_q\|_{\mathrm{HS}}^2 \le (1 - C^2)^{-1}\|F_q^\delta|_{\Omega^c} - F_q|_{\Omega^c}\|_{\mathrm{HS}}^2\,. \tag{5.4b}$$

5.1.2. Completion by solving an $\ell^1 \times \ell^1$ minimization problem

If a priori knowledge of the size R of the scatterer is not available, but at least its approximate position $\boldsymbol{c}$ is known, we can as before replace the least squares problem (5.2) by an associated *(weighted)* $\ell^1 \times \ell^1$ *minimization problem.* Let

$$F_q|_{\Omega^c} \approx \widetilde{F}_q^0 + \widetilde{B}_q^0$$

be an approximate decomposition of the exact restricted far field operator with $\widetilde{F}_q^0 \in \mathcal{V}_N^{\boldsymbol{c}}$ and $\widetilde{B}_q^0 \in \mathcal{V}_\Omega$, e.g., obtained by solving the least squares problem (5.2). Furthermore, let $F_q^\delta|_{\Omega^c}$ denote a noisy version of the restricted far field operator and define the objective function by

$$\Psi : (\mathrm{HS}(L^2(S^{d-1})))^2 \to [0,\infty)\,,\ \Psi(\widetilde{F}_q, \widetilde{B}_q) := \begin{cases} \|\mathcal{T}_{\boldsymbol{c}}\widetilde{F}_q\|_{\ell^1 \times \ell^1} & \text{if } d = 2\,, \\ \|\mathcal{T}_{\boldsymbol{c}}\widetilde{F}_q\|_{\ell^1_{\sqrt{2n+1}} \times \ell^1_{\sqrt{2n+1}}} & \text{if } d = 3\,. \end{cases} \tag{5.5}$$

Theorem 5.8. *Suppose that* $F_q \in \mathrm{HS}(L^2(S^{d-1}))$, $\Omega \subseteq S^{d-1} \times S^{d-1}$, $N \in \mathbb{N}$ *with* $N \gtrsim kR$ *and* $\boldsymbol{c} \in \mathbb{R}^d$ *such that* $C < 1$, *where*

$$C := \begin{cases} \frac{(2N+1)|\Omega|}{\pi^2} & \text{if } d = 2\,, \\ \frac{(N+1)^4|\Omega|}{4\pi^2} & \text{if } d = 3\,. \end{cases}$$

We set $F_q|_{\Omega^c} := (I - \mathcal{P}_{\mathcal{V}_\Omega})F_q$, *and we assume that* $\widetilde{F}_q^0 \in \mathcal{V}_N^{\boldsymbol{c}}$ *and* $\widetilde{B}_q^0 \in \mathcal{V}_\Omega$ *are such that*

$$\|F_q|_{\Omega^c} - (\widetilde{F}_q^0 + \widetilde{B}_q^0)\|_{\mathrm{HS}} < \delta_0$$

for some $\delta_0 > 0$. *Moreover, suppose that* $F_q^\delta|_{\Omega^c} := (I - \mathcal{P}_{\mathcal{V}_\Omega})F_q^\delta$ *for some* $F_q^\delta \in \mathrm{HS}(L^2(S^{d-1}))$ *and* $\delta \ge 0$ *satisfies*

$$\delta \ge \delta_0 + \|F_q|_{\Omega^c} - F_q^\delta|_{\Omega^c}\|_{\mathrm{HS}}$$

and let $(\widetilde{F}_q^\delta, \widetilde{B}_q) \in \mathrm{HS}(L^2(S^{d-1}))^2$ *denote the solution to*

$$\underset{(\widetilde{F}_q, \widetilde{B}_q)}{\text{minimize}} \quad \Psi(\widetilde{F}_q, \widetilde{B}_q) \quad \text{subject to} \quad \|\widetilde{F}_q^\delta|_{\Omega^c} - (\widetilde{F}_q + \widetilde{B}_q)\|_{\mathrm{HS}} \le \delta \tag{5.6}$$

with Ψ *from* (5.5)*. Then,*

$$\|\widetilde{F}_q^0 - \widetilde{F}_q^\delta\|_{\mathrm{HS}}^2 \leq (1-C)^{-1} 4\delta^2 \qquad \textit{and} \qquad \|\widetilde{B}_q^0 - \widetilde{B}_q^\delta\|_{\mathrm{HS}}^2 \leq (1-C)^{-1} 4\delta^2 \,. \tag{5.7}$$

Proof. This proof is structured as the ones of Theorems 3.23 and 3.24. We set $\widetilde{F} := \widetilde{F}_q^0 - \widetilde{F}_q^\delta$ and $\widetilde{B} := \widetilde{B}_q^0 - \widetilde{B}_q^\delta$, and we denote the $\ell^0 \times \ell^0$-support of $\mathcal{T}_{\boldsymbol{c}} \widetilde{F}_q^0$ by W. As in the proof of Theorem 3.23, we can show for $d = 2$ (cf. (3.32))

$$\|\mathcal{T}_{\boldsymbol{c}} \widetilde{F}\|_{\ell^1 \times \ell^1} \leq 2 \|\mathcal{T}_{\boldsymbol{c}} \widetilde{F}\|_{\ell^1 \times \ell^1(W)}$$

and for $d = 3$ (cf. (3.36))

$$\|\mathcal{T}_{\boldsymbol{c}} \widetilde{F}\|_{\ell^1_{\sqrt{2n+1}} \times \ell^1_{\sqrt{2n+1}}} \leq 2 \|\mathcal{T}_{\boldsymbol{c}} \widetilde{F}\|_{\ell^1_{\sqrt{2n+1}} \times \ell^1_{\sqrt{2n+1}}(W)} \,.$$

Proceeding as in the proof of the same theorem, further yields

$$4\delta^2 \geq \|\widetilde{F}\|_{\mathrm{HS}}^2 + \|\widetilde{B}\|_{\mathrm{HS}}^2 - 2|\langle \widetilde{F}, \widetilde{B} \rangle_{\mathrm{HS}}| = \|\widetilde{F}\|_{\mathrm{HS}}^2 + \|\widetilde{B}\|_{\mathrm{HS}}^2 - 2|\langle \mathcal{T}_{\boldsymbol{c}} \widetilde{F}, \mathcal{T}_{\boldsymbol{c}} \widetilde{B} \rangle_{\mathrm{HS}}| \,.$$

For $d = 2$, we conclude with Hölder's inequality, (2.52) and the mapping property (2.55) that

$$\begin{aligned}
4\delta^2 &\geq \|\widetilde{F}\|_{\mathrm{HS}}^2 + \|\widetilde{B}\|_{\mathrm{HS}}^2 - 2\|\mathcal{T}_{\boldsymbol{c}} \widetilde{F}\|_{L^\infty} \|\mathcal{T}_{\boldsymbol{c}} \widetilde{B}\|_{L^1} \geq \|\widetilde{F}\|_{\mathrm{HS}}^2 + \|\widetilde{B}\|_{\mathrm{HS}}^2 - \frac{1}{\pi} \|\mathcal{T}_{\boldsymbol{c}} \widetilde{F}\|_{\ell^1 \times \ell^1} \|\widetilde{B}\|_{L^1} \\
&\geq \|\widetilde{F}\|_{\mathrm{HS}}^2 + \|\widetilde{B}\|_{\mathrm{HS}}^2 - \frac{2}{\pi} \|\mathcal{T}_{\boldsymbol{c}} \widetilde{F}\|_{\ell^1 \times \ell^1(W)} \|\widetilde{B}\|_{L^1} \geq \|\widetilde{F}\|_{\mathrm{HS}}^2 + \|\widetilde{B}\|_{\mathrm{HS}}^2 - \frac{2}{\pi} \sqrt{|W||\Omega|} \|\widetilde{F}\|_{\mathrm{HS}} \|\widetilde{B}\|_{\mathrm{HS}} \\
&\geq (1-C) \|\widetilde{F}\|_{\mathrm{HS}}^2 + \left(\|\widetilde{B}\|_{\mathrm{HS}} - \frac{1}{\pi} \sqrt{|W||\Omega|} \|\widetilde{F}\|_{\mathrm{HS}} \right)^2 .
\end{aligned}$$

For $d = 3$, we obtain with the same calculations due to Hölder's inequality, (2.59) and (2.62) that

$$\begin{aligned}
4\delta^2 &\geq \|\widetilde{F}\|_{\mathrm{HS}}^2 + \|\widetilde{B}\|_{\mathrm{HS}}^2 - 2\|\mathcal{T}_{\boldsymbol{c}} \widetilde{F}\|_{L^\infty} \|\mathcal{T}_{\boldsymbol{c}} \widetilde{B}\|_{L^1} \geq \|\widetilde{F}\|_{\mathrm{HS}}^2 + \|\widetilde{B}\|_{\mathrm{HS}}^2 - \frac{1}{2\pi} \|\mathcal{T}_{\boldsymbol{c}} \widetilde{F}\|_{\ell^1_{\sqrt{2n+1}} \times \ell^1_{\sqrt{2n+1}}} \|\widetilde{B}\|_{L^1} \\
&\geq \|\widetilde{F}\|_{\mathrm{HS}}^2 + \|\widetilde{B}\|_{\mathrm{HS}}^2 - \frac{1}{\pi} \|\mathcal{T}_{\boldsymbol{c}} \widetilde{F}\|_{\ell^1_{\sqrt{2n+1}} \times \ell^1_{\sqrt{2n+1}}(W)} \|\widetilde{B}\|_{L^1} \\
&\geq \|\widetilde{F}\|_{\mathrm{HS}}^2 + \|\widetilde{B}\|_{\mathrm{HS}}^2 - \frac{1}{\pi} \Bigg(\sum_{(m,n) \in W} (2m+1)(2n+1) \Bigg)^{\frac{1}{2}} \sqrt{|\Omega|} \|\widetilde{F}\|_{\mathrm{HS}} \|\widetilde{B}\|_{\mathrm{HS}} \\
&\geq \|\widetilde{F}\|_{\mathrm{HS}}^2 + \|\widetilde{B}\|_{\mathrm{HS}}^2 - \frac{1}{\pi} \sum_{n=0}^{N} (2n+1) \sqrt{|\Omega|} \|\widetilde{F}\|_{\mathrm{HS}} \|\widetilde{B}\|_{\mathrm{HS}} \\
&= \|\widetilde{F}\|_{\mathrm{HS}}^2 + \|\widetilde{B}\|_{\mathrm{HS}}^2 - \frac{1}{\pi} (N+1)^2 \sqrt{|\Omega|} \|\widetilde{F}\|_{\mathrm{HS}} \|\widetilde{B}\|_{\mathrm{HS}} \\
&\geq (1-C) \|\widetilde{F}\|_{\mathrm{HS}}^2 + \left(\|\widetilde{B}\|_{\mathrm{HS}} - \frac{1}{2\pi} (N+1)^2 \sqrt{|\Omega|} \|\widetilde{F}\|_{\mathrm{HS}} \right)^2 ,
\end{aligned}$$

where we used (2.38) in the last equality. In both cases, dropping the second summand yields the first inequality and interchanging the roles of $\widetilde{F}$ and $\widetilde{B}$ in the last estimate the second inequality. □

In the following remark, we collect some observations related to the question of how the low rank property of F_q can be utilized to solve the far field operator completion problem.

Remark 5.9. It is ongoing research to adapt techniques from the proofs in Subsection 3.4.2 for developing an uncertainty principle that involves $\mathcal{W}_N^{\mathfrak{c}}$ and $\mathcal{V}_\Omega$ or equivalently for bounding $\|\mathcal{P}_{\mathcal{W}_N^{\mathfrak{c}}} \mathcal{P}_{\mathcal{V}_\Omega}\|$. In particular, this would be necessary to investigate the stability of an associated (coupled or non-coupled) nuclear norm minimization problem in the manner of the previous stability theorems. In this remark, some approaches are collected to derive such an uncertainty principle, and it is

explained why they are not appropriate.

Suppose $G \in \mathcal{W}_N^{\boldsymbol{c}}$ and $H \in \mathcal{V}_\Omega$. On the one hand, we can estimate that

$$|\langle G, H\rangle_{\mathrm{HS}}| \;\le\; \|G\|_{\mathrm{nuc}}\|H\| \;\le\; \sqrt{\operatorname{rank} G}\|G\|_{\mathrm{HS}}\|H\|\,,$$

where $\operatorname{rank} G \le 2N+1$ for $d=2$ and $\operatorname{rank} G \le (N+1)^2$ for $d=3$ (see Lemma 3.26 and Remarks 2.10 (iii) and 2.18 (v)). However, it is not clear how to bound $\|H\|$ in terms of $\|H\|_{\mathrm{HS}}$ for generating a prefactor smaller than one. One the other hand, Lemmas 2.24 (d) and 2.25 (d) suggest to start estimating

$$|\langle G, H\rangle_{\mathrm{HS}}| \;\le\; \|G\|_{L^\infty}\|H\|_{L^1} \;\le\; \begin{cases} \frac{\sqrt{|\Omega|}}{2\pi}\|\mathcal{T}_{\boldsymbol{c}}G\|_{\ell^1\times\ell^1}\|H\|_{\mathrm{HS}} & \text{if } d=2\,,\\ \frac{\sqrt{|\Omega|}}{4\pi}\|\mathcal{T}_{\boldsymbol{c}}G\|_{\ell^1_{\sqrt{2n+1}}\times\ell^1_{\sqrt{2n+1}}}\|H\|_{\mathrm{HS}} & \text{if } d=3\,. \end{cases}$$

Unfortunately, this produces, compared with the proofs of Propositions 3.27 or 3.28, two additional sums over infinite dimensional index sets, which cannot be controlled. The most promising attempt is the following. For simplicity we consider $d=2$ but the same can be done for $d=3$. Given a singular system $(\sigma_n; u_n, v_n)_{1\le n\le \operatorname{rank} G}$ for G, we can expand u_n and v_n in terms of $(T_{-\boldsymbol{c}}\boldsymbol{e}_m)_m$ and $(T_{-\boldsymbol{c}}\boldsymbol{e}_l)_l$ and compare the resulting formula with (2.24) to conclude that

$$u_n(\widehat{\boldsymbol{x}})\overline{v_n(\boldsymbol{\theta})} \;=\; \sum_{|m|\le N}\sum_{l\in\mathbb{Z}} \lambda^n_{m,l} T_{-\boldsymbol{c}}\boldsymbol{e}_m(\widehat{\boldsymbol{x}})\overline{T_{-\boldsymbol{c}}\boldsymbol{e}_l(\boldsymbol{\theta})} + \sum_{|m|>N}\sum_{|l|\le N} \lambda^n_{m,l} T_{-\boldsymbol{c}}\boldsymbol{e}_m(\widehat{\boldsymbol{x}})\overline{T_{-\boldsymbol{c}}\boldsymbol{e}_l(\boldsymbol{\theta})}$$

for some coefficients $\lambda^n_{m,l} \in \mathbb{C}$. Again according to Lemma 2.24 (d) this yields

$$|\langle G, H\rangle_{\mathrm{HS}}| \;\le\; \|G\|_{L^\infty}\|H\|_{L^1} \;\le\; \frac{\sqrt{|\Omega|}}{2\pi}\sum_{n=1}^{\operatorname{rank} G}\|(\lambda^n_{m,l})_{m,l}\|_{\ell^1\times\ell^1}\|H\|_{\mathrm{HS}}\,.$$

By Parseval's identity we have that

$$\|(\lambda^n_{m,l})_{m,l}\|_{\ell^2\times\ell^2} \;=\; \|u_n\|_{L^2(S^1)}\|v_n\|_{L^2(S^1)} \;=\; 1 \quad \text{for } 1\le n\le \operatorname{rank} G\,,$$

but, unfortunately, it is not clear how to use this for bounding the factor $\sum_{n=1}^{\operatorname{rank} G}\|(\lambda^n_{m,l})_{m,l}\|_{\ell^1\times\ell^1}$ in terms of $\|G\|_{\mathrm{HS}}$. All in all, the problem lies in the combination of G being only expandable as finite sum along one dimension and of the additional sums that come into play when not starting with

$$|\langle G, H\rangle_{\mathrm{HS}}| \le \|\mathcal{T}_{\boldsymbol{c}}G\|_{\ell^\infty\times\ell^\infty}\|\mathcal{T}_{\boldsymbol{c}}H\|_{\ell^1\times\ell^1}\,,$$

which is not appropriate in this situation, since we know nothing about the support of the Fourier coefficients ($d=2$) or of the spherical harmonics components ($d=3$) of H. ◊

So far we have not yet been able to develop a stability theory for a nuclear norm minimization problem for far field operator completion. However, we have investigated another third scheme, which we describe in the next subsection.

5.1.3. Completion by solving a coupled L^1 and $\ell^1\times\ell^1$ minimization problem

If in addition to the unknown size R of the scatterer the non-observable set Ω is unknown as well, we can adapt Theorem 5.8 in the sense that we add a penalty term to the objective function that prevents the L^0-support of $\widetilde{B}^\delta_q$ from becoming too large. Doing so, we follow [55, Cor. 6.4] and

define for some coupling parameter $\lambda > 0$

$$\Psi_\lambda : \mathrm{HS}(L^2(S^{d-1}))^2 \to [0,\infty)\,,\ \Psi_\lambda(\widetilde{F}_q,\widetilde{B}_q) := \begin{cases} \frac{1}{\lambda}\|\mathcal{T}_{\boldsymbol{c}}\widetilde{F}_q\|_{\ell^1\times\ell^1} + \lambda\|\widetilde{B}_q\|_{L^1} & \text{if } d=2\,,\\ \frac{1}{\lambda}\|\mathcal{T}_{\boldsymbol{c}}\widetilde{F}_q\|_{\ell^1_{\sqrt{2n+1}}\times\ell^1_{\sqrt{2n+1}}} + \lambda\|\widetilde{B}_q\|_{L^1} & \text{if } d=3\,. \end{cases} \tag{5.8}$$

Corollary 5.10. *Suppose that $F_q \in \mathrm{HS}(L^2(S^{d-1}))$, $\Omega \subseteq S^{d-1}\times S^{d-1}$, $N\in\mathbb{N}$ with $N \gtrsim kR$ and $\boldsymbol{c}\in\mathbb{R}^d$ such that it holds $C_\lambda, C_{\lambda,\Omega} < 1$, where*

$$C_\lambda := \begin{cases} \frac{2(2N+1)^2}{\pi\lambda^2} & \text{if } d=2\,,\\ \frac{(N+1)^4}{\pi\lambda^2} & \text{if } d=3\,, \end{cases} \qquad \text{and} \qquad C_{\lambda,\Omega} := \begin{cases} \frac{2\lambda^2|\Omega|}{\pi} & \text{if } d=2\,,\\ \frac{\lambda^2|\Omega|}{\pi} & \text{if } d=3\,. \end{cases}$$

We set $F_q|_{\Omega^c} := (I-\mathcal{P}_{\mathcal{V}_\Omega})F_q$, and we assume that $\widetilde{F}_q^0 \in \mathcal{V}_N^{\boldsymbol{c}}$ and $\widetilde{B}_q^0 \in \mathcal{V}_\Omega$ are such that

$$\|F_q|_{\Omega^c} - (\widetilde{F}_q^0 + \widetilde{B}_q^0)\|_{\mathrm{HS}} < \delta_0$$

for some $\delta_0 \geq 0$. Moreover, suppose that $F_q^\delta|_{\Omega^c} := (I-\mathcal{P}_{\mathcal{V}_\Omega})F_q^\delta$ for some $F_q^\delta \in \mathrm{HS}(L^2(S^{d-1}))$ and $\delta\geq 0$ satisfy

$$\delta \geq \delta_0 + \|F_q|_{\Omega^c} - F_q^\delta|_{\Omega^c}\|_{\mathrm{HS}}$$

and let $(\widetilde{F}_q^\delta,\widetilde{B}_q) \in \mathrm{HS}(L^2(S^{d-1}))^2$ denote the solution to

$$\underset{(\widetilde{F}_q,\widetilde{B}_q)}{\text{minimize}} \quad \Psi_\lambda(\widetilde{F}_q,\widetilde{B}_q) \quad \text{subject to} \quad \|F_q^\delta|_{\Omega^c} - (\widetilde{F}_q+\widetilde{B}_q)\|_{\mathrm{HS}} \leq \delta \tag{5.9}$$

with Ψ_λ from (5.8). Then,

$$\|\widetilde{F}_q^0 - \widetilde{F}_q^\delta\|_{\mathrm{HS}}^2 \leq (1-C_\lambda)^{-1}4\delta^2 \qquad \text{and} \qquad \|\widetilde{B}_q^0 - \widetilde{B}_q^\delta\|_{\mathrm{HS}}^2 \leq (1-C_{\lambda,\Omega})^{-1}4\delta^2\,. \tag{5.10}$$

Proof. As before we set $\widetilde{F} := \widetilde{F}_q^0 - \widetilde{F}_q^\delta$ and $\widetilde{B} := \widetilde{B}_q^0 - \widetilde{B}_q^\delta$. For the case $d=2$ we obtain similar to the derivation of (3.32)

$$\Psi_\lambda(\widetilde{F},\widetilde{B}) \leq 2\left(\frac{1}{\lambda}\|\widetilde{F}\|_{\ell^1\times\ell^1(W)} + \lambda\|\widetilde{B}\|_{L^1(\Omega)}\right). \tag{5.11}$$

Proceeding as in the proof of Theorem 5.8 yields the result since using (2.55), $4ab \leq (a+b)^2$ for $a,b\geq 0$ and (5.11) we can bound

$$\begin{aligned} 2|\langle\mathcal{T}_{\boldsymbol{c}}\widetilde{F},\mathcal{T}_{\boldsymbol{c}}\widetilde{B}\rangle_{\mathrm{HS}}| &\leq 2\|\mathcal{T}_{\boldsymbol{c}}\widetilde{F}\|_{L^\infty}\|\mathcal{T}_{\boldsymbol{c}}\widetilde{B}\|_{L^1} \leq \frac{1}{\pi}\|\mathcal{T}_{\boldsymbol{c}}\widetilde{F}\|_{\ell^1\times\ell^1}\|\widetilde{B}\|_{L^1} = \frac{1}{\pi}\frac{1}{\lambda}\|\mathcal{T}_{\boldsymbol{c}}\widetilde{F}\|_{\ell^1\times\ell^1}\lambda\|\widetilde{B}\|_{L^1}\\ &\leq \frac{1}{4\pi}\left(\frac{1}{\lambda}\|\mathcal{T}_{\boldsymbol{c}}\widetilde{F}\|_{\ell^1\times\ell^1} + \lambda\|\widetilde{B}\|_{L^1}\right)^2 = \frac{1}{4\pi}\Psi_\lambda^2(\widetilde{F},\widetilde{B})\\ &\leq \frac{1}{\pi}\left(\frac{1}{\lambda}\|\mathcal{T}_{\boldsymbol{c}}\widetilde{F}\|_{\ell^1\times\ell^1(W)} + \lambda\|\widetilde{B}\|_{L^1(\Omega)}\right)^2\\ &\leq \frac{1}{\pi}\left(\frac{\sqrt{|W|}}{\lambda}\|\mathcal{T}_{\boldsymbol{c}}\widetilde{F}\|_{\mathrm{HS}} + \lambda\sqrt{|\Omega|}\|\widetilde{B}\|_{\mathrm{HS}}\right)^2\\ &\leq \frac{2}{\pi}\left(\frac{|W|}{\lambda^2}\|\mathcal{T}_{\boldsymbol{c}}\widetilde{F}\|_{\mathrm{HS}}^2 + \lambda^2|\Omega|\|\widetilde{B}\|_{\mathrm{HS}}^2\right). \end{aligned}$$

Here, for last step we used the second bound in Lemma 3.22. The case $d=3$ follows immediately by adapting the corresponding mapping properties of the translation operator. □

Remark 5.11. As explained in [55] the coupling parameter λ balances how good or bad the approxi-

mation quality of $\widetilde{F}_q^\delta$ and $\widetilde{B}_q^\delta$ should be at the cost of the other.

Furthermore, it can be increased for compensating a large N and decreased for compensating a large $|\Omega|$, provided the other of these two quantities is comparable small at the same time, respectively.

A symmetric choice that ensures $C_\lambda = C_{\lambda,\Omega}$ is given by

$$\lambda^2 = \frac{2N+1}{\sqrt{|\Omega|}} \text{ for } d=2 \qquad \text{and} \qquad \lambda^2 = \frac{(N+1)^2}{\sqrt{|\Omega|}} \text{ for } d=3\,.$$

◊

5.2. Splitting and completion

In this section we solve the **far field operator splitting and completion** problem simultaneously, i.e., we aim to recover the far field operator F_q or the far field operators F_{q_1} and F_{q_2} corresponding to the two components of the scatterer from the observable far field operator $F_q|_{\Omega^c}$. For this purpose, we combine the results from Section 5.1 with those of Chapter 3, and we suppose that Assumptions 3.1, 5.1 and 5.3 are fulfilled. We directly restrict ourselves to the framework of Section 3.5, and we recap the second order Born series expansion of F_q, cf. (3.66), which was the core equation of Section 3.5, namely

$$F_q^{(\leq 2)} = F_{q_1}^{(\leq 2)} + F_{q_2}^{(\leq 2)} + \left(F_{q_1,q_2}^{(2)} + F_{q_2,q_1}^{(2)}\right).$$

We further recap that for $l \neq j$ the component $F_{q_j}^{(\leq 2)}$ can be well approximated in $\mathcal{V}_{N_j}^{\boldsymbol{c}_j}$, while the component $F_{q_j,q_l}^{(2)}$ can be well approximated in $\mathcal{V}_{N_j,N_l}^{\boldsymbol{c}_j,\boldsymbol{c}_l}$. By writing $F_q^{(\leq 2)}|_{\Omega^c} := (I - \mathcal{P}_{\mathcal{V}_\Omega})F_q^{(\leq 2)}$ and $B_q^{(\leq 2)} := F_q^{(\leq 2)}|_{\Omega^c} - F_q^{(\leq 2)}$ the expansion above reads

$$F_q^{(\leq 2)}|_{\Omega^c} = F_{q_1}^{(\leq 2)} + F_{q_2}^{(\leq 2)} + \left(F_{q_1,q_2}^{(2)} + F_{q_2,q_1}^{(2)}\right) + B_q^{(\leq 2)}\,, \tag{5.12}$$

where $B_q^{(\leq 2)} \in \mathcal{V}_\Omega$.

Example 5.12. We extend the far field operator split from Example 5.5 for illustrating the far field operator splitting and completion problem. Here, we directly assume Ω to be symmetric in the sense of reciprocity. By setting $\boldsymbol{D} := \boldsymbol{F}_q - (\boldsymbol{F}_{q_1} + \boldsymbol{F}_{q_2})$, which is the component that models multiple scattering effects involving both scatterer's components (cf. Example 3.2), we have that

$$\boldsymbol{F}_q|_{\Omega^c} = \boldsymbol{F}_{q_1} + \boldsymbol{F}_{q_2} + \boldsymbol{D} + \boldsymbol{B}_q\,.$$

The discretized far field operators components in this equation are shown in Figure 5.3. ◊

5.2.1. Splitting and completion by solving a least squares problem

The following proposition gives an uncertainty principle involving a generalized subspace $\mathcal{V}_{M,N}^{\boldsymbol{b},\boldsymbol{c}}$ and the subspace $\mathcal{V}_\Omega$.

Proposition 5.13. *Suppose that $G \in \mathcal{V}_{M,N}^{\boldsymbol{b},\boldsymbol{c}}$ and $H \in \mathcal{V}_\Omega$ for some $\boldsymbol{b},\boldsymbol{c} \in \mathbb{R}^d$, $M,N \in \mathbb{N}$, and $\Omega \subseteq S^{d-1} \times S^{d-1}$. Then,*

$$\frac{|\langle G,H\rangle_{\mathrm{HS}}|}{\|G\|_{\mathrm{HS}}\|H\|_{\mathrm{HS}}} \leq \begin{cases} \frac{\sqrt{(2M+1)(2N+1)|\Omega|}}{2\pi} & \text{if } d=2\,, \\ \frac{(M+1)(N+1)\sqrt{|\Omega|}}{4\pi} & \text{if } d=3\,. \end{cases}$$

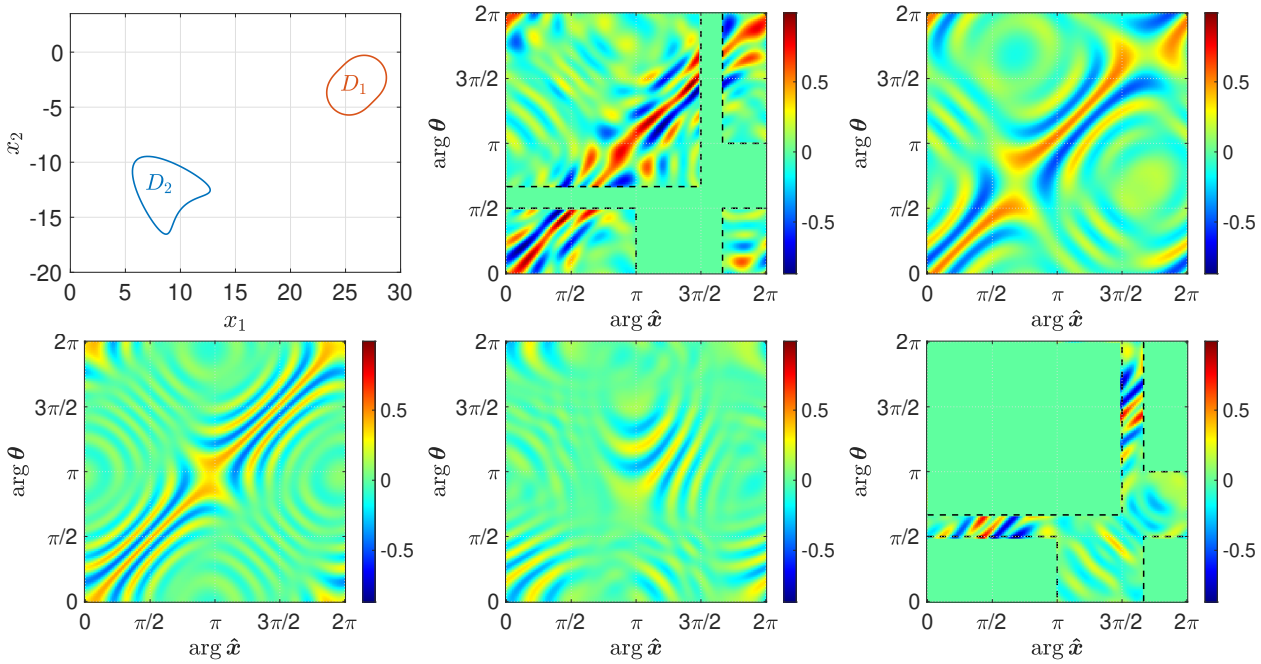

FIGURE 5.3. Top left: Supports of the scatterer's components. Real parts of discretized observable far field operator $\boldsymbol{F}_q|_{\Omega^c}$ (top middle), of discretized far field operator components $\boldsymbol{F}_{q_1}$ (top right) and $\boldsymbol{F}_{q_2}$ (bottom left), of difference $\boldsymbol{D} = \boldsymbol{F}_q - (\boldsymbol{F}_{q_1} + \boldsymbol{F}_{q_2})$ and of discretized non-observable far field operator $\boldsymbol{B}_q$

Proof. We proceed as in the proof of Proposition 5.6 and obtain for $d = 2$

$$|\langle G, H\rangle_{\mathrm{HS}}| \leq \frac{\sqrt{\|\mathcal{T}_{\boldsymbol{b},\boldsymbol{c}}G\|_{\ell^0\times\ell^0}\|H\|_{L^0}}}{2\pi}\|\mathcal{T}_{\boldsymbol{b},\boldsymbol{c}}G\|_{\ell^2\times\ell^2}\|H\|_{L^2} \leq \frac{\sqrt{(2M+1)(2N+1)|\Omega|}}{2\pi}\|G\|_{\mathrm{HS}}\|H\|_{\mathrm{HS}}\,.$$

For $d = 3$, we set $W := \|\mathcal{T}_{\boldsymbol{c}}G\|_{\ell^0\times\ell^0}$ and conclude

$$\begin{aligned}|\langle G, H\rangle_{\mathrm{HS}}| &\leq \frac{1}{4\pi}\|\mathcal{T}_{\boldsymbol{c}}G\|_{\ell^1_{\sqrt{2n+1}}\times\ell^1_{\sqrt{2n+1}}}\|H\|_{L^1} \leq \frac{\sqrt{|\Omega|}}{4\pi}\Big(\sum_{(m,n)\in W}(2m+1)(2n+1)\Big)^{\frac{1}{2}}\|G\|_{\mathrm{HS}}\|H\|_{\mathrm{HS}}\\ &\leq \frac{\sqrt{|\Omega|}}{4\pi}\Big(\sum_{m=0}^{M}(2m+1)\sum_{n=0}^{N}(2n+1)\Big)^{\frac{1}{2}}\|G\|_{\mathrm{HS}}\|H\|_{\mathrm{HS}}\\ &= \frac{(M+1)(N+1)\sqrt{|\Omega|}}{4\pi}\|G\|_{\mathrm{HS}}\|H\|_{\mathrm{HS}}\,.\end{aligned}$$

□

Based on representation (5.12) we modify Theorem 5.7 in the sense that we no longer search an approximation of F_q in $\mathcal{V}_N^{\boldsymbol{c}}$, but in the subspace $\mathcal{V}_{N_1}^{\boldsymbol{c}_1} + \mathcal{V}_{N_2}^{\boldsymbol{c}_2} + \mathcal{V}_{N_1,N_2}^{\boldsymbol{c}_1,\boldsymbol{c}_2} + \mathcal{V}_{N_2,N_1}^{\boldsymbol{c}_2,\boldsymbol{c}_1}$.

The following can be deduced from Theorem 3.15 by making the choice $J = 5$ with

$$\mathcal{V}_1 = \mathcal{V}_{N_1}^{\boldsymbol{c}_1}\,,\ \mathcal{V}_2 = \mathcal{V}_{N_2}^{\boldsymbol{c}_2}\,,\ \mathcal{V}_3 = \mathcal{V}_{N_1,N_2}^{\boldsymbol{c}_1,\boldsymbol{c}_2}\,,\ \mathcal{V}_4 = \mathcal{V}_{N_2,N_1}^{\boldsymbol{c}_2,\boldsymbol{c}_1} \text{ and } \mathcal{V}_5 = \mathcal{V}_\Omega\,.$$

Here, we use the related uncertainty principles from Propositions 3.37, 3.38 and 5.13.

Theorem 5.14. *Suppose* $F_q, F_q^\delta \in \mathrm{HS}(L^2(S^{d-1}))$, $\boldsymbol{c}_1, \boldsymbol{c}_2 \in \mathbb{R}^d$, $N_1, N_2 \in \mathbb{N}$ *with* $N_1 \gtrsim kR_1$

and $N_2 \gtrsim kR_2$ *and* $\Omega \subseteq S^{d-1} \times S^{d-1}$. *We define*

$$C := \begin{cases} \frac{(2N_1+1)(2N_2+1)}{(k|\boldsymbol{c}_1-\boldsymbol{c}_2|)^{\frac{2}{3}}} & \text{if } d=2\,, \\ \frac{16}{9}\frac{\prod_{i=1}^{3}(N_1+\frac{i}{2})(N_2+\frac{i}{2})}{(k|\boldsymbol{c}_1-\boldsymbol{c}_2|)^{\frac{5}{3}}} & \text{if } d=3\,, \end{cases} \quad \text{and} \quad C_{j,l} := \begin{cases} \frac{\sqrt{(2N_j+1)(2N_l+1)|\Omega|}}{2\pi} & \text{if } d=2\,, \\ \frac{(N_j+1)(N_l+1)\sqrt{|\Omega|}}{4\pi} & \text{if } d=3\,, \end{cases}$$

where $(j,l) \in \{1,2\}^2$. *We assume that, for all* $(j,l) \in \{1,2\}^2$,

$$M_{j,l} := \sqrt{C}\Big(\sqrt{C} + (2N_j+1) + (2N_l+1)\Big) + C_{j,l} < 1\,,$$
$$C_{1,1} + 2C_{1,2} + C_{2,2} < 1\,.$$

Denote by $\widetilde{F}_{q_1}, \widetilde{F}_{q_2}, \widetilde{F}_{q_1,q_2}, \widetilde{F}_{q_2,q_1}, \widetilde{B}_q$ *and* $\widetilde{F}^{\delta}_{q_1}, \widetilde{F}^{\delta}_{q_2}, \widetilde{F}^{\delta}_{q_1,q_2}, \widetilde{F}^{\delta}_{q_2,q_1}, \widetilde{B}^{\delta}_q$ *the solutions to the least squares problems*

$$F_q|_{\Omega^c} \overset{\text{LS}}{=} \widetilde{F}_{q_1} + \widetilde{F}_{q_2} + \widetilde{F}_{q_1,q_2} + \widetilde{F}_{q_2,q_1} + \widetilde{B}_q\,, \qquad \widetilde{F}_{q_j} \in \mathcal{V}^{\boldsymbol{c}_j}_{N_j}\,,\ \widetilde{F}_{q_j,q_l} \in \mathcal{V}^{\boldsymbol{c}_j,\boldsymbol{c}_l}_{N_j,N_l}\,,\ \widetilde{B}_q \in \mathcal{V}_\Omega\,, \tag{5.13a}$$

$$F^{\delta}_q|_{\Omega^c} \overset{\text{LS}}{=} \widetilde{F}^{\delta}_{q_1} + \widetilde{F}^{\delta}_{q_2} + \widetilde{F}^{\delta}_{q_1,q_2} + \widetilde{F}^{\delta}_{q_2,q_1} + \widetilde{B}^{\delta}_q\,, \qquad \widetilde{F}^{\delta}_{q_j} \in \mathcal{V}^{\boldsymbol{c}_j}_{N_j}\,,\ \widetilde{F}^{\delta}_{q_j,q_l} \in \mathcal{V}^{\boldsymbol{c}_j,\boldsymbol{c}_l}_{N_j,N_l}\,,\ \widetilde{B}^{\delta}_q \in \mathcal{V}_\Omega\,, \tag{5.13b}$$

respectively. Then,

$$\|\widetilde{F}_{q_j} - \widetilde{F}^{\delta}_{q_j}\|^2_{\text{HS}} \leq \big(1-(M_{j,j}+C_{j,j})\big)^{-1}\|F_q - F^{\delta}_q\|^2_{\text{HS}}\,, \qquad j=1,2\,, \tag{5.14a}$$

$$\|\widetilde{B}_q - \widetilde{B}^{\delta}_q\|^2_{\text{HS}} \leq \big(1-(C_{1,1}+2C_{1,2}+C_{2,2})\big)^{-1}\|F_q - F^{\delta}_q\|^2_{\text{HS}}\,. \tag{5.14b}$$

Remark 5.15. (i) Provided $k|\boldsymbol{c}_1 - \boldsymbol{c}_2| < 2(N_1+N_2+d/2)$ the stability estimate (5.14) can be improved by replacing $C<1$ by $\widetilde{C}<1$ with

$$\widetilde{C} := \begin{cases} \frac{(2N_1+1)(2N_2+1)}{k|\boldsymbol{c}_1-\boldsymbol{c}_2|} & \text{if } d=2\,, \\ \frac{16}{9}\frac{\prod_{i=1}^{3}(N_1+\frac{i}{2})(N_2+\frac{i}{2})}{(k|\boldsymbol{c}_1-\boldsymbol{c}_2|)^2} & \text{if } d=3\,. \end{cases}$$

(ii) Considering the same scattering object we always have that $N > N_1+N_2$ when comparing Theorems 5.7 and 3.39. For sufficiently large $|\boldsymbol{c}_1-\boldsymbol{c}_2|$ the stability constants in (5.14) become smaller than the one in (5.4). Consequently, for the scatterer's components being near to each other it makes sense to solve problem (5.3), whereas for them being far away from each other it makes sense to solve (5.13).

(iii) As described in Section 3.6.1, we can further improve the stability of problem (5.16) by taking the reciprocity relation into account, i.e. by replacing $\mathcal{V}^{\boldsymbol{c}_1}_{N_1}$, $\mathcal{V}^{\boldsymbol{c}_2}_{N_2}$ and $\mathcal{V}^{\boldsymbol{c}_1,\boldsymbol{c}_2}_{N_1,N_2} \oplus \mathcal{V}^{\boldsymbol{c}_2,\boldsymbol{c}_1}_{N_2,N_1}$ by $\widetilde{\mathcal{V}}^{\boldsymbol{c}_1}_{N_1}$, $\widetilde{\mathcal{V}}^{\boldsymbol{c}_2}_{N_2}$ and $\widetilde{\mathcal{V}}^{\boldsymbol{c}_1,\boldsymbol{c}_2}_{N_1,N_2}$. ◊

5.2.2. Splitting and completion by solving an $\ell^1 \times \ell^1$ minimization problem

Let

$$F_q|_{\Omega^c} \approx \widetilde{F}^0_{q_1} + \widetilde{F}^0_{q_2} + \widetilde{F}^0_{q_1,q_2} + \widetilde{F}^0_{q_2,q_1} + \widetilde{B}^0_q$$

be an approximate decomposition of the exact restricted far field operator with $\widetilde{F}^0_{q_j} \in \mathcal{V}^{\boldsymbol{c}_j}_{N_j}$ and $\widetilde{F}^0_{q_j,q_l} \in \mathcal{V}^{\boldsymbol{c}_j,\boldsymbol{c}_l}_{N_j,N_l}$ for $j \neq l$ and $\widetilde{B}^0_q \in \mathcal{V}_\Omega$, e.g., obtained by solving the least squares problem from Theorem 5.14. We slightly modify our objective function Ψ from (3.72) according

to $\Psi : \mathrm{HS}(L^2(S^{d-1}))^5 \to [0,\infty)$ by for $d = 2$

$$\Psi(\widetilde{F}_{q_1}, \widetilde{F}_{q_2}, \widetilde{F}_{q_1,q_2}, \widetilde{F}_{q_2,q_1}, \widetilde{B}_q) := \sum_{\substack{j,l=1 \\ j\neq l}}^{2} \left(\|\mathcal{T}_{\boldsymbol{c}_j} \widetilde{F}_{q_j}\|_{\ell^1\times\ell^1} + \|\mathcal{T}_{\boldsymbol{c}_j,\boldsymbol{c}_l} \widetilde{F}_{q_j,q_l}\|_{\ell^1\times\ell^1} \right) \tag{5.15a}$$

and for $d = 3$

$$\Psi(\widetilde{F}_{q_1}, \widetilde{F}_{q_2}, \widetilde{F}_{q_1,q_2}, \widetilde{F}_{q_2,q_1}, \widetilde{B}_q) := \sum_{\substack{j,l=1 \\ j\neq l}}^{2} \left(\|\mathcal{T}_{\boldsymbol{c}_j} \widetilde{F}_{q_j}\|_{\ell^1_{\sqrt{2n+1}}\times\ell^1_{\sqrt{2n+1}}} + \|\mathcal{T}_{\boldsymbol{c}_j,\boldsymbol{c}_l} \widetilde{F}_{q_j,q_l}\|_{\ell^1_{\sqrt{2n+1}}\times\ell^1_{\sqrt{2n+1}}} \right). \tag{5.15b}$$

Theorem 5.16. *Suppose that $F_q \in \mathrm{HS}(L^2(S^{d-1}))$, $\Omega \subseteq S^{d-1}\times S^{d-1}$, $N_1, N_2 \in \mathbb{N}$ with $N_1 \gtrsim kR_1$ and $N_2 \gtrsim kR_2$ and $\boldsymbol{c}_1, \boldsymbol{c}_2 \in \mathbb{R}^d$ such that it holds for $j,l = 1,2$ that*

$$C_{j,l} := \begin{cases} \frac{12(2N_j+1)(2N_l+1)}{(k|\boldsymbol{c}_1-\boldsymbol{c}_2|)^{\frac{1}{3}}} + \frac{1}{\pi}\sqrt{(2N_j+1)(2N_l+1)|\Omega|} < 1 & \text{if } d = 2\,, \\ \frac{48}{3}\frac{\prod_{i=1}^{3}(N_j+\frac{i}{2})(N_l+\frac{i}{2})}{(k|\boldsymbol{c}_1-\boldsymbol{c}_2|)^{\frac{5}{6}}} + \frac{4}{3\pi}(N_j+1)(N_l+1)\sqrt{|\Omega|} < 1 & \text{if } d = 3\,, \end{cases}$$

and

$$C_\Omega := \begin{cases} \frac{1}{\pi}\sum_{j,l=1}^{2}\sqrt{(2N_j+1)(2N_l+1)|\Omega|} < 1 & \text{if } d = 2\,, \\ \frac{4}{3\pi}\sum_{j,l=1}^{2}(N_j+1)(N_l+1)\sqrt{|\Omega|} < 1 & \text{if } d = 3\,. \end{cases}$$

We set $F_q|_{\Omega^c} := (I - \mathcal{P}_{\mathcal{V}_\Omega})F_q$, and we assume that $\widetilde{F}^0_{q_j} \in \mathcal{V}^{\boldsymbol{c}_j}_{N_j}$ and $\widetilde{F}^0_{q_j,q_l} \in \mathcal{V}^{\boldsymbol{c}_j,\boldsymbol{c}_l}_{N_j,N_l}$ for $j \neq l$ and $\widetilde{B}^0_q \in \mathcal{V}_\Omega$ are such that

$$\|F_q|_{\Omega^c} - (\widetilde{F}^0_{q_1} + \widetilde{F}^0_{q_2} + \widetilde{F}^0_{q_1,q_2} + \widetilde{F}^0_{q_2,q_1} + \widetilde{B}^0_q)\|_{\mathrm{HS}} < \delta_0$$

for some $\delta_0 > 0$. Moreover, suppose that $F^\delta_q|_{\Omega^c} := (I - \mathcal{P}_{\mathcal{V}_\Omega})F^\delta_q$ for some $F^\delta_q \in \mathrm{HS}(L^2(S^2))$ and $\delta > 0$ satisfy

$$\delta \geq \delta_0 + \|F_q|_{\Omega^c} - F^\delta_q|_{\Omega^c}\|_{\mathrm{HS}}$$

and let $(\widetilde{F}^\delta_{q_1}, \widetilde{F}^\delta_{q_2}, \widetilde{F}^\delta_{q_1,q_2}, \widetilde{F}^\delta_{q_2,q_1}, \widetilde{B}^\delta_q) \in \mathrm{HS}(L^2(S^2))^5$ denote the solution to

$$\begin{aligned} \underset{(\widetilde{F}^\delta_{q_1}, \widetilde{F}^\delta_{q_2}, \widetilde{F}^\delta_{q_1,q_2}, \widetilde{F}^\delta_{q_2,q_1}, \widetilde{B}^\delta_q)}{\text{minimize}} \quad & \Psi(\widetilde{F}^\delta_{q_1}, \widetilde{F}^\delta_{q_2}, \widetilde{F}^\delta_{q_1,q_2}, \widetilde{F}^\delta_{q_2,q_1}, \widetilde{B}^\delta_q) \\ \text{subject to} \quad & \|\widetilde{F}^\delta_q|_{\Omega^c} - (\widetilde{F}^\delta_{q_1} + \widetilde{F}^\delta_{q_2} + \widetilde{F}^\delta_{q_1,q_2} + \widetilde{F}^\delta_{q_2,q_1} + \widetilde{B}^\delta_q)\|_{\mathrm{HS}} \leq \delta \end{aligned} \tag{5.16}$$

with Ψ from (5.15). Then, for $j = 1,2$

$$\|\widetilde{F}^0_{q_j} - \widetilde{F}^\delta_{q_j}\|^2_{\mathrm{HS}} \leq (1 - C_{j,j})^{-1} 4\delta^2 \qquad \text{and} \qquad \|\widetilde{B}^0_q - \widetilde{B}^\delta_q\|^2_{\mathrm{HS}} \leq (1 - C_\Omega)^{-1} 4\delta^2\,. \tag{5.17}$$

Proof. We proceed as in the proof of [55, Thm. SM4.4]. We set $F := F_q - F^\delta_q$, $\widetilde{B} := \widetilde{B}^0_q - \widetilde{B}^\delta_q$ and for $j,l = 1,2$, $j \neq l$, $\widetilde{F}_j := \widetilde{F}^0_{q_j} - \widetilde{F}^\delta_{q_j}$ and $\widetilde{F}_{j,l} := \widetilde{F}^0_{q_j,q_l} - \widetilde{F}^\delta_{q_j,q_l}$, and we denote the $\ell^0\times\ell^0$-support of $\mathcal{T}_{\boldsymbol{c}_j}\widetilde{F}^0_{q_j}$ and $\mathcal{T}_{\boldsymbol{c}_j,\boldsymbol{c}_l}\widetilde{F}^0_{q_j,q_l}$ by W_j and $W_{j,l}$, respectively. Similar to (3.76) and (3.77) we can show for $d = 2$ that

$$\begin{aligned} \Psi(\widetilde{F}_1, \widetilde{F}_2, \widetilde{F}_{1,2}, \widetilde{F}_{2,1}, \widetilde{B}) \leq 2\big(&\|\mathcal{T}_{\boldsymbol{c}_1}\widetilde{F}_1\|_{(\ell^1\times\ell^1)(W_1)} + \|\mathcal{T}_{\boldsymbol{c}_2}\widetilde{F}_2\|_{(\ell^1\times\ell^1)(W_2)} \\ &+ \|\mathcal{T}_{\boldsymbol{c}_1,\boldsymbol{c}_2}\widetilde{F}_{1,2}\|_{(\ell^1\times\ell^1)(W_{1,2})} + \|\mathcal{T}_{\boldsymbol{c}_2,\boldsymbol{c}_1}\widetilde{F}_{2,1}\|_{(\ell^1\times\ell^1)(W_{2,1})}\big) \end{aligned} \tag{5.18}$$

and for $d = 3$ that

$$\Psi(\widetilde{F}_1,\widetilde{F}_2,\widetilde{F}_{1,2},\widetilde{F}_{2,1}) \le 2(\|\mathcal{T}_{\boldsymbol{c}_1}\widetilde{F}_1\|_{(\ell^1_{\sqrt{2n+1}}\times\ell^1_{\sqrt{2n+1}})(W_1)} + \|\mathcal{T}_{\boldsymbol{c}_2}\widetilde{F}_2\|_{(\ell^1_{\sqrt{2n+1}}\times\ell^1_{\sqrt{2n+1}})(W_2)} + \|\mathcal{T}_{\boldsymbol{c}_1,\boldsymbol{c}_2}\widetilde{F}_{1,2}\|_{(\ell^1_{\sqrt{2n+1}}\times\ell^1_{\sqrt{2n+1}})(W_{1,2})} + \|\mathcal{T}_{\boldsymbol{c}_2,\boldsymbol{c}_1}\widetilde{F}_{2,1}\|_{(\ell^1_{\sqrt{|2n+1}}\times\ell^1_{\sqrt{2n+1}})(W_{2,1})}) . \quad (5.19)$$

Using the same arguments as before yields

$$\begin{aligned}4\delta^2 \ge\ & \|\widetilde{F}_1\|_{\mathrm{HS}}^2 + \|\widetilde{F}_2\|_{\mathrm{HS}}^2 + \|\widetilde{F}_{1,2}\|_{\mathrm{HS}}^2 + \|\widetilde{F}_{2,1}\|_{\mathrm{HS}}^2 + \|\widetilde{B}\|_{\mathrm{HS}}^2 \\ & - 2|\langle\widetilde{F}_1,\widetilde{F}_2\rangle_{\mathrm{HS}}| - 2|\langle\widetilde{F}_1,\widetilde{F}_{1,2}\rangle_{\mathrm{HS}}| - 2|\langle\widetilde{F}_1,\widetilde{F}_{2,1}\rangle_{\mathrm{HS}}| - 2|\langle\widetilde{F}_1,\widetilde{B}\rangle_{\mathrm{HS}}| \\ & - 2|\langle\widetilde{F}_2,\widetilde{F}_{1,2}\rangle_{\mathrm{HS}}| - 2|\langle\widetilde{F}_2,\widetilde{F}_{2,1}\rangle_{\mathrm{HS}}| - 2|\langle\widetilde{F}_2,\widetilde{B}\rangle_{\mathrm{HS}}| \\ & - 2|\langle\widetilde{F}_{1,2},\widetilde{F}_{2,1}\rangle_{\mathrm{HS}}| - 2|\langle\widetilde{F}_{1,2},\widetilde{B}\rangle_{\mathrm{HS}}| - 2|\langle\widetilde{F}_{2,1},\widetilde{B}\rangle_{\mathrm{HS}}| .\end{aligned}$$

For $d=2$ we obtain due to Hölder's inequality, (3.7) and the mapping properties (3.8) and (2.55) that

$$\begin{aligned}4\delta^2 \ge\ & \|\widetilde{F}_1\|_{\mathrm{HS}}^2 + \|\widetilde{F}_2\|_{\mathrm{HS}}^2 + \|\widetilde{F}_{1,2}\|_{\mathrm{HS}}^2 + \|\widetilde{F}_{2,1}\|_{\mathrm{HS}}^2 + \|\widetilde{B}\|_{\mathrm{HS}}^2 \\ & - \frac{2}{(k|\boldsymbol{c}_1-\boldsymbol{c}_2|)^{\frac{2}{3}}}(\|\mathcal{T}_{\boldsymbol{c}_1}\widetilde{F}_1\|_{\ell^1\times\ell^1}\|\mathcal{T}_{\boldsymbol{c}_2}\widetilde{F}_2\|_{\ell^1\times\ell^1} + \|\mathcal{T}_{\boldsymbol{c}_1,\boldsymbol{c}_2}\widetilde{F}_{1,2}\|_{\ell^1\times\ell^1}\|\mathcal{T}_{\boldsymbol{c}_2,\boldsymbol{c}_1}\widetilde{F}_{2,1}\|_{\ell^1\times\ell^1}) \\ & - \frac{2}{(k|\boldsymbol{c}_1-\boldsymbol{c}_2|)^{\frac{1}{3}}}(\|\mathcal{T}_{\boldsymbol{c}_1}\widetilde{F}_1\|_{\ell^1\times\ell^1}\|\mathcal{T}_{\boldsymbol{c}_1,\boldsymbol{c}_2}\widetilde{F}_{1,2}\|_{\ell^1\times\ell^1} + \|\mathcal{T}_{\boldsymbol{c}_1}\widetilde{F}_1\|_{\ell^1\times\ell^1}\|\mathcal{T}_{\boldsymbol{c}_2,\boldsymbol{c}_1}\widetilde{F}_{2,1}\|_{\ell^1\times\ell^1} \\ & \qquad + \|\mathcal{T}_{\boldsymbol{c}_2}\widetilde{F}_2\|_{\ell^1\times\ell^1}\|\mathcal{T}_{\boldsymbol{c}_1,\boldsymbol{c}_2}\widetilde{F}_{1,2}\|_{\ell^1\times\ell^1} + \|\mathcal{T}_{\boldsymbol{c}_2}\widetilde{F}_2\|_{\ell^1\times\ell^1}\|\mathcal{T}_{\boldsymbol{c}_2,\boldsymbol{c}_1}\widetilde{F}_{2,1}\|_{\ell^1\times\ell^1}) \\ & - \frac{1}{\pi}\Psi(\widetilde{F}_1,\widetilde{F}_2,\widetilde{F}_{1,2},\widetilde{F}_{2,1},\widetilde{B})\|\widetilde{B}\|_{L^1} .\end{aligned}$$

As in the proof of Theorem 3.41, we use $2\sum_i\sum_{j<i}a_ia_j = \sum_i\sum_{j\neq i} \le \frac{3}{4}(\sum_i a_i)^2 \le 3\sum_i a_i^2$ for $a_1,a_2,a_3,a_4\in\mathbb{R}$, (5.18) and the Cauchy Schwarz inequality to bound

$$\begin{aligned}& - \frac{2}{(k|\boldsymbol{c}_1-\boldsymbol{c}_2|)^{\frac{2}{3}}}\left(\|\mathcal{T}_{\boldsymbol{c}_1}\widetilde{F}_1\|_{\ell^1\times\ell^1}\|\mathcal{T}_{\boldsymbol{c}_2}\widetilde{F}_2\|_{\ell^1\times\ell^1} + \|\mathcal{T}_{\boldsymbol{c}_1,\boldsymbol{c}_2}\widetilde{F}_{1,2}\|_{\ell^1\times\ell^1}\|\mathcal{T}_{\boldsymbol{c}_2,\boldsymbol{c}_1}\widetilde{F}_{2,1}\|_{\ell^1\times\ell^1}\right) \\ & - \frac{2}{(k|\boldsymbol{c}_1-\boldsymbol{c}_2|)^{\frac{1}{3}}}\Big(\|\mathcal{T}_{\boldsymbol{c}_1}\widetilde{F}_1\|_{\ell^1\times\ell^1}\|\mathcal{T}_{\boldsymbol{c}_1,\boldsymbol{c}_2}\widetilde{F}_{1,2}\|_{\ell^1\times\ell^1} + \|\mathcal{T}_{\boldsymbol{c}_1}\widetilde{F}_1\|_{\ell^1\times\ell^1}\|\mathcal{T}_{\boldsymbol{c}_2,\boldsymbol{c}_1}\widetilde{F}_{2,1}\|_{\ell^1\times\ell^1} \\ & \qquad + \|\mathcal{T}_{\boldsymbol{c}_2}\widetilde{F}_2\|_{\ell^1\times\ell^1}\|\mathcal{T}_{\boldsymbol{c}_1,\boldsymbol{c}_2}\widetilde{F}_{1,2}\|_{\ell^1\times\ell^1} + \|\mathcal{T}_{\boldsymbol{c}_2}\widetilde{F}_2\|_{\ell^1\times\ell^1}\|\mathcal{T}_{\boldsymbol{c}_2,\boldsymbol{c}_1}\widetilde{F}_{2,1}\|_{\ell^1\times\ell^1}\Big) \\ \ge\ & -\frac{2}{(k|\boldsymbol{c}_1-\boldsymbol{c}_2|)^{\frac{1}{3}}}\Big(\|\mathcal{T}_{\boldsymbol{c}_1}\widetilde{F}_1\|_{\ell^1\times\ell^1}\|\mathcal{T}_{\boldsymbol{c}_2}\widetilde{F}_2\|_{\ell^1\times\ell^1} + \|\mathcal{T}_{\boldsymbol{c}_1,\boldsymbol{c}_2}\widetilde{F}_{1,2}\|_{\ell^1\times\ell^1}\|\mathcal{T}_{\boldsymbol{c}_2,\boldsymbol{c}_1}\widetilde{F}_{2,1}\|_{\ell^1\times\ell^1} \\ & \qquad + \|\mathcal{T}_{\boldsymbol{c}_1}\widetilde{F}_1\|_{\ell^1\times\ell^1}\|\mathcal{T}_{\boldsymbol{c}_1,\boldsymbol{c}_2}\widetilde{F}_{1,2}\|_{\ell^1\times\ell^1} + \|\mathcal{T}_{\boldsymbol{c}_1}\widetilde{F}_1\|_{\ell^1\times\ell^1}\|\mathcal{T}_{\boldsymbol{c}_2,\boldsymbol{c}_1}\widetilde{F}_{2,1}\|_{\ell^1\times\ell^1} \\ & \qquad + \|\mathcal{T}_{\boldsymbol{c}_2}\widetilde{F}_2\|_{\ell^1\times\ell^1}\|\mathcal{T}_{\boldsymbol{c}_1,\boldsymbol{c}_2}\widetilde{F}_{1,2}\|_{\ell^1\times\ell^1} + \|\mathcal{T}_{\boldsymbol{c}_2}\widetilde{F}_2\|_{\ell^1\times\ell^1}\|\mathcal{T}_{\boldsymbol{c}_2,\boldsymbol{c}_1}\widetilde{F}_{2,1}\|_{\ell^1\times\ell^1}\Big) \\ \ge\ & -\frac{3}{4(k|\boldsymbol{c}_1-\boldsymbol{c}_2|)^{\frac{1}{3}}}\Psi^2(\widetilde{F}_1,\widetilde{F}_2,\widetilde{F}_{2,1},\widetilde{F}_{2,1},\widetilde{B}) \\ \ge\ & -\frac{3}{(k|\boldsymbol{c}_1-\boldsymbol{c}_2|)^{\frac{1}{3}}}\Big(\|\mathcal{T}_{\boldsymbol{c}_1}\widetilde{F}_1\|_{(\ell^1\times\ell^1)(W_1)} + \|\mathcal{T}_{\boldsymbol{c}_2}\widetilde{F}_2\|_{(\ell^1\times\ell^1)(W_2)} \\ & \qquad + \|\mathcal{T}_{\boldsymbol{c}_1,\boldsymbol{c}_2}\widetilde{F}_{1,2}\|_{(\ell^1\times\ell^1)(W_{1,2})} + \|\mathcal{T}_{\boldsymbol{c}_2,\boldsymbol{c}_1}\widetilde{F}_{2,1}\|_{(\ell^1\times\ell^1)(W_{2,1})}\Big)^2 \\ \ge\ & -\frac{3}{(k|\boldsymbol{c}_1-\boldsymbol{c}_2|)^{\frac{1}{3}}}\left(\sqrt{|W_1|}\|\widetilde{F}_1\|_{\mathrm{HS}} + \sqrt{|W_2|}\|\widetilde{F}_2\|_{\mathrm{HS}} + \sqrt{|W_{1,2}|}\|\widetilde{F}_{1,2}\|_{\mathrm{HS}} + \sqrt{|W_{2,1}|}\|\widetilde{F}_{2,1}\|_{\mathrm{HS}}\right)^2\end{aligned}$$

$$\geq -\frac{12}{(k|\boldsymbol{c}_1-\boldsymbol{c}_2|)^{\frac{1}{3}}}\left(|W_1|\|\widetilde{F}_1\|_{\mathrm{HS}}^2+|W_2|\|\widetilde{F}_2\|_{\mathrm{HS}}^2+|W_{1,2}|\|\widetilde{F}_{1,2}\|_{\mathrm{HS}}^2+|W_{2,1}|\|\widetilde{F}_{2,1}\|_{\mathrm{HS}}^2\right).$$

Furthermore, we estimate due to the Cauchy Schwarz inequality, (5.18) and $2ab \leq a^2+b^2$ for $a,b\in\mathbb{R}$

$$\begin{aligned}
&-\frac{1}{\pi}\Psi(\widetilde{F}_1,\widetilde{F}_2,\widetilde{F}_{1,2},\widetilde{F}_{2,1},\widetilde{B})\|\widetilde{B}\|_{L^1} \geq -\frac{1}{\pi}\Psi(\widetilde{F}_1,\widetilde{F}_2,\widetilde{F}_{1,2},\widetilde{F}_{2,1},\widetilde{B})\sqrt{|\Omega|}\|\widetilde{B}\|_{\mathrm{HS}}\\
&\geq -\frac{2}{\pi}\Big(\|\mathcal{T}_{\boldsymbol{c}_1}\widetilde{F}_1\|_{(\ell^1\times\ell^1)(W_1)}+\|\mathcal{T}_{\boldsymbol{c}_2}\widetilde{F}_2\|_{(\ell^1\times\ell^1)(W_2)}\\
&\qquad+\|\mathcal{T}_{\boldsymbol{c}_1,\boldsymbol{c}_2}\widetilde{F}_{1,2}\|_{(\ell^1\times\ell^1)(W_{1,2})}+\|\mathcal{T}_{\boldsymbol{c}_2,\boldsymbol{c}_1}\widetilde{F}_{2,1}\|_{(\ell^1\times\ell^1)(W_{2,1})}\Big)\sqrt{|\Omega|}\|\widetilde{B}\|_{\mathrm{HS}}\\
&\geq -\frac{2}{\pi}\Big((|\Omega||W_1|)^{\frac{1}{4}}\|\mathcal{T}_{\boldsymbol{c}_1}\widetilde{F}_1\|_{\mathrm{HS}}(|\Omega||W_1|)^{\frac{1}{4}}\|\widetilde{B}\|_{\mathrm{HS}}+(|\Omega||W_2|)^{\frac{1}{4}}\|\mathcal{T}_{\boldsymbol{c}_2}\widetilde{F}_2\|_{\mathrm{HS}}(|\Omega||W_2|)^{\frac{1}{4}}\|\widetilde{B}\|_{\mathrm{HS}}\\
&\quad+(|\Omega||W_{1,2}|)^{\frac{1}{4}}\|\mathcal{T}_{\boldsymbol{c}_1,\boldsymbol{c}_2}\widetilde{F}_{1,2}\|_{\mathrm{HS}}(|\Omega||W_{1,2}|)^{\frac{1}{4}}\|\widetilde{B}\|_{\mathrm{HS}}+(|\Omega||W_{2,1}|)^{\frac{1}{4}}\|\mathcal{T}_{\boldsymbol{c}_2,\boldsymbol{c}_1}\widetilde{F}_{2,1}\|_{\mathrm{HS}}(|\Omega||W_{2,1}|)^{\frac{1}{4}}\|\widetilde{B}\|_{\mathrm{HS}}\Big)\\
&\geq -\frac{\sqrt{|\Omega|}}{\pi}\Big(\sqrt{|W_1|}\|\widetilde{F}_1\|_{\mathrm{HS}}^2+\sqrt{|W_2|}\|\widetilde{F}_2\|_{\mathrm{HS}}^2+\sqrt{|W_{2,1}|}\|\widetilde{F}_{1,2}\|_{\mathrm{HS}}^2+\sqrt{|W_{2,1}|}\|\widetilde{F}_{2,1}\|_{\mathrm{HS}}^2\\
&\qquad+\left(\sqrt{|W_1|}+\sqrt{|W_2|}+\sqrt{|W_{1,2}|}+\sqrt{|W_{2,1}|}\right)\|\widetilde{B}\|_{\mathrm{HS}}^2\Big).
\end{aligned}$$

Altogether, we obtain for the case $d=2$ that

$$4\delta^2 \geq (1-C_{1,1})\|\widetilde{F}_1\|_{\mathrm{HS}}^2+(1-C_{2,2})\|\widetilde{F}_2\|_{\mathrm{HS}}^2+(1-C_{1,2})\left(\|\widetilde{F}_{1,2}\|_{\mathrm{HS}}^2+\|\widetilde{F}_{2,1}\|_{\mathrm{HS}}^2\right)+(1-C_\Omega)\|\widetilde{B}\|_{\mathrm{HS}}^2.$$

For $d=3$ we do the same calculations replacing (3.8) by (3.9) and (2.55) by (2.62) and using in the last step

$$\left(\sum_{(m,n)\in W_j}(2m+1)(2n+1)\right)^{\frac{1}{2}} \leq (N_j+1)^2 \quad\text{and}\quad \left(\sum_{(m,n)\in W_{j,l}}(2m+1)(2n+1)\right)^{\frac{1}{2}} \leq (N_j+1)(N_l+1),$$

(cf. (2.38)) for $j,l=1,2$, $j\neq l$. This yields the result. □

Remark 5.17. We make similar observations as in Remark 5.15.

(i) Provided $k|\boldsymbol{c}_1-\boldsymbol{c}_2| \leq 2(N_1+N_2+d/2)$ the stability estimate (5.17) can be improved by replacing $C_{j,l}<1$ by $\widetilde{C}_{j,l}<1$ with

$$\widetilde{C}_{j,l} := \begin{cases} \frac{12(2N_j+1)(2N_l+1)}{(k|\boldsymbol{c}_1-\boldsymbol{c}_2|)^{\frac{1}{2}}}+\frac{1}{\pi}\sqrt{(2N_j+1)(2N_l+1)|\Omega|} & \text{if } d=2,\\ \frac{48}{3}\frac{\prod_{i=1}^3(N_j+\frac{i}{2})(N_l+\frac{i}{2})}{k|\boldsymbol{c}_1-\boldsymbol{c}_2|}+\frac{4}{3\pi}(N_j+1)(N_l+1)\sqrt{|\Omega|} & \text{if } d=3. \end{cases}$$

(ii) When comparing Theorems 5.8 and 5.16 we recognize that the first is more stable for small $|\boldsymbol{c}_1-\boldsymbol{c}_2|$ and the latter is more stable for sufficiently large $|\boldsymbol{c}_1-\boldsymbol{c}_2|$.

(iii) Our findings from Section 3.6 for far field operator splitting remain valid when considering far field operator completion and splitting. Particularly, this involves the generalizations to $J\geq 2$ components and to higher scattering orders. As described in Remark 5.15 (iii), we can further improve the stability of problem (5.16) by taking the reciprocity relation into account. ◊

CHAPTER 6

NUMERICAL TESTS FOR FAR FIELD OPERATOR COMPLETION

In this section, we provide numerical examples to illustrate the performance of our far field operator (splitting and) completion methods from Chapter 5. We first apply them to synthetic data in Section 6.2, as we already did in Section 4.2 for the far field operator completion problem. In Section 6.3 we test our methods on real data provided by the Fresnel Institute, see [7]. Finally, in Section 6.4, we combine our methods with the factorization method for solving the inverse problem of reconstructing the shape of the scatterer on the base of incomplete far field data.

6.1. REMARKS ON THE IMPLEMENTATION

6.1.1. SIMULATION OF THE NON-OBSERVABLE SET

Let in the following $d = 2$. We simulate the exact far field operator as described in Example 2.5 and Section 4.1.1 by choosing $L \in \mathbb{N}$ sufficiently large and even, equally distributed illumination and observation directions

$$\widehat{\boldsymbol{x}}_l := \boldsymbol{\theta}_l := (\cos\psi_l, \sin\psi_l)^\top \qquad \text{with } \psi_l := (l-1)\frac{2\pi}{L} \text{ for } l = 1, \dots, L\,.$$

The resulting matrix is denoted by $\boldsymbol{F}_q \in \mathbb{C}^{L\times L}$, and by adding complex uniformly distributed random relative noise $\boldsymbol{N}$ at relative noise level $\delta_{\text{rel}} \in [0, 1)$ we obtain a noisy version $\boldsymbol{F}_q^\delta := \boldsymbol{F}_q + \boldsymbol{N}$ of $\boldsymbol{F}_q$. Of course, it is also possible to choose different numbers of illumination and observation directions, as will be the case with the real data in Section 6.3, but we do not consider this here for simplification.

Let $\Omega \subset S^1 \times S^1$ model the non-observable set. On the discrete level, the associated orthogonal projection $\mathcal{P}_\Omega : \mathbb{C}^{L\times L} \to \mathbb{C}^{L\times L}$ is given by the pointwise multiplication with the matrix

$$\boldsymbol{P}_\Omega := (\chi_\Omega(\widehat{\boldsymbol{x}}_m; \boldsymbol{\theta}_n))_{1\le m,n\le L} \in \{0,1\}^{L\times L}\,,$$

by means of which we can write the observable part of $\boldsymbol{F}_q^\delta$, i.e. the given data, as $\boldsymbol{F}_q^\delta|_{\Omega^c} := \boldsymbol{F}_q^\delta - \mathcal{P}_\Omega \boldsymbol{F}_q^\delta$ and its non-observable part as $\boldsymbol{B}_q := -\mathcal{P}_\Omega \boldsymbol{F}_q^\delta$.

According to Assumption 5.3 we suppose that the complement Ω^c of Ω, which models the observable set, is symmetric in the sense of reciprocity, i.e., it satisfies (5.1). As a consequence, $\mathbf{1} - \boldsymbol{P}_\Omega$ is a symmetric matrix after swapping either the two halves of each column or of each row, which can be realized by either using the MATLAB functions fftshift$(\cdot, 1)$ or fftshift$(\cdot, 2)$. Here, $\mathbf{1}$ denotes the $L \times L$ matrix whose entries are all equal to one. If this symmetry of the observable data is not given, we can complete Ω^c and the observable far field data $\boldsymbol{F}_q^\delta|_{\Omega^c}$ according to (3.79), i.e., we replace $\boldsymbol{P}_\Omega$ and $\boldsymbol{F}_q^\delta|_{\Omega^c}$ by

$$\text{fftshift}(\mathbf{1} + \text{fftshift}(\boldsymbol{P}_\Omega - \mathbf{1}, 1) + \text{fftshift}(\boldsymbol{P}_\Omega - \mathbf{1}, 1)^\top - \text{fftshift}(\boldsymbol{P}_\Omega - \mathbf{1}, 1) .* \text{fftshift}(\boldsymbol{P}_\Omega - \mathbf{1}, 1)^\top, 1)$$

Algorithm 4 Far field operator splitting and completion by conjugate gradient method

Input: Noisy observed far field matrix $\boldsymbol{F}_q^\delta|_{\Omega^c}$, projection $\mathcal{P}_\Omega$ on non-observable set, wave number k, a priori knowledge on locations $\boldsymbol{c}_1$, $\boldsymbol{c}_2$, R_1 and R_2, maximum number of cg iterations $l_{\max}$, absolute noise level $\delta > 0$ and fudge parameter $\tau > 1$.

Output: Approximations $\widetilde{\boldsymbol{F}}_q$ and $\widetilde{\boldsymbol{B}}_q$ to $\boldsymbol{F}_q$ and $\boldsymbol{B}_q$.

Set $N_j = \lceil ekR_j/2 \rceil$ for $j = 1, 2$.
Initialize $\boldsymbol{R}^{(0)} = [\boldsymbol{0}, \mathcal{P}_1\boldsymbol{F}_q^\delta|_{\Omega^c}, \mathcal{P}_2\boldsymbol{F}_q^\delta|_{\Omega^c}, \mathcal{P}_{1,2}\boldsymbol{F}_q^\delta|_{\Omega^c}, \mathcal{P}_{2,1}\boldsymbol{F}_q^\delta|_{\Omega^c}]$,
$\boldsymbol{D}^{(0)} = \boldsymbol{R}^{(0)}$ and
$\boldsymbol{F}^{(0)} = [\boldsymbol{0}, \boldsymbol{0}, \boldsymbol{0}, \boldsymbol{0}, \boldsymbol{0}]$.
for $l = 0, 1, 2, \cdots, l_{\max}$ **do**
  Update $\alpha_l = \|\boldsymbol{R}^{(l)}\|_{\mathrm{HS}}^2 / \langle \boldsymbol{D}^{(l)}, \mathcal{M}\boldsymbol{D}^{(l)} \rangle_{\mathrm{HS}}$,
  $\boldsymbol{F}^{(l+1)} = \boldsymbol{F}^{(l)} + \alpha_l \boldsymbol{D}^{(l)}$,
  $\boldsymbol{R}^{(l+1)} = \boldsymbol{R}^{(l)} - \alpha_l \mathcal{M}\boldsymbol{D}^{(l)}$,
  $\beta_l = \|\boldsymbol{R}^{(l+1)}\|_{\mathrm{HS}}^2 / \|\boldsymbol{R}^{(l)}\|_{\mathrm{HS}}^2$ and
  $\boldsymbol{D}^{(l+1)} = \boldsymbol{R}^{(l+1)} + \beta_l \boldsymbol{D}^{(l)}$.
  if $\|\boldsymbol{R}^{(l+1)}\|_{\mathrm{HS}} \leq \tau\delta$ **then**
    Set $l_{\max} = l$.
  end if
end for
Set $[\widetilde{\boldsymbol{B}}_q, \widetilde{\boldsymbol{F}}_{q_1}, \widetilde{\boldsymbol{F}}_{q_2}, \widetilde{\boldsymbol{F}}_{q_1,q_2}, \widetilde{\boldsymbol{F}}_{q_2,q_1}] = \boldsymbol{F}^{(l_{\max}+1)}$ and
  $\widetilde{\boldsymbol{F}}_q = \widetilde{\boldsymbol{F}}_{q_1} + \widetilde{\boldsymbol{F}}_{q_2} + \widetilde{\boldsymbol{F}}_{q_1,q_2} + \widetilde{\boldsymbol{F}}_{q_2,q_1}$.

and

$$\mathrm{fftshift}(\mathrm{fftshift}(\boldsymbol{F}_q^\delta|_{\Omega^c}, 1) + \mathrm{fftshift}(\boldsymbol{F}_q^\delta|_{\Omega^c}, 1)^\top - \mathrm{fftshift}(\boldsymbol{F}_q^\delta|_{\Omega^c}, 1) .* \mathrm{fftshift}(\boldsymbol{F}_q^\delta|_{\Omega^c}, 1)^\top, 1)\,,$$

respectively, where $.*$ denotes the elementwise matrix product. The last summands remove the doubly counted already symmetric parts of $\boldsymbol{P}_\Omega$ and $\boldsymbol{F}_q^\delta|_{\Omega^c}$ in above representations. In case of case of noisy data, so $\delta_{\mathrm{rel}} > 0$, this procedure further implements noise filtering.

We evaluate the relative errors

$$\varepsilon_{\mathrm{rel}} := \frac{\|\boldsymbol{F}_q - \widetilde{\boldsymbol{F}}_q\|_{\mathrm{HS}}}{\|\boldsymbol{F}_q\|_{\mathrm{HS}}} \qquad \text{and} \qquad \varepsilon_{\mathrm{rel}}^\Omega := \frac{\|\boldsymbol{B}_q - \widetilde{\boldsymbol{B}}_q\|_{\mathrm{HS}}}{\|\boldsymbol{B}_q\|_{\mathrm{HS}}} \tag{6.1}$$

for the reconstructed far field operator $\widetilde{\boldsymbol{F}}_q$ and for the reconstructed non-observable part $\widetilde{\boldsymbol{B}}_q$.

In the following, we briefly explain how we modify our algorithms from Subsections 4.1.4 and 4.1.5 for (additionally) solving the far field operator completion problem, and we present additional methods for solving this problem. As before, we assume the scatterer $D = D_1 \cup D_2$ to consist of two well-separated components, i.e., $D_j \subset B_{R_j}(\boldsymbol{c}_j)$ for some $\boldsymbol{c}_j \in \mathbb{R}^2$ and $R_j > 0$, $j = 1, 2$, with $|\boldsymbol{c}_1 - \boldsymbol{c}_2| > R_1 + R_2$. Moreover, we set $q_j := \chi_{D_j} q$ for $j = 1, 2$, and we assume $D \subset B_R(\boldsymbol{c})$ for some $\boldsymbol{c} \in \mathbb{R}^2$ and $R > 0$. For instance, we can always choose

$$\boldsymbol{c} = \boldsymbol{c}_1 + \frac{\boldsymbol{c}_2 - \boldsymbol{c}_1}{2|\boldsymbol{c}_1 - \boldsymbol{c}_2|}\left(|\boldsymbol{c}_1 - \boldsymbol{c}_2| + R_2 - R_1\right) \qquad \text{and} \qquad R = \frac{1}{2}\left(|\boldsymbol{c}_1 - \boldsymbol{c}_2| + R_1 + R_2\right).$$

6.1.2. (Splitting and) Completion by the conjugate gradient method

To solve the least squares problem (5.3b) of far field operator completion, we assume a priori knowledge on the location $B_R(\boldsymbol{c})$ of the whole scatterer and on the non-observable set Ω. According

to (3.13) solving problem (5.3b) is equivalent to solve the block system

$$\begin{bmatrix} \boldsymbol{I} & \mathcal{P}_\Omega\mathcal{P} \\ \mathcal{P}\mathcal{P}_\Omega & \boldsymbol{I} \end{bmatrix} \begin{bmatrix} \boldsymbol{B} \\ \boldsymbol{F} \end{bmatrix} = \begin{bmatrix} \boldsymbol{0} \\ \mathcal{P}\boldsymbol{F}_q^\delta|_{\Omega^c} \end{bmatrix} \tag{6.2}$$

with $\mathcal{P}$ denoting the orthogonal projection onto $\mathcal{V}_N^c$. We use $N = \lceil \frac{e}{2}kR \rceil$. With our notations from Subsection 4.1.4 we solve the least squares problem (5.13) of the far field operator splitting and completion by extending the linear block system (4.3) according to

$$\begin{bmatrix} \boldsymbol{I} & \mathcal{P}_\Omega\mathcal{P}_1 & \mathcal{P}_\Omega\mathcal{P}_2 & \mathcal{P}_\Omega\mathcal{P}_{1,2} & \mathcal{P}_\Omega\mathcal{P}_{2,1} \\ \mathcal{P}_1\mathcal{P}_\Omega & \boldsymbol{I} & \mathcal{P}_1\mathcal{P}_2 & \mathcal{P}_1\mathcal{P}_{1,2} & \mathcal{P}_1\mathcal{P}_{2,1} \\ \mathcal{P}_2\mathcal{P}_\Omega & \mathcal{P}_2\mathcal{P}_1 & \boldsymbol{I} & \mathcal{P}_2\mathcal{P}_{1,2} & \mathcal{P}_2\mathcal{P}_{2,1} \\ \mathcal{P}_{1,2}\mathcal{P}_\Omega & \mathcal{P}_{1,2}\mathcal{P}_1 & \mathcal{P}_{1,2}\mathcal{P}_2 & \boldsymbol{I} & \mathcal{P}_{1,2}\mathcal{P}_{2,1} \\ \mathcal{P}_{2,1}\mathcal{P}_\Omega & \mathcal{P}_{2,1}\mathcal{P}_1 & \mathcal{P}_{2,1}\mathcal{P}_2 & \mathcal{P}_{2,1}\mathcal{P}_{1,2} & \boldsymbol{I} \end{bmatrix} \begin{bmatrix} \boldsymbol{B} \\ \boldsymbol{F}_1 \\ \boldsymbol{F}_2 \\ \boldsymbol{F}_{1,2} \\ \boldsymbol{F}_{2,1} \end{bmatrix} = \begin{bmatrix} \boldsymbol{0} \\ \mathcal{P}_1\boldsymbol{F}_q^\delta|_{\Omega^c} \\ \mathcal{P}_2\boldsymbol{F}_q^\delta|_{\Omega^c} \\ \mathcal{P}_{1,2}\boldsymbol{F}_q^\delta|_{\Omega^c} \\ \mathcal{P}_{2,1}\boldsymbol{F}_q^\delta|_{\Omega^c} \end{bmatrix}. \tag{6.3}$$

Here, we mention that $\mathcal{P}_\Omega\boldsymbol{F}_q^\delta|_{\Omega^c} = \boldsymbol{0}$. This involves a priori knowledge on the locations $B_{R_j}(\boldsymbol{c}_j)$ of the scatterer's components, $j = 1, 2$, and on the non-observable set Ω. Since the operators on the left hand sides of (6.2) and (6.3) are again hermitian and under the assumptions of Theorems 5.7 and 5.14 positive definite (cf. Section 3.3), we can approximate the corresponding solutions by the cg method. For the latter system we denote this operator by $\mathcal{M}$. The resulting method in that case is described in Algorithm 4.

6.1.3. (Splitting and) Completion by Fast Iterative Soft Thresholding

If additionally to the non-observable set Ω only knowledge on the position $\boldsymbol{c}$ of the whole scatterer (in case of far field operator completion) or knowledge on the positions $\boldsymbol{c}_j$, $j = 1, 2$, of the scatterer's components (in case of far field operator splitting and completion) is available, one can solve the $\ell^1 \times \ell^1$ minimization problem (5.6) or (5.16), respectively. The related Tikhonov functionals are given by

$$\boldsymbol{F} \mapsto \|\boldsymbol{F}_q^\delta|_{\Omega^c} - (\boldsymbol{I} - \mathcal{P}_\Omega)\boldsymbol{F}\|_{\mathrm{HS}}^2 + \mu\|\mathcal{T}_{\boldsymbol{c}}\boldsymbol{F}\|_{\ell^1\times\ell^1}$$

and

$$\begin{aligned}(\boldsymbol{F}_1, \boldsymbol{F}_2, \boldsymbol{F}_{1,2}, \boldsymbol{F}_{2,1}) \mapsto\ & \|\boldsymbol{F}_q^\delta|_{\Omega^c} - (\boldsymbol{I} - \mathcal{P}_\Omega)(\boldsymbol{F}_1 + \boldsymbol{F}_2 + \boldsymbol{F}_{1,2} + \boldsymbol{F}_{2,1})\|_{\mathrm{HS}}^2 \\ & + \mu\Big(\|\mathcal{T}_{\boldsymbol{c}_1}\boldsymbol{F}_1\|_{\ell^1\times\ell^1} + \|\mathcal{T}_{\boldsymbol{c}_2}\boldsymbol{F}_2\|_{\ell^1\times\ell^1} + \|\mathcal{T}_{\boldsymbol{c}_1,\boldsymbol{c}_2}\boldsymbol{F}_{1,2}\|_{\ell^1\times\ell^1} + \|\mathcal{T}_{\boldsymbol{c}_2,\boldsymbol{c}_1}\boldsymbol{F}_{2,1}\|_{\ell^1\times\ell^1}\Big)\end{aligned}$$

with $\|\cdot\|_{\ell^1\times\ell^1}$ given as in Subsection 4.1.3. As elaborated in Section 4.1.5, the unique minimizers $\widetilde{\boldsymbol{F}}_q$ and $(\widetilde{\boldsymbol{F}}_{q_1}, \widetilde{\boldsymbol{F}}_{q_2}, \widetilde{\boldsymbol{F}}_{q_1,q_2}, \widetilde{\boldsymbol{F}}_{q_2,q_1})$ of these functionals can, for suitably chosen regularization parameters $\mu > 0$, be approximated by FISTA. The related non-observable part can be approximated by setting

$$\widetilde{\boldsymbol{B}}_q := -\mathcal{P}_\Omega\widetilde{\boldsymbol{F}}_q \qquad \text{and} \qquad \widetilde{\boldsymbol{B}}_q := -\mathcal{P}_\Omega(\widetilde{\boldsymbol{F}}_{q_1} + \widetilde{\boldsymbol{F}}_{q_2} + \widetilde{\boldsymbol{F}}_{q_1,q_2} + \widetilde{\boldsymbol{F}}_{q_2,q_1}),$$

respectively. Compared to Algorithm 2 we only have to modify the evaluations of the residuum, which result in the algorithm that is described in Algorithm 5.

6.1.4. Splitting and completion by RPCP with a FISTA type method

Suppose only a priori knowledge on the position $\boldsymbol{c}_2$ of the second scatterer's component and on the non-observable set Ω is available, we modify our scheme from Subsection 4.1.6 to additionally solve the far field operator completion problem. This leads for suitably chosen $\mu > 0$ to minimizing the Tikhonov functional

$$(\boldsymbol{L}, \boldsymbol{S}) \mapsto \|\boldsymbol{F}_q^\delta|_{\Omega^c} - (\boldsymbol{I} - \mathcal{P}_\Omega)(\boldsymbol{L} + \boldsymbol{S})\|_{\mathrm{HS}}^2 + \mu\Big(\|\boldsymbol{L}\|_{\mathrm{nuc}} + \lambda\|\mathcal{T}_{\boldsymbol{c}_2}\boldsymbol{S}\|_{\ell^1\times\ell^1}\Big).$$

Algorithm 5 Far field operator splitting and completion by FISTA

Input: Noisy observed far field matrix $\boldsymbol{F}_q^\delta|_{\Omega^c}$, projection $\mathcal{P}_\Omega$ on non-observable set, wave number k, a priori knowledge on positions $\boldsymbol{c}_1$ and $\boldsymbol{c}_2$, maximum number of FISTA iterations $l_{\max}$, regularization parameter $\mu > 0$, initial guess $\boldsymbol{F} = [\boldsymbol{F}_1, \boldsymbol{F}_2, \boldsymbol{F}_{1,2}, \boldsymbol{F}_{2,1}]$, tolerance $\varepsilon > 0$.

Output: Approximation $\widetilde{\boldsymbol{F}}_q$ to $\boldsymbol{F}_q$.

Set $\omega = 1/5$.
Initialize $\boldsymbol{H}^{(1)} = [\boldsymbol{H}_1^{(1)}, \boldsymbol{H}_2^{(1)}, \boldsymbol{H}_{1,2}^{(1)}, \boldsymbol{H}_{2,1}^{(1)}] = \boldsymbol{F}$,
$\boldsymbol{F}^{(0)} = [\boldsymbol{F}_1^{(0)}, \boldsymbol{F}_2^{(0)}, \boldsymbol{F}_{1,2}^{(0)}, \boldsymbol{F}_{2,1}^{(0)}] = \boldsymbol{F}$
$\boldsymbol{R}^{(1)} = \boldsymbol{F}_q^\delta|_{\Omega^c} - (\boldsymbol{I} - \mathcal{P}_\Omega)(\boldsymbol{H}_1^{(1)} + \boldsymbol{H}_2^{(1)} + \boldsymbol{H}_{1,2}^{(1)} + \boldsymbol{H}_{2,1}^{(1)})$ and
$t_1 = 1$.
for $l = 1, 2, \cdots, l_{\max}$ **do**
  Update $\boldsymbol{F}^{(l)} = [\boldsymbol{F}_1^{(l)}, \boldsymbol{F}_2^{(l)}, \boldsymbol{F}_{1,2}^{(l)}, \boldsymbol{F}_{2,1}^{(l)}]$ with $\boldsymbol{F}_1^{(l)} = \mathcal{M}_{\omega\mu,\boldsymbol{c}_1,\boldsymbol{c}_1}(\boldsymbol{H}_1^{(l)} + \omega\boldsymbol{R}^{(l)})$,
  $\boldsymbol{F}_2^{(l)} = \mathcal{M}_{\omega\mu,\boldsymbol{c}_2,\boldsymbol{c}_2}(\boldsymbol{H}_2^{(l)} + \omega\boldsymbol{R}^{(l)})$,
  $\boldsymbol{F}_{1,2}^{(l)} = \mathcal{M}_{\omega\mu,\boldsymbol{c}_1,\boldsymbol{c}_2}(\boldsymbol{H}_{1,2}^{(l)} + \omega\boldsymbol{R}^{(l)})$ and
  $\boldsymbol{F}_{2,1}^{(l)} = \mathcal{M}_{\omega\mu,\boldsymbol{c}_2,\boldsymbol{c}_1}(\boldsymbol{H}_{2,1}^{(l)} + \omega\boldsymbol{R}^{(l)})$,
  $t_{l+1} = \frac{1+\sqrt{1+4t_l^2}}{2}$,
  $\boldsymbol{H}^{(l+1)} = [\boldsymbol{H}_1^{(l+1)}, \boldsymbol{H}_2^{(l+1)}, \boldsymbol{H}_{1,2}^{(l+1)}, \boldsymbol{H}_{2,1}^{(l+1)}] = \boldsymbol{F}^{(l)} + \frac{t_l - 1}{t_{l+1}}(\boldsymbol{F}^{(l)} - \boldsymbol{F}^{(l-1)})$ and
  $\boldsymbol{R}^{(l+1)} = \boldsymbol{F}_q^\delta|_{\Omega^c} - (\boldsymbol{I} - \mathcal{P}_\Omega)(\boldsymbol{H}_1^{(l+1)} + \boldsymbol{H}_2^{(l+1)} + \boldsymbol{H}_{1,2}^{(l+1)} + \boldsymbol{H}_{2,1}^{(l+1)})$.
  if $\|\boldsymbol{R}^{(l+1)}\|_{\mathrm{HS}} \leq \varepsilon$ **then**
    Set $l_{\max} = l$.
  end if
end for
Set $[\widetilde{\boldsymbol{F}}_{q_1}, \widetilde{\boldsymbol{F}}_{q_2}, \widetilde{\boldsymbol{F}}_{q_1,q_2}, \widetilde{\boldsymbol{F}}_{q_2,q_1}] = \boldsymbol{F}^{(l_{\max})}$ and
  $\widetilde{\boldsymbol{F}}_q = \widetilde{\boldsymbol{F}}_{q_1} + \widetilde{\boldsymbol{F}}_{q_2} + \widetilde{\boldsymbol{F}}_{q_1,q_2} + \widetilde{\boldsymbol{F}}_{q_2,q_1}$.

The resulting method is described in Algorithm 6. Compared to Algorithm 3 again only a modification of the evaluations of the residuum is required.

6.1.5. (SPLITTING AND) COMPLETION BY COUPLED L^1 AND $\ell^1 \times \ell^1$ MINIMIZATION WITH A FISTA TYPE METHOD

Suppose we have no a priori knowledge on the non-observable set Ω but still on the center $\boldsymbol{c}$ of a ball that contains the whole scatterer. Then, one can tackle far field operator completion by solving the coupled minimization problem (5.9). For suitably chosen $\mu > 0$ it is equivalent to minimize the related Tikhonov functional

$$(\boldsymbol{F}, \boldsymbol{B}) \mapsto \|\boldsymbol{F}_q^\delta|_\Omega - (\boldsymbol{F} + \boldsymbol{B})\|_{\mathrm{HS}}^2 + \mu\Big(\tfrac{1}{\lambda}\|\mathcal{T}_{\boldsymbol{c}}\boldsymbol{F}\|_{\ell^1\times\ell^1} + \lambda\|\boldsymbol{B}\|_{L^1}\Big),$$

cf. [49, Prop. 2.2]. We note that $\|\cdot\|_{L^1}$ is given as in Subsection 4.1.3. Due to (D.2) with $J = 2$ and Example D.2 (i)–(ii) the unique minimizer of this functional solves for $0 < \omega < 1/2$ the fixed point equation

$$\begin{bmatrix} \boldsymbol{F} \\ \boldsymbol{B} \end{bmatrix} = \begin{bmatrix} \mathcal{M}_{\frac{\omega\mu}{\lambda},\boldsymbol{c},\boldsymbol{c}}(\boldsymbol{F} + \omega(\boldsymbol{F}_q^\delta|_\Omega - \boldsymbol{F} - \boldsymbol{B})) \\ \mathcal{S}_{\omega\lambda\mu}(\boldsymbol{B} + \omega(\boldsymbol{F}_q^\delta|_\Omega - \boldsymbol{F} - \boldsymbol{B})) \end{bmatrix}$$

with $\mathcal{M}_{\frac{\omega\mu}{\lambda},\boldsymbol{c},\boldsymbol{c}}$ given as in (4.5) and $\mathcal{S}_{\omega\lambda\mu}$ as in (D.3). It can be approximated by a modified version of FISTA (cf. [34, Subsubsec. 1.4.2]). As before, we have to use the proximal operator of $\omega\mu/\lambda\|\mathcal{T}_{\boldsymbol{c}}(\cdot)\|_{\ell^1\times\ell^1}$ in direction $\boldsymbol{F}$, but additionally the proximal operator of $\omega\mu\lambda\|\cdot\|_{L^1}$ in direction $\boldsymbol{B}$. Far field operator splitting and completion for an unknown non-observable set Ω, but a priori

Algorithm 6 Far field operator splitting and completion by RPCP via FISTA type method

Input: Noisy observed far field matrix $\boldsymbol{F}_q^\delta|_{\Omega^c}$, projection $\mathcal{P}_\Omega$ on non-observable set, wave number k, a priori knowledge on position $\boldsymbol{c}_2$, maximum number of proximal gradient iterations $l_{\max}$, regularization parameter $\mu > 0$, coupling parameter $\lambda > 0$, initial guess $\boldsymbol{F} = [\boldsymbol{F}_{1,2}, \boldsymbol{F}_2]$, tolerance $\varepsilon > 0$.

Output: Approximation $\widetilde{\boldsymbol{F}}_q$ to far field matrix $\boldsymbol{F}_q$.

Set $\omega = 1/3$.
Initialize $\boldsymbol{H}^{(1)} = [\boldsymbol{H}_L^{(1)}, \boldsymbol{H}_S^{(1)}] = \boldsymbol{F}$,
$\boldsymbol{F}^{(1)} = [\boldsymbol{L}^{(1)}, \boldsymbol{S}^{(1)}] = \boldsymbol{F}$,
$\boldsymbol{R}^{(1)} = \boldsymbol{F}_q^\delta|_{\Omega^c} - (\boldsymbol{I} - \mathcal{P}_\Omega)(\boldsymbol{H}_L^{(1)} + \boldsymbol{H}_S^{(1)})$ and
$t_1 = 1$.
for $l = 1, 2, \cdots, l_{\max}$ **do**
  Update $\boldsymbol{F}^{(l)} = [\boldsymbol{L}^{(l)}, \boldsymbol{S}^{(l)}]$ with $\boldsymbol{L}^{(l)} = \mathcal{D}_\mu(\boldsymbol{H}_L^{(l)} + \omega \boldsymbol{R}^{(l)})$ and
  $\boldsymbol{S}^{(l)} = \mathcal{M}_{\lambda\mu, \boldsymbol{c}_2, \boldsymbol{c}_2}(\boldsymbol{H}_S^{(l)} + \omega \boldsymbol{R}^{(l)})$,
  $t_{l+1} = \frac{1+\sqrt{1+4t_l^2}}{2}$,
  $\boldsymbol{H}^{(l+1)} = [\boldsymbol{H}_L^{(l+1)}, \boldsymbol{H}_S^{(l+1)}] = \boldsymbol{F}^{(l)} + \frac{t_l - 1}{t_{l+1}}(\boldsymbol{F}^{(l)} - \boldsymbol{F}^{(l-1)})$ and
  $\boldsymbol{R}^{(l+1)} = \boldsymbol{F}_q^\delta|_{\Omega^c} - (\boldsymbol{I} - \mathcal{P}_\Omega)(\boldsymbol{H}_L^{(l+1)} + \boldsymbol{H}_S^{(l+1)})$.
  if $\|\boldsymbol{R}^{(l+1)}\|_{\mathrm{HS}} \leq \varepsilon$ **then**
    Set $l_{\max} = l$.
  end if
  Set $[\widetilde{\boldsymbol{F}}_{q_1,q_2}, \widetilde{\boldsymbol{F}}_{q_2}] = \boldsymbol{F}^{(l_{\max})}$ and
  $\widetilde{\boldsymbol{F}}_q = \widetilde{\boldsymbol{F}}_{q_1,q_2} + \widetilde{\boldsymbol{F}}_{q_2}$.
end for

known positions $\boldsymbol{c}_j$ of the scatterer's components, $j = 1, 2$, can be tackled in a similar way. This leads to the Tikhonov functional

$$(\boldsymbol{F}_1, \boldsymbol{F}_2, \boldsymbol{F}_{1,2}, \boldsymbol{F}_{2,1}, \boldsymbol{B}) \mapsto \|\boldsymbol{F}_q^\delta|_\Omega - (\boldsymbol{F}_1 + \boldsymbol{F}_2 + \boldsymbol{F}_{1,2} + \boldsymbol{F}_{2,1} + \boldsymbol{B})\|_{\mathrm{HS}}^2 + \mu\Big(\lambda\|\boldsymbol{B}\|_{L^1} + \frac{1}{\lambda}(\|\mathcal{T}_{\boldsymbol{c}_1}\boldsymbol{F}_1\|_{\ell^1\times\ell^1} + \|\mathcal{T}_{\boldsymbol{c}_2}\boldsymbol{F}_2\|_{\ell^1\times\ell^1} + \|\mathcal{T}_{\boldsymbol{c}_1,\boldsymbol{c}_2}\boldsymbol{F}_{1,2}\|_{\ell^1\times\ell^1} + \|\mathcal{T}_{\boldsymbol{c}_2,\boldsymbol{c}_1}\boldsymbol{F}_{2,1}\|_{\ell^1\times\ell^1})\Big),$$

whose unique minimizer is, for suitably chosen $\mu > 0$ and all $0 < \omega < 1/5$, characterized by the fixed point equation

$$\begin{bmatrix} \boldsymbol{F}_1 \\ \boldsymbol{F}_2 \\ \boldsymbol{F}_{1,2} \\ \boldsymbol{F}_{2,1} \\ \boldsymbol{B} \end{bmatrix} = \begin{bmatrix} \mathcal{M}_{\frac{\omega\mu}{\lambda}, \boldsymbol{c}_1, \boldsymbol{c}_1}(\boldsymbol{F}_1 + \omega(\boldsymbol{F}_q^\delta|_\Omega - (\boldsymbol{F}_1 + \boldsymbol{F}_2 + \boldsymbol{F}_{1,2} + \boldsymbol{F}_{2,1} + \boldsymbol{B}))) \\ \mathcal{M}_{\frac{\omega\mu}{\lambda}, \boldsymbol{c}_2, \boldsymbol{c}_2}(\boldsymbol{F}_2 + \omega(\boldsymbol{F}_q^\delta|_\Omega - (\boldsymbol{F}_1 + \boldsymbol{F}_2 + \boldsymbol{F}_{1,2} + \boldsymbol{F}_{2,1} + \boldsymbol{B}))) \\ \mathcal{M}_{\frac{\omega\mu}{\lambda}, \boldsymbol{c}_1, \boldsymbol{c}_2}(\boldsymbol{F}_{1,2} + \omega(\boldsymbol{F}_q^\delta|_\Omega - (\boldsymbol{F}_1 + \boldsymbol{F}_2 + \boldsymbol{F}_{1,2} + \boldsymbol{F}_{2,1} + \boldsymbol{B}))) \\ \mathcal{M}_{\frac{\omega\mu}{\lambda}, \boldsymbol{c}_2, \boldsymbol{c}_1}(\boldsymbol{F}_{2,1} + \omega(\boldsymbol{F}_q^\delta|_\Omega - (\boldsymbol{F}_1 + \boldsymbol{F}_2 + \boldsymbol{F}_{1,2} + \boldsymbol{F}_{2,1} + \boldsymbol{B}))) \\ \mathcal{S}_{\omega\lambda\mu}(\boldsymbol{B} + \omega(\boldsymbol{F}_q^\delta|_\Omega - (\boldsymbol{F}_1 + \boldsymbol{F}_2 + \boldsymbol{F}_{1,2} + \boldsymbol{F}_{2,1} + \boldsymbol{B}))) \end{bmatrix}.$$

This also follows from (D.2) with $J = 5$ and Example D.2 (i)–(ii) The resulting method for far field operator splitting and completion is described in Algorithm 7. In comparison to Algorithm 2, a fifth matrix is added to the cell-structure, which models the non-observable part.

6.1.6. Completion by Singular Value Thresholding

Although we have no stability analysis for this problem formulation we further approximate the solution of the far field operator completion problem for some noise level $\delta > 0$ by the solution of

Algorithm 7 Far field operator splitting and completion by coupled L^1 and $\ell^1 \times \ell^1$ minimization via FISTA type method

Input: Noisy observed far field matrix $\boldsymbol{F}_q^\delta|_{\Omega^c}$, wave number k, a priori knowledge on positions $\boldsymbol{c}_1$ and $\boldsymbol{c}_2$, maximum number of proximal gradient iterations $l_{\max}$, regularization parameter $\mu > 0$, coupling parameter $\lambda > 0$, initial guess $\boldsymbol{F} = [\boldsymbol{F}_1, \boldsymbol{F}_2, \boldsymbol{F}_{1,2}, \boldsymbol{F}_{2,1}, \boldsymbol{B}]$, tolerance $\varepsilon > 0$.

Output: Approximations $\widetilde{\boldsymbol{F}}_q$ and $\widetilde{\boldsymbol{B}}_q$ to $\boldsymbol{F}_q$ and $\boldsymbol{B}_q$.

Set $\omega = 1/6$.
Initialize $\boldsymbol{H}^{(1)} = [\boldsymbol{H}_1^{(1)}, \boldsymbol{H}_2^{(1)}, \boldsymbol{H}_{1,2}^{(1)}, \boldsymbol{H}_{2,1}^{(1)}, \boldsymbol{H}_B^{(1)}] = \boldsymbol{F}$,
  $\boldsymbol{F}^{(0)} = [\boldsymbol{F}_1^{(0)}, \boldsymbol{F}_2^{(0)}, \boldsymbol{F}_{1,2}^{(0)}, \boldsymbol{F}_{2,1}^{(0)}, \boldsymbol{B}^{(0)}] = \boldsymbol{F}$
  $\boldsymbol{R}^{(1)} = \boldsymbol{F}_q^\delta|_{\Omega^c} - (\boldsymbol{H}_1^{(1)} + \boldsymbol{H}_2^{(1)} + \boldsymbol{H}_{1,2}^{(1)} + \boldsymbol{H}_{2,1}^{(1)} + \boldsymbol{H}_B^{(1)})$ and
  $t_1 = 1$.
for $l = 1, 2, \cdots, l_{\max}$ **do**
  Update $\boldsymbol{F}^{(l)} = [\boldsymbol{F}_1^{(l)}, \boldsymbol{F}_2^{(l)}, \boldsymbol{F}_{1,2}^{(l)}, \boldsymbol{F}_{2,1}^{(l)}, \boldsymbol{B}^{(l)}]$ with $\boldsymbol{F}_1^{(l)} = \mathcal{M}_{\frac{\omega\mu}{\lambda}, \boldsymbol{c}_1, \boldsymbol{c}_1}(\boldsymbol{H}_1^{(l)} + \omega \boldsymbol{R}^{(l)})$,
    $\boldsymbol{F}_2^{(l)} = \mathcal{M}_{\frac{\omega\mu}{\lambda}, \boldsymbol{c}_1, \boldsymbol{c}_1}(\boldsymbol{H}_2^{(l)} + \omega \boldsymbol{R}^{(l)})$,
    $\boldsymbol{F}_{1,2}^{(l)} = \mathcal{M}_{\frac{\omega\mu}{\lambda}, \boldsymbol{c}_1, \boldsymbol{c}_1}(\boldsymbol{H}_{1,2}^{(l)} + \omega \boldsymbol{R}^{(l)})$ and
    $\boldsymbol{F}_{2,1}^{(l)} = \mathcal{M}_{\frac{\omega\mu}{\lambda}, \boldsymbol{c}_1, \boldsymbol{c}_1}(\boldsymbol{H}_{2,1}^{(l)} + \omega \boldsymbol{R}^{(l)})$,
    $\boldsymbol{B}^{(l)} = \mathcal{S}_{\omega\lambda\mu}(\boldsymbol{H}_B^{(l)} + \omega \boldsymbol{R}^{(l)})$,
  $t_{k+1} = \frac{1+\sqrt{1+4t_l^2}}{2}$,
  $\boldsymbol{H}^{(l+1)} = [\boldsymbol{H}_1^{(l+1)}, \boldsymbol{H}_2^{(l+1)}, \boldsymbol{H}_{1,2}^{(l+1)}, \boldsymbol{H}_{2,1}^{(l+1)}, \boldsymbol{H}_B^{(l+1)}] = \boldsymbol{F}^{(l)} + \frac{t_l - 1}{t_{l+1}}(\boldsymbol{F}^{(l)} - \boldsymbol{F}^{(l-1)})$,
  $\boldsymbol{R}^{(l+1)} = \boldsymbol{F}_q^\delta|_{\Omega^c} - (\boldsymbol{H}_1^{(l+1)} + \boldsymbol{H}_2^{(l+1)} + \boldsymbol{H}_{1,2}^{(l+1)} + \boldsymbol{H}_{2,1}^{(l+1)} + \boldsymbol{H}_B^{(l+1)})$.
  if $\|\boldsymbol{R}^{(l+1)}\|_{\mathrm{HS}} \leq \varepsilon$ **then**
    Set $l_{\max} = l$.
  end if
end for
Set $[\widetilde{\boldsymbol{F}}_{q_1}, \widetilde{\boldsymbol{F}}_{q_2}, \widetilde{\boldsymbol{F}}_{q_1,q_2}, \widetilde{\boldsymbol{F}}_{q_2,q_1}, \widetilde{\boldsymbol{B}}_q] = \boldsymbol{F}^{(l_{\max})}$ and
  $\widetilde{\boldsymbol{F}}_q = \widetilde{\boldsymbol{F}}_{q_1} + \widetilde{\boldsymbol{F}}_{q_2} + \widetilde{\boldsymbol{F}}_{q_1,q_2} + \widetilde{\boldsymbol{F}}_{q_2,q_1} + \widetilde{\boldsymbol{B}}_q$.

Algorithm 8 Far field operator completion by SVT

Input: Noisy observable far field matrix $\boldsymbol{F}_q^\delta|_{\Omega^c}$, projection $\mathcal{P}_\Omega$ on non-observable set, maximum number of SVT iterations $l_{\max}$, threshold parameter $\tau > 0$, step size $\delta > 0$ and tolerance $\varepsilon > 0$.

Output: Approximation $\widetilde{\boldsymbol{F}}_q$ to far field matrix $\boldsymbol{F}_q$.

Set $\kappa = \left\lfloor \tau / (\delta \|\boldsymbol{F}_q^\delta|_{\Omega^c}\|_{\mathrm{HS}}) \right\rfloor$.
Initialize $\boldsymbol{H}^{(0)} = \kappa\delta \boldsymbol{F}_q^\delta|_{\Omega^c}$.
for $l = 1, 2, \cdots, l_{\max}$ **do**
  Update $\boldsymbol{F}^{(l)} = \mathcal{D}_{2\tau}(\boldsymbol{H}^{(l-1)})$,
    $\boldsymbol{H}^{(l)} = (I - \mathcal{P}_\Omega)(\boldsymbol{H}^{(l-1)} + \delta(\boldsymbol{F}_q^\delta|_{\Omega^c} - \boldsymbol{F}^{(l)}))$ and
    $\boldsymbol{R}^{(l)} = \boldsymbol{F}_q^\delta|_{\Omega^c} - (I - \mathcal{P}_\Omega)\boldsymbol{F}^{(l)}$.
  if $\|\boldsymbol{R}^{(l)}\|_{\mathrm{HS}} \leq \varepsilon$ **then**
    Set $l_{\max} = l$.
  end if
  Set $\widetilde{\boldsymbol{F}}_q = \boldsymbol{F}^{(l_{\max})}$.
end for

the nuclear norm minimization problem

$$\underset{\boldsymbol{F} \in \mathbb{C}^{L \times L}}{\text{minimize}} \quad \|\boldsymbol{F}\|_{\mathrm{nuc}} \quad \text{subject to} \quad \|\boldsymbol{F}_q^\delta|_{\Omega^c} - (\boldsymbol{I} - \mathcal{P}_\Omega)\boldsymbol{F}\|_{\mathrm{HS}} \leq \delta \tag{6.4}$$

with $\|\cdot\|_{\mathrm{nuc}}$ denoting the nuclear norm, i.e. the ℓ^1 norm of singular values. Here, in contrast to the previous formulations, a priori knowledge on the non-observable set Ω, but not on the scatterer's geometry is taken into account. From Definition D.1 we know, that the proximity operator $\mathcal{D}_{2\tau}(\boldsymbol{F})$ of $\tau\|\cdot\|_{\mathrm{nuc}}$ given as in Example D.2 (iii) minimizes for all $\tau > 0$ the functional

$$\boldsymbol{F} \mapsto \tau\|\boldsymbol{F}\|_{\mathrm{nuc}} + \frac{1}{2}\|\boldsymbol{F}_q^\delta|_{\Omega^c} - (\boldsymbol{I} - \mathcal{P}_\Omega)\boldsymbol{F}\|_{\mathrm{HS}}^2\,,$$

see also [15, Thm. 2.1]. This motivates to perform the *Singular Value Thresholding (SVT) algorithm* as it is proposed in [15, Alg. 1] for step sizes $(\delta_k)_k$ and described in Algorithm 8. In [15, Thm. 4.2] it is shown that for $1 < \inf \delta_k \leq \sup \delta_k < 2$ for all k the SVT iterates converge to the unique solution of the problem

$$\underset{\boldsymbol{F}\in\mathbb{C}^{L\times L}}{\text{minimize}} \quad \tau\|\boldsymbol{F}\|_{\mathrm{nuc}} + \frac{1}{2}\|\boldsymbol{F}\|_{\mathrm{HS}}^2 \quad \text{subject to} \quad \|\boldsymbol{F}_q^\delta|_{\Omega^c} - (\boldsymbol{I} - \mathcal{P}_\Omega)\boldsymbol{F}\|_{\mathrm{HS}} \leq \delta\,,$$

and that for a sufficiently large threshold parameter $\tau > 0$ this solution approximates a minimizer of problem (6.4), see [15, Thm. 3.1]. The here stated version of the SVT algorithm is slightly simplified in the sense that no adaptive step width control is implemented and a full singular value decomposition is calculated in each step. In case of large matrices, it may be extended by implementing the acceleration from [15, Alg. 1], which allows us to calculate the singular value decomposition of smaller matrices in each step. Since the matrices of our problem class are relatively small, we have not realized this in our implementation. In [15, p. 1973] it is proposed to choose $\tau = 5L$ as well as a constant step size $\delta_k = \overline{\delta} = 1.2L^2/m$ for all k with m denoting the number of non-zero entries of $\boldsymbol{P}_\Omega$. The latter choice turned out to be unsuitable for our purposes in numerical experiments. Instead we set $\overline{\delta} = \min\{1.2L^2/m, 1.99\}$. Given the approximation $\widetilde{\boldsymbol{F}}_q$, the related non-observable part can again be approximated by setting $\widetilde{\boldsymbol{B}}_q := -\mathcal{P}_\Omega\widetilde{\boldsymbol{F}}_q$.

6.2. Numerical tests using synthetic data

We choose the wave number $k = 0.5$ and fix a similar geometrical setup as in our numerical tests on far field operator splitting in Section 4.2, i.e., we assume the scatterer $D = D_1 \cup D_2$ to consist of two well-separated components, a nut shaped scatterer D_1 and a kite shaped scatterer D_2 as depicted in Figure 6.1. Furthermore, let the associated contrast function $q := -0.5\chi_{D_1} + \chi_{D_2}$ be piecewise constant. We simulate the associated far field operator $\boldsymbol{F}_q$ as described in Example 2.5 and Subsection 4.1.1 using $L = 100$ equidistant distributed illumination and observation directions. From Example 6.1 we know that the whole scatterer is contained in a ball of radius $R = 14.25$, so the number of discretization points is large enough to resolve the $\boldsymbol{F}_q$ with sufficient accuracy, see also Example 4.1.

On the one hand, we investigate the performance of our methods for varying size $|\Omega|$ and varying structure of the non-observable set Ω. On the other hand, we analyze how much the results improve if, instead of solving only the completion problem (cf. Example 6.1), we split and complete at the same time (cf. Example 6.2). In the last Example 6.3 we consider a different scatterer with missing backscattering data within a certain angular range for different wave numbers. This should serve as a benchmark for our tests with the experimental data in the following section. As was the case in Chapter 4, the assumptions of our corresponding stability theorems are not satisfied in any of the examples because the scatterers are too close to each other relative to their size. Nevertheless, our methods provide useful reconstructions in most of the cases.

Example 6.1 (Completion for varying size $|\Omega|$ of Ω)**.** We study the accuracy of our numerical reconstructions depending on the size $|\Omega|$ of the non-observable set Ω. To examine how the quality of our reconstructions depends not only on the size of Ω, but also on its geometric structure, we analyze three different test scenarios. For our first test, we assume that the missing data segment $\Omega_1(\alpha)$

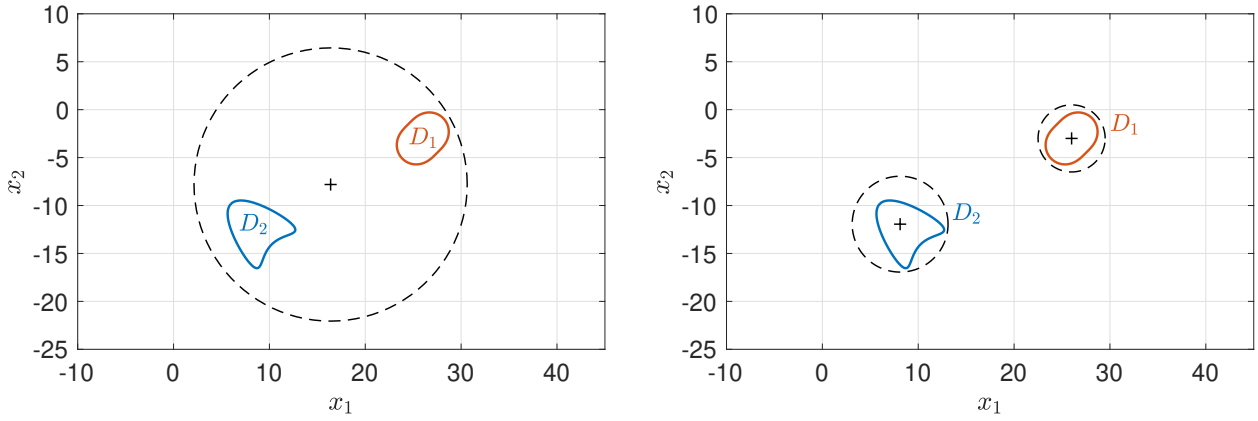

FIGURE 6.1. Geometry of scatterer (solid) and a priori information on its location and size (dashed). Left: For completion only in Example 6.1. Right: For splitting and completion in Example 6.2.

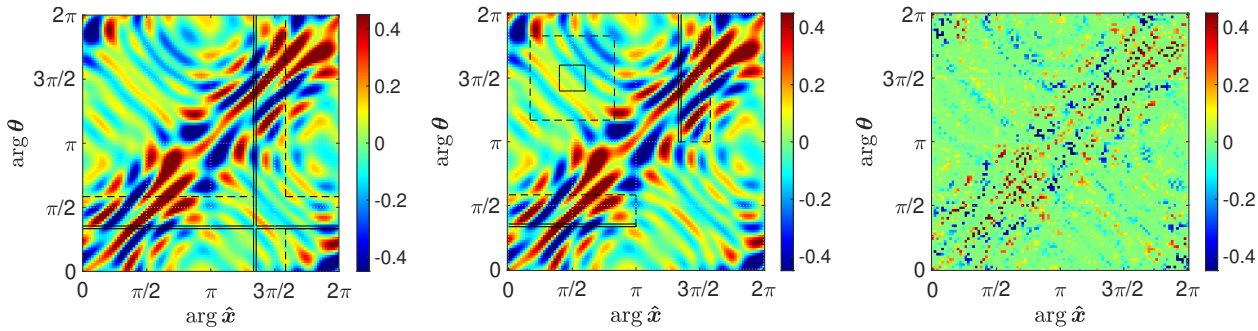

FIGURE 6.2. Real part of discretized far field operator $\boldsymbol{F}_q$ together with different missing data segments. Left: Smallest (solid, 2.7% missing data) and largest (dashed, 23.7% missing data) cross-shaped missing data segment $\Omega = \Omega_1$. Middle: Smallest (solid, 2.3% missing data) and largest (dashed, 23.3% missing data) disconnected missing data segment $\Omega = \Omega_2$. Right: Largest (75.1% missing data) randomly chosen missing data segment $\Omega = \Omega_3$.

is supported on a union of two stripes of width α. This is shown in Figure 6.2 (left) in polar coordinates for the smallest value $\alpha = 1/48$ (solid) and largest value $\alpha = 1/4$ (dashed) of α, and it leads to missing data of between 2.7% and 23.7%. In our second test, we suppose that the missing data segment $\Omega_2(\alpha)$ is supported on a union of two stripes of width α and length π and a square with side length $\sqrt{\alpha(2\pi - \alpha)}$. This is shown in Figure 6.2 (middle) for the smallest value $\alpha = 1/48$ (solid) and largest value $\alpha = 1/4$ (dashed) of α, and it leads to missing data of between 2.3% and 23.3%. In our third test, we choose Ω_3 randomly by computing between 2250 and 45000 equally independent and uniformly distributed indices, that are assigned to Ω. This leads to missing data of between 8.3% and 75.1%. The resulting observable far field operator for the latter is shown in Figure 6.2 (right).

We use the cg method, FISTA, SVT and the version of FISTA for coupled L^1 and $\ell^1 \times \ell^1$ minimization from Subsections 5.1.1, 5.1.2, 6.1.6 and 6.1.5, respectively, for solving far field operator completion. For the cg method we assume the dashed ball $B_R(\boldsymbol{c})$ in Figure 6.1 (left) and the non-observable set Ω to be known a priori. The choice $R = 14.25$ leads to the subspace dimension $2N + 1 = 2\lceil ekR/2 \rceil + 1 = 21$, according to (4.1). For FISTA we use the regularization parameter $\mu = 5 \times 10^{-5}$, and we assume that the position $\boldsymbol{c}$ of the scatterer, marked by a cross in Figure 6.1 (left), as well as the non-observable set Ω is given. SVT only requires knowledge of the non-observable set Ω. We use the proposed parameter choices of τ and $\overline{\delta}$ from Subsection 6.1.6.

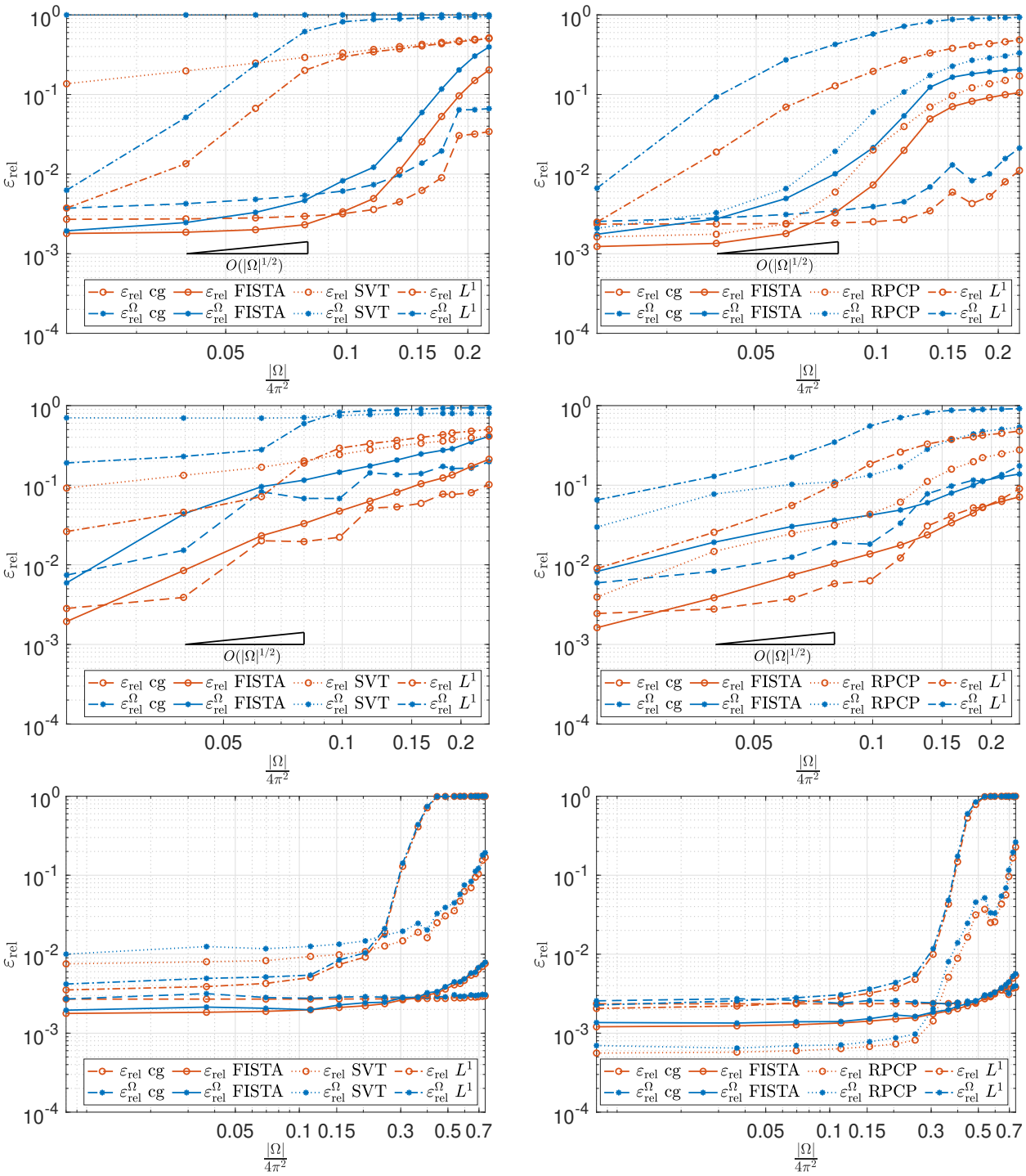

FIGURE 6.3. Relative errors of far field operator completion (left) and far field operator completion and splitting (right) for varying size of the missing data segment.
Top: For cross-shaped missing data segment $\Omega = \Omega_1$. Middle: For disconnected missing data segment $\Omega = \Omega_2$. Bottom: For randomly chosen missing data segment $\Omega = \Omega_3$.

For the modified version of FISTA, solving the coupled L^1 and $\ell^1 \times \ell^1$ minimization problem setting $\lambda = 8$ and $\mu = 8 \times 10^{-4}$ turns out to be appropriate, where only the position $\boldsymbol{c}$ is supposed to be given.

The results are shown in Figure 6.3 (left) on a logarithmic scale. As suggested by the associated stability estimates (5.4), (5.7) and (5.10), all relative errors decay in $|\Omega|$. In all tests, the cg method

and FISTA yield the best results, with FISTA providing the most accurate approximations for a small number of missing entries. However, for larger values of $|\Omega|$, the performance of FISTA deteriorates earlier than the one of the cg method. For the first test, the cg method generates satisfying results up to about 14% missing data, FISTA up to about 10% missing data and the fourth method only for the first data point, so about 3% missing data. SVT does not provide a useful reconstruction for all considered sets Ω_1. In the second test, all reconstructions are worse than in the first test, for comparable sizes of Ω. Since Ω_1 as well as Ω_2 are supported on the two stripes, this worsening is due to the additional square in the support of Ω_2. It seems that not only the size $|\Omega|$ of Ω plays a role, but also something like the radius of the largest ball that is completely contained in Ω. In the second test, the cg method and FISTA only yield satisfying results for the smallest missing data segment of about 3% missing data. The other two methods do not provide satisfying approximations. When deleting randomly chosen entries of the far field operator $\boldsymbol{F}_q$ in the third test, even in the case of about 75% missing data the reconstructions of the cg method and FISTA are surprisingly good. This further confirms our hypothesis that the geometric structure of Ω in the previous mentioned form influences how good the reconstructions are. In that test, the fourth method and SVT are successful for up to 20%, which particularly implies that SVT can only compete with the other approaches in the third test, and even there, it provides the worst results. A convergence order with respect to $|\Omega|$ is not identifiable for all curves. ◊

Example 6.2 (Splitting and completion for varying size $|\Omega|$ of Ω)**.** We consider the same setting as in the previous example, but instead of solving only the completion problem, we solve the splitting and the completion problem simultaneously. Here, we use the cg method as described in Algorithm 4, FISTA as described in Algorithm 5 and the FISTA type method solving RPCP as described in Algorithm 6 as well as the FISTA version solving the coupled problem as described in Algorithm 7. For the cg method we assume the dashed circles in Figure 6.1 (right) and the non-observable set Ω to be known a priori, where, according to (4.1), the choices $R_1 = 3.5$ and $R_2 = 5$ lead to the subspace dimensions $2N_1 + 1 = 2\lceil ekR_1/2\rceil + 1 = 5$ and $2N_2 + 1 = 2\lceil ekR_2/2\rceil + 1 = 7$, respectively. For FISTA we assume the positions $\boldsymbol{c}_1$ and $\boldsymbol{c}_2$ of both dashed circles and Ω to be given, and we choose the regularization parameter $\mu = 4 \times 10^{-5}$. For the RPCP formulation we only assume the position $\boldsymbol{c}_2$ of the kite shaped scatterer and Ω to be known a priori, and we set $\lambda = 10^{-4}$ and $\mu = 10^{-5}/\lambda$. Finally, for the fourth method we suppose the positions $\boldsymbol{c}_1$ and $\boldsymbol{c}_2$ of both scatterer's components to be given, and we set $\lambda = 8$ and $\mu = 8 \times 10^{-5}\lambda$.

The results are shown in Figure 6.3 (right). In the first two tests, we obtain significantly better reconstructions by using the cg method compared to the previous example. This appears reasonable recalling our stability estimate (5.14) since $R_1 + R_2 = 8.5 < 14.25 = R$. For FISTA this improvement is only observable in the second test, although the related stability estimate (5.17) also suggests this in the first test. The third method provides reconstructions of approximately the same quality as FISTA in the first test, and the fourth only convinces in the first data point, so for about 3% missing data in that case. Concerning the second test, these two methods also only perform well for about 3% missing data. When removing randomly chosen entries in the third test, the fourth method yields good approximations for up to 30% missing entries, the third method for up to 40% missing entries and the cg method and FISTA for all considered sets Ω_3, as it was already the case in the previous example. ◊

To link our tests with synthetic data to the tests with real data, in the next section we consider a further example with missing backscattering data and a single scattering object of similar size for the same wave numbers k. Since both SVT and the modified version of FISTA solving the coupled L^1 and $\ell^1 \times \ell^1$ minimization problem have proven to be clearly at a disadvantage compared to the cg method and FISTA in Example 6.1, we only use the latter two methods for far field operator completion in this example as well as in the tests in Section 6.3.

Example 6.3 (Completion with missing backscattering data)**.** We consider a kite shaped scatterer D as shown in Figure 6.4 (left) with a contrast function given by $q = 2\chi_D$. The associated

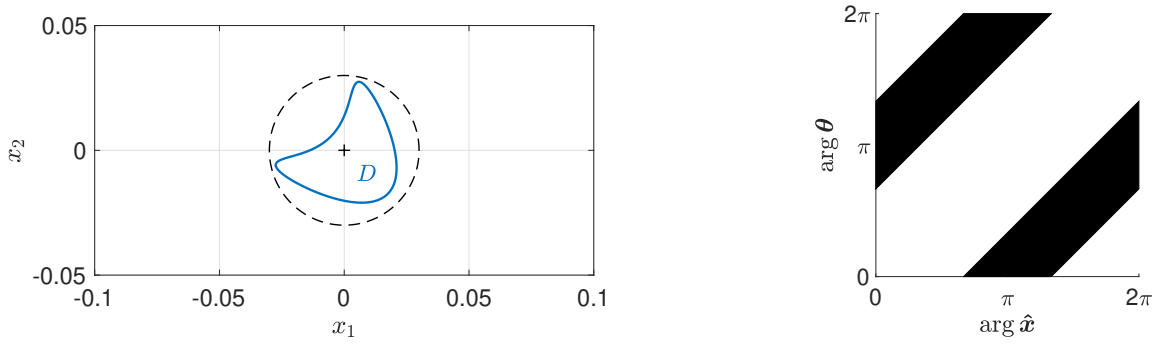

FIGURE 6.4. Left: Geometry of kite shaped scatterer (solid) and a priori information on location $\boldsymbol{c} = (0,0)^\top$ and size $R = 0.03$ (dashed). Right: Non-observable set Ω.

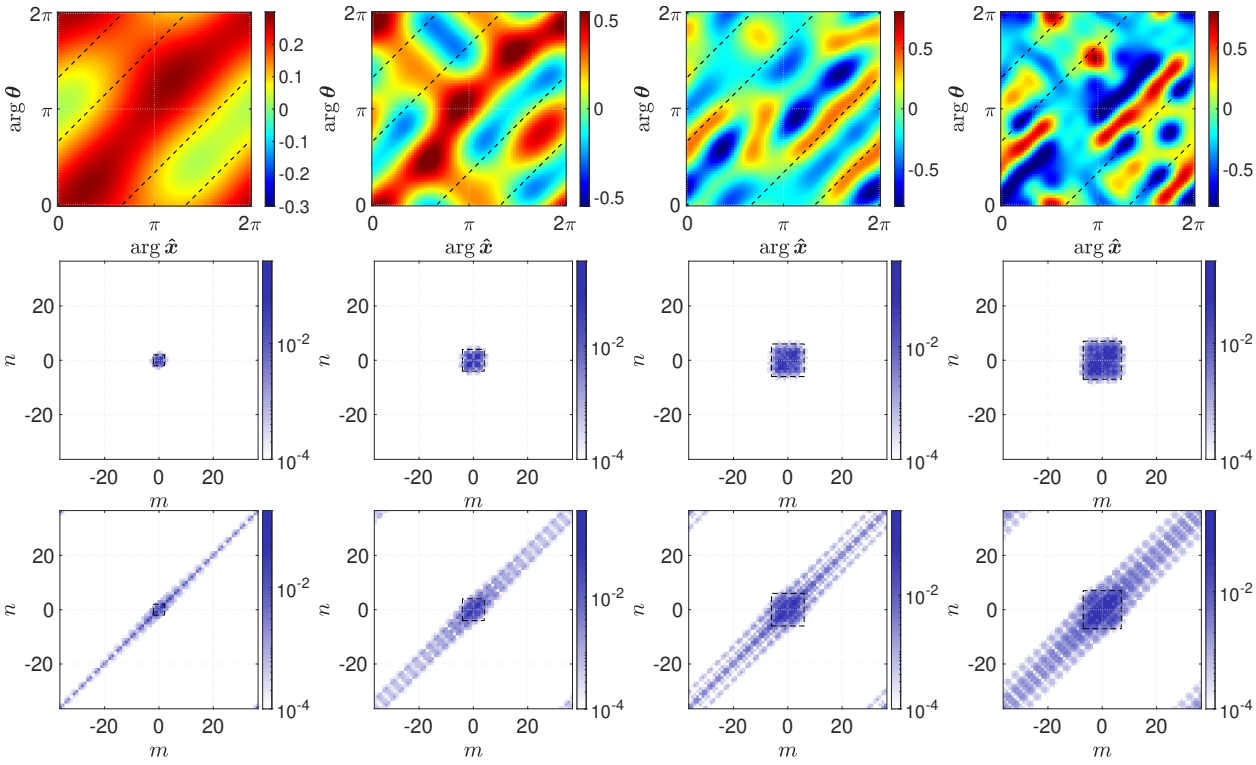

FIGURE 6.5. Top: Real part of discretized far field operator $\boldsymbol{F}_q$ for kite shaped scatterer and different values of k together with dashed marked non-observable set Ω. Middle: Absolute values of Fourier coefficients of $\boldsymbol{F}_q$. Bottom: Absolute values of Fourier coefficients of discretized observable far field operator $\boldsymbol{F}_q|_{\Omega^c}$. Left: $k = 41.9$. Middle left: $k = 83.8$. Middle right: $k = 125.8$. Right: $k = 167.7$.

discretized far field operator $\boldsymbol{F}_q$ is simulated for the four wave numbers from Section 6.3 below, so $k \in \{41.9, 83.8, 125.8, 167.7\}$. Furthermore, we suppose missing backscattering data within an angular range of 120°, i.e., the non-observable set Ω is given by

$$\Omega := \left\{ (\hat{\boldsymbol{x}}, \boldsymbol{\theta}) \in S^1 \times S^1 \,|\, |\arg \boldsymbol{\theta} - (\arg \hat{\boldsymbol{x}} + \pi)| \leq \tfrac{\pi}{3} \right\}, \tag{6.5}$$

which is plotted in Figure 6.4 (right) and corresponds to about 33% missing data. Such type of a non-observable set Ω is considered in Example 5.4. Here, we observed that no reduction of the missing data is possible by taking reciprocity into account. The discretized far field operator $\boldsymbol{F}_q$ together with the dashed marked non-observable set Ω is shown in Figure 6.5 (top). Since the

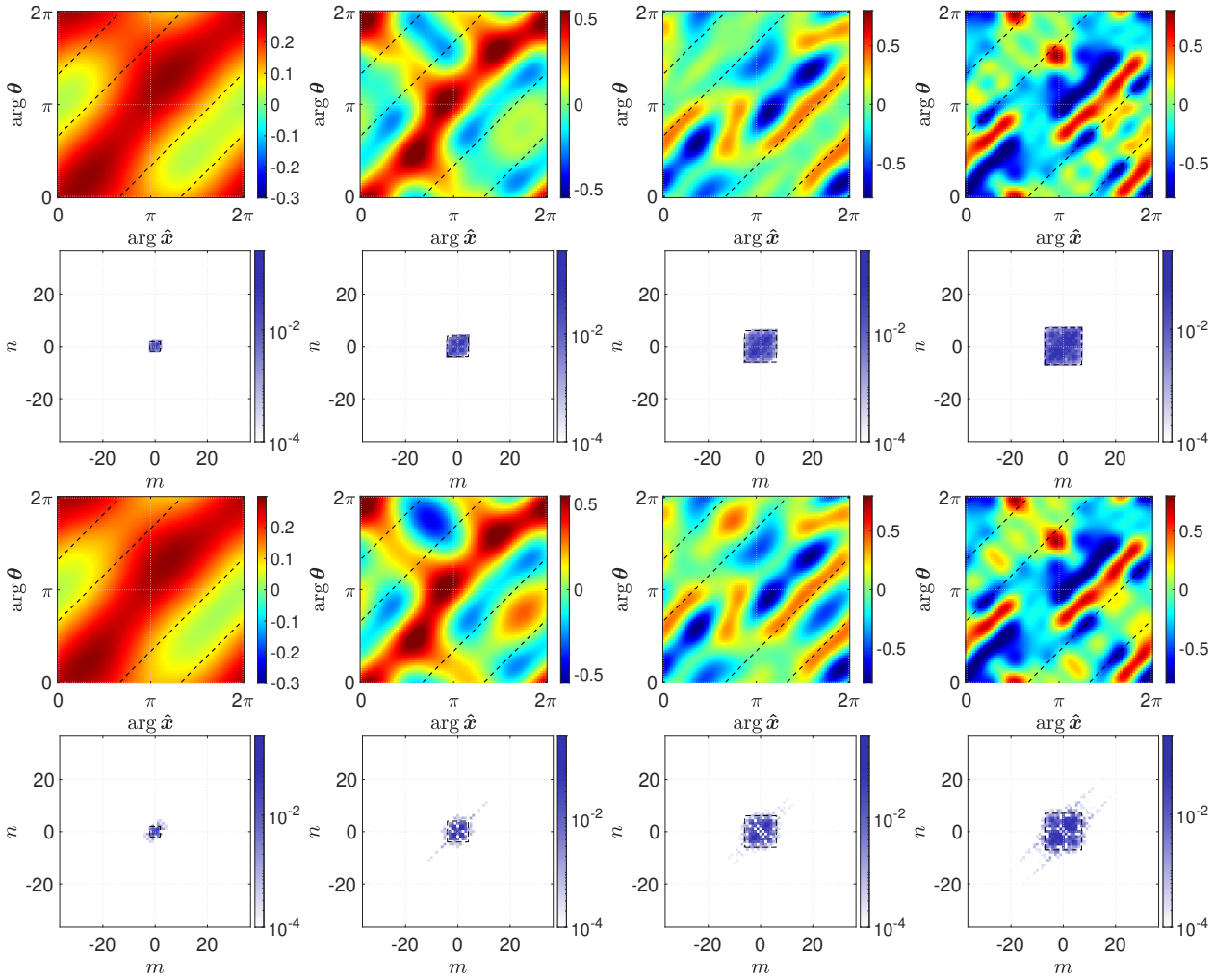

FIGURE 6.6. Real part of reconstructed far field operator $\widetilde{\boldsymbol{F}}_q$ for kite shaped scatterer and different values of k. First row: cg method. Third row: FISTA. Absolute values of Fourier coefficients $(a_{m,n})_{m,n}$ of $\widetilde{\boldsymbol{F}}_q$. Second row: cg method. Fourth row: FISTA. Left: $k = 41.9$. Middle left: $k = 83.8$. Middle right: $k = 125.8$. Right: $k = 167.7$.

scatterer is located in the origin, the translation operator $\mathcal{T}_{\boldsymbol{c}}$ can be omitted. Thus, we compute the Fourier coefficients of $\boldsymbol{F}_q$ and those of the observable part $\boldsymbol{F}_q|_{\Omega^c} = \boldsymbol{F}_q - \mathcal{P}_\Omega \boldsymbol{F}_q$, which are plotted in Figure 6.5 (middle, bottom) on a logarithmic scale. Here, we add dashed squares marking the $\ell^0 \times \ell^0$-support of operators in $\mathcal{V}_N$ for $N = \lceil ekR/2 \rceil \in \{2, 4, 6, 7\}$ with $R = 0.03$. It can clearly be seen in all plots that the essential support of the coefficients is concentrated in the marked square, but in case of $\boldsymbol{F}_q|_{\Omega^c}$ it also spreads on a diagonal stripe of a width corresponding to the diagonal of the marked square. In this sense, the special shape of Ω seems to correspond to a certain support of noise in the associated Fourier coefficients. We use the cg method and FISTA for solving the related far field operator completion problem. For the cg method we assume the dashed circle in Figure 6.4 (left) to be known a priori, which leads to the subspace dimensions $2N + 1 \in \{5, 9, 13, 15\}$. For FISTA, we choose in all tests the regularization parameter $\mu = 10^{-4}$. The results are shown in Figure 6.6. We evaluate the relative errors ε_{rel} and $\varepsilon_{\text{rel}}^{\Omega}$ as introduced in (6.1). In case of the cg method they are given by

$$\varepsilon_{\text{rel}} \in \{0.01, 0.25, 0.25, 0.21\} \qquad \text{and} \qquad \varepsilon_{\text{rel}}^{\Omega} \in \{0.02, 0.87, 0.88, 0.69\},$$

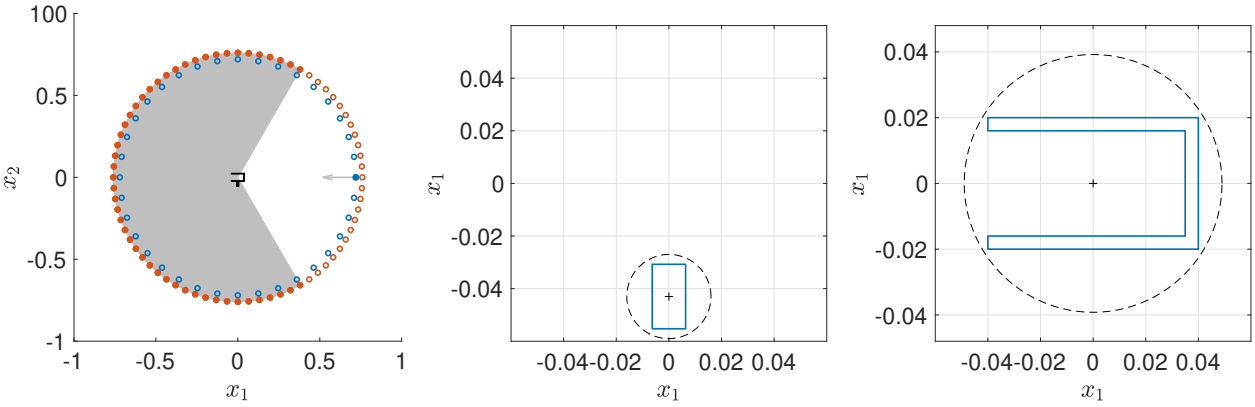

Figure 6.7. Left: Sketch of geometrical setup with emitter positions marked in red, receiver positions marked in blue and two scatterers marked in black (emitter for illumination direction $(-1,0)^\top$ highlighted together with associated observing receivers and observable area in gray). Geometry of scatterers (solid) and a priori information on their location $\boldsymbol{c} \in \mathbb{R}^2$ and size $R > 0$ (dashed). Middle: Rectangular shaped scatterer with $\boldsymbol{c} = (0\text{m}, -0.043\text{m})^\top$ and $R = 0.016\text{m}$. Right: U-shaped scatterer with $\boldsymbol{c} = (0\text{m}, 0\text{m})^\top$ and $R = 0.049\text{m}$.

and in case of FISTA by

$$\varepsilon_{\text{rel}} \in \{0.02, 0.09, 0.21, 0.22\} \qquad \text{and} \qquad \varepsilon_{\text{rel}}^{\Omega} \in \{0.07, 0.32, 0.76, 0.73\}\,.$$

From these relative errors we conclude our methods to fail for all wave numbers k except for the smallest one, and we observe the FISTA reconstructions to be a bit better for the other test cases. Since we are interested to build a benchmark for our tests on real data in the next section, we consider these extreme situations, in which we cannot expect our methods to work well. In fact, the assumptions from both stability Theorems 5.7 and 5.8 are not fulfilled even for the smallest value of k. We further calculate the relative errors by

$$\varepsilon_{\text{rel}}^{0} := \frac{\|\mathcal{P}_\Omega \boldsymbol{F}_q\|_{\text{HS}}}{\|\boldsymbol{F}_q\|_{\text{HS}}} \in \{0.31, 0.28, 0.28, 0.31\}$$

of approximating $\boldsymbol{F}_q$ by $\boldsymbol{F}_q|_{\Omega^c}$. Comparing $\varepsilon_{\text{rel}}^{0}$ to ε_{rel}, we observe that applying our methods consistently leads to an improvement over completing the non-observable entries by zero for all values of k. By further comparing the plots in Figure 6.5 to those in Figure 6.6, we recognize that the observable parts of all reconstructions visually match the given data $\boldsymbol{F}_q|_{\Omega^c}$, while their non-observable parts differ noticeably, except for $k = 41.9$. Visually, however, the impaintings also look reasonable for higher frequencies. Applying FISTA further removes most of the diagonal stripe outside the marked square. ◊

6.3. Numerical tests using experimental data

Next we test our methods on experimental data, which is provided by the Institute Fresnel, see [7]. The experimental setup is shown in Figure 6.7 (left). A cylindrical metallic scatterer (approximately) sitting in the origin is irradiated by microwaves from a linearly polarized fixed antenna acting as an emitter and positioned $R_E = 0.72\text{m}$ away from the origin. The incident wave propagates perpendicular to the axis of the cylinder and is polarized perpendicular to the axis of the cylinder. This means that its magnetic field has no component along the propagation axis, which makes this incident wave a Transverse Magnetic (TM) wave. Consequently, this three-dimensional

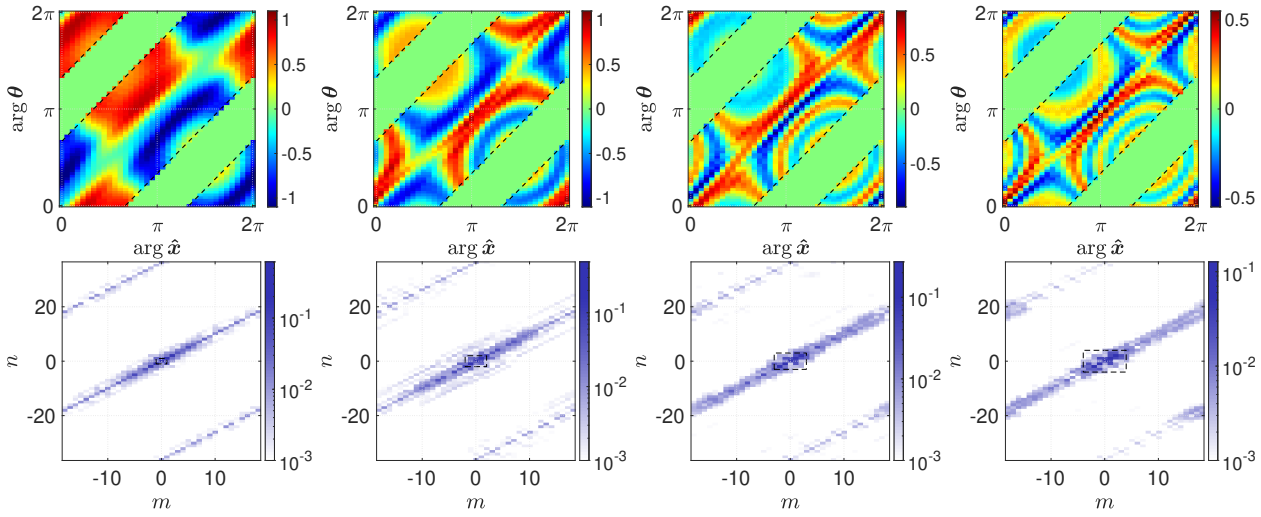

FIGURE 6.8. Top: Real part of measured far field operator $\boldsymbol{F}_q$ for rectangular scatterer and different values of k. Bottom: Absolute values of Fourier coefficients $(a_{m,n})_{m,n}$ of $\mathcal{T}_c \boldsymbol{F}_q^\delta|_{\Omega^c}$. Left: $k = 41.9\text{m}^{-1}$. Middle left: $k = 83.8\text{m}^{-1}$. Middle right: $k = 125.8\text{m}^{-1}$. Right: $k = 167.7\text{m}^{-1}$.

scattering problem can be modeled by a two-dimensional Helmholtz equation as it is derived in detail in [16, Sec. 5.1], see also [23, 82]. Here, a two-dimensional bistatic measurement system is used, i.e., additionally to the transmitter a second rotatable antenna acts as a receiver and is positioned $R_R = 0.76\text{m}$ away from the origin. Changes of the illumination direction $\boldsymbol{\theta}$ are realized by rotating the scatterer. We consider two metallic scatterers, a rectangular shaped scatterer (see Example 6.4) and a U shaped scatterer (see Example 6.5) as shown in Figure 6.7 (middle, right) together with the assumed a priori knowledge on their locations, respectively. In three dimensions this corresponds to two cylindrical scatterers with a rectangular shaped and a U-shaped cross section, respectively. We mention, that all lengths are given in decimeter. Since both the receiver and the emitter are far away from the origin compared to the size of the scatterer, cf. Figure 6.7 (left), we assume far field data, which can be obtained by multiplying the scattered field data with $R_R e^{-\mathrm{i}kR_R}/C_2$, see (2.4). Moreover, we assume the incident wave to be a plane wave given by

$$u^i(\boldsymbol{x};\boldsymbol{\theta}) \;=\; A_k e^{\mathrm{i}k\boldsymbol{x}\cdot\boldsymbol{\theta}}\,, \qquad \boldsymbol{x} \in \mathbb{R}^2\,.$$

This model of the incident wave is not clear from the data and has for example been discussed in [23, Sec. 5.1]. The constant $A_k > 0$ models the amplitude of the incident field measured in front of the emitter. Consequently, we observe that we have to divide the measured far field data by A_k to obtain far field data fitting in the framework, as it is introduced in Section 2.2, i.e., for the incident wave $u^i(\boldsymbol{x};\boldsymbol{\theta}) = e^{\mathrm{i}k\boldsymbol{x}\cdot\boldsymbol{\theta}}$, $\boldsymbol{x} \in \mathbb{R}^2$. Since we do not know the values of A_k from the data, we ignore this scaling in our numerical tests. As it can be seen in Figure 6.7 (left), measurements of the far field pattern for $L_{\widehat{\boldsymbol{x}}} = 72$ equally distributed observation and $L_{\boldsymbol{\theta}} = 36$ equally distributed illumination directions are given, i.e.,

$$\widehat{\boldsymbol{x}}_l \;:=\; (\cos\theta_l, \sin\theta_l)^\top \qquad \text{with } \theta_l \;:=\; (l-1)\frac{2\pi}{L_{\widehat{\boldsymbol{x}}}} \text{ for } l = 1,\dots,L_{\widehat{\boldsymbol{x}}}$$

and

$$\boldsymbol{\theta}_l \;:=\; (\cos\phi_l, \sin\phi_l)^\top \qquad \text{with } \phi_l \;:=\; (l-1)\frac{2\pi}{L_{\boldsymbol{\theta}}} \text{ for } l = 1,\dots,L_{\boldsymbol{\theta}}\,.$$

Since $L_{\widehat{\boldsymbol{x}}} \neq L_{\boldsymbol{\theta}}$, this leads to a non-square discretized far field operator

$$\boldsymbol{F}_q = \frac{2\pi}{L_{\boldsymbol{\theta}}} \left(u_q^\infty(\widehat{\boldsymbol{x}}_m; \boldsymbol{\theta}_n) \right)_{\substack{1 \le m \le L_{\widehat{\boldsymbol{x}}}, \\ 1 \le n \le L_{\boldsymbol{\theta}}}} \in \mathbb{C}^{L_{\widehat{\boldsymbol{x}}} \times L_{\boldsymbol{\theta}}} .$$

Due to physical limitations, the two antennas cannot be positioned closer to another than in an angle of 60°. This results in missing backscattering data within an angular range of 120° as it is considered in Example 6.3. The associated non-observable set Ω given as in (6.5) is shown in Figure 6.4 (right). For both scatterers, we consider measurements for four different frequencies f, so for four different wave numbers k, which can be related to each other by $k = 2\pi f/c$, where $c = 299792458\text{m/s}$ denotes the speed of light in vacuum. In both cases we obtain

$$f \in \{2\text{GHz}, 4\text{GHz}, 6\text{GHz}, 8\text{GHz}\}, \qquad \text{so} \qquad k \in \{41.9\text{m}^{-1}, 83.8\text{m}^{-1}, 125.8\text{m}^{-1}, 167.7\text{m}^{-1}\}.$$

These are exactly the wave numbers from Example 6.3. The size of the scatterer from Example 6.3 is similar to the size of the rectangle and the size of the U shaped scatterer. Consequently, up to unknown model errors and unknown noise, the situation in Example 6.3 is comparable to that of Example 6.4 and 6.5 below. We again emphasize that we cannot expect our methods to work well in these extreme situations. Nevertheless, also with regard to the next section, where we couple our methods with a shape identification method, we want to test if we can achieve improvements.

Example 6.4 (Completion for rectangular scatterer)**.** First, we consider the rectangular scatterer from Figure 6.7 (middle). The measured far field operator $\boldsymbol{F}_q^\delta|_{\Omega^c}$ for the different values of k is shown in Figure 6.8 (top). We further compute the Fourier coefficients of $\mathcal{T}_{\boldsymbol{c}} \boldsymbol{F}_q^\delta|_{\Omega^c}$ for $\boldsymbol{c} = (0\text{m}, -0.043\text{m})^\top$. These are plotted in Figure 6.8 (bottom) together with a dashed square corresponding to the support of the Fourier coefficients of operators in $\mathcal{V}_N^{\mathrm{c}}$ with $N = \lceil ekR/2 \rceil \in \{1, 2, 3, 4\}$ with $R = 0.016\text{m}$. It can clearly be seen in all plots that the essential support of the coefficients is concentrated in the marked square, but it also spreads on a diagonal stripe of a width corresponding to the diagonal of the marked square, which is due to the shape of Ω, see Example 6.3. We use the cg method and FISTA for completing the far field operators, which yield approximations $\widetilde{\boldsymbol{F}}_q$. Here, we assume the dashed a priori knowledge from Figure 6.7 (middle) to be given. This leads to the subspace dimensions $2N + 1 \in \{3, 5, 7, 9\}$ in the cg method. For FISTA we use the regularization parameters $\mu \in \{10^{-4}, 10^{-4}, 10^{-3}, 2 \times 10^{-3}\}$. The results are shown in Figure 6.9. While the observable parts of the FISTA reconstructions (see Figure 6.9 (third row)) visually coincide with the given data $\boldsymbol{F}_q^\delta|_{\Omega^c}$ (see Figure 6.8 (top)), the associated parts differ for the cg reconstructions (see Figure 6.9 (first row)). The support of the Fourier coefficients of the FISTA reconstructions (see Figure 6.9 (fourth row)), which should theoretically be essentially contained in $[-N, N]^2$, still spreads along the diagonal stripe, but is more concentrated after the completion with FISTA, compared to Figure 6.8 (bottom). Especially for the two larger values of k the impainting $\mathcal{P}_\Omega \widetilde{\boldsymbol{F}}_q$ of the non-observable part integrate well into the images as a whole for both methods. ◊

Example 6.5 (Completion for U-shaped scatterer)**.** As a second example, we consider the U-shaped scatterer from Figure 6.7 (right). The measured far field operator $\boldsymbol{F}_q^\delta|_{\Omega^c}$ for different values of k is plotted in Figure 6.10 (top) together with the associated Fourier coefficients $(a_{m,n})_{m,n}$ in Figure 6.10 (bottom) and the $\ell^0 \times \ell^0$-support of operators in $\mathcal{V}_N$, where $N = \lceil ekR/2 \rceil \in \{3, 6, 9, 12\}$ with $R = 0.049\text{m}$. We mention that the U-shaped scatterer is located in the origin, so the translation operator $\mathcal{T}_{\boldsymbol{c}}$ can be omitted. As in the previous example, we observe the essential support of the Fourier coefficients to spread on a diagonal stripe, centered in the marked square, caused by the shape of Ω. We obtain approximations $\widetilde{\boldsymbol{F}}_q$ by solving the related far field operator completion problem with the cg method and FISTA. These are shown in Figure 6.11 (first row, third row). For the cg method we assume the dashed circle from Figure 6.7 (right) to be known a priori, which leads to the subspace dimensions $2N + 1 \in \{7, 13, 19, 25\}$. For FISTA we assume $\boldsymbol{c} = (0\text{m}, 0\text{m})^\top$ and choose as regularization parameters $\mu \in \{10^{-4}, 10^{-4}, 10^{-3}, 2 \times 10^{-3}\}$. In Figure 6.11 (second

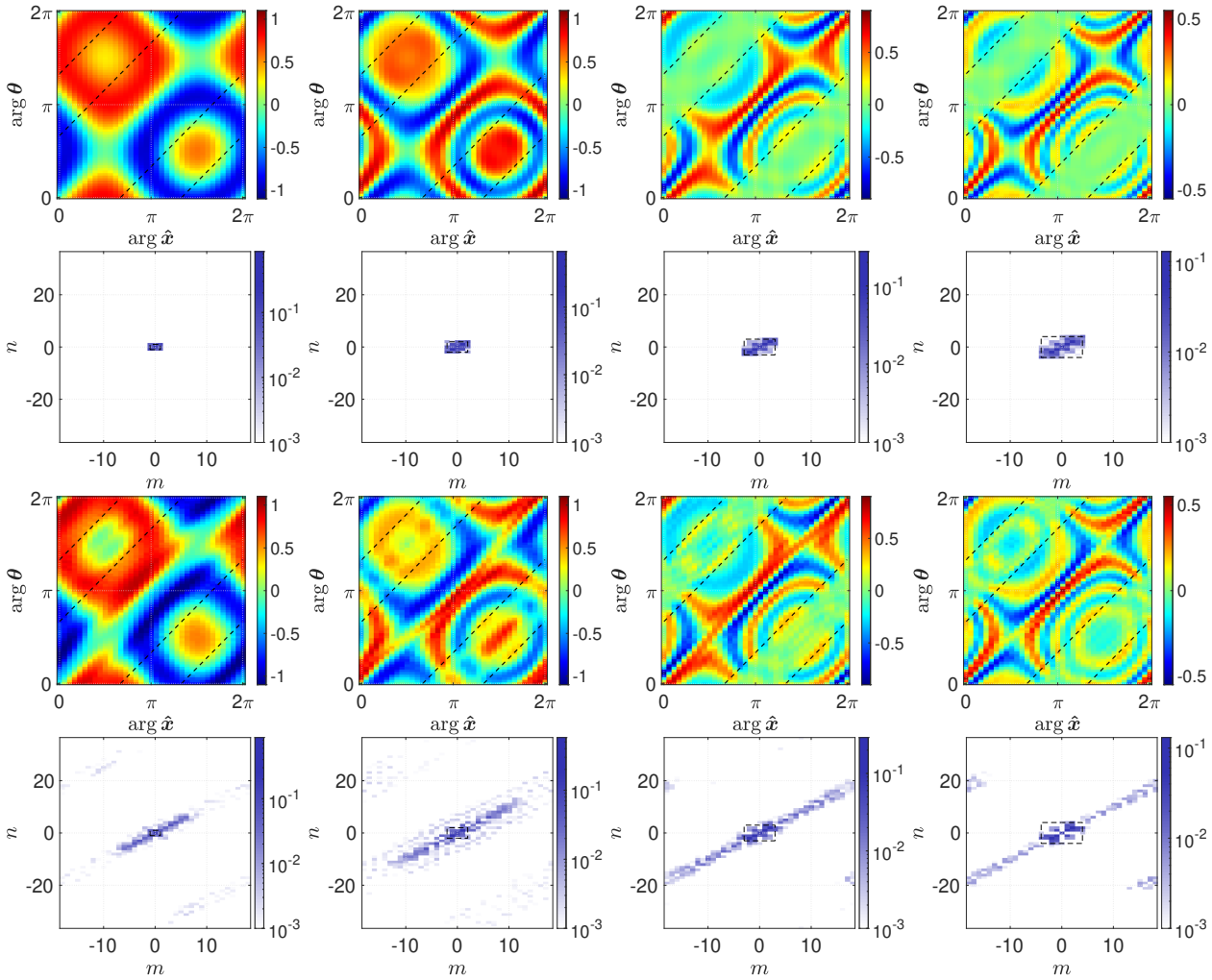

FIGURE 6.9. Real part of reconstructed far field operator $\widetilde{\boldsymbol{F}}_q$ for rectangular shaped scatterer and different values of k. First row: cg method. Third row: FISTA. Absolute values of Fourier coefficients $(a_{m,n})_{m,n}$ of $\mathcal{T}_c\widetilde{\boldsymbol{F}}_q$. Second row: cg method. Fourth row: FISTA. Left: $k = 41.9\text{m}^{-1}$. Middle left: $k = 83.8\text{m}^{-1}$. Middle right: $k = 125.8\text{m}^{-1}$. Right: $k = 167.7\text{m}^{-1}$.

row, fourth row) we further plot the Fourier coefficients of $\widetilde{\boldsymbol{F}}_q$. Compared to Example 6.4, the essential supports of the Fourier coefficients of the FISTA reconstructions are more concentrated in the marked square, as is expected theoretically. Furthermore, the observable part of the cg reconstruction visually fits better to the actually observed far field data. Actually, we would have assumed worse reconstructions compared to the previous example, since the U-shaped scatterer is larger than the rectangular scatterer, while choosing the same non-observable set Ω and the same wave numbers k. This leads us to assume that there is better signal to noise ratio on the data of the U-shaped scatterer than on those of the rectangular scatterer. In all cases, the reconstructions $\mathcal{P}_\Omega\widetilde{\boldsymbol{F}}_q$ of the non-observable part integrate well into the images as a whole, but they differ for the two methods.

◊

6.4. COMBINING OUR METHODS WITH THE FACTORIZATION METHOD

In this section, we investigate whether our reconstructions are a suitable input for solving another well known inverse problem related to (2.1), the *shape identification problem*. Here, given the far

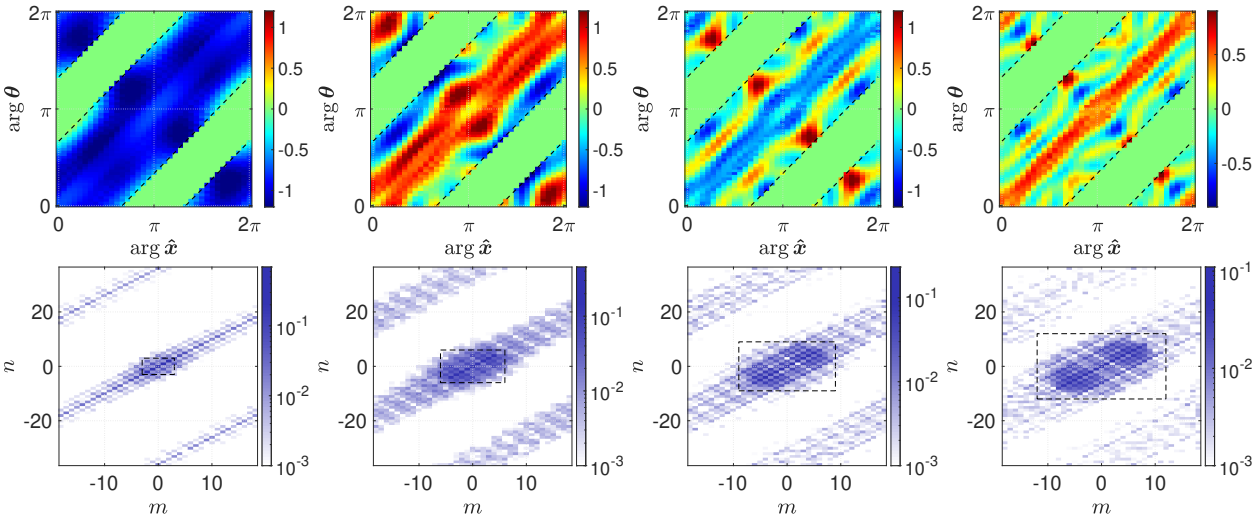

Figure 6.10. Top: Real part of measured far field operator $\boldsymbol{F}_q^\delta|_{\Omega^c}$ for U-shaped scatterer and different values of k. Bottom: Absolute values of Fourier coefficients $(a_{m,n})_{m,n}$ of $\boldsymbol{F}_q^\delta|_{\Omega^c}$. Left: $k = 41.9\mathrm{m}^{-1}$. Middle left: $k = 83.8\mathrm{m}^{-1}$. Middle right: $k = 125.8\mathrm{m}^{-1}$. Right: $k = 167.7\mathrm{m}^{-1}$.

field operator F_q or a noisy version F_q^δ of F_q, the aim is to recover the shape of the scatterer D. As we already discussed in the beginning of Chapter 5 this problem is uniquely solvable, but ill-posed and nonlinear. A common class of related solvers are sampling methods, see e.g. [31, Sec. 11.5] or [30, Sec. 6] for an overview. For our numerical tests we choose the *factorization method* by Kirsch, cf. [69, Chap. 4], [65, Sec. 4] and [66]. We briefly repeat the most important concepts of this procedure. The basis is a factorization

$$F_q \;=\; G_q T_q G_q^*$$

of the far field operator F_q with

$$\begin{aligned}
&G_q : L^2(D) \to L^2(S^{d-1})\,, && (G_q f)(\widehat{\boldsymbol{x}}) \;:=\; \int_D f(y) e^{-\mathrm{i}k\widehat{\boldsymbol{x}}\cdot y}\,\mathrm{d}\boldsymbol{y}\,, && \widehat{\boldsymbol{x}} \in S^{d-1}\,,\\
&T_q : L^2(D) \to L^2(D)\,, && (T_q f)(\boldsymbol{y}) \;:=\; k^2(q(I-L_q)^{-1}f)(\boldsymbol{y})\,, && \boldsymbol{y} \in D\,,\\
&G_q^* : L^2(S^{d-1}) \to L^2(D)\,, && (G_q^* g)(\boldsymbol{y}) \;:=\; \int_{S^{d-1}} g(\widehat{\boldsymbol{x}}) e^{-\mathrm{i}k\widehat{\boldsymbol{x}}\cdot\boldsymbol{y}}\,\mathrm{d}s(\widehat{\boldsymbol{x}})\,, && \boldsymbol{y} \in D\,,
\end{aligned}$$

where L_q is given by (2.12) (cf. [66, Thm. 3.1]). Defining the test functions $\Phi_{\boldsymbol{z}}(\widehat{\boldsymbol{x}}) := e^{-\mathrm{i}k\widehat{\boldsymbol{x}}\cdot\boldsymbol{z}}$, $\widehat{\boldsymbol{x}} \in S^{d-1}$, for $\boldsymbol{z} \in \mathbb{R}^d$ we have the following characterization of D, cf. [66, Thm. 3.2], namely

$$\boldsymbol{z} \in D \qquad \text{if and only if} \qquad \Phi_{\boldsymbol{z}} \in \mathcal{R}(G_q)\,.$$

Since the far field operator F_q is normal, see Proposition 2.4 (c), the spectral theorem for compact normal operators (see e.g. [27, Thm. 17.7]) yields

$$F_q \;=\; \sum_{n=1}^{\infty} \lambda_n \langle\,\cdot\,, \psi_n\rangle_{L^2(S^{d-1})}\psi_n$$

for an orthonormal basis $(\psi_n)_n$ of $L^2(S^{d-1})$ consisting of eigenfunctions of F_q with corresponding eigenvalues $(\lambda_n)_n$. Consequently, we have a second factorization

$$F_q \;=\; (F_q^* F_q)^{\frac{1}{4}} R_q (F_q^* F_q)^{\frac{1}{4}}$$

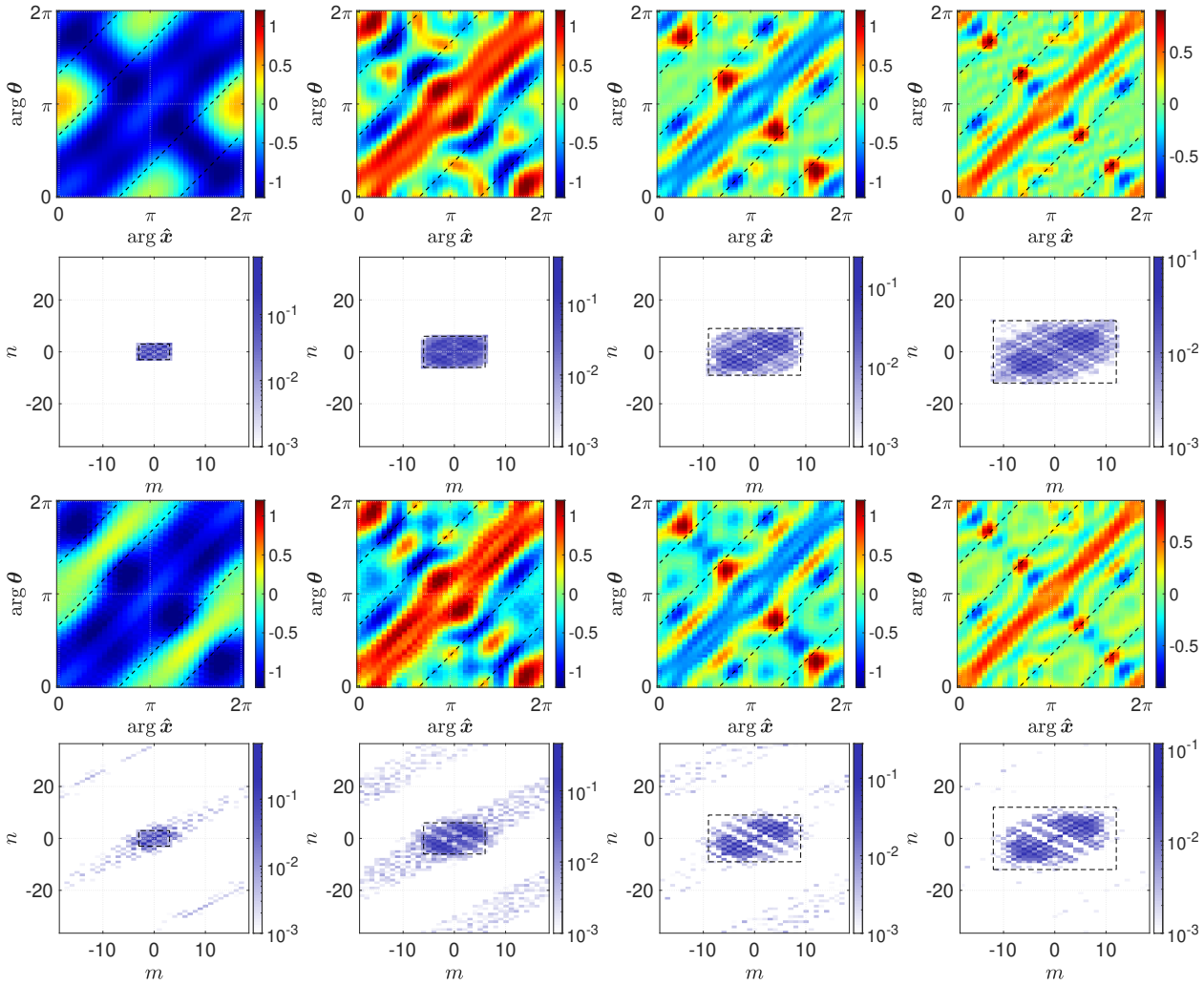

FIGURE 6.11. Real part of reconstructed discretized far field operator $\widetilde{\boldsymbol{F}}_q$ for U-shaped scatterer and different values of k. First row: cg method. Third row: FISTA. Absolute values of Fourier coefficients $(a_{m,n})_{m,n}$ of $\mathcal{T}_{\boldsymbol{c}}\widetilde{\boldsymbol{F}}_q$. Second row: cg method. Fourth row: FISTA. Left: $k = 41.9\text{m}^{-1}$. Middle left: $k = 83.8\text{m}^{-1}$. Middle right: $k = 125.8\text{m}^{-1}$. Right: $k = 167.7\text{m}^{-1}$.

of the far field operator F_q with

$$(F_q^* F_q)^{\frac{1}{4}} : L^2(S^{d-1}) \to L^2(S^{d-1}), \qquad (F_q^* F_q)^{\frac{1}{4}} := \sum_{n=1}^{\infty} \sqrt{|\lambda_n|}\langle \cdot, \psi_n\rangle_{L^2(S^{d-1})}\psi_n,$$

$$R_q : L^2(S^{d-1}) \to L^2(S^{d-1}), \qquad R_q := \sum_{n=1}^{\infty} \frac{\lambda_n}{|\lambda_n|}\langle \cdot, \psi_n\rangle_{L^2(S^{d-1})}\psi_n.$$

Since one can show that $\mathcal{R}(G_q) = \mathcal{R}((F_q^* F_q)^{1/4})$ provided k^2 is not interior transmission eigenvalue, see [65, Thm. 4.3], we obtain

$$\boldsymbol{z} \in D \qquad \text{if and only if} \qquad \Phi_{\boldsymbol{z}} \in \mathcal{R}((F_q^* F_q)^{\frac{1}{4}}) \qquad \text{if and only if} \qquad \sum_{n=1}^{\infty} \frac{|\langle \Phi_{\boldsymbol{z}}, \psi_n\rangle_{L^2(S^{d-1})}|^2}{|\lambda_n|} < \infty,$$

see [65, Thm. 4.4]. The second equivalence holds due to the Picard criterion from Theorem A.2. This can be reformulated in terms of a singular system $(\sigma_n; u_n, v_n)_n$ for F_q, where $\sigma_n = |\lambda_n|$, $u_n = \lambda_n/|\lambda_n|\psi_n$

and $v_n = \psi_n$ for $n \in \mathbb{N}$. Thus, we have that

$$\boldsymbol{z} \in D \qquad \text{if and only if} \qquad \sum_{n=1}^{\infty} \frac{|\langle \Phi_{\boldsymbol{z}}, v_n \rangle_{L^2(S^{d-1})}|^2}{\sigma_n} < \infty \,.$$

Therefore, discretizing an a priori known region of interest containing D, evaluating the singular value decomposition of F_q and truncating and plotting the inverse of this series for each discretization point $\boldsymbol{z}$ gives an approximation of D. In the plot, we obtain values close to zero outside of D and values strictly greater than zero within D.

In the following we compare the reconstructions of the scatterer's shape obtained by the factorization method. As input we use either the cg or the FISTA reconstructions $\widetilde{\boldsymbol{F}}_q$ of $\boldsymbol{F}_q$ or the measurable far field operator $\boldsymbol{F}_q^{\delta}|_{\Omega^c}$ extended by zeros. Here, we consider $d = 2$ and use the reconstructions from Example 6.3 for synthetic data and the ones from Examples 6.4 and 6.5 for experimental data. This procedure also makes sense for a nonsquare $\boldsymbol{F}_q$, as it is the case for the experimental data. Since in that case we have that $L_{\boldsymbol{\theta}} < L_{\widehat{\boldsymbol{x}}}$, we compute a thin singular value decomposition $\boldsymbol{F}_q = \boldsymbol{U}\boldsymbol{S}\boldsymbol{V}^*$ of $\boldsymbol{F}_q$ with $\boldsymbol{U} \in \mathbb{C}^{L_{\widehat{\boldsymbol{x}}} \times L_{\boldsymbol{\theta}}}$, $\boldsymbol{S} = \operatorname{diag}(\sigma_1, \ldots, \sigma_{L_{\boldsymbol{\theta}}}) \in \mathbb{C}^{L_{\boldsymbol{\theta}} \times L_{\boldsymbol{\theta}}}$ and $\boldsymbol{V} = (\boldsymbol{v}_1, \ldots, \boldsymbol{v}_{L_{\boldsymbol{\theta}}}) \in \mathbb{C}^{L_{\boldsymbol{\theta}} \times L_{\boldsymbol{\theta}}}$, cf. e.g. [47, Subsec. 2.4.3]. Here we distinguish the thin from the usual singular value decomposition by the fact that zero columns of $\boldsymbol{U}$ and zero diagonal entries of $\boldsymbol{S}$ are not stored. The criterion from above then can be implemented by plotting for each discretization point $\boldsymbol{z}$ the value

$$\left(\sum_{n=1}^{L_{\boldsymbol{\theta}}} \frac{1}{\sigma_n} |\boldsymbol{\phi}_{\boldsymbol{z}} \cdot \overline{\boldsymbol{v}_n}|^2 \right)^{-1} ,$$

where $\boldsymbol{\phi}_{\boldsymbol{z}} = (e^{\mathrm{i}k\boldsymbol{\theta}_1 \cdot \boldsymbol{z}}, \ldots, e^{\mathrm{i}k\boldsymbol{\theta}_{L_{\boldsymbol{\theta}}} \cdot \boldsymbol{z}})^\top \in \mathbb{C}^{L_{\boldsymbol{\theta}}}$. The experimental data provided by the Institute Fresnel has been used for testing sampling methods several times, and hereby, it is common to use the data extended by zeros as an input, see e.g. [82, Sec. IV.A] for a discussion or [9]. In all three examples below we have 33% missing backscattering data and the wave numbers $k \in \{4.19, 8.38, 12.58, 16.77\}$, and we choose the region of interest $[-0.07, 0.07]^2$.

Example 6.6 (Shape identification for kite shaped scatterer)**.** We consider the kite shaped scatterer from Example 6.3. As a first test, we apply the factorization method to the exact but incomplete observable far field operator $\boldsymbol{F}_q|_{\Omega^c}$. The results are shown in Figure 6.12 (top) for the different values of k. We further apply the factorization method to the cg and FISTA reconstructions $\widetilde{\boldsymbol{F}}_q$ from Figure 6.6 (second row, third row). The results are plotted for the different values of k in Figure 6.12 (middle) for the cg method and in Figure 6.12 (bottom) for FISTA. Comparing the first and the third row, we recognize a clear improvement of the kite's shape for all values of k when applying FISTA, and this improvement is more noticeable for small values of k. In case of the cg method we observe a clear improvement for the two smaller values of k, and the results achieved here are even better than for FISTA. For the two larger values of k the reconstructed scatterer's shape shrinks to a ball centered in the a priori assumed location $\boldsymbol{c} = (0, 0)^\top$, that is used for constructing the subspace $\mathcal{V}_N^{\boldsymbol{c}}$ in the cg method. Thus, in these situations the cg reconstructions clearly do not provide a meaningful input for solving the shape identification problem. Numerical tests show that this cannot be prevented by performing less cg iterations. Even after performing one cg iteration, the factorization method still produces a ball afterwards for both values of k. ◊

Example 6.7 (Shape identification for rectangular shaped scatterer)**.** As a first test on experimental data, we turn to the rectangular shaped scatterer from Example 6.4, and we again first apply the factorization method to the noisy observable far field operator $\boldsymbol{F}_q^{\delta}|_{\Omega^c}$ from Figure 6.8 (top). The results are shown in Figure 6.13 (top). Especially for the two larger values of k the reconstructions of the rectangle already look surprisingly good, but we observe small circular artifacts with the scatterer in their center. Next, we apply the factorization method to the cg reconstructions from Figure 6.9 (middle) and to the FISTA reconstructions from Figure 6.9 (bottom), and we plot

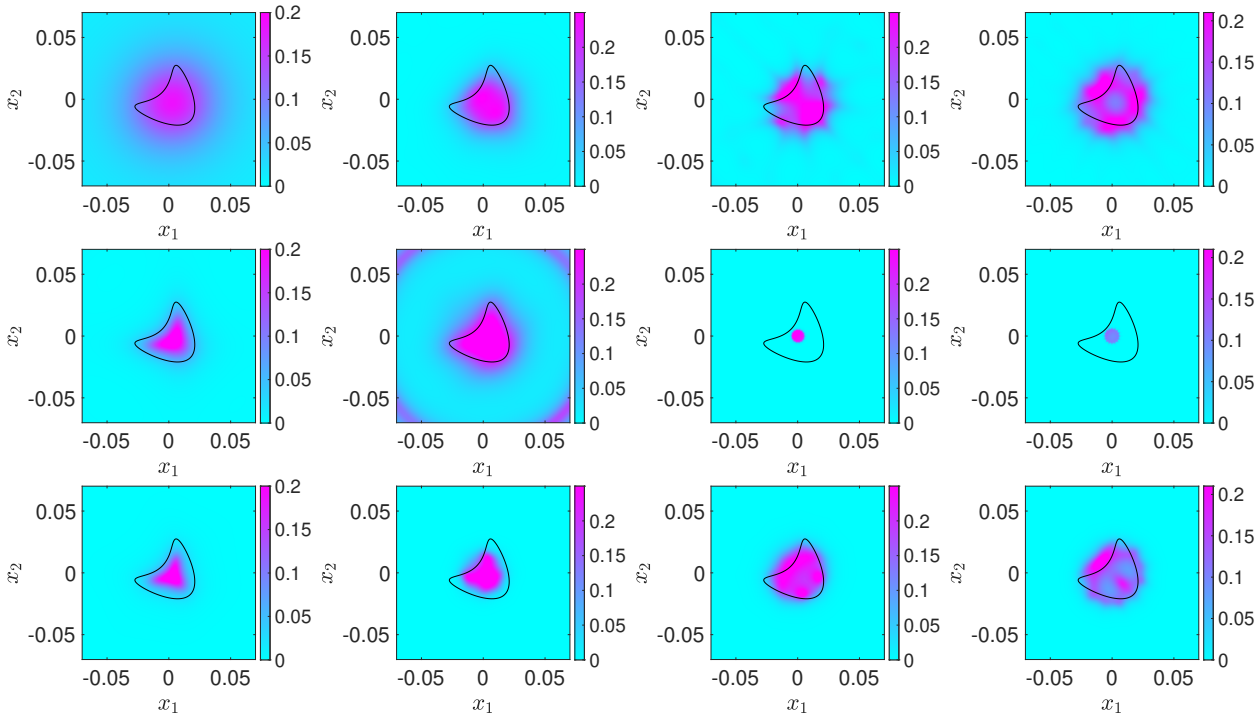

FIGURE 6.12. Reconstruction of kite by factorization method for different input and different values of k. Top: By zero completed observable far field operator $\boldsymbol{F}_q|_{\Omega^c}$ as input. Middle: cg reconstruction $\widetilde{\boldsymbol{F}}_q$ as input. Bottom: FISTA reconstruction $\widetilde{\boldsymbol{F}}_q$ as input. Left: $k = 41.9$. Middle left: $k = 83.8$. Middle right: $k = 125.8$. Right: $k = 167.7$.

the results in Figure 6.13 (middle, bottom). In case of FISTA we observe improvements on the rectangle's shape compared to the top row of Figure 6.13, which are again the larger the smaller k is. In case of the cg method we also observe improvements of the rectangle's shape, but additionally, the circular artifacts are strongly increased. Nevertheless, if enough a priori knowledge on the scatterer's location is available, which is already needed for performing the cg method and can be obtained by applying the factorization method to the original data $\boldsymbol{F}_q^\delta|_{\Omega^c}$, one can argue to just zoom in to remove these artifacts. Since the wave fronts move closer to the scatterer for larger values of k, this becomes more difficult for larger k. ◊

Example 6.8 (Shape identification for U-shaped scatterer)**.** Finally we consider the U-shaped scatterer from Example 6.5, the shape of which we first reconstruct by applying the factorization method to the noisy observable far field operator $\boldsymbol{F}_q^\delta|_{\Omega^c}$ from Figure 6.10 (top), and we plot the results in Figure 6.14 (top). The reconstructions obtained by applying the factorization method on the cg reconstructions from Figure 6.11 (first row) and on the FISTA reconstructions from Figure 6.11 (third row) are shown in Figure 6.14 (middle) and Figure 6.14 (bottom), respectively. For the smaller two values of k we observe an improvement when applying both methods compared to the data completed by zero. For the larger two values of k, all three reconstructions look relatively good. In case of the cg method we again observe increased artifacts at the edge of the region of interest as we already did in the example before. By applying FISTA, the artifacts outside the scatterer seem to be reduced. ◊

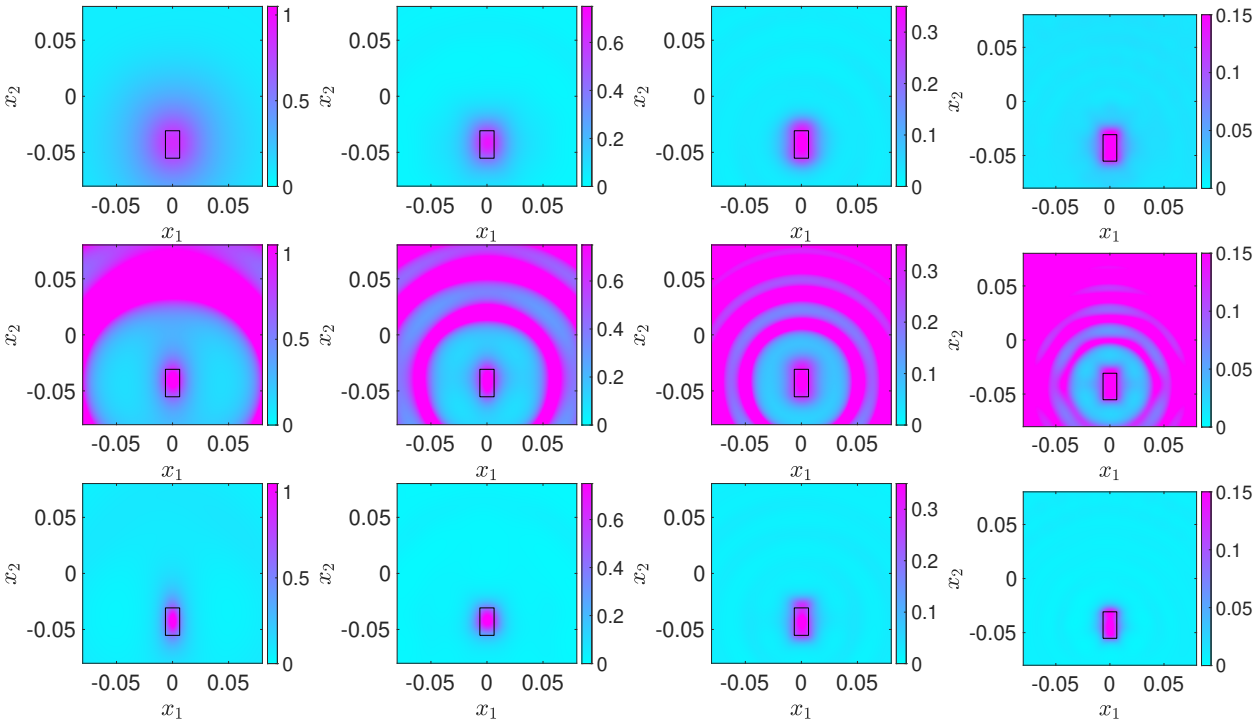

Figure 6.13. Reconstruction of rectangle by factorization method for different input and different values of k. Top: By zero completed observable far field operator $\boldsymbol{F}_q^\delta|_{\Omega^c}$ as input. Middle: cg reconstruction $\widetilde{\boldsymbol{F}}_q$ as input. Bottom: FISTA reconstruction $\widetilde{\boldsymbol{F}}_q$ as input. Left: $k = 41.9\text{m}^{-1}$. Middle left: $k = 83.8\text{m}^{-1}$. Middle right: $k = 125.8\text{m}^{-1}$. Right: $k = 167.7\text{m}^{-1}$.

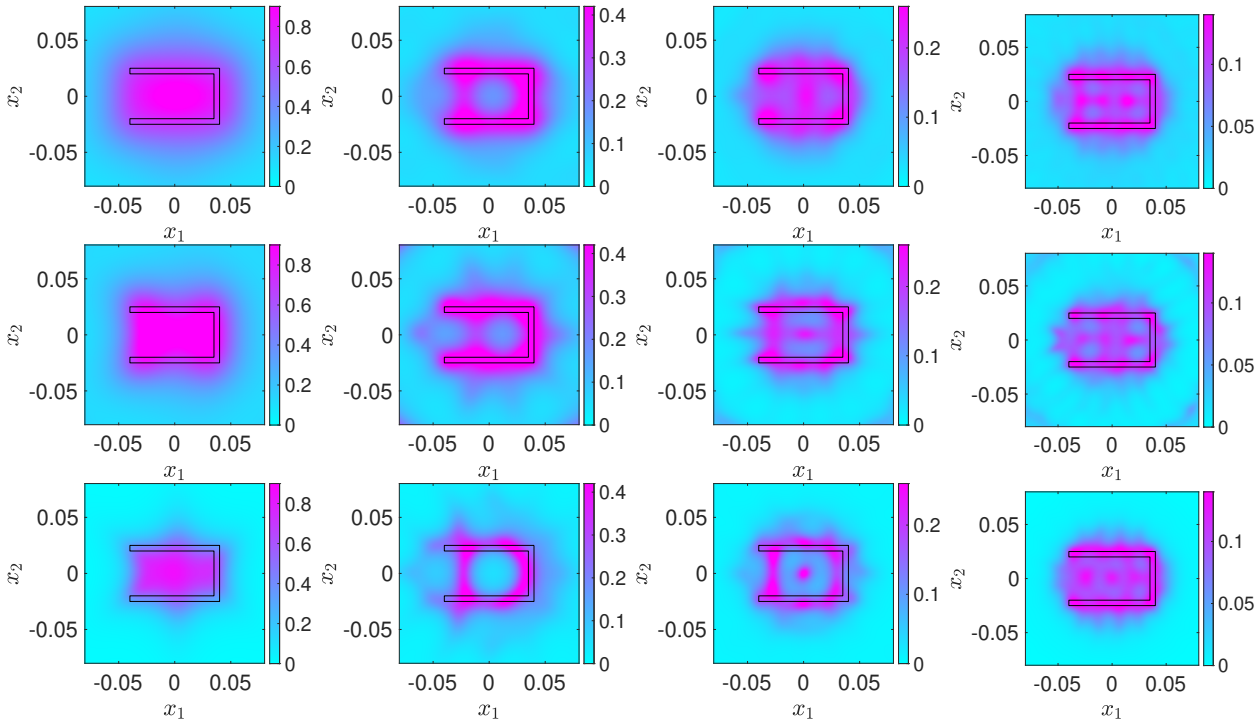

FIGURE 6.14. Reconstruction of U by factorization method for different input and different values of k. Top: By zero completed observable far field operator $\boldsymbol{F}_q^\delta|_{\Omega^c}$ as input. Middle: cg reconstruction $\widetilde{\boldsymbol{F}}_q$ as input. Bottom: FISTA reconstruction $\widetilde{\boldsymbol{F}}_q$ as input. Left: $k = 41.9\text{m}^{-1}$. Middle left: $k = 83.8\text{m}^{-1}$. Middle right: $k = 125.8\text{m}^{-1}$. Right: $k = 167.7\text{m}^{-1}$.

APPENDIX A

HILBERT–SCHMIDT INTEGRAL OPERATORS

The results in this appendix can be found e.g. in [90].

We denote by $\mathcal{L}(L^2(S^{d-1}))$ the space of linear bounded operators on the separable Hilbert space $L^2(S^{d-1})$, i.e., the space of all linear operators $G : L^2(S^{d-1}) \to L^2(S^{d-1})$ with finite operator norm

$$\|G\| := \|G\|_{\|\cdot\|_{L^2(S^{d-1})} \to \|\cdot\|_{L^2(S^{d-1})}} := \sup_{\substack{g \in L^2(S^{d-1}), \\ g \neq 0}} \frac{\|Gg\|_{L^2(S^{d-1})}}{\|g\|_{L^2(S^{d-1})}} . \tag{A.1}$$

We further denote by $\mathcal{K}(L^2(S^{d-1})) \subset \mathcal{L}(L^2(S^{d-1}))$ the space of compact linear bounded operators $L^2(S^{d-1}) \to L^2(S^{d-1})$.

The following theorem can for example be found in [90, Thm. VI.17] or [67, Def. A.52, Thm. A.53].

Theorem A.1. *Let $\sigma_1 \geq \sigma_2 \geq \ldots \geq 0$ denote the ordered sequence of the positive* singular values *of $G \in \mathcal{K}(L^2(S^{d-1}))$. These are the nonnegative square roots of the eigenvalues of the nonnegative self-adjoint operator $G^*G \in \mathcal{K}(L^2(S^{d-1}))$. Then, there exist complete orthonormal systems $(u_n)_n$ in $\overline{\mathcal{R}(G)}$ and $(v_n)_n$ in $\mathcal{N}(G)^\perp$ such that*

$$Gv_n = \sigma_n u_n \qquad \text{and} \qquad G^*u_n = \sigma_n v_n \qquad \text{for all } n \in \mathbb{N} .$$

The triple $(\sigma_n; u_n, v_n)_n$ is called a singular system *for G. There further holds that*

$$Gg = \sum_{n \in \mathbb{N}} \sigma_n u_n \langle g, v_n \rangle_{L^2(S^{d-1})} \qquad \text{for all } g \in L^2(S^{d-1}) . \tag{A.2}$$

The following theorem gives a characterization of the range of a compact operator in terms of a corresponding singular system, which we refer to as the *Picard criterion*.

Theorem A.2. *[67, Thm. A.54] Let $(\sigma_n; u_n, v_n)_n$ denote a* singular system *for $G \in L^2(S^{d-1})$ and suppose $f \in \overline{\mathcal{R}(G)} = \mathcal{N}(G^*)^\perp$. Then, the equation*

$$Gg = f$$

is solvable, i.e., there holds $f \in \mathcal{R}(G)$, if and only if

$$\sum_{n \in \mathbb{N}} \frac{1}{\sigma_n^2} |\langle f, v_n \rangle_{L^2(S^{d-1})}|^2 < \infty ,$$

and in this case

$$g = \sum_{n \in \mathbb{N}} \frac{1}{\sigma_n} \langle f, v_n \rangle_{L^2(S^{d-1})}$$

is a solution of above equation.

From Theorem A.1 we conclude, that $(\sigma_n)_n$ are the eigenvalues of $|G| := \sqrt{G^*G}$, which is the uniquely determined nonnegative operator $|G|$ such that $G^*G = |G|^2$ (see e.g. [90, Thm. VI.9]). With the notation of Theorem A.1 it further holds for all $g \in L^2(S^{d-1})$ that

$$|G|g = \sum_{n\in\mathbb{N}} \sigma_n v_n \langle g, v_n\rangle_{L^2(S^{d-1})} \qquad \text{and} \qquad G^*Gg = \sum_{n\in\mathbb{N}} \sigma_n^2 v_n \langle g, v_n\rangle_{L^2(S^{d-1})}\,, \tag{A.3}$$

so, in particular, $(v_n)_n$ are the eigenfunctions of $|G|$ and of G^*G.

Definition A.3. [90, Thm. VI.18, Thm. VI.20] Let $G \in \mathcal{K}(L^2(S^{d-1}))$ and $(g_n)_n$ be an arbitrary orthonormal basis in $L^2(S^{d-1})$.

(i) We define the *trace* of G by

$$\operatorname{tr} G := \sum_{n\in\mathbb{N}} \langle g_n, Gg_n\rangle_{L^2(S^{d-1})}\,. \tag{A.4}$$

This definition is independent on the choice of $(g_n)_n$.

(ii) We call G *trace class* or *nuclear* if and only if $\operatorname{tr}|G| < \infty$ and denote by $\mathcal{N}(L^2(S^{d-1}))$ the space of all nuclear operators, which forms a Banach space together with the *nuclear norm* $\|G\|_{\mathrm{nuc}} := \operatorname{tr}|G|$.

Let $(\widetilde{v}_n)_n$ be an extension of $(v_n)_n$ to an orthonormal basis of $L^2(S^{d-1})$. By choosing $g_n = \widetilde{v}_n$ in (A.4) and inserting the singular value decompositions (A.2) and (A.3) of G and $|G|$ we obtain

$$\operatorname{tr} G = \sum_{n\in\mathbb{N}} \sigma_n \langle v_n, u_n\rangle_{L^2(S^{d-1})} \qquad \text{and} \qquad \|G\|_{\mathrm{nuc}} = \sum_{n\in\mathbb{N}} \sigma_n = \|(\sigma_n)_n\|_{\ell^1}\,. \tag{A.5}$$

One can show that (A.2) together with the definition of the operator norm (A.1) implies

$$\|G\| = \sup_{n\in\mathbb{N}} \sigma_n = \sigma_1 \qquad \text{and therefore} \qquad \|G\| \le \|G\|_{\mathrm{nuc}}\,.$$

Definition A.4. [90, Thm. VI.22] We call an operator $G \in \mathcal{K}(L^2(S^{d-1}))$ *Hilbert–Schmidt* if and only if $\operatorname{tr} G^*G < \infty$ and denote the space of such operators by $\mathrm{HS}(L^2(S^{d-1}))$, which forms a Hilbert space together with the inner product $\langle G, H\rangle_{\mathrm{HS}} := \operatorname{tr}(G^*H)$ and the norm $\|G\|_{\mathrm{HS}} := \sqrt{\langle G, G\rangle_{\mathrm{HS}}}$.

The definition of the trace (A.4) and plugging the singular value decomposition of G^*G (A.3) into (A.4) while choosing $g_n = v_n$ for the second identity yields

$$\|G\|_{\mathrm{HS}}^2 = \sum_{n\in\mathbb{N}} \|Gg_n\|_{L^2(S^{d-1})}^2 \qquad \text{and} \qquad \|G\|_{\mathrm{HS}}^2 = \sum_{n\in\mathbb{N}} \sigma_n^2 = \|(\sigma_n)_n\|_{\ell^2}^2\,. \tag{A.6}$$

From $\|\cdot\|_{\ell^\infty} \le \|\cdot\|_{\ell^2} \le \|\cdot\|_{\ell^1}$, (A.5) and (A.6) we can conlude that

$$\|\cdot\| \le \|\cdot\|_{\mathrm{HS}} \le \|\cdot\|_{\mathrm{nuc}}\,, \tag{A.7}$$

so $\mathcal{N}(L^2(S^{d-1})) \subseteq \mathrm{HS}(L^2(S^{d-1}))$.

Remark A.5 (Infinite dimensional matrices). Let $G \in \mathrm{HS}(L^2(S^{d-1}))$ and $(g_n)_n$, $(f_n)_n$ be two arbitrary complete orthonormal systems in $L^2(S^{d-1})$. We expand Gg_n in terms of $(g_n)_n$ and obtain with the first identity of (A.6)

$$\begin{aligned}\|G\|_{\mathrm{HS}}^2 = \sum_{n\in\mathbb{N}} \langle Gg_n, Gg_n\rangle_{L^2(S^{d-1})}^2 &= \sum_{m,n\in\mathbb{N}} \langle Gg_n, f_m\rangle_{L^2(S^{d-1})} \langle f_m, Gg_n\rangle_{L^2(S^{d-1})} \\ &= \sum_{m,n\in\mathbb{N}} |\langle Gg_n, f_m\rangle_{L^2(S^{d-1})}|^2\,.\end{aligned}$$

Accordingly, we can expand G in terms of $(\langle\,\cdot\,, g_n\rangle_{L^2(S^{d-1})} f_m)_{m,n}$ via

$$Gg = \sum_{m\in\mathbb{N}} f_m \Big\langle G\Big(\sum_{n\in\mathbb{N}} g_n \langle g, g_n\rangle_{L^2(S^{d-1})}\Big), f_m\Big\rangle_{L^2(S^{d-1})} = \sum_{m,n\in\mathbb{N}} f_m \langle Gg_n, f_m\rangle_{L^2(S^{d-1})} \langle g, g_n\rangle_{L^2(S^{d-1})}\,, \qquad g \in L^2(S^{d-1})\,.$$

The fact that G is Hilbert–Schmidt ensures the norm convergence of this expansion. By fixing the choice of the two orthonormal systems the Hilbert–Schmidt operator G can be interpreted as infinite dimensional matrix $(a_{m,n})_{m,n} := (\langle Gg_n, f_m\rangle_{L^2(S^{d-1})})_{m,n}$, whose matrix entries are square summable. In this sense the Hilbert–Schmidt norm is the infinite dimensional generalization of the Frobenius norm for matrices.

Definition A.6. An operator $G \in \mathcal{L}(L^2(S^{d-1}))$ has *finite rank* if and only if the range of G is finite dimensional, i.e., there exists some $N \in \mathbb{N}$ and a family $(g_n)_{n=1,\dots,N}$ in $L^2(S^{d-1})$ such that for every $g \in L^2(S^{d-1})$ we can write $Gg = \sum_{n=1}^{N} \lambda_n g_n$ for some $\lambda_n \in \mathbb{C}$, $n = 1, \dots, N$. If N is chosen minimal, then $\operatorname{rank} G := N$ is called the *rank* of G. In particular, G is nuclear, so also Hilbert–Schmidt and compact.

Corollary A.7. *The finite rank operators are $\|\cdot\|$-dense in $\mathcal{K}(L^2(S^{d-1}))$, as well as $\|\cdot\|_{\mathrm{HS}}$-dense in $\mathrm{HS}(L^2(S^{d-1}))$ and $\|\cdot\|_{\mathrm{nuc}}$-dense in $\mathcal{N}(L^2(S^{d-1}))$.*

Finally, the next theorem states that $\mathrm{HS}(L^2(S^{d-1}))$ cannot only be identified with the space $\ell^2 \times \ell^2$ (cf. Remark A.5) but also with $L^2(S^{d-1} \times S^{d-1})$, so it has additional structure.

Theorem A.8. *[90, Thm. VI.23] A operator $G \in \mathcal{K}(L^2(S^{d-1}))$ is Hilbert–Schmidt if and only if there is a function $\kappa_G \in L^2(S^{d-1} \times S^{d-1})$ such that*

$$Gg = \int_{S^{d-1}} \kappa_G(\,\cdot\,, \theta) g(\theta)\, \mathrm{d}s(\theta)\,, \qquad h \in L^2(S^{d-1})\,.$$

In that context, G is referred to as a Hilbert–Schmidt integral operator *with associated* Hilbert–Schmidt integral kernel *κ_G. It holds*

$$\|G\|_{\mathrm{HS}} = \|\kappa_G\|_{L^2(S^{d-1}\times S^{d-1})} \qquad \textit{and} \qquad \langle G, H\rangle_{\mathrm{HS}} = \langle \kappa_G, \kappa_H\rangle_{L^2(S^{d-1}\times S^{d-1})}$$

with κ_H denoting the kernel of $H \in \mathrm{HS}(L^2(S^{d-1}))$.

APPENDIX B

SPHERICAL HARMONICS AND BESSEL FUNCTIONS

Approximations of functions on the unit sphere S^{d-1} or for our purposes, since far field patterns are $L^2(S^{d-1} \times S^{d-1})$, on $S^{d-1} \times S^{d-1}$ naturally lead to expansions in terms of a certain orthonormal system, namely spherical harmonics. Let

$$\mathbb{H}_n^d := \left\{ p : \mathbb{R}^d \to \mathbb{C} \ : \ p(\boldsymbol{x}) = \sum_{|\boldsymbol{\alpha}|=n} a_{\boldsymbol{\alpha}} \boldsymbol{x}^{\boldsymbol{\alpha}}, a_{\boldsymbol{\alpha}} \in \mathbb{C} \right\}$$

define the space of homogeneous polynomials of degree $n \in \mathbb{N}$ in d dimensions. Here, we use the multi-index notation $\boldsymbol{\alpha} = (\alpha_1, \ldots, \alpha_d) \in \mathbb{N}_0^d$, $|\boldsymbol{\alpha}| := \sum_{j=1}^d \alpha_d$ and $\boldsymbol{x}^{\boldsymbol{\alpha}} := x_1^{\alpha_1} \ldots x_d^{\alpha_d}$ for $\boldsymbol{x} \in \mathbb{R}^d$.

We now can define the space of spherical harmonics of degree n

$$\mathbb{Y}_n^d := \mathbb{Y}_n(\mathbb{R}^d)|_{S^{d-1}}, \qquad \text{where} \qquad \mathbb{Y}_n(\mathbb{R}^d) := \{ p \in \mathbb{H}_n^d \ : \ \Delta p = 0 \} \tag{B.1}$$

denotes the space of harmonic homogeneous polynomials of degree n. By definition every spherical harmonic $Y_n \in \mathbb{Y}_n^d$ can be related to a harmonic homogeneous polynomial $H_n \in \mathbb{H}_n^d$ via

$$H_n(\boldsymbol{x}) := |\boldsymbol{x}|^n Y_n(\widehat{\boldsymbol{x}}) . \tag{B.2}$$

One can show that $\dim \mathbb{Y}_n^2 = \dim \mathbb{Y}_n(\mathbb{R}^2) = 2$ and $\dim \mathbb{Y}_n^3 = \dim \mathbb{Y}_n(\mathbb{R}^3) = 2n+1$ (see [1, p. 15-19]). Furthermore, there holds

$$L^2(S^{d-1}) = \bigoplus_{n=0}^{\infty} \mathbb{Y}_n^d \qquad \text{and} \qquad \mathbb{Y}_n^d \perp \mathbb{Y}_m^d, \ n \neq m . \tag{B.3}$$

In the following we introduce a concrete example of an orthonormal basis for $\mathbb{Y}_n^d$ in case of $d = 2, 3$ and deduce suitable solutions of the Helmholtz equation.

B.1. THE CASE $d = 2$ AND BESSEL FUNCTIONS

The results of this section can be found in [31, Sec. 3.5]. We set $p^{\pm}(\boldsymbol{x}) := (x_1 \pm \mathrm{i} x_2)^n$ and conclude from the binomial theorem that $p^{\pm} \in \mathbb{H}_n^2$ and further from direct calculation that $p^{\pm} \in \mathbb{Y}_n(\mathbb{R}^2)$. By introducing polar coordinates $\boldsymbol{x} = r(\cos\varphi, \sin\varphi)^\intercal$, $r \geq 0$, $\varphi \in (-\pi, \pi]$ there holds

$$p^{\pm}(\boldsymbol{x}) = r^n (\cos\varphi \pm \mathrm{i} \sin\varphi)^n = r^n e^{\pm \mathrm{i} n \varphi} ,$$

which implies due to (B.2) that $e^{\pm \mathrm{i} n \varphi} \in \mathbb{Y}_n^2$ and since $\dim \mathbb{Y}_n^2 = 2$ that $\mathbb{Y}_n^2 = \operatorname{span}\{e^{\mathrm{i} n \varphi}, e^{-\mathrm{i} n \varphi}\}$ is the space of trigonometric polynomials of order n.

We are now interested in solutions of the Helmholtz $\Delta u + k^2 u = 0$, for which we make the ansatz $u(\boldsymbol{x}) := f(kr) e^{\pm \mathrm{i} n \varphi}$. By the chain rule and the Laplace operator in polar coordinates u solves

the Helmholtz equation if and only if

$$\frac{1}{r}\left(\frac{\partial}{\partial r}\left(r\frac{\partial}{\partial r}\right)+\frac{1}{r}\frac{\partial^2}{\partial\varphi^2}\right)f(kr)e^{\pm in\varphi}+k^2f(kr)e^{\pm in\varphi}=0\,,$$

so if and only if

$$e^{\pm in\varphi}\left(\frac{k}{r}f'(kr)+k^2f''(kr)+\left(k^2-\frac{n^2}{r^2}\right)f(kr)\right)=0\,.$$

By multiplying by r^2 and setting $t=kr$ this is equivalent to f satisying the *Bessel differential equation of order n*

$$t^2f''(t)+tf'(t)+\left(t^2-n^2\right)f(t)=0\,. \tag{B.4}$$

Two linearly independent solutions of (B.4) are given by the *Bessel function* J_n and *Neumann function* Y_n *of order n*. For explicit series expansions of J_n and Y_n see e.g. [87, (10.2.2), (10.8.1)]. Whereas J_n is analytic on $\mathbb{R}$, Y_n is analytic on $(0,\infty)$. Of course all linear combinations of J_n and Y_n are solutions of (B.4) as well, the special linear combinations

$$H_n^{(1)}:=J_n+\mathrm{i}Y_n\qquad\text{and}\qquad H_n^{(2)}:=J_n-\mathrm{i}Y_n\,, \tag{B.5}$$

which are called *Hankel function of the first and second kind of order n*, respectively. The function $H_0^{(1)}$ is the fundamental solution of the differential equation considered in this work, see (2.2), and consequently has special significance for our purposes. In the rest of this subsection we list the basic properties of these four special functions, that are needed throughout this work.

For $n\in\mathbb{Z}$ and $a,z\in\mathbb{C}$ there holds the product formula (cf. [87, (10.22.5)])

$$\int zJ_n^2(az)\,\mathrm{d}z=\frac{1}{2}z^2\left(J_n^2(az)-J_{n-1}(az)J_{n+1}(az)\right)\,. \tag{B.6}$$

as well as the connection formula (cf. [87, (10.4.1)])

$$J_{-n}(z)=(-1)^nJ_n(z)\,. \tag{B.7}$$

Formula (B.6) remains true for Bessel functions J_ν of order $\nu\in\mathbb{R}$, which are defined in the same manner as solutions of (B.4) when replacing $n\in\mathbb{N}$ by $\nu\in\mathbb{R}$. By [77, p. 199] we have the following monotonically decreasing bound

$$|J_n(t)|<b_0t^{-\frac{1}{3}}\,,\qquad n\in\mathbb{Z},\,t>0,\,b_0\approx0.7857\,, \tag{B.8}$$

which can be improved even further for special choices of t and n. Let $t>2(M+1)$ for some $M\in\mathbb{N}$ and $|n|\le M$. Then, proceeding as in the proof of [55, Thm. 4.6] using [72, Thm. 2] gives

$$|J_n(t)|\le b_1t^{-\frac{1}{2}}\qquad\text{with } b_1\approx0.7595\,. \tag{B.9}$$

We further have the following consequence of Neumann's addition theorem, cf [87, (10.23.3)]

$$\sum_{n\in\mathbb{Z}}J_n^2(z)=1\,,\qquad z\in\mathbb{C}\,. \tag{B.10}$$

For given $\boldsymbol{\theta}\in S^1$ and $\boldsymbol{x}\in\mathbb{R}^2$ the *Jacobi–Anger expansion* (see [31][(3.112)]) reads

$$e^{\pm\mathrm{i}k\boldsymbol{x}\cdot\boldsymbol{\theta}}=J_0(k|\boldsymbol{x}|)+2\sum_{n=1}^{\infty}\mathrm{i}^nJ_n(k|\boldsymbol{x}|)\cos(n\vartheta) \tag{B.11}$$

with ϑ denoting the angle between $\pm\boldsymbol{\theta}$ and $\widehat{\boldsymbol{x}}$. By using polar coordinates for $\pm\boldsymbol{\theta}$ and $\widehat{\boldsymbol{x}}$ we

rewrite $\vartheta = \arg(\pm\boldsymbol{\theta}) - \arg\widehat{\boldsymbol{x}} + 2\pi m\mathrm{i}$ for some $m \in \mathbb{Z}$ and consequently since $\arg(-\boldsymbol{\theta}) = \arg\boldsymbol{\theta} + \pi + 2\pi m\mathrm{i}$ for some $m \in \mathbb{Z}$

$$\cos(n\vartheta) = \frac{1}{2}(e^{\mathrm{i}n\vartheta} + e^{-\mathrm{i}n\vartheta}) = \frac{1}{2}\left((\pm 1)^n e^{\mathrm{i}n\arg\boldsymbol{\theta}} e^{-\mathrm{i}n\arg\widehat{\boldsymbol{x}}} + (\pm 1)^{-n} e^{-\mathrm{i}n\arg\boldsymbol{\theta}} e^{\mathrm{i}n\arg\widehat{\boldsymbol{x}}}\right).$$

Plugging this into (B.11) yields together with $J_{-n}(k|x|) = (-1)^n J_n(k|x|)$, $n \in \mathbb{Z}$,

$$e^{\pm\mathrm{i}k\boldsymbol{x}\cdot\boldsymbol{\theta}} = \sum_{n\in\mathbb{Z}} (\pm\mathrm{i})^n e^{\mathrm{i}n\arg\boldsymbol{\theta}} J_n(k|\boldsymbol{x}|) e^{-\mathrm{i}n\arg\widehat{\boldsymbol{x}}} = \sum_{n\in\mathbb{Z}} \mathrm{i}^{\pm n} e^{\mathrm{i}n\arg\boldsymbol{\theta}} J_n(k|\boldsymbol{x}|) e^{-\mathrm{i}n\arg\widehat{\boldsymbol{x}}}. \tag{B.12}$$

This provides an expansion of plane waves $e^{\pm\mathrm{i}k(\cdot)\cdot\boldsymbol{\theta}}$ in terms of spherical waves $J_n(k|\cdot|)e^{-\mathrm{i}n\arg(\cdot)}$ for $n \in \mathbb{Z}$ and it converges uniformly in $\boldsymbol{x}$ on compact subsets of $\mathbb{R}^2$.

B.2. The case $d = 3$ and spherical Bessel functions

For a more detailed discussion of the results below we refer to [31, Sec. 2.3, 2.4]. We introduce spherical coordinates $\boldsymbol{x} = r(\sin\vartheta\cos\varphi, \sin\vartheta\sin\varphi, \cos\vartheta)^\intercal$, $r \geq 0$, $\vartheta \in [0, \pi]$, $\varphi \in (-\pi, \pi]$. By using the relation (B.2) together with $\Delta H_n = 0$ and the Laplace operator in spherical coordinates Y_n is a spherical harmonic of order n if and only if it solves

$$\left(\frac{1}{\sin\vartheta}\frac{\partial}{\partial\vartheta}\left(\sin\vartheta\frac{\partial}{\partial\vartheta}\right) + \frac{1}{\sin^2\vartheta}\frac{\partial^2}{\partial\varphi^2}\right) Y_n = -n(n+1)Y_n. \tag{B.13}$$

One can show that $\{Y_n^m : m = -n, \ldots, n,\ n \in \mathbb{N}_0\}$ with

$$Y_n^m(\vartheta, \varphi) := \sqrt{\frac{2n+1}{4\pi}\frac{(n-|m|)!}{(n+|m|)!}} P_n^{|m|}(\cos\vartheta) e^{\mathrm{i}m\varphi} \tag{B.14}$$

forms an orthonormal basis for the related solution space, i.e. for $\mathbb{Y}_n^3$ (cf. [31, Thm. 2.8]). Here, P_n^m denotes the *mth associated Legendre function of order n*, given by

$$P_n^m(t) := (1-t^2)^{m/2}\frac{\mathrm{d}^m P_n(t)}{\mathrm{d}t^m}, \qquad m = 0, \ldots, n,\ t \in [-1, 1],$$

and P_n the *Legendre polynomial of degree n*, given by

$$P_n(t) := \frac{1}{2^n n!}\frac{\mathrm{d}^n}{\mathrm{d}t^n}(t^2-1)^n, \qquad t \in [-1, 1]. \tag{B.15}$$

The following lemma is typically referred to as *addition theorem*.

Lemma B.1. *Let $n \in \mathbb{N}$ and $\{Y_n^m : m = -n, \ldots, n\}$ be a system of orthonormal spherical harmonics of order n. Then, for all $\widehat{\boldsymbol{x}}, \boldsymbol{\omega} \in S^2$ it holds*

$$\sum_{m=-n}^{n} Y_n^m(\widehat{\boldsymbol{x}})\overline{Y_n^m(\boldsymbol{\omega})} = \frac{2n+1}{4\pi} P_n(\widehat{\boldsymbol{x}}\cdot\boldsymbol{\omega}). \tag{B.16}$$

Proof. See [1, Thm. 2.9] or [31, Thm. 2.9]. □

Remark B.2. Lemma B.1 in particular implies that $P_n^{\widehat{\boldsymbol{x}}}$, which is defined by $P_n^{\widehat{\boldsymbol{x}}}(\boldsymbol{\omega}) := P_n(\widehat{\boldsymbol{x}}\cdot\boldsymbol{\omega})$, is also a spherical harmonic of order $n \in \mathbb{N}$ for fixed $\widehat{\boldsymbol{x}} \in S^2$. Furthermore, it satisfies (cf. [1, (2.39), (2.40)])

$$\|P_n^{\widehat{\boldsymbol{x}}}\|_{L^2(S^2)} = \sqrt{\frac{4\pi}{2n+1}} \qquad \text{and} \qquad \|P_n^{\widehat{\boldsymbol{x}}}\|_{L^\infty(S^2)} = 1. \tag{B.17}$$

Theorem B.3. *Every $\alpha \in L^2(S^2 \times S^2)$ can be expanded as a Fourier–Laplace series*

$$\alpha(\widehat{\boldsymbol{x}}, \boldsymbol{\theta}) = \sum_{m=0}^{\infty} \sum_{n=0}^{\infty} \alpha_{m,n}(\widehat{\boldsymbol{x}}, \boldsymbol{\theta}) \,. \tag{B.18}$$

Here, $\alpha_{m,n}$ is called (m,n)th spherical harmonics component *of α, which satisfies*

$$\alpha_{m,n}(\widehat{\boldsymbol{x}}, \boldsymbol{\theta}) = \frac{(2m+1)(2n+1)}{16\pi^2} \int_{S^2} P_m(\widehat{\boldsymbol{x}} \cdot \boldsymbol{\omega}) \int_{S^2} P_n(\theta \cdot \boldsymbol{\upsilon}) \alpha(\boldsymbol{\omega}, \boldsymbol{\upsilon}) \, \mathrm{d}s(\boldsymbol{\upsilon}) \, \mathrm{d}s(\boldsymbol{\omega}) \,, \tag{B.19}$$

and it is the orthogonal projection of α on $\mathbb{Y}_m^3 \times \mathbb{Y}_n^3$.

Proof. Let $\{Y_n^m : m = -n, \dots, n\}$ be an arbitrary system of orthonormal spherical harmonics of order n, e.g. the one defined in (B.14). Since $L^2(S^2) = \bigoplus_{n=0}^{\infty} \mathbb{Y}_n^3$ we have

$$L^2(S^2 \times S^2) = \left(\bigoplus_{m=0}^{\infty} \mathbb{Y}_m^3 \right) \times \left(\bigoplus_{n=0}^{\infty} \mathbb{Y}_n^3 \right) = \bigoplus_{m,n=0}^{\infty} (\mathbb{Y}_m^3 \times \mathbb{Y}_n^3)$$

(cf. [90, Sec. II.4]), and we can expand any $\alpha \in L^2(S^2 \times S^2)$ according to (B.18) with

$$\alpha_{m,n}(\widehat{\boldsymbol{x}}, \boldsymbol{\theta}) = \sum_{o=-m}^{m} \sum_{p=-n}^{n} \int_{S^2} \overline{Y_m^o(\boldsymbol{\omega})} \int_{S^2} \overline{Y_n^p(\boldsymbol{\upsilon})} \alpha(\boldsymbol{\omega}, \boldsymbol{\upsilon}) \, \mathrm{d}s(\boldsymbol{\upsilon}) \, \mathrm{d}s(\boldsymbol{\omega}) Y_m^o(\widehat{\boldsymbol{x}}) Y_n^p(\boldsymbol{\theta}) \,.$$

By the monotone convergence theorem and (B.16) we can conclude representation (B.19). □

The following lemma adapts [56, Lemma C.1] and provides an orthogonality property of triple products of the here needed spherical harmonic constructions.

Lemma B.4. *Suppose that $\alpha_{m,n} \in \mathbb{Y}_m^3 \times \mathbb{Y}_n^3$, $\beta_{o,p} \in \mathbb{Y}_o^3 \times \mathbb{Y}_p^3$ and $\gamma_{r,s} \in \mathbb{Y}_r^3 \times \mathbb{Y}_s^3$ for some $m, n, o, p, r, s \in \mathbb{N}_0$. If $m > o + r$ or $n > p + s$ or $m < |o - r|$ or $n < |p - s|$, then it holds*

$$\int_{S^2} \int_{S^2} \alpha_{m,n}(\widehat{\boldsymbol{x}}, \boldsymbol{\theta}) \beta_{o,p}(\widehat{\boldsymbol{x}}, \boldsymbol{\theta}) \gamma_{r,s}(\widehat{\boldsymbol{x}}, \boldsymbol{\theta}) \, \mathrm{d}s(\boldsymbol{\theta}) \, \mathrm{d}s(\widehat{\boldsymbol{x}}) = 0 \,.$$

As before, we are interested in solutions of the Helmholtz $\Delta u + k^2 u = 0$, for which we this time make the ansatz $u(\boldsymbol{x}) := f(kr) Y_n^m(\widehat{\boldsymbol{x}})$. Using the chain rule, the Laplace operator in spherical polar coordinates and (B.13) we can conclude that u solves the Helmholtz equation if and only if

$$\frac{1}{r^2} \left(\frac{\partial}{\partial r} \left(r^2 \frac{\partial}{\partial r} \right) + \frac{1}{\sin \vartheta} \frac{\partial}{\partial \vartheta} \left(\sin \vartheta \frac{\partial}{\partial \vartheta} \right) + \frac{1}{\sin^2 \vartheta} \frac{\partial^2}{\partial \varphi^2} \right) f(kr) Y_n^m(\widehat{\boldsymbol{x}}) + k^2 f(kr) Y_n^m(\widehat{\boldsymbol{x}}) = 0 \,,$$

so if and only if

$$Y_n^m(\widehat{\boldsymbol{x}}) \left(2 \frac{k}{r} f'(kr) + k^2 f''(kr) + \left(k^2 - \frac{n(n+1)}{r^2} \right) f(kr) \right) = 0 \,.$$

We multiply by r^2 and set $t = kr$ to obtain the equivalent *spherical Bessel differential equation of order n*

$$t^2 f''(t) + 2t f'(t) + \Big(t^2 - n(n+1) \Big) f(t) = 0 \,. \tag{B.20}$$

Two linearly independent solutions of (B.20) are given by the *spherical Bessel function j_n* and the *spherical Neumann function y_n of order n*. For explicit series expansions of j_n and y_n see e.g. [31, (2.32), (2.33)]. Again, whereas j_n is analytic on $\mathbb{R}$, y_n is analytic on $(0, \infty)$. Their special linear combinations

$$h_n^{(1)} := j_n + \mathrm{i} y_n \qquad \text{and} \qquad h_n^{(2)} := j_n - \mathrm{i} y_n$$

are the *spherical Hankel functions of the first* and *second kind of order* n.

Bessel functions and spherical Bessel function are related by the following formula. For $n \in \mathbb{Z}$ and $z \in \mathbb{C}$ there holds

$$j_n(z) = \sqrt{\frac{\pi}{2z}} J_{n+\frac{1}{2}}(z)\,. \tag{B.21}$$

By using this relation we can deduce from the bound (B.8) for $n \in \mathbb{Z}$ and $t \in \mathbb{R} \setminus \{0\}$ that

$$|j_n(t)| = \sqrt{\frac{\pi}{2t}} |J_{n+\frac{1}{2}}(t)| \leq \sqrt{\frac{\pi}{2}} b_0 |t|^{-\frac{1}{2}-\frac{1}{3}} \leq b_2 |t|^{-\frac{5}{6}}\,, \qquad b_2 \approx 0.9848\,. \tag{B.22}$$

As in the two-dimensional case, this bound can be improved even further for special choices of t and n. Let $t > 2(M + \frac{3}{2})$ for some $M \in \mathbb{N}$ and $0 \leq n \leq M$. Then, using relation (B.21) together with the associated bound (B.9) gives

$$|j_n(t)| = \sqrt{\frac{\pi}{2t}} |J_{n+\frac{1}{2}}(t)| \leq \sqrt{\frac{\pi}{2}} b_1 t^{-\frac{1}{2}-\frac{1}{2}} \leq b_3 t^{-1} \qquad \text{with } b_3 \approx 0.9519\,. \tag{B.23}$$

Here, (B.9) is applicable due to $n + \frac{1}{2} \leq M + \frac{1}{2}$ and $t > 2((M + \frac{1}{2}) + 1)$.

For given $\boldsymbol{\theta} \in S^2$ and $\boldsymbol{x} \in \mathbb{R}^3$ the *Jacobi–Anger expansion* (see [31, (2.46)]) reads

$$e^{\pm \mathrm{i} k \boldsymbol{x} \cdot \boldsymbol{\theta}} = \sum_{n=0}^{\infty} \mathrm{i}^n (2n+1) j_n(k|\boldsymbol{x}|) P_n(\pm \widehat{\boldsymbol{x}} \cdot \boldsymbol{\theta}) = \sum_{n=0}^{\infty} (\pm \mathrm{i})^n (2n+1) j_n(k|\boldsymbol{x}|) P_n(\widehat{\boldsymbol{x}} \cdot \boldsymbol{\theta})\,, \tag{B.24}$$

which again is an expansion of plane waves $e^{\pm \mathrm{i} k (\,\cdot\,) \cdot \boldsymbol{\theta}}$ in terms of spherical waves $j_n(k|\,\cdot\,|) P_n((\,\cdot\,) \cdot \boldsymbol{\theta})$ for $n \in \mathbb{Z}$, and it converges uniformly in $\boldsymbol{x}$ on compact subsets of $\mathbb{R}^3$. Here, we used the symmetry property $P_n(-\widehat{\boldsymbol{x}} \cdot \boldsymbol{\theta}) = (-1)^n P_n(\widehat{\boldsymbol{x}} \cdot \boldsymbol{\theta})$, cf. [87, (18.6.1)].

APPENDIX C

TWO SUBGRADIENTS

In the following we restrict ourselves to the two-dimensional case.

For the results in this appendix we refer to [91, Chap. 5] and [92, Chap. 8], as a standard reference for the theory of convex non-differentiable functions on $\mathbb{R}^N$, $N \in \mathbb{N}$, and to [5, Chap. 16], which covers the generalization of these results when replacing $\mathbb{R}^N$ by an arbitrary Hilbert space.

Definition C.1. We call an operator $H \in \mathrm{HS}(L^2(S^1))$ *subgradient* of a norm $\|\cdot\|_{\mathcal{V}}$ on $\mathrm{HS}(L^2(S^1))$ at $H^* \in \mathrm{HS}(L^2(S^1))$ if

$$\|H^* + G\|_{\mathcal{V}} \geq \|H^*\|_{\mathcal{V}} + \langle H, G\rangle_{\mathrm{HS}} \qquad \text{for all } G \in \mathrm{HS}(L^2(S^1))\,. \tag{C.1}$$

The set of all subgradients of $\|\cdot\|_{\mathcal{V}}$ at H^* is called *subdifferential* of $\|\cdot\|_{\mathcal{V}}$ at H^* and denoted by $\partial\|H^*\|_{\mathcal{V}}$.

The above definition has the following equivalent characterization. There holds $H \in \partial\|H^*\|_{\mathcal{V}}$ if and only if

$$\|H^*\|_{\mathcal{V}} = \langle H^*, H\rangle_{\mathrm{HS}} \qquad \text{and} \qquad \|H\|_{\mathcal{V}}^* \leq 1\,, \tag{C.2}$$

cf. [99]. Here, $\|\cdot\|_{\mathcal{V}}^*$ denotes the *dual norm* of $\|\cdot\|_{\mathcal{V}}$, which is given by

$$\|H\|_{\mathcal{V}}^* := \max_{\|G\|_{\mathcal{V}} \leq 1} \langle G, H\rangle_{\mathrm{HS}}\,. \tag{C.3}$$

Example C.2. (i) We set $\mathcal{V} = \mathcal{N}(L^2(S^1))$, i.e., we consider the nuclear norm. Let $(\sigma_n, v_n, u_n)_{n\in\mathbb{N}}$ be a singular system for some $H^* \in \mathcal{N}(L^2(S^1))$. We define

$$\mathcal{W} := \left\{ G \in \mathrm{HS}(L^2(S^1)) \;\middle|\; G = \sum_{n\in\mathbb{N}} \Big(u_n \langle\,\cdot\,, \alpha_n\rangle_{L^2(S^1)} + \beta_n \langle\,\cdot\,, v_n\rangle_{L^2(S^1)} \Big)\,,\ \alpha_n, \beta_n \in L^2(S^1) \right\}.$$

Then, all subgradients $H \in \partial\|H^*\|_{\mathrm{nuc}}$ of the nuclear norm at H^* are of the form

$$H = \sum_{n\in\mathbb{N}} u_n \langle\,\cdot\,, v_n\rangle_{L^2(S^1)} + W \qquad \text{with} \quad \mathcal{P}_{\mathcal{W}} W = 0 \qquad \text{and} \qquad \|W\| \leq 1\,,$$

cf. [99, Ex. 2]. This can be seen by checking (C.2). Since $\mathcal{P}_{\mathcal{W}} W = 0$ the operators W and H^* are orthogonal and we obtain

$$\langle H^*, H\rangle_{\mathrm{HS}} = \sum_{m,n\in\mathbb{N}} \sigma_n \langle v_n, v_m\rangle_{L^2(S^1)} \langle u_n, u_m\rangle_{L^2(S^1)} = \sum_{n\in\mathbb{N}} \sigma_n = \|H^*\|_{\mathrm{nuc}}\,.$$

Furthermore, for $g \in L^2(S^1)$, $V := \mathrm{span}\{v_n\}$ and $V^\perp$ denoting the orthogonal complement

of V with respect to $\langle \cdot, \cdot \rangle_{L^2(S^1)}$ we can write

$$Hg = H(\mathcal{P}_V g + \mathcal{P}_{V^\perp} g) = \sum_{n\in\mathbb{N}} u_n \langle \mathcal{P}_V g, v_n \rangle_{L^2(S^1)} + W(\mathcal{P}_{V^\perp} g)$$

and obtain with Parseval's identity and $\|W\| \leq 1$ that

$$\begin{aligned} \|Hg\|^2_{L^2(S^1)} &= \| \sum_{n\in\mathbb{N}} u_n \langle \mathcal{P}_V g, v_n \rangle_{L^2(S^1)} \|^2_{L^2(S^1)} + \|W(\mathcal{P}_{V^\perp} g)\|^2_{L^2(S^1)} \\ &\leq \|\mathcal{P}_V g\|^2_{L^2(S^1)} + \|\mathcal{P}_{V^\perp} g\|^2_{L^2(S^1)} = \|g\|^2_{L^2(S^1)}, \end{aligned}$$

so $\|H\| \leq 1$. Since the operator norm is the dual norm of $\|\cdot\|_{\mathrm{nuc}}$ this yields the result.

(ii) We consider $\mathcal{V} = \mathrm{HS}(L^2(S^1)) \cap \ell^1 \times \ell^1$. Let $(a_{m,n})_{m,n}$ denote the Fourier coefficients of $H^* \in \mathrm{HS}(L^2(S^1)) \cap \ell^1 \times \ell^1$. Furthermore, we set

$$\mathcal{W} := \{G \in \mathrm{HS}(L^2(S^1)) \,|\, supp_{\ell^0\times\ell^0} G \subset \mathrm{supp}_{\ell^0\times\ell^0} H\}$$

with $\ell^0\times\ell^0$-support $\mathrm{supp}_{\ell^0\times\ell^0}(\cdot)$ given as in Notation 2.7. Then, all subgradients $H \in \partial\|H^*\|_{\ell^1\times\ell^1}$ of the $\ell^1 \times \ell^1$ norm at H^* are of the form

$$H = \sum_{m,n\in\mathbb{Z}} \frac{\overline{a_{m,n}}}{|a_{m,n}|} \boldsymbol{e}_m \langle \cdot, \boldsymbol{e}_n \rangle_{L^2(S^1)} + F \qquad \text{with} \qquad \mathcal{P}_{\mathcal{W}} F = 0 \qquad \text{and} \qquad \|F\|_{\ell^\infty\times\ell^\infty} \leq 1\,. \tag{C.4}$$

As before, we prove this by checking (C.2). We calculate

$$\begin{aligned} \langle H^*, H \rangle_{\mathrm{HS}} &= \sum_{m,n,\tilde{m},\tilde{n}\in\mathbb{Z}} a_{m,n} \frac{\overline{a_{\tilde{m},\tilde{n}}}}{|a_{\tilde{m},\tilde{n}}|} \langle \boldsymbol{e}_m, \boldsymbol{e}_{\tilde{m}} \rangle_{L^2(S^1)} \langle \boldsymbol{e}_n, \boldsymbol{e}_{\tilde{n}} \rangle_{L^2(S^1)} \\ &= \sum_{m,n\in\mathbb{Z}} a_{m,n} \frac{\overline{a_{m,n}}}{|a_{m,n}|} = \sum_{m,n\in\mathbb{Z}} |a_{m,n}| = \|H^*\|_{\ell^1\times\ell^1}. \end{aligned}$$

Since $\|\cdot\|_{\ell^\infty\times\ell^\infty}$ is the dual norm of $\|\cdot\|_{\ell^1\times\ell^1}$ due to the disjoint supports of the two summands in (C.4) we further have

$$\|H\|_{\ell^\infty\times\ell^\infty} = \max\left\{ \| \left(\tfrac{\overline{a_{m,n}}}{|a_{m,n}|} \right)_{m,n} \|_{\ell^\infty\times\ell^\infty}, \|F\|_{\ell^\infty\times\ell^\infty} \right\} \leq 1\,.$$

Lemma C.3 (Calculation of subgradients)**.** *(a) Given two norms $\|\cdot\|_{\mathcal{V}}$ and $\|\cdot\|_{\mathcal{W}}$ the subgradient of their sum at some $H^* \in \mathrm{HS}(L^2(S^1))$ is given by*

$$\partial(\|H^*\|_{\mathcal{V}} + \|H^*\|_{\mathcal{W}}) = \partial\|H^*\|_{\mathcal{V}} + \partial\|H^*\|_{\mathcal{W}} := \{G + H \,|\, G \in \partial\|H^*\|_{\mathcal{V}}, H \in \partial\|H^*\|_{\mathcal{W}}\}.$$

(b) Given a norm $\|\cdot\|_{\mathcal{V}}$ and $\lambda > 0$ the subgradient of $\lambda\|\cdot\|_{\mathcal{V}}$ at some $H^* \in \mathrm{HS}(L^2(S^1))$ is given by

$$\partial(\lambda\|H^*\|_{\mathcal{V}}) = \lambda\partial\|H^*\|_{\mathcal{V}} := \{\lambda H \,|\, H \in \partial\|H^*\|_{\mathcal{V}}\}.$$

APPENDIX D

SOME PROXIMITY OPERATORS AND RELATED SPLITTING METHODS

Most of our problem formulations in Chapters 4 and 6 and thus resulting methods are of the same structure.

In this appendix we consequently consider the general convex but non-differentiable minimization problem

$$\underset{(\boldsymbol{F}_1,\dots,\boldsymbol{F}_J)\in(\mathbb{C}^{L\times L})^J}{\text{minimize}} \qquad \sum_{j=1}^{J} \mathscr{A}_j(\boldsymbol{F}_j) + \frac{1}{2}\|\mathcal{R}(\boldsymbol{F}_1,\dots,\boldsymbol{F}_J)\|_{\text{HS}}^2\,, \tag{D.1}$$

where $J, L \in \mathbb{N}$, and $\mathscr{A}_j : \mathbb{C}^{L\times L} \to \mathbb{R}$ are proper, lower semi-continuous and convex functions, whose specific choices are discussed later in Example D.2. We either further have for the residual function $\mathcal{R}$ that

$$\mathcal{R}(\boldsymbol{F}_1,\dots,\boldsymbol{F}_J) \;=\; \boldsymbol{F}_q^\delta - \sum_{j=1}^{J} \boldsymbol{F}_j$$

in case of far field operator splitting or that

$$\mathcal{R}(\boldsymbol{F}_1,\dots,\boldsymbol{F}_J) \;=\; \boldsymbol{F}_q^\delta|_{\Omega^c} - (\boldsymbol{I}-\mathcal{P}_\Omega)\sum_{j=1}^{J} \boldsymbol{F}_j$$

in case of far field operator completion. Here, $\boldsymbol{F}_q^\delta$ or $\boldsymbol{F}_q^\delta|_{\Omega^c}$ is the given noisy observable far field operator, respectively. The definition below can be e.g. found in [33, Subsec. 2.3].

Definition D.1. The *Moreau envelope* of a proper, lower semi-continuous and convex function $\mathscr{A} : \mathbb{C}^{L\times L} \to \mathbb{R}$ at index $\omega > 0$ is the continuous and convex function

$$\boldsymbol{F} \;\mapsto\; \inf_{\boldsymbol{G}\in\mathbb{C}^{L\times L}} \left(\mathscr{A}(\boldsymbol{G}) + \frac{1}{2\omega}\|\boldsymbol{F}-\boldsymbol{G}\|_{\text{HS}}^2\right).$$

This infimum is achieved at a unique point called $\text{prox}_{\omega\mathscr{A}}\,\boldsymbol{F}$ with *proximity operator* of $\omega\mathscr{A}$ given by

$$\text{prox}_{\omega\mathscr{A}} : \mathbb{C}^{L\times L} \to \mathbb{C}^{L\times L}\,, \qquad \boldsymbol{F} \;\mapsto\; \text{argmin}_{\boldsymbol{G}\in\mathbb{C}^{L\times L}} \left(\omega\mathscr{A}(\boldsymbol{G}) + \frac{1}{2}\|\boldsymbol{F}-\boldsymbol{G}\|_{\text{HS}}^2\right).$$

From [33, Prop. 3.1] and [34, Prop. 8] we know that the unique solution of above minimization problem (D.1) is for all $0 < \omega < 1/J$ characterized by the fixed point equation

$$\begin{bmatrix} \boldsymbol{F}_1 \\ \vdots \\ \boldsymbol{F}_J \end{bmatrix} = \begin{bmatrix} \text{prox}_{\omega\mathscr{A}_1}\left(\boldsymbol{F}_1 - \omega\mathcal{R}(\boldsymbol{F}_1,\dots,\boldsymbol{F}_J)\right) \\ \vdots \\ \text{prox}_{\omega\mathscr{A}_J}\left(\boldsymbol{F}_J - \omega\mathcal{R}(\boldsymbol{F}_1,\dots,\boldsymbol{F}_J)\right) \end{bmatrix}. \tag{D.2}$$

We mention that this choice of ω ensures $\|\omega\mathcal{K}^*\mathcal{K}\| \leq \omega J < 1$ for

$$\mathcal{K} : (\mathbb{C}^{L\times L})^J \to \mathbb{C}^{L\times L}\,, \qquad (\boldsymbol{F}_1,\dots,\boldsymbol{F}_J) \mapsto \sum_{j=1}^{J} \boldsymbol{F}_j$$

in case of far field operator splitting or

$$\mathcal{K} : (\mathbb{C}^{L\times L})^J \to \mathbb{C}^{L\times L}\,, \qquad (\boldsymbol{F}_1,\dots,\boldsymbol{F}_J) \mapsto (\boldsymbol{I}-\mathcal{P}_\Omega)\sum_{j=1}^{J} \boldsymbol{F}_j$$

in case of far field operator completion, see also [54, pp. 716f]. In our numerical tests we always choose $\omega = 1/(J+1)$. The following example provides those proximity operators that are relevant in this work, which are all deduced from the $\ell^1 \times \ell^1$ norm since they all enforce the related solution to be sparse in some sense.

Example D.2. (i) Let $\mathscr{A} := \mu\|\cdot\|_{\ell^1\times\ell^1}$ for some $\mu > 0$ and $\|\cdot\|_{\ell^1\times\ell^1}$ given as in Subsection 4.1.3. Then, $\operatorname{prox}_{\mathscr{A}} = \mathcal{F}_L^{-1} \circ \mathcal{S}_{2\mu} \circ \mathcal{F}_L$ with nonlinear *thresholding function* $\mathcal{S}_{2\mu} : \mathbb{C}^{L\times L} \to \mathbb{C}^{L\times L}$ given by

$$(\mathcal{S}_{2\mu}\boldsymbol{F})_{m,n} := \begin{cases} (|f_{m,n}| - \mu)\, e^{\mathrm{i}\arg f_{m,n}} & \text{if } |f_{m,n}| \geq \mu\,, \\ 0 & \text{else}\,, \end{cases} \qquad \boldsymbol{F} = (f_{m,n})_{1\leq m,n\leq L} \in \mathbb{C}^{L\times L}\,, \tag{D.3}$$

see e.g. [33, Exas. 2.16, 2.20].

(ii) Let $\mathscr{A} := \mu\|\boldsymbol{U}(\cdot)\|_{\ell^1\times\ell^1}$ for some $\mu > 0$ and some unitary matrix $\boldsymbol{U} \in \mathbb{C}^{L\times L}$. Then,

$$\operatorname{prox}_{\mathscr{A}} = \boldsymbol{U}^*(\mathcal{F}_L^{-1} \circ \mathcal{S}_{2\mu} \circ \mathcal{F}_L)(\boldsymbol{U}(\cdot))\,,$$

see e.g. [33, Lem. 2.8, Exas. 2.16, 2.20].

(iii) Let $\mathscr{A} := \mu\|\cdot\|_{\mathrm{nuc}}$ for some $\mu > 0$. Then, $\operatorname{prox}_{\mathscr{A}} = \mathcal{D}_{2\mu}$, where the singular value thresholding function $\mathcal{D}_{2\mu}$ is given by

$$\mathcal{D}_{2\mu} : \mathbb{C}^{L\times L} \to \mathbb{C}^{L\times L}\,, \qquad \mathcal{D}_{2\mu}\boldsymbol{F} := \boldsymbol{U}\mathcal{S}_{2\mu}(\boldsymbol{S})\boldsymbol{V}^* \tag{D.4}$$

with $\boldsymbol{F} = \boldsymbol{U}\boldsymbol{S}\boldsymbol{V}^*$ denoting a singular value decomposition of $\boldsymbol{F}$, see e.g. [15, pp. 1959f]. Here, $\mathcal{D}_{2\mu}$ is independent of the choice of $(\boldsymbol{U},\boldsymbol{S},\boldsymbol{V})$ and thus well-defined.

Given a start iterate $\boldsymbol{F}^{(0)} = (\boldsymbol{F}_1^{(0)},\dots,\boldsymbol{F}_J^{(0)}) \in \mathbb{C}^{L\times L}$ the fixed point equation (D.2) suggests to approximate the solution of (D.2) by the associated fixed point iteration

$$\begin{bmatrix} \boldsymbol{F}_1^{(k+1)} \\ \vdots \\ \boldsymbol{F}_J^{(k+1)} \end{bmatrix} = \begin{bmatrix} \operatorname{prox}_{\omega\mathscr{A}_1}\left(\boldsymbol{F}_1^{(k)} - \omega\mathcal{R}(\boldsymbol{F}_1^{(k)},\dots,\boldsymbol{F}_J^{(k)})\right) \\ \vdots \\ \operatorname{prox}_{\omega\mathscr{A}_J}\left(\boldsymbol{F}_J^{(k)} - \omega\mathcal{R}(\boldsymbol{F}_1^{(k)},\dots,\boldsymbol{F}_J^{(k)})\right) \end{bmatrix}, \tag{D.5}$$

which is known in literature *proximal forward-backward splitting algorithm*. In each iteration it is performed a gradient step forwards and a proximal step backwards. The choices for $\mathscr{A}_j$ as in Example D.2 lead to versions of the *iterative thresholding algorithm*, see e.g. [34]. We refer to [34, Prop. 2.1] and to [33, Thm. 3.4] for related convergence results.

Bibliography

[1] K. Atkinson and W. Han. *Spherical harmonics and approximations on the unit sphere: an introduction*, volume 2044 of *Lecture Notes in Mathematics*. Springer, Heidelberg, 2012. doi:10.1007/978-3-642-25983-8.

[2] L. Audibert and H. Haddar. A generalized formulation of the linear sampling method with exact characterization of targets in terms of farfield measurements. *Inverse Problems*, 30(3):035011, 20, 2014. doi:10.1088/0266-5611/30/3/035011.

[3] M. Aussal, Y. Boukari, and H. Haddar. Data completion method for the Helmholtz equation via surface potentials for partial Cauchy data. *Inverse Problems*, 36(5):055012, 17, 2020. doi:10.1088/1361-6420/ab730c.

[4] D. Baffet and M. J. Grote. On wave splitting, source separation and echo removal with absorbing boundary conditions. *J. Comput. Phys.*, 387:589–596, 2019. doi:10.1016/j.jcp.2019.03.004.

[5] H. H. Bauschke and P. L. Combettes. *Convex analysis and monotone operator theory in Hilbert spaces*. CMS Books in Mathematics/Ouvrages de Mathématiques de la SMC. Springer, Cham, second edition, 2017. With a foreword by Hédy Attouch. doi:10.1007/978-3-319-48311-5.

[6] A. Beck and M. Teboulle. A fast iterative shrinkage-thresholding algorithm for linear inverse problems. *SIAM J. Imaging Sci.*, 2(1):183–202, 2009. doi:10.1137/080716542.

[7] K. Belkebir and M. Saillard, editors. *Special section: Testing inversion algorithms against experimental data*. Institute of Physics Publishing, Bristol, 2001. Inverse Problems 17 (2001), no. 6. doi:10.1088/0266-5611/17/6/301.

[8] F. ben Hassen, J. Liu, and R. Potthast. On source analysis by wave splitting with applications in inverse scattering of multiple obstacles. *J. Comput. Math.*, 25(3):266–281, 2007.

[9] M. T. Bevacqua and R. Palmeri. Qualitative methods for the inverse obstacle problem: A comparison on experimental data. *Journal of Imaging*, 5(4), 2019. URL: https://www.mdpi.com/2313-433X/5/4/47, doi:10.3390/jimaging5040047.

[10] N. Bleistein and J. K. Cohen. Nonuniqueness in the inverse source problem in acoustics and electromagnetics. *J. Mathematical Phys.*, 18(2):194–201, 1977. doi:10.1063/1.523256.

[11] L. Borcea, V. Druskin, A. V. Mamonov, and M. Zaslavsky. Untangling the nonlinearity in inverse scattering with data-driven reduced order models. *Inverse Problems*, 34(6):065008, 35, 2018. doi:10.1088/1361-6420/aabb16.

[12] Y. Boukari and H. Haddar. A convergent data completion algorithm using surface integral equations. *Inverse Problems*, 31(3):035011, 21, 2015. doi:10.1088/0266-5611/31/3/035011.

[13] T. Bouwmans and E. H. Zahzah. Robust PCA via principal component pursuit: A review for a comparative evaluation in video surveillance. *Computer Vision and Image Understanding*, 122:22–34, 2014. doi:10.1016/j.cviu.2013.11.009.

[14] A. L. Bukhgeim. Recovering a potential from Cauchy data in the two-dimensional case. *J. Inverse Ill-Posed Probl.*, 16(1):19–33, 2008. doi:10.1515/jiip.2008.002.

[15] J.-F. Cai, E. J. Candès, and Z. Shen. A singular value thresholding algorithm for matrix completion. *SIAM J. Optim.*, 20(4):1956–1982, 2010. doi:10.1137/080738970.

[16] F. Cakoni and D. Colton. *A qualitative approach to inverse scattering theory*, volume 188 of *Applied Mathematical Sciences*. Springer, New York, 2014. doi:10.1007/978-1-4614-8827-9.

[17] F. Cakoni, D. Colton, and H. Haddar. *Inverse scattering theory and transmission eigenvalues*, volume 98 of *CBMS-NSF Regional Conference Series in Applied Mathematics*. Society for Industrial and Applied Mathematics (SIAM), Philadelphia, PA, 2023. Second edition.

[18] E. J. Candès. Mathematics of sparsity (and a few other things). In *Proceedings of the International Congress of Mathematicians—Seoul 2014. Vol. 1*, pages 235–258. Kyung Moon Sa, Seoul, 2014.

[19] E. J. Candès, X. Li, Y. Ma, and J. Wright. Robust principal component analysis? *J. ACM*, 58(3):Art. 11, 37, 2011. doi:10.1145/1970392.1970395.

[20] E. J. Candès and Y. Plan. Matrix completion with noise. *Proceedings of the IEEE*, 98(6):925–936, 2010. doi:10.1109/JPROC.2009.2035722.

[21] E. J. Candès and B. Recht. Exact matrix completion via convex optimization. *Found. Comput. Math.*, 9(6):717–772, 2009. doi:10.1007/s10208-009-9045-5.

[22] E. J. Candès, J. Romberg, and T. Tao. Robust uncertainty principles: exact signal reconstruction from highly incomplete frequency information. *IEEE Trans. Inform. Theory*, 52(2):489–509, 2006. doi:10.1109/TIT.2005.862083.

[23] A. Carpio, M. Pena, and M. L. Rapún. Processing the 2D and 3D Fresnel experimental databases via topological derivative methods. *Inverse Problems*, 37(10):Paper No. 105012, 30, 2021. doi:10.1088/1361-6420/ac21c8.

[24] V. Chandrasekaran, S. Sanghavi, P. A. Parrilo, and A. S. Willsky. Sparse and low-rank matrix decompositions. *IFAC Proceedings Volumes*, 42(10):1493–1498, 2009. doi:10.3182/20090706-3-FR-2004.00249.

[25] V. Chandrasekaran, S. Sanghavi, P. A. Parrilo, and A. S. Willsky. Rank-sparsity incoherence for matrix decomposition. *SIAM J. Optim.*, 21(2):572–596, 2011. doi:10.1137/090761793.

[26] S. S. Chen, D. L. Donoho, and M. A. Saunders. Atomic decomposition by basis pursuit. *SIAM Rev.*, 43(1):129–159, 2001. doi:10.1137/S003614450037906X.

[27] C. Clason. *Introduction to functional analysis*. Compact Textbooks in Mathematics. Birkhäuser/Springer, Cham, 2020. doi:10.1007/978-3-030-52784-6.

[28] S. Cogar, D. Colton, S. Meng, and P. Monk. Modified transmission eigenvalues in inverse scattering theory. *Inverse Problems*, 33(12):125002, 31, 2017. doi:10.1088/1361-6420/aa9418.

[29] D. Colton and A. Kirsch. A simple method for solving inverse scattering problems in the resonance region. *Inverse Problems*, 12(4):383–393, 1996. doi:10.1088/0266-5611/12/4/003.

[30] D. Colton and R. Kress. Looking back on inverse scattering theory. *SIAM Rev.*, 60(4):779–807, 2018. doi:10.1137/17M1144763.

[31] D. Colton and R. Kress. *Inverse acoustic and electromagnetic scattering theory*, volume 93 of *Applied Mathematical Sciences*. Springer, Cham, fourth edition, 2019. doi:10.1007/978-3-030-30351-8.

[32] D. Colton and P. Monk. The inverse scattering problem for time-harmonic acoustic waves in an inhomogeneous medium. *Quart. J. Mech. Appl. Math.*, 41(1):97–125, 1988. doi:10.1093/qjmam/41.1.97.

[33] P. L. Combettes and V. R. Wajs. Signal recovery by proximal forward-backward splitting. *Multiscale Model. Simul.*, 4(4):1168–1200, 2005. doi:10.1137/050626090.

[34] I. Daubechies, M. Defrise, and C. De Mol. An iterative thresholding algorithm for linear inverse problems with a sparsity constraint. *Comm. Pure Appl. Math.*, 57(11):1413–1457, 2004. doi:10.1002/cpa.20042.

[35] N. DeFilippis, S. Moskow, and J. C. Schotland. Born and inverse Born series for scattering problems with Kerr nonlinearities. *Inverse Problems*, 39(12):Paper No. 125015, 20, 2023. doi:10.1088/1361-6420/ad07a5.

[36] F. Deutsch. The angle between subspaces of a Hilbert space. In *Approximation theory, wavelets and applications (Maratea, 1994)*, volume 454 of *NATO Adv. Sci. Inst. Ser. C: Math. Phys. Sci.*, pages 107–130. Kluwer Acad. Publ., Dordrecht, 1995.

[37] D. L. Donoho. Compressed sensing. *IEEE Trans. Inform. Theory*, 52(4):1289–1306, 2006. doi:10.1109/TIT.2006.871582.

[38] D. L. Donoho, M. Elad, and V. N. Temlyakov. Stable recovery of sparse overcomplete representations in the presence of noise. *IEEE Trans. Inform. Theory*, 52(1):6–18, 2006. doi:10.1109/TIT.2005.860430.

[39] D. L. Donoho and X. Huo. Uncertainty principles and ideal atomic decomposition. *IEEE Trans. Inform. Theory*, 47(7):2845–2862, 2001. doi:10.1109/18.959265.

[40] D. L. Donoho and P. B. Stark. Uncertainty principles and signal recovery. *SIAM J. Appl. Math.*, 49(3):906–931, 1989. doi:10.1137/0149053.

[41] F. Dou, X. Liu, S. Meng, and B. Zhang. Data completion algorithms and their applications in inverse acoustic scattering with limited-aperture backscattering data. *J. Comput. Phys.*, 469:Paper No. 111550, 17, 2022. doi:10.1016/j.jcp.2022.111550.

[42] V. Druskin, A. V. Mamonov, A. E. Thaler, and M. Zaslavsky. Direct, nonlinear inversion algorithm for hyperbolic problems via projection-based model reduction. *SIAM J. Imaging Sci.*, 9(2):684–747, 2016. doi:10.1137/15M1039432.

[43] V. Druskin, A. V. Mamonov, and M. Zaslavsky. A nonlinear method for imaging with acoustic waves via reduced order model backprojection. *SIAM J. Imaging Sci.*, 11(1):164–196, 2018. doi:10.1137/17M1133580.

[44] H. W. Engl, M. Hanke, and A. Neubauer. *Regularization of inverse problems*, volume 375. Springer Science & Business Media, 1996.

[45] L. C. Evans. *Partial differential equations*, volume 19 of *Graduate Studies in Mathematics*. American Mathematical Society, Providence, RI, 1998. doi:10.1090/gsm/019.

[46] D. Gilbarg and N. S. Trudinger. *Elliptic partial differential equations of second order*. Classics in Mathematics. Springer-Verlag, Berlin, 2001. Reprint of the 1998 edition.

[47] G. H. Golub and C. F. Van Loan. *Matrix computations*. Johns Hopkins Studies in the Mathematical Sciences. Johns Hopkins University Press, Baltimore, MD, fourth edition, 2013.

[48] M. Graff, M. J. Grote, F. Nataf, and F. Assous. How to solve inverse scattering problems without knowing the source term: a three-step strategy. *Inverse Problems*, 35(10):104001, 20, 2019. doi:10.1088/1361-6420/ab2d5f.

[49] M. Grasmair, M. Haltmeier, and O. Scherzer. Necessary and sufficient conditions for linear convergence of ℓ^1-regularization. *Comm. Pure Appl. Math.*, 64(2):161–182, 2011. doi:10.1002/cpa.20350.

[50] R. Griesmaier, M. Hanke, and J. Sylvester. Far field splitting for the Helmholtz equation. *SIAM J. Numer. Anal.*, 52(1):343–362, 2014. doi:10.1137/120891381.

[51] R. Griesmaier and B. Harrach. Monotonicity in inverse medium scattering on unbounded domains. *SIAM J. Appl. Math.*, 78(5):2533–2557, 2018. doi:10.1137/18M1171679.

[52] R. Griesmaier, N. Hyvönen, and O. Seiskari. A note on analyticity properties of far field patterns. *Inverse Probl. Imaging*, 7(2):491–498, 2013. doi:10.3934/ipi.2013.7.491.

[53] R. Griesmaier and L. Schätzle. Far field operator splitting and completion in inverse medium scattering. *Inverse Problems*, 40(11):Paper No. 115010, 32, 2024.

[54] R. Griesmaier and J. Sylvester. Far field splitting by iteratively reweighted ℓ^1minimization. *SIAM J. Appl. Math.*, 76(2):705–730, 2016. doi:10.1137/15M102839X.

[55] R. Griesmaier and J. Sylvester. Uncertainty principles for inverse source problems, far field splitting, and data completion. *SIAM J. Appl. Math.*, 77(1):154–180, 2017. doi:10.1137/16M1086157.

[56] R. Griesmaier and J. Sylvester. Uncertainty principles for three-dimensional inverse source problems. *SIAM J. Appl. Math.*, 77(6):2066–2092, 2017. doi:10.1137/17M111287X.

[57] R. Griesmaier and J. Sylvester. Uncertainty principles for inverse source problems for electromagnetic and elastic waves. *Inverse Problems*, 34(6):065003, 37, 2018. doi:10.1088/1361-6420/aab45c.

[58] M. J. Grote, M. Kray, F. Nataf, and F. Assous. Time-dependent wave splitting and source separation. *J. Comput. Phys.*, 330:981–996, 2017. doi:10.1016/j.jcp.2016.10.021.

[59] P. Henrici. *Applied and computational complex analysis. Vol. 1*. Wiley Classics Library. John Wiley & Sons, Inc., New York, 1988. Power series—integration—conformal mapping—location of zeros, Reprint of the 1974 original, A Wiley-Interscience Publication.

[60] M. R. Hestenes and E. Stiefel. Methods of conjugate gradients for solving linear systems. *J. Research Nat. Bur. Standards*, 49:409–436, 1952.

[61] L. Hörmander. *An introduction to complex analysis in several variables*, volume Vol. 7 of *North-Holland Mathematical Library*. North-Holland Publishing Co., Amsterdam-London; American Elsevier Publishing Co., Inc., New York, revised edition, 1973.

[62] K. Kilgore, S. Moskow, and J. C. Schotland. Inverse Born series for scalar waves. *J. Comput. Math.*, 30(6):601–614, 2012. doi:10.4208/jcm.1205-m3935.

[63] K. Kilgore, S. Moskow, and J. C. Schotland. Convergence of the Born and inverse Born series for electromagnetic scattering. *Appl. Anal.*, 96(10):1737–1748, 2017. doi:10.1080/00036811.2017.1292349.

[64] A. Kirsch. Characterization of the shape of a scattering obstacle using the spectral data of the far field operator. *Inverse Problems*, 14(6):1489–1512, 1998. doi:10.1088/0266-5611/14/6/009.

[65] A. Kirsch. Factorization of the far-field operator for the inhomogeneous medium case and an application in inverse scattering theory. *Inverse Problems*, 15(2):413–429, 1999. doi:10.1088/0266-5611/15/2/005.

[66] A. Kirsch. The MUSIC algorithm and the factorization method in inverse scattering theory for inhomogeneous media. *Inverse Problems*, 18(4):1025–1040, 2002. doi:10.1088/0266-5611/18/4/306.

[67] A. Kirsch. *An introduction to the mathematical theory of inverse problems*, volume 120 of *Applied Mathematical Sciences*. Springer, New York, second edition, 2011. doi:10.1007/978-1-4419-8474-6.

[68] A. Kirsch. Remarks on the Born approximation and the factorization method. *Appl. Anal.*, 96(1):70–84, 2017. doi:10.1080/00036811.2016.1188286.

[69] A. Kirsch and N. Grinberg. *The factorization method for inverse problems*, volume 36 of *Oxford Lecture Series in Mathematics and its Applications*. Oxford University Press, Oxford, 2008.

[70] A. Kirsch and F. Hettlich. *The mathematical theory of time-harmonic Maxwell's equations*, volume 190 of *Applied Mathematical Sciences*. Springer, Cham, 2015. Expansion-, integral-, and variational methods. doi:10.1007/978-3-319-11086-8.

[71] D. E. Knuth. Johann Faulhaber and sums of powers. *Math. Comp.*, 61(203):277–294, 1993. doi:10.2307/2152953.

[72] I. Krasikov. Uniform bounds for Bessel functions. *J. Appl. Anal.*, 12(1):83–91, 2006. doi:10.1515/JAA.2006.83.

[73] R. Kress. *Linear integral equations*, volume 82 of *Applied Mathematical Sciences*. Springer, New York, third edition, 2014. doi:10.1007/978-1-4614-9593-2.

[74] R. Kreß and G. F. Roach. Transmission problems for the Helmholtz equation. *J. Mathematical Phys.*, 19(6):1433–1437, 1978. doi:10.1063/1.523808.

[75] S. Kusiak and J. Sylvester. The scattering support. *Comm. Pure Appl. Math.*, 56(11):1525–1548, 2003. doi:10.1002/cpa.3038.

[76] S. Kusiak and J. Sylvester. The convex scattering support in a background medium. *SIAM J. Math. Anal.*, 36(4):1142–1158, 2005. doi:10.1137/S0036141003433577.

[77] L. J. Landau. Bessel functions: monotonicity and bounds. *J. London Math. Soc. (2)*, 61(1):197–215, 2000. doi:10.1112/S0024610799008352.

[78] M. M. Lavrent'ev, V. G. Romanov, and S. P. Shishatskii. *Ill-posed problems of mathematical physics and analysis*, volume 64 of *Translations of Mathematical Monographs*. American Mathematical Society, Providence, RI, 1986. Translated from the Russian by J. R. Schulenberger. doi:10.1090/mmono/064.

[79] Z. Lin, A. Ganesh, J. Wright, L. Wu, M. Chen, and Y. Ma. Fast convex optimization algorithms for exact recovery of a corrupted low-rank matrix. *Coordinated Science Laboratory Report no. UILU-ENG-09-2214, DC-246*, 2009.

[80] X. Liu and J. Sun. Data recovery in inverse scattering: from limited-aperture to full-aperture. *J. Comput. Phys.*, 386:350–364, 2019. doi:10.1016/j.jcp.2018.10.036.

[81] W. McLean. *Strongly elliptic systems and boundary integral equations*. Cambridge University Press, Cambridge, 2000.

[82] P. Monk, M. Pena, and V. Selgas. Multifrequency linear sampling method on experimental datasets. *IEEE Transactions on Antennas and Propagation*, 71(11):8788–8798, 2023. doi:10.1109/TAP.2023.3298974.

[83] S. Moskow and J. C. Schotland. Convergence and stability of the inverse scattering series for diffuse waves. *Inverse Problems*, 24(6):065005, 16, 2008. doi:10.1088/0266-5611/24/6/065005.

[84] A. I. Nachman. Reconstructions from boundary measurements. *Ann. of Math. (2)*, 128(3):531–576, 1988. doi:10.2307/1971435.

[85] F. Natterer. An error bound for the Born approximation. *Inverse Problems*, 20(2):447–452, 2004. doi:10.1088/0266-5611/20/2/009.

[86] R. G. Novikov. A multidimensional inverse spectral problem for the equation $-\Delta\psi+(v(x)-Eu(x))\psi=0$. *Funktsional. Anal. i Prilozhen.*, 22(4):11–22, 96, 1988. doi:10.1007/BF01077418.

[87] F. W. J. Olver, D. W. Lozier, R. F. Boisvert, C. W. Clark, and eds. Nist digital library of mathematical functions, 2010. URL: https://dlmf.nist.gov/.

[88] R. Potthast, F. M. Fazi, and P. A. Nelson. Source splitting via the point source method. *Inverse Problems*, 26(4):045002, 17, 2010. doi:10.1088/0266-5611/26/4/045002.

[89] A. G. Ramm. Recovery of the potential from fixed-energy scattering data. *Inverse Problems*, 4(3):877–886, 1988. URL: http://stacks.iop.org/0266-5611/4/877.

[90] M. Reed and B. Simon. *Methods of modern mathematical physics. I. Functional analysis*. Academic Press, New York-London, 1972.

[91] R. T. Rockafellar. *Convex analysis*. Princeton Landmarks in Mathematics. Princeton University Press, Princeton, NJ, 1997. Reprint of the 1970 original, Princeton Paperbacks.

[92] R. T. Rockafellar and R. J.-B. Wets. *Variational analysis*, volume 317 of *Grundlehren der mathematischen Wissenschaften [Fundamental Principles of Mathematical Sciences]*. Springer-Verlag, Berlin, 1998. doi:10.1007/978-3-642-02431-3.

[93] J. Saranen and G. Vainikko. *Periodic integral and pseudodifferential equations with numerical approximation*. Springer Monographs in Mathematics. Springer-Verlag, Berlin, 2002. doi:10.1007/978-3-662-04796-5.

[94] I. E. Schochetman, R. L. Smith, and S.-K. Tsui. On the closure of the sum of closed subspaces. *Int. J. Math. Math. Sci.*, 26(5):257–267, 2001. doi:10.1155/S0161171201005324.

[95] J. Sylvester. Notions of support for far fields. *Inverse Problems*, 22(4):1273–1288, 2006. doi:10.1088/0266-5611/22/4/010.

[96] J. Sylvester. An estimate for the free Helmholtz equation that scales. *Inverse Probl. Imaging*, 3(2):333–351, 2009. doi:10.3934/ipi.2009.3.333.

[97] G. Vainikko. Fast solvers of the Lippmann-Schwinger equation. In *Direct and inverse problems of mathematical physics (Newark, DE, 1997)*, volume 5 of *Int. Soc. Anal. Appl. Comput.*, pages 423–440. Kluwer Acad. Publ., Dordrecht, 2000. URL: https://doi.org/10.1007/978-1-4757-3214-6_25, doi:10.1007/978-1-4757-3214-6_25.

[98] T. von Petersdorff. Boundary integral equations for mixed Dirichlet, Neumann and transmission problems. *Math. Methods Appl. Sci.*, 11(2):185–213, 1989. doi:10.1002/mma.1670110203.

[99] G. A. Watson. Characterization of the subdifferential of some matrix norms. *Linear Algebra Appl.*, 170:33–45, 1992. doi:10.1016/0024-3795(92)90407-2.

[100] J. Wright, A. Ganesh, S. Rao, Y. Peng, and Y. Ma. Robust principal component analysis: Exact recovery of corrupted low-rank matrices via convex optimization. In Y. Bengio, D. Schuurmans, J. Lafferty, C. Williams, and A. Culotta, editors, *Advances in Neural Information Processing Systems*, volume 22. Curran Associates, Inc., 2009.

[101] Z. Zhou, X. Li, J. Wright, E. Candès, and Y. Ma. Stable principal component pursuit. In *2010 IEEE International Symposium on Information Theory*, pages 1518–1522, 2010. doi:10.1109/ISIT.2010.5513535.

Notation

Basic notation

$\mathbb{N}$, $\mathbb{N}_0$	natural numbers, $\mathbb{N}_0 = \mathbb{N} \cup \{0\}$	
$\mathbb{Z}$	integer numbers	
$\mathbb{R}^d$	$d-$dimensional real Euclidean space	
$\mathbb{C}^d$	$d-$dimensional complex Euclidean space	
$\boldsymbol{x}$	point $\boldsymbol{x} = (x_1, \ldots, x_d)^\top$ in $\mathbb{R}^d$	
$\lvert\boldsymbol{x}\rvert$	Euclidean norm of $\boldsymbol{x}$	
$\boldsymbol{x} \cdot \boldsymbol{y}$	dot product of $\boldsymbol{x}, \boldsymbol{y} \in \mathbb{R}^d$	
D	scatterer, open set in $\mathbb{R}^d$ with Lipschitz boundary	8, 9
D_1, D_2	disjointly supported scatterer's components	37
$\boldsymbol{x}'$	point $\boldsymbol{x}' = (x_1, \ldots, x_{d-1})^\top$ in $\mathbb{R}^{d-1}$	7
$B'_R(\boldsymbol{c}')$	open ball in $\mathbb{R}^{d-1}$ of radius R centered at $\boldsymbol{c}' \in \mathbb{R}^{d-1}$	8
S^{d-1}	unit sphere in $\mathbb{R}^d$	8
$\widehat{\boldsymbol{x}}$	direction $\boldsymbol{x}/\lvert\boldsymbol{x}\rvert \in S^{d-1}$ of $\boldsymbol{x}$, observation direction	9, 10
$\boldsymbol{\theta}$	illumination direction of incident plane wave u^i	9
Ω	non-observable set in $S^{d-1} \times S^{d-1}$	103
$\Omega^{c,r}$	subset of $S^{d-1} \times S^{d-1}$ on which observable far field data can be extended according reciprocity	104
$\boldsymbol{\alpha}$	multi-index in $\mathbb{N}_0^d$ of order $\lvert\boldsymbol{\alpha}\rvert = \alpha_1 + \ldots + \alpha_d$	143
$\boldsymbol{x}^{\boldsymbol{\alpha}}$	multi-index notation for power, $\boldsymbol{x}^{\boldsymbol{\alpha}} = x_1^{\alpha_1} \ldots x_d^{\alpha_d}$	143
$\lvert D\rvert$, $\lvert\Omega\rvert$	volume of $D \subseteq \mathbb{R}^d$, surface area of $\Omega \subseteq S^{d-1} \times S^{d-1}$	
k	real-valued and positive wave number	9
c	speed of light in vacuum, $c = 299792458$m/s	130
f	frequency	130
$N \gtrsim kR$	$N = N(kR)$ is somewhat larger than kR	16
δ_n^m	Kronecker delta	21, 76

Function spaces

$C^m(D)$	m times continuously differentiable functions on $D \subseteq \mathbb{R}^d$	7
$C_0^m(D)$	C^m functions with compact support on $D \subseteq \mathbb{R}^d$	7
$L^p(D)$	Lebesgue space on $D \subseteq \mathbb{R}^d$	7
$L^p(D, \mathbb{C}^3)$	vector-valued Lebesgue space on $D \subseteq \mathbb{R}^d$	7
$L^p(S^{d-1})$, $L^p(S^{d-1} \times S^{d-1})$	Lebesgue space on unit sphere	9

$H^1(D)$	Sobolev space of weakly differentiable functions on $D \subseteq \mathbb{R}^d$	7
$H^1_{\mathrm{loc}}(\mathbb{R}^d)$	Sobolev space of H^1 functions on compact subsets of $\mathbb{R}^d$	8
$\mathbb{H}^d_n$	homogeneous polynomials of degree n in $\mathbb{R}^d$	143
$\mathbb{Y}_n(\mathbb{R}^d)$	harmonic homogeneous polynomials of degree n in $\mathbb{R}^d$	143
$\mathbb{Y}^d_n$	spherical harmonics of degree n in $\mathbb{R}^d$, $\mathbb{Y}^d_n \subseteq L^2(S^{d-1})$	143

Spaces of sequences

$\ell^p \times \ell^p$, $\|\cdot\|_{\ell^p \times \ell^p}$	$\ell^p \times \ell^p$ space of Fourier coefficients $(a_{m,n}) \in \mathbb{C}^{\mathbb{Z}\times\mathbb{Z}}$	15
$\ell^p \times \ell^p(W)$, $\|\cdot\|_{\ell^p \times \ell^p(W)}$	$\ell^p \times \ell^p$ sequences with $\ell^0 \times \ell^0$-support in $W \subseteq \mathbb{Z}^2$	16
$(\ell^p \times \ell^p)(L^2(S^2 \times S^2))$, $\|\cdot\|_{\ell^p \times \ell^p}$	$\ell^p \times \ell^p$ space of spherical harmonic components $(\alpha_{m,n}) \in (L^2(S^2 \times S^2))^{\mathbb{N}_0 \times \mathbb{N}_0}$	22
$(\ell^p_w \times \ell^p_v)(L^2(S^2 \times S^2))$, $\|\cdot\|_{\ell^p_w \times \ell^p_v}$	weighted $(\ell^p \times \ell^p)(L^2(S^2 \times S^2))$ space	22
$(\ell^p_w \times \ell^p_v)(L^2(S^2 \times S^2))(W)$, $\|\cdot\|_{\ell^p \times \ell^p(W)}$	$(\ell^p_w \times \ell^p_v)(L^2(S^2 \times S^2))$ sequences with $\ell^0 \times \ell^0$-support in $W \subseteq \mathbb{N}_0^2$	22

Spaces of operators

$\mathcal{L}(L^2(S^{d-1}))$, $\|\cdot\|$	linear bounded operators $L^2(S^{d-1}) \to L^2(S^{d-1})$	139
$\mathcal{K}(L^2(S^{d-1}))$	compact operators in $\mathcal{L}(L^2(S^{d-1}))$	139
$\mathcal{N}(L^2(S^{d-1}))$, $\|\cdot\|_{\mathrm{nuc}}$	nuclear operators in $\mathcal{L}(L^2(S^{d-1}))$	140
$\mathrm{HS}(L^2(S^{d-1}))$, $\|\cdot\|_{\mathrm{HS}}$	Hilbert–Schmidt operators in $\mathcal{L}(L^2(S^{d-1}))$	140
$\mathcal{V}_N$, $\mathcal{V}_N^{\boldsymbol{c}}$	subspace of sparse far field operators, $\mathcal{V}_N = \mathcal{V}_N^{\boldsymbol{0}}$	16, 23, 29
$\mathcal{W}_N$, $\mathcal{W}_N^{\boldsymbol{c}}$	subspace of low rank far field operators, $\mathcal{W}_N = \mathcal{W}_N^{\boldsymbol{0}}$	16, 23, 29
$\mathcal{V}_{M,N}$, $\mathcal{V}_{M,N}^{\boldsymbol{b},\boldsymbol{c}}$	generalized subspace of sparse far field operators, $\mathcal{V}_{M,N} = \mathcal{V}_{M,N}^{\boldsymbol{0},\boldsymbol{0}}$, $\mathcal{V}_{N,N}^{\boldsymbol{c},\boldsymbol{c}} = \mathcal{V}_N^{\boldsymbol{c}}$	40
$\widetilde{\mathcal{V}}_N$, $\widetilde{\mathcal{V}}_N^{\boldsymbol{c}}$, $\widetilde{\mathcal{V}}_{M,N}$, $\widetilde{\mathcal{V}}_{M,N}^{\boldsymbol{b},\boldsymbol{c}}$	sparse far field operators satisfying reciprocity	76
$\mathcal{V}_\Omega$	non-observable far field operators ass. to Ω	103
$\mathrm{HS}(L^2(S^{d-1})) \cap L^p(S^{d-1} \times S^{d-1})$, $\|\cdot\|_{L^p}$	operators in $\mathrm{HS}(L^2(S^{d-1}))$ with L^p integral kernel	15, 22
$\mathrm{HS}(L^2(S^1)) \cap \ell^p \times \ell^p$, $\|\cdot\|_{\ell^p \times \ell^p}$	operators in $\mathrm{HS}(L^2(S^1))$ with Fourier coefficients in $\ell^p \times \ell^p$	15
$\mathrm{HS}(L^2(S^2)) \cap \ell^p \times \ell^p$, $\|\cdot\|_{\ell^p \times \ell^p}$	operators in $\mathrm{HS}(L^2(S^2))$ with spherical harmonic components in $\ell^p \times \ell^p$	22

Functions

Φ_k	fundamental solution of the Helmholtz equation at wave number k	9
$q_{\boldsymbol{c}}$, q	by $\boldsymbol{c}$ shifted and unshifted contrast function	9, 28
n^2	index of refraction	9
u^i	incident plane wave	9
u^s_q	scattered wave that results from scattering of u^i on q	9
u_q	total wave, $u_q = u^i + u^s_q$	9
u^∞_q	far field pattern	10

$u_q^{s,(l)}$, $u_{q_{j_1},\dots,q_{j_l}}^{s,(l)}$	scattered wave components associated to scattering processes of order l	13
$u_q^{\infty,(l)}$, $u_{q_{j_1},\dots,q_{j_l}}^{\infty,(l)}$	far field components associated to scattering processes of order l	13, 38
$u_q^{\infty,(\leq p)}$, $u_{q_j}^{\infty,(\leq p)}$	Born far field of order p	13
J_n	Bessel function of order n	144
Y_n	Neumann function of order n	144
$H_n^{(1)}$, $H_n^{(2)}$	Hankel function of first and second kind and of order n	144
$(\boldsymbol{e}_n)_n$	trigonometric monomials of order n, ONB of $L^2(S^1)$	15
$(\boldsymbol{e}_{m,n})_{m,n}$	ONB of $L^2(S^1 \times S^1)$, $\boldsymbol{e}_{m,n}(\widehat{\boldsymbol{x}},\boldsymbol{\theta}) = \boldsymbol{e}_m(\widehat{\boldsymbol{x}})\boldsymbol{e}_{-n}(\boldsymbol{\theta})$	15
P_n	Legendre polynomial of order n	145
P_n^m	associated Legendre function of order n	145
$P_n^{\widehat{\boldsymbol{x}}}$	spherical harmonic of order n, $P_n^{\widehat{\boldsymbol{x}}} = P_n(\widehat{\boldsymbol{x}} \cdot (\,\cdot\,))$	145
j_n	spherical Bessel function of order n	146
y_n	spherical Neumann function of order n	146
$h_n^{(1)}$, $h_n^{(2)}$	spherical Hankel function of first and second kind and order n	146
$(Y_n^m)_{m,n}$	mth spherical harmonics of order n, ONB of $L^2(S^2 \times S^2)$	145
$a_{m,n}$, $a_{m,n}^{(l)}$, $a_{m,n}^{\boldsymbol{c}}$	(m,n)th Fourier coefficient of u_q^∞, $u_q^{\infty,(l)}$, $u_{q_{\boldsymbol{c}}}^\infty$, …	16, 31
$\alpha_{m,n}$, $\alpha_{m,n}^{(l)}$, $\alpha_{m,n}^{\boldsymbol{c}}$	(m,n)th spherical harmonic component of u_q^∞, $u_q^{\infty,(l)}$, $u_{q_{\boldsymbol{c}}}^\infty$, …	23, 32
$\mathcal{F}_L$	discrete L-point two-dimensional Fourier transform	86
$\mathcal{Q}_{M,N}$, $\mathcal{Q}_N$	truncation or cut-off function on $\mathbb{C}^{L\times L}$	86
$\mathcal{S}_\mu$	nonlinear thresholding function on $\mathbb{C}^{L\times L}$	152
$\mathcal{M}_{\mu,\boldsymbol{b},\boldsymbol{c}}$	thresholding function in modulated Fourier bases on $\mathbb{C}^{L\times L}$	89
$\mathcal{D}_\mu$	singular value thresholding function on $\mathbb{C}^{L\times L}$	152
χ_D	characteristical function of $D \subseteq \mathbb{R}^d$	

OPERATORS

$\operatorname{rank} G$	rank of $G \in \mathcal{L}(L^2(S^{d-1}))$	141
$\operatorname{tr} G$	trace of $G \in \mathcal{K}(L^2(S^{d-1}))$	140
$\mathcal{R}(G)$	range of $G \in \mathcal{L}(L^2(S^{d-1}))$	
$\mathcal{N}(G)$	null space of $G \in \mathcal{L}(L^2(S^{d-1}))$	
$\operatorname{supp} u$	support of function u	7
$\operatorname{supp}_{L^0} G$	L^0-support of $G \in \mathrm{HS}(L^2(S^{d-1}))$	16, 22
$\operatorname{supp}_{\ell^0\times\ell^0} G$	$\ell^0 \times \ell^0$-support of $G \in \mathrm{HS}(L^2(S^{d-1}))$	16, 22
F_q, F_{q_j}	far field operator	10, 37
$F_q^{(l)}$, $F_{q_{j_1},\dots,q_{j_l}}^{(l)}$	far field operator component associated to scattering processes of order l	
$F_q^{(\leq p)}$, $F_{q_j}^{(\leq p)}$	Born far field operator of order p	
B_q	non-observable part of F_q	103

$F_q\|_{\Omega^c}$	restricted or observable far field operator	103
S_q	scattering operator	11
L_q, $L_{q,j,l}$	operator modeling Lippmann–Schwinger equation	13, 38
$T_{\boldsymbol{c}}$	translation operator on $L^2(S^{d-1})$	29
$\mathcal{T}_{\boldsymbol{c}}$	translation operator on $\mathrm{HS}(L^2(S^{d-1}))$ or $\mathbb{C}^{L\times L}$	29, 86
$\mathcal{T}_{\boldsymbol{b},\boldsymbol{c}}$	generalized translation operator on $\mathrm{HS}(L^2(S^{d-1}))$ or $\mathbb{C}^{L\times L}$	40, 86
$\mathcal{P}_{\mathcal{V}}$	orthogonal projection on $\mathcal{V} \subset \mathrm{HS}(L^2(S^{d-1}))$	
$\mathcal{V}^{\perp}$	orthogonal complement of $\mathcal{V}$ in $\mathrm{HS}(L^2(S^{d-1}))$	
$\widetilde{G}$	approximation to $G \in \mathrm{HS}(L^2(S^{d-1}))$	
$\widetilde{G}^0$	approximation to $G \in \mathrm{HS}(L^2(S^{d-1}))$ in a subspace, reference solution for $\ell^1 \times \ell^1$ minimization	
$\widetilde{G}^{\delta}$	approximation to $G \in \mathrm{HS}(L^2(S^{d-1}))$ given noisy data	
$\boldsymbol{G}$	discretization of $G \in \mathrm{HS}(L^2(S^{d-1}))$	
$\partial\|G\|_{\mathcal{V}}$	subdifferential of norm $\|\cdot\|_{\mathcal{V}}$ at $G \in \mathrm{HS}(L^2(S^1))$	149
$\mathrm{prox}_{\mathscr{A}}$	proximity operator of $\mathscr{A} : \mathbb{C}^{L\times L} \to \mathbb{R}$	151

CONSTANTS

C_d	prefactor in far field expansion, $C_2 = e^{\mathrm{i}\pi/4}/\sqrt{8\pi}$, $C_3 = 1/(4\pi)$	10
b_0	prefactor in upper bound for $\|J_n(\|\cdot\|)\|_{L^2(B_{kR}(0))}$, $b_0 \approx 0.7928$	19
b_1	prefactor in upper bound for $\|j_n(\|\cdot\|)\|^2_{L^2(B_{kR}(0))}$, $b_1 \approx 4.791$	27
b_2	prefactor in upper bound for $\|j_n(t)\| = O(t^{-5/6})$, $b_2 \approx 0.9848$	147
b_3	prefactor in upper bound for $\|j_n(t)\| = O(t^{-1})$, $b_3 \approx 0.9519$	147

Index

Symbols

A

B

C

D

F

H

J

L

M

N

O